INVESTIGATION OF A HIGH EFFICIENCY LOW EMISSIONS GAS ENGINE

A Thesis submitted for the degree of Doctor of Philosophy

by

Karl Joseph Sean Mendis

Department of Mechanical Engineering, Brunel University

February 1994

ABSTRACT

The purpose of this project was to optimise a diesel engine converted to operate on natural gas, to suit the requirements for: low emissions, a high efficiency and sufficient power delivery within the constraints of cogeneration (combined heat and power) systems. Cogeneration Installations seek to improve the efficiency of power generation by utilising waste heat from the prime mover, as well as the production of electricity. Many small scale systems are based on open chamber gas engines, and, to reduce the payback time for the installation, the overall engine efficiency is of prime importance.

Stationary engines can be subject to strict standards for emissions, the greatest challenge being presented by the control of NO_x emissions. The main difficulty is that the highest efficiency operating point of a spark ignition engine is also the point of maximum NO_x emissions. The extent of this problem was analysed by conducting tests across the entire operating map of the baseline engine at the required speed of 1500 rpm. The solution, in the form of a new high compression ratio combustion system was based on the following: An extensive literature review, the previous Brunel experience with gas engines, an evaluation of the baseline combustion and emissions performance, and the predictions of the Integrated Spark Ignition engine Simulation (ISIS) thermodynamic model.

Tests were conducted on the new Fast Burn High Compression Ratio combustion system at compression ratios of 15:1 and 13:1, which demonstrated an extended lean burn capability such that an operating point was identified, that satisfied the conflicting requirements of: low emissions (less than 1g NOx/kWh or 360mg/m^3), and a high brake efficiency (above 30%), as well as particular cogeneration criteria. The bmep was mostly above 6 bar.

After further tuning and calibration with experimental data, the ISIS model was used to predict the engine power output, efficiency and emissions (NOx and CO) for the compression ratio of 15:1, across the entire operating map for both naturally aspirated and turbocharged configurations. The naturally aspirated results showed good agreement with the results of the experimental 15:1 FBHCR combustion system. The turbocharged engine was simulated with a bmep of 10 bar. The results identified much larger operating areas and all emissions limits were met above a brake efficiency of 36%.

The conclusions are, that an open chamber fast burn high compression ratio combustion system can achieve very low emissions, particularly of NOx, and a high efficiency by having the capability of operating with lean enough mixtures. Further improvement in the efficiency is likely if other engine parameters (such as the valve timing) were to be optimised for 1500 rpm. The results from the turbocharged simulation show that turbocharging, whilst restoring the output can also achieve low emissions, and a higher efficiency than a naturally aspirated engine.

ACKNOWLEDGEMENTS

I am indebted to Dr Richard Stone for his guidance, supervision, support and endless patience throughout the course of this project.

I am grateful for the assistance and supervision of Dr Nicos Ladommatos, and the assistance and valuable discussions with Mr Graham Weller and Mr Mehdi Daragheh.

I am also grateful to the workshop and engineering technicians, particularly Mr John Langdon, Mr Leslie Newell, Mr Clive Barrett, Mr Brian Morgan and Mr Brian Dear for their assistance.

I wish to acknowledge the support of British Gas and the SERC.

I wish to thank Razmik Balian, my friends, research fellows and students for their valued advice and encouragement.

Finally I would like to thank Michael DeSilva for bringing this project to my attention, and my mother and all my family for their help, encouragement and support throughout the course of this project.

NOMENCLATURE

abdc	After bottom dead centre	
AFR	Air fuel ratio	
atdc	After top dead centre	
bdc	Bottom dead centre	
bmep	Brake mean effective pressure	bar
bsfc	Brake specific fuel consumption	g/kWh
°ca	Degrees crank angle	°ca
CalValg	Gravimetric calorific value	J/kg
CI	Compression ignition	
CNC	Computer numerical control	
CoV	Coefficient of variation	%
EGR	Exhaust gas recirculation	
Eta	Efficiency	%
Evc	Exhaust valve closes	
Evo	Exhaust valve opens	
FBHCR	Fast burn high compression ratio	
F.E.	Finite element	
fmep	Frictional mean effective pressure	bar
IC	Internal combustion	
imep	Indicated mean effective pressure	bar
Ivc	Inlet valve closes	
Ivo	Inlet valve opens	
λ	Actual AFR / stoichiometric AFR	
LML	Lean mixture limit	
MBT	Minimum ignition timing advance for best torque	°ca
mfb	Mass fraction burnt	°ca
Mgas	Molecular weight of natural gas	kg /kmol
MIG	Metal inert gas	
NTP	Normal temperature and pressure	
Pabs	Absolute pressure	bar
Pbaro	Barometric pressure	mm
Pgdn	Gas pressure downstream of regulator	inches
Pivc	Pressure at inlet valve closure	bar
Pmax	Maximum cylinder pressure	bar
ppm	Parts per million	ppm
RAZ	Intermediate variable used in the fortran code to denote a fuel composition dependent constant	
RON	Research octane number	

SI	spark ignition	
TALuft	Technische Anleitung zure Reinhaltung der Luft (German Emissions Regulations)	
TAOx	Oxygen in the exhaust	%
TCI	Engine coolant temperature	
tdc	Top dead centre	
θ	Ignition timing	°btdc
UHC	Unburnt hydrocarbons	
VITU	Variable ignition timing unit	
WOT	Wide open throttle	

CONTENTS

CONTENTS

CHAPTER 1

LITERATURE REVIEW

1.1 INTRODUCTION TO THE CONCEPT OF COGENERATION

Combined Heat and Power or cogeneration are names given to systems that produce both electricity and useful heat concurrently. Conventional electricity generating plant comprises a prime mover and a generator. The prime mover requires an input of heat energy in order to produce useful work to drive the generator. The heat energy is usually obtained by burning a fossil fuel. Not all of this heat is converted into work. Some heat is lost, for example in the flue gases of a boiler, and some heat must be rejected to the surroundings. Cogeneration systems in contrast, make use of this waste heat in order to provide either process steam for industrial use, or hot water for space heating requirements. A cogeneration system then, would comprise a prime mover, a generator, and a comprehensive heat recovery system. (see figure 1.1). Large scale cogeneration systems (by a common convention these are systems that produce 500kW or more of electrical output) are based on gas turbine, or combined cycle, (ie. gas turbine and steam turbine), or large reciprocating engines. These reciprocating engines may be of the compression ignition or spark ignition type. Small scale cogeneration systems (systems producing under 500kW of electrical output), are invariably based on the reciprocating SI engine. In this particular range of prime mover, the SI engine offers the best all-round advantage, not least in terms of mechanical, and hence electricity generating efficiency, and the capital cost of buying and installing such a unit, but one of simplicity too. Large scale cogeneration plant have existed for many years, one of the oldest being at the Mogden sewage works which was built over fifty years ago.

Interest in small scale cogeneration plant, which is what this project is primarily concerned with, was stimulated after the 1983 energy act which relaxed the laws concerning connecting and running generators in parallel with the National Grid network. Linnell(1990), has provided several typical examples of small scale systems. Cogeneration systems may be used whenever there is a need for both electricity and heat. Hospitals are a particularly good example, requiring a constant supply of both. The benefits of cogeneration schemes are outlined in the following section.

1.2 BENEFITS OF COGENERATION SCHEMES

1.2.1 Economic Benefits

The electricity generating efficiency of the best conventional plant, at present is in the range 30%-40% (Davies Johnson and Weller 1990), whilst the majority of plant in the UK have generating efficiencies at the lower end of this range. The best combined cycle plant has a generating efficiency of not more than 50%. Modern boiler plant used for space heating purposes usually have efficiencies in the range 70%-85%. A well matched cogeneration plant in comparison, is capable of an useful energy conversion efficiency of 90%. Thus substantial savings can be made on heating and electricity costs provided high utilisation is made of cogeneration. Packer(1990) has described the major and marginal cost savings to be made from such schemes. These cost savings can be offset against the initial capital cost and the running costs to give a payback

period of typically two to three years. Thus the principal motive for installing a cogeneration scheme is an economic one.

1.2.2 Energy Conservation

Also for economic reasons, which will be discussed in section 1.3, the majority of cogeneration schemes are matched to the heating requirement and not the electrical load. However, owing to the concurrent production of electricity, the energy saving comes from displacing electricity that would otherwise be produced by the less efficient centralised conventional power stations.

1.2.3 Environmental Benefits

Generally whatever the choice of fuel, cogeneration systems burn less fuel and emit fewer emissions whilst achieving the same energy output as conventional sources. Hence they are much kinder to the environment. Natural gas is an ideal choice of fuel for stationary applications, as it is cheap and conveniently piped, and being a cleaner burning fuel, offers a greater potential for the reduction of emissions than most commonly used fuels. Emissions are currently a very important issue and although there is not at present legislation in the UK, regarding small scale stationary sources, there is proposed EEC legislation. For NOx emissions, the Swiss target of $4g/m^3$ and the German TALuft target of $500mg/m^3$ currently appears to be the most stringent for Europe, Thomas(1991). The types of exhaust emissions and the benefits of natural gas as a fuel are discussed further in the two following sections.

1.3 FACTORS AFFECTING SI ENGINE POWERED COGENERATION.

1.3.1 Availability

As mentioned previously, small scale cogeneration schemes are invariably based on the reciprocating engine. The majority of SI engine based cogeneration units are derived from CI engines and converted to run on Natural gas. The thermal and mechanical loadings experienced in a gas engine are much lower, compared with its diesel equivalent, and can therefore be expected to be inherently more reliable. Cogeneration also requires a fixed or constant engine speed (usually at 1500 rpm and coupled to a four pole generator to give a 50 Hz electricity supply that is compatible with the National Grid). From past experience, constant speed engines wear considerably slower than their vehicle mounted counterparts. Consequently they enjoy a longer lifespan and the ability to run at maximum availability with reduced downtimes for repair and maintenance. Maximum availability is desirable to maximize financial returns. Maximum availability at this stage means maximum usage (continuous usage if possible) at maximum load conditions and hence high energy utilisation efficiencies.

1.3.2 Energy Weighting and Sizing of Plant

As two forms of energy are produced concurrently in cogeneration schemes, there are now economic as well as thermodynamic aspects to consider, and a value weighting may be attached to each energy type Horlock(1987). Electricity is more versatile than the heat energy. It can be

exported to the National Grid. Therefore it would command a higher price. High grade heat (above 80°C) is more valuable than low grade heat, however if this is in excess it has to be dumped giving no financial gain. The ratio of heat to electrical output from an SI engine powered cogeneration system is characteristically 2:1. Not many applications require heat and power in exactly this ratio, (sewage treatment works being a notable exception), therefore careful sizing is essential. Provided there are no fuel supply limitations the best payback occurs when cogeneration is used solely to meet the baseload heating requirement which is ideally a constant heating requirement, for which the corresponding electricity generation still leads to an import of electricity. Thus it is desirable to shift the production ratio in favour of the electricity which will amongst other things strongly influence the payback period.

1.3.3 Improving Electricity Production Efficiency

The electricity generating efficiency is directly dependant on the brake thermal efficiency of the engine. Stone and Ladommatos(1991) have shown from work done on a gas engine that raising the compression ratio is likely to benefit the brake efficiency. It is envisaged that a compression ratio of 15:1 would be acceptable for this engine, using Natural gas, without the incurring knock. A higher compression ratio would also benefit an active lean burn combustion system. Lean burn combustion is desirable because it can be used to give a low bsfc (fuel efficiency) and low specific emissions without resorting to a catalytic converter and its associated efficiency penalties. More is said about compression ratio selection in section 1.7.

1.3.4 Fuel Cost

The cost of fuel energy is yet another factor that will strongly influence the payback period. Natural gas is offered at competitive prices compared to petrol, diesel or any other type of fuel. It also has several other attributes which are listed below. When an energy balance is considered, it must be remembered that in calculating the calorific value of natural gas, the water vapour is allowed to condense. As the latent heat of water is accounted for, it is thus the higher, or gross calorific value that is used.

Advantages :

Natural gas is readily piped and it is therefore good for stationary applications.

No vaporisation or atomization problems as with a liquid fuel, so it should be easier to achieve more homogeneous mixtures of air and fuel and facilitate easier starting.

Burns more cleanly (no SOx or emission of lead compounds) and offers a greater potential for the reduction of NOx, CO2, UHCs, and CO.

Has the equivalent of a very high octane rating enabling a higher compression ratio to be used.

Offers the user the choice of switching to bio-gas.

Disadvantages :

Methane concentration in the natural gas supply is subject to slight variations, (ie between about 90% and 97%). This may lead to experimental errors owing to the possibility of an inconsistent

air to fuel ratio.

Burns more slowly than petrol (Burn rates for typical air fuel ratios (λ) (and with 20% exhaust gas recirculation, EGR), are given for atmospheric conditions of pressure and temperature, (from Heywood(1988)).

Fuel type	Air fuel ratio λ	Laminar flame speed (cm/s)
Petrol	1.25	52
	1.0	75
	1.0+20%EGR	23
Methane	1.25	30
	1.0	40
	0.870	45

1.4 EMISSIONS

1.4.1 Types Of Emission And Effects

SI engines, in common with all internal combustion engines, produce work by converting the chemical energy in a fuel, (in this case methane), into heat by combusting it directly within their cylinders. The resulting expansion of the burning gases produces the work output. Under ideal conditions methane will burn completely in air to give carbon dioxide, water vapour or steam, and nitrogen (see equation below for stoichiometric combustion). However the combustion parameters in an engine are far from ideal and combustion is always incomplete. The products of incomplete combustion, in addition to the gases mentioned above are carbon monoxide, partially burnt and unburnt hydrocarbons, and oxides of nitrogen. The oxides of nitrogen

$$CH_4 + 2(O_2+\frac{79}{21}N_2) \rightarrow CO_2 + 2H_2O + 2(\frac{79}{21})N_2$$

consist mainly of nitric oxide (NO), with small amounts of nitrogen dioxide (NO_2) and are collectively referred to as NOx. It is the emission these gases, the products of incomplete combustion, that give rise to most concern. For a petrol SI engine the relative emission of each, per kilogram of fuel burnt as given by Heywood, are of the order 20g NO_x, 200g CO, and 25g unburnt hydrocarbons. Emissions from an untreated gas burning engine, running at a relatively low fixed speed are likely to be less given the lower carbon to hydrogen ratio of methane. This provides a good base to introduce emission control techniques, and these are discussed in section 1.5.

1.4.2 Nitrogen Oxides

NOx is considered to be the major pollutant from SI gas engines. It is formed during combustion where temperatures can rise high enough to cause atmospheric nitrogen, which is normally inert, to oxidise to NO, NO_2, and N_2O_5 (nitrogen pentoxide). About 98% of the NOx formed initially consists of NO, with about 2% of NO_2; (the level of N_2O_5 is negligible). With regard to health effects NO is only mildly harmful, but converts rapidly in the presence of air to NO_2. NO_2 is a poisonous gas which causes a wide range of respiratory problems. It is particularly harmful to asthmatics. In the presence of ultra violet light (present in sunlight), NO_2 and UHCs lead via complex chemical reactions to the formation of a photochemical oxidant, collectively known as smog, which together with sulphur dioxide is associated with acid rain. The reduction of NOx emissions without seriously compromising the power output of the engine is fundamentally difficult, and although the reduction of the other gaseous emissions is also important, NOx control methods currently draw the focus of attention.

1.4.3 Unburnt Hydrocarbons

Exhaust gases consist of a wide variety of unburnt and partially burnt hydrocarbons such as alkanes, alkenes, and aromatic compounds. Some products are the result of thermal cracking, caused by the high combustion temperatures; this is most applicable to the heavier liquid fuels such as petrol and diesel, whose molecules consist of long carbon atom chains. However, Natural gas consists almost entirely of methane. (A typical volumetric composition would be 93% methane, 3% ethane, 3% nitrogen, and traces of propane, butane, pentane, and helium). Methane is a relatively simple molecule which is completely saturated, and polymerisation reactions are unlikely to occur during combustion; (the reverse is true for heavier fuels). Therefore it is reasonable to assume that the unburnt fraction consists mainly of unreacted methane (see Davies Johnson and Weller (1990)). Past experience with gas engines suggests that a small proportion of formaldehyde, (the result of partially burnt hydrocarbons) is also present. Unburnt hydrocarbons can be objectionable because they cause irritation to the mucous membranes, particularly affecting the eyes and the nose. Of much greater significance is the reaction of these with NOx in sunlight to give the irritant ozone. Ozone is one of the constituents of what is commonly known as smog. Goldsmith (1989).

1.4.4 Carbon Monoxide

Carbon monoxide is a colourless and odourless gas. It is a primary pollutant and the first stage in the complete oxidation of carbon in the fuel. It is particularly dangerous to the health because it is more easily absorbed into the bloodstream than the oxygen (which it displaces), and inhalation of as little as 0.5% by volume can cause death in under 30 minutes. Goldsmith (1989), and the department of the environment report on global atmosphere and air quality (1991), provide a descriptive account of the primary and secondary pollutants and their effect on the environment .

1.4.5 Sources Of Unburnt Methane And CO Emission

CO emissions together with methane are considered to be a measure of the completeness of combustion and are primarily dependant on the air to fuel ratio; (its influence on emissions is examined in section 1.5). However, even at very lean mixtures (excess oxygen) there will be some CO and HC emission. At weak air to fuel ratios, CO emission is attributed to: incomplete mixing, insufficient combustion temperature, and the combustible mixture not being exposed to moderately high temperatures for long enough to effect complete oxidation to CO_2.

With regard to unburnt HC emissions, three possible sources have been identified. The largest of these (considered to be 40%-50%) is from the crevice volume, (the thin annulus formed between the piston crown, topmost piston ring, and cylinder), which is too narrow for the flame to enter. The other sources are from the quench layer, which consists of partially burnt and unburnt hydrocarbons, and from the thin lubricating oil layer which is capable of absorbing and desorbing hydrocarbons during the compression and expansion strokes respectively. These sources for both CO and Methane, can be minimised in a lean burn engine. Also of benefit is the likely operating envelope of this engine (to be discussed in the following section).

1.5 EFFECT OF AIR TO FUEL RATIO ON EMISSIONS

Figure 1.2 qualitatively shows typical variations of CO, NOx and unburnt HC emission with changing equivalence ratio, (the lambda (λ) is defined as the actual air fuel ratio divided by the stoichiometric air fuel ratio). At $\lambda<1$ (rich air to fuel ratios) emissions of CO and methane are very high owing to the scarcity of oxygen to facilitate complete oxidation. NOx emissions are low, but the fuel efficiency is also low. As the air to fuel ratio is weakened, both CO and methane emission levels fall rapidly until at around $\lambda=1$ or $\lambda=1.1$ the rate of decrease is slowed down. SI engines are normally operated at stoichiometric air to fuel ratios ($\lambda=1$) or slightly rich of stoichiometric to ensure smooth and reliable combustion, which is manifested in a high maximum torque range and a reasonably good fuel economy. However NOx emissions are high. The peak NOx emissions level is attained at a slightly weak mixture setting (about $\lambda=1.1$) owing to the combined effect of a high concentration of oxygen, and a high temperature. As the air fuel ratio is progressively weakened beyond $\lambda=1.1$ emissions of NOx fall rapidly until a combustion limit is reached, where owing to the large percentage of diluents present (ie.excess air or exhaust gas), the flame is either extinguished, or combustion is so slow that only a fraction of the mixture is consumed prior to the exhaust valve opening. Both these limits are manifested in erratic operation and a sharp increase in the unburnt HC emission and the fuel consumption.

One of the few disadvantages of natural gas is its relatively slow burn rate or flame speed. This limitation becomes a decisive factor in operating modes either side of the stoichiometric mixture setting. However, this is outweighed by its advantages (these are listed later in this section), and the operating envelope of a gas fuelled cogeneration unit which offers considerable potential for the optimisation of the specific fuel consumption with emission control. A fully vaporised fuel and

air mixture together with almost complete homogeneity, by definition, is said to possess the highest mixture quality. Methane being gaseous will contribute towards the achievement of such a mixture quality. This is desirable, as increased homogeneity has the effect of shifting the peak NOx position towards the right, Brown(1991). Operation is at wide open throttle (WOT) and although transient load conditions are expected, any mismatching that may occur owing to transient speed conditions, which only serve to exacerbate emissions of all three pollutants, are eliminated. There are currently two main operating modes for gas fuelled cogeneration units in order to reduce emissions of all three pollutants to acceptable levels. These are:

a) Operation with a stoichiometric air fuel ratio and a 3 way catalyst.
b) Operation with a sufficiently weak air fuel ratio such that NOx emissions are reduced to acceptable levels.

1.5.1 Stoichiometric Operation With a 3 Way Catalyst

A rapid ignition and a fast flame speed are more easily achievable with stoichiometric mixtures than lean mixtures. Thus, this mode of operation generally gives a higher brake work output and lower cyclic variability (ie CoV of imep), than with lean burn engines (less than a CoV of 5% for the purpose of electricity generation). Nevertheless, the main drawback is that peak temperatures are high. This leads to high NOx emissions and possible thermal overloading of engine components (and catalyst), which in turn increases the tendency for knock, and restricts the use of advanced ignition timings and turbocharging. See figure 1.3. Hundleby(1989) shows the limits of ignition timing with stoichiometric mixtures. An effective means of reducing peak temperatures is to apply exhaust gas recirculation. Seppen(1987) states that a 70% reduction in engine out emissions of NOx is achievable with only a 3% increase in fuel consumption and no loss of power. Further NOx reductions are possible with the use of a catalyst (more is said about this later). The Swiss NOx emission target of $4g/m^3$ for gas engines and the stricter German TALuft target of 500mg NO_x/m^3 currently appears to be the most stringent for Europe. Apart from the problem of peak temperatures, combustion efficiency is somewhat lower with stoichiometric operation than with lean burn operation, and consequently CO and HC emissions are higher. A common and very effective solution is the employment of a 3-way catalyst. Generally the 3-way catalyst gas engine gives the lowest emissions of all three pollutants provided it is operated within the catalyst "window" Thomas(1991).

The function of a 3-way catalyst is to oxidise CO and unburnt hydrocarbons to CO_2 and water, and to reduce NO to N_2 and O_2. The active catalytic material (platinum for oxidising, rhodium for reducing) must present the largest surface area (usually called the catalyst bed) to the stream of exhaust gas that is directed over it, in order to achieve the highest conversion efficiencies. Three-way catalysts employ a single catalyst bed for the conversion of all three pollutants. Heywood has shown that conversion efficiencies are of the order of 80%, providing the engine is operated at all times with an air fuel ratio at, or close to stoichiometric. Whilst this is true for the hydrocarbon oxidation of heavier molecular weight fuels, conversion efficiencies for methane

are not higher than 50% owing to the relative difficulty of oxidising saturated hydrocarbons. Furthermore ammonia can be produced during the reduction process of NO in the catalyst (Thomas). Also, running outside 0.5% to 1% richer (equivalent to λ=0.952 to λ=0.903) than stoichiometric will give strongly increased emissions and will result in damage to the catalyst (Seppen). This operating window is too narrow for the control capabilities of an ordinary carburettor, and a complex closed loop control system with oxygen and air fuel ratio sensors is required. Not withstanding these limitations and the costs involved, exhaust catalysts can be extremely effective for a given operating envelope, but may present difficulties for engines that place a greater reliance on the variability of the air fuel ratio as a means of compensating for changes in load.

1.5.2 Lean Burn Operation

An important (but difficult to meet) requirement for lean burn engines operating with natural gas, is the ability to achieve reliable ignition and fast flame propagation with very weak mixtures (ie weaker than λ=1.5), such that NOx levels are low enough to meet legislation (without resorting to a catalyst), and that cyclic variability does not exceed 5% CoV of imep (as dictated by generator stability limits). The emission of CO is negligible from a lean burn gas engine, and providing that the lean combustion limit is not approached, unburnt HC (or methane) can also be minimised by using compact combustion chambers in which the crevice volumes are minimised. Compact combustion chambers that are more tolerant of lean mixtures are desirable; this is examined in greater detail in section 1.7. Generally a lean combustion system gives a lower isfc than a stoichiometric combustion system with EGR. This is because the combustion efficiency is greater, and the chemical energy associated with catalytic conversion of unburnt fuel could be utilised in the combustion chamber instead. Stone and Ladommatos have shown that as the mixture strength is weakened there is a reduction in the indicated sfc. However, there is a penalty, as a relatively low brake power output can be expected from a lean burn engine; the use of turbocharging may have to be considered in order to raise this. It has already been stated that charge dilution is very effective in reducing NOx levels, and also for extending the onset of knock by reducing the peak temperatures. This implies that a higher compression ratio and/or turbocharging may be used to raise the power output without thermally overloading engine components. Raising the compression ratio should increase the imep and enable the lean misfire limit to be extended. A lower combustion temperature would also lead to less heat transfer to the cylinder and improve the thermal efficiency. Thus lean burn combustion offers a simpler, more cost effective solution with scope for the lowest fuel consumption.

1.6 NITROGEN OXIDE CONTROL METHODS

1.6.1 Sources

As mentioned in section 1.4.2 the predominant oxide (about 98%) that comprises NOx is NO. The main source of NO is from the oxidation of atmospheric nitrogen which occurs at high temperatures. (The oxidation of nitrogen present in the fuel is an additional source only when

it is chemically bonded for example in an aromatic compound in the fuel, but as these are present only in trace form this source of nitrogen may be considered insignificant). Weaving(1990) shows the relationship of NO formation rates with temperature. Superimposed is the thermal efficiency curve (see figure 1.4). Reducing the temperature will reduce total NO emissions but not without also incurring a thermal efficiency penalty, and a compromise is required between efficiency and emissions.

The formation of NO is described by the extended Zeldovich mechanism:

$$O + N_2 \rightleftharpoons NO + N$$
$$N + O_2 \rightleftharpoons NO + O$$
$$N + OH \rightleftharpoons NO + H$$

These mechanisms are deemed to be sufficient for most computer model predictions. All three reactions are reversible and will reach an equilibrium given sufficient time. However owing to the rapid changes within the engine cylinders these reactions freeze, since during the expansion stroke the temperature of the burnt gas falls, and the reverse reaction rates become too slow for equilibrium to be attained, and this gives rise to a larger concentration of the products (ie.NO), than predicted by equilibrium considerations. Thus, it is interesting to observe the variance of the kinetically controlled NO concentration, and concentrations predicted by equilibrium considerations when plotted as a function of crank angle (see figure 1.4a (taken from Raine 1993)).

Combustion of the fuel and air mixture occurs through a flame propagation process, which originates in the vicinity of the spark plug and travels rapidly across the combustion chamber. This rapid flame propagation depending on the ignition timing, usually occurs before TDC of the piston is reached, hence that proportion of the mixture that is consumed initially is compressed further and attains a higher temperature than immediately after combustion. The time scale for NO reactions are relatively slow compared to the speed of the flame front (HC oxidation), therefore the NO formation can be decoupled from the combustion reaction, and it is assumed that the NO formation is predominantly behind the flame front, in the burnt gas region where all of the above radicals are present. Heywood has introduced equilibrium concentrations for the reactants (denoted by $[\ ]_e$) in each of the three equations, and together with their respective reaction rate constants, he gives a single equation for predicting the rate of NO formation which is given below.

$$\frac{d[NO]}{dt} = \frac{6\times10^{16}}{T^{1/2}} \exp\left(\frac{-69090}{T}\right) [O_2]_e^{1/2} [N_2]_e \qquad mol/cm^3 s$$

It is clear that the rate of reaction varies exponentially with temperature. Weaving shows that the predictions compare well with experimental results, but at maximum NO concentrations the model required some adjustment in order to give comparable values. Raine(1993) has presented data

from a computer model developed from Ferguson(1986) by Stone et al(1993) which uses either a single burnt zone, or a user specified number of zones in which the average temperature of an adjacent zone would differ from the next. The predicted NO values are very close to experimental values, particularly when using multiple burnt gas zones. The comparisons are discussed fully in chapter 5.

1.6.2 NOx Control Methods : EGR

Mixture dilution is a very effective means of reducing peak temperatures because the percentage of extra diluents present such as air or exhaust gas, not only displace the fresh charge, but also absorbs the heat released during combustion, without in any way contributing to it. This reduces the flame temperature and the NO. The NO reducing capacity of the diluents is directly related to their specific heat capacity. CO_2 is the best available and exhaust gas is almost as good, Thomas. Exhaust gases contain a proportion of water. Provided this is cooled to the air temperature prior to induction (this is necessary in order to maintain the volumetric efficiency but not always possible.), then the latent heat effect provides an important cooling facility. Also at higher temperatures water dissociates endothermically into its constituents, hydrogen and oxygen and re-associates when the temperatures fall. This negates the effect of its lower heat capacity compared with CO_2. Reductions of as much as 70% and 80% in engine out emissions of NOx have been achieved by using sophisticated control equipment and various ratios of exhaust gas and excess air. Seppen has described three different situations where these may be applied. The level of EGR used for gas engines operating with a stoichiometric charge and exhaust catalyst is generally between 25% and 30%

1.6.3 NOx Control Methods : Excess Air

EGR may also be used with lean burn gas engines, however if the NOx emissions targets can be met with the use of excess air alone then this should lead to a lower specific fuel consumption. Stone(1989) has shown how the fuel-air efficiency increases with weakening equivalence ratios (figure 1.5). (ie. Assuming the LML is not approached, the efficiency increases as the mixture is weakened). Generally for a given NOx reduction it is necessary to use a greater percentage of excess air than exhaust gas owing to the lower molecular weight and lower heat capacity of its constituents (this difference increases as the temperatures rise during compression and will improve the cycle efficiency). There are some gas engines running with as much as 60% to 90% excess air. Thomas. The peak NOx levels in SI gas engines occur at a slightly weak air fuel ratio (λ). This is because the extra oxygen available initially offsets the falling combustion temperatures, and it is where an optimum of combustion temperature. oxygen availability and time is reached. So although it may be argued that the oxygen in excess air is a contributant to NOx at close to stoichiometric mixtures, at very weak air fuel ratios the temperature has a disproportionately greater effect on NOx formation than the oxygen. Hundleby(1989) has compared EGR with excess air (0% EGR), on engine out emissions of NOx. As discussed in section 1.3.3, the use of excess air would also lead to a capital cost saving as a lean burn combustion system does not require a catalyst and an EGR control system.

1.6.4 NOx Control Methods : Ignition Retardation

The phasing of the spark discharge relative to the position of the piston is vital for obtaining the greatest amount of work from the burning fuel. If the spark occurs too early in the compression stroke the amount of (negative) work the piston has to impart on the burning gas increases drastically. That is, a larger volume of burnt gas is compressed to a higher pressure and temperature than immediately after combustion, and this gives rise to high levels of NO formation. If the spark occurs at, or too close to TDC the pressure rise due to combustion is offset by the increasing cylinder volume as the piston retracts towards BDC, and is manifested in higher exhaust temperatures and loss of heat energy. Between these extremes exists an optimum timing (MBT), which maximises the bmep or net work output. The bmep is relatively insensitive to spark timing around the optimum timing value. If a slightly retarded spark timing to the optimum value is chosen (as is sometimes done in practice), this will result in only a small loss of net work (often less than 1% (Brown 1991)), but a significant reduction in the tendency for knock to occur. Generally EGR and exhaust gas catalysts operating with a stoichiometric mixture, or a lean burn combustion system using a very weak air fuel ratio may be used in the first instance to reduce emissions of NO. (As the percentage of diluents increase the flame speed decreases, hence the spark timing needs to be advanced to give more burn time duration. The best combustion chambers have features that will promote a faster burn so that very advanced timings are unnecessary. See section 1.7). If further NOx reductions are required retarding the ignition is very effective. Some engines are better able to tolerate retarded ignition at maximum loads owing to the higher cylinder pressures and the resultant faster burn rates, but this should be used as a last resort as the efficiency is reduced also.

1.7 COMBUSTION SYSTEMS

1.7.1 Principles

In a spark ignition engine the combustible charge of fuel and air is pre-mixed in the intake system, inducted through the inlet valve into the cylinder and compressed prior to being combusted. The quantity of fuel is controlled so that the air fuel ratio can be richened or weakened within the combustible range in response to the load placed on the engine, or the emission control requirements. Combustion is normally started towards the end of the compression stroke by a spark which initiates burning in a small region, forming a roughly spherical shape (flame kernel), close to the spark plug electrodes. The flame kernel grows slowly at first with no detectable pressure rise in the cylinder; this period is usually referred to as the ignition delay (or flame development) period. The flame speeds at this stage are close to the laminar flame speeds, because the flame kernel is smaller than the typical turbulent length scales within the cylinder. Because of its size it is also more easily influenced by the air motion. If the flame kernel is displaced towards the centre of the combustion system than towards a surface, then the development of the flame frontal area is less likely to be inhibited by early contact with the combustion chamber walls. (Displacement of the flame kernel is thought to be a primary source of cyclic variation because of the resultant effects of heat transfer to the combustion

chamber walls, development of the flame frontal area, and the peak temperature and pressure attained in combustion). As the flame grows in size, and turbulence becomes much more significant, the flame speed increases rapidly to a value that is much higher than the laminar flame speed. This is called the rapid flame propagation stage and is accompanied by a rapid rate of change of temperature and pressure. The flame frontal area continues to grow in a spherical manner until the combustion chamber walls are encountered. The entire process then begins to slow down until the remainder of the charge (or end gas), is consumed. During the rapid flame propagation stage the temperature and pressure of the end gas also increases rapidly. Its temperature is further increased due to radiation from the flame front. If sufficient time is spent at these high temperatures, elements of the end gas are liable to spontaneously ignite. This process is known as knock or auto-ignition and results in a sudden increase in pressure and the familiar high pitched ringing sound.

1.7.2 Factors Affecting Combustion

It has been considered historically that for best engine performance the mixture of fuel and air should be completely gaseous and homogeneously mixed. As examined previously the air fuel ratio affects several aspects of engine performance. The main aspect is the rate at which the flame front is established and thereafter propagates through the unburnt charge. Brown(1991) has shown the effect of the air fuel ratio on laminar flame speeds. Due to dissociation effects, the maximum flame speed occurs with slightly richer than stoichiometric air fuel ratios. If the air fuel ratio is richened or weakened beyond this optimum, the combustion temperature is lowered (ie heat is absorbed by the excess fuel or excess air respectively), which in turn lowers the flame speed. When the mixture is progressively richened an ignition limit is ultimately reached where the spark can no longer initiate a self sustaining chemical reaction. When the mixture is progressively weakened, then again a limit is reached. Either ignition can fail to occur, or the flame is extinguished (this is called the lean misfire limit (LML) and is deemed to have been reached when flame propagation fails in a certain percentage of cycles), or flame propagation is so slow that the mixture is only partially burnt before exhaustion.

The mixture pressure and temperature just prior to ignition have a significant effect on the flame speed. Both cause a higher reaction front temperature and consequently greater flame speed. Another factor is mixture motion or turbulence within the cylinder. Turbulence has the effect of wrinkling the flame front. (During the initial flame development phase too much turbulence may be detrimental because the flame front may be strained severely enough to extinguish it). This increases the flame frontal area and reduces the time required to consume the entire charge. In this engine, factors that increase the flame speed are highly desirable as they extend the LML and the partial-burn limit and they also reduce the tendency for knock mechanisms to occur. Increasing the turbulence intensity will increase the burn rate over all air fuel ratios. Thus the critical mixture at which slow burning has a result on efficiency is made leaner. Overington(1990) has presented graphical results showing the effect of air dilution and increased turbulence on engine performance. He has shown that the lean running limit is considerably extended from an

an air fuel ratio λ of 1.35 to 1.49, giving better fuel efficiency, and lower NOx emissions whilst still maintaining reasonably low levels of unburnt HC emissions.

1.7.3 Cyclic Variation In Combustion

The problem of cyclic variation in the imep is fundamentally a problem of variation in combustion from one cycle to the next owing to variations (it is widely believed), in the initial flame development period. Brown has shown by means of a turbulent combustion model that cycle to cycle variation in imep is largely due to the random variation in the initial position of the flame kernel after detachment from the spark plug gap. If the flame kernel is detached towards the chamber walls, heat transfer to the walls lowers the burn rate and peak cylinder pressure. The reverse is true if the kernel is detached towards the centre.

The mixture strength in the immediate vicinity of the spark plug also has an influence on flame development. It is clear from the preceding arguments that what is required is low turbulence in the vicinity of the spark plug and high turbulence in the main bulk of the charge to enhance the rate of combustion. Charge stratification is one method used with very lean mixtures (this is discussed in the section on divided chambers), but is not possible in all cases. Brown has outlined the effects of a number of parameters on flame development and propagation which have been summarised by Germane et al(1983) and are as shown in table 1.1.

Table 1.1. Effects of a number of parameters on flame kernel development and flame propagation. Adapted from Germane et al(1983).

Ignition Parameter	Flame kernel development	Flame propagation
Increased spark energy	Increases	No effect
Hotter spark plug	Increases	No effect
Increased compression ratio	Increases	Increases
Turbulence	Decreases	Increases
Charge dilution	Decreases	Decreases
Increased flame travel (ie. non centralised ignition source)	No effect	Decreases

1.7.4 Design Features Of Active Combustion Systems

The arguments so far, have outlined that low emissions and a reasonably high efficiency, can be achieved with a fast burn combustion system because it is better able to tolerate the burning of weak mixtures. These 'active' combustion systems have a variety of design features to promote 'fast burn' and these are discussed below.

The spark plug and the combustion chamber are centred around the hottest part of the combustion chamber (ie. near the exhaust valve), so that the end gas is burnt in the coolest part of the chamber (ie. near the inlet valve or squish area), thus minimising the risk of self-ignition. Flame travel is also shorter, thus the time taken to consume the entire charge is reduced.

A high thermal efficiency is achieved by: a) Using the highest practicable compression ratio (ie. just avoiding the onset of knock or self-ignition), b) minimising the heat loss to the combustion chamber walls. The lowest surface-to-volume ratio (hence smaller quench area), is achieved with spherical combustion chambers, but this may not be usually possible owing to the need to accommodate other essential features such as efficient port shapes and a large valve area.

Crevice volumes are kept to a minimum (ie. around the spark plug electrodes, between the cylinder head and block, and the annulus between piston, piston ring and cylinder wall) in order to minimise emissions of unburnt hydrocarbons. Most combustion chambers have a squish clearance. This is very effective in generating turbulence when it is most required; that is close to TDC during the rapid flame propagation phase. A large valve area is beneficial to the volumetric efficiency. A significant increase in valve area per bore size can be achieved with four rather than two valves.

The careful design and positioning of the inlet port will improve the induction flow characteristics which will in turn influence the subsequent mixture motion within the cylinder during the compression stroke. This is sometimes enhanced by including special features in the valve or piston crown geometry, as with the Nebula combustion chamber, see section 1.7.6. If a regular and uniform flow is induced in the cylinder and it is possible to conserve its kinetic energy until the very last moment, then this is an important source for generating turbulence during the rapid flame propagation phase. The induced mixture motion is usually a swirling motion whose axis is either in the same plane as that of the cylinder (swirl), or perpendicular to the cylinder axis (tumble). In the design of combustion chambers, it is never possible to accommodate the best of every feature. Thus a compromise has to be made which takes into account the operating envelope of the engine, manufacturing constraints, and other constraints.

It has already been mentioned that low emissions can be achieved by operating with either a stoichiometric mixture and an exhaust catalyst, or a very lean mixture. The reasons for adopting lean burn combustion have been stated. Lean burn combustion systems can generally be divided

into two different types. They are: a) Open chamber. b) Divided chamber. These are described in the following two sections.

1.7.5 Divided Chambers

Charge stratification is one method employed to ensure the reliable ignition of overall very weak air fuel ratios. This is facilitated by using a combustion system comprising two chambers; a small pre-chamber and a main chamber which are connected together by one or more narrow passages (See figure 1.6). A predominantly rich mixture is introduced into the pre-chamber which is initially too rich to burn. This is brought close to a stoichiometric composition during compression, when part of the very lean mixture in the main chamber is forced into the pre-chamber at high velocities. The resulting turbulence ensures good mixing and once ignited the flame that exhausts from the pre-chamber (which is of considerably higher energy than could be obtained from a spark plug), acts as a torch, igniting the more difficult to ignite charge in the main chamber. The overall effect of this arrangement is to enhance early flame development and increase subsequent flame speeds, without relying on mixture motion induced during the induction period. A large fraction of the air can be utilised, and operation with much weaker air fuel ratios (eg. λ=1.96 or greater, (Kingston Jones and Heaton(1989)), is possible than with open chamber combustion systems.

It is common to find that there is a wide range of diesel engines that lend themselves readily for conversion to gas operation. The central diesel fuel injector is replaced by an assembly comprising a small pre-chamber, a spark plug, and a gas admission valve. Pohl(1988) presents sectioned views of some conversions. Installation of the pre-chamber assembly is only suitable for engines with a cylinder bore size of say 160mm and above. Kingston Jones and Heaton state that for bore sizes below this figure the conversion is not so easily accommodated owing to smaller injector sizes and inadequate space.

Serve(1982) presents results showing the effect of various parameters on NOx emission and the bsfc. These parameters are: charge dilution, charge air cooling, and ignition retardation. Development of the divided combustion system resulted in a design whose pre-chamber volume is less than 2% of the swept volume. The outcome is a reduction of 93% NOx with a concurrent fuel consumption improvement ranging from 2% to 8%. This translates to 2.68g NO_x/kWh at the rated speed and load. A further reduction to 1g NO_x/kWh is possible whilst incurring a 3% fuel penalty and a reduced full torque speed range.

Pohl presents results from a pre-chamber combustion system. Very lean mixtures were used (up to 80% excess air), in order to meet targeted emission levels of 2.0g/kWh, 3.35g/kWh, and 1.34g/kWh of NOx, CO, and HC respectively. A three hole nozzle was used between the pre-chamber and the main chamber. A compression ratio of 9:1 was used and the engine had a bmep rating of 13.1 bar. Operation was at fixed speeds which ranged from 750rpm to 1000rpm.

This review shows that pre-chamber combustion systems are well proven in their ability to control NOx emissions, and return a high knock free bmep by operating at very lean air fuel ratios. However, pre-chamber combustion systems are not without problems. Improvements in thermal efficiency are hindered by high heat transfer coefficients caused by the high gas velocities between chambers. This and the inherently higher surface-to-volume ratio causes air temperatures to be reduced. Also the susceptibility of nozzle hole erosion is increased. Control of the air fuel ratio is complex. Stone and Ladommatos state that *the most demanding control* requirements are starting, and transient load acceptance in electrical generation systems. It has also been suggested that it is difficult to make a system suitable for operating over a wide range of speeds and loads. Consequently there is merit in the use of an open chamber combustion system, that will operate with a sufficiently lean mixture.

1.7.6 Open Chambers

Open chamber combustion systems have been widely used in the conversion of diesel engines to operation with Natural gas, because modifications are generally simpler and consequently cheaper. This may also be more appropriate as many production diesel engines in the cylinder bore range up to 160mm have only two valves and swirling combustion systems. The modifications required are: substitution of a spark plug for the diesel fuel injector, installation of a gas carburettor and ignition system, and some dimensional changes to the combustion chamber. The design of the combustion system is limited by certain practical constraints, (ie. location of the spark plug is largely dictated by the fuel injector position, and the combustion chamber itself is usually limited to a hollow in the piston). However, Stone and Ladommatos present encouraging results from just such a combustion system and there is scope for much more development. Generally there has been little specific interest in developing an open chamber combustion system for gas operation with low emissions. However a notable exception is the adaptation of the Ricardo 'Nebula' open chamber for lean burn gas operation.

1.7.7 Choice Of Compression Ratio

One way of improving the thermal efficiency is by raising the compression ratio. In petrol SI engines the maximum practicable compression ratio is about 12:1. Active combustion chambers and alteration to the timing will delay the onset of knock to a certain extent but ultimately it is the fuel quality (octane rating), that is the limiting factor. The properties of Natural gas are such that it is the equivalent of using a petrol of a much higher octane rating. (ie. about 120 RON rather than 97 RON). Thus it is possible to raise the compression ratio closer to its optimum; even if the fuel is not a limiting factor and the onset of knock could be avoided, there is an optimum compression ratio above which there is no appreciable gain in overall cycle efficiency owing to thermal and mechanical losses (see figure 1.7). At a higher compression ratio peak temperatures and turbulence intensity will generally be higher and the combustion chamber shape will be influenced by other constraints. Thus the surface to volume ratio will not be the ideal for thermal efficiency. Consequently there will be greater heat losses. The reduction in mechanical efficiency is due to higher pressure loadings on the bearings. Hence the optimum compression ratio is

around 16:1, although this figure has been arrived at somewhat arbitrarily by considering parameters such as: the cylinder swept volume, the air fuel ratio, the combustion system design, and the operating speed in question, it is consistent with the work of others. Muranaka et al(1987), have published data on the optimisation of compression ratio. The fact that some IDI diesel engines operate at a compression ratio above 20:1 is to achieve reliable ignition of the fuel at all conditions, particularly in the starting of a cold engine, and it does not necessarily give the peak efficiency for either economy or power. Early methods of NOx control were to lower the compression ratio, and retard the ignition timing in order to limit peak temperatures, but this also reduced the thermal efficiency. The modern approach is to operate with a very weak air fuel ratio whilst maintaining a high compression ratio. This should give the duel benefits of reduced NOx emissions and improved fuel efficiency.

1.7.8 Review Of Open Chambers

It has been mentioned that divided chambers employ a degree of charge stratification to facilitate the burning of overall very weak mixtures. Its effect on open chambers is examined by Ozasa et al(1991), who present results obtained from a research petrol engine with a helical port and a swirl ratio of 2.6. Three types of combustion chamber were examined using a gas sampling technique. It was found that greater mixture homogeneity had the effect of reducing NOx emissions. The mixing effect was most substantial with the "figure of 8" shape combustion chamber as even with an induced heterogeneous charge, mixture strengths latterly in the compression stroke were almost uniform throughout the cylinder.

Weaving presents results on four types of petrol lean burn combustion chamber. Lowest NOx and unburnt HC emissions were obtained from the Nebula combustion system at a compression ratio of 9:1 and a best air fuel ratio of λ=1.35.

Kingston Jones and Heaton have evaluated the Nebula combustion chamber for Natural gas. At 9.4 bar bmep and 1800 rpm the engine achieved 0.7g/m^3 NOx within the target gas consumption of 9900 kJ/kWh and at an excess air ratio of λ=1.62. At 9.4 bar bmep and 1200 rpm the engine achieved 0.5g/m^3 NOx within the same target gas consumption.

The results presented by Stone and Ladommatos are also for a lean burn gas engine. The combustion chamber was a bowl in piston Heron shape, and offset to reduce swirl and increase turbulence. The swirl ratio was 1.79. Operation was at 1500rpm, wide open throttle WOT, at a bmep of 6.4 bar. With an equivalence ratio of 0.6 the brake specific emissions of NO_x were 3g/kWh. They state that there is yet more scope for reductions in emissions with further development of this combustion system.

1.7.9 Benefits Of Turbocharging

The drawback of operation with a very weak air fuel ratio is a lower brake work output. A low output usually leads to a decrease in efficiency since the fmep (largest contribution is thought to

be from the piston ring and cylinder) which is assumed to remain constant over a given range now forms a significant percentage of the imep. Turbocharging is often used to compensate for falling output because it is a very cost effective solution. Turbocharging would usually lead to an improvement in efficiency, as better use is now being made of the exhaust energy whilst increasing the brake work output. However, owing to the greater air requirement of a lean burn combustion system and the fact that there is less energy available in the exhaust to drive the turbine, it is now most important to maximise turbocharger efficiency. With fixed speed operation there is considerable potential, by use of better matching, for maximising turbocharged engine efficiency.

CHAPTER 2

EXPERIMENTAL SYSTEM

2.1 INTRODUCTION

An engine test facility was installed and commissioned to carry out the experimental work. This involved setting up a Natural gas conversion of a Ford Dover six cylinder 6.2 litre spark ignition engine on a test frame and coupling it to a water brake. Provision was also made for fuelling, cooling, electrical and instrumentation systems. See appendix A for the engine specification. Figure 2.1 is a schematic diagram of the test facility.

The cooling water supplied to the heat exchanger is also used for the water brake. Fuelling is directly from the Natural gas supply via a gas meter, according to the code of practice for Natural gas fuelled spark ignition engines (British Gas publication IM/17,first edition 02.81). Flexible connections are used to isolate the gas supply, the cooling water supply, and the exhaust system from test bed vibrations.

Exhaust emissions are measured with three types of exhaust analyser. Combustion analysis is facilitated by a piezo-electric cylinder pressure transducer and a high speed data acquisition software package. Provision is made for the measurement and control of the power output and speed of the engine.

2.2 DESIGN, FABRICATION, AND INSTALLATION OF THE TEST FACILITY

The test bed was designed as a welded structure using readily available standard mild steel sections. The sections were welded together using the MIG arc welding process. A rigorous analysis of stresses (such as an F.E. analysis), experienced in the structure and the welds was not carried out, as this would be time consuming and complicated. Instead a large factor of safety was adhered to, and the structural dimensions to achieve adequate rigidity are based on previous experience. Stress calculations are based on simplifying assumptions and were deemed sufficient for this application. The torsional load resulting from the engine torque is small compared to the total weight of the engine and dynamometer (ie. 386Nm compared to approximately 10kN). Therefore stresses are based solely on the bending moment derived from the overall weight of the engine and dynamometer. The weight of the steel members is neglected and the total weight of the engine and dynamometer is assumed to act on the centre of the beams. Thus by assuming the worst possible case, a large factor of safety is allowed for.

The test bed is installed on the test cell floor on four rubber cushioned mounts. The engine is mounted on the test bed on front and rear supports fabricated from standard lengths of mild steel angle. The supports are secured to the bed by four M24 bolts.

The dynamometer stand is fabricated from standard lengths of angle and also serves as a support for the shell and tube heat exchanger. The dynamometer is bolted to the stand and the entire assembly is located using dowel pins, and bolted to the test bed. See figure 2.2.

2.2.1 Engine and Dynamometer Coupling

In order to measure the engine speed, torque, and power output it is necessary to connect the engine to a dynamometer. This facilitates control of the above variables by altering the dynamometer load. A flexible coupling is used as an interface to absorb any vibrations (arising from variations in the balance caused by slight misalignment of the engine with respect to the dynamometer), and torque fluctuations. A commercially available coupling was chosen, which gave the widest tolerance on shaft misalignment in its specification. See appendix A, (The specification gave a maximum speed rating of 2500 rpm, a maximum torque rating of 2712 Nm, and allowance for radial and axial misalignment of 0.6 mm and 3.5° respectively).

2.2.2 Flywheel and Dynamometer Flanges

The flexible coupling could not be bolted directly on to the engine flywheel and the dynamometer driving flange. Therefore two flanges were designed to interface between the engine and the coupling, and the coupling and the dynamometer respectively. The engine flywheel has a machined face with tapped holes to secure the clutch pressure plate. This face provides a good locating point for a flange to connect with the flexible coupling. The dynamometer driving flange also has bolt holes to facilitate the location of a similar flange. Thus, both the coupling flanges are machined from 40 mm thick mild steel plate. A reasonable assumption made here is that the material is homogeneous, in which case the flanges will be in balance. See figure 2.3.

2.3 QUASI-STEADY MEASUREMENTS

2.3.1 Engine Speed Measurement and Control

The engine speed is controlled by a Heenan and Froude DPX3 water brake dynamometer. This type of dynamometer consists of a vaned rotor which turns adjacent to a pair of vaned stators. Sluice gates separate the stators from the rotor, and it is these which control the load absorbed by the dynamometer. See figure 2.4.

All tests were to be carried out at wide open throttle and a constant speed of 1500 rpm. The dynamometer is used to vary the torque presented to the engine in order to maintain a constant speed over the entire operating equivalence ratio range. The dynamometer drive shaft is fitted with a sixty tooth gear wheel, which is used in conjunction with a magnetic pick-up in order to sense the engine speed. The engine speed is displayed to the user on a digital display unit. An analogue output is also provided, and this is used to drive an analogue indicator in the test cell. An accuracy of $\pm$ 0.25% (4rpm) of full scale reading is quoted as being obtainable. This has been checked with a digital counter sourced at the instrument input. An accuracy of $\pm$ 1rpm is possible thus vindicating the manufacturer's quoted figure.

2.3.2 Engine Torque Measurement and Control

When the air fuel ratio is enriched to increase the torque and power output from the engine, it is necessary to increase the load in order to maintain a constant speed of 1500 rpm. The engine output torque is measured by the reaction on the dynamometer casing, by a strain gauge type of load cell. The signals produced are fed back to the control panel to be displayed in units of torque (Nm), or power (kW) on a digital display unit. Units of torque are preferred to kW due to the inherent inaccuracy of the instrument power calculation. A calibration check is carried out by attaching a calibration arm (of known length), and hanging weights (of known value; see following section on calibration data) and taking a torque reading from the instrument at each addition. On attaining full scale reading (500Nm, which is slightly above the maximum torque developed by the engine), a further set of readings is taken as weights are removed from the calibration arm. Comparison of the readings taken in either direction will give an indication of the hysteresis and repeatability of the system. Generally an accuracy of better than $\pm$ 0.25% has been quoted as being obtainable (which corresponds to $\pm$ 1.25Nm), and from inspection of the results below this is largely true.

2.3.3 Calibration Data

A typical set of readings is presented in table 2.1 for the static loading and unloading of the Dynamometer during calibration checks. The beam span is 2250mm and the scale is 1lb ≡ 5Nm.

Table 2.1 Dynamometer calibration results during loading and unloading tests

Load(lb)	Equivalent torque(Nm)	Display(Nm)	Comments
0	0	-2.9	Loading
25	125	120.6	
50	250	247.2	
75	375	374.0	
100	500	500.0	
75	375	374.4	Offloading
50	250	250.6	
25	125	121.4	
0	0	-1.9	

2.3.4 Gas Flow and Equivalence Ratio Control

Generally, control of the gas flow and hence the equivalence ratio is achieved in two possible ways: 1) The inlet gas pressure can be varied by means of a gas pressure regulator which is fitted downstream of the gas meter. 2) The gas flow rate to the engine can be varied by a butterfly valve which lies immediately upstream of the Impco gas carburettor. Either one, or both may be used in order to achieve the desired result. Further control of the equivalence ratio is possible by making use of modifications in the carburettor which allow extra air to be bled in and/or less gas to be admitted. See figures 2.5, and 2.6 and appendix A.

The inlet gas pressure can be varied from 127 mm or 152 mm water gauge to under 25 mm but this usually leads to erratic engine operation. The gas flow is measured in cubic feet per minute with the use of a stop watch to time the consumption of a fixed volume (10 cubic feet) of gas.

2.3.5 Blowby Gas Flow Measurement

The flow of combustion chamber gases past the piston rings into the sump, which largely occurs during the compression stroke is termed blowby. A suitable mid range operating point (1500rpm, λ=1.3 and MBT ignition timing), is chosen for this measurement. The gas flow is measured in cubic feet per minute using a Roots type gas flow meter and stopwatch. The blowby gas line is connected to the Roots meter using a short length of rubber hose and clips to ensure no leakages, and the elapsed time is recorded for 10 cubic feet. The ambient pressure and the gas temperature are also recorded.

The blowby emissions are passed through the Richard Oliver analyser in order to determine its composition. The results (0.02% CO, 0.76% CO_2, 37280ppm HC, 18.2% O_2), establish that it largely comprises unburnt mixture. If the mass fraction of the combustion products in the blowby flow is calculated then this places an upper bound on the exhaust residuals trapped in the cylinder.

2.3.6 Air Flow Measurement

The air flow was measured by a Lucas Dawe air mass flowmeter which was connected immediately upstream of the air filter. The display unit gave the air flow in g/s. At the present moment the air flow is entirely influenced by the inlet manifold depression. The throttle setting is WOT in order to improve the volumetric efficiency, and the speed is constant at 1500 rpm. The advantage of this flowmeter is that it gives an instantaneous measurement of the air flow. Cockshott et al,(1983) have described the operating principles. The flowmeter has an air duct in which an electrode is placed centrally. This electrode is maintained at about 10kV (by using mains electricity and an amplifier) so that a corona discharge is formed. The exact voltage is varied so that the sum of the currents flowing to the two collector electrodes is constant. When air flows through the duct, the ion flow is deflected, and this causes an imbalance in the current flowing to the two collector electrodes. Cockshott et al show that the difference in the current flow is proportional to the air mass flow rate. The flowmeter has a response time of about 1 ms and

is bi-directional, but the length of the measuring section leads to a slight averaging effect. The disadvantage of this meter is its sensitivity to air temperature and humidity. A more accurate way of evaluating the air flow rate is to measure the fuel flow rate, and to calculate the air fuel ratio from an exhaust gas analysis. Latterly all calculations were based on the fuel flow rate measurements and the air flowmeter was not used at all.

2.3.7 Temperature Measurement and Control

Thermocouples are used extensively for monitoring the oil, cooling water, fuel, air, and exhaust temperatures (see figure 2.1). (If the exhaust manifold was watercooled, its low surface temperature could lead to an underestimate of the exhaust temperature, in which case it would be appropriate to use a radiation shield over the thermocouple). The thermocouples require a reference or cold junction, which is provided electronically for temperature measurement. However this has to be properly calibrated by inserting each thermocouple in a water/ice mixture and observing the corresponding reading. The calibration is checked at the ice and steam points, and at intermediate temperatures (by insertion in boiling water and allowing it to cool), by a mercury in glass thermometer with 0.2K resolution. In the temperature range 20°C - 100°C, the accuracy of the thermocouples were within $\pm$ 1K. Further checks were undertaken on the coolant thermocouples, and in the relevant temperature range there was mostly no difference in the readings.

Engine cooling is achieved using an externally mounted shell and tube heat exchanger. The engine coolant temperature is controlled by varying the flow rate of engine coolant passing through the heat exchanger and also the flow rate of the heat exchanger cooling water. The heat transfer to the cooling water is found from the temperature rise in the coolant as it passes through the engine and the mass flow rate of the coolant. The flow rate is given as a volumetric flow rate by a flow meter installed between the engine outlet and the inlet to the heat exchanger. Three thermocouples are used to measure the engine coolant circuit temperatures. An additional sensor is provided for operating the safety circuit which automatically stops the engine from operating if the temperature was to rise above a pre-determined value.

2.3.8 Pressure Measurement

Oil pressure in the engine oil gallery is monitored by means of a Bourdon gauge, which is linked to the engine safety cut out circuit in case of an oil pressure drop. The inlet air pressure, or depression prior to entry to the carburettor is also monitored by a Bourdon gauge. Gas pressure is measured by means of a simple U tube manometer and a Bourdon gauge connected upstream and downstream of the gas pressure regulator respectively. Thus, it is possible to measure the gas pressure immediately prior to its entry to the carburettor. Also in accordance with the British Gas code of practice for Natural gas fuelled SI engines, a low pressure cut off switch is fitted upstream of the carburettor and linked to the safety cut out circuit. The cylinder pressure is monitored by a piezo-electric pressure transducer. This measurement is described more fully in section 2.5.3.

2.4 EXHAUST EMISSIONS

Exhaust gas emissions are harmful to the environment. They need to be measured because of legislation, and also because of the insights the measurements provide into engine performance. The emissions governed by legislation are: carbon monoxide (measured by infra-red absorption) and nitrogen oxides (measured by chemiluminescence). Unburnt hydrocarbons are also governed by legislation and if carbon dioxide (also measured by infra-red absorption) and oxygen (measured by a chemical cell) are also analysed, then it is possible to calculate the air fuel ratio. Each of these measuring techniques will be mentioned in the following sections.

2.4.1 Richard Oliver Gas Analyser Operating Principles

This analyser is capable of measuring the emissions of CO, unburnt HC (methane), and additionally CO_2 and O_2.

2.4.1.1 Infra-Red Absorption

Infra-red radiation is absorbed by a wide range of gas molecules, each of which has a characteristic absorption spectrum. The fraction of radiation transmitted (τ_λ) at a particular wavelength (λ) is given by Beer's Law

$$\tau_\lambda = \exp(-\rho\alpha_\lambda L)$$

where ρ is the gas density, α_λ is the absorptivity and L is the path length.

Figure 2.7 shows the key components in a non-dispersive infra-red gas analyser. The detector cells are filled with the gas that is to be measured (for example carbon monoxide), so that they absorb the radiation in the wavelength band associated with that gas.

Figure 2.8 shows the absorption spectra of carbon monoxide and carbon dioxide. This shows that in the region of 4.4 microns, infra-red radiation is absorbed by both carbon dioxide and carbon monoxide. In other words, for the simple arrangement shown in figure 2.8, if radiation of 4.4 micron wavelength is present when carbon dioxide is present in the sample, then this will affect slightly the readings of carbon monoxide, and vice versa when carbon dioxide is being measured. This problem can be eliminated by using a 'filter' cell between the infra red sources and the sample and the detector. If carbon monoxide is to be measured, then the filter cell could be filled with carbon dioxide, and any carbon dioxide in the sample should not then lead to any further infra-red absorption.

The non-dispersive infra-red analyser has a solid-state infra-red detector, using lead selenide. The chopper disc between the sample cell and the detector rotates. The chopper disc has an aperture, so that the infra red detector is exposed to: the infra-red from the sample cell, the reference cell, and no direct infra-red. This enables a single detector cell to establish the background signal level, and then make a comparative measurement between the reference cell

and the sample cell. Thin film filters can also be used instead of reference gas cells, and by moving appropriate filters between the sample and the detector, then a single cell can be used for measuring different species. If the filters are incorporated into the chopper disc apertures then a particularly simple arrangement is achieved.

The windows in the analyser have to be transparent to infra-red, so are made from materials such as mica and quartz. Obviously readings would be invalidated by fouling of the windows in the sample cell. To minimise this risk, the sample is filtered to remove particulates, and condensation (of water vapour or high molecular weight hydrocarbons) is avoided by either:

i) heating the sample lines and analyser

or ii) cooling and removing the condensate, then warming the sample to ambient temperature.

Non-dispersive infra-red absorption (NDIR) can be used for measuring the unburned hydrocarbons. However, this is not entirely satisfactory, as different hydrocarbon species have different absorption spectra. Ideally, when quantitative measurements of hydrocarbons are required a flame ionisation detection system should be used. However, when Natural gas is being used as a fuel the unburnt hydrocarbons can be assumed to be methane, and the analyser is calibrated using a known concentration of methane in nitrogen.

2.4.1.2 Oxygen and Air Fuel Ratio Analyser

Oxygen is obviously not an undesirable exhaust emission, but its measurement is very useful when evaluating the air fuel ratio. The lowest cost oxygen analysers are usually based around a galvanic cell. A typical galvanic cell comprises a PTFE membrane with a gold coating that acts as the cathode. Also immersed in the electrolyte (potassium chloride gel) is a silver or lead anode. A potential is applied across the electrodes. When the oxygen diffuses through the membrane it is reduced electrochemically, and a current flows that is proportional to the partial pressure of the oxygen in the sample. The galvanic cell also responds to other gases, and the gas of greatest significance with combustion is carbon dioxide. However a 12% carbon dioxide concentration would only give an output equivalent to that of 0.1% oxygen.

The Cussons Lamdascan unit also measures the oxygen and air to fuel ratio, but this works on a different principle which will be mentioned in section 2.4.3.

2.4.1.3 Richard Oliver Gas Analyser Calibration

The analyser is calibrated by means of a certified bottled gas cocktail containing CO, CO_2, H_2, and Methane (CH_4) in nitrogen. A separate certified mixture of 3.6% O_2 in N_2 is used for calibrating the oxygen cell. A gas bottle pressure regulator is required that is capable of supplying gas at approximately 0.3 bar to the gas analyser. The calibration procedure is in three

major stages, each taking less than three minutes. During each stage it is necessary to finely adjust the potentiometers that correspond to the CO_2, CO, CH_4, and O_2 measurements. Access to these is obtained by removing a side panel. The analyser will take 30 minutes to warm-up and auto-calibrate after being switched on. The gas bottle is connected to the analyser calibration port on the rear panel and the supply pressure set to approximately 0.3 bar.

For stage 1, the calibrate switch is depressed and held until the displays go blank. When the switch is released the displays will re-illuminate. The HC, CO and CO_2 zero potentiometers may now be adjusted so that the displays read between -4.95 and -5.05, and the O_2 span potentiometer adjusted to give between +4.95 and +5.05. When adjustment is complete, the calibrate switch is pressed and released in order to enter stage 2. Three minutes is allowed for this stage within the internal clock, after which time the analyser will revert to normal operation.

Once stage 2 is entered the pump will stop and a new three minute period will begin. The "CAL" valve on the rear panel is depressed to bleed in the gas, and the HC, CO and CO_2 cal potentiometers are adjusted to display the bottle CH_4, CO and CO_2 values and, the O_2 zero potentiometer adjusted to give 00.0 on the display. The calibrate switch is then pressed and released to enter stage 3.

The pump restarts and a new three minute period commences. It is now necessary to adjust the HC, CO, and CO_2 E-span potentiometers to display between +6.99 and +7.01 and the O_2 span to read between +4.95 and +5.05 (when steady). When complete, the calibrate switch is pressed and released for the last time and the analyser will enter its normal mode of operation.

If the settings are within tolerance, the displays will show "OP" indicating that the analyser is operational. Should "???" be displayed, this indicates that the E-span settings have not been set within the tolerance, in which case the gas calibration procedure should be repeated. The accuracy of the displays can now be checked by introducing the calibration gas to the analyser through the normal exhaust sampling port. The pressure is regulated such that a slight bypass flow of the calibration gas can be detected via a T piece. (Periodic checks for air leaks is recommended). The displayed readings are recorded in the next section. Accuracy is stated to be within + 0.1% and the results mostly vindicate this.

2.4.1.4 Richard Oliver Calibration Data

The calbration gas comprises 6.20% CO, 12.29% CO_2, 550ppm CH_4 in Nitrogen. The display readings are arranged chronologically and may be compared directly with the gas bottle values. The important readings are the CH_4 and CO and the calibration results are satisfactory. The O_2 readings are the least accurate but no direct use was made of these data except in the evaluation of the thermal energy of the exhaust, for which an explanation is given in section 2.8. When the oxygen level in the exhaust was needed, this was calculated from the value of lambda and the emissions of CO, CO_2 and CH_4 in the engine output analysis program. The consistency of the

emissions data was also checked by calculating the air fuel ratio using a carbon balance and a hydrogen/oxygen balance. The self consistency of these data were also checked by a comparison with the air fuel ratio calculated by the lambdascan.

Table 2.2 Emissions Analyser periodic calibration test results

Date	CO(%)	CO_2(%)	CH_4(ppm)	O_2(%)	Comments
-	6.20	12.29	550	0	Calibration gas values
Dec 91	6.13	11.72	500	- 1.7	Before calibration.
	6.29	12.30	520	- 2.3	After calibration.
Mar 92	6.15	12.36	600	0	After calibration.
Jun 92	6.23	12.30	580	0	After calibration.
Jul 92	6.34	13.09	560	0	Before calibration.
	6.22	12.18	650	0	After calibration.
Nov 92	5.74	12.00	580	1.8	Before calibration.
Feb 93	6.08	12.87	540	0	Before calibration.
	6.27	12.30	580	0	After calibration.

2.4.2. NOx Measurement by Chemiluminescence

The chemiluminescence technique depends on the emission of light. Nitric oxide (NO) reacts with ozone (O_3) to produce nitrogen dioxide in an activated state (NO^*_2), which in due course can emit light as it converts to its normal state

$$NO + O_3 \rightarrow NO^*_2 + O_2 \rightarrow NO_2 + O_2 + \text{photon}$$

The nitrogen dioxide can also be deactivated by a collision with another molecule. Ferguson (1986) shows that if:

(a) the reactor is sufficiently large,

(b) the ozone flow rate is steady and high compared with a steady sample flow, and

(c) the reactor is at a fixed temperature,

then the light emitted is proportional to the concentration of nitric oxide in the sample stream.

Both nitric oxide and nitrogen dioxide can exist in the exhaust of an engine, and NO_x is used to denote the sum of the nitrogen oxides. Nitrogen dioxide can be measured by passing the sample through an oven that converts the nitrogen dioxide to nitric oxide. By switching the converter in and out of the sample line, then the concentrations of NO and (NO + NO_2) can be found in the exhaust sample.

Figure 2.9 shows the arrangement of a NO_x analyser. The vacuum pump controls the pressure in the reaction chamber, and is responsible for drawing in the ozone and exhaust sample. The ozone is generated by an electrical discharge in oxygen at low pressure, and the flow of ozone is controlled by the oxygen supply pressure and the critical flow orifice (a short length of capillary tube). The sample can either bypass or flow through the nitrogen dioxide converter. The sample flow rate is regulated by two critical flow orifices. The bypass flow is drawn through by a sample pump. This arrangement ensures a high flow rate of sample gas, so as to minimise the instrument response to a change in NO_x concentration in the sample. The flow of sample into the reactor is controlled by the pressure differential across the critical flow orifice upstream of the NO_x converter; this pressure differential is controlled by a differential pressure regulator.

The light emission in the reactor is measured by a photomultiplier, and then amplified. In view of variations in gain that might occur with the photomultiplier, and in the other parameters that affect the light emission, then it is essential to calibrate the NO_x analyser regularly. Calibration gases are used to set the zero and check the span.

2.4.2.1 NO_x Analyser Calibration

The analyser ozone generator requires an air supply set at a minimum specified humidity (-40°C dew point or lower). Although room air may be used together with a drying assembly it is more convenient (as recommended) to use a cylinder of zero (minimum impurities) air since the dew point for such air is normally below -40°C. The air delivery pressure is set at 0.6 $\pm$0.3 bar.

The power supply to the analyser and the external sample bypass pump is switched on. The vacuum gauges and the oxygen pressure gauges are allowed to stabilise at their correct respective pressures. Power is switched on to the NOx converter, which is set at a temperature of 650°C. Once this has "warmed-up" and the high voltage supply to the photomultiplier is switched on the instrument is ready for calibrating. The NO_x indicator on the control panel is checked for zero and full scale deflection and a background noise suppression potentiometer is provided for adjustment. A suitable range, with regard to the reference gas (in this case 241ppm NO in N_2), is selected. The ozone generator is switched on and the sample pressure is adjusted to give the required gas flow through the instrument. If necessary the "calibrate" potentiometer may be fine tuned to obtain agreement with the named value of the nitric oxide calibration gas. There is provision for two modes of measurement; the "NO mode" readings should agree within

$\pm$ 0.5% of the values measured in the "NO_x mode". When the instrument is in continuous use during engine testing the NO_x reading is found to be repeatable and accurate. Thus initial calibration was sufficient. The sample gas is turned off and the analyser switched to measure the exhaust gas stream from the engine. Care is exercised to ensure that the instrument resolution is maximised by always using the most appropriate range.

2.4.3 Air Fuel Ratio Measurement by Lamdascan

Exhaust gas oxygen sensors can be used as the basis of an oxygen analyser with a comparatively fast response. The two options are to either mount the sensor in the exhaust stream, or to take a sample of the exhaust to the analyser. If a sample of the exhaust is fully oxidised, then it is also possible to deduce the air fuel ratio.

In the Cussons Lamdascan, a sample of the exhaust is taken to an analyser. If a rich mixture is being burned, then a controlled amount of oxygen is blended into the exhaust. This way, there is always oxygen present in the sample being analysed. The sample is passed through a heated catalyst to fully oxidise any partial products of combustion. For rich mixtures, one of several levels of dope air is added, so that there is a low level of oxygen in the diluted sample. If the hydrogen/carbon/oxygen ratio of the fuel is known, and the quantity of any dope air is known, then the equivalence ratio or air fuel ratio can be deduced.

2.4.3.1 Lamdascan Calibration

Before calibration tests are carried out the instrument must be switched on and left to "warm-up" in accordance with the routine operating instructions. The pump is then switched on and the unit left for a further period to ensure all operating temperatures have stabilised, (ie. cell temperature, catalyst temperature, oven temperature and heated line temperature).

The oxygen sensor (Zirconia cell), can be calibrated by means of atmospheric air, and bottled nitrogen. The control panel is set to measure "air" and of the three available modes of measurement, O_2, AFR and λ, O_2 is selected. The unit will display the percentage of atmospheric oxygen, (21% or thereabouts).

A more accurate check of the oxygen sensor is made using a certified nitrogen/oxygen calibration gas, with a low level of oxygen (3.60%), as might be encountered in the exhaust gas. The hydrogen/carbon and oxygen/carbon ratios are set to 0.00 by operating the switches at the rear of the unit. The calibration gas is introduced to the sample handling unit directly via the CAL2 port. The respective switch (CAL2), is engaged on the control panel which enables a solenoid operated valve to feed the gas to the instrument. The displayed oxygen readings are presented in table 2.3. These results indicate the maximum error in the oxygen measurement is not greater than 0.05%. Another verification of the oxygen cell performance is to run the system in the O_2 display mode with zero dope (ie no.1 dope ratio) so that nitrogen is admitted to the oxygen cell. The O_2 display should read less than 0.04% oxygen, (ie. no oxygen). Dope ratios from 1 to 8 are

selected and the respective oxygen readings are checked to correspond within $\pm$0.04% O_2. At higher levels, say 5 to 8 a greater deviation $\pm$0.08% is acceptable. When sampling rich mixtures, as will be seen by the results in the next section, the best instrument resolution is achieved with a low residual level of between 1% and 2% O_2.

The performance of the catalyst and the dope air system can be checked by a calibration gas cocktail as mentioned in 2.4.1.4 that represents the combustion products of a rich mixture. It is connected to the CAL1 port and the respective switch engaged on the control unit. Due to the high storage pressure of the gas cylinder (200 bar), care must be exercised to regulate the gas flow within the range of the instrument internal controllers, (ie. The supply pressure is slowly increased whilst observing the bypass flowmeter. The correct setting is achieved when the flowmeter indicates the recommended excess of normal bypass flow. The hydrogen/carbon and the oxygen/carbon ratios are set (rear of control unit), in accordance with the fuel sample that is used. For the calibration gas cocktail this has been calculated to be 1.53 and 0.00 respectively, see section 2.4.3.2. Starting with a dope ratio of 3 (the minimum level required here in order to ensure residual oxygen), "dope update" and "dope check" are selected, the dope rate is allowed to stabilise after each selection to within $\pm$0.04% O_2 for the lower levels and $\pm$0.08% O_2 for the higher levels. Each of the three measuring modes is then selected in turn to give the residual oxygen level, λ, and the AFR. The λ and the AFR are consistently accurate over the entire range of dope levels up to 8. The maximum error in the displayed readings is about 0.5%. The results of the calibrations are shown in table 2.3. These data are arranged chronologically, and may be compared with the actual gas bottle values. These are 3.60% O_2 in Nitrogen, and for the gas cocktail λ = 0.812, AFR = 11.45.

Table 2.3 Lambdascan periodic calibration test results

Date	O_2 in N_2 (%)	Dope ratio	λ	AFR
Nov 91	3.61	3 - 4	-	11.46-11.48
March 92	3.60	-	0.816	11.49
June 92	3.64	-	0.807	11.37
July 92	3.61	1 - 8	0.810	11.40
Sept 92	3.60	4 - 7	0.802-0.807	11.29-11.36
Jan 93	3.60	3 - 8	0.809-0.814	11.39-11.46

2.4.3.2 AFR And λ Calculation of the Calibration Gas Cocktail

The calibration gas bottle comprises the following:

CH_4 - 0.055%

H_2 - 3.23%

CO - 6.20%

CO_2 - 12.29%

N_2 - Balance (78.22%)

For 100kmol of dry products:

$$C_xH_y + z(O_2 + \frac{79}{21}N_2) \rightarrow 0.055CH_4 + 3.23H_2 + 6.20CO + 12.29CO_2 + 78.22N_2 + gH_2O$$

C balance: $x = 0.055 + 6.20 + 12.29$; $x = 18.545$

N_2 balance: $z(79/21) = 78.22$; $z = 20.793$

O_2 balance: $z = 6.20/2 + 12.29 + f/2$; $f = 10.806$

H balance: $y = (0.055)4 + (3.23)2 + 2f = 28.292$

$H/C = y/x = 1.526$

If M is the molar mass for each species, then the AFR is:

$$xM_C + yM_H \ : \ z(M_{O2} + 79/21M_{N2})$$

$$250.8 \ : \ 2871.4$$

$$1 \ : \ 11.45$$

For stoichiometric combustion the stoichiometric air fuel ratio (AFRs) is:

$$C_xH_y + q(O_2 + \frac{79}{21}N_2) \rightarrow xCO_2 + \frac{y}{2}H_2O + q\frac{79}{21}N_2$$

O_2 balance: $q = x + y/4$

$$\therefore \ xM_C + yM_H : (x+y/4)M_{air}\times\frac{100}{21}$$

$$250.8 : 3537.72$$

$$\text{AFRs} = \underline{1 : 14.11}$$

$$\text{and } \lambda = 11.45/14.11$$

$$\lambda = \underline{0.812}$$

2.5 CYCLIC MEASUREMENTS

2.5.1 Crankshaft Encoder

2.5.1.1 Installation

A crankshaft encoder is attached to the crankshaft pulley on the engine. This is used to produce output signals in the form of clock and trigger information for use with monitoring in-cylinder pressures. The mounting arrangements for the encoder are described as follows, with reference to figure 2.10.

A driver is designed to interface between the crankshaft pulley and the encoder shaft. The driver is located and bolted on to the crankshaft pulley taking care to ensure concentricity of the driver spigot and the pulley. The driver spigot is attached to the encoder shaft by means of a diaphragm coupling. Both the encoder shaft and the driver spigot have flats machined to give a positive location for the coupling. The body of the encoder is supported in a circular plate and secured by means of two semi-circular collars. Hexagonal bars are bolted on to three equidistant bolt holes on the engine, around the crankshaft pulley. These bars serve as a three point mounting arrangement for the circular plate and the encoder. A mandrel having the same dimensions of the encoder and the driver spigot is used to align the circular plate. All

components are assembled with the mandrel in place, thus correct alignment is assured.

2.5.1.2 Calibration

The shaft encoder used here is an opto-electronic device. Eight output pins out of a total of twelve are used, see figure 2.11. Two are used for the power supply to the encoder. Four are used for clock signalling channels. (ie. a pulse is generated every 2°, 1°, ½°, or ¼° of crankshaft rotation). Only one of these channels may be used at a time in conjunction with other data (eg. cylinder pressure signal), and selection is by means of a four way switch. The switch is situated in a panel. The two remaining pins are used for the tdc and bdc marker flags. These two flags are 180° out of phase. Therefore it is only necessary to synchronise one with the actual tdc of the piston. This was done in the following way:

Firstly it was necessary to make visual angular markers on the crankshaft pulley with some degree of accuracy. With the cylinder head removed, a dial indicator is placed above no.1 cylinder. The crankshaft is rotated until the piston reaches a predetermined height which corresponds to say 30° before tdc. A line is scribed along the pulley with reference to a stationary pointer on the engine block. The pulley is removed from the crankshaft and placed in an indexing head. Six marks are made corresponding to tdc, bdc, 30° and 15° before tdc, and after tdc respectively. The indexing facility and a height gauge are used to scribe the lines along the front face and sides of the pulley using the original marker as a datum. The pulley is replaced, the crankshaft is rotated until the piston is again at the 30° btdc position. The pointer is finely adjusted to coincide with the 30° btdc mark on the pulley. This procedure is repeated, at exactly the same height which corresponds to 30° atdc in order to verify the positional accuracy of the tdc marker, See figure 2.12. This method of creating a tdc marker is inherently more accurate than trying to position the engine with the piston at the end of its stroke.

To check the tdc flag position and the ignition timing a strobe light was connected to the HT lead of cylinder number one. By using the 20° and 30° timing pulley marks it was possible to check the ignition timing. Furthermore, by monitoring the HT signal and the encoder outputs, it was possible to check the tdc flag position. Some corroboration was also achieved by recording the cylinder pressure and tdc flag from a motoring test; as expected the cylinder pressure was a maximum just before tdc.

The panel, as mentioned earlier in this section is connected to the encoder by a multi-core lead which carries the power supply and has DIN connectors for the signals. The DIN sockets on the front of the panel may be used with an oscilloscope or data acquisition unit.

2.5.2 Ignition Timing Control

A very wide range of ignition timings was employed in the testing of this engine. An electronic variable ignition timing unit (VITU), developed at Brunel by Hudson et al (1990), was used to remotely advance or retard the timing.

2.5.3 Cylinder Pressure Transducer

2.5.3.1 Installation

In order to monitor in-cylinder pressures, it was necessary to install a pressure transducer in one of the six cylinders. The normal practice is to house the transducer in a water cooled holder, and locate the entire assembly in the cylinder head. However, the positioning of this transducer necessitated penetrating the cooling water jacket of the engine itself. This was used to advantage, as it eliminated the separate cooling arrangements for the pressure transducer, thus simplifying the design and manufacture of the holder. Drawings of the holder and the cylinder head have been included in figure 2.13.

The pressure transducer is secured in the holder, and the whole assembly is located in the cylinder head above number one cylinder. (Number one cylinder was chosen purely for convenience). Proper installation warrants the sensing face of the transducer to be almost flush with that of the flame deck. The internal dimensions of the holder were dictated by a D-BIT cutter which provides appropriate clearances for the external dimensions of the pressure transducer. External flats were machined on the holder (ie. A/F 17mm) to facilitate its installation and removal with a socket spanner. Actual positioning of the assembly was largely dictated by the available space, allowance for adequate cooling, and the need for easy access to the transducer and the holder. The cooling water jacket is sealed with a malleable copper washer at the bottom end, and a rubber O-ring at the top. Previous experience suggests that temperatures in this area (about 100°C) can be tolerated by an O-ring. The pressure transducer cable exits through a core plug hole (via the rocker box), at the top of the cylinder head. The transducer cable and the top of the holder are enclosed in a rubber boot to minimise oil contamination. The transducer used is a Kistler piezo-electric type 6001.

2.5.3.2 Operating Principles

The pressure transducer requirements are very demanding because of the high temperature and pressures, and the need for a high frequency response. The piezo-electric transducer, as used here, has a metal diaphragm which is displaced by the pressure. The displacement is to be measured by a piezo-electric crystal. See appendix A. Piezo-electric transducers respond only to the rate of change of pressure; thus they have to be used in conjunction with a charge amplifier that integrates the signal. The electrical charge that is produced is proportional to pressure (typically between 2 and 50 pC/bar). When the signal is integrated it is necessary to define the pressure/voltage datum, and although this can be done in a variety of ways, a cycle simulation program such as SPICE might be used to define the pressure at a particular crank angle.

For calculations such as imep it is not necessary to know the absolute values of pressure, and for peak pressures (invariably above 30 bar) uncertainty of 0.3 bar or so in the datum will not be significant.

The electrical charge is prone to both leakage and accumulation, and this causes the voltage output from the charge amplifier to drift. By using a coupling with an appropriate time constant, the effect of the drift is eliminated. However, when the pressure transducer is calibrated by static pressures, then a long time constant is needed, so that a steady pressure corresponds to a steady voltage. This places considerable demands on the input resistance of the charge amplifier, the internal resistance of the pressure transducer, and the interconnecting cable. To prevent the electrical charge being dissipated, a resistance greater than 10e9 Ohms is required.

2.5.3.3 Calibration

The transducer was connected to a charge amplifier by a teflon-coated low capacitance coaxial cable. (The connectors must be kept clean and dry in order to maintain as high an impedance as possible and avoid charge leakage). Both transducer and amplifier were calibrated under steady pressure conditions, by means of a dead-weight tester and a digital voltmeter.

The dead weight tester is prepared by ensuring that the hydraulic oil reservoir is full, and free of any air pockets. The pressure transducer assembly is then located in the dead weight tester. The electrical equipment is switched on and allowed to stabilise. The multimeter is set to read DC mV with a typical range of 1 - 20 mV/pC. The charge amplifier is set to give a zero reading at 100psi (approximately 6.9 bar). Additional weights are now added and the corresponding readings taken up to a maximum of about 1200psi (approximately 80 bar). This figure is deemed sufficient for this engine and corresponded to a reading of 7.33V. A calibration is conducted by incrementing and decrementing the pressure. The results have been tabulated and a calibration curve plotted. See figure 2.14, and table 2.4.

Table 2.4 Kistler pressure transducer and charge amplifier calibration test results.

Pressure (psi)	Pressure (mVolts)	
	Loading	Offloading
100	0.0	-0.12
200	0.67	0.55
300	1.34	1.22
400	2.02	1.90
500	2.69	2.57
600	3.36	3.24
700	4.03	3.92
800	4.69	4.60
900	5.35	5.28
1000	6.02	5.96
1100	6.68	6.64
1200	7.33	7.33

2.5.4 Morse Test

A Morse test is conducted at the same mid-range operating point, as for the blowby measurement. The motoring pressure is recorded with the use of a high speed data acquisition card. Thus a direct comparison can be made of the calculated and the "Morse test" imeps for cylinder no.1. This is a good check of the inter-cylinder variability of the imep. This is useful since the pressure transducer was only installed in cylinder no.1. Attempts at using a Kistler spark plug mounted pressure transducer were unsatisfactory. When calculating the imep for these readings it became evident that the transducer was subject to thermal drift.

2.6 COMPUTER BASED DATA ACQUISITION

The computer based data acquisition system used here is a Computerscope data acquisition card installed in a Compaq 386/25e personal computer; the resulting specification is in table 2.5. When selecting a data acquisition card, it is necessary to decide on:

i) the resolution and accuracy (e.g. 10 bit)

ii) the number of channels

iii) the maximum sampling rate

iv) how much data are to be collected

Firstly, the lower the resolution of the card, then the lower the cost for a given sampling rate. An analogue to digital converter (ADC) with 8 bits might appear adequate, as this will give a

Table 2.5. The specification of a computer based data acquisition system comprising a Computerscope data acquisition card, and a Compaq 386/25e personal computer.

Channels	1,2,4,8 or 16	
Multiplexing Overhead	1 μs	
Resolution	12 bits	
Input voltage range	± 10V	
	Max. Sampling Rate	Available Memory
Computerscope on-board memory	1 MHz	256 k
System RAM	200 kHz	10 MB
Hard Disk	100 kHz	60 MB

resolution of 1 part in 256. In other words, the ADC will cause an uncertainty of about 0.4%, and this is comparable with the accuracy of a piezo-electric pressure transducer. However, to achieve this ADC accuracy it is necessary to use the full dynamic voltage range of the input, and this may not be convenient. Consider the cylinder pressure transducer which might have a response that is within 1% of linear to a frequency of 10 kHz. This might suggest that the maximum useful sampling rate is 20 kHz. However, if a phenomenon such as knock is being investigated, then a higher sampling rate will be wanted, even though the non-linearity of the transducer is becoming significant. In general, the sampling will be controlled by a shaft encoder on the engine that presents a signal to the 'external clock' input of the data acquisition system. This arrangement has the advantage, that the angular position of each reading will be known. Thus the sampling rate will also be influenced by the engine crank angle resolution that is required. For example, the injector needle lift might be wanted with a ¼ degree resolution to determine the start of injection.

Thus:

Sampling Rate (k sample/s) = 6 x engine speed (rpm)
x number of readings/degree
x number of channels enabled

For example, with the gas engine operating at 1500 rpm, with 2 channels enabled and readings taken every ¼ degree, there would be 72 k samples/s.

Finally, the amount of data to be collected has to be identified, as this influences the maximum sampling rate. Large quantities of data need to be written to some form of disk, and this is slower

than writing to RAM (random access memory). Consider measurements of cycle-by-cycle variation in a four-stroke spark-ignition engine. The requirement for memory is:

Memory = number of cycles x number of channels x number of readings/degrees x (180 number of strokes) x number of bytes/sample

For example if 300 cycles of a four stroke engine are to be recorded from 2 channels, with readings every ½ degree and 2 bytes are required for each reading (for a 12 bit reading), then about 1.7 MB of memory will be required.

The trade-offs between the sampling rate and the storage capacity have been illustrated by table 2.5 for a particular system. In this case, the 1.7 MB of memory would require the use of the RAM or the hard disk, and the engine speeds corresponding to the maximum sampling rates would be 8333 or 4166 rpm. These two examples illustrate that the system described in table 2.5 is capable of acquiring large amounts of data very quickly. This can then lead to analysis and archiving problems unless the combustion analysis software is quick to run.

There are other issues to be considered with computer based data acquisition systems. Firstly, when channels are being multiplexed, then the channels are not all being read at the same time. For example, table 2.5 shows that the Computerscope system has a delay of 1 microsecond between reading successive channels. This becomes significant with high sampling rates, but it can be corrected for in software, that either assigns the correct angle to the reading or interpolates between readings to give the value at a specific crank angle. Secondly, it is essential that the ADC is coupled to a sample/hold circuit. If this is not the case, then slight changes in the signal during the analogue to digital conversion process can lead to large errors.

2.7 COMPUTER BASED COMBUSTION ANALYSIS

There are essentially two types of combustion analysis undertaken:

i) Burn rate analysis - usually associated with SI engines.

ii) Heat release analysis - usually associated with diesel engines, hence this will not be described here.

2.7.1 Burn Rate Analysis

A burn rate analysis is usually applied to the combustion data from spark ignition engines to calculate the mass fraction burnt (mfb). A widely used technique is the approach devised by Rassweiler and Withrow (1938). After the start of combustion, the pressure rise (Δp) during a crank angle interval ($\Delta\theta$) is assumed to be made of two parts: a pressure rise due to combustion (Δp_c) and a pressure change due to the volume change (Δp_v):

$$\Delta p = \Delta p_c + \Delta p_v$$

As the crank angle (θ_i) increments to its next value (θ_{i+1}) the volume changes from V_i to V_{i+1}, and the pressure changes from p_i to p_{i+1}. It is assumed that the pressure change due to the change in volume can be modelled by a polytropic process with an exponent k. Substituting for p_v, the above equation becomes:

$$p_{i+1} - p_i = \Delta p_c + p_i[(\frac{V_i}{V_{i+1}})^k - 1]$$

from which Δp_c can be evaluated:

$$\Delta p_c = p_{i+1} - p_i(\frac{V_i}{V_{i+1}})^k$$

The pressure rise due to combustion is not directly proportional to the mass of fuel burned, as the combustion process is not occurring at constant volume. The pressure rise due to combustion has to be referenced to a datum volume, for example the clearance volume at tdc, V_c

$$\Delta p_c^{\cdot} = \Delta p_c V_i / V_c$$

The end of combustion occurs after N increments, and is defined by the pressure rise due to combustion becoming zero. If it is assumed that the referenced pressure rise due to combustion is proportional to the mass/fraction burned, then

$$mfb = \frac{\Sigma_0^i \Delta p_{c\cdot}}{\Sigma_0^N \Delta p_{c\cdot}}$$

which is the summation of the referenced pressure due to combustion.

Since the volume change is small when the piston is in the region of tdc, the computed mass fraction burned is insensitive to slight errors in the positioning of tdc. However, the method does depend on using an appropriate value of the polytropic index, k. Rassweiler and Withrow evaluated the polytropic index for before and after combustion and used an appropriately averaged value for during combustion. If the polytropic index is only evaluated during compression then this will lead to a fall in the referenced pressure due to combustion and the mass fraction burned after the end of combustion, as the polytropic index is lower during the expansion process than during compression. This is a consequence of the heat transfer and the presence of combustion products.

During compression the polytropic index is usually within the range of 1.2 to 1.3 for a spark ignition engine, and is evaluated from the compression process prior to ignition. By evaluating

the logarithmic values of pressure and volume, a least squares straight line fit can be used to determine the polytropic index. However, care is needed because of two reasons:

1) there might be errors in the pressure datum
2) during the initial part of compression the pressure rise is small, and discretisation errors from the ADC are more significant.

Both effects are minimised if the initial part of the compression is ignored; for example, the polytropic index could be evaluated up to ignition, from half way between the inlet valve closure and ignition.

The Rassweiler and Withrow method contains several assumptions. It is assumed that the referenced pressure rise due to combustion is proportional to the mass fraction burned in each increment. There is no explicit allowance for heat transfer, dissociation or change in composition of the gases. Though to some extent an allowance is made, as the polytropic index is allowed to vary from the ratio of the gas specific heat capacities. These shortcomings have been investigated by Stone and Green-Armytage (1987), who used a thermodynamic analysis to make a direct comparison with the same data being analysed by the Rassweiler and Withrow method. The thermodynamic model divided the combustion chamber into two zones, and took into account dissociation and heat transfer within the combustion process. Notwithstanding the substantial differences between the two approaches, the results were in surprisingly close agreement. This was attributed to the temperature of the burnt gas being almost constant during combustion, so that the effects of dissociation and heat transfer had an almost uniform influence throughout combustion.

Since the Rassweiler and Withrow method is simple to calculate, it is an appropriate and popular method when cycle-by-cycle variations in combustion are to be analysed.

2.8 PROGRAM FOR ANALYSING ENERGY, EMISSIONS AND COMBUSTION DATA

The program to be described here was written in fortran code. A listing is in appendix B. The terms used here are not always identical to those used in the code. For example, the letter H, used to denote humidity, (page 47) is different to the abbreviation 'hmdty' which is used in the fortran code. However an explanation is given wherever this is the case. Firstly, all variables that are real are declared as such at the beginning of the program followed by a recognition of the input and output files. This is followed by an array (definition of all elements), for calculating the heat flow to the exhaust. Next are a series of "read" and "write" statements for user and machine inter-action. These provide basic information about the program and prompts the user for input information and file names. The "open" statements enable the appropriate input and output files

to be recognized and read. Following this is a definition of constants used such as Pi, the British Gas reference temperature and the molecular weights of the major constituents of the fuel. There are two input files; the engine file contains constants for a given engine configuration of which there are three. The data file which should have a suffix ".dat" contains all the raw experimental data including outputs from the combustion analysis, and these vary with each operating point for a given engine configuration within its operating envelope.

The "read" statement enables the engine file to be read in. The contents can be displayed ("write" statement), for the benefit of the user, in order to check the value of these constants and verify correct matching of the input files.

Natural gas is subject to slight variations in its composition and calorific value. Typical values have been obtained for the particular region and period in question, (see appendix B). The molecular weight of the gas naturally varies with its composition and this is calculated in the

Table 2.6 Example: This table shows the Natural gas composition in 100kmols measured from a sample taken in february 1993 :

Nat.Gas composition (vol %) (eg. Feb 1993)		Atoms of each (vol %) C	H	O	N
N_2	2.34				4.68
CO_2	0.31	0.31		0.62	
CH_4	93.45	93.45	373.80		
C_2H_6	2.97	5.94	17.82		
C_3H_8	0.60	1.80	4.80		
C_4H_{10}	0.23	0.92	2.30		
C_5H_{12}	0.10	0.50	1.20		
Total		102.92	399.92	0.62	4.68

following way. Using the atomic proportions contained in table 2.6 for example 1kmol of natural gas would have the following formula:

$$C_{1.0292}\, H_{3.9992}\, O_{0.0062}\, N_{0\,0468}$$

Clearly this is almost the same as pure methane (CH_4). The atomic ratios (eg. Cbn, (Carbon) Hdn, (Hydrogen) etc. as contained in the engine file in appendix B), multiplied by the atomic weights gives the molecular weight M_{gas}, of 1kmol of natural gas.

$$M_{gas} = Cbn \times M_{Cbn} + Hdn \times M_{Hdn} + Oxn \times M_{Oxn} + Ntn \times M_{Ntn}$$

The value of Mgas normally lies between 19kg/kmol and 15kg/kmol. The user's attention is drawn if the computed value lies outside this range indicating that its composition has varied beyond the likely limits. Thus the specific gas constant for natural gas R is obtained from:

$$R = \frac{R_0}{M_{gas}} \qquad \textit{Where } R_0 \textit{ is the Universal gas constant}$$

$AFR_{sv/sg}$

$AFR_{sv/sg}$ is the notation for the air to fuel ratio on a volumetric/gravimetric basis. The stoichiometric AFR will vary with the fuel molecular formula (gas composition), and is calculated for each engine configuration. Thus consider a fuel of generalised known composition $C_\alpha H_\beta O_\gamma N_\delta$. For stoichiometric combustion with air:

$$C_\alpha H_\beta O_\gamma N_\delta + x(O_2 + \frac{79.05}{20.95} N_2) \rightarrow \alpha CO_2 + \frac{\beta}{2} H_2O + \frac{79.05}{20.95} N_2$$

An oxygen balance gives:

$$\gamma + 2x = 2\alpha + \frac{\beta}{2}$$

$$2x = 2\alpha + \frac{\beta}{2} - \gamma$$

$$x = \alpha + \frac{\beta}{4} - \frac{\gamma}{2}$$

The AFR_{sv} (or volume of air) =

$$(\alpha + \frac{\beta}{4} - \frac{\gamma}{2})(1 + \frac{79.05}{20.95}) = (\alpha + \frac{\beta}{4} - \frac{\gamma}{2}) \times \frac{100}{20.95}$$

The equivalent Fortran code = (Cbn + Hdn/4 + Oxn/2) / 0.2095

The AFR_{sg} of air (mass) =

$$AFR_{sv} \times \frac{M_{air}}{M_{gas}} \qquad \textit{Where } M_{air} = 28.96 \textit{ kg kmol}$$

CalValg

The gross calorific value of the fuel (MJ/m^3), is read in from the engine file and multiplied by R (specific gas constant), and standard conditions to give the gravimetric value.

$$CalVal_g = CalVal \times \frac{R \times T_{Ref}}{Std.atm.pressure}$$

Where Std. Pressure = 101325 Pa, R = 8314.3/Mgas J/kgK

T_{Ref} = 288.15 K (Brit.Gas reference temperature)

Input File

This contains all the raw experimental data including outputs from the combustion analysis program.

Dynamometer Offset

This offset decreases with increasing output torque and in the usual operating range amounts to 0.5% error. As this is very near the instrument resolution and subject to slight fluctuations anyway, it was omitted from the program.

Power/Torque Input

The engine output may be entered in units of power or torque. The power output varies in the range 30 to 70 kW and the equivalent torque varies between 180 to 450 Nm. As the power output never exceeds the value 100 (kW), and the useful torque will always be above 100 (Nm), this figure is used as a determining criterion in order to differentiate between the two. Ideally because of the inherent instrument inaccuracy in the power calculation, all inputs (as they have been for the last two engine rebuilds), should be in units of torque, in which case the need for this loop will be obviated.

Power

The Power output can be calculated from the Torque and the angular speed (in rad/s).

$$Hence\ Power\ (kW) = \frac{Torque \times 2 \times \pi \times speed(rpm)}{60 \times 1000}$$

$$Torque\ (Nm) = \frac{Power \times 60 \times 1000}{2 \times \pi \times speed(rpm)}$$

Bmep

This is defined as:

$$Bmep = \frac{Brake\ work\ output\ per\ cylinder\ per\ mechanical\ cycle}{Swept\ volume\ per\ cylinder}$$

$$= \frac{Power \times 1000}{\frac{V_s}{1000} \times \frac{speed}{60 \times 2}} \qquad V_s = litres, \quad \frac{speed}{60 \times 2} = cycles\ per\ sec.$$

$$Thus\ the\ bmep = \frac{Power \times 1.2 \times 10^8}{V_s \times speed}\ (pa) \qquad = \frac{Power \times 1200}{V_s \times speed}\ (bars)$$

Imep

This is evaluated from the pressure data (no.1 cylinder), by the combustion analysis package.

Fmep

The fmep is the difference between the bmep (derived from the brake work output), and the imep (calculated from the cylinder pressure data).

imep - bmep = fmep

η_m

The mechanical efficiency determines the proportion of indicated power that is transferred to the crankshaft after subtraction of the frictional and mechanical losses. It is defined as:

$$\eta_m = \frac{brake\ power}{indicated\ power} = \frac{bmep}{imep}$$

P_{abs}

The absolute pressure is defined as the atmospheric pressure P_{baro} (mm Hg), plus the gauge pressure P_{gdn} (inches of water). Heywood gives a conversion factor (x 1.333224 x 10^2 to go from mm Hg to Pascal), which multiplied by 10^{-5} gives units of bar. No conversion factor was readily available for the gauge pressure, which was measured in inches of water, therefore this was converted to metres (x 25.4), multiplied by ρg (1000 x 9.81), and (10^{-5}) to give units of bar.

V_{fuel}

The volumetric fuel flow rate is calculated by dividing 10 cubic feet of gas by the time taken for its consumption, and converting the result (conversion factor = 0.02831685) into m^3/s.

M_{fuel}

The characteristic equation for an ideal gas, for a mass m, occupying a volume v is:

where R = specific gas constant, T = gas temperature, p = absolute gas pressure

$$pv = mRT$$

$$\text{This may be rewritten as:} \qquad m = \frac{vp}{RT}$$

where v and m can represent flow rates V_{fuel} and M_{fuel} respectively.

η_b

The brake efficiency is a measure of the fuel energy conversion efficiency, ie brake power divided by the incoming fuel energy. The fuel energy is determined by the mass flow rate of fuel and its gravimetric calorific value.

$$\eta_b = \frac{Power}{M_{fuel} \times CalVal_g}$$

η_i

Having obtained the brake efficiency and the mechanical efficiency it is possible to deduce the indicated efficiency:

$$\eta_i = \frac{\eta_b}{\eta_m}$$

AFRV

The instantaneous (volumetric) equivalence ratio may be found by dividing the stoichiometric AFR by the instantaneous AFR. The inverse of this is λ. Thus the instantaneous AFRV is found by multiplying the AFR_{sv} by λ

AFRG

This represents the gravimetric AFR and is calculated in a similar way as the AFRV.

$M_{exhaust}$

If the mass flow rate of the fuel m_{fuel}, and the gravimetric air fuel ratio AFRG, are known then the mass flow rate of the exhaust products can be deduced:

$$m_{exhaust} = m_{fuel} \times (1 + AFRG)$$

AirfIrt

This too is calculated from the mass flow rate of the fuel and the air fuel ratio. The result is expressed in g/s.

η_v

The Volumetric efficiency is a measure of the inducting and exhausting efficiency in an engine. It is arbitrarily defined as (assuming air obeys the Gas Laws),

$$\eta_v = \frac{vol\ of\ ambient\ pressure\ air\ inhaled\ per\ cyl.\ per\ cycle}{cylinder\ volume}$$

This may also be expressed as "mass flow rate of air" over "induction cycles per second".

$$\eta_v = \frac{V_{fuel} \times AFRV}{\frac{V_s}{1000} \times \frac{speed}{60 \times 2}} \qquad \eta_v = \frac{V_{fuel} \times AFRV \times 120000}{V_s \times speed}$$

v_{fuel} x AFRV is the volumetric air flow rate into the engine. V_{swept} is converted from litres to m^3 and the speed is divided by 60 x 2 to give induction cycles per second.

Tcl

The temperature of the engine coolant TCI, for the purpose of calculating the specific heat capacity is taken as the average of the inlet temperature TCI_{in}, and outlet temperature TCI_{out}.

CpEg

The specific heat capacity of ethylene glycol is temperature dependant and follows the relationship

$$CpEg = Cp_0 + K \times T$$

Cp_0 is 2.474 (see appendix B), which corresponds to the bottom of the appropriate range, say 40° to 100°C.

$$Thus\ the\ gradient\ K = \frac{2.742 - 2.474}{100 - 40}$$

and T = (TCI - 40).

CpW

This is the specific heat capacity of water (also temperature dependant), and is calculated for the same range as ethylene glycol.

CpCl

The specific heat capacity of the mixture is calculated taking into account its particular composition of ethylene glycol and water, as read in from the engine file.

Rhocool

The density of the coolant varies with its composition and temperature. The weakest concentration of ethylene glycol is 52% by weight (this does not vary by more than +15%). The operating temperatures are in the range 50° to 90°C. The corresponding slope for this range, say between 100° to 200°F (see appendix B) is:

$$\rho_{cool} = \rho_0 + K \times T$$

K is calculated to be 0.701 and ρ_0 is 1084 for the above concentration.
Variations in the coolant composition are accounted for by the additional term

$$(Cl_{comp} - 52) \times 1.025$$

where 1.025 is the gradient of the appropriate isotherm.

QCI

The heat flow to the coolant is calculated in the following way:

$$QCI = \frac{Coolant\ flowrate \times \rho_{cool} \times CpCl \times (TCl_{out} - TCl_{\epsilon})}{1000 \times 60}$$

The coolant flow rate is divided by 1000 x 60 for converting from litres/min to m^3/s.

The amount of nitric oxide chemically formed in combustion is very sensitive to the humidity of the inlet air. The SAE handbook (vol 3 section 25 item 3) provides the following data and equations for correcting NO_x emissions to reference humidity standards ie. 10.71g water/kg dry air (75 grains per pound) (see appendix B).

$$NO_{xcorr}\ (ppm) = \frac{NO_x\ (ppm)}{K}$$

Where K (*also known as ABK*) $= 1 + (7A(H-10.714)) + (1.8B(T_{air}-29.444))$

$$A = \frac{0.044}{air{:}fuel\ ratio} - 0.0038 \qquad B = \frac{-0.116}{air{:}fuel\ ratio} + 0.0053$$

H (*also known as hmdty*) = *Specifichumidity* (*g water/kg dry air*)

Calculation of Brake Specific Emissions

The stoichiometric combustion of a fuel of generalised known composition with oxygen will be:

$$C_\alpha H_\beta O_\gamma N_\delta \quad (\alpha\ \beta/4\ \gamma/2)O_2 \rightarrow products$$

When the fuel is burned with air and the equivalence ratio is λ, then:

$$y[C_\alpha H_\beta O_\gamma N_\delta + \lambda(\alpha+\beta/4-\gamma/2)\{O_2 + \frac{79.05}{20.95}N_2\}] \rightarrow 100 kmol\ of\ prodts.$$

$$where \quad \alpha M_C+\beta M_H+\gamma M_O+\delta M_N = M_{gas} \quad kg/kmol$$

The temporary variable 'y' is such as to give 100 kmol of exhaust products, and it will be seen later that the products can be measured either wet or dry. To produce 100 kmol of products the mass of reactants, m_R (which will also be equal to the mass of products m_P) is given by:

$$m_R = m_P = y[\alpha M_C+\beta M_H+\gamma M_O+\delta M_N + \lambda(\alpha+\beta/4-\gamma/2)M_{air}/0.2095]$$

The temporary variable, y can be found by an atomic balance. Since the carbon balance is considered the most reliable atomic balance:

$$y\alpha = \%CO + \%CO_2 + ppmCH_4/10^4$$

where %CO = measured value in the exhaust etc.

$$y = \frac{(\%CO + \%CO_2 + ppmCH_4/10^4)}{\alpha}$$

The mass flow rate of the exhaust (m_{ex}) can be found from the measured fuel mass flow rate (m_{fuel}) and the gravimetric air fuel ratio (AFRG):

$$m_{ex} \quad m_{fuel}(1 + AFRG) \quad kg/h$$

where AFRG = λ x AFR_{sg}

If the power output W_b (kW), the brake specific output of species i will be:

$$mass\ fraction\ of\ exhaust\ species\ i \times \frac{m_{ex}}{W_b} \quad kg/kWh$$

or

$$\frac{n_i M_i}{M_R} \times \frac{m_{ex}}{W_b} \quad kg/kWh$$

where n_i = % of species i in the exhaust.

Substituting for m_{ex} and m_R gives:

$$\frac{\%i \times M_i}{y \times (M_{gas} + \lambda(\alpha+\beta/4-\gamma/2)M_{air}/0.2095)} \times \frac{m_{fuel}(1 + AFRG)}{W_b}$$

$$But: \quad AFRG{:}1 = (\lambda\ AFR_{sg}){:}1 = (\lambda\ (\alpha+\beta/4+\gamma/2)M_{air} \times \frac{100}{20.95}) : M_{gas}$$

Re-writing the above equation, the mass fraction of exhaust species i will be:

$$\frac{\%i \times M_i}{y \times M_{gas}(1 + AFRG)} \times \frac{m_{fuel}(1 + AFRG)}{W_b}$$

As bsfc = m_{fuel}/W_b this simplifies to:

$$\frac{\%i \times M_i}{y \times M_{gas}} \times bsfc$$

The equivalent fortran code is:

$$Species\ i\ (g/kWh) = \%i \times M_i \times \frac{bsfc}{RAZ \times M_{gas}} = \%i \times M_i \times IAN$$

$$RAZ = y = \frac{(\%CO + \%CO_2 + ppmCH_4/10^4)}{\alpha}$$

Conversion to g/MJ (thermal)

The above equation may be re-written as:

$$\frac{\%i \times M_i}{RAZ \times M_{gas}} \times \frac{1000}{CalVal_g/1000}$$

where $CalVal_g$ = MJ/kg

$$Thus: \quad i\ (g/MJ\ thermal) = \frac{i(g/kWh) \times 10^6}{bsfc \times CV}$$

TA Luft Calculations

The final formulation, is that used in the German TA Luft regulations (see appendix B), in which the concentration is referred back to a specified level of oxygen in the exhaust. Thus if the emissions level is specified at A % oxygen whilst the measured oxygen level was B %, then:

$$[\%i]_A = [\%i]_B \times \frac{20.95 - A\%}{20.95 - B\%}$$

To convert to a gravimetric basis, it is necessary to multiply by the density (kg/m^3) of species i at NTP conditions (760mm Hg, 0°C).

$$i\ (Kg/m^3) = \frac{[\%i]_A}{100} \times [\rho]_{NTP}$$

$$i\ (g/m^3) = 10 \times [\%i]_A \times [\rho]_{NTP}$$

In the work reported here the $\%O_2$ was only measured by a chemical cell, so for weak mixtures the oxygen level, TAOx was estimated from a carbon balance as follows:

$$y[C_\alpha H_\beta O_\gamma N_\delta + \lambda(\alpha+\beta/4-\gamma/2)(O_2+\frac{79}{21}N_2)] \rightarrow aCO_2 + bCO + cO_2 + dH_2O + eCH_4 + fNO + gN_2$$

where a = $\%CO_2$, b = %CO, c = $\%O_2$ etc.

and y = a+b+c+e+f+g = 100kmols; d is not included because the products are dry.

Carbon balance: $\alpha y = a+b+c$; $y = \frac{a+b+c}{\alpha}$ ---------- 1

Oxygen balance: $y(\gamma + \lambda(\alpha+\beta/4-\gamma/2)2) = 2a+b+2c+d+f$ ---------- 2

Hydrogen balance: $y\beta = 2d + 4e$; $d = \frac{y\beta - 4e}{2}$ ---------- 3

Rearranging 2: $2c = y(\gamma+\lambda(\alpha+\beta/4-\gamma/2)2) - 2a-b-d-f$

Substituting for d, from 3:

$$2c = y(\gamma+\lambda(\alpha+\beta/4-\gamma/2)2) - (\frac{y\beta-4e}{2}) - 2a-b-f$$

$$= y(\gamma+\lambda(\alpha+\beta/4-\gamma/2)2) - \frac{y\beta}{2} - (2a+b+f-2e)$$

$$= y(\gamma + \lambda(\alpha+\beta/4-\gamma/2)2 - \beta/2) - (2a+b+f-2e)$$

Substituting for these two:

$$But \quad y = \frac{a+b+c}{\alpha} \quad \text{----- 1 ;} \qquad AFRV = \lambda(\alpha+\beta/4-\gamma/2)\frac{100}{20.95}$$

$$2c = (\frac{a+b+c}{\alpha})(\gamma + AFRV\times\frac{20.95}{100}\times 2 - \beta/2) - (2a+b+f-2e)$$

$$c = 1/2\ \{(\frac{a+b+c}{\alpha})(\gamma-\beta/2+0.418AFRV) - (2a+b+f-2e)\}$$

Substituting for a, b, c, e and f:

$$\%O_2 = 1/2\ \{(\frac{\%CO_2 + \%CO + ppmCH_4/10^4}{\alpha})(\gamma - \beta/2 + 0.418AFRV)$$

$$- 2\times\%CO_2 + \%CO + ppmNO_x/10^4 - 2\times ppmCH_4/10^4\}$$

Substituting with terms used in the fortran code:

$$\%O_2 = 1/2\ \{RAZ(Cbn - Hdn/2 + 0.418AFRV) - T_{ax}\}$$

Power Correction

The SAE handbook (vol 3 section 25 item 3) provides formulae to correct the measured power output for SI engines, to reference inlet air conditions. The equation in SI units is:

$$Power_{corr} = Power \times 1.18(\frac{99}{P_{dry}})\sqrt{(\frac{T_{air} + 273}{298} - 0.18)}$$

$$where \quad P_{dry} = \frac{P_{baro} \times 0.133224}{(1 + (\frac{humidity}{1000}\times\frac{M_{air}}{M_{water}}))}$$

Calculation of the Heat Flow to the Exhaust

The heat flow to the exhaust, Q_{ex} may be calculated with reference to the following relationship.

$$Q_{ex} = \Sigma \text{ molar flow rate x enthalpy (exhaust gases)}$$

However it is first necessary to determine the proportions of all the exhaust gas constituents in order to apportion the corresponding enthalpies. Thus for a fuel $C_\alpha H_\beta O_\gamma N_\delta$:

$$C_\alpha H_\beta O_\gamma N_\delta + AFRV \rightarrow aCO_2 + bCO + cO_2 + dH_2O + eCH_4 + fNO + gN_2 + hH_2$$

where a, b, c, e and f are measured percentages.

d and h are in proportion to each other.

g = 100 - (a+b+c+e+f+g+h)

For weak mixtures it is assumed that there is no H_2 present; only H_2O. Therefore using the hydrogen to carbon proportion:

$$\frac{H}{C} = \frac{\beta}{\alpha} = \frac{2d+4e}{a+b+e}$$

$$\alpha(a+b+e) = 2\beta(2e+d) \; ; \quad \frac{\alpha}{2\beta}(a+b+e) = 2e+d$$

$$d = \frac{\alpha}{2\beta}(a+b+e)-2e; \quad h = 0 \quad (ie.\ no\ H_2)$$

For rich mixtures (λ less than 1), it is assumed that both H_2 and H_2O are present.

$$Thus: \quad \frac{H}{C} = \frac{\beta}{\alpha} = \frac{4e+2d+2h}{a+b+e}$$

$$d + h = \frac{\beta}{2\alpha}(a+b+e)-2e \quad \text{---------- 1}$$

From the water gas constant (spindt 1965):

$$wg = 3.5 = \frac{\%CO \times \%H_2O}{\%CO_2 \times \%H_2} = \frac{bd}{ah} \; ; \qquad d = \frac{3.5ah}{b} \quad \text{---------- 2}$$

Substituting 2 in 1 gives:

$$\frac{3.5ah}{b} + h = \frac{\beta}{2\alpha}(a+b+e) - 2e$$

$$h(b + 3.5a) = \{\frac{\beta}{2\alpha}(a+b+e) - 2e\}b$$

All percentages (a, b, c, etc.) must be converted to kmol/s. The conversion factor CF (having the

$$h = \{\frac{\beta}{2\alpha}(a+b+e) - 2e\} \{\frac{b}{b + 3.5a}\} \quad \text{---------- 3}$$

same units) is evaluated in the following way:

$$\frac{m_{fuel}}{M_{gas}} \times \alpha = kmols\ of\ carbon/\text{sec} = CF \times (a+b+e)$$

where m_{fuel} = kg/s

and M_{gas} = kg/kmol

$$\therefore \quad CF = \frac{m_{fuel} \times \alpha}{M_{gas}\ (a+b+e)}$$

Thus: *species i*(%) × *CF* = *species i*(*kmol/s*)

The conversion factor CF, as above, converts all percentage flow rates to kmols per second. An array is created for all these species, such that Nmol x (1 to 8) (fortran code) is the equivalent of CF x (species 1 to 8).

Stone 1992, adapted from Reid et al. (1977) provides data for calculating the molar heat capacity at constant volume. The sum of the internal energies can be calculated from the following expression.

$$U(T) = U_0 + Cv_0T + \frac{1}{2}Cv_1T^2 + \frac{1}{3}Cv_2T^3 + \frac{1}{4}Cv_3T^4$$

The above expression simplifies to:

$$U(T) = U_0 + T\,(Cv_0 + T\,(\frac{1}{2}Cv_1 + T\,(\frac{1}{3}Cv_2 + \frac{1}{4}Cv_3T\,)))$$

where U_0 = Integration constant for setting the datum.

R_0 = 8.3143 kJ/kmol

$$As \quad H = U + pV \equiv U + R_0T$$

$$then \quad H(T) = U_0 + T(Cv_0 + R_0 + T(\frac{1}{2}Cv_1 + T(\frac{1}{3}Cv_2 + \frac{1}{4}Cv_3T\,)))$$

Thus the specific enthalpy of all the exhaust gas constituents is Σ H(T). When this is multiplied by the molar flow rate (kmol/s), the heat output (kW), is obtained.

An array is created with the values of the c_v. In the evaluation of the thermal energy of the

exhaust gas the measured percentage of oxygen was used. It might have been more accurate to use the computed value as derived for the TALuft calculations. However the difference in the oxygen levels was in most cases below 2%, and this causes a negligible (less than 100W), difference in the heat output. This is because an over-estimate of the oxygen leads to a corresponding under-estimate of the nitrogen and there is only a small difference in their respective molar heat capacities.

KDtm is the datum temperature for the exhaust gases (80°C). With a finite sized heat exchanger and a cooling medium that is above the ambient temperature, it is clearly impossible to cool the exhaust gases to the ambient temperature. The datum temperature of 80°C was selected to reflect these considerations, and to ensure that the exhaust gases remained above their dewpoint temperature. If a condensing heat exchanger was used it would need to be very large and made from material that would be resistant to corrosion. Since the exhaust gases are not considered to be cooled to the ambient temperature, then this adds to the "unaccounted heat loss" term, albeit to a small extent. The major sources of "heat loss" will be the radiation from the exhaust manifold, and convection from all the surfaces of the engine.

Q_{chem}

Oxidation reactions would not normally be taken into account. However they are considered for two reasons.

a) There is a need to account for all energy outputs.

b) Lean burn cogeneration systems have the option of an exhaust oxidation catalyst, which would enable the chemical energy to be released thermally.

Thus the specific enthalpy of combustion of CO, CH_4, NO and H_2 are used to evaluate the thermal energy associated with these reactions:

$$Q_{chem} = CO \times 282990 + HC \times 802310 + NO_x \times 90290 + H_2 \times 241830$$

where CO, HC, NO_x and H_2 are in kmol/s, and ΔH_0 is in kJ/kmol, giving Q_{chem} in kW.

Q_{cond}

Q_{cond} is the latent heat of water and this is included in the energy balance because the higher calorific value of the fuel is used.

Energy Balance

All the heat and work outputs can be expressed as fractions and percentages of the fuel energy. The fuel energy can be quoted in units of kW by multiplying the mass flow rate of fuel by its gravimetric calorific value: Therefore to express as a percentage:

$$\frac{Heat\ /\ Work\ (kW)}{Fuel\ energy\ (kW)} \times 100\%$$

Some energy losses cannot be easily calculated (ie. radiation losses, noise, kinetic energy etc.). However these may be deduced by subtracting all the known outputs. Thus:

$$Q_{Unaccounted} = \{\ 1\ -\ (\frac{work\ +\ heat}{fuelenergy})\} \times 100\%$$

Mass Fraction Burn Durations

These are outputs from the combustion analysis software. The 0-1%, 0-10% and 0-90% burn durations are expressed in degrees crank angle, with bdc of the piston as the start or reference. Thus absolute burn duration values are obtained by subtracting 180° and adding the ignition timing offset.

$$MFB1\ -\ 180\ +\ Tmg.offset\ =\ 0\text{–}1\%\ burn\ duration$$

The 10-90% burn duration is not calculated by the software but obtained by subtracting the 0-10% from the 0-90% mass fraction burn durations. This is probably the most representative burn time as it covers the duration where the bulk of the mixture is consumed by the rapid flame propagation phase, (ie. a more uniform burn rate).

The Wiebe Function

The Wiebe function is used to simulate the "s" shaped curve that is produced when calculating the cumulative mass fraction burnt (mfb), in an SI engine. It is defined by the equation:

$$mfb\ =\ 1\ -\ \exp(-a \times \theta^{(m+1)})$$

where theta(θ) is the fraction of the burn duration and a and m are constants with typical values of 5 and 2.

Output Files

There are four output files; the measurements, the combustion analysis output, the emissions and the energy balance.

The measurements file consists largely of regurgitated experimental data such as engine coolant and oil temperatures, gas pressure and humidity. The computed wiebe constants and burn periods are also included for later use in engine modelling programs. The λ number and the ignition timing provide a reference and are common to all output files.

The second output file consists of data produced by the combustion analysis software such as the CoVimep, Pmax, Imep etc. and the MFB durations (from which the Wiebe parameters are evaluated. The indicated, brake, mechanical and volumetric efficiencies are also included together with the fmep.

The third output file deals with the exhaust emissions. The harmful emissions such as NO_x, HC, and CO, as well as CO_2 are expressed on a volumetric and gravimetric basis. The grams per cubic metre are expressed in accordance with the TALuft regulations in which the concentration of exhaust species is referred back to a specified oxygen level and NTP conditions.

The fourth output file gives the energy balance. Energy outputs of heat and work are expressed in kW and also as a percentage of the in-coming fuel energy. The efficiencies are duplicated in this file for convenience.

CHAPTER 3

BASELINE EXPERIMENTAL RESULTS

3.1 BASELINE TESTING

Apart from providing a criterion against which to judge subsequent combustion systems, the baseline tests also provide data with which to calibrate a computer model, see section 3.4. The results discussed here were obtained at a constant speed of 1500 rpm and full throttle, for a range of air/fuel ratios or lambda (air fuel ratio /stoichiometric air fuel ratio), and ignition timings which encompassed the lean operating limit of the engine. The tests were conducted with systematic variation of the ignition timing and lambda. (see page 57a). The ignition timings were measured and controlled by a Variable ignition Timing Unit designed and developed at Brunel (Hudson, Stone 1990). The air fuel ratio was obtained and controlled from an exhaust gas analysis using the Lamdascan system.

3.1.1 Engine Specification

The test data were obtained from a 6.2 litre naturally aspirated gas engine, for which the specification is in Table 3.1.

Table 3.1 Specification of the gas engine

Configuration		in-line 6 cylinder
bore (mm)		107
stroke (mm)		115
compression ratio		10.3
valve timing:	evo 53	(° bbdc)
	ivo 20	(° btdc)
	evc 12	(° atdc)
	ivc 45	(° abdc)

The engine was a proprietary conversion of the Ford Dover diesel engine, which had been modified by replacing the injectors with spark plugs, adding a distributor and electronic ignition system, machining the existing diesel engine pistons and modifying the inlet manifold to take an Impco gas carburettor. The pistons were machined, so as to increase the squish clearance to 5.26 mm, and create a concentric flat bowl 19.7 mm deep in the piston, with a 47% squish area.

3.2 BASELINE RESULTS

The results are presented as a series of contour plots, in which the dots (see page 57a), represent individual operating points at which test data were recorded. As the mixture was weakened the engine would only operate over a progressively narrower range of ignition timings. With mixtures slightly rich of stoichiometric, the ignition advance of 65° btdc led to knock being just visible on the cylinder pressure trace but not audible.

3.1 BASELINE TESTING

Apart from providing a criterion against which to judge subsequent combustion systems, the baseline tests also provide data with which to calibrate a computer model, see section 3.3. The results discussed here were obtained at a constant speed of 1500 rpm and full throttle, for a range of air/fuel ratios or lambda (air fuel ratio /stoichiometric air fuel ratio), and ignition timings which encompassed the lean operating limit of the engine. The tests were conducted with systematic variation of the ignition timing and lambda. The ignition timings were measured and controlled by a Variable ignition Timing Unit designed and developed at Brunel(Hudson, Stone 1990). For each air/fuel ratio (lambda), the ignition timing θ was varied in steps of 3° to cover the range -18°>MBT>+18°. The lambda was obtained and controlled from an exhaust gas analysis using the lamdascan system and it was varied in steps of 0.06 in the range $0.800>\lambda>1.000$, and in steps of 1.00 thereafter until the lean limit was encountered. Each test point is represented on the contour plots as a dot. The 3d plotting facility used was called 'Unimap' and is part of the 'Uniras graphics software package'. A choice of interpolations are provided and in this case the one that gave the 'best fit contour' was chosen. Both, the contour and the individual data point can be labelled, and therefore the positional accuracy of the contour is easily determined. Areas with no data can be blanked off so that the interpolation is not carried out in these areas.

The computer based data acquisition system used here has been described fully in section 2.6. Data was recorded on two Channels (ie. one for cylinder pressure and the other for crankshaft encoder signals such as the tdc marker), and this enabled a sampling rate of 360 cycles for each test condition λ and θ. The data once recorded was processed using Biceri's 'Biccas' combustion analysis software which is based on the Rassweiler and Withrow method; this is described in section 2.7.1. The Wiebe function constants which are used to define the burn rate curves in the ISIS thermodynamic model were verified against the actual 10-90% mass fraction burned curves plotted by Biccas (see also page 55 and appendix B for an explanation of the Wiebe function).

The ISIS thermodynamic model is based on the 'Arbitrary Heat Release' subroutine presented by Ferguson(1986), (see also sections 3.2 and 5.1). Despite its name 'ahr' takes into account the equilibrium composition of the burnt gases and their real thermodynamic behaviour. By using the Wiebe function as an input, the arbitrary nature of the heat release is eliminated.

3.1.1 Engine Specification

3.2.1 Bmep

Figure 3.1 shows the bmep as measured, while figure 3.2 shows the bmep when corrected to datum conditions of 0.99 bar and 25°C according to the SAE handbook (vol 3 section 25 item 3), on a contour plot of ignition timing and lambda. A comparison of figures 3.1 and 3.2 shows that there is a negligible difference, since the test conditions were always close to the datum. The response of the bmep to variations in the air/fuel ratio are as expected, although at very lean mixtures (λ=1.5), the timing was advanced by as much as 45° btdc in order to achieve MBT. The maximum bmep was produced slightly rich of stoichiometric at around MBT. The contours show a fairly broad peak or plateau at the richer mixture settings (λ 0.8 to 1.1), and the slope of least gradient corresponds to the MBT ignition timing schedule. Generally, the weak mixtures led to a significant reduction in the bmep at all ignition timings. For the rich mixtures the bmep reduces significantly only at the very retarded, and very advanced timings. These results agree with the general trends. For the very rich mixtures there is insufficient oxygen to facilitate complete burning, and at the weaker mixture settings there is less fuel to be burnt. Both lead to a falling bmep. Advancing the timing will increase the burn time duration, but if the timing is advanced greatly beyond the optimum (MBT), the negative work increases drastically. Retarding the timing greatly beyond MBT will reduce the burn time duration. Both these measures effectively reduce the bmep.

3.2.2 Brake Efficiency

Figure 3.3 shows the brake efficiency, (η_b) on a similar plot of ignition timing and lambda. The brake efficiency increases as the fuel/air rich mixture is made leaner from lambda 0.8 to lambda 1.0. A maximum efficiency plateau of about 30% is reached just lean of lambda 1.0, and this is maintained at approximately the same level along the MBT ignition timing schedule. As the bmep reduces the frictional losses become more significant, and this is normally manifest as a reduction in the brake efficiency. However when the bmep reduces as a consequence of weakening the mixture, the weaker mixture leads to a higher indicated efficiency, thus compensating for the increasing significance of the mechanical losses. Hence a falling bmep does not show a falling efficiency until extremely weak air/fuel ratios are encountered, such as lambda 1.5 and lambda 1.6. At this point, owing to the occurrence of misfire and the increasing effect of the fmep, the brake efficiency begins to fall. Generally, the brake efficiency contours show a very broad peak efficiency plateau, which indicates that the brake efficiency is not sensitive to small variations (up to 10°), in the ignition timing either side of MBT. A sharp decrease in the brake efficiency is only experienced at $\lambda < 1.0$, due to the falling bmep and the rising fuel flow rate. Greatly advancing or retarding the ignition timing has a similar effect, because of negative work or insufficient burn time duration respectively. The general trends of brake efficiency are as expected.

3.2.3 Exhaust Temperature

Figure 3.4 is a plot of the exhaust gas temperatures measured at the exhaust manifold. As the air/fuel ratio is weakened with fixed ignition timing, the available energy in the mixture is reduced. Thus the exhaust temperatures will be lower than for the weaker air fuel ratios. At the retarded

timings, say Ignition timing < 10° (with fixed air fuel ratio), the exhaust temperatures can be expected to rise owing to the later burning of the fuel, and the exhaust valve opening closer to the end of combustion. At the more advanced timings temperatures are lower because more heat is transferred to the coolant and less heat energy is dissipated in the exhaust gases. As the mixture is made richer from about lambda 1.2 the exhaust temperatures become increasingly more sensitive to variations in the ignition timing. A maximum sensitivity band may be seen between lambda 1.0 and 1.2, where the flame speed is fast enough to enable engine operation at very retarded timings. However the extremely high temperatures of 800°C and 900°C suggest that the combustion is incomplete within the cylinder, and that the gases are continuing to burn in the exhaust system. The results conform to the usual trends.

3.2.4 CoV of Imep

Figure 3.5 shows the Coefficient of Variation (mean value/standard deviation) of the imep. The Coefficient of Variation (CoV) of imep has been selected as it is the most appropriate means of characterising the cycle-by-cycle variations. Ultimately, variations in the imep of individual cycles will lead to engine speed fluctuations. It is generally accepted that if the CoV of imep is less than 5%, then this will lead to satisfactory speed regulation in electrical generation applications. The largest variations of CoV of imep are to be found at the extremities of the operating envelope, at the very advanced ignition timings and at the very retarded ones. As the timing is varied towards MBT the CoV of imep falls steadily until, a minimum value is reached in the area covering the MBT ignition timing. The CoV of imep shows a steady increase as the timing is moved away from MBT. The contours show that weakening the mixture tends to increase the cycle-by-cycle variations, especially as the weak mixture limit is approached.

3.2.5 Maximum Pressure

Figure 3.6 shows the maximum cylinder pressure plotted against ignition timing and lambda. The maximum cylinder pressure, as expected is produced with the richer air fuel ratios (λ < 1.1), where the highest laminar burn velocities are produced giving a shorter burn duration (ie. the pv diagram is less rounded giving a larger area and consequently a larger work output). Varying the ignition timing in this area has a significantly greater effect on the maximum pressure, than at the weaker air fuel ratios. The maximum pressure rises steadily as the timing is advanced towards MBT. Thereafter, although the maximum pressure continues to rise with advancing timing there is less effect. This is because when combustion is phased to occur at tdc, then this produces the highest maximum pressure as the combustion chamber is then compact. When the mixture is weakened beyond λ 1.1 (fixed timing), there is a decrease in the maximum pressure, whence lambda begins to have a greater effect on pmax than the ignition timing, due to the slower burn rate of the mixture.

3.2.6 CoV of Maximum Pressure

Figure 3.7 shows the Coefficient of Variation of the maximum combustion pressure. The Coefficient of Variation of the Maximum Pressure, CoV of pmax is another way of characterising the cycle-by-cycle variations and these contours show the same basic trends as the CoV of imep. A mean low value is reached in an area covering the MBT ignition timing schedule. Advancing the timing with fixed air fuel ratio causes the CoV of pmax to fall significantly. At advanced timings the gradient is less steep. Advancing the ignition timing lowers the CoV of Pmax since the maximum cylinder pressure will be higher. Furthermore, there will be less variation in the maximum cylinder pressure since the combustion will be closer to completion. Generally, there will be less cyclic variation of maximum pressure at the richer air fuel ratios ($\lambda<1.1$ and fixed ignition timing), and this in part will be due to the higher maximum cylinder pressures.

3.2.7 0-10% Burn Duration

The mass fraction burnt was calculated on a cycle-by-cycle basis, using the Rassweiler and Withrow (1938), method. Three burn rate plots are presented here. The 0-10% burn rate (figure 3.8), reflects the value of the laminar burning velocity at the time of ignition. The laminar burning velocity is a maximum slightly rich of stoichiometric, so when the mixture is weakened (with a fixed ignition timing), the 0-10% burn duration increases. When ignition occurs earlier in the compression stroke (that is advanced timings) the mixture temperature is lower. This leads to a lower laminar burning velocity and a longer burn duration. This is most apparent with the weaker slower burning mixtures.

3.2.8 0-90% Burn Duration

Figure 3.9 shows there is less variation in the 0-90% mass fraction burn duration than in the 0-10% burn duration, as the latter is more dependant on the in-cylinder conditions just prior to ignition. The 0-90% burn contours show that the burn rate decreases steadily with advancing ignition timing. However, both the 0-10% and the 0-90% burn duration minima coincide just rich of stoichiometric for MBT ignition timings.

3.2.9 10-90% Burn Duration

The 10-90% mass fraction burn duration (figure 3.10), is representative of the turbulent burn rate in the cylinder. This is because the 10-90% burn time is dominated by turbulent combustion, and the turbulence intensity will not vary much in the region of tdc; for the MBT ignition timings. The 10-90% mass fraction burn occurs within the period from about 10°btdc to 20°atdc. It also appears that the MBT timing is such that the 10-90% burn period is close to the minimum value for each ignition timing. The 10-90% burn period is a minimum in the region of the stoichiometric air fuel ratio. Weakening the mixture (at a fixed ignition timing), beyond stoichiometric increases the 10-90% burn duration for two reasons. Firstly, the weaker mixture has a lower laminar burning velocity, and this leads to a later start for the 10-90% burn period, so that (secondly) the turbulence will have decayed more during the compression stroke. In general, advancing the ignition timing (for a fixed air fuel ratio) reduces the 10-90% burn time, since the earlier phasing

of this part of combustion results in the turbulence having decayed less.

3.2.10 NOx Emissions

The emissions of Nitrogen Oxides were measured as NOx and calculated as NO_2 (equations for calculating gravimetric values are presented in section 2.8), and they are summarised by figures 3.11 to 3.14. The NOx emissions respond in the usual way to variations in the ignition timing and the air fuel ratio. The formation of the NOx is very temperature dependant, so that when the ignition timing is advanced (with a fixed air fuel ratio) then the high temperatures during the main part of combustion, lead to an increase in the NOx emissions. The dependence of the NOx formation on the air fuel ratio is more complex as there are two competing factors. The formation of NOx depends on both the oxygen concentration in the burnt gas and the burnt gas temperature. Weakening the air fuel ratio increases the oxygen concentration, but reduces the temperature in the burnt gas region. The result is that the maximum NOx formation occurs slightly weak of stoichiometric, close in fact to the air fuel ratio for the maximum brake efficiency. The volumetric NOx contours in figure 3.11 are more indicative of the influence of the ignition timing and the air fuel ratio on the NOx formation as these values are not related to the power output of the engine. Figure 3.12 and 3.13 show how the brake specific output can be reduced at a particular air fuel ratio, by retarding the ignition timing. However this leads to a fall in the brake efficiency and the bmep. Alternately the NOx emissions can be reduced by using a much weaker air fuel ratio. The brake efficiency only falls slightly with the weaker air fuel ratio (figure 3.2) but the bmep (figure 3.1) is reduced significantly. However the bmep can be restored by turbocharging, and this would also increase the brake efficiency for the weak mixtures. In figure 3.14 the contours represent grams of NOx per cubic metre. The NOx concentration is referred back to a specified level of oxygen in the exhaust in accordance with the German TA Luft regulations. The rationale for this, is to prevent an apparent reduction in emissions being obtained by mere dilution with air. The TA Luft requirement (at present the most stringent in Europe), for NOx is $0.5g/m^3$ It is possible to achieve this target only at the extremities of this operating envelope (ie. with the standard combustion system).

3.2.11 Unburnt Hydrocarbon Emissions

The unburnt hydrocarbon emissions were assumed to be only methane, as explained in section 1.4. For these results also it is necessary to refer to four different plots (figures 3.15 to 3.18), giving identical units as for the NOx. Figure 3.16 which is the brake specific counterpart of figure 3.15, shows a large region around the MBT ignition timing schedule, for which the brake specific methane emissions are below 4.5 g/kWh (0.412 g/MJthermal). With retarded ignition timings the emissions rise rapidly, because the slower burning cycles will not have finished before the exhaust valve starts to open. As the mixture is weakened the ignition timing has to be steadily advanced to compensate for the slower burning velocity of the mixture, and the range for which the emissions are below 4.5g/kWh considerably narrows. As the mixture is weakened further ($\lambda > 1.4$) the emissions increase rapidly as the weak mixture limit is approached. The TA Luft requirement is $0.15g/m^3$ non-methane hydrocarbon emissions; the non-methane hydrocarbons

from this engine is assumed to be zero. Thus it is possible considering only the NOx and the UHCs to satisfy the TA Luft targets but the operating points are too close to the extremities of the operating envelope to be of practical use.

3.2.12 Carbon Monoxide Emissions

The emissions of carbon monoxide (figure 3.19) is considered here because it forms part of the TA Luft requirements which state a limit of 0.65g/m^3 along with the other limits mentioned in sections 3.2.9 and 3.2.10. Generally the the CO emission for a lean burn engine is low provided it is operated in the lean regime. The contours in figure 3.19 show high CO emission at λ=0.8 which decreases rapidly as the oxygen availability is increased by weakening the air fuel ratio. A large region of under 1.5g/m^3 is maintained at air fuel ratios weaker than stoichiometric. However in order to satisfy the TA Luft limit of 0.65g/m^3 it would necessitate operating in a narrow band between λ 1.1 and 1.3. But as this would mean unacceptable NOx emissions (figure 3.14) of well over 0.5g/m^3 it is clear that both these requirements cannot be satisfied with the present combustion system. However, a simple oxidation catalyst for the CO may suffice.

3.2.13 Energy Balance; Exhaust Energy

Figures 3.20 to 3.24 represent an energy balance expressed as percentages of the total energy present in the fuel. Figure 3.20 shows the exhaust energy. With fixed ignition timing, the contours show the heat energy increasing, from λ=0.8, with weakening air fuel ratio until at stoichiometric conditions (also the condition for the fastest burn duration and the highest efficiency) a value of 27% is reached. This is maintained well into the lean region particularly along the MBT ignition timing schedule until the onset of slow burn. The ignition timing has a significantly greater effect on the exhaust energy than lambda. Retarding the ignition timing causes the exhaust energy to increase, until at the extremely retarded timings due to late burning, the energy percentage is very high.

3.2.14 Energy Balance; Coolant Energy

Figure 3.21 shows the coolant energy contours expressed as a percentage, and this shows results that are consistent with the exhaust energy. The heat transferred to the coolant is a maximum at stoichiometric mixtures. With richening air fuel ratio (λ < 1), and fixed ignition timing the heat output steadily decreases, this is because less of the chemical energy is available with rich mixtures. Also with weakening air fuel ratio (λ > 1.1), the percentage of heat transferred decreases until very weak air fuel ratios are encountered, where higher heat transfer rates are experienced due to increased burn duration. When the ignition timing is retarded at a fixed air fuel ratio the heat absorbed by the coolant decreases. The greatest heat transfer occurs at the very advanced ignition timings as expected, which also coincides with the least heat dissipated in the exhaust gases. Generally, the time of ignition with respect to the position of the piston in its compression stroke have a much greater effect on the heat output than lambda.

3.2.15 Energy Balance; Chemical Energy

Figure 3.22 shows the potential heat energy that might be utilised from the unburnt methane if an exhaust oxidation catalyst was fitted. With mixtures richer than stoichiometric the chemical energy is very high owing to the high proportion of incompletely burnt fuel; because there is less oxygen with the rich mixtures this energy could only be converted if there was air injection upstream of the catalyst. When the oxygen availability is sufficient for complete combustion ($\lambda > 1$), the proportion of unburnt methane in the exhaust system is low, and the energy that might be released thermally is correspondingly low. The general trends are as expected. The ignition timing has no significant effect except at the extremes of the operating envelope.

3.2.16 Energy Balance; Condensate Energy

In figure 3.23 the condensate energy (latent heat of condensation of water vapour), is directly proportional to the mass of water (along with all of the other products), being produced by the reactants. The results follow expected trends in that the condensate energy is a maximum for stoichiometric mixtures (ie. in the region where the bsfc is high for the amount of fuel being burnt completely). As the mixture is weakened the condensate energy decreases because the mass of fuel burnt is being lessened; for the rich mixtures the condensate energy is less because there is insufficient oxygen for complete combustion. Varying the ignition timing has little effect, until at timings retarded of MBT the values are below average. Generally the variation is less than 15% over the entire operating range of the engine.

3.2.17 Energy Balance; Unaccounted Energy

Finally the contours in figure 3.24 show the percentage of fuel energy not accounted for in the previous figures. The lowest value occurs just weak of stoichiometric, which is also the region of highest efficiency (figures 3.2 and 3.3), and NOx formation. There is a general trend in which the unaccounted losses increase as the air fuel ratio is weakened (from λ=1.1 to λ=1.5). It can be argued that the convective heat transfer from the engine will be almost independent of the operating point. (Higher exhaust temperatures will of course lead to increased radiation and convective losses from the exhaust manifold). When the air fuel ratio is weakened the energy flux into the engine is reduced, and thus the (almost invariant), convective losses will become a larger proportion of the input. Generally the largest fraction (30%), of the fuel energy may be apportioned to the brake work output, the second largest (27%), to the exhaust gases and the smallest fraction (24%), to the engine coolant.

3.3 THE FAST BURN HIGH COMPRESSION RATIO COMBUSTION SYSTEM

With the standard compression ratio of 10.3, the engine would only exhibit trace knock with a mixture that was slightly rich of stoichiometric, and an ignition timing 45° advanced from MBT. This very high knock margin indicates that a significantly higher compression ratio could be utilised. A previous study for an engine with a similar cylinder capacity, concluded that a compression ratio of about 15:1 would be optimum (Stone and Ladommatos 1991). A report on

very comprehensive tests by Lee and Schafer (1982), indicates that for high output and low fuel consumption at full load:

* the squish area should be 50-60%
* there is little benefit in reducing the squish clearance below 2 mm
* the ignition point should be close to the centre of the bowl

Lee and Schafer investigated various bowl positions and obtained good results with the bowl centred around the exhaust valve.

Tests on the cylinder head using a blowing rig and a swirl torque meter, had established that the Ricardo swirl ratio was 2.01 (AVL swirl ratio = 2.75), see appendix B. This comparatively high level of swirl implied that an offset bowl in the piston should be used, as this would tend to disrupt the swirl and generate turbulence, (McKinley and Primus 1988).

3.3.1 Design of the FBHCR Combustion Chamber

The combustion system selected for testing first had: a 1 mm squish clearance, a bowl diameter of 68 mm (giving a 60% squish area), and a bowl depth of 17.5 mm. Other attributes were: the eccentric bowl centred around the exhaust valve and an inlet valve cut-out to provide a clearance of 1.3 mm. The combustion system (shown in Figure 3.25) was designed so as to avoid any thin sections that might overheat. Pistons with un-machined crowns were machined on a CNC mill, and the bowl volume was measured afterwards to check the compression ratio.

The spark plug mounting position could not be readily changed, so different spark plugs were obtained. In the standard engine the spark plug gap is positioned slightly recessed into the cylinder head. For the high compression ratio tests, some spark plugs with the same heat rating were obtained, which enabled the spark plug gap to be projected up to 10 mm further into the combustion bowl. An investigation with a phenomenological turbulent combustion model (Stone Brown and Beckwith 1992), indicated that igniting the mixture away from the cylinder head should lead to a faster burn. Various tests were conducted in order to find the most suitable ignition system and the effect of these combustion system parameters are studied in chapter 4.

3.4 MODEL PREDICTIONS

The spark ignition engine model used here is an extension (developed by Stone et al 1993), of the model presented by Ferguson (1986). Ferguson provides full details of the relevant differential equations, and how the equilibrium combustion products are evaluated. The model used here includes the NO kinetics, a choice of in-cylinder heat transfer correlations, and estimates of the friction and gas exchange losses.

The extended Zeldovich mechanism is used to describe the NO formation; full details of the

method and relevant rate constants are provided by Heywood (1988). The formation of NO_2 is not considered in the model, but when the engine-out emissions are calculated on a specific basis, then it is assumed that all the NO will oxidise to NO_2. The emissions of carbon monoxide and hydrogen are computed by freezing the composition of the cylinder contents at a user specified temperature, assumed here to be 1800 K. (See page 65a).

The heat transfer is calculated from either: the Woschni correlation, the Eichelberg correlation, the Hohenberg correlation, or a user provided heat transfer coefficient; fine tuning is by means of a scaling factor. The frictional losses are computed from the Chen and Flynn correlation (1965), with a weighting factor here of 0.8; the gas exchange losses are determined from the work by Bishop (1968).

For each engine operating point, the experimental 10% and 90% mass fraction burn durations were used to define the variables in the Wiebe burn rate equation. The pressure at inlet valve closure was varied in order to obtain the correct engine output. The inlet valve was assumed to close instantaneously half way between bottom dead centre, and its true closure angle. This was to allow for the pressure rise in the cylinder prior to inlet valve closure. The Hohenberg heat transfer correlation was used, with a 1.2 weighting factor, as this was found to give good agreement with the experimental data. The model was tuned for a lambda of 1.2 with an ignition timing of 25° btdc; the model was not re-tuned for any other operating point (see page 65a).

3.4.1 *Baseline Performance Predictions*

Figure 3.26 shows the computed value of the bmep for the range of ignition timings and air fuel ratios. When this is compared with the experimental data in figure 3.1, it can be seen that the model predicts a slightly higher maximum bmep (about 0.3 bar), but that this difference reduces as the mixture is weakened. It should be remembered that the only parameters varied in the model were: the ignition timing, the air fuel ratio, and the burn rate.

The computed brake efficiency in figure 3.27 also compares well with the experimental data in figure 3.2. The predicted efficiencies are mostly about 1 percentage point higher than the experimental data. The exception is in the region around stoichiometric with retarded ignition timings, for which cases the efficiency is significantly over-predicted. However, this is not a region of interest for the current work - if it was, then the model could of course be tuned to simulate this region. Although it is not presented here, there was close agreement between the measured and predicted values of the maximum cylinder pressure.

Figure 3.28 shows the predictions of the brake specific NOx emissions, and a comparison should be made with the experimental data in figure 3.12. The model gives the most reliable predictions in the regions where the NOx emissions are predicted to be less than 20 g/kWh. The predictions become particularly unreliable with over advanced ignition timings, which fortunately are not a region of importance. When looking at the discrepancies between the measurements and

predictions, it should be remembered that:

1) Only a two-zone combustion model has been used
2) There is uncertainty over the rate constants for calculating the NO kinetics
3) When brake specific emissions are calculated, there is a compounding of the errors Associated with predicting the emissions and the brake efficiency.
4) A mean cycle has been modelled which will not necessarily be the same as an average of all the individual cycles.

None the less, the predictions of the brake specific NOx emissions show the correct trends.

3.4.2 FBHCR Combustion system performance predictions

For reasons explained in section 3.3, the engine was rebuilt with a new compact combustion system, and a compression ratio of 14.7. A new set of pistons were machined on a CNC mill (see section 3.3.1). The computer model was then used (without changing any of the tuning variables) to predict the high compression ratio engine performance with:

1) the same burn duration
2) a burn duration reduced by 30% to simulate the expected effects of the faster burn.

Figure 3.29 shows the predicted dependence of the bmep ignition timing and air fuel ratio for both the standard (-) and fast burn (- - -) combustion systems at a compression ratio of 14.7. The fast burn combustion system has a less advanced MBT ignition timing schedule, and the bmep also reduces more rapidly as the ignition timing departs from MBT. If a comparison is made with the low compression ratio (10.3:1) predictions (see figure 3.26), then there is an almost uniform gain in bmep of about 0.3 bar.

The predicted dependence of the brake efficiency on ignition timing and air fuel ratio, is shown in figure 3.30 for both the standard and fast burn combustion systems. As with the bmep (figure 3.29), the brake efficiency is more sensitive to ignition timing in the fast burn case; the faster burn does not lead to any significant changes in efficiency. When a comparison is made with the baseline predictions of the brake efficiency (figure 3.27), it can be seen that there is an almost uniform 2 percentage points increase in the brake efficiency.

Figure 3.31 shows the predicted dependence of the brake specific NOx emissions on variations in the air fuel ratio and ignition timing, for both the standard and fast burn combustion systems at the high compression ratio (14.7:1). The fast burn combustion system leads to higher peak pressures and temperatures, so this might be expected to cause higher NOx emissions. However, this trend appears to be balanced by the faster burn combustion having a shorter duration at the temperatures that permit NOx formation. Thus, when a comparison is made between the brake specific NOx emissions on the respective MBT ignition timing schedules, then

there is only a small difference between the fast and standard burn rate systems. However, when comparisons are made on the basis of absolute ignition timings that are in advance of MBT, then the fast burn combustion system does give higher brake specific NOx emissions.

When a comparison is made with the low compression ratio (10.3:1) predictions of the brake specific NOx emissions (figure 3.28), then there are no discernible differences (except at very advanced ignition timings) with the predictions for the standard burn system at the high compression ratio. The higher compression ratio leads to higher temperatures during compression and all subsequent processes, so this might be expected to give higher NOx emissions (indeed, on a volumetric basis it does). However, the higher compression ratio also reduces the brake specific fuel consumption, and this balances the tendency for the higher compression ratio to give greater NOx emissions. If the standard and fast burn combustion systems are compared in figure 3.31, then at a given ignition timing, the fast burn combustion system gives greater NOx emissions. This is because a fixed ignition timing is more advanced on a relative basis for a fast burn combustion system.

The results discussed in figures 3.29, 3.30 and 3.31 have implied that the faster burn combustion system offers only slight advantages in efficiency and output. Indeed the greater sensitivity to departures from MBT ignition timing might be considered a disadvantage. However, the modelling discussed here, has not taken into account cycle-by-cycle variations in combustion. The faster burn will in fact lead to lower cycle-by-cycle variations in combustion, and this will be most evident and important for the combustion of weak air fuel mixtures. Also a faster burn enables combustion to be complete whilst the piston is still very close to tdc. Thus any variations in the burn rate have a small effect on the work output.

One of the origins of cycle-by-cycle variation in combustion is from the displacements of the flame kernel away from the spark plug during the early burn period. These displacements are random, because of cycle-by-cycle variations in the mean flow around the spark plug at the time of ignition. The flame kernel displacements continue until the flame kernel is of comparable scale to the turbulence. Thus the concentrations of air, fuel and residuals close to the spark plug influence the cycle-by-cycle variations, since weak air fuel mixtures or a high concentration of residuals cause a low laminar burning velocity. In turn, the low laminar burning velocity means that it takes the flame kernel longer to reach a size at which it is no longer displaced by the mean flow. Finally, the greater these flame kernel displacements, then the higher the level of cycle-by-cycle variations in the combustion. The high compression ratio, fast burn combustion system will lead to lower cycle-by-cycle variations in combustion, since the in-cylinder temperature with the less advanced ignition timings will be higher, and this increases the laminar burning velocity. Furthermore, with fast burn combustion systems, even the slow burning cycles will have been completed before the piston moves significantly away from tdc. In other words, a fast burn combustion system means that a greater percentage of the cycles will approach the ideal of constant volume combustion.

CHAPTER 4

FAST BURN HIGH COMPRESSION RATIO EXPERIMENTAL RESULTS

4.1 FAST BURN HIGH COMPRESSION RATIO RESULTS

For the FBHCR combustion system tests two compression ratios were tested, one at 14.7:1 the other at 13:1. The engine had to be rebuilt with a new set of pistons each time. Initial tests with the 14.7:1 compression ratio combustion system were conducted to optimise the ignition system as this was the first compact combustion chamber to be installed in the engine.

4.2 IGNITION SYSTEM OPTIMISATION

In order to identify the most suitable ignition system, tests were conducted at full throttle, fixed speed (1500 rpm) and a fixed air/fuel ratio (λ = 1.5) for a span of ignition timings. Tests were undertaken with different spark plug types, spark plug gap, spark plug electrode protrusion and ignition coil. The weak air fuel ratio (λ = 1.5) was chosen, since this was close to the limit for stable combustion with the original combustion system. The effect of combustion system parameters was studied with reference to:

the brake mean effective pressure (bmep)
the brake efficiency (Etab)
the emissions (NOx and HC)
the 1%, 10% and 90% mass fraction burn duration
and the cycle-by-cycle variations (as shown by the CoV of the imep and maximum cylinder pressure)

4.2.1 The Influence of the Spark Plug

Figure 4.1 shows the different spark plug types tested. The original spark plug (figure 4.1a) has no protrusion of the central electrode into the main part of the combustion chamber, the long nose spark plug (fig. 4.1b) has the centre of the spark plug electrode gap project about 2 mm into the combustion chamber (the effect of the electrode gap size and its position in the combustion chamber will be seen later). Figure 4.1c shows a long reach plug (7 mm) that was made by removing part of the thread on a spark plug with 18 mm of thread.

Figure 4.2 shows the bmep and combustion stability (CoV of imep) for the different ignition systems across the range of ignition timings. (Not all the systems would operate stably over the full ignition timing span of 0-40° btdc). The bmep shows the usual response to the ignition timing, and the coefficient of variation (CoV) of the imep is (as expected) a minimum in the region of the MBT ignition timing. The bmep shows that the long nose spark plug (figure 4.1b) gives the best performance and this is also reflected by the slightly lower level of the CoV of imep. Since the engine is operating with a fixed air fuel ratio at full throttle, then the fuel flow rate into the engine should be constant. Thus the brake efficiency and bmep are linked to one another, and show the same trends, with the long nose spark plug giving the highest brake efficiency of 34.5%.

The brake specific emissions of the nitrogen oxides (NOx) and unburnt hydrocarbons (HC) are shown in figure 4.3. The brake specific NOx emissions are principally dependent on the ignition timing, with the retarded ignition timings giving lower NOx emissions. The spark plug (figure 4.1b) that gave the highest bmep and efficiency and lowest cycle-by-cycle variations in combustion gave a slightly higher brake specific NOx emissions for a particular ignition timing. However, at the respective MBT ignition timings there was no discernible difference in the brake specific NOx emissions. It will be seen later (fig. 4.4) that this spark plug also gave the fastest burn. However, if the ignition timing with the long nose spark plug (fig. 4.1b) is retarded, to give the same bmep or brake efficiency as another spark plug, then the long nose spark plug gives the lowest brake specific NOx emissions.

The brake specific HC emissions (figure 4.3) are lowest for the long nose spark plug, and this spark plug also permits the widest range of ignition timings before the HC emissions start to rise rapidly (above say 7 g/kWh). The brake specific HC emissions rise rapidly with the onset of unstable combustion, and this accounts for the similarity with the cycle-by-cycle variations of the imep shown in figure 4.2. By the time the brake specific HC emissions have reached 7 g/kWh, the CoV of imep is starting to rise rapidly and is at or above 5%.

Finally, figure 4.4 shows that the long nose spark plug gave the fastest burn; as usual the 0-90% burn duration is a minimum in the region of MBT ignition timing. The differences between the various spark plugs are greatest at the extremes of ignition timing. The 0-90% burn durations show the greatest differences between the spark plugs, and these differences are consistent with the cycle-by-cycle variations in combustion.

The fastest burn is associated with the most efficient engine operation, the highest bmep, the lowest cycle-by-cycle variations and the lowest HC emissions. There is also the greatest tolerance to changes in ignition timing. The long nose spark plug also appeared to give the highest emissions of NOx. However, the differences in NOx emissions (at a given ignition timing) are slight, and for a given brake specific fuel consumption, the long nose spark plug (figure 4.1b) gives the lowest brake specific NOx emissions.

Referring back to figure 4.1, it shows that the standard spark plug would lead to a flame kernel that was likely to be adversely affected by the cavity in the cylinder head. In contrast, the long reach plug projects 7 mm into the combustion chamber in the bowl. There will thus be high mean velocities (from the swirl) and turbulence (from the squish). Too high a mean velocity will cause too much stretching of the arc, and detachment of the arc from the spark plug before the ignition system is fully discharged. The high mean velocity and turbulence will also lead to significant flame stretching, and this can cause a flame kernel to be extinguished shortly after ignition. The arc can be detached from the spark plug electrodes when the mean velocity is about 15 m/s (at 1 bar), and this is the velocity level that can be predicted by modelling the swirl during the induction and compression processes. Thus the long nose spark plug (figure 4.1b) gives the best

performance because:

a) it avoids the cavity associated with the standard spark plug, and
b) it avoids the activity associated with the flow away from the combustion chamber surfaces

Subsequent tests showed that even the long nose spark plug performance was affected by arc detachment. The normal arc duration is typically 1 ms, but arc detachment, and subsequent re-striking of the arc, was observed after about 0.5 ms.

4.2.2 The Effect of Spark Plug Gap

Some previous work (Stone and Steele, 1989) on ignition systems had shown that cycle-by-cycle variations were reduced by increasing the spark plug gap. However, when a small gap was used, the cycle-by-cycle variations were reduced by increasing the energy stored in the coil. Since these data were obtained with a different ignition system, and a lower compression ratio (10:1) at part load (3.2 bar bmep), then no direct use can be made of the data and an experimental investigation was needed.

A consequence of increasing the compression ratio, is that at a given ignition timing, the in-cylinder pressure will be higher. Furthermore, the fast burn combustion system also requires a less advanced ignition timing, and again this means a higher cylinder pressure at ignition. The higher cylinder pressure causes a higher breakdown voltage and a higher arc voltage. Because of losses due to the spark gap in the distributor, and the internal resistance of the HT windings in the coil, then too large a spark plug gap results in less energy per unit volume being dissipated in the spark plug gap.

To investigate the influence of the spark plug gap, a series of tests was conducted with the long nose spark plug. Some tests were subsequently conducted with a low energy coil at the optimum spark plug gap of 0.46 mm. Table 4.1 summarises the properties and performance of the two coils. It can be seen that the lower impedance of the low energy coil leads to a higher current at coil-off, and a marginally greater energy storage. However, the standard coil has a higher mutual inductance, and this should lead to higher breakdown voltage being available.

Figure 4.5 shows the effect of the spark plug gap on the bmep and CoV of the imep for full throttle tests at 1500 rpm and a lambda of 1.5. The spark plug gap has a discernible and consistent effect on the engine performance. Firstly, it should be noted, that as the spark plug gap is increased the misfire ignition timing becomes more advanced. As the ignition timing is moved towards tdc, then the cylinder pressure rises. The onset of misfire indicates that there was insufficient voltage and energy to form a spark across large spark plug gaps. The bmep results show that in the region of MBT ignition timing (say 15-20° btdc), the standard and low energy coils gave comparable results when the spark plug gap was 0.46 mm.

Table 4.1 Comparison between the standard (high performance) and low energy coils.

Type	Standard	Low Performance
Primary Resistance (Ω)	2.7	1.8
Primary Inductance (mH)	9.45	5.93
Current at Coil-Off (A)	2.8	3.8
Theoretical Energy-stored in Primary (mJ)	37	43
Resistance of HT Winding (kΩ)	9.00	8.68
Secondary Inductance (H)	68.1	53.9

The CoV of the imep in figure 4.5 shows negligible differences, for the most part. With ignition timings retarded from MBT the low energy coil does not provide a satisfactory spark, and the cycle-by-cycle variations rise more rapidly than with the standard coil.

Figure 4.6 shows the dependence of the brake specific emissions on the spark plug gap and ignition timing. The spark plug gap has a negligible effect in most cases. However, the onset of misfiring as the ignition timing is retarded, is preceded by a sudden rise in the hydrocarbon emissions (in the same way as the CoV of imep rose). The brake specific NOx emissions all show the same trend, with the emissions rising sharply as the ignition timing is advanced. As there were only slight differences in the burn rate for the different spark plug gaps, these data are not plotted here.

To summarise, the best performance was obtained using the long nose spark plug with a 0.46 mm gap in conjunction with the standard (high energy) coil. Compared with the original spark plug at MBT ignition timings, this combination gave:

a 2% increase in bmep (and reduction in specific fuel consumption)
a 3% reduction in the 0-90% burn duration
no change in the brake specific NOx or HC emissions
a slightly lower level of cycle-by-cycle variations in combustion

4.3 FBHCR COMBUSTION SYSTEM RESULTS

As with the baseline results, tests with the 14.7:1 (hereafter referred to as 15:1) and the 13:1 FBHCR engines were conducted at full throttle and 1500 rpm. The air fuel ratio was varied in the range $0.8<\lambda<1.9$ displaying the ability of the new combustion system to operate at a much weaker

air fuel ratio than the baseline engine. The ignition timing (θ) was varied systematically in steps of 3° from θ=3° to θ=35° btdc. Extending the timing beyond this range, for the weak mixtures, led to no appreciable advantage in either the efficiency or specific NOx, whilst enriching the air fuel ratio from about λ=1.3 caused a progressively narrower range of ignition timings, in advance of the MBT ignition timing schedule, to be used due to the onset of knock.

The results to be presented here will show comparisons between the FBHCR and the baseline engine. As the FBHCR combustion systems are of more interest, the baseline results are presented with a shifted ignition timing axis (Y axis), and an extended air fuel ratio axis (X axis), to facilitate comparison with the new data.

4.3.1 Bmep

Figure 4.7a shows that the corrected peak bmep in the baseline data occurs slightly rich of stoichiometric with an MBT ignition timing of 25° btdc. The bmep then falls in the usual way when: the ignition timing is either advanced or retarded, or if the mixture is further enrichened or weakened. Away from the maximum bmep air fuel ratio, the minimum advance for best torque (MBT) ignition timing becomes more advanced. With the new data, both the 15:1 FBHCR (figure 4.7b), and the 13:1 FBHCR (figure 4.7c), combustion systems show the same general trends, except that the MBT ignition timing schedule is less advanced, (about 10°) together with a retarded ignition timing operating range, which is characteristic of a faster burn and as a result shows an extended lean burn tolerance. Compared with the original combustion system, the maximum bmep has been increased by 0.5 bar while with the weak mixtures (say $\lambda \geq 1.4$), the bmep has been increased by about 0.45 bar. The difference between the FBHCR combustion systems are more subtle. Although both maxima occur at a slightly richer than stoichiometric air fuel ratio, the 15:1 FBHCR bmep contours extend well into the lean operating regime, particularly along the MBT ignition timing schedule, such that for a given air fuel ratio (in the stoichiometric region), the 15:1 FBHCR bmep is about 0.25 bar higher than the 13:1 FBHCR bmep. In the lean region (say λ>1.3) this difference increases to 0.5 bar. Achieving a high bmep in the lean region is particularly important in order to maintain a high efficiency (as will be seen in figure 4.8b), due to the proportionally greater effect of the fmep.

4.3.2 Brake Efficiency

Figure 4.8a shows that the original brake efficiency had a maximum at a slightly weaker than stoichiometric air fuel ratio of λ=1.1. The efficiency falls in the usual way if the mixture is richened or further weakened, or if the ignition timing is moved away from the MBT schedule. The FBHCR results show that an efficiency of above 0.34 can be achieved with the 15:1 compression ratio (figure 4.8b), and an efficiency of above 0.33 can be achieved with the 13:1 compression ratio; figure 4.8c (ie. 10% and 6.5% higher than the base line results respectively). Also the maximum efficiency in both FBHCR combustion systems occurred at a weaker mixture setting of λ=1.2 and covered a wider range of air fuel ratios than the baseline engine. Comparing the maximum efficiency range in the baseline engine, the 15:1 combustion system will maintain

0.31 at λ=1.6 (and weaker still), while for the 13:1 combustion system 0.31 can be achieved at λ=1.5. It will be seen later, when these contours are overlapped with the bmep and the brake specific NOx emissions, the importance of maintaining a high bmep in the lean burn region in order to give as wide a operating envelope within the required constraints as possible.

4.3.3 Exhaust Temperature

Figure 4.9a shows that the maximum exhaust temperatures occur near stoichiometric conditions. As the air fuel ratio is weakened or enriched from the stoichiometric condition (with fixed ignition timing), the temperature falls in the usual way because: a) there is less fuel being burnt b) or there is insufficient oxygen to facilitate maximum heat release. At very retarded timings in the stoichiometric region, the exhaust temperatures are particularly high owing to a) the later burning of the fuel b) the shorter time duration between ignition, and exhaust valve opening events means less time available for heat transfer to the engine. Figures 4.9b and 4.9c show the FBHCR data. Both combustion systems show *the same trends as the baseline engine.* Temperatures along the respective MBT ignition timing schedules are comparable (if not lower), for the new combustion system while peak temperatures are definitely lower. This indicates that the higher compression ratio active combustion system's faster burn rate (being closer to the ideal of constant volume combustion), leads to a greater heat to work transfer than in the baseline engine. The differences between the 15:1 and the 13:1 FBHCR combustion systems are less noticeable. Both show similar temperature variation patterns although the intervals between the two, for a given air fuel ratio (weaker than say λ=1.2), are about 20°C higher for the 13:1 FBHCR combustion system. It may be argued that this again indicates a greater heat to work transfer for the 15:1 compression ratio combustion system which is manifest in a higher bmep and an extended weak air fuel ratio brake efficiency. Also, the higher coolant energy (figure 4.27), means that there is greater heat transfer to the engine due to the adverse volume:area ratio with the 15:1 FBHCR combustion chamber when the piston is at the top of its stroke.

4.3.4 COV of Imep

Figure 3.5 showed that the baseline Coefficient of Variation of imep (CoV of imep), was below 5% (the generally accepted limit for electricity generation applications), for the major part of the operating envelope. In its truncated form, (figure 4.10a), the COV of imep is somewhat misleading as so much data are omitted. Figure 4.10b and 4.10c show the FBHCR data for the 15:1 and the 13:1 combustion systems respectively. Here the CoV of imep limits are better defined. There is a larger area in which the CoV of imep is below 5%. When the air fuel ratio is made leaner than λ=1.55 for the 15:1, and λ=1.50 for the 13:1 combustion systems, then the CoV of imep increases rapidly. At this stage the CoV of imep is almost entirely dependent on the air fuel ratio. The 15:1 FBHCR combustion system offers slightly weaker CoV of imep air fuel ratio limits than the 13:1 FBHCR combustion system. Also the ignition timing has a marginally greater effect on the 15:1 results. However, the sensitivity to ignition timing is weak compared to the air fuel ratio. A comparison with figures 4.24 to 4.25 shows that the hydrocarbon emissions anticipates the rise in the CoV of imep. If the unburnt methane emissions are limited by

legislation then it is likely to be these that impose a limit on the operating envelope.

4.3.5 Maximum Pressure

Figure 4.11a is the truncated version of figure 3.6 and shows the baseline maximum cylinder pressure plotted against ignition timing and lambda. The contours follow the general trends. Peak pressures for the FBHCR engine (figures 4.11b and 4.11c) are around 75 to 80 bar, and occur as expected slightly rich of stoichiometric where the burn velocities and energy content are higher. This gives a shorter burn duration, a higher pressure rise (ie. a more pointed PV diagram), and consequently a greater work output. The relative differences between the original and the fast burn combustion systems amount to 10 to 15 bar higher for the maximum peak pressures (only apparent from a comparison of the original data in figure 3.7). Along the respective MBT ignition timing schedules the FBHCR combustion systems show an increase of 5-15 bar over the baseline engine. Both FBHCR data sets are plotted using identical increments of 5 bar per contour interval, and maximum and minimum limits. Therefore the differences are easily comparable. The 15:1 compression ratio combustion system shows consistently higher peak pressures (about 5 bar) over the 13:1 combustion system. The peak pressure contours also indicate that this combustion system continues to function with leaner mixtures and more retarded ignition timings than the 13:1 combustion system which is important, because apart from aiding the bmep and the efficiency in the lean region, the facility of retarding the timing in order to control the NOx level is still retained.

4.3.6 CoV of Maximum Pressure

Figure 4.12a shows the baseline CoV of maximum pressure (the complete operating range is shown in figure 3.7). There is a large area where the CoV of maximum pressure is low. Retarding the ignition timing causes the peak pressure to decrease and the variation to increase (ie as Pmax, the denominator decreases, the CoV of Pmax being equal to σ/Pmax increases). Weakening the air fuel ratio increases the burn duration. This means there is a larger volume change due to piston motion, and any difference in burn rate will lead to a larger pressure variation. The FBHCR results (figure 4.12b and 4.12c) show the same trends, as the baseline data and the sudden increase in the CoV of maximum pressure at the extremities of the operating envelope are very clearly defined and are similar to the variation of the CoV of imep.

Generally the faster the burn rate, the higher the peak pressure (and the larger the denominator), which will in part lead to a lower CoV of maximum pressure because the combustion will be closer to completion at tdc. Although generally similar, the 15:1 FBHCR (figure 4.12b), exhibits lower CoV of maximum pressure at very weak mixtures (λ>1.4), than the 13:1 FBHCR (figure 4.12c). With weak mixtures and retarded ignition timing (ie the region bounded by θ=3, λ=1.4 and θ=15, and λ=1.8), the CoV of Pmax falls. This occurs because the combustion process is phased so late, that the maximum pressure is primarily due to piston motion, and the maximum value is not affected much by combustion. The influence of the ignition timing on the laminar burn velocities may be seen more clearly in the following burn rate figures 4.13a to 4.13c.

4.3.7 0-1% Burn Duration

The burn rate has been characterised (figures 4.13a to 4.16c) by the duration (° ca), for burning the first 1%, 10%, and 90% of the fuel. A comparison of the original combustion system with the fast burn combustion systems is best made at the corresponding MBT ignition timings. The 0-1% burn duration (figure 4.13a), shows that the laminar burn velocity in the original combustion system is a maximum slightly rich of stoichiometric (giving the shortest burn duration of 12° ca) along the MBT ignition timing schedule. The burn time steadily increases with weakening air fuel ratio, and as the ignition timing is advanced from MBT. This is most noticeable with the weaker slower burning mixtures. For the 13:1 FBHCR (figure 4.13b), and in particular the 15:1 FBHCR (figure 4.13c), combustion systems the 0-1% burn time is clearly shorter. Between the FBHCR combustion systems, this difference is most apparent at the lean burn limit where the 15:1 high FBHCR burn durations are consistently shorter by 2-3° ca. As the air fuel ratio is weakened from stoichiometric the burn durations increase in the proportion 1° ca per λ until the lean misfire limit is approached. At this stage the burn durations increase rapidly for the 13:1 FBHCR and more gradually for the 15:1 FBHCR.

4.3.8 0-10% Burn Duration

The 0-10% burn duration encompasses laminar and transition to fully turbulent combustion. Figures 4.14a to 4.14c show the laminar 0-10% burn durations for the three combustion systems respectively. The trends are basically the same as the 0-1%, however the burn durations are longer by 6° ca for the baseline engine and 4° ca for the FBHCR engines.

4.3.9 0-90% Burn Duration

The 0-90% burn durations (figures 4.15a to 4.15c) are more representative of the total burn period than the previous figures. The differences are more striking. The air fuel ratio is more influential in the 0-90% burn durations than in the laminar burn rates in figures 4.13 and 4.14. The ignition timing has little influence except at the extremities of its range. The 15:1 FBHCR combustion system has the shortest burn duration for all air fuel ratios. Compared with the baseline results the 15:1 FBHCR (figure 4.15b) is reduced by about 40% and the 13:1 FBHCR (figure 4.15c) is reduced by about 35%.

4.3.10 10-90% Burn Duration

The 10-90% mass fraction burn times are illustrated in figures 4.16a to 4.16c respectively and represent the rapid, turbulent flame propagation period. The reduction in the turbulent burn durations are about 40% compared with the baseline combustion system. However the differences between the two FBHCR combustion systems are less obvious. In the stoichiometric and slightly weak of stoichiometric region the 13:1 exhibits shorter turbulent scale burn durations than the 15:1 FBHCR. However in the weak operating regime (say λ>1.5), the burn durations are of similar value.

To summarise, the 15:1 FBHCR exhibits a quicker laminar burn rate (a reduction of about 20-25%

in the laminar burn durations compared with the 13:1 combustion system), and a comparable if not slightly longer turbulent scale burn duration. In all cases the 15:1 FBHCR exhibits the shortest lean mixture burn durations. The overall reduction in the FBHCR burn time is about 40% compared with the original combustion system. As the in-cylinder thermodynamic state is more influential on the laminar burn phase (ie. the initial flame development phase), just prior to ignition, and because these conditions are more favourable with the higher compression ratio, then this combustion system (15:1), will have the shortest total burn period (ie. 0-90% burn durations). The consequence of this is that the main part of combustion will be more closely centred around tdc, and is thus a closer approximation to the ideal of constant volume combustion. As seen in figures 4.10b, and 4.12b, the effects of cycle-by-cycle variations will be reduced, and this will lead to a significant improvement in the efficiency (figure 4.8b), particularly in the lean burn region where a high efficiency is most required.

4.3.11 NOx Emissions

The emissions of Nitrogen oxides were measured as NOx ($NO+NO_2$), but calculated as NO_2 since the Nitric oxide oxidises to Nitrogen dioxide in the environment. As with the baseline emissions, four units of measurement are presented here: ppm, g/kWh, g/MJ(th), and g/m^3. The calculation of these and the corrections for the changes in humidity and temperature (Mendis et al 1993), have been presented in section 2.8.

Figure 4.17a to 4.17d are the truncated plots of the baseline NOx emissions. (The full operating range can be found in figures 3.11 to 3.14). The contours follow the expected trends. Peak NOx emissions are produced at a slightly weak of stoichiometric air fuel ratio where the competing factors of high combustion temperature and oxygen concentration are at an optimum. As the air fuel ratio is further weakened or enriched the NOx concentration falls. Retarding the ignition timing also causes the NOx concentration to fall, but when large excursions away from MBT are made the efficiency falls also. Thus within a given brake efficiency contour, varying the air fuel ratio will have a bigger influence on the NOx formation than the ignition timing.

Figures 4.18a to 4.18d shows the 15:1 FBHCR NOx emissions. Peak ppm values are slightly higher, but on a brake specific basis (figure 4.18b), because of the improved brake efficiency, they are lower than the baseline values for a given air fuel ratio, and ignition timings away from the respective MBT ignition timing schedules. When this is combined with the extended lean burn capability of this combustion system, it becomes viable to achieve very low brake specific NOx emissions. The brake specific targets were initially 5g NOx/kWh, and 3g/kWh with subsequent development of the combustion system. These targets were met without the need for further modifications, and if the gain in efficiency is traded entirely for a reduction in NOx, then further reductions are possible, such that the stringent TA Luft limits of 500mg NOx/m^3 are also satisfied.

Figure 4.19a shows that the 13:1 FBHCR volumetric NOx emissions are of similar magnitude to the 15:1 results, but the contours in the lean burn MBT region (say λ>1.3) are displaced slightly

towards the stoichiometric air fuel ratio indicating that advancing the ignition timing has less of an influence on the NOx output in this combustion system. This effect is visible to a lesser extent in the brake specific plots (figures 4.19b and 4.19c). Thus when the NOx emission targets, an unburnt hydrocarbon limit of say 10g CH_4/kWh, and a CoV of imep of 5% are overlaid on the brake efficiency contours (see Mendis et al 1993), this will identify various operating windows (figures 4.20 and 4.21). Consider the target of 5g NOx/kWh. Only the 15:1 FBHCR combustion system achieves this target whilst still returning a brake efficiency of 0.33. Next consider the target of 3g NOx/kWh. Both combustion systems can achieve this target at an efficiency of above 0.32; the 15:1 FBHCR window is slightly larger. Next consider the TA Luft target of 0.5g NOx/m^3. Both combustion systems achieve this target at a brake efficiency of above 0.30. However, the 13:1 FBHCR system has the larger operating window, mainly because the NOx formation is less sensitive to variations in the ignition timing in the lean burn regime. This is also true for the efficiency, hence the existence of a more retarded MBT ignition timing schedule allowing a larger operating window.

4.3.12 Unburnt Hydrocarbons

The original combustion system (see figures 4.22a to 4.22d for Unburnt Hydrocarbons in ppm, g/kWh, g/MJ(th), and g/m^3 respectively), has low emissions only in the region of MBT for mixtures richer than λ=1.2 (see also figures 3.15 to 3.18). Moving the ignition timing away from MBT, or having too weak a mixture (λ>1.4), leads to incipient misfire or slow burning, so that the hydrocarbon emissions rise rapidly.

Figures 4.23 and 4.24 show that the fast burn combustion systems can lead to lower hydrocarbon emissions and this is most significant with weak mixtures. For example, the 13:1 FBHCR system has less than 4.5g CH_4/kWh at λ=1.4 for any ignition timing, and it is not until the mixtures are weaker than λ=1.5 in the 13:1, and λ=1.6 in the 15:1 that the unburnt hydrocarbon emissions rise rapidly. In both cases 4.5g CH_4/kWh amounts to about 2% of the fuel consumption, and is thus a comparatively small loss in the efficiency. However, the sudden increase in the hydrocarbon emissions is a pre-cursor of the rise in cycle-by-cycle variations in combustion, and will constitute an increasing efficiency penalty. Thus, even if the hydrocarbon emission constraint of 10g CH_4/kWh was relaxed either as a consequence of using an oxidation catalyst, or because the non-methane content is very low (Shaw,1992), the 5% CoV of imep constraint will impose a limit on the operating window (see figures 4.20 and 4.21), owing to the increasing number of non-optimised cycles in combustion (this limiting effect is clearer in the 15:1 FBHCR operating window, probably because of its greater deviation from MBT).

4.3.13 Energy Balance; Exhaust Energy

As with the baseline results, the thermal energy distribution expressed as percentages of the total energy available in the fuel, will be divided between the coolant, the exhaust, the chemical and latent heat energy in the exhaust, and the brake energy. The brake energy percentage is equivalent to the brake efficiency and is dealt with in section 4.3.2.

The baseline exhaust energy is shown in figure 4.25a (adapted from 3.20). The FBHCR data (figures 4.25b and 4.25c), follow the same basic trends as the original data. The contours show the exhaust energy increasing with weakening air fuel ratio until stoichiometric conditions are reached (ie. the products are more fully oxidised owing to the increasing proportion of oxygen). Thereafter (with fixed ignition timing), the exhaust energy remains largely unchanged until the weak mixture limit is encountered. With mixtures weaker than stoichiometric, retarding the ignition timing causes the exhaust energy to increase. The late burning leads to increased heat output to the exhaust because of a lower heat to work transfer rate, and a lower heat transfer to the coolant (due to less time and lower combustion temperatures). Over-advancing the ignition timing causes the exhaust energy to decrease because the heat transferred to the coolant is now relatively much higher. For MBT ignition timings in the lean burn region, the FBHCR exhaust energy is lower by about 20%. Almost all of this energy is utilised in a higher heat to work transfer rate which leads to a higher bmep and brake efficiency. However, there is also a slight increase in the coolant energy indicating a slightly higher heat transfer rate. Even though the exhaust energy percentage is somewhat lower for the FBHCR combustion systems, there is potential for turbocharging the engine in the lean burn region (ie $1.2>\lambda>1.6$ and MBT ignition timings is the region of most interest), in order to boost the bmep where it is likely to be of most benefit (turbocharging is discussed more fully in chapter 5).

4.3.14 Energy Balance; Coolant Energy

The thermal energy dissipated in the coolant is shown for all combustion systems in figures 4.26a to 4.26c. Generally the trends and the values are approximately the same for the original and the FBHCR combustion systems. When the air fuel ratio is weakened from $\lambda=0.8$ to $\lambda=1$ the oxygen availability increases. Thus an increasing proportion of the fuel can be burnt. This increases in-cylinder temperatures and pressures and consequently the heat transferred to the engine. Thereafter, with weakening air fuel ratio (and fixed ignition timing), the fuel and hence the energy flux into the engine steadily decreases (combustion temperatures will be lower too). However the convective losses do not decrease in proportion, (probably due to the increased burn duration in the mixture), and as a consequence the energy dissipated to the coolant is seen to decrease only gradually. The highest convective losses to the coolant, in proportion to the brake work and the heat output to the exhaust, occurs at the very advanced timings where the combustion is completed quite early in the cycle giving higher burnt and unburnt mixture temperatures and ample time for heat transfer to the combustion system walls. Generally, as the compression ratio is raised the volume:surface area ratio changes adversely with regard to heat transfer.

4.3.15 Energy Balance; Chemical Energy

Figures 4.27a to 4.27c represents the chemical energy in the exhaust for all the combustion systems. All have the same basic patterns of variation. In the rich region the percentage of chemical energy flux in the exhaust is high owing to the higher proportion of incompletely oxidised exhaust products and unburnt methane. It must be remembered that this energy can only be

utilised by means of a catalyst and an additional supply of air in the exhaust system. With mixtures weaker than stoichiometric, there is a large area where the energy is very low (ie. less than 4%). It increases above this value only when the weak mixture limit is approached due to the rise in the unburnt hydrocarbons. Figures 4.27b and 4.27c show that the chemical energy is primarily a function of the air fuel ratio. The ignition timing does not have much influence except at the extremities of the operating envelope, and at the weak MBT ignition timing limit.

4.3.16 Energy Balance; Condensate Energy

The condensate energy percentages remain largely unchanged for the FBHCR combustion systems (see figures 4.28a to 4.28c). As with the chemical energy in the exhaust, the condensate energy is largely a function of the air fuel ratio, and not of the ignition timing. When the air fuel ratio is close to the stoichiometric air fuel ratio, the fuel flow rate is high and consequently the water being produced is high. As the air fuel ratio is weakened the fuel flow decreases, and the oxygen concentration increases. The amount of water being produced does not fall immediately, because a greater proportion of the fuel is now being burnt more completely (this also depends on how readily the other products are oxidised with respect to H_2O). In the limiting case with perfect combustion of methane the enthalpy of the water condensation represents 9.9% of the higher (gross) calorific value of the fuel. This represents an upper bound on the condensate energy in the exhaust. For the most part, the experimental condensate energy results are very close to 9%. The only notable trend that occurs for all compression ratios, is that as the mixture weakens the condensate energy percentage decreases. Examination of the unburnt hydrocarbon figures (figure 4.22) shows that this is due to less of the fuel being burnt, and in consequence there being less water vapour in the exhaust. The water vapour content and hence the condensate energy only drops significantly when the lean misfire limit is approached at around λ=1.6.

4.3.17 Energy Balance; Unaccountable Energy losses

Figures 4.29a to 4.29c show the unaccounted energy losses. These are on average about 10% and were reconciled with measurements of air flow and temperature rise in the test cell (see appendix B). As with the original data there is a general trend in the FBHCR results, in which the unaccounted energy losses increase with weakening air fuel ratio. This is probably because the energy influx to the engine is decreasing, and the unaccounted losses form a greater proportion of the fuel energy, with weakening air fuel ratio. Generally the unaccounted losses in the FBHCR combustion system are lower in the region of most interest (ie The lean burn region to say λ=1.5), and it is thus possible to operate here with overall efficiencies of above 87%. Compared with the baseline energy distribution (section 3.2.13), the 15:1 FBHCR brake energy is about 10% higher; the 13:1 about 7% higher (for an air fuel ratio of say λ=1.5). As a consequence the FBHCR exhaust energy is about 18% lower. The thermal energy distributed to the coolant is also reduced by about 8%.

CHAPTER 5

MATHEMATICAL MODEL PREDICTIONS

5.1 CALIBRATION OF THE MODEL WITH FBHCR EXPERIMENTAL RESULTS

FBHCR performance predictions have been presented in section 3.4.2 for: the efficiency, the bmep, and the specific NO_2 output. See figures 5.1, 5.2, and 5.3 (which are in fact the FBHCR contours using the reduced burn duration; these have been adapted from figures 3.29, 3.30, and 3.31). These results were obtained, using a model that was calibrated with the original experimental data, and an estimate of the reduction in the burn duration; and not re-tuned with any of the FBHCR experimental data. Consequently, although the model was correct, there was scope for improving the accuracy of the predicted brake efficiency, and in particular the specific NO_2 emissions, which were over-predicted by about 100 per cent (compare with figures 4.7b, 4.8b, and 4.18d). The most likely reasons for this is an under-estimate of the heat transfer coefficients or shortcomings in the reaction rates used in the extended Zeldovich equations. (Mendis et al 1993).

5.1.1 The ISIS Thermodynamic In-cylinder Model

Thermodynamic models such as ISIS (Stone et al 1993), must start with specified conditions at the start of compression. These are known with some degree of accuracy, and include the properties of the gas mixture such as the: pressure, temperature, composition, and calorific value. In addition to the gas conditions, the cylinder dimensions and the speed at which the engine is operating are required. Also important is the surface temperature distribution in the cylinder, and this is represented in the model by a single temperature that is independent of position and time. From this information, it is then possible to calculate the amount of energy that is inducted into the cylinder. Once the model has these details, it can proceed to increment through the compression process. The rate of change of volume with crank angle can be calculated from the dimensions already entered. The change of pressure in the cylinder can then be calculated with respect to crank angle.

The combustion process is modelled using burn rate laws that have been fitted to experimental data. The calculation of the heat released from the fuel air mixture as it burns is used to predict the pressure and temperature in the cylinder during combustion. Then, once the compression process is complete, the expansion process must be modelled, taking into account the changes in thermodynamic properties due to combustion. Once the expansion process is complete, details of the exhaust gas can be calculated. Details of the emissions themselves are calculated from the very start of combustion, using knowledge of the fuel and the pressure and temperature of the burnt zone within the cylinder. The indicated work and efficiency can be calculated given the rate of heat loss from the cylinder during the cycle.

5.1.2 Model Re-tuning and Simulation Results

The ISIS thermodynamic model is based on the "Arbitrary Heat Release" subroutine presented by Ferguson(1986). (see section 3.4 and page 57a). The extended Zeldovich mechanism and rate constants used to describe the NO formation are provided by Heywood(1988). The model does not consider the formation of NO_2 but assumes that all of the NO will oxidise to NO_2 outside

the engine. The fact that this might have led to some inaccuracies in the rich region was considered, but operation was with lean mixtures for the most part, and the model was tuned originally for a lambda of 1.2. A choice of heat transfer correlations are provided, and these together with the frictional and gas exchange losses, were mentioned in section 3.4. The variables in the Wiebe equation which are used to generate the burn rates were defined from the experimental 10% and 90% mass fraction burn durations. The FBHCR predictions produced thus far, are from a model tuned with data from the original combustion system at a fixed air fuel ratio and ignition timing. The model has been developed since then to include multiple burnt and unburnt zones. Fine tuning with FBHCR data such as 10-90% burn durations, NO formation reaction rates, equilibrium freezing temperatures, heat transfer correlations, and the temperature of the combustible gas at inlet valve closure has had a significant effect on the accuracy and trends of the ensuing plots (Stone 1993).

5.1.3 Bmep and Brake Efficiency

The results to be presented here are from the re-tuned simulation of the 14.7:1 fast burn compression ratio engine operating at full throttle and 1500 rpm. They are plotted within the same axes frame to facilitate comparison with the experimental 14.7:1 FBHCR data.

Figure 5.4 shows the bmep from the FBHCR simulation as a function of the air fuel ratio λ, and the ignition timing θ. The model contours follow the expected trends, but no areas are blanked out due to the occurrence of knock (at the richer air fuel ratios and very advanced timings), or the lean misfire limit where engine operation is erratic. Therefore, when a direct comparison is made with the experimental FBHCR bmep (figure 4.7b), a reasonable margin should be allowed at the extremities of engine operation. The model trends are very good indeed, and there is almost exact agreement with the experimental data for the MBT ignition timing, when the bmep is in the range 5.5 to 7.5 bar. Thereafter, the agreement between the experimental and modelled bmep is mostly better than 0.25 bar.

Figure 5.5 shows the brake efficiency, which rises with weakening air fuel ratio, initially following the trend of the indicated efficiency. The brake efficiency peaks slightly weak of stoichiometric, but thereafter as the bmep reduces (as a result of weakening the mixture), due to the proportionally increasing effect of the fmep, the brake efficiency begins to fall. Once again allowance has to be made when drawing a comparison with the experimental FBHCR brake efficiency (figure 4.8b), for the blanked out knock, and retarded timing, lean mixture operating regions. Peak brake efficiencies are of a similar contour area, with a slight overestimate of 0.5 percentage points. In the range $1.0>\lambda<1.4$ and $7°>\theta<25°$ the difference rises to about 1 percentage point. Thereafter the differences increase with weakening or richening air fuel ratio because the experimental brake efficiency falls away more rapidly (particularly with the richer than stoichiometric mixtures, and the very lean air fuel ratios), than the simulation. This divergence between the model and the experimental data coincides with: the rise in unburnt hydrocarbons outside the range $0.9<\lambda<1.4$, and the increase in cycle by cycle variations with weak mixtures

(λ>1.6). Neither the unburnt hydrocarbons nor cycle by cycle variations are considered in the current simulation. Nonetheless there is a significant improvement over the previous predictions (figures 5.1 and 5.2).

5.1.4 Imep and Indicated Efficiency

Figure 5.6 shows the indicated efficiency as a function of the ignition timing and the air fuel ratio from which it can be seen that the indicated efficiency is a maximum for weak mixtures, and the MBT ignition timing becomes more advanced as the mixture is weakened. This is a consequence of the weaker mixtures being slower to burn. The imep (figure 5.7), follows the same MBT trend but the maximum imep occurs with a mixture just rich of stoichiometric. The difference between the imep and the bmep (figure 5.4), is almost constant, varying from an fmep of 1.25 bar at stoichiometric to about 1 bar at λ = 1.8. As seen before, the fall in bmep with weak mixtures means that the frictional losses become more significant with weak mixtures, and the maximum brake efficiency *(figure 5.5) occurs just weak of stoichiometric. Thus with very weak mixtures the* rise in indicated efficiency is not sufficient to offset the fall in mechanical efficiency due to the increasing significance of the fmep.

5.1.5 NOx Emissions

The simulated Nitrogen Oxide emissions are shown on a volumetric basis (as ppm in figure 5.8) and on a brake specific basis (as gNO_2/kWh in figure 5.9). Consider figures 5.8 and 4.18a (the experimental volumetric NOx emissions). Both plots have common contour intervals of 500 ppm above 500 ppm, and contour intervals of 50 ppm below. A direct comparison shows close agreement at 3000ppm on the weak side of the stoichiometric air fuel ratio. At weaker air fuel ratios away from this contour, the model under-predicts the output of NOx, and at richer air fuel ratios there is an over-prediction. In both cases the differences between the model and the experimental NOx output are not more than about 500ppm; so long as θ<25°btdc. In the brake specific plots (figures 5.9, and 4.18b) the best correlation is found with the 15g NOx/kWh contour just weak of stoichiometric, and at ignition timings retarded from θ=15°btdc. There is also a trend towards close agreement at air fuel ratios richer than λ=0.9. At air fuel ratios in between, the differences are mostly about 2g/kWh higher than the experimental values, rising to an over-estimate of about 5g/kWh at the NO_x peak. As the air fuel ratio is weakened beyond the 15g/kWh NOx contour air fuel ratio, the predicted NOx output reduces more rapidly than the experimental output, such that a maximum difference of 2g/kWh is observed. In both cases the general trends of the model are very good, particularly in the range 0.8>λ<1.2. However, it must be remembered that the differences in the simulated brake specific emissions are compounded by the discrepancies (between the experimental and modelled results) found in the brake efficiency as well as those in the volumetric predictions.

5.1.6 Maximum Pressure

Figure 5.10 shows the simulated maximum pressure contours. Comparison with the experimental counterpart (figure 4.11b), shows agreement mostly within $\pm$2 bar (that is within the stable

operating regime of the engine) particularly in the air fuel ratio range $1.1<\lambda<1.4$ and an ignition timing range $10°<\theta<20°$.

5.1.7 Energy Balance

The thermal energy in the exhaust is plotted as a function of the air fuel ratio and the ignition timing (figures 5.11a and 5.11b). Figure 5.11b assumes the lower calorific value for the fuel. The experimental results (figure 4.25b) show for the rich mixtures, that as the air fuel ratio is weakened towards stoichiometric, the exhaust energy increases because more of the fuel is combusted with the increasing oxygen availability. Thereafter, with fuel efficient burning the exhaust energy percentage forms almost a constant proportion of the incoming fuel energy. Retarding the ignition timing (with fixed air fuel ratio) leads to later burning, a reduction of the brake work, less heat transfer to the coolant, and in consequence a rise in the exhaust temperature and energy percentage in the exhaust stream. The simulation (figure 5.11a) generally follows similar trends (with an inclination towards the MBT ignition timing schedule). At a particular air fuel ratio, the change in the ignition timing predicts much the same change in the simulated exhaust energy as the experimental data. For example at an air fuel ratio of about $\lambda=1.4$, varying the ignition timing from $\theta=25°$ to 5° btdc results in a 6 percentage point increase in the measured exhaust energy, and this compares with a prediction of a 7 percentage point increase. However, for the weak mixtures the experimental data show the energy flow to the coolant to be almost independent of λ (with θ fixed), whilst the prediction shows an increase in the exhaust energy as the mixture is weakened. If the absolute values of the simulated exhaust energy percentages are considered (figure 5.11b), and this is compared with the experimental result (figure 4.25b), then these too at first appear to be over-estimated. The difference varies from about 1 percentage point in the rich region to about 8 percentage points at the lean air fuel ratios. The significant overprediction in the lean region is probably due to the cycle by cycle variations and unburnt hydrocarbons not being modelled in the simulation. Also, the experimental condensate energy term (figure 4.28b), is not included in the experimental exhaust energy term, whilst the model does. It could also be argued that the extraneous heat transfer from the engine will be most significant from the exhaust system, since this is at the highest temperatures. Figures 5.12a and 5.12b show the exhaust energy on an absolute basis, figure 5.12a is the simulation output and figure 5.12b is the FBHCR experimental output. In this comparison, the contours have much more similar trends, than in the previous comparison on the percentage basis, figures 5.11a and 5.11b. There appears to be a constant offset of about 8kW between the experimental and predicted exhaust energy values. This difference corresponds closely to the experimental unaccounted for energy term. The unaccounted term is simply a term used to balance the total energy outflow from the engine with the total energy flow into the engine.

The coolant energy is shown in figure 5.13. Like the experimental results in figure 4.26b, the contours tend to follow the MBT ignition timing schedule. In the rich region the coolant energy reduces systematically with richening air fuel ratios, because the chemical energy (figure 5.14) increases. As the mixture is weakened beyond the stoichiometric air fuel ratio, the influence of

the air fuel ratio reduces, and that of the ignition timing increases. Advancing the ignition timing from MBT increases the heat transfer to the coolant, because the earlier phased combustion allows more time for heat transfer to occur. Retarding the timing reduces the heat flow. The general trends are similar to the experimental results in figure 4.26b for most of the operating envelope, for say $\lambda<1.6$. The closest matching of the experimental and simulated results occur in the range $0.8>\lambda>1.2$ and $\theta>10°$btdc where the difference is at best 2 percentage points (comparing the 22%-27% contour intervals in figure 5.14 with the equivalent contours 20%-25% in 4.26b), and at worst about 4 percentage points; thereafter the results are slightly more divergent.

In figure 5.14 it can be seen that the chemical energy increases rapidly from stoichiometric as the air fuel ratio is richened (because of partially oxidised exhaust products and unburnt fuel in the exhaust system), and that it is largely independent of the ignition timing. Realising this energy would necessitate the introduction of air into the exhaust system downstream of the exhaust manifold. The simulation follows experimental trends and values (figure 4.27b) very closely indeed over the majority of the operating regime. However the simulation takes no account of the unburnt hydrocarbons and thus there is a uniform under-prediction of about 2 percentage points for most of the operating envelope. When the unburnt hydrocarbon emissions rise (in particular as the lean mixture limit is reached) then the experimental chemical energy term increases rapidly but there is no change in the model predictions.

5.1.8 Conclusions

Perhaps the most useful comparison of the model and the simulation is made, if the brake specific NO_x contours are overlaid on the brake efficiency plot, in order to identify an operating window. Figure 5.15 shows the same NO_x emissions limits of 5g/kWh, 3g/kWh, and the TALuft limit of 0.5g/m^3 as mentioned in the *previous chapter (figure 4.20)*. The maximum pressure contour of 70 bar has also been overlaid. The CoV of imep and the Unburnt Hydrocarbon emissions are not available from the simulation, however if these are imported from the experimental 14.7:1 FBHCR data, and superimposed on the simulated plots a useful comparison may be drawn. The 5g NOx/kWh limit permits the largest operating window above a brake efficiency of 34% compared with an efficiency of 33% in figure 4.20. The other NOx limits also permit a generous area above the same brake efficiency contour. The lean limitation is the UHC limit of 10g CH_4/kWh. In reality the deterioration of combustion stability as the lean misfire limit is approached, and the consequent rise in the CoV of imep and the Unburnt Hydrocarbons will lead to an efficiency penalty. Thus, unless the lean burn capability is enhanced, the lean high efficiency region would not be as extensive. Generally the larger operating windows permitted in the simulation are the result of variations in the brake specific NOx contours (ie simulation NOx contours are inclined at a steeper angle than the equivalent experimental contours thus enclosing a larger operating area). Nonetheless, allowing for these limitations, the model predictions and the positional accuracy of the identified areas (they fall within the same range $1.3<\lambda<1.6$ as the experimental data) are very good indeed.

The unaccounted losses in figure 4.29b are between 7% and 10% for the majority of the operating regime. These are mostly radiation and convective heat losses from the engine and correspond to measurements made of the air flow and the temperature rise in the test cell (see appendix C). In the simulation the fuel energy is completely balanced with the brake work, the coolant, the exhaust, and the chemical energy. Thus, part of the radiation loss (about 3-5%), and the condensate energy would be included in the simulation exhaust energy term.

5.2 TURBOCHARGED ENGINE SIMULATION

The function of a turbocharger is: by utilising a portion of the exhaust energy, to increase the charge pressure, thereby increasing the density of the charge induced into the cylinders. This is manifest in a higher bmep and a higher brake work output from the engine. By altering the pressure and temperature at the start of compression in ISIS, it is possible to model the effect of a turbocharged engine at various boost pressures. In the example to be discussed here a turbocharged engine has been simulated with a bmep of 10 bar. Since the bmep is directly dependent on the air fuel ratio λ it is immediately apparent that to maintain a bmep of 10 bar at a weak air fuel ratio (say λ=1.6) would necessitate a higher boost pressure or Pivc than that required at a richer setting (say λ=0.95). The bmep 10 bar maps will correspond to a range of turbocharger boost pressures, but it is not possible to obtain these data directly from the ISIS simulations. Instead, to obtain values of the various engine parameters at these specific operating points, it was necessary to interpolate the values from runs with ISIS obtained at discrete values of boost pressure. In the simulation, it was assumed that the turbocharger efficiency was such that there was no change from the pumping work of the naturally aspirated engine. In other words, it was assumed that the mean inlet manifold boost pressure corresponded to the mean back pressure from the turbine. In order to obtain the same pumping loss, the pressure at inlet valve closure was always kept at 0.1 bar below the inlet manifold pressure. Table 5.1 shows the input conditions that were varied when the turbocharged engine was simulated.

Table 5.1 Changes in the inputs to the FBHCR model to simulate a turbocharged engine.

Manifold pressure (bar)	Pressure at IVC (bar)	Estimated comp. delivery temp. (K)	Temp at IVC (K)
1.00	0.90	295	350
1.35	1.25	339	365
1.60	1.50	366	380

The temperature at inlet valve closure IVC, rises due to the rise in temperature within the compressor. However as the boost pressure increases, the rise in the compressor delivery

temperature is greater than the rise in the temperature at inlet valve closure. This is because the temperature at inlet valve closure is influenced by the: coolant, inlet port, and inlet valve temperatures. Since the coolant temperature is about 360K (and the combustion chamber temperatures were estimated as 450K), then the temperature at inlet valve closure with a naturally aspirated engine is significantly above ambient. In contrast, if the compressor delivery temperature is above the cylinder head temperatures, then the gases would be cooled by the cylinder head. Table 5.1 includes estimates of the compressor delivery temperatures (assuming gamma γ=1.4 and a compressor isentropic efficiency of 0.60), and it can be seen that the difference between these temperatures and the temperature at inlet valve closure reduces as the boost pressure increases.

The assumption of a compressor isentropic efficiency of 0.6, and the compressor pressure only equalling the exhaust back pressure, may appear somewhat pessimistic. However, with a carburetted gas engine it would be undesirable for the compressor boost pressure to be above the exhaust back pressure, as during valve overlap this would lead to an increase in the short circuiting of fuel. This would adversely affect both the brake efficiency and the emissions of unburnt hydrocarbons. If the compressor boost pressure is too high, then it can readily be controlled by throttling or by using an exhaust waste gate.

In the modelling of the turbocharged engine, it was possible to obtain accurate results for a range of turbocharged engine configurations (whilst saving considerable computing time) by using an interpolation technique to generate the full range of performance parameters. In many cases, linear interpolation is adequate given the co-ordinates of two discrete points (see the equation below and figure 5.16).

$$f(x) = y_1 + \left(\frac{y_2-y_1}{x_2-x_1}\right)(x-x_1) = y$$

However, if a polynomial Lagrangian interpolation technique is used instead, the accuracy of the desired result is significantly enhanced with not much more computing effort. The equations for parabolic Lagrangian interpolation are given below:

$$f(x)=\frac{(x-x_2)(x-x_3)}{(x_1-x_2)(x_1-x_3)}y_1 + \frac{(x-x_1)(x-x_3)}{(x_2-x_1)(x_2-x_3)}y_2 + \frac{(x-x_1)(x-x_2)}{(x_3-x_1)(x_3-x_2)}y_3 = y$$

The use of polynomial Lagrangian interpolation is best described with reference to the following example, in which the aim is to interpolate data corresponding to a bmep of 10 bar, from data generated at three discrete values of the pressure at inlet valve closure (Pivc).

ISIS will have been run for a combination of air fuel ratios (λ) and ignition timings (θ) at the three specified pressures Pivc. The output from such a run is illustrated by table 5.2. For each value

of Pivc there is a "page" of data, in which each line of data comprises a different λ and θ combination. These are the "X" and "Y" variables needed for the subsequent contour plots. The other columns of data represent the "Z" parameters for the contour plots, such as: bmep, NOx, Maximum Pressure etc; the "Z" parameters also include the Pivc (which is the "page" variable, the variable which is constant for each 'page' of data).

The first stage in the interpolation procedure is to find the Pivc at a particular λ,θ (λ_i,θ_i) that gives the desired value of the demand variable (in this case a bmep of 10 bar). This is illustrated by figure 5.17a, which shows interpolation using data from the same "line" (the lines on each page with the same values of λ_i and θ_i) obtained from the three different "pages" (the data suffix "1", "2", and "3" come from pages 1,2,3). Thus for this particular "line" the Pivc has been found that is needed to give the "demand" of 10 bar bmep. The next stage (as shown by figure 5.17b), is to use this value of the Pivc to interpolate the values of all the other "Z" parameters, for this particular value of Pivc that gives the required bmep of 10 bar.

Table 5.2 ISIS data for use in the interpolation program

Page 1, Pressure at inlet valve closure (Pivc) of 0.9 bar

λ	θ	"Z" Parameters					
X	Y	Pivc	Imep	Bmep	Eta i	Pmax	.....
0.80		35.0	0.90	8.74	7.49	28.37	86.68 .....
0.90		35.0	0.90	9.01	7.75	32.42	88.62 .....
			to				
1.90		2.0	0.90	4.54	3.51	32.64	27.27 .....

Page 2, Pressure at inlet valve closure (Pivc) of 1.25 bar

λ	θ	"Z" Parameters					
X	Y	Pivc	Imep	Bmep	Eta i	Pmax	.....
0.80		35.0	1.25	11.69	10.32	28.49	116.54 .....
0.90		35.0	1.25	12.05	10.67	32.55	119.12 .....
			to				
1.90		2.0	1.25	6.03	4.96	32.54	37.46 .....

Page 3, Pressure at inlet valve closure (Pivc) of 1.60 bar

λ	θ	"Z" Parameters				
X	Y	Pivc	Imep	Bmep	Eta i	Pmax .....
0.80	35.0	1.60	14.39	12.92	28.53	144.49 .....
0.90	35.0	1.60	14.83	13.34	32.60	147.67 .....
		to				
1.90	2.0	1.60	7.38	6.27	32.41	47.44 .....

Thus a new "line" of data can be generated that contains each Z parameter. Once these interpolations have been completed for a particular line, they are repeated for the next line. Although the demand variable remains the same (bmep = 10 bar), the value of the page variable will change. The outputs that are generated for each "line" of data, with interpolation for a bmep of 10 bar, for all the other Z parameters, together with pages 1, 2, and 3 are shown in appendix C.

It should be noted that in going from the first stage to the second stage of interpolation, that the page variable has moved from the y axis to the x axis. This means that included in the interpolated z parameters will be the demand variable (in this case the bmep of 10 bar). As the interpolation assumes a parabolic relationship between all variables, then errors will be introduced. These errors are indicated by the interpolated values of the demand variable not being exactly equal to the demand value. Fortunately for small changes in the Pivc the engine performance is close to linear so that parabolic interpolation leads to very small errors. It has been found that the errors are only significant when extrapolation occurs (see appendix C).

5.2.1 Turbocharged Simulation Brake Efficiency

Figure 5.18 shows the turbocharged engine brake efficiency as a function of the ignition timing and the air fuel ratio. Comparison with figure 5.5 (naturally aspirated) indicates a considerable shift in the peak brake efficiency towards the leaner air fuel ratios and more advanced ignition timings. Because the same bmep is maintained across the operating envelope by increasing the boost pressure (pressure at inlet valve closure), the significance of the fmep (around 1 bar) does not increase as the mixture is weakened. Thus with frictional losses that are almost invariant, the brake efficiency follows the indicated efficiency (figure 5.19) closely, and the peak of 35.5% is achievable over a large area of the lean operating envelope. The differences between the turbocharged simulation and the naturally aspirated simulation are about 0.5 percentage points in the range $0.8>\lambda>1.1$, and a maximum of 2 percentage points in the lean burn peak efficiency

region. The burn duration increases as the mixture is weakened, but not indefinitely, because in practice a lean mixture limit would be encountered. In a turbocharged engine the lean mixture limit would normally be extended due to the higher density of the charge and combustion temperatures and pressures. Thus, if the experimental 5% Coefficient of Variation limit is adopted as a guide to combustion stability then this may be viewed as a rich bound in the region of deteriorating operating stability. For this reason the experimental 15:1 FBHCR 5% CoV contour and 10g/kWh hydrocarbon emissions contour will be superimposed on the turbocharged engine simulated outputs in figure 5.24.

5.2.2 Turbocharged Simulated Indicated Efficiency and Imep

The turbocharged simulated indicated efficiency (figure 5.19) shows a very similar response when compared with the naturally aspirated simulation (figure 5.6). In contrast to this the turbocharged imep (figure 5.20) and the naturally simulated imep (figure 5.7) bear no resemblance. It can be seen from figure 5.20 that the turbocharged imep follows the pattern of variation of the pressure at inlet valve closure (figure 5.25) and this in turn is dictated by the requirement of maintaining a constant bmep over the whole range. In figure 5.7 the imep falls as the mixture is weakened, and the fmep being largely invariant, constitutes a greater significance and this leads to an increasingly rapid fall in the bmep (figure 5.6). In contrast the turbocharged simulation shows a relatively constant imep of approximately 11.2 bar over the entire air fuel ratio range. However, because the fmep is approximately constant in absolute terms, the trends show that as the ignition timing is advanced it becomes necessary to increase the imep in order to maintain the same 10 bar bmep, since at these higher cylinder pressures the frictional losses are also higher.

5.2.3 Turbocharged Simulated NOx Emissions

As with the experimental and naturally aspirated simulation, the turbocharged simulated NO_x emissions are shown on a volumetric basis (figure 5.21), and on a brake specific basis (figure 5.22). Both plots show almost identical outputs with the naturally aspirated simulations (figures 5.8 and 5.9 respectively) in the rich region, as the mixture is weakened to say λ=1.0 (or the volumetric NOx contour of 3500ppm). Thereafter as the mixture is weakened further, to say λ=1.1 the turbocharged outputs match the naturally aspirated simulations only at ever advancing ignition timing angles from tdc. Thereafter the turbocharged NOx output shows a later response to weakening the air fuel ratio such that comparable NO_x levels of 5g/kWh and under (or 1000ppm NO_x and under) occur at leaner air fuel ratios (ie leaner by about λ=0 05). The agreement between the naturally aspirated and the turbocharged results is mostly within 500ppm or 2.5g/kWh. In a turbocharged engine, an increase in the NO_x levels would not be unexpected due to the invariable increase in the density of the fuel air mixture (see table 5.1) (represented in the model by using a higher temperature at inlet valve closure) and the increased flow rate of the reactants and the products. Lower NOx emissions could be achieved if a suitable cooling medium was available for an intercooler to cool the flow leaving the compressor.

5.2.4 Turbocharged Simulated Maximum Pressure

Figure 5.23 shows the peak cylinder pressure against the ignition timing and lambda. Where as the FBHCR experimental peak pressures and those of the naturally aspirated simulation gave comparable results (ie about 80 bar), the turbocharged simulation gives a maximum peak pressure of 112 bar. The contours do not bear much similarity with the trends in the naturally aspirated simulation (figure 5.10), but follow the pattern of the pressure at inlet valve closure (figure 5.25). Along the MBT ignition timing schedule and in the weak mixture range of say $1.2<\lambda<1.6$ (the most likely operating region) peak pressures are in the range 70 to 95 bar. As the timing is advanced away from the MBT schedule peak pressures rise to above 100 bar. Though pressures of 100 bar and above might appear to be excessive, it is unlikely that the engine will be operated in these areas due to knock and other constraints. There is little doubt about the mechanical strength of the Dover engine, as its Diesel parent has been known to be heavily boosted in offshore powerboat racing applications, such that peak combustion pressures of 125 bar and 160 bar are attained using standard cylinder heads from the turbocharged mass production variants, Kaye(1989). However, in order to retain an adequate thermal and pressure loading margin (and for reliability), it might be beneficial to lower the compression ratio.

5.2.5 Conclusions

Figure 5.24 shows the operating windows that are identified by superimposing the experimental FBHCR constraints of 5% CoV and the 10g CH_4/kWh and the simulated NOx contours on the turbocharged brake efficiency contour plot in a similar way as figure 5.15. Figure 5.15 (the naturally aspirated engine simulation) shows that all NOx limits can be satisfied above a brake efficiency of 34%. In the turbocharged simulation (figure 5.24), due to a displaced peak efficiency region which is biased towards the leaner air fuel ratios, all NOx limits are achievable above a brake efficiency of 36%.

CHAPTER 6

CONCLUSIONS AND RECOMMENDATIONS

6.1 LITERATURE REVIEW : SUMMARY AND CONCLUSIONS

The literature review has shown that the case for gas powered cogeneration based on the spark ignition engine is well established. The economic and environmental benefits associated with cogeneration are considerable when compared with conventional plant. Based on the characteristic energy production ratio, the best payback occurs when the cogeneration plant is matched to the heat requirement, and ideally this would be a constant heat requirement. Since the energy value weighting is biased towards the electricity, then there is a case for optimising the electricity production efficiency. Because emissions legislation is becoming increasingly stringent for stationary power sources it is thus necessary to reduce emissions, particularly those of NOx. The two modes of operating gas engines in order to give low emissions have been discussed, and the advantage of "leanburn" over "stoichiometric operation with catalyst" have been stated. Open chamber and divided chamber combustion systems have been reviewed. The open chamber combustion system is arguably simpler to implement, and facilitates starting and transient load acceptance in the size range of electrical generation systems considered here. A review of open chamber systems has shown that reliable lean burn operation is possible such that emissions are reduced to the required limits.

The open chamber combustion system considered here (in a gas engine based on the Ford Dover 6.2 litre diesel), is typical of one used in small scale cogeneration applications (up to 100kWe). Thus it was appropriate to use this engine in order to investigate methods of reducing emissions, as well as optimising the power output and efficiency.

6.2 EXPERIMENTAL AND SIMULATED RESULTS : SUMMARY AND CONCLUSIONS

6.2.1 Baseline Results

The baseline results showed that all low emissions targets (ie below 5g NOx/kWh and 10g CH_4/kWh) could not be met simultaneously for a single operating condition.

During the tests it was observed that even at the conditions most likely to induce knock, the engine exhibited only trace knock. This indicated that a significantly higher compression ratio could be utilised. It was concluded from previous work (Stone and Ladommatos 1991) that a compression ratio of about 15:1 would be optimum.

Tests carried out on the cylinder head prior to testing established that the Ricardo swirl ratio was 2.01 (method and calculations are in appendix C). This comparatively high level of swirl indicated that an offset bowl in the piston should be used as this would tend to disrupt the swirl and generate turbulence.

Previous work with a phenomenological turbulent combustion model (Stone, Brown and Beckwith 1992) indicated that igniting the mixture away from the cylinder head should lead to a faster burn. This was investigated later by using different spark plugs, spark plug electrode protrusions, spark plug electrode gaps, and ignition coil energy. In the event it was found that too much protrusion

was disadvantageous, for the reasons discussed in section 4.2.

The work of Lee and Schafer (1982) indicated that increasing the squish area, reducing the squish clearance and placing the ignition point closer to the centre of the bowl would benefit the brake efficiency at full load.

The Ricardo Nebula head (Thomas 1991) demonstrated that an active combustion system enhanced lean combustion and extended the lean misfire limit such that harmful exhaust emissions, particularly those of NOx are reduced to very low levels.

The results from the baseline tests were used to calibrate a thermodynamic model (Stone et al 1992, based on Ferguson 1986). Baseline simulations showed close similarities for the bmep and the brake efficiency, but not for the brake specific NOx. Notwithstanding this limitation the model was re-run for a compression ratio of 15:1 with an estimate of the likely reduction in burn time that could be attained. The results showed a significant increase in the bmep and the brake efficiency.

The Fast Burn High Compression Ratio combustion system was designed with the above observations and criteria in mind.

6.2.2 FBHCR Results

The factors influencing the design of the FBHCR combustion system have been stated in section 3.3. The first series of tests conducted were to optimise the combustion system with respect to the bmep, brake efficiency, CoV of imep, 1%, 10%, and 90% burn durations and the brake specific methane and NOx emissions. The FBHCR combustion system was evaluated at compression ratios of 13:1 and 14.7:1.

The long nose spark plug gave the best performance. The conclusions drawn from this was that it avoided the cavity (and possible heat transfer) associated with the standard spark plug, and it avoided the high mean velocity (and possible arc re-striking and flame stretching) experienced by the long reach spark plug due to the greater mixture motion away from the combustion chamber surfaces. The improvements are listed thus:

The bmep was increased by 0.5 bar. The differences in the bmep between the 15:1 and the 13:1 FBHCR combustion systems varied between 0.5 and 0.25 bar.

This accounted for the improvement in the brake efficiency from 31% (baseline) to above 34% for the 15:1 FBHCR. and above 33% for the 13:1 FBHCR combustion systems.

FBHCR maximum peak pressures were 75 to 80 bar compared to 65 bar in the baseline engine. The 15:1 FBHCR maximum peak pressures are about 5 bar higher than the 13:1 FBHCR values.

Examination of the burn durations showed that the 15:1 FBHCR total burn time (0-90% mfb) was reduced by 40% and the 13:1 FBHCR by 35%. Whilst both FBHCR turbulent burn rates are of comparable time duration (particularly with weak mixtures), the 15:1 FBHCR exhibits a quicker laminar (0-1% and 0-10% mfb) burn duration compared with the 13:1 FBHCR combustion system.

The faster burn led to a reduction in the cyclic variation. The improved combustion stability meant that the rise in the unburnt hydrocarbons and the CoV of imep was at a weaker air fuel ratio (λ>1.55) than previously attained. A wider ignition timing range was also retained and very low NOx emissions (below 1g/kWh) were obtainable when the ignition timing was retarded from MBT.

Thus the proposed low emissions target of 5g NOx/kWh at an efficiency above 33% was met. Because the lean burn capability was extended it was possible to obtain very low emissions of NOx (below 1g/kWh) such that the TALuft 500mg/m^3 (or 1.3g/kWh) limit was met and surpassed whilst meeting the other operational constraints of a CoV of imep below 5%, a brake efficiency of above 30% and an unburnt hydrocarbon limit of below 10g CH_4/kWh. (Present limits are worth noting as TALuft dictates 150mg of non-methane hydrocarbons/m^3).

Examination of the overlaid plots (figures 4.20 and 4.21) showed that the 13:1 FBHCR exhibits a slightly larger lean operating area, in the case of NOx emissions below 500mg/m^3. Therefore it is doubtful if further improvements are to be gained in the brake specific emissions for a given efficiency by increasing the compression ratio above 15:1.

The difference in the laminar burn durations suggests that the combustion system might benefit from a slightly larger squish clearance (say 2mm compared with the present value of 1mm). This should give slightly lower turbulence and less stretching of the flame front. If the total burn duration can be reduced as a result of a shorter laminar burn time then this will benefit lean combustion and should extend the LML.

6.2.3 Model Predictions

The ISIS simulation (Stone et al 1993) was re-tuned with 15:1 FBHCR experimental data. Considering that the model was tuned for a specific operating point, and with a single burnt zone, and that the effect of cyclic variation and unburnt hydrocarbons was not modelled, comparisons with the actual values were good for the bmep, the brake efficiency, peak pressure and brake specific NOx emissions. On the whole the energy balance also gave good agreement. These were a significant improvement over the previous predictions.

One of the drawbacks of operating with lean mixtures is a lower power output (bmep is below 6 bar). However, turbocharging can restore the output. The effect of turbocharging was modelled by specifying a constant output bmep of 10 bar in the simulation. Superpositioning the

corresponding brake efficiency and brake specific NOx emissions showed that all NOx limits were achievable above an efficiency of 36% (figure 5.24; see section 5.2.5 for a more detailed explanation). Since the accuracy of the model is good (compare figure 4.20 with 5.15) then the case for turbocharging is clear.

6.3 RECOMMENDATIONS

The reasons for turbocharging have been stated. The ISIS simulation for a lean burn turbocharged gas engine identified distinct improvements in the brake efficiency and brake specific NOx. However this can only be verified with experimental data.

Valve overlap in the gas engine is 32°. Reducing the overlap period is likely to reduce fuel shortcircuiting, thereby reducing the fuel consumption and the brake specific hydrocarbon emissions.

Assuming that the valve timing events were optimised (ivc = 45°abdc) in the diesel parent for maximum power at 2600 rpm, the volumetric efficiency (see appendix B) at 1500 rpm for the gas variant is likely to benefit from earlier closing of the inlet valve (say 20°abdc). This could increase the output and reduce the fuel consumption.

The blow-by gases consist mostly of unburnt methane. If these gases can be re-admitted to the engine with the fresh charge (as per standard practice with vehicles) then this would result in about a 1% lower fuel consumption.

A more central ignition source which is likely to experience a lower mean velocity past the spark plug electrodes could eliminate arc re-striking, reduce flame stretching and extinguishing, and thereby reduce the cyclic variation and hydrocarbon emissions as the weak mixture limit is approached.

REFERENCES

Beard C.A. 'Inlet and exhaust systems' ch 6 in Diesel Engine Reference Book, ed LRC Lilly, Butterworth, 1984.

Bishop I.N. Effects of design variables on friction and economy SAE Trans. Vol 73 pp334-358, 1968.

British Gas Publication - Code of practice for Natural gas fuelled spark ignition and duel-fuel engines, Publication IM/17, 1st edition, February 1981.

Brown A.G. Measurement and Modelling of Combustion in a Spark Ignition Engine. PhD Thesis, Brunel University, 1991.

Brown C.N. Mixture Preparation in a Fuel-Injected Spark-Ignition Engine at Low Load and Low Speed. PhD Thesis, Brunel University, 1991.

Chen S.K., and Flyn P. Development of a compression ignition research engine, SAE Paper, 650733, 1965.

Cockshott C.P., Vernon J.P., and Chambers P. An air mass flowmeter for test cell instrumentation, 4th Int. Conference on Automotive Electronics, IMechE Conf. Proc.,MEP, London, 1983.

Davies R.M., Johnson C.A., and Weller G.B. The environmental implications of gas fired power generation and combined heat and power - communication 1443, presented at the 56th meeting and gas 90 exhibition, 1990.

Department of the Environment Report on 'global atmosphere and air quality' 1992-93

Federal Ministry for Environment, Nature Conservation and Reactor Safety, Bonn 1986. Technische Anleitung zure Reinhaltung der Luft (TA Luft) vom 27 February 1986.

Ferguson C.R. Internal Combustion Engines - Applied Thermosciences. Wiley, New York, 1986.

Germane G.J., Wood C.G. and Hess C.C. Lean Combustion in Spark Ignition Engines - A review. SAE 831694, 1983.

Goldsmith R. Passenger Car Exhaust Emissions - Mechanical Incorporated Engineer, 1989.

Gould J., and Stone C.R. Factors Limiting the Efficiency and Output of Natural Gas Fuelled Engines, British Gas report, 1993.

Heywood J.B. Internal Combustion Engine Fundamentals, 1st edition. (McGraw Hill, New York) 1988.

Hood S. The V grooved electrode spark plug. Ortech International. 1989.

Horlock J.H. Cogeneration: combined heat and power, 1st edition. (Pergamon Press, Oxford) 1987.

Hudson C., Stone C.R., Denham M.J., and Bradbury I. Ignition Control System for Fuel Testing, International Conference on Automotive Diagnostics, I.Mech E. Conference Proceedings, 1990.

Hundleby G.E. Low emissions approach for heavy-duty gas-powered urban vehicles, SAE paper 892134, 1989.

Jeffrey A., Reinhold V.N. Mathematics for Engineers and Scientists. 4th edition.

Kaye G.C. The evolution of the Sabre 'Marathon' diesel engine for offshore powerboat racing, I.Mech.E. Seminar, 1989.

Kingston Jones M.G., and Heaton D.M. Nebula combustion system for lean burn spark ignited gas engines, SAE paper 890211, 1989.

Lee W., and Schafer H.J. Verbrauchsreduzierung am ottomotor optimierung von Drennraumform und Verdictungsverhaltnis. MTZ Motortechnische Zeitschrift, 1982, 279-284.

Linnel C.J. The first 10 years on the UK market for packaged co-generation plant - a review, IMechE Seminar: Gas Engines and Cogeneration, MEP, 1990.

McKinley T.L., and Primus R.J., The Influence of bowl offset on Motion in a Direct Injection Diesel Engine, SAE Paper 881611, 1988

Mendis K.J.S., Stone C.R., Ladommatos N., and Weller G.B. Modelling and Measurements from a Natural Gas Fuelled Engine, SAE paper 930927, 1993.

Mendis K.J.S., Stone C.R., Ladommatos N., and Daragheh M.M. A lean burn low emissions gas engine, I.Mech.E, Seminar, 1993.

Moore, S.G. An investigation into running a gas engine at a high compression ratio fuelled by bio-gas. Project report, Brunel University, 1989.

Muranaka S., Takagi Y., and Ishida T. Factors limiting the improvement in thermal efficiency of S.I. engine at higher compression ratio, *SAE paper 870548, 1987.*

Overington M.T. Combustion in Spark Ignition Engines, Chapter 1, 1st edition, 1990.

Ozasa T., Suzuki S., Kondo H., Takahashi H., Kataoka M. and Oshima, Y. *Effect of* Combustion Chamber Shape on a Lean-Burn SI Engine - Measurement of In-Cylinder Mixture Strength Using a Gas Sampling Technique. JSAE review, 1991.

Packer J.P. Advanced packaged co-generation, IMechE Seminar: Gas Engines and Co-generation, MEP, 1990.

Pohl J.M. NOx reduction on large bore turbocharged SI engines, ASME 82-DGP-16, Energy Sources Technology Conference, January 1988.

Raine R.R. SERC report on Visiting Fellowship GR/H88138, Brunel University, 1993.

Rassweiler G.M., and Withrow L. Motion pictures of engine flame correlated with pressure cards, SAE Paper 800131, (originally presented in January 1938).

Seppen J.J. Optimising gas fuelled engines using modern computer techniques and dedicated fuel supply systems, EAEC International Conference on New Developments in Power train and Chassis Engineering, Vol 2, 1987.

Serve J.V. NOx reduction on large bore turbocharged SI engines, ASME 82-DGP-16, Energy Sources Technology Conference, March 1982.

Shaw T.O.R. The Law's Demands. Proc. Seminar Stationary Combustion Engines and the Environmental Protection Act, I.Mech.E, 1992.

Spindt R.S. Air-Fuel Ratios from Exhaust Gas Analysis, SAE Paper 650507, May, 1965.

Stone C.R. Introduction to Internal Combustion Engines, 2nd edition, 1992.

Stone C.R. Introduction to Internal Combustion Engines, 2nd edition, 1992, - p369, adapted from **Reid R.C., Prausnitz J.M., Sherwood T.K.** The Properties of Gases and Liquids, 3rd edition (1977)

Stone C.R., Brown A.G., and Beckwith P. A Turbulent Combustion Model Used to Give Insights Into Cycle-by-Cycle Variations in Spark Ignition Engine Combustion, Paper C448/013 Int. Conf.on Combustion in Engines 1-3 December 1992, I.Mech.E, London, 1992.

Stone C.R., Gould J., and Podmore I. ISIS User Manual 2nd Edition, Brunel University 1993

Stone C.R., and Green-Armytage D.I. Comparison of methods for the calculation of mass fraction burnt from engine pressure-time diagrams, Proc.IMechE, Vol 201, No. D1, 1987.

Stone C.R., and Ladommatos N. Design and Evaluation of a Fast Burn Spark Ignition Combustion System for Gaseous Fuels at High Compression Ratio, Journal of the Institute of Energy, Vol 64, December 1991.

Stone C.R., and Steele A.B. Measurement and Modelling of Ignition System Energy and its Effect on Engine Performance, Proc I.Mech.E. Vol 203 pp 277-284, 1989.

Thomas J.R. Low emissions gas engines for stationary and vehicle uses: Lean burn, 3-way catalysts or any other technique? Ricardo Consulting Engineers Ltd, Enserve Symposium 1991.

Weaving J.H. and Pouille J.P. Internal Combustion Engineering Science and Technology, Chapter 15, 1st edition, 1990.

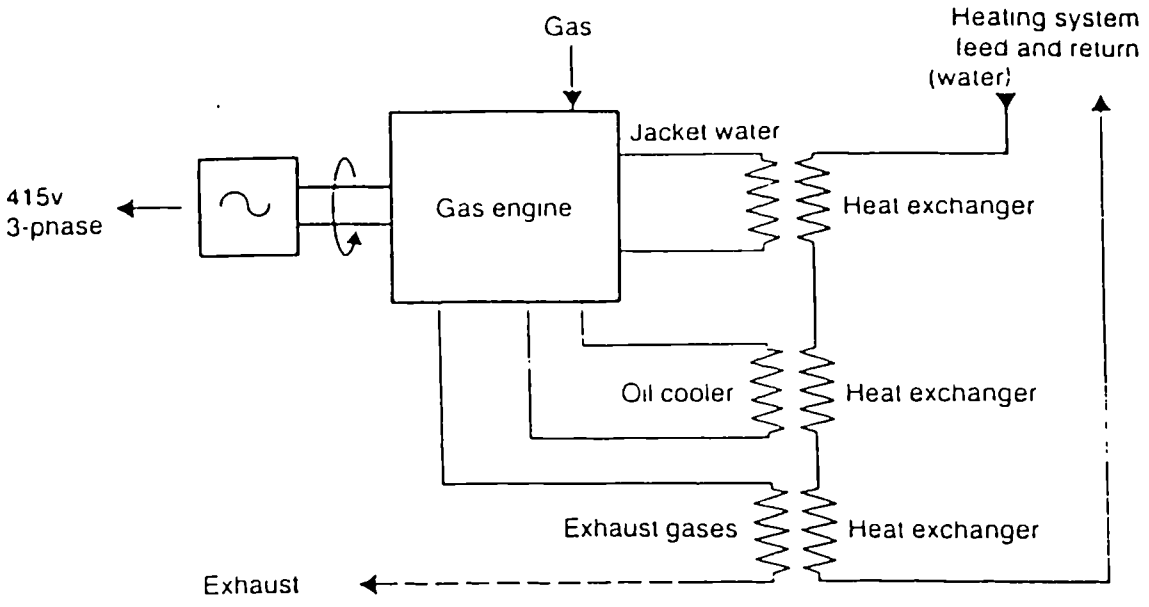

Figure 1.1 Layout of a cogeneration plant.

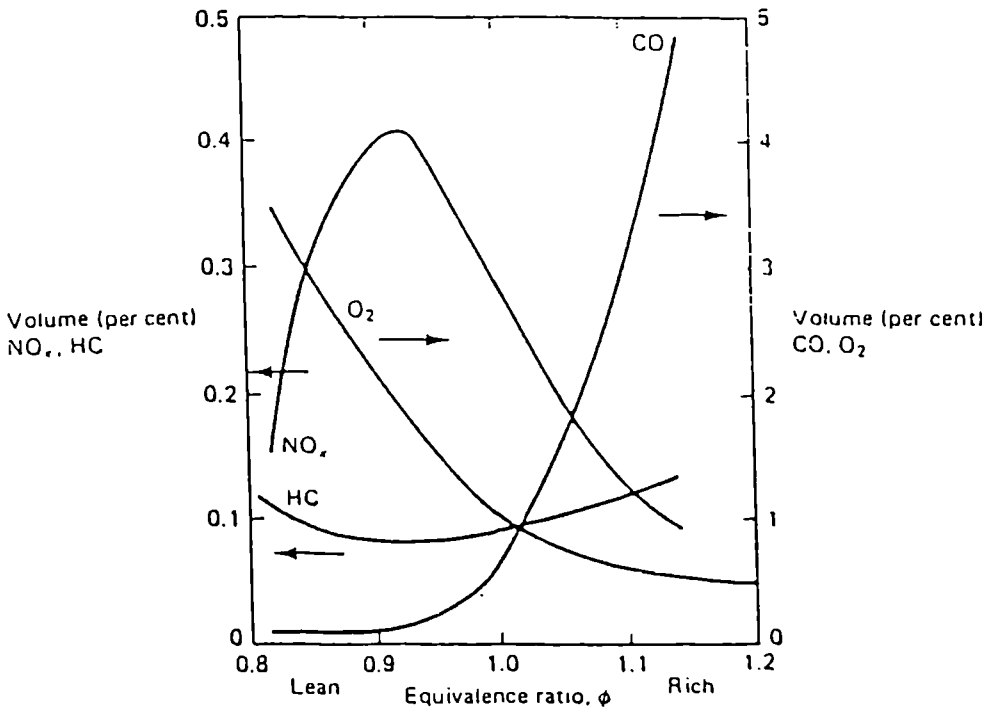

Figure 1.2 Emissions versus equivalence ratio (taken from Stone (1989), courtesy of Johnson Matthey).

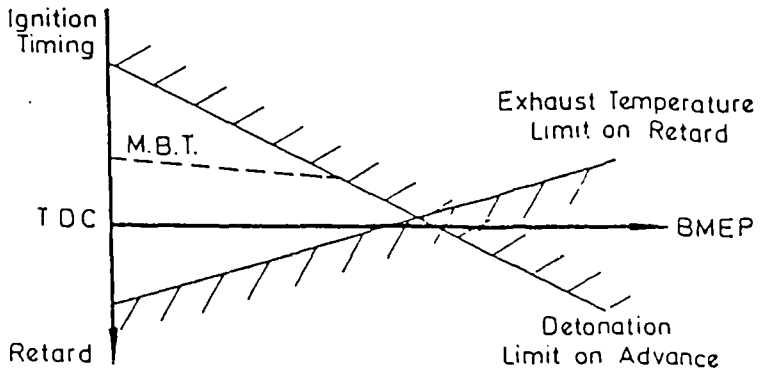

Figure 1.3 Limitations on stoichiometric engine operation (taken from Hundleby (1989)).

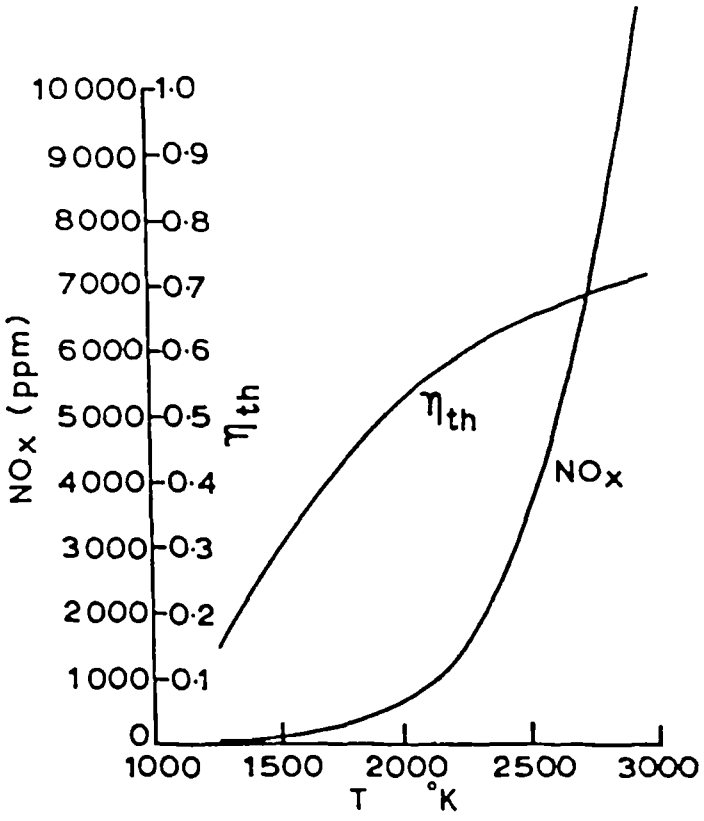

Figure 1.4 Variation of NOx emissions and thermal efficiency versus temperature (taken from Weaving (1990)).

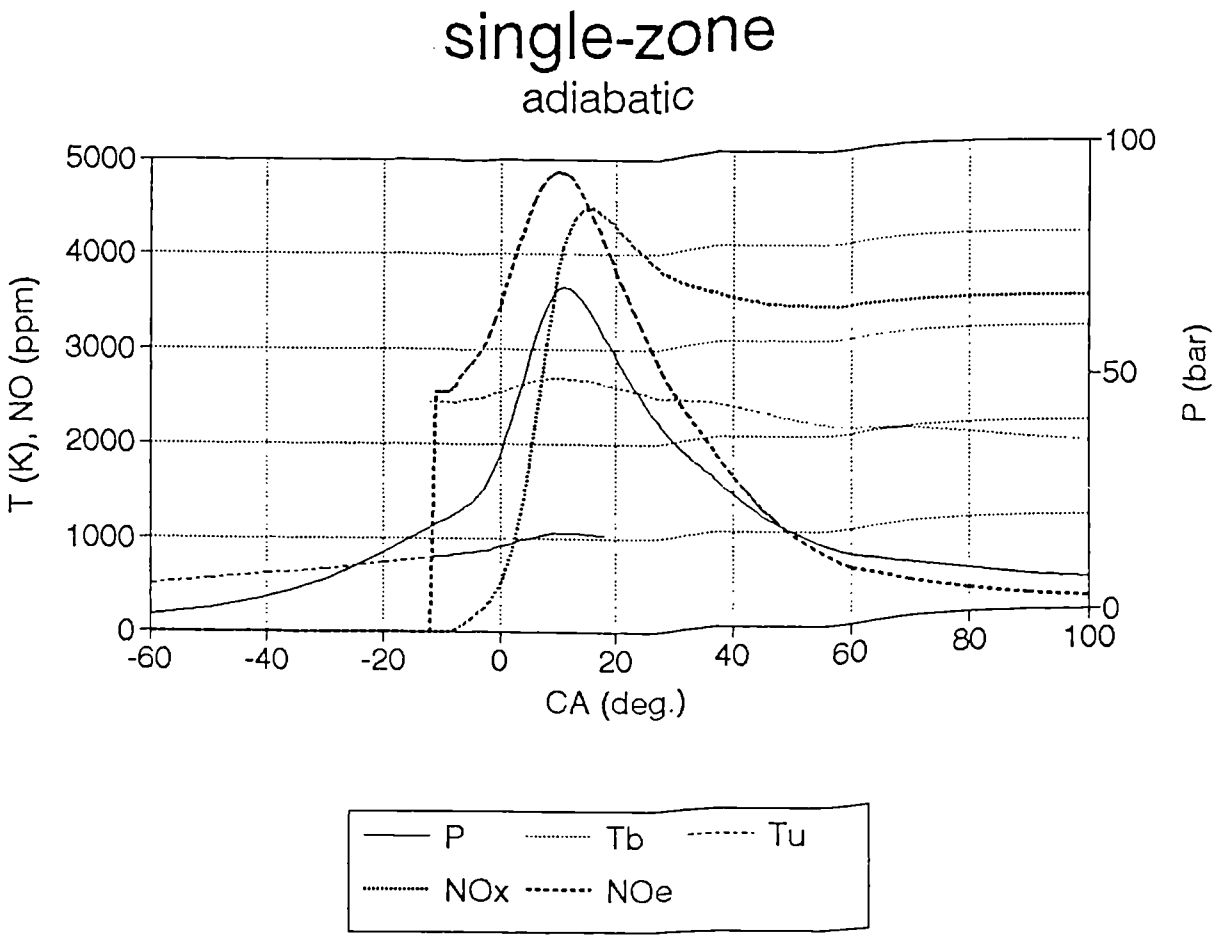

Figure 1.4a Model results for adiabatic cases using a single burnt gas zone; pressure (P), burnt gas temperature (Tb), unburnt gas temperature (Tu), and kinetic (NOx) and equilibrium (NOe) nitric oxide concentrations as a function of crank angle. (Taken from Raine (1993)).

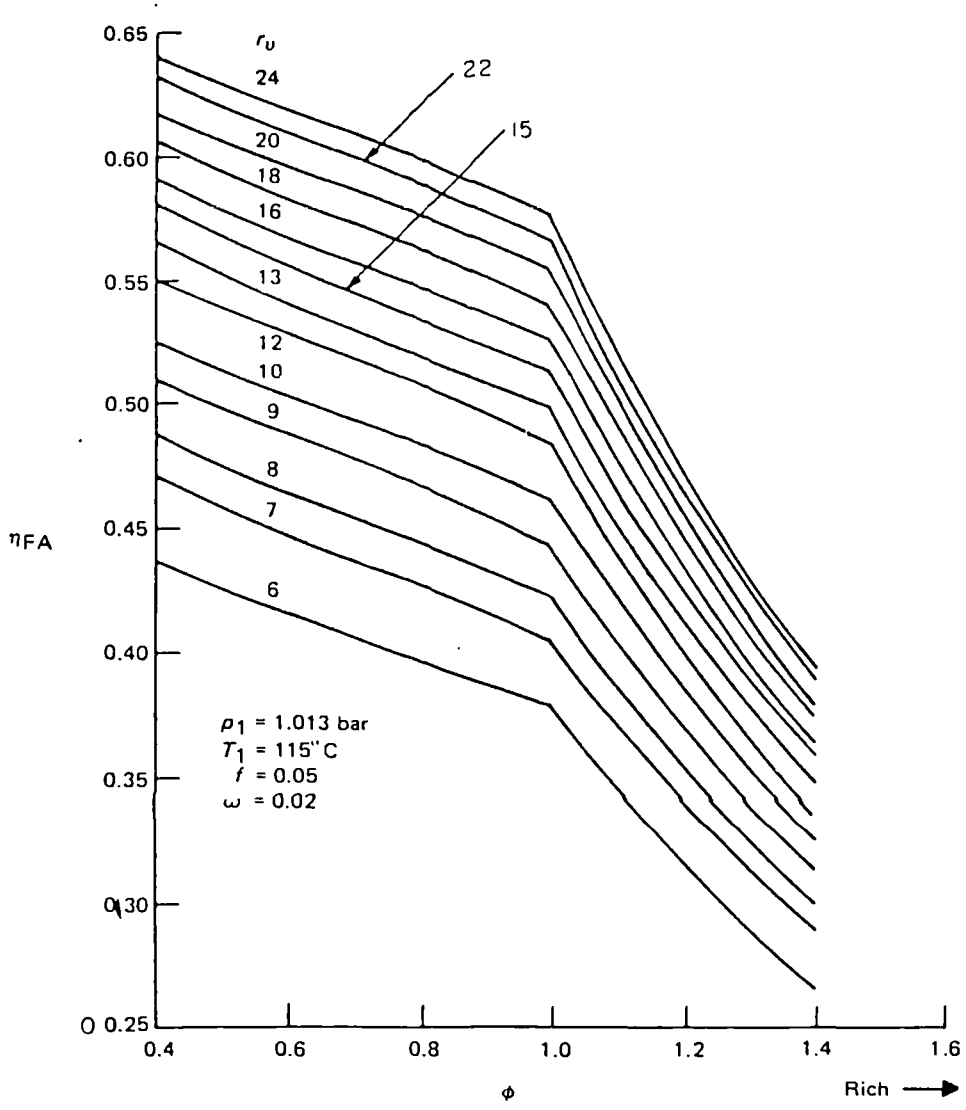

Figure 1.5 Variation of efficiency with equivalence ratio for a constant volume fuel-air cycle with 1-octene fuel for different compression ratios (taken from Stone (1989) adapted from Taylor (1966)).

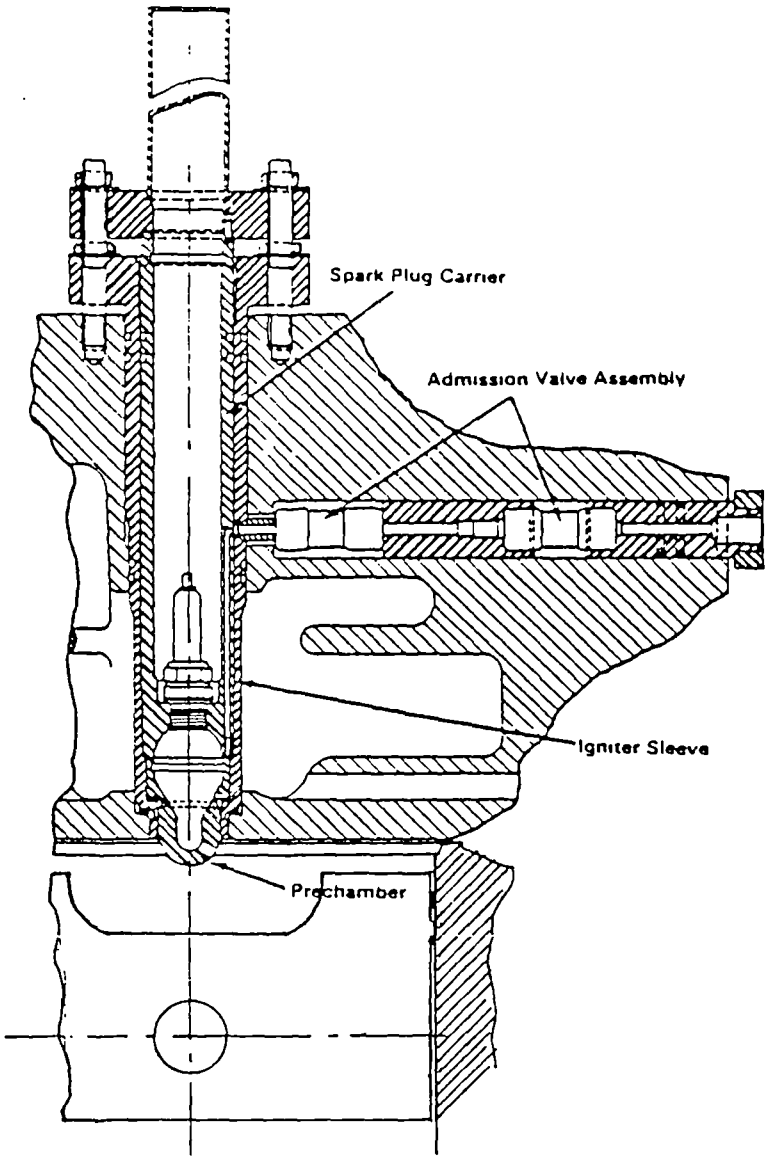

Figure 1.6 Cross-section of a divided combustion chamber (adapted from Pohl (1988)).

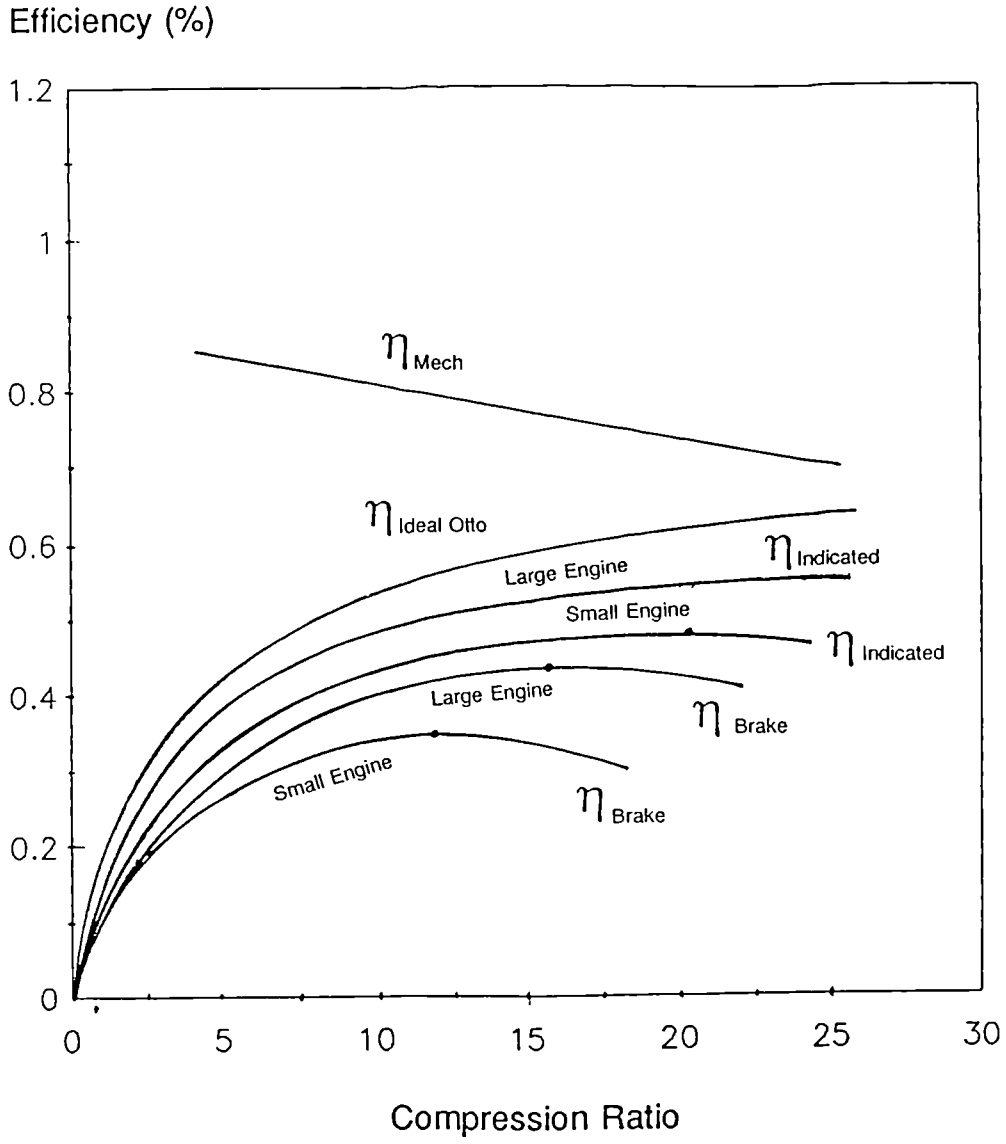

Figure 1.7 Variation in efficiency with compression ratio for large engines (say > 0.75 litres per cylinder), and small engines (say < 0.50 litres per cylinder).

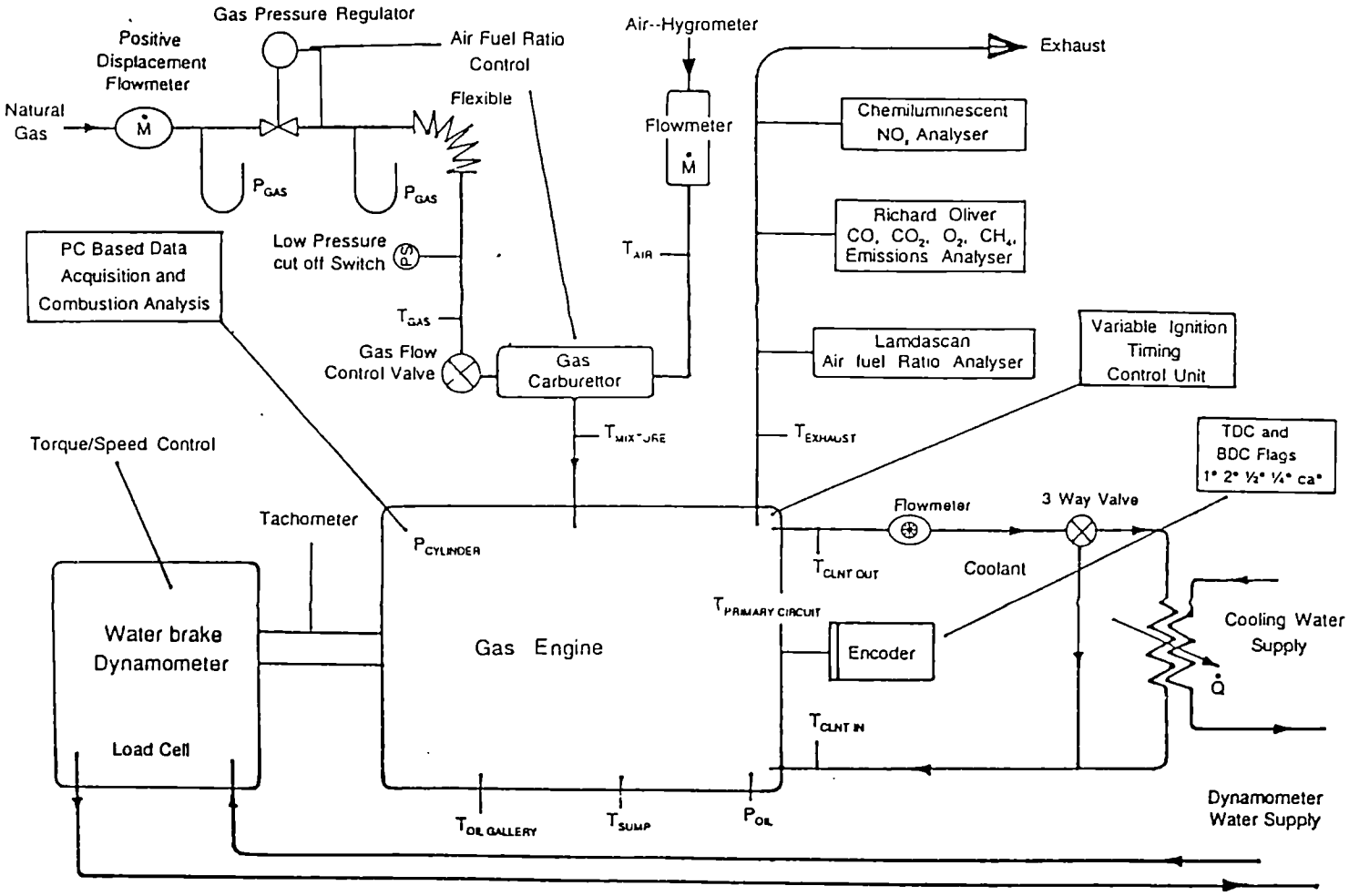

Figure 2.1 The Dover gas engine and associated instrumentation.

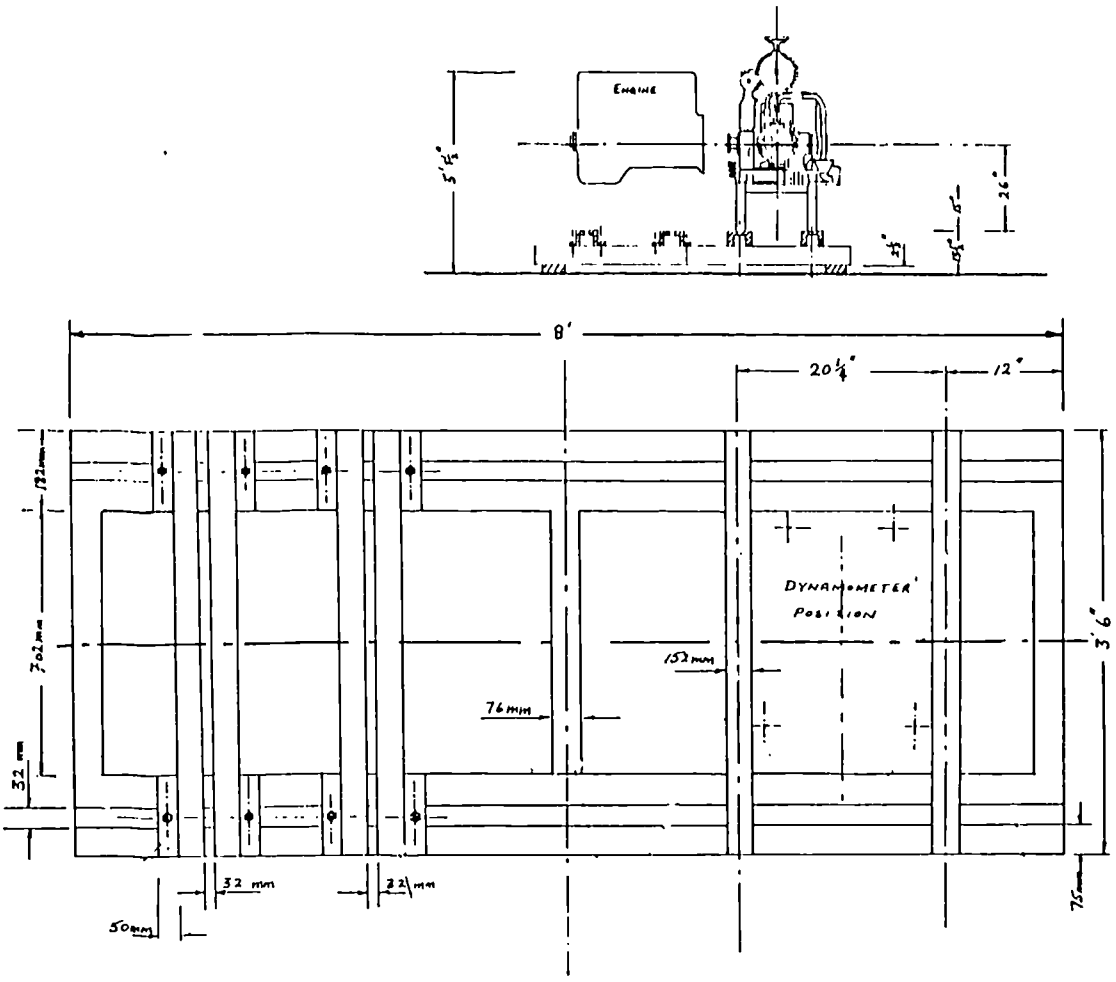

Figure 2.2 Plan view of the test bed. Inset is the side elevation of the engine and dynamometer

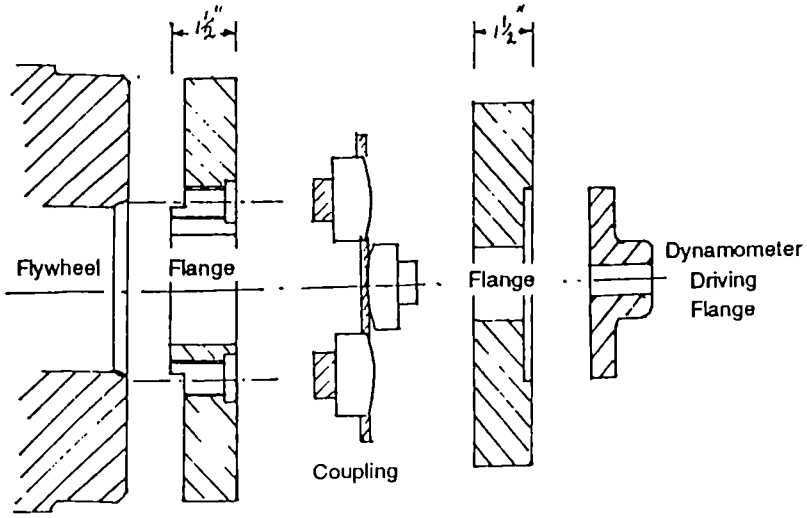

Figure 2.3 The engine and dynamometer coupling assembly.

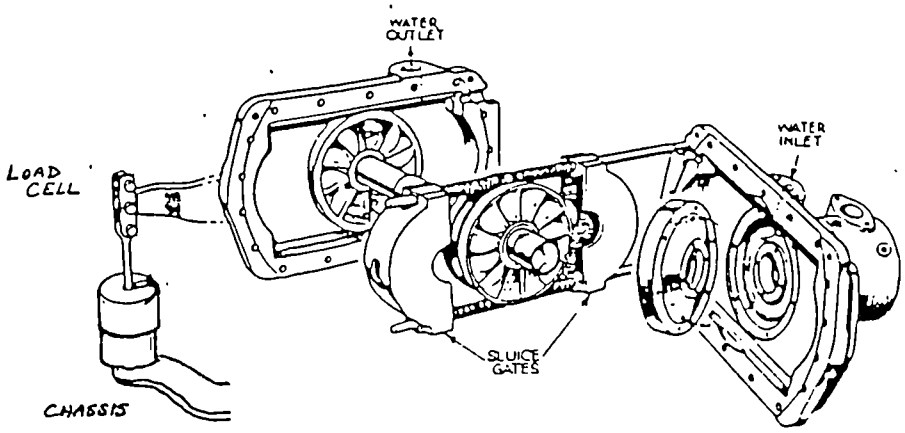

Figure 2.4 Water brake (courtesy of Froude Consine Ltd).

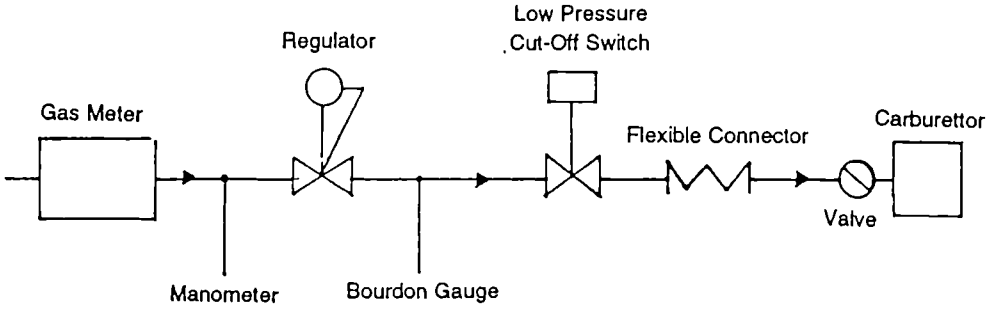

Figure 2.5 Schematic diagram of the gas supply to the engine (with regard to British Gas standards of good practice), showing the pressure regulator and other control devices.

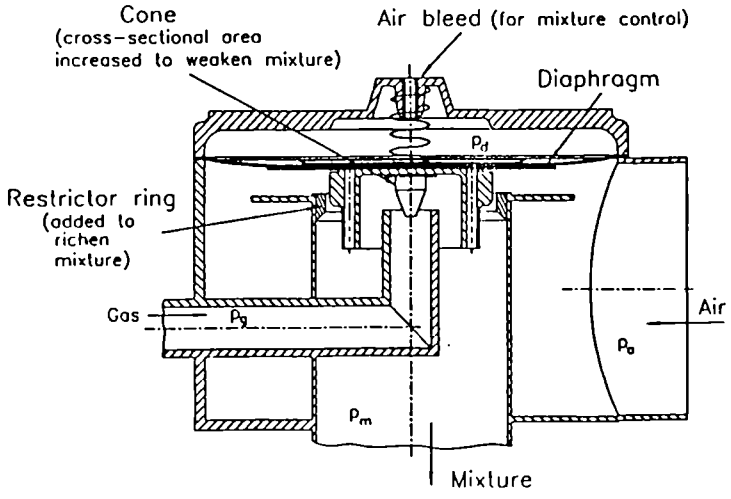

Figure 2.6 Modifications to the Impco carburettor for extended air fuel ratio control.

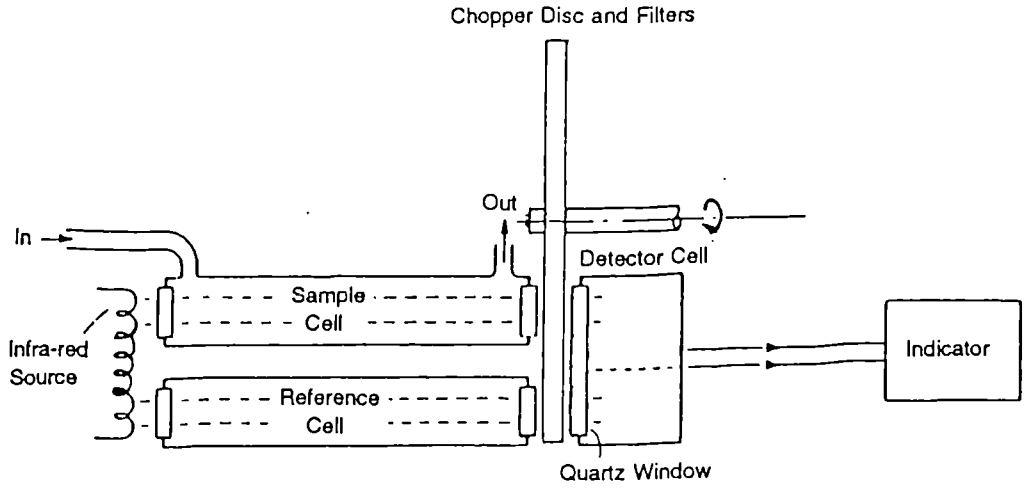

Figure 2.7 The key components in a nondispersive infra-red (NDIR) gas analyser (adapted from Stone 1992).

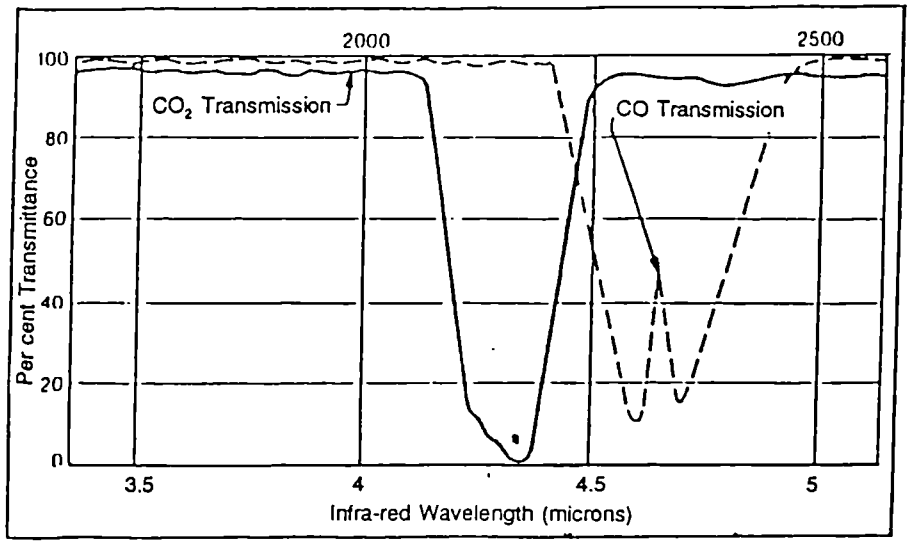

Figure 2.8 Transmittance of infra-red through gaseous carbon dioxide and carbon monoxide (taken from Stone 1992).

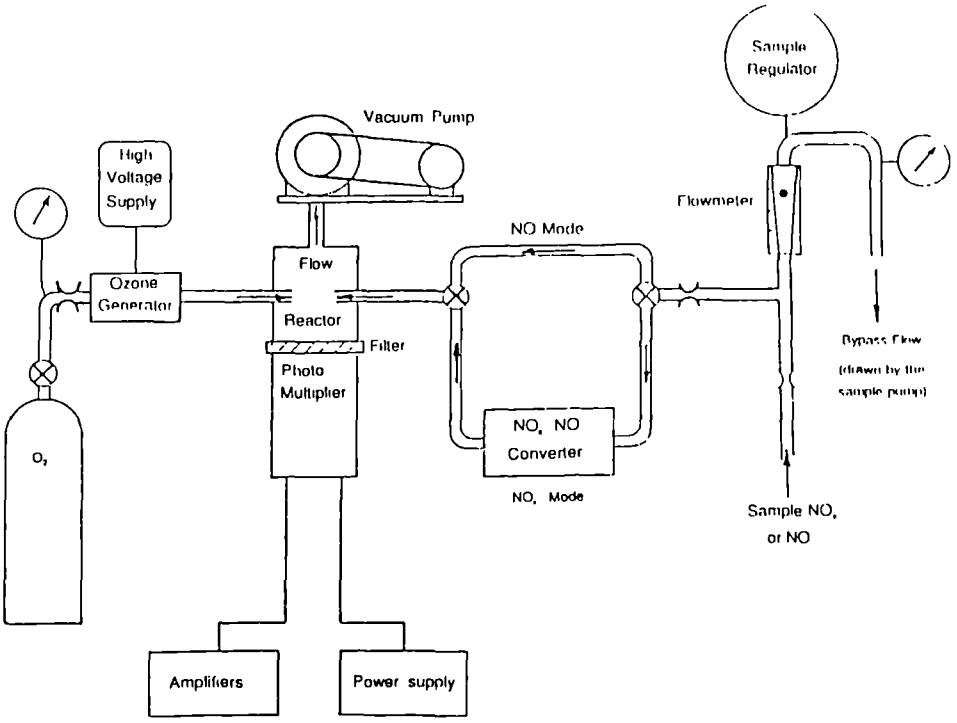

Figure 2.9 Key elements in a chemiluminescent NOx analyser (taken from Stone 1992).

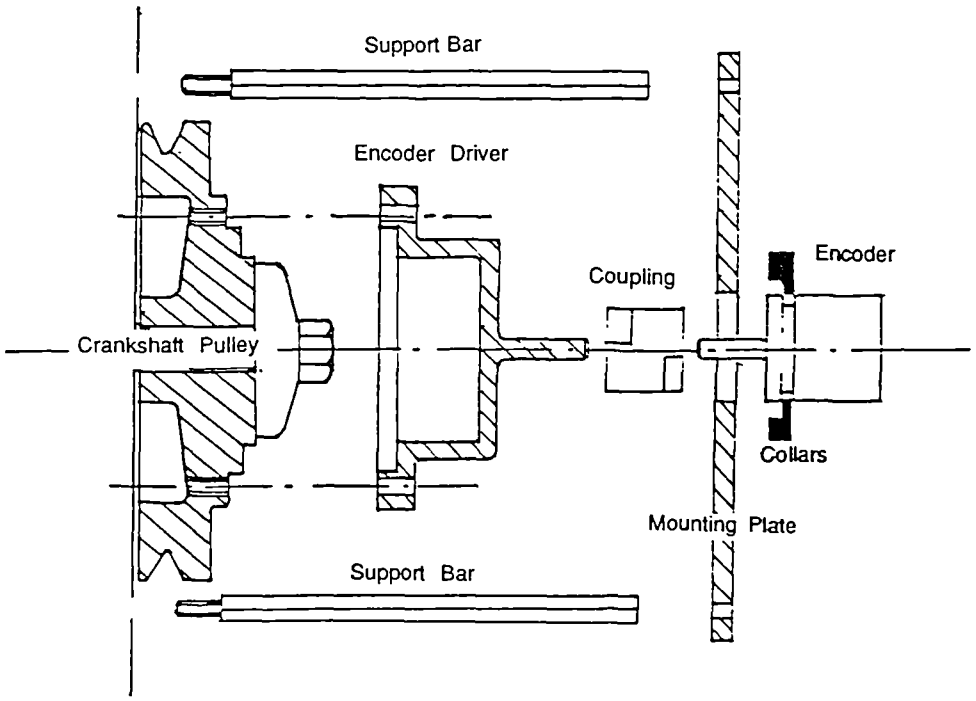

Figure 2.10 Shaft encoder drive and mounting assembly.

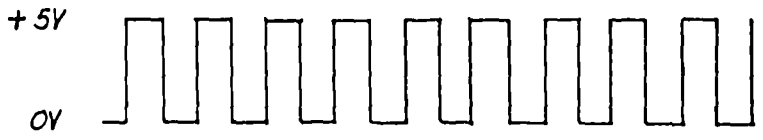

(a) Equivalent to degrees of crank angle output

(b) TDC/BDC flag

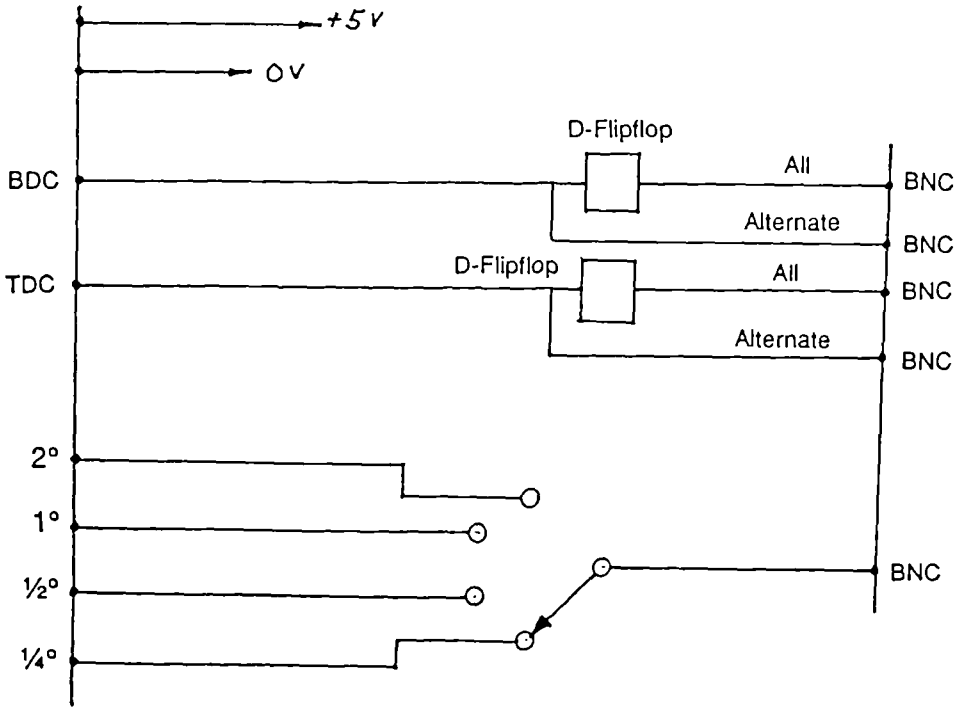

Figure 2.11 Encoder outputs.

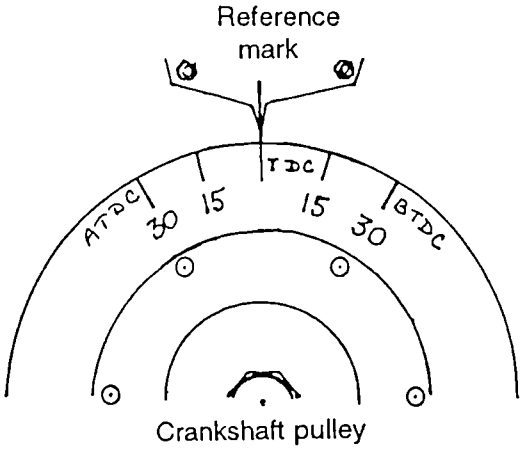

Figure 2.12 TDC and crankshaft angular markers.

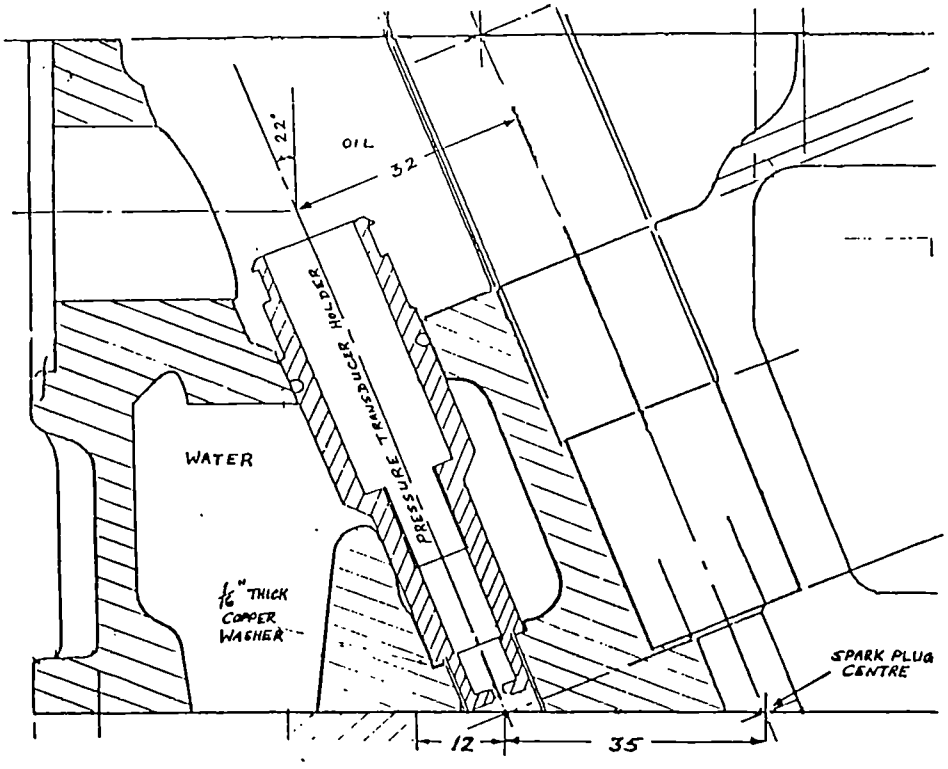

Figure 2.13 Cylinder head cross-section showing positions for the spark plug and pressure transducer.

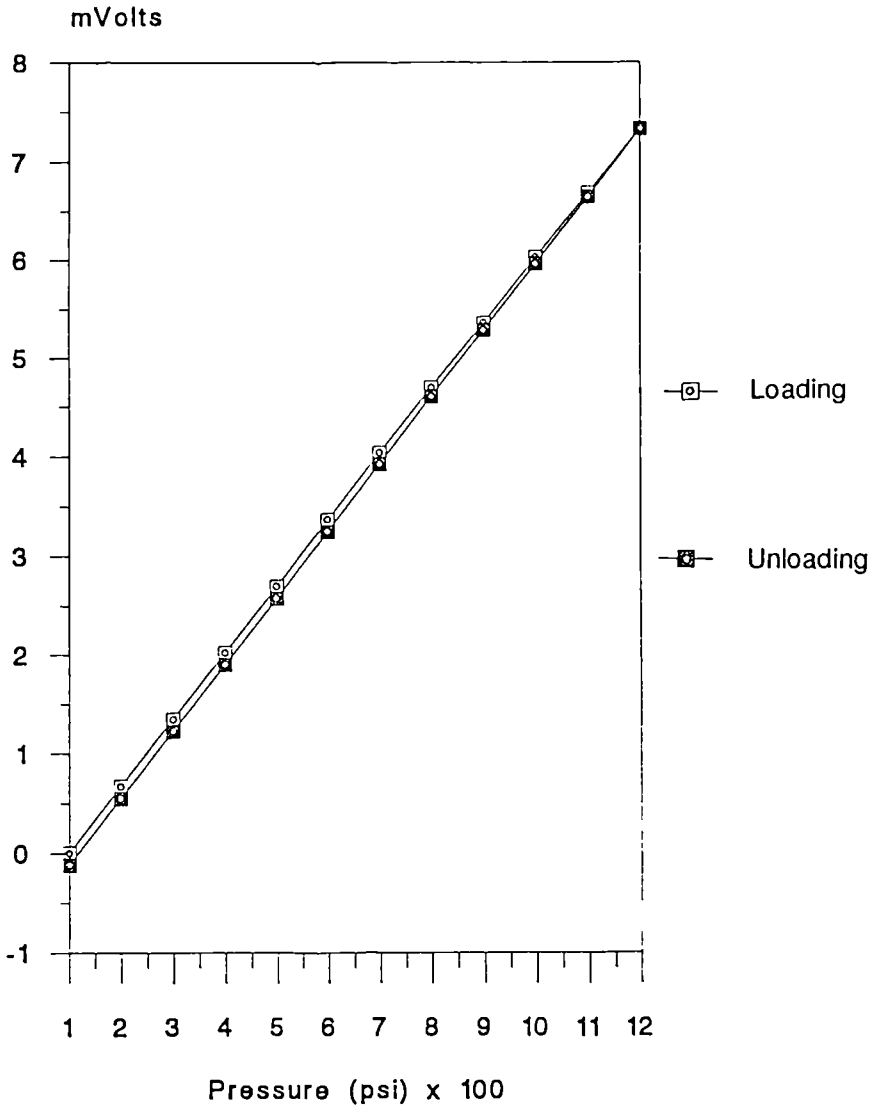

Figure 2.14 Pressure transducer calibration curve.

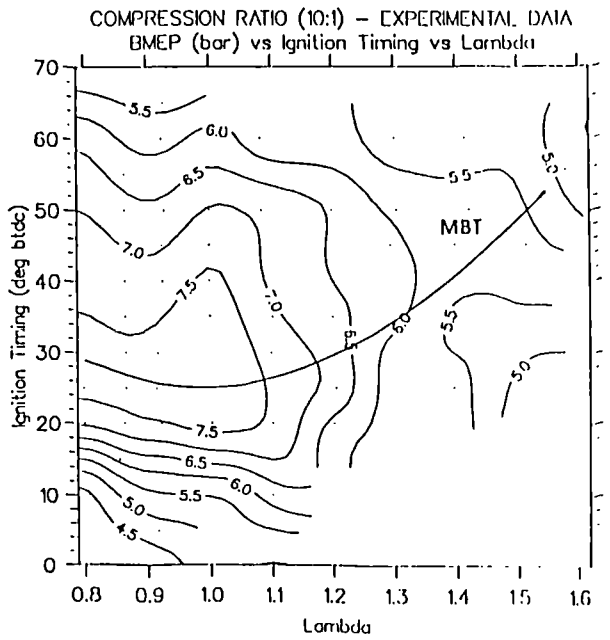

Fig. 3.1 The baseline bmep (bar) with a compression ratio of 10.3, as a function of the air fuel ratio and the ignition timing. The points in all of the figures represent engine experimental operating points.

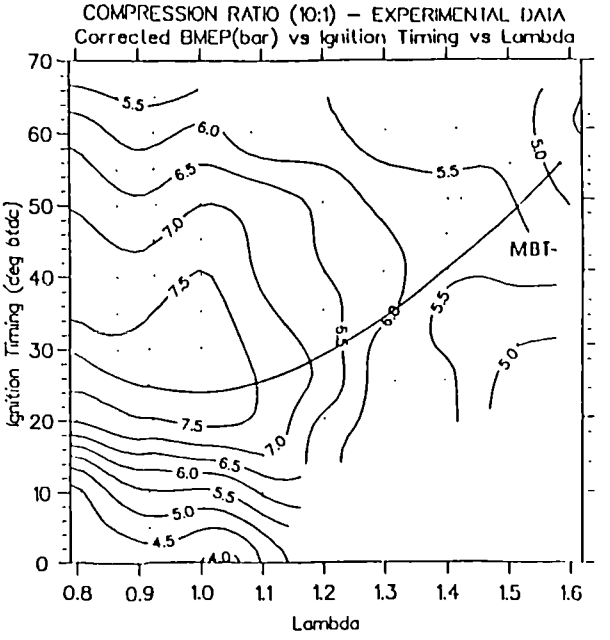

Fig. 3.2 The baseline bmep (bar) corrected for standard conditions, with a compression ratio of 10.3, as a function of the air fuel ratio and the ignition timing, shows negligible differences from figure 3.1

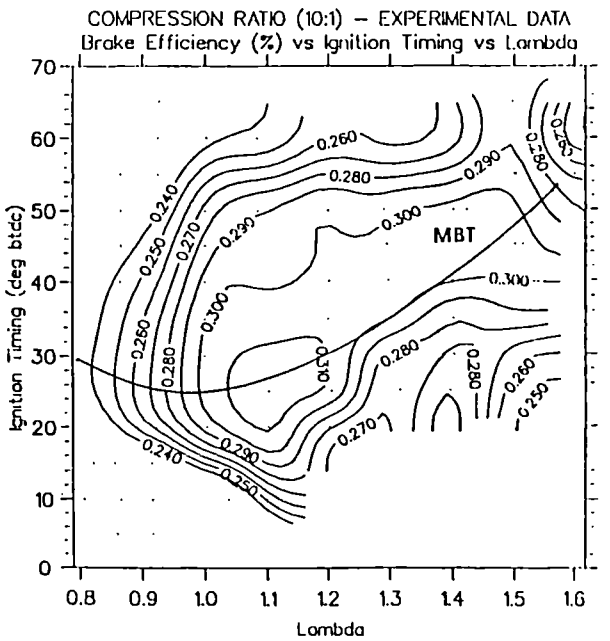

Fig. 3.3 The baseline brake efficiency (%) with a compression ratio of 10.3, as a function of the air fuel ratio and the ignition timing. Also shown as in the previous figure and in others, is the MBT ignition timing Schedule.

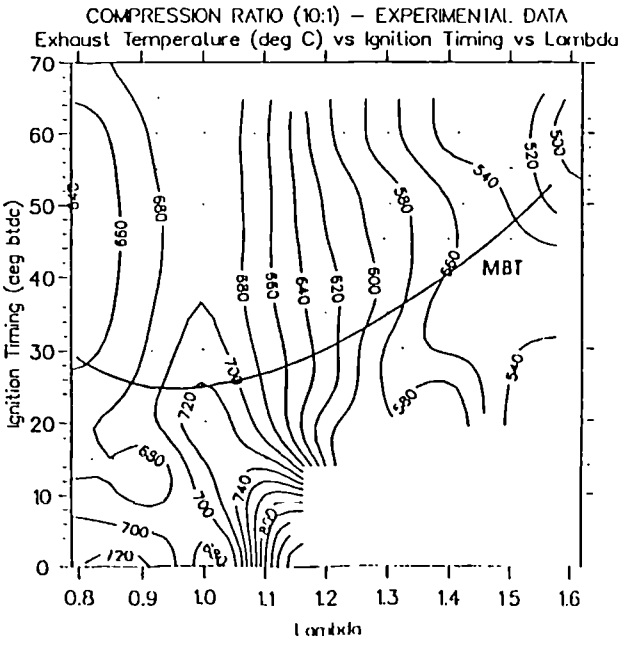

Fig. 3.4 The baseline exhaust temperature (°C) with a compression ratio of 10.3, as a function of the air fuel ratio and the ignition timing.

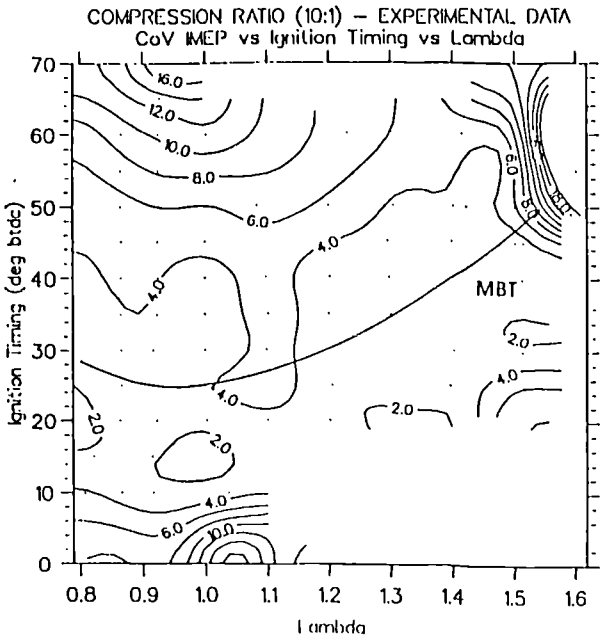

Fig. 3.5 The baseline CoV of imep (%) with a compression ratio of 10.3, as a function of the air fuel ratio and the ignition timing. A 5% CoV of imep is the generally accepted limit for satisfactory speed regulation.

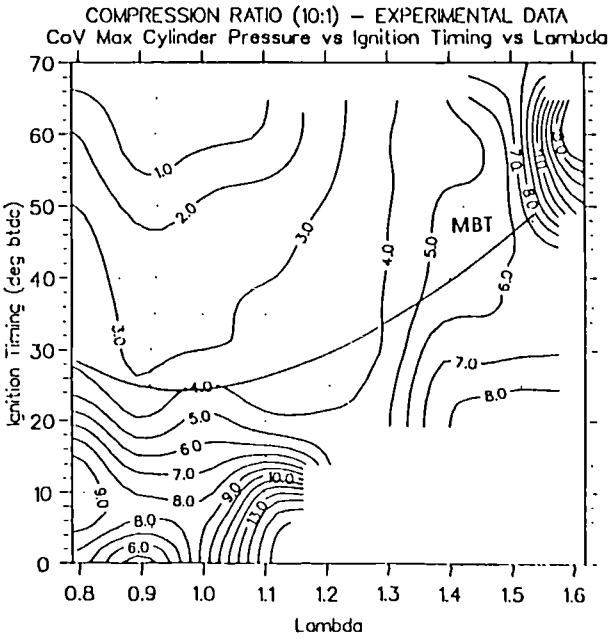

Fig. 3.7 The baseline CoV of maximum pressure (%) with a compression ratio of 10.3, as a function of the air fuel ratio and the ignition timing.

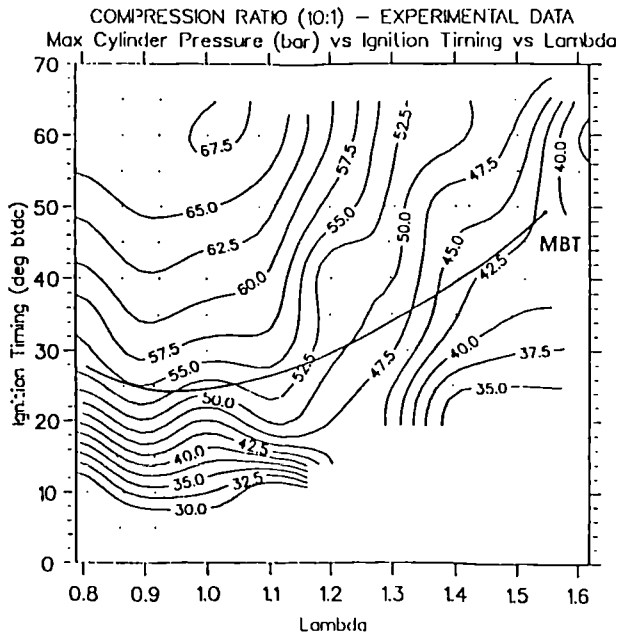

Fig. 3.6 The baseline maximum pressure (bar) with a compression ratio of 10.3, as a function of the air fuel ratio and the ignition timing.

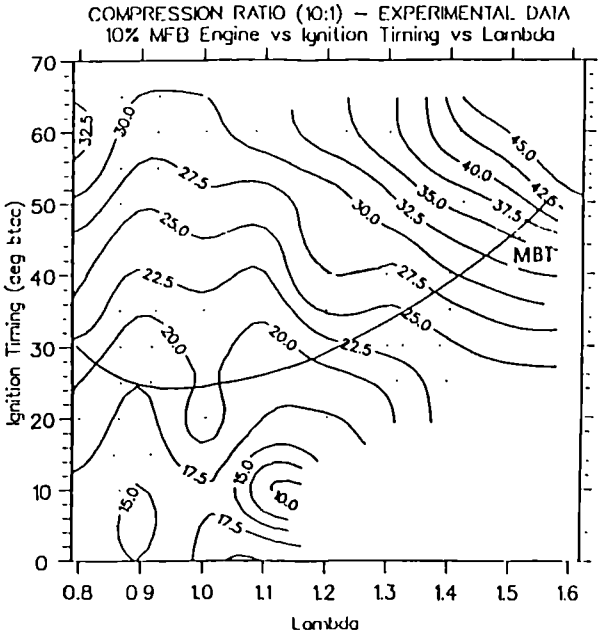

Fig. 3.8 The baseline 0-10% burn duration (°ca) with a compression ratio of 10.3, as a function of the air fuel ratio and the ignition timing.

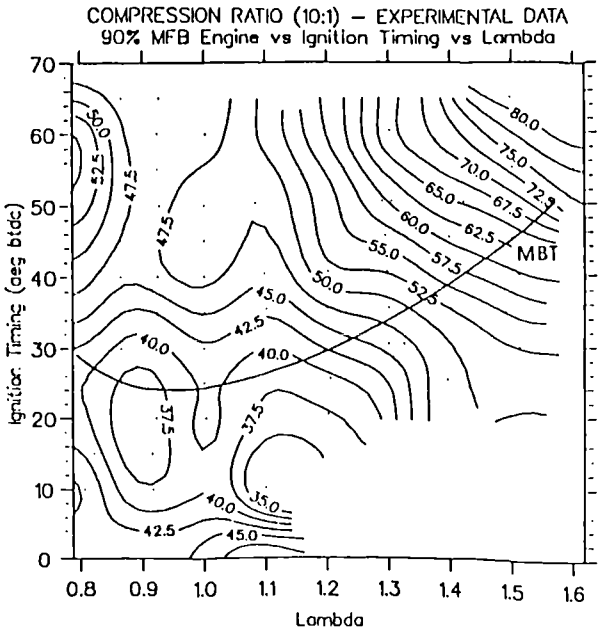

Fig. 3.9 The baseline 0-90% burn duration (°ca) with a compression ratio of 10.3, as a function of the air fuel ratio and the ignition timing.

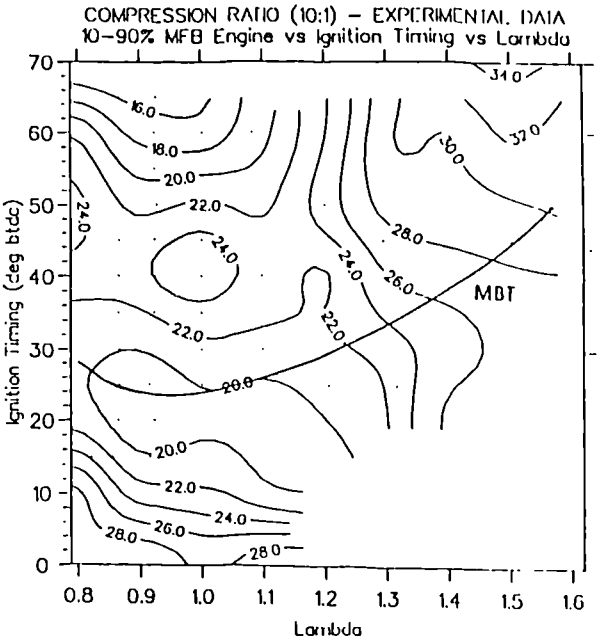

Fig. 3.10 The baseline 10-90% burn duration (°ca) representative of the turbulent burn rate, with a compression ratio of 10.3, as a function of the air fuel ratio and the ignition timing.

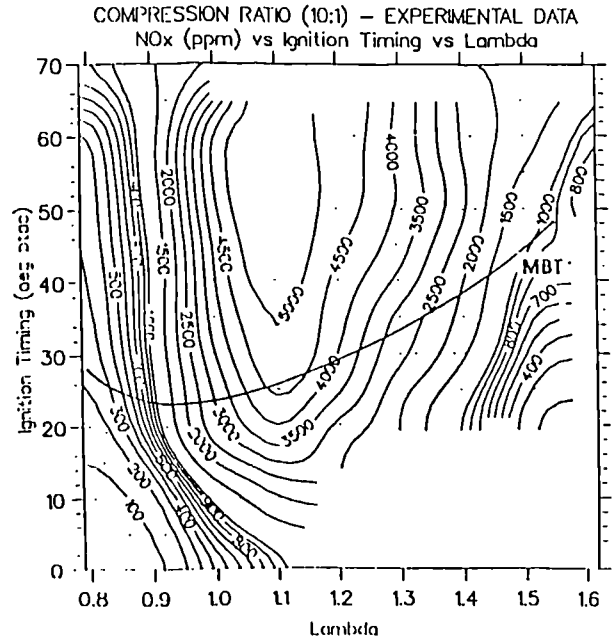

Fig. 3.11 The baseline volumetric NOx emissions (ppm) with a compression ratio of 10.3, as a function of the air fuel ratio and the ignition timing.

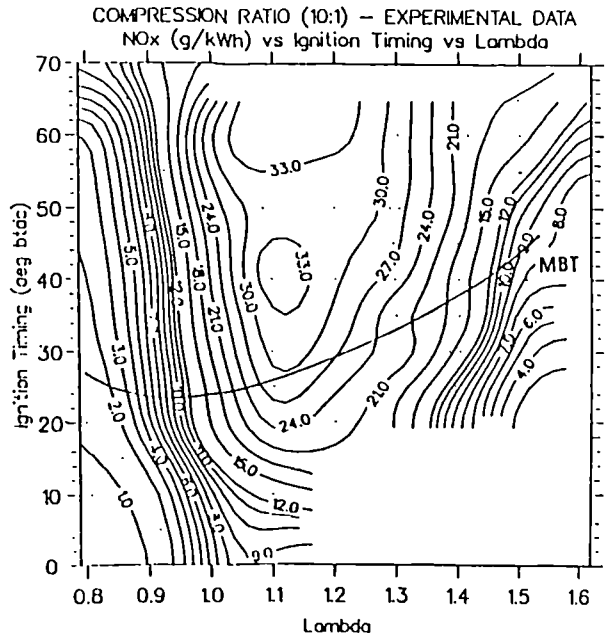

Fig. 3.12 The baseline gravimetric NOx emissions (g/kWh).

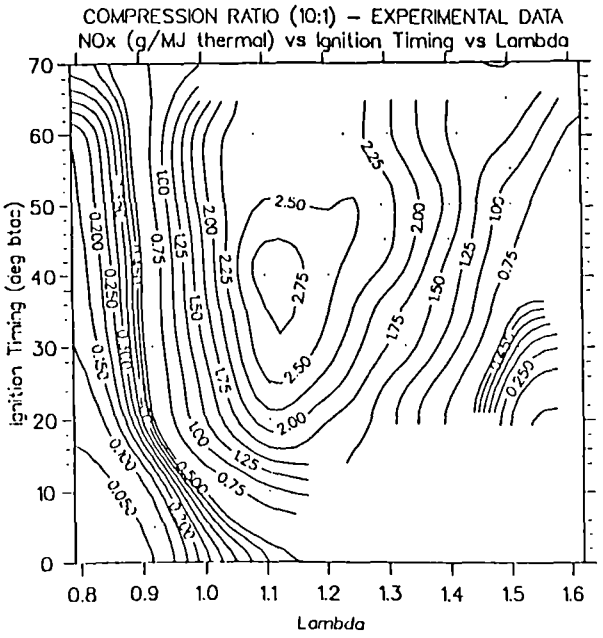

Fig. 3.13 The baseline gravimetric NOx emissions (g/MJ thermal).

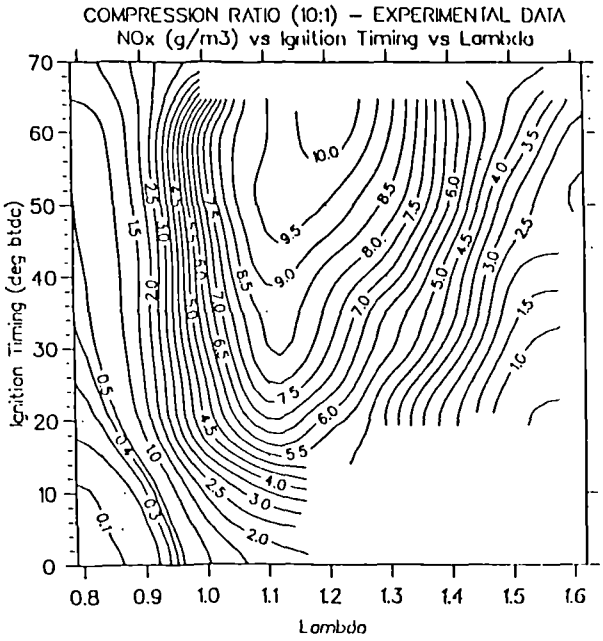

Fig. 3.14 *The baseline NOx emissions (g/m³).*

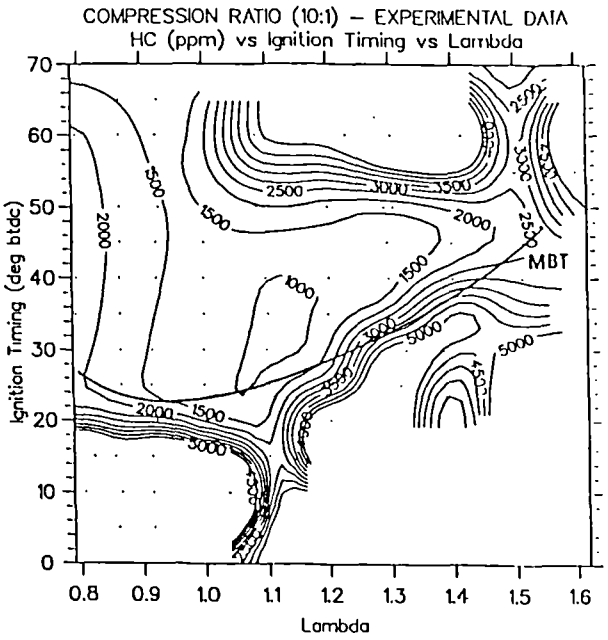

Fig. 3.15 The baseline volumetric hydrocarbon emissions (ppm) with a compression ratio of 10.3, as a function of the air fuel ratio and the ignition timing.

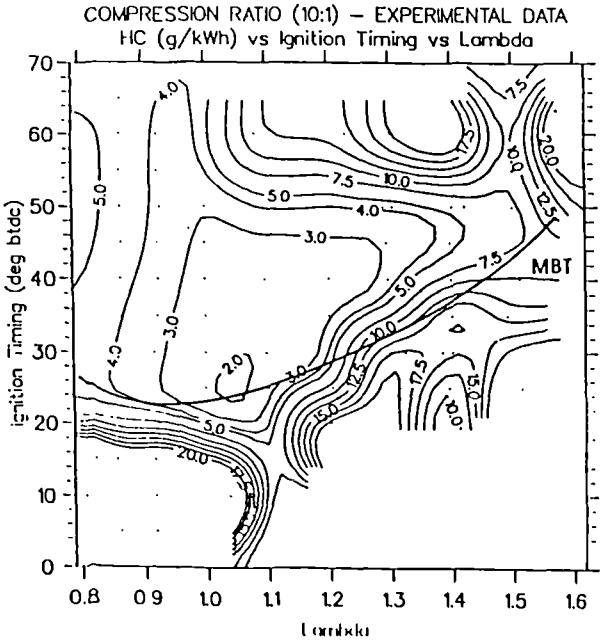

Fig. 3.16 The baseline gravimetric hydrocarbon emissions (g/kWh).

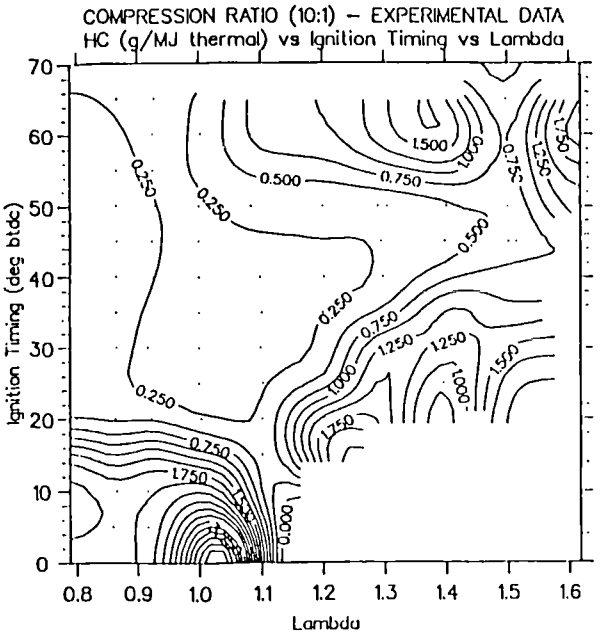

Fig. 3.17 The baseline gravimetric hydrocarbon emissions (g/MJ thermal).

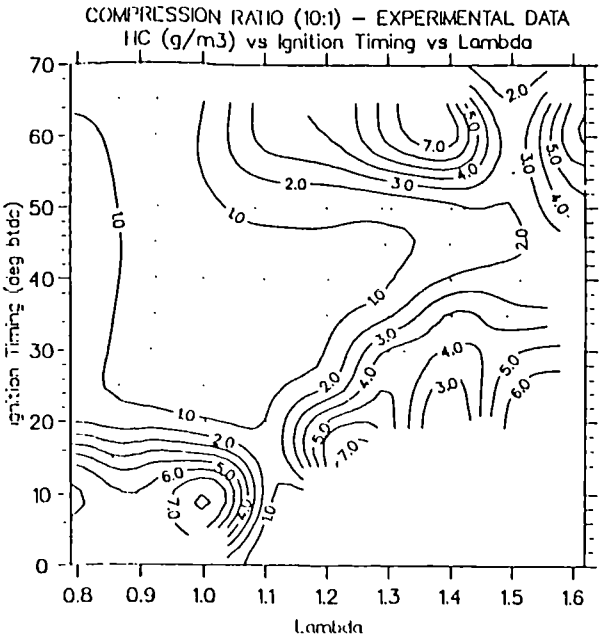

Fig. 3.18 The baseline hydrocarbon emissions (g/m^3).

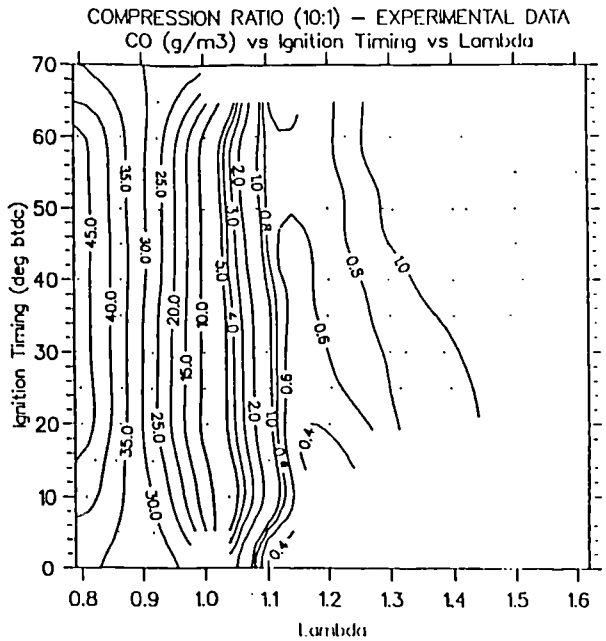

Fig. 3.19 The baseline carbon monoxide emissions (g/m^3) with a compression ratio of 10.3, as a function of the air fuel ratio and the ignition timing.

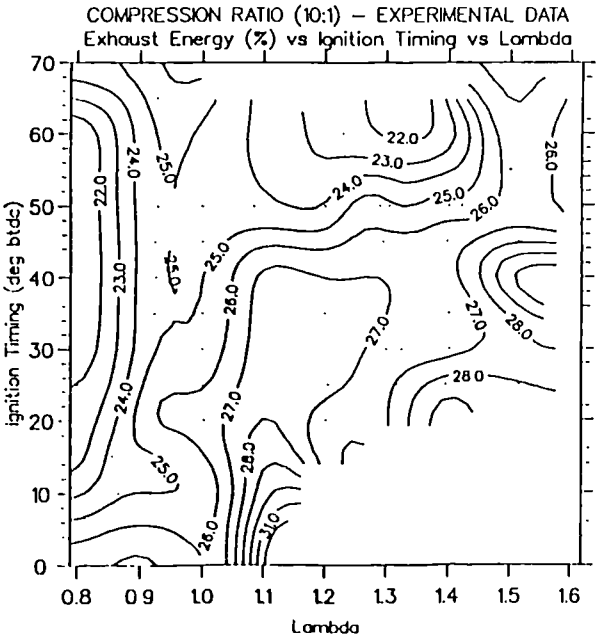

Fig. 3.20 The baseline exhaust energy (%) as a function of the air fuel ratio and the ignition timing.

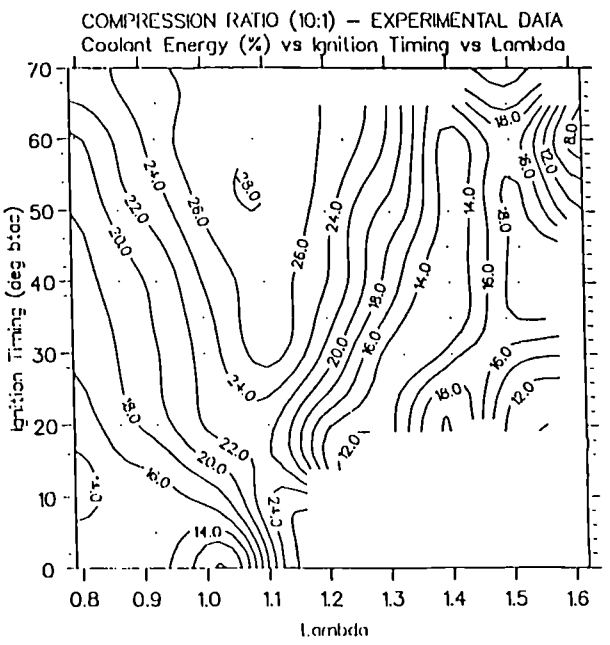

Fig. 3.21 The baseline coolant energy (%) as a function of the air fuel ratio and the ignition timing.

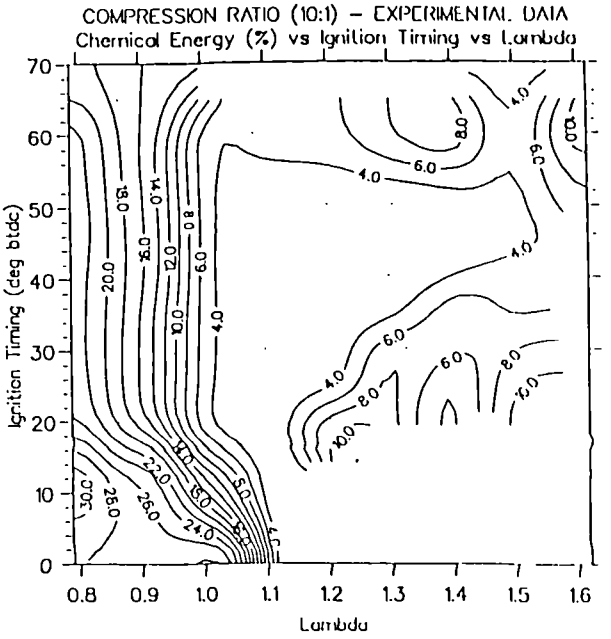

Fig. 3.22 The baseline chemical energy (%) as a function of the air fuel ratio and the ignition timing.

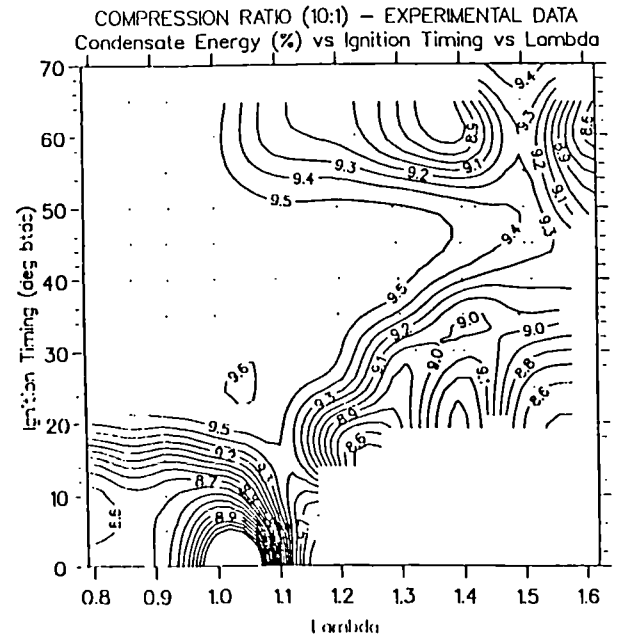

Fig. 3.23 The baseline condensate energy (%) as a function of the air fuel ratio and the ignition timing.

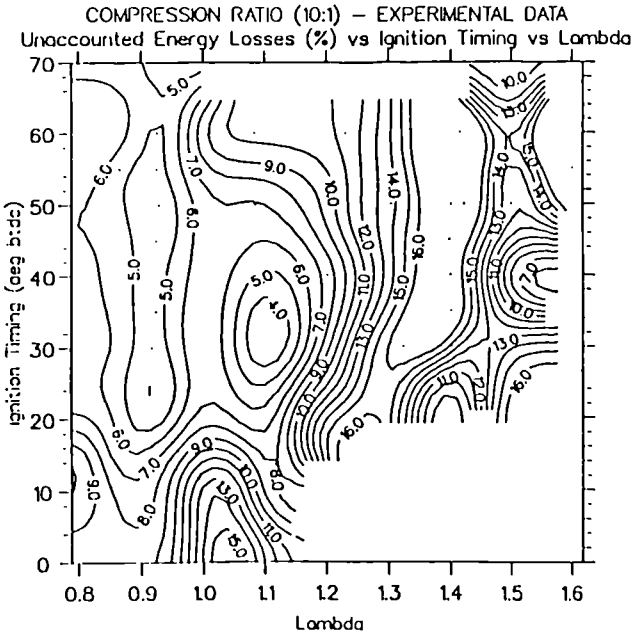

Fig. 3.24 The baseline unaccounted energy (%) as a function of the air fuel ratio and the ignition timing. This completes the balance of the converted energy sum.

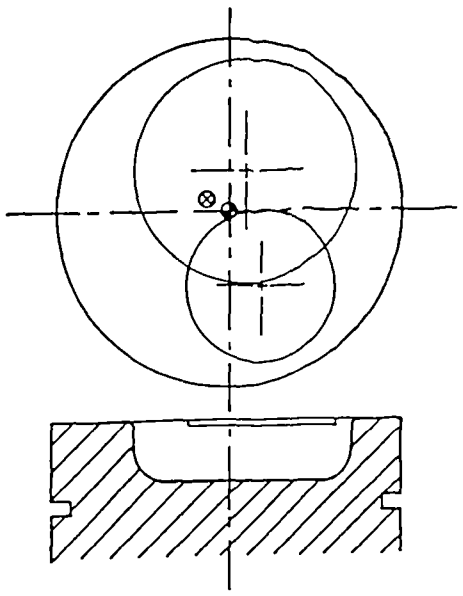

Fig. 3.25 The key features of the FBHCR combustion chamber showing the position of the bowl, the inlet valve and the spark plug electrodes.

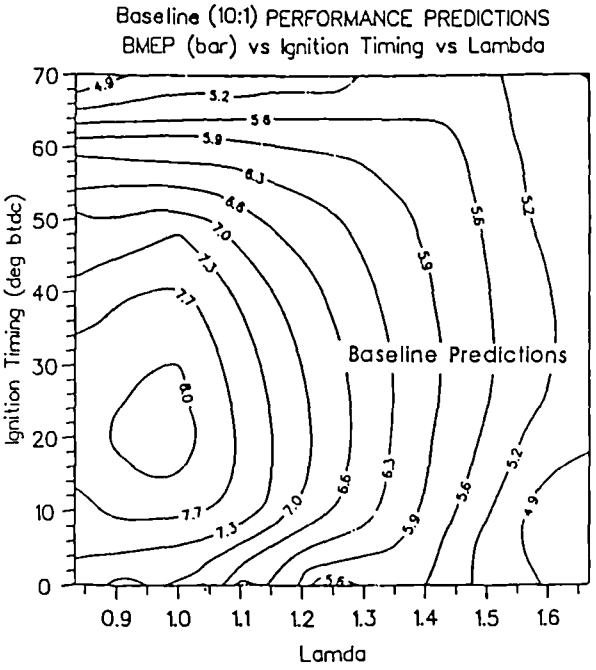

Fig. 3.26 The simulation bmep (bar) for the baseline engine (compression ratio = 10.3), as a function of the air fuel ratio and the ignition timing.

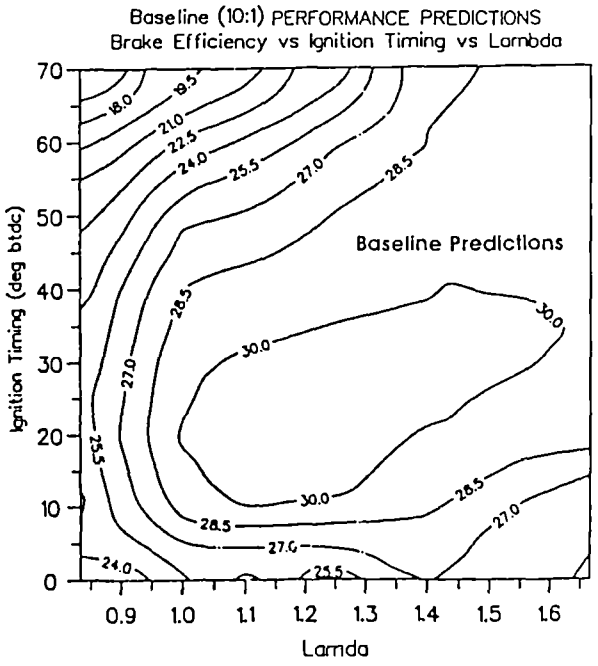

Fig. 3.27 The simulation brake efficiency (%) for the baseline engine (compression ratio = ,10.3), as a function of the air fuel ratio and the ignition timing.

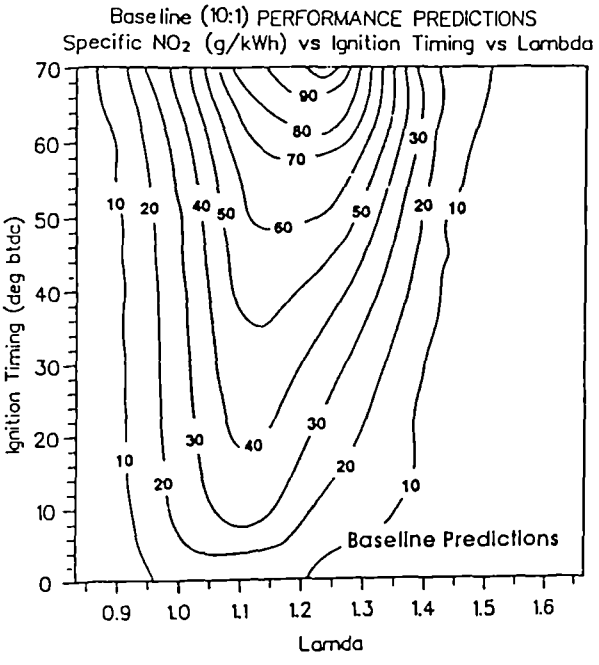

Fig. 3.28 The simulation brake specific NOx emissions (g/kWh) for the baseline engine (compression ratio = 10.3), as a function of the air fuel ratio and the ignition timing.

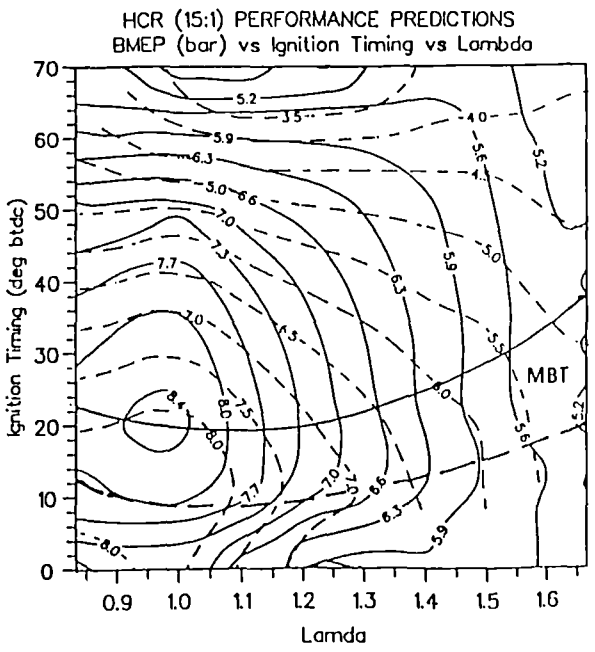

Fig. 3.29 The simulation bmep (bar) for the high compression engine (compression ratio = 14.7), as a function of the air fuel ratio and the ignition timing, for the standard (-) and fast burn (--).

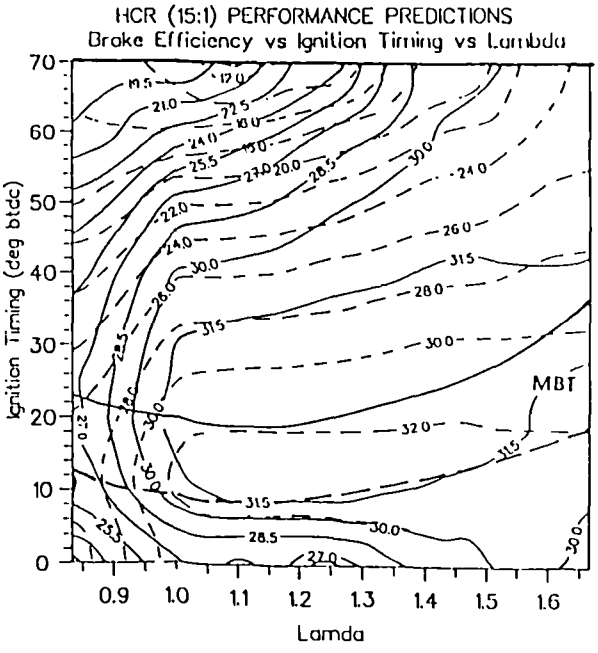

Fig. 3.30 The simulation brake efficiency (%) for the high compression engine (compression ratio = 14.7), as a function of the air fuel ratio and the ignition timing, for the standard (-) and fast burn (--).

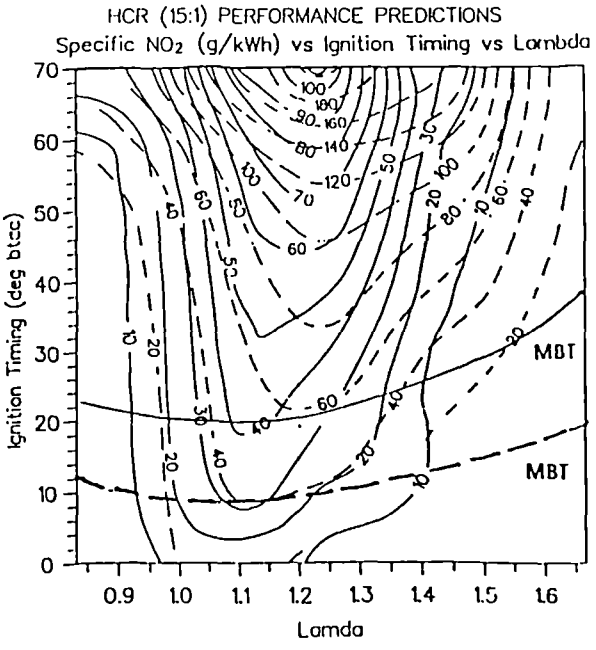

Fig. 3.31 The simulation brake specific NOx emissions (g/kWh) for the high compression engine (compression ratio = 14.7), as a function of the air fuel ratio and the ignition timing, for the standard (-) and fast burn (--).

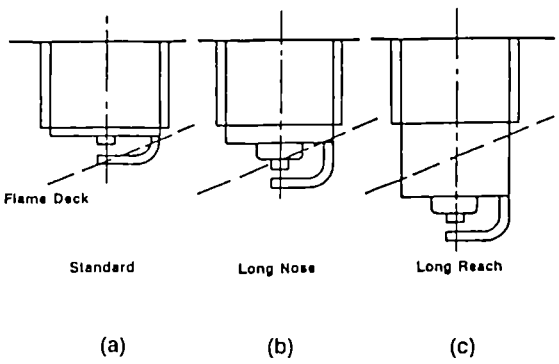

Fig 4.1 The different spark plug geometries used in the Fast Burn High Compression (FBHCR) combustion system.

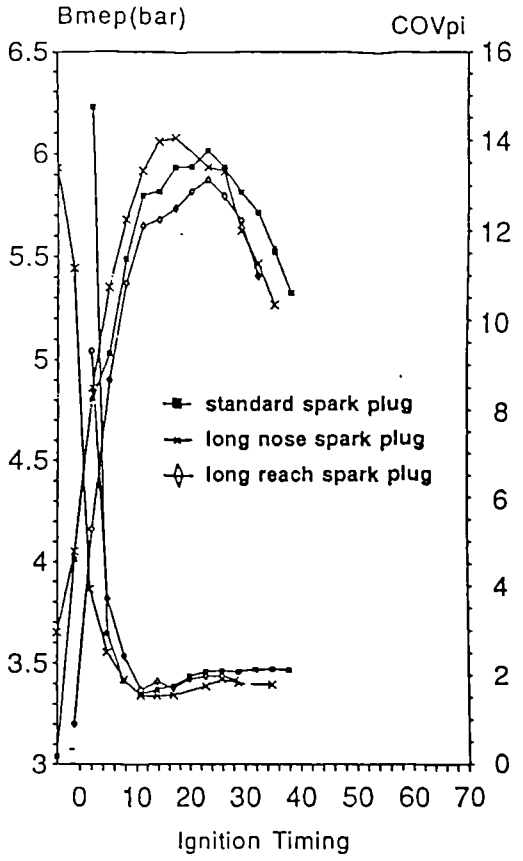

Fig 4.2 The bmep (bar) and coefficient of variation of the imep (%), as a function of ignition timing for different spark plugs.

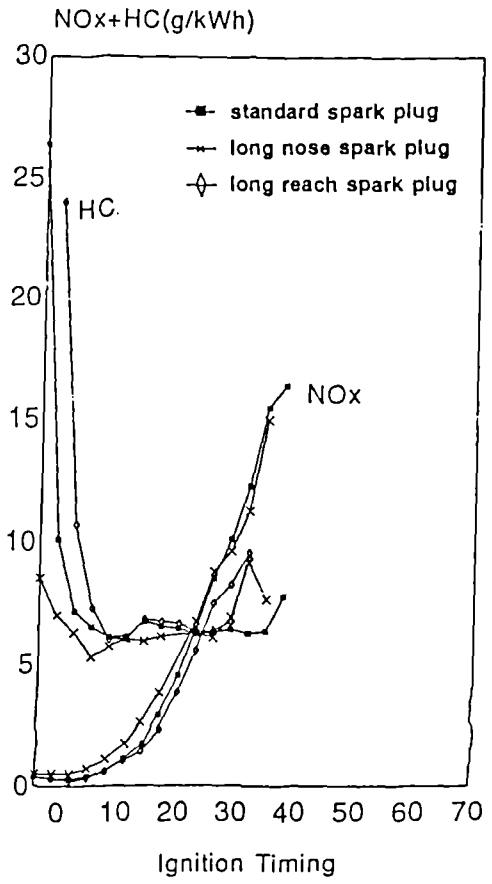

Fig 4.3 The brake specific NOx emissions and unburnt hydrocarbon emissions, as a function of ignition timing for different spark plugs.

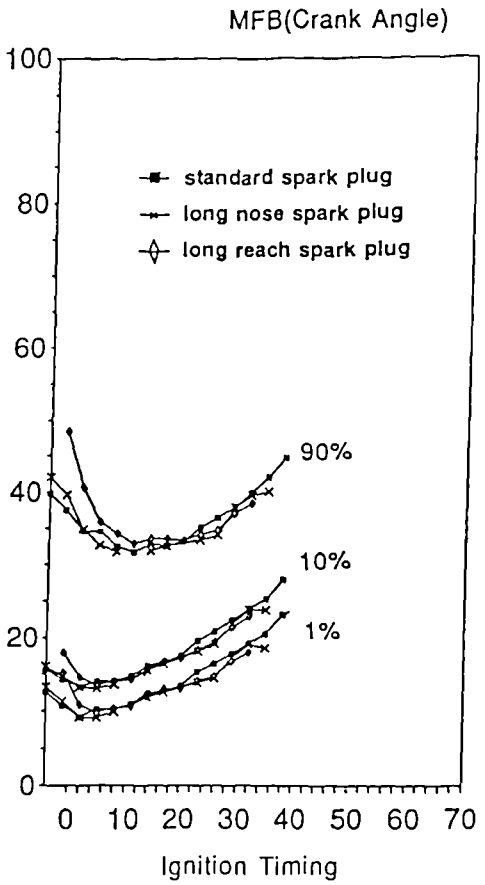

Fig 4.4 The 0-1%, 0-10%, and 0-90%, burn duration (°ca), as a function of ignition timing for different spark plugs.

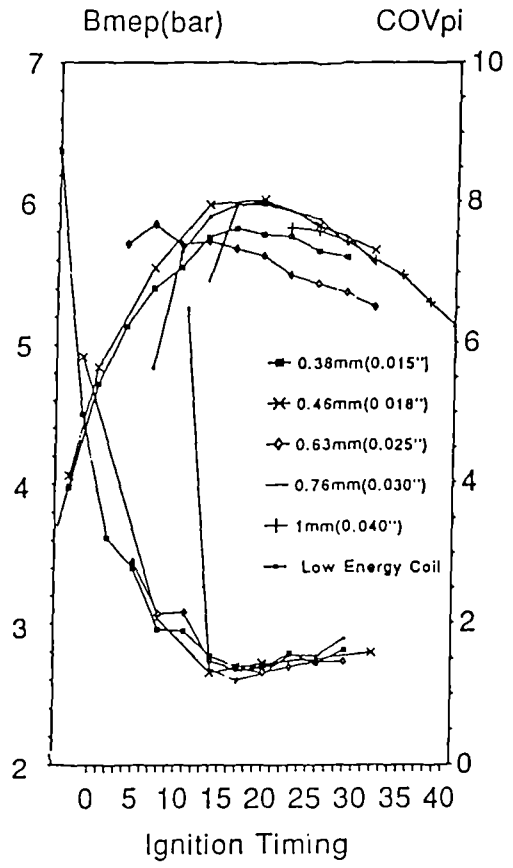

Fig 4.5 The effect of the spark plug gap and coil energy on the bmep and the coefficient of variation of the imep for a range of ignition timings.

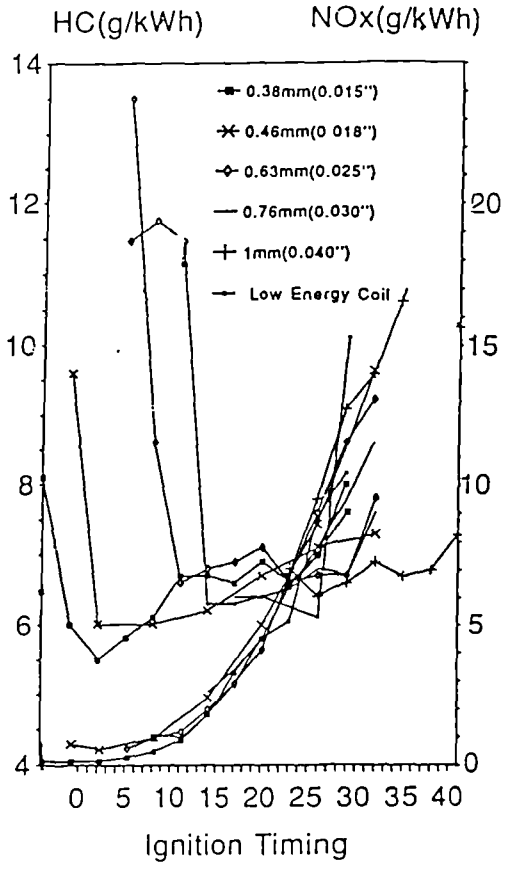

Fig 4.6 The effect of the spark plug gap and coil energy on the brake specific NOx and unburnt hydrocarbon emissions for a range of ignition timings.

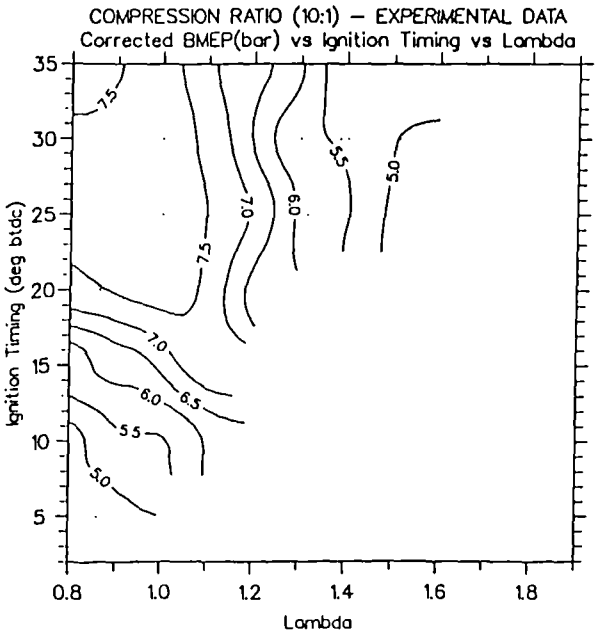

Fig. 4.7a The baseline bmep (bar) with a compression ratio of 10.3, as a function of the air fuel ratio and the ignition timing.

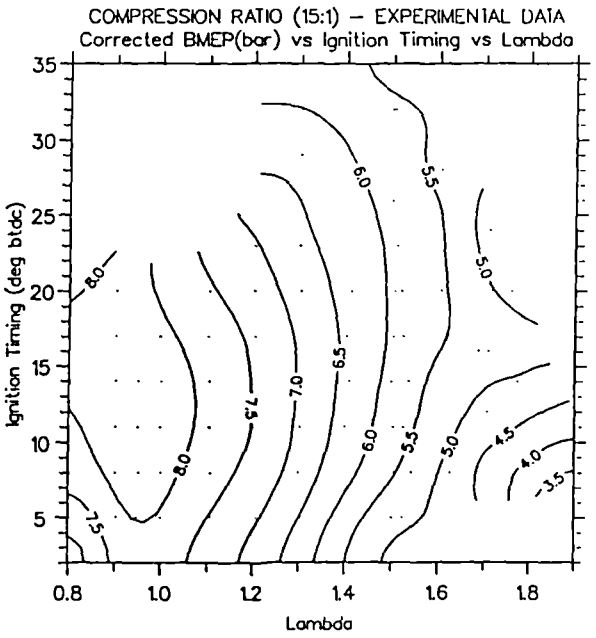

Fig. 4.7b The FBHCR bmep (bar) with a compression ratio of 14.7, as a function of the air fuel ratio and the ignition timing.

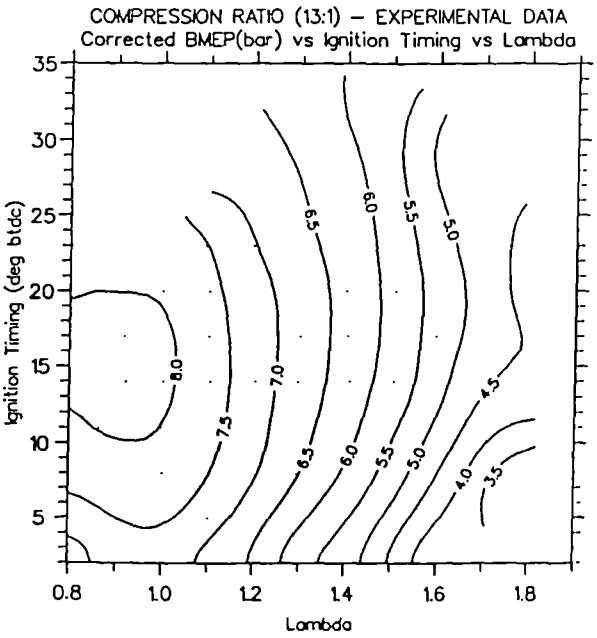

Fig. 4.7c The FBHCR bmep (bar) with a compression ratio of 13.0, as a function of the air fuel ratio and the ignition timing.

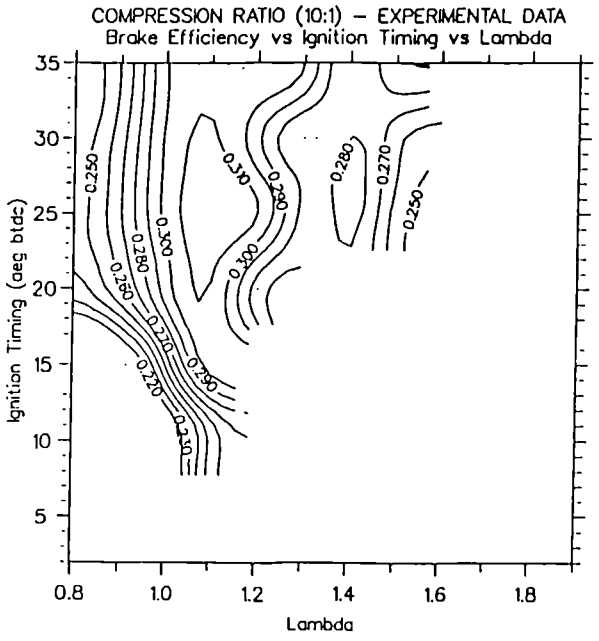

Fig. 4.8a The baseline brake efficiency (%) with a compression ratio of 10.3, as a function of the air fuel ratio and the ignition timing.

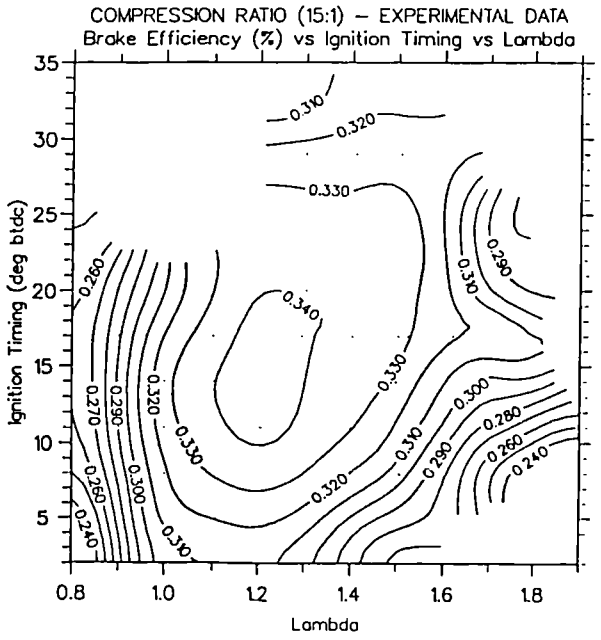

Fig. 4.8b The FBHCR brake efficiency (%) with a compression ratio of 14.7, as a function of the air fuel ratio and the ignition timing.

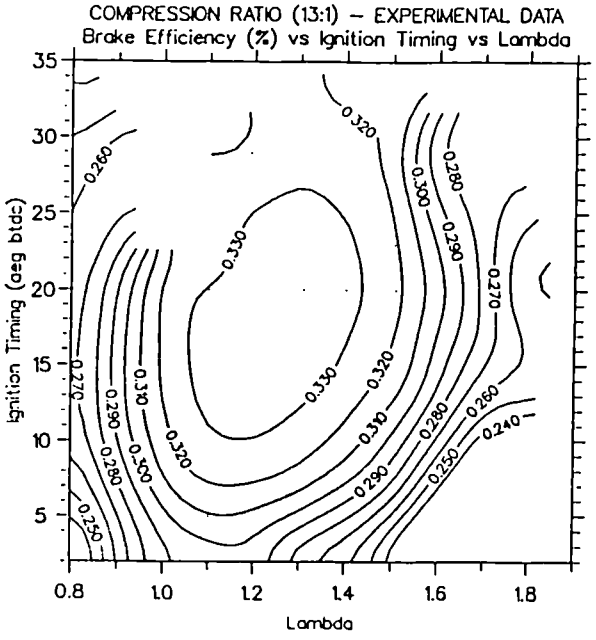

Fig. 4.8c The FBHCR brake efficiency (%) with a compression ratio of 13.0, as a function of the air fuel ratio and the ignition timing.

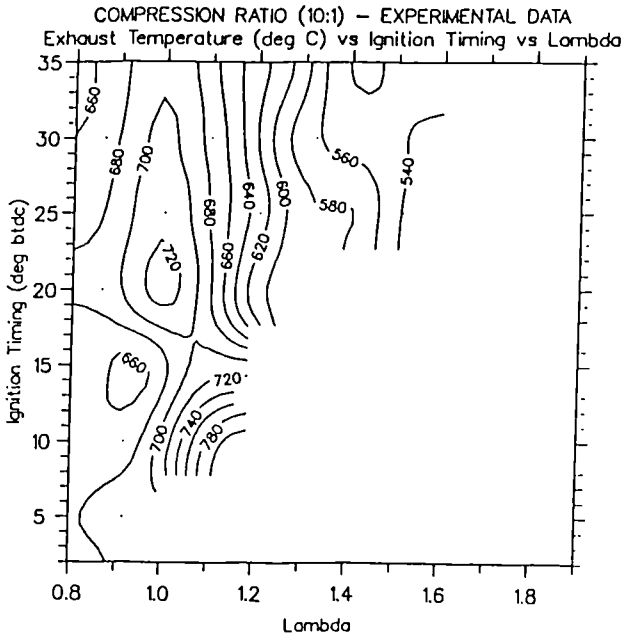

Fig. 4.9a The baseline exhaust temperature (°C) with a compression ratio of 10.3, as a function of the air fuel ratio and the ignition timing.

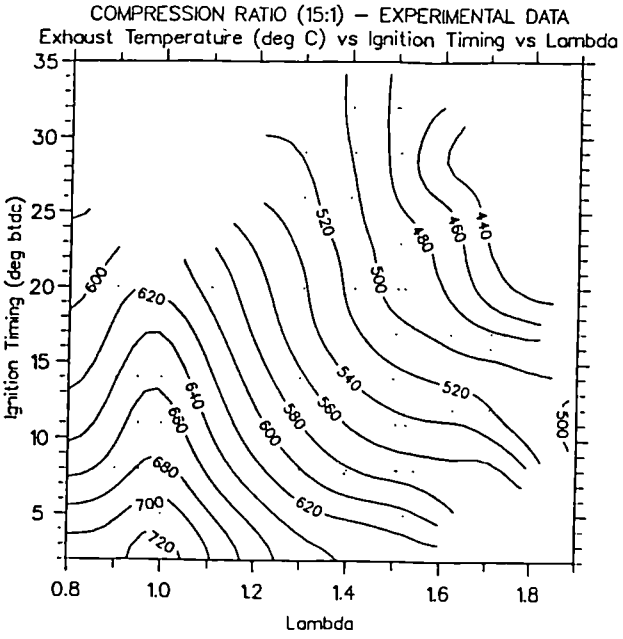

Fig. 4.9b The FBHCR exhaust temperature (°C) with a compression ratio of 14.7, as a function of the air fuel ratio and the ignition timing.

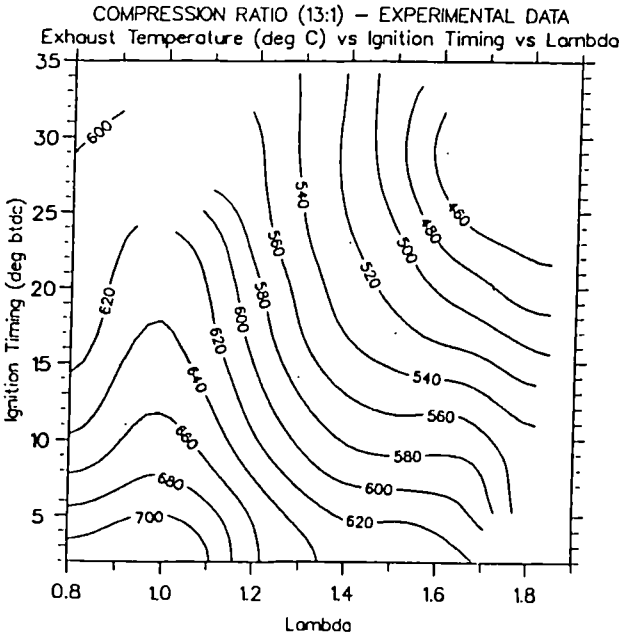

Fig. 4.9c The FBHCR exhaust temperature (°C) with a compression ratio of 13.0, as a function of the air fuel ratio and the ignition timing.

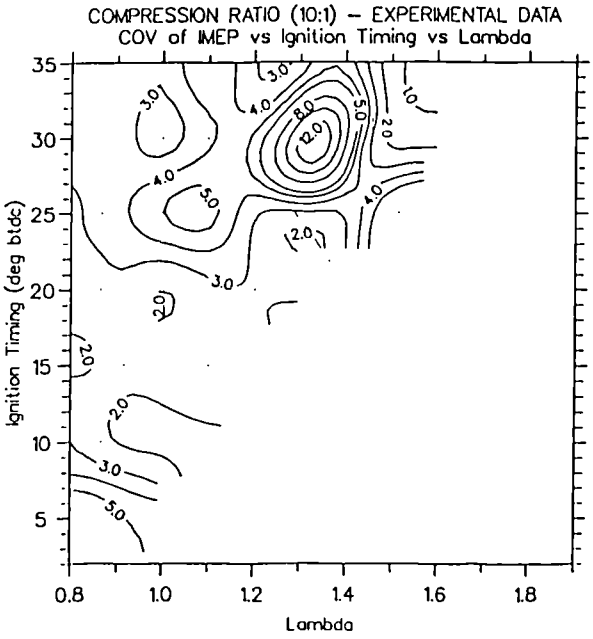

Fig. 4.10a The baseline CoV of imep (%) with a compression ratio of 10.3, as a function of the air fuel ratio and the ignition timing.

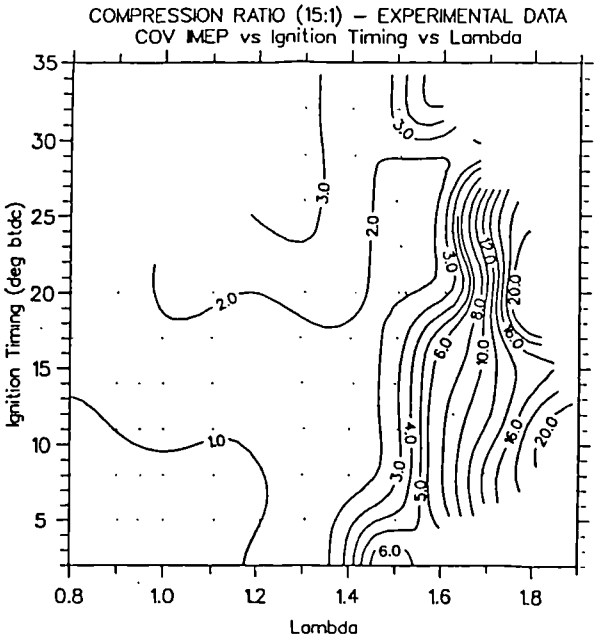

Fig. 4.10b The FBHCR CoV of imep (%) with a compression ratio of 14.7, as a function of the air fuel ratio and the ignition timing.

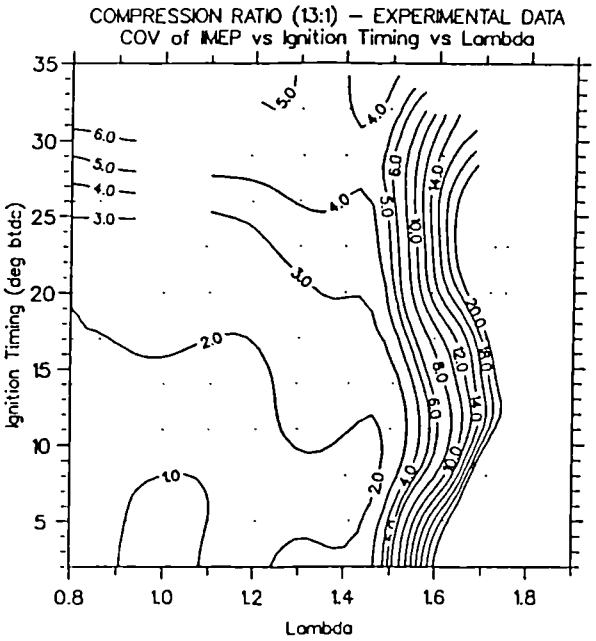

Fig. 4.10c The FBHCR CoV of imep (%) with a compression ratio of 13.0, as a function of the air fuel ratio and the ignition timing.

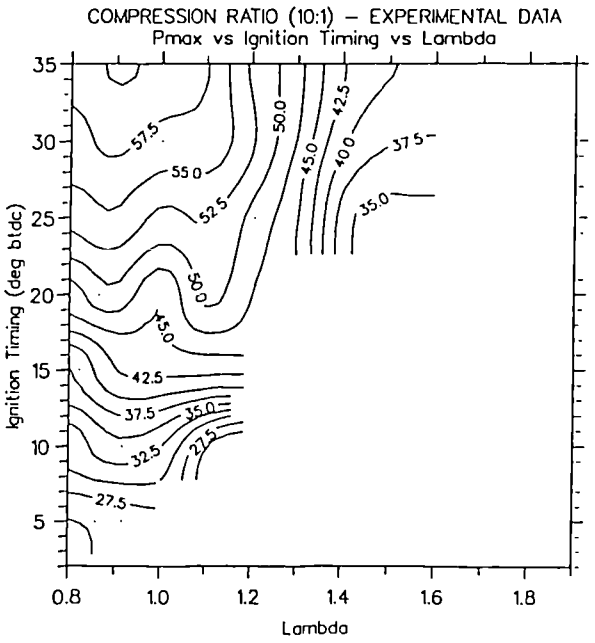

Fig. 4.11a The baseline maximum pressure (bar) with a compression ratio of 10.3, as a function of the air fuel ratio and the ignition timing.

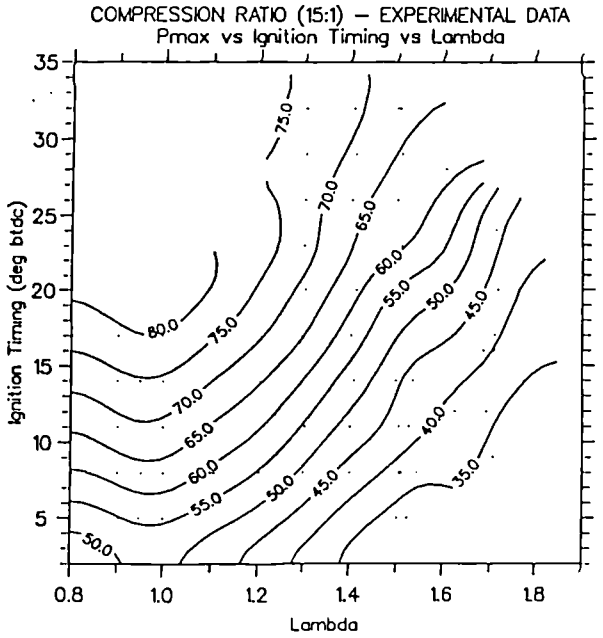

Fig. 4.11b The FBHCR maximum pressure (bar) with a compression ratio of 14.7, as a function of the air fuel ratio and the ignition timing.

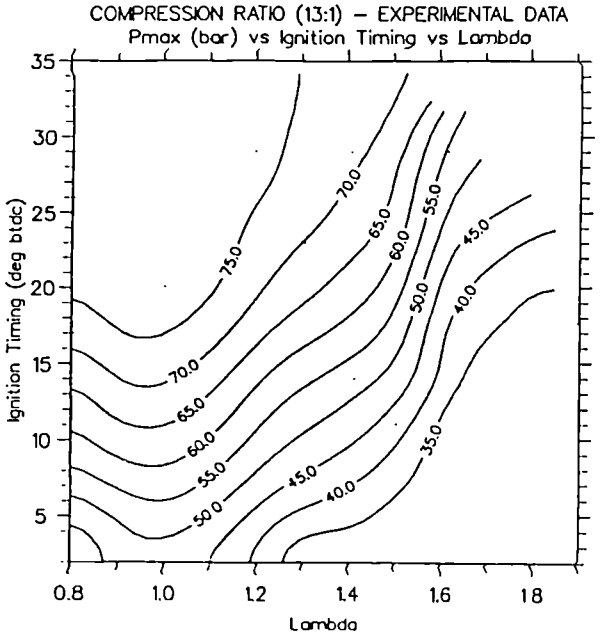

Fig. 4.11c The FBHCR maximum pressure (bar) with a compression ratio of 13.0, as a function of the air fuel ratio and the ignition timing.

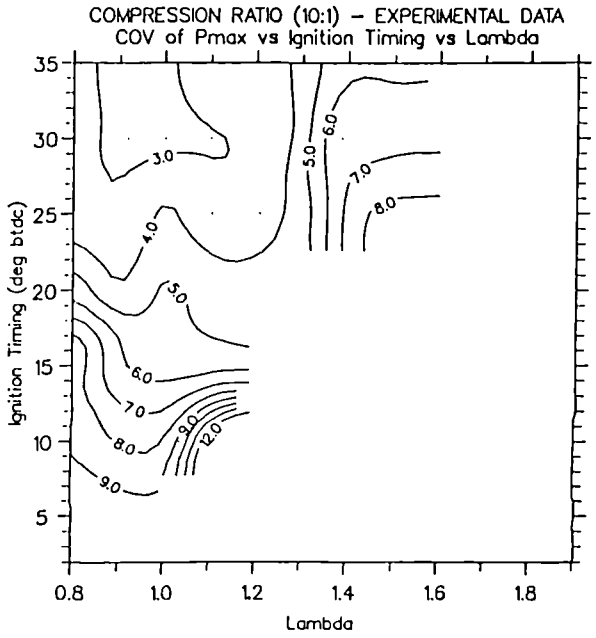

Fig. 4.12a The baseline CoV of maximum pressure (%) with a compression ratio of 10.3, as a function of the air fuel ratio and the ignition timing.

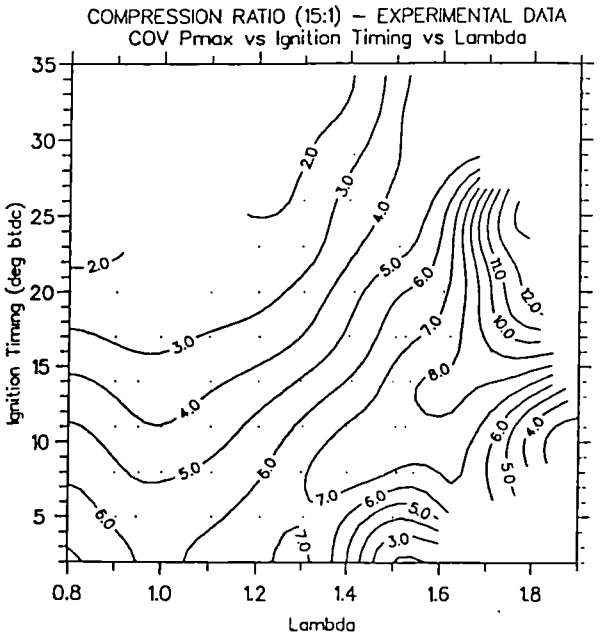

Fig. 4.12b The FBHCR CoV of maximum pressure (%) with a compression ratio of 14.7, as a function of the air fuel ratio and the ignition timing.

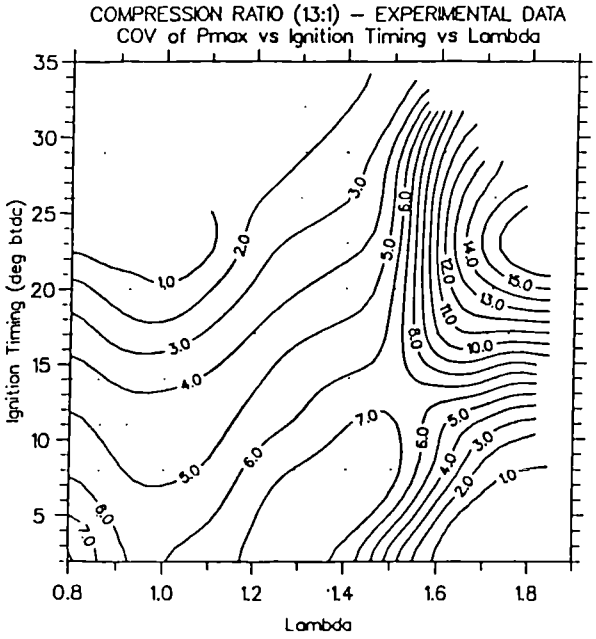

Fig. 4.12c The FBHCR CoV of maximum pressure (%) with a compression ratio of 13.0, as a function of the air fuel ratio and the ignition timing.

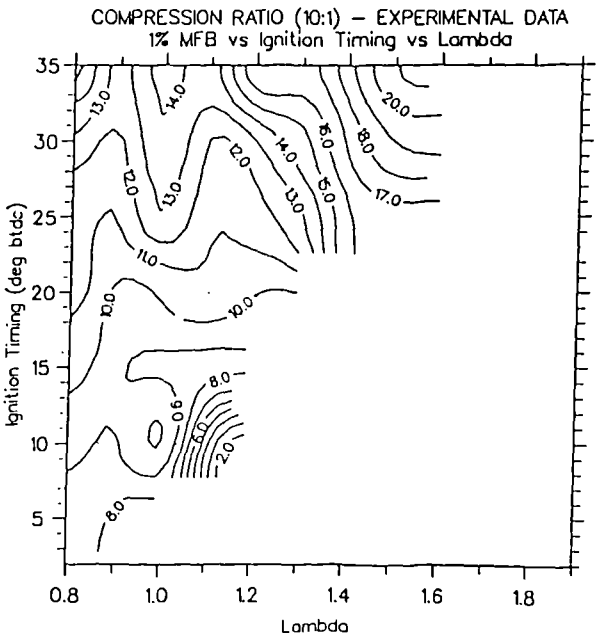

Fig. 4.13a The baseline 0-1% burn duration (°ca) with a compression ratio of 10.3, as a function of the air fuel ratio and the ignition timing.

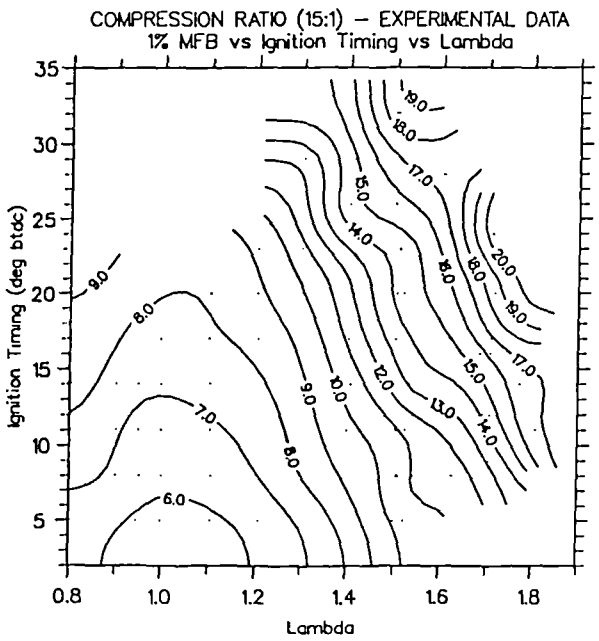

Fig. 4.13b The FBHCR 0-1% burn duration (°ca) with a compression ratio of 14.7, as a function of the air fuel ratio and the ignition timing.

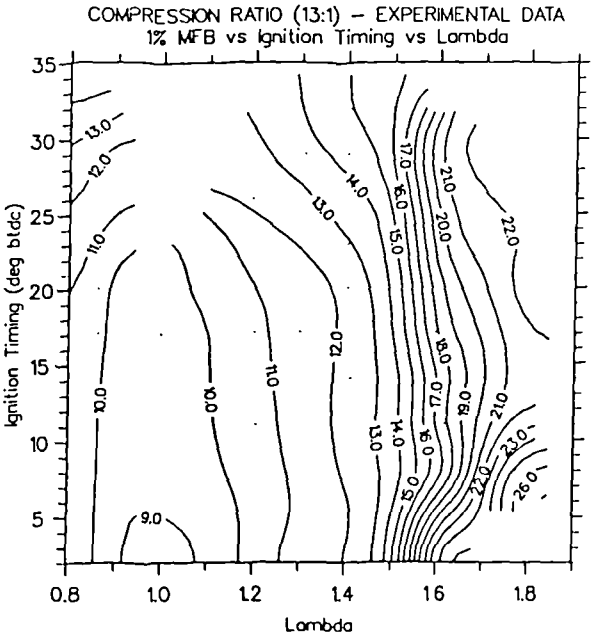

Fig. 4.13c The FBHCR 0-1% burn duration (°ca) with a compression ratio of 13.0, as a function of the air fuel ratio and the ignition timing.

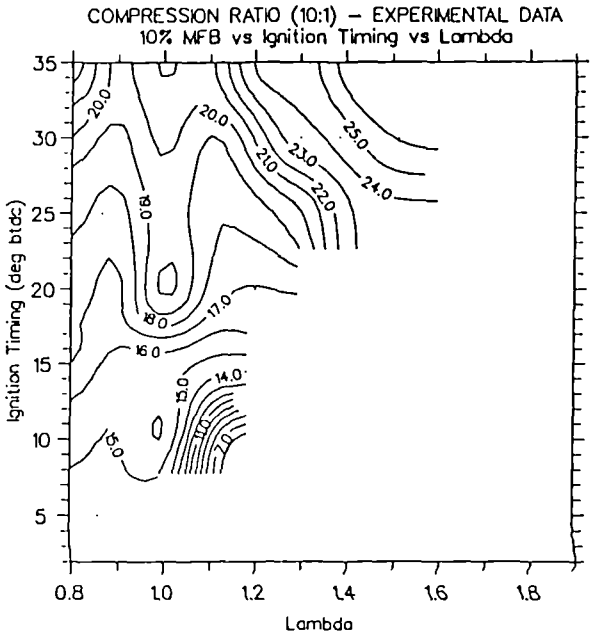

Fig. 4.14a The baseline 0-10% burn duration (°ca) with a compression ratio of 10.3, as a function of the air fuel ratio and the ignition timing.

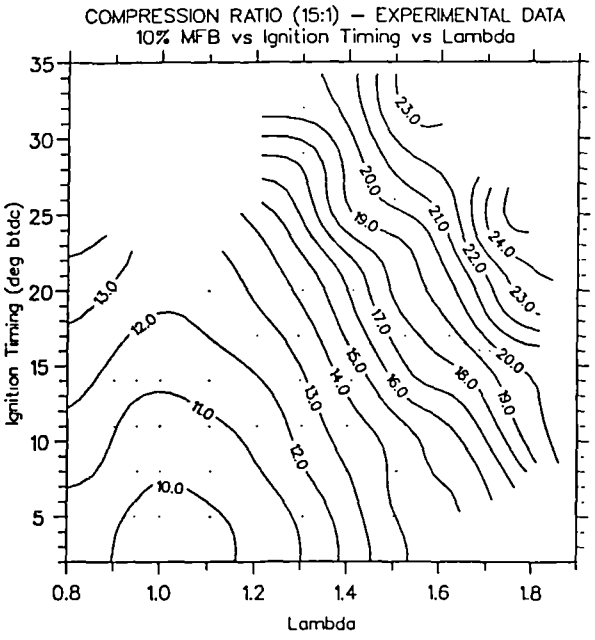

Fig. 4.14b The FBHCR 0-10% burn duration (°ca) with a compression ratio of 14.7, as a function of the air fuel ratio and the ignition timing.

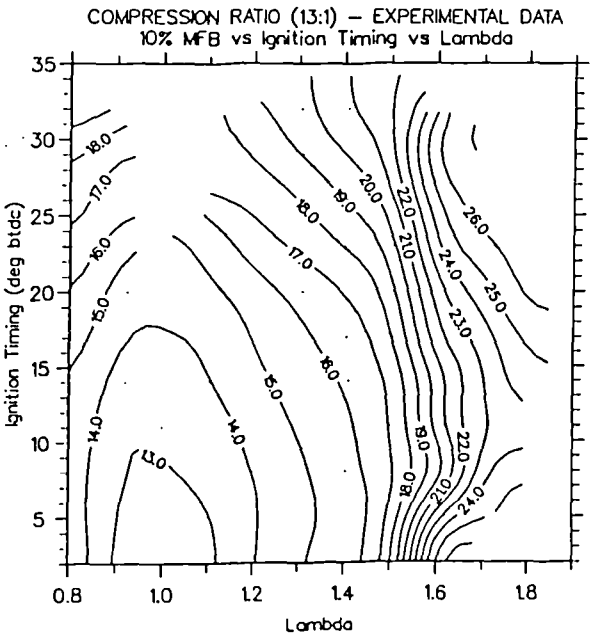

Fig. 4.14c The FBHCR 0-10% burn duration (°ca) with a compression ratio of 13.0, as a function of the air fuel ratio and the ignition timing

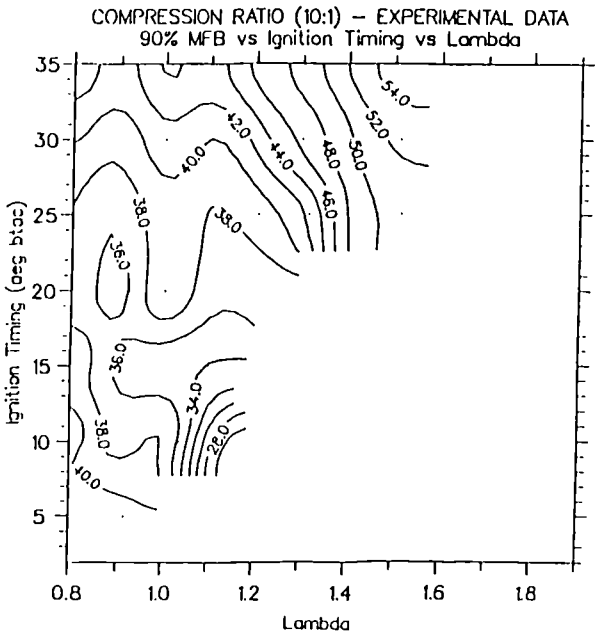

Fig. 4.15a The baseline 0-90% burn duration (°ca) with a compression ratio of 10.3, as a function of the air fuel ratio and the ignition timing.

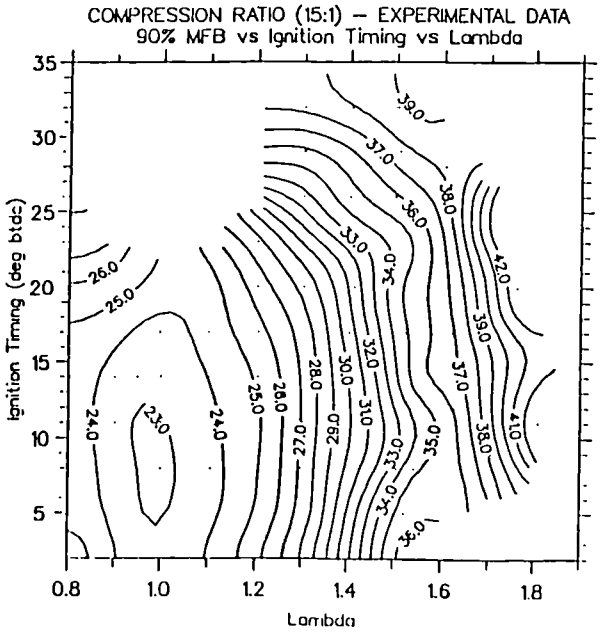

Fig. 4.15b The FBHCR 0-90% burn duration (°ca) with a compression ratio of 14.7, as a function of the air fuel ratio and the ignition timing.

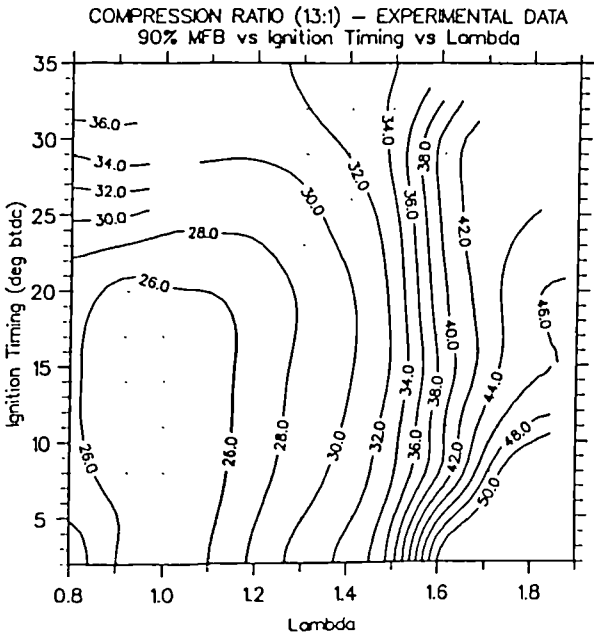

Fig. 4.15c The FBHCR 0-90% burn duration (ca) with a compression ratio of 13 0, as a function of the air fuel ratio and the ignition timing.

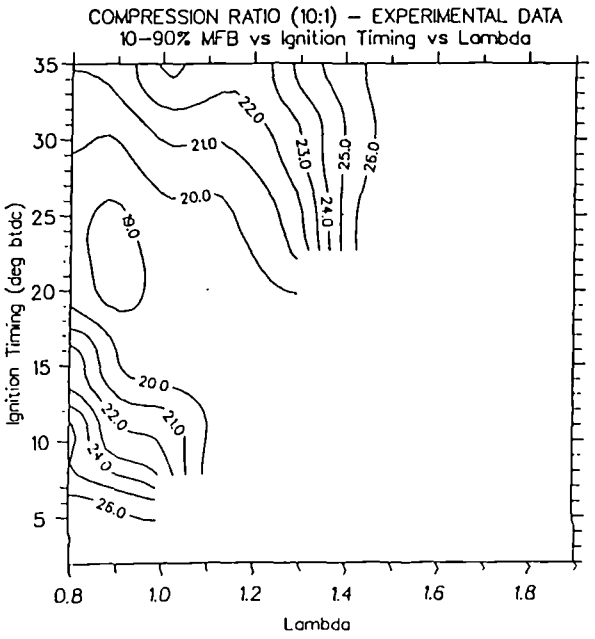

Fig. 4.16a The baseline 10-90% burn duration (°ca) with a compression ratio of 10.3. as a function of the air fuel ratio and the ignition timing.

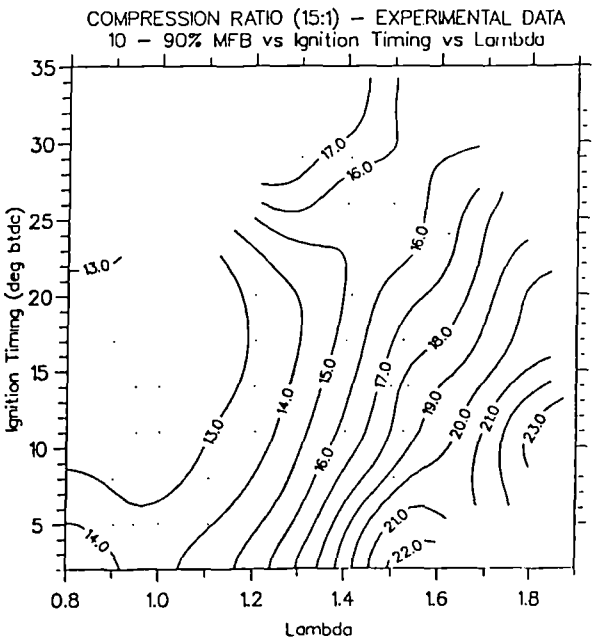

Fig. 4.16b The FBHCR 10-90% burn duration (°ca) with a compression ratio of 14.7, as a function of the air fuel ratio and the ignition timing.

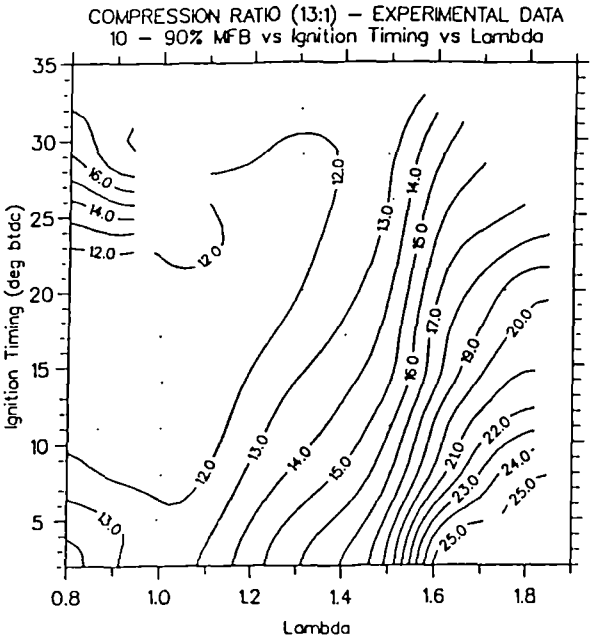

Fig. 4.16c The FBHCR 10-90% burn duration (°ca) with a compression ratio of 13.0, as a function of the air fuel ratio and the ignition timing.

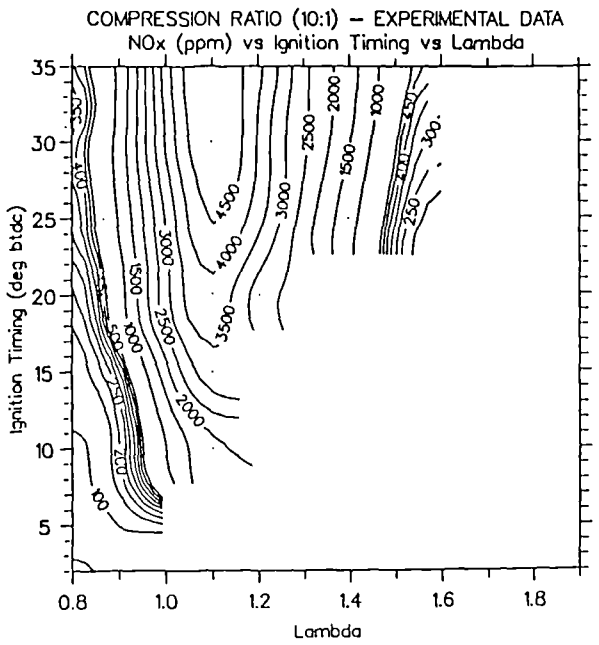

Fig. 4.17a The baseline volumetric NOx emissions (ppm) with a compression ratio of 10.3, as a function of the air fuel ratio and the ignition timing.

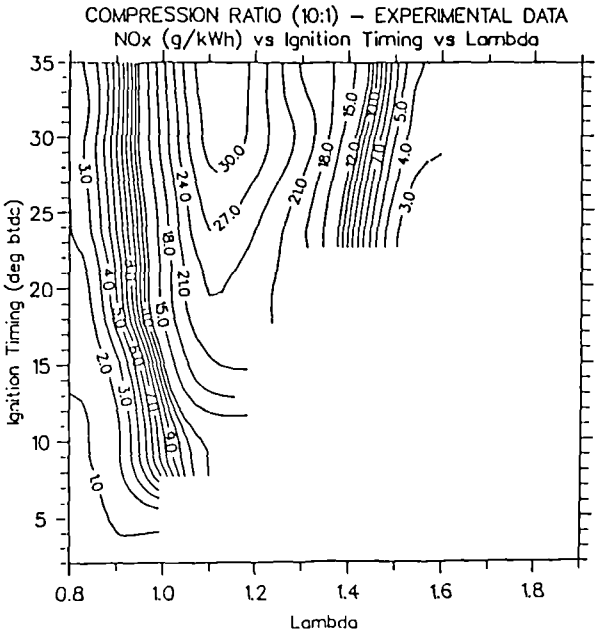

Fig. 4.17b The baseline gravimetric NOx emissions (g/kWh).

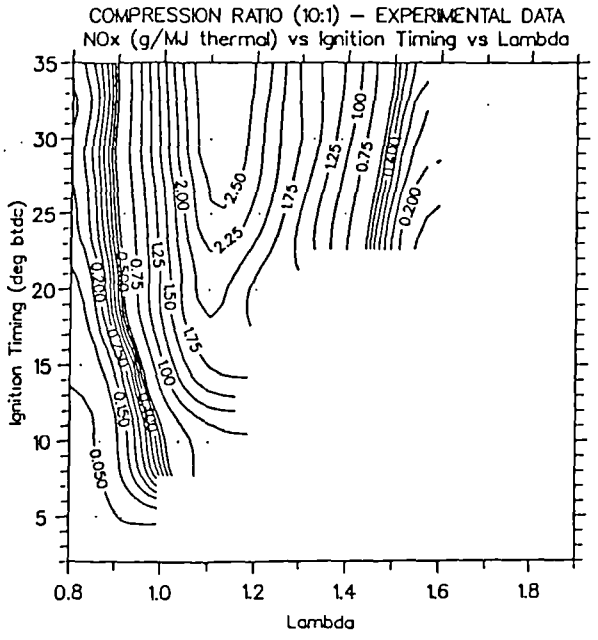

Fig. 4.17c The baseline gravimetric NOx emissions (g/MJ thermal).

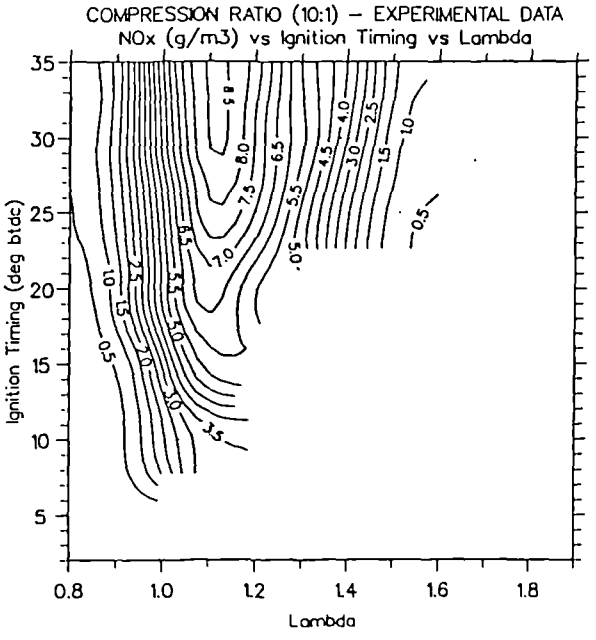

Fig. 4.17d The baseline NOx emissions (g/m^3).

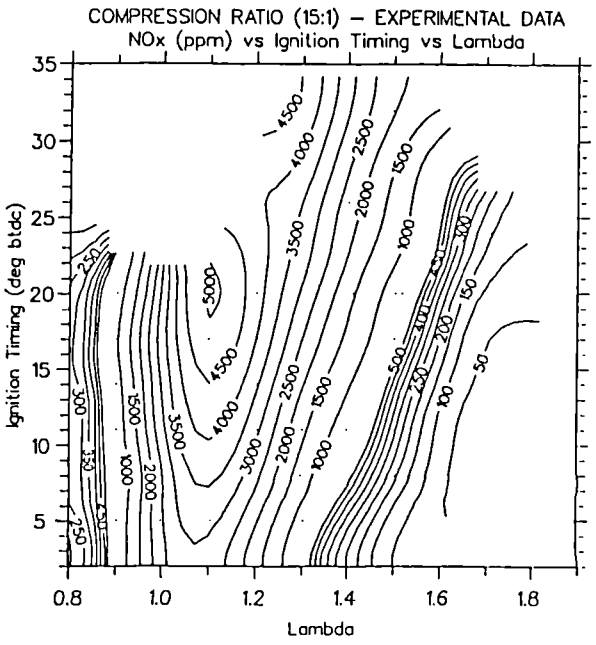

Fig. 4.18a The FBHCR volumetric NOx emissions (ppm) with a compression ratio of 14.7, as a function of the air fuel ratio and the ignition timing.

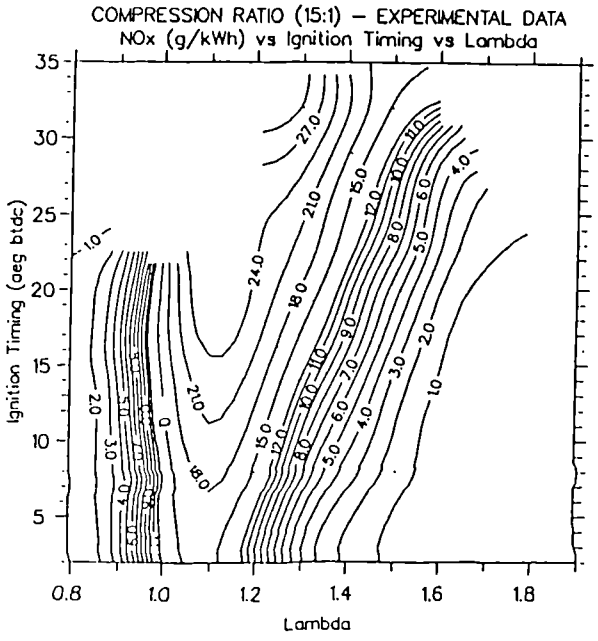

Fig. 4.18b The FBHCR gravimetric NOx emissions (g/kWh).

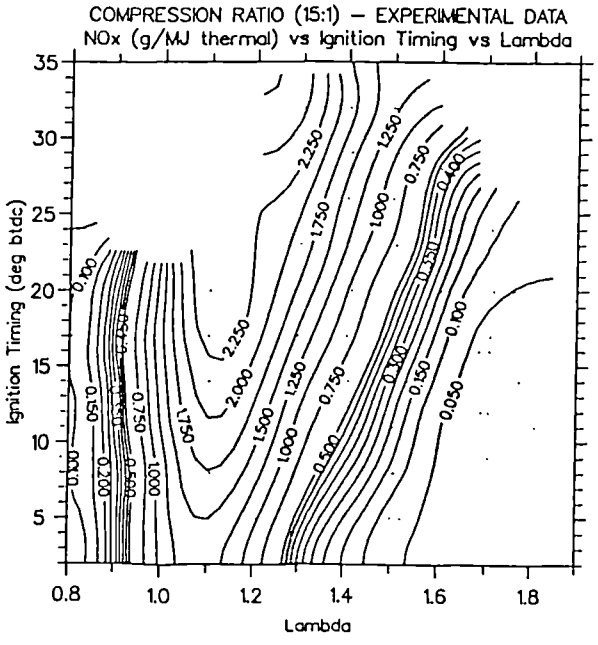

Fig. 4.18c The FBHCR gravimetric NOx emissions (g/MJ thermal).

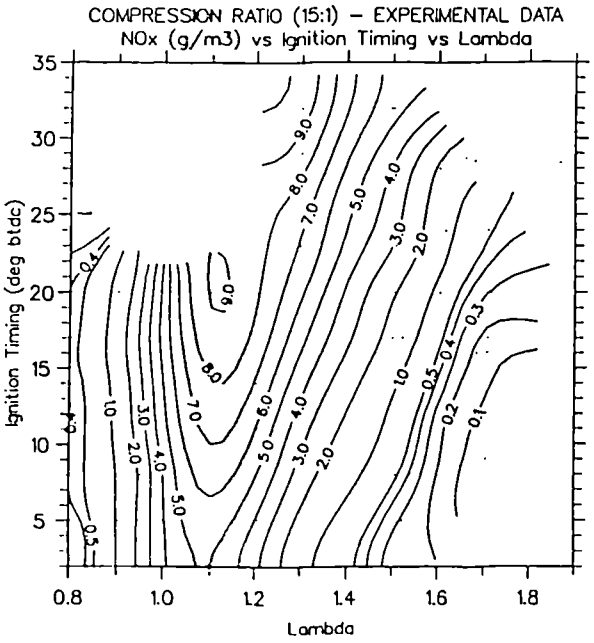

Fig. 4.18d The FBHCR NOx emissions (g/m^3).

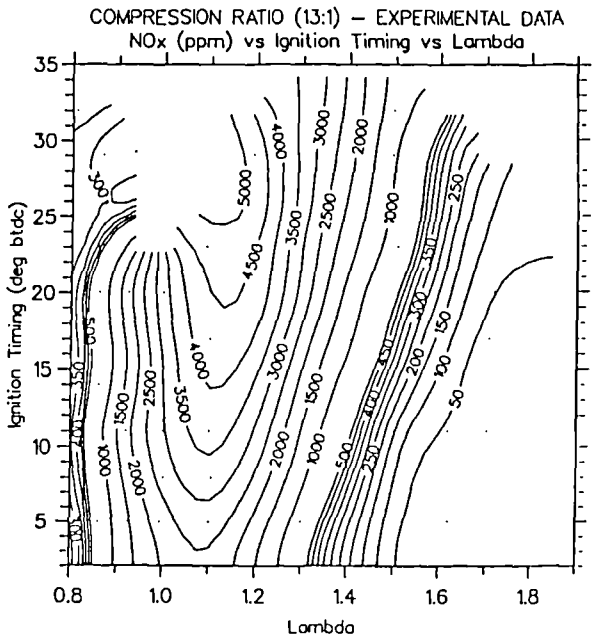

Fig. 4.19a The FBHCR volumetric NOx emissions (ppm) with a compression ratio of 13.0, as a function of the air fuel ratio and the ignition timing.

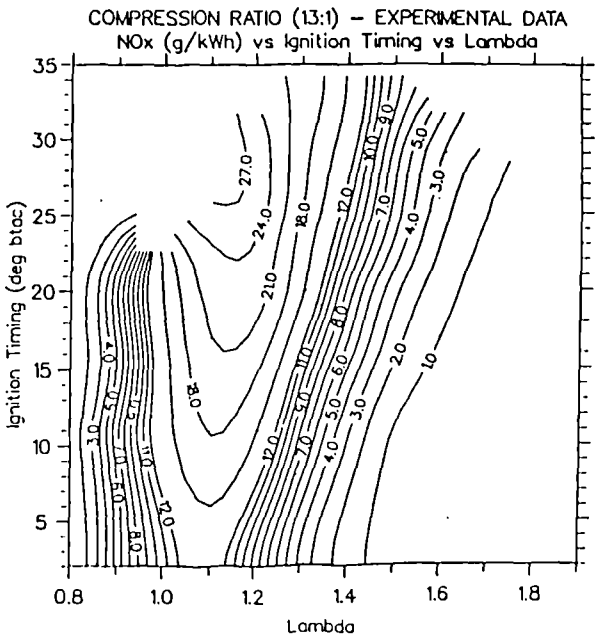

Fig. 4.19b The FBHCR gravimetric NOx emissions (g/kWh).

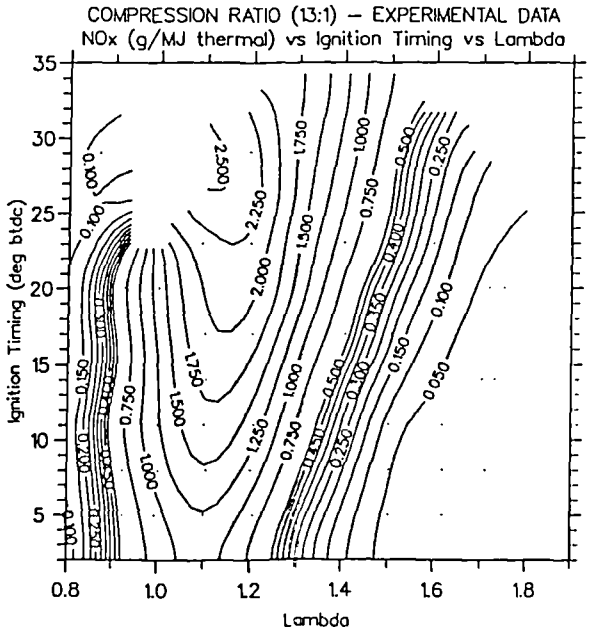

Fig. 4.19c The FBHCR gravimetric NOx emissions (g/MJ thermal).

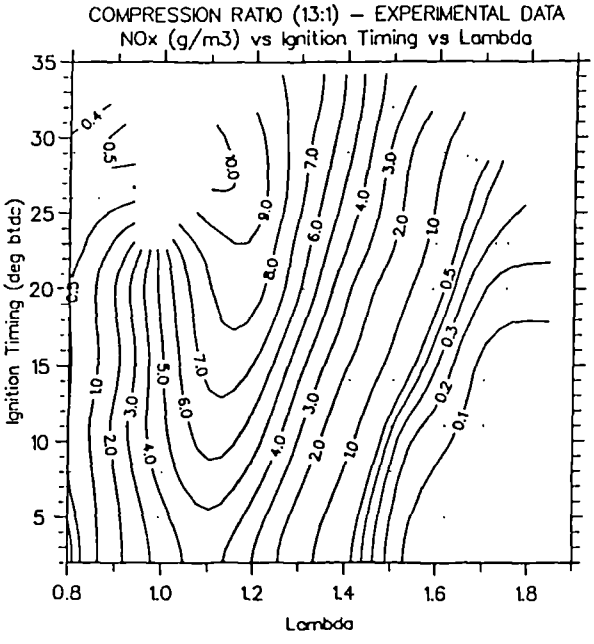

Fig. 4.19d The FBHCR NOx emissions (g/m^3).

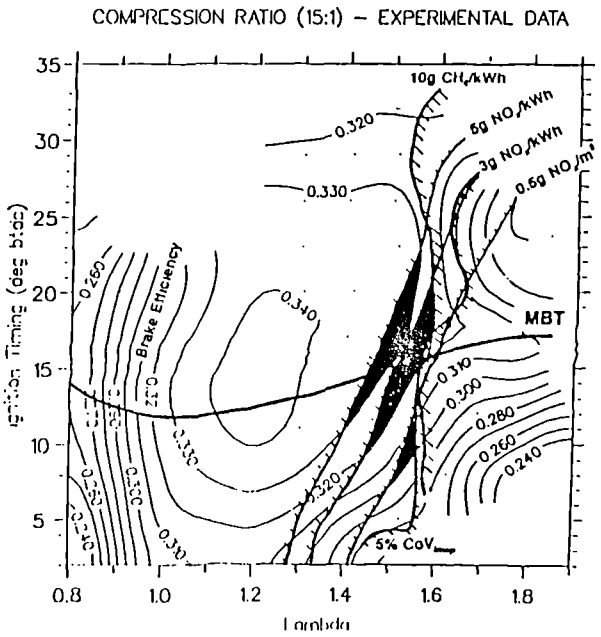

Fig. 4.20 Identifying operating windows with the FBHCR 14.7:1 compression ratio, within typical operational and emissions constraints.

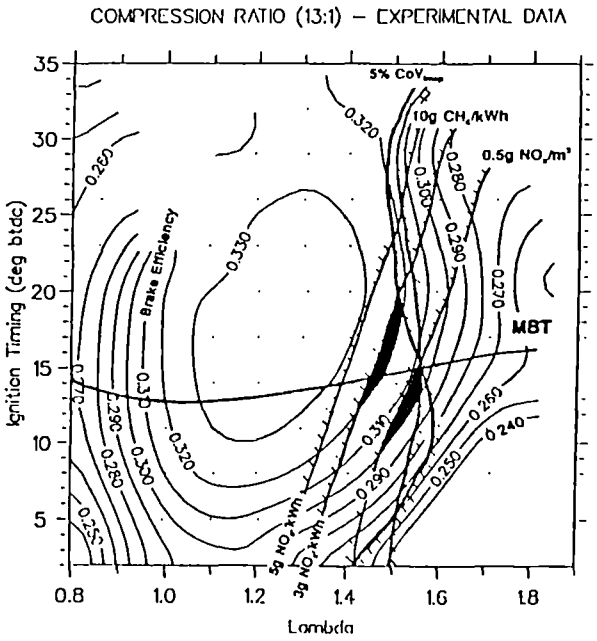

Fig. 4.21 Identifying operating windows with the FBHCR 13.0:1 compression ratio, within typical operational and emissions constraints.

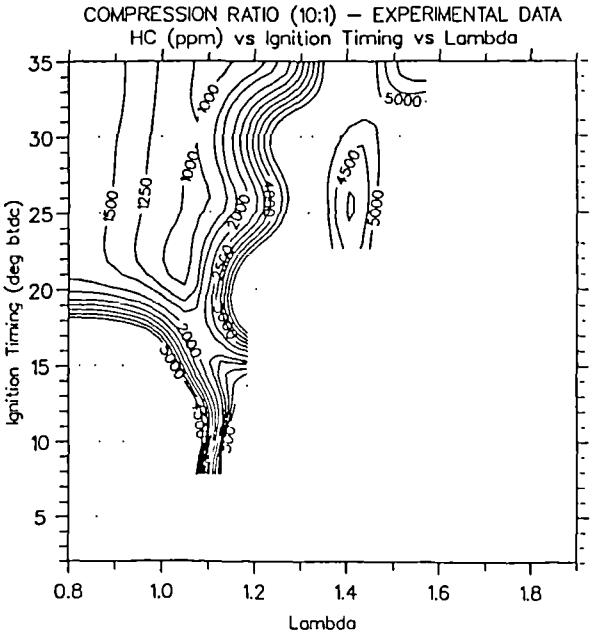

Fig. 4.22a The baseline volumetric hydrocarbon emissions (ppm) with a compression ratio of 10.3, as a function of the air fuel ratio and the ignition timing.

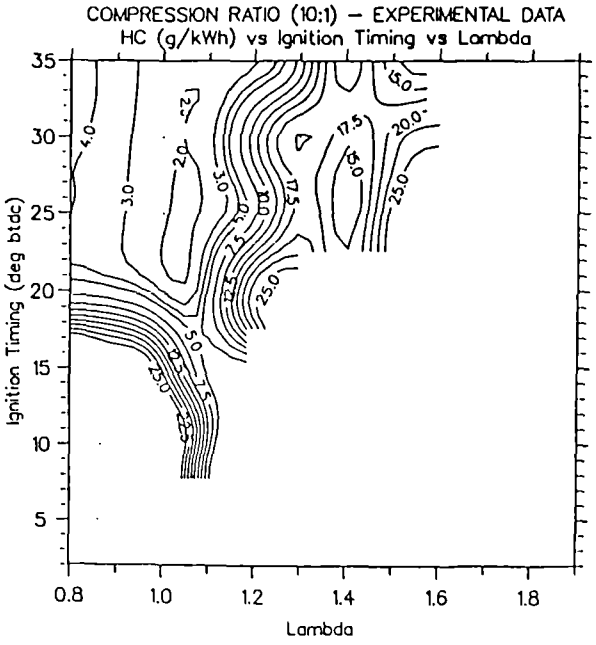

Fig. 4.22b The baseline gravimetric hydrocarbon emissions (g/kWh).

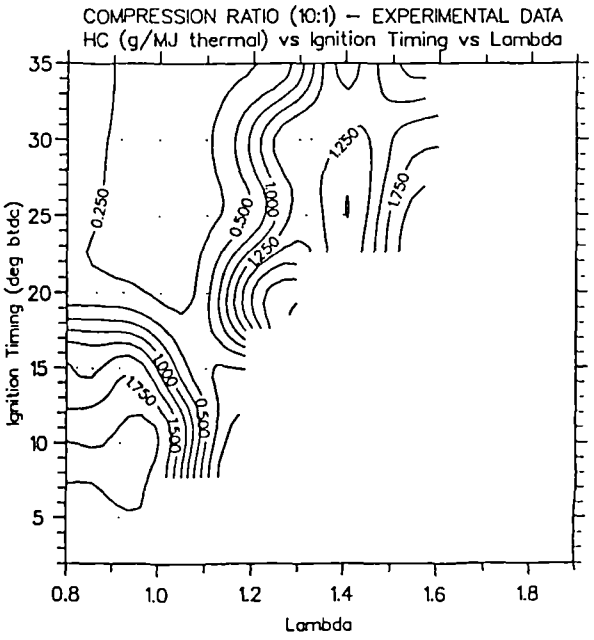

Fig. 4.22c The baseline gravimetric hydrocarbon emissions (g/MJ thermal).

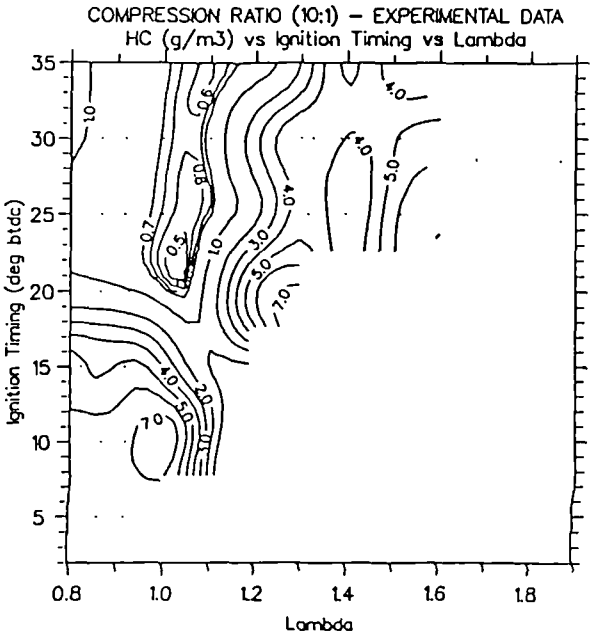

Fig. 4.22d The baseline hydrocarbon emissions (g/m^3).

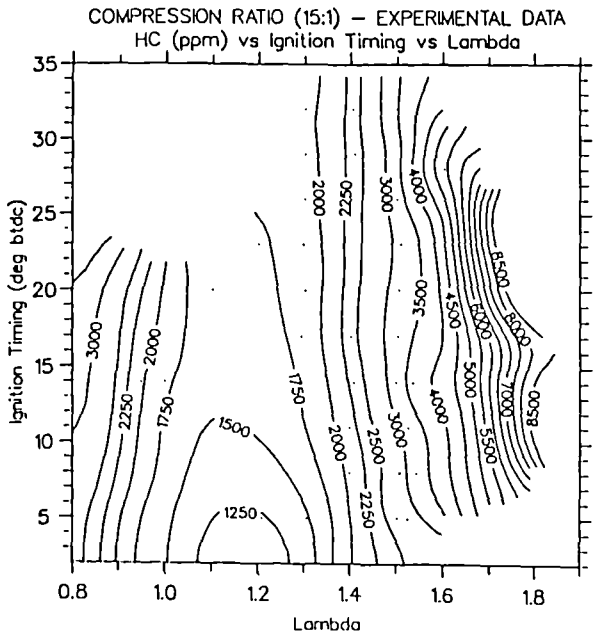

Fig. 4.23a The FBHCR volumetric hydrocarbon emissions (ppm) with a compression ratio of 14.7, as a function of the air fuel ratio and the ignition timing.

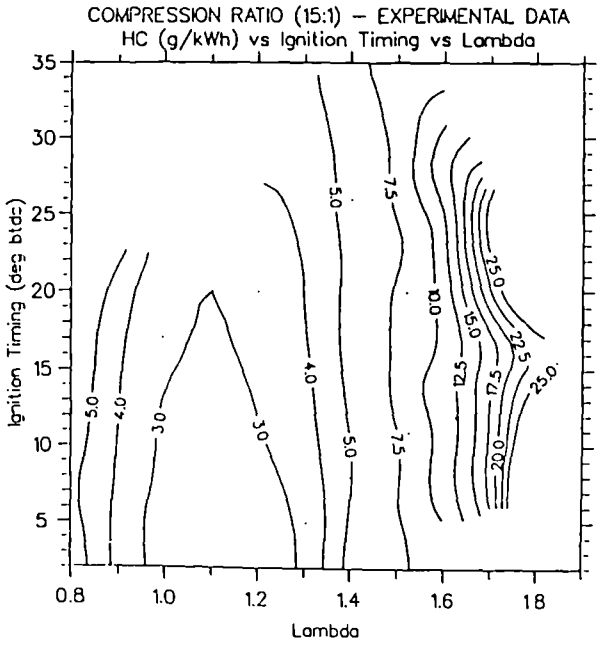

Fig. 4.23b The FBHCR gravimetric hydrocarbon emissions (g/kWh).

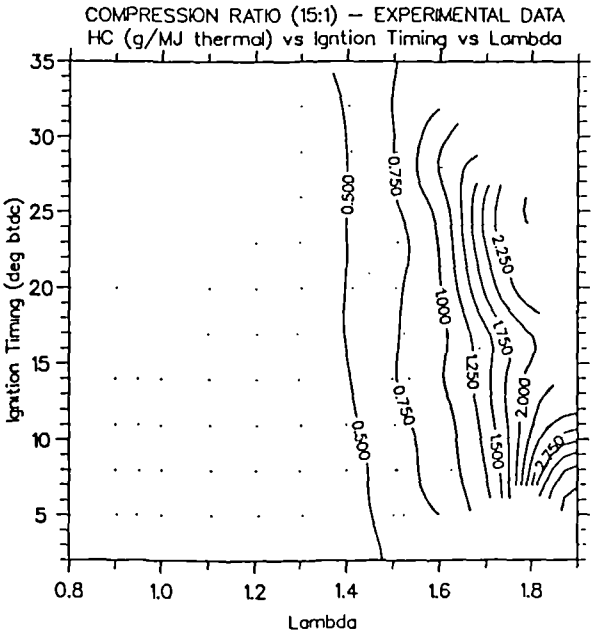

Fig. 4.23c The FBHCR gravimetric hydrocarbon emissions (g/MJ thermal).

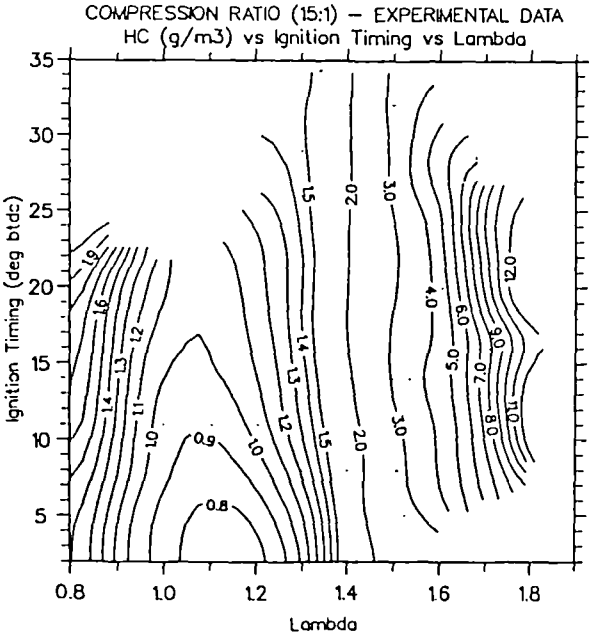

Fig. 4.23d The FBHCR hydrocarbon emissions (g/m^3).

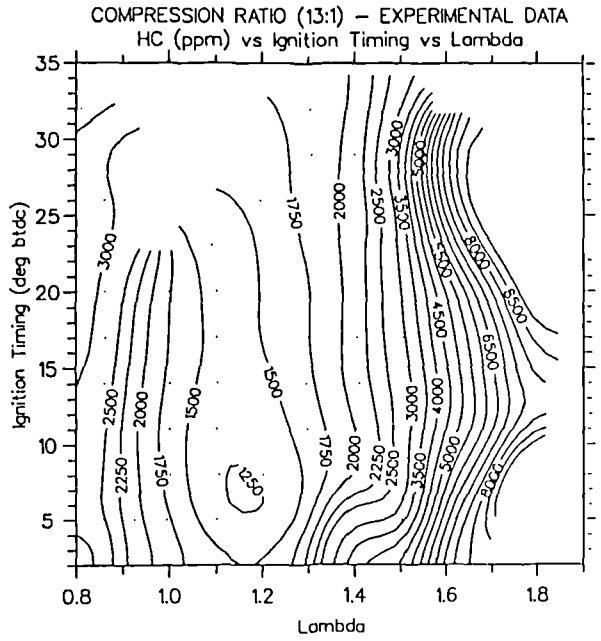

Fig. 4.24a The FBHCR volumetric hydrocarboon emissions (ppm) with a compression ratio of 13.0, as a function of the air fuel ratio and the ignition timing.

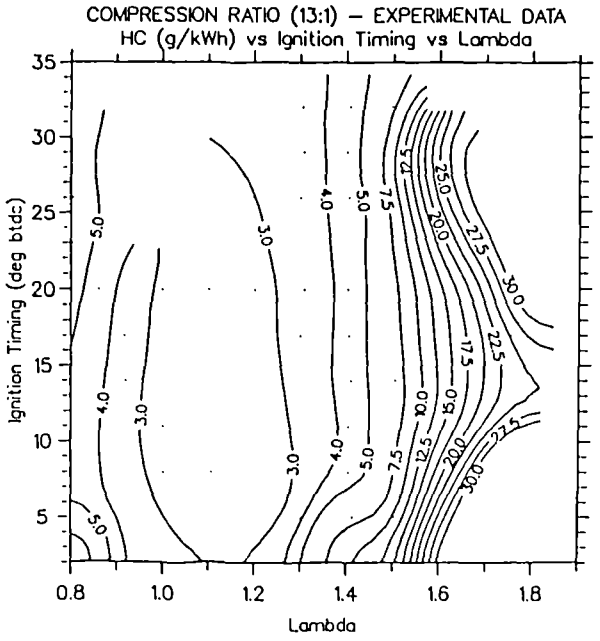

Fig. 4.24b The FBHCR gravimetric hydrocarbon emissions (g/kWh).

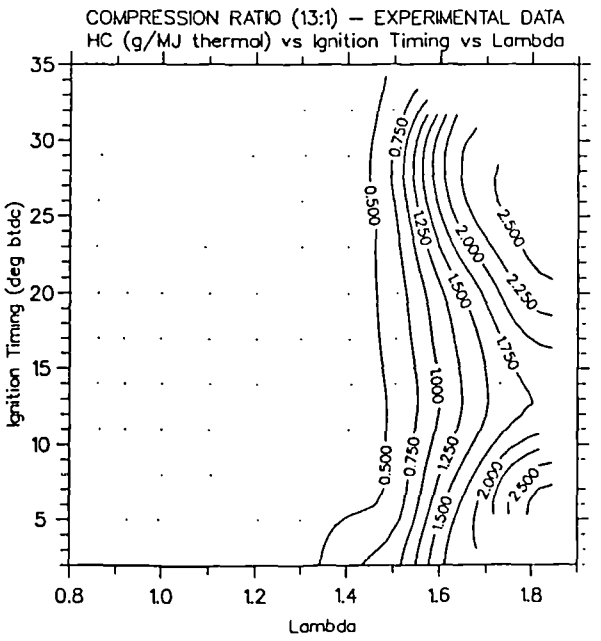

Fig. 4.24c The FBHCR gravimetric hydrocarbon emissions (g/MJ thermal).

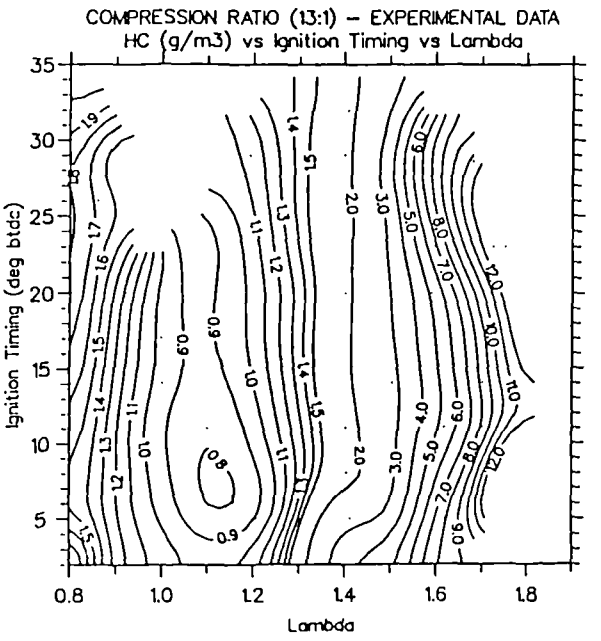

Fig. 4.24d The FBHCR hydrocarbon emissions (g/m^3).

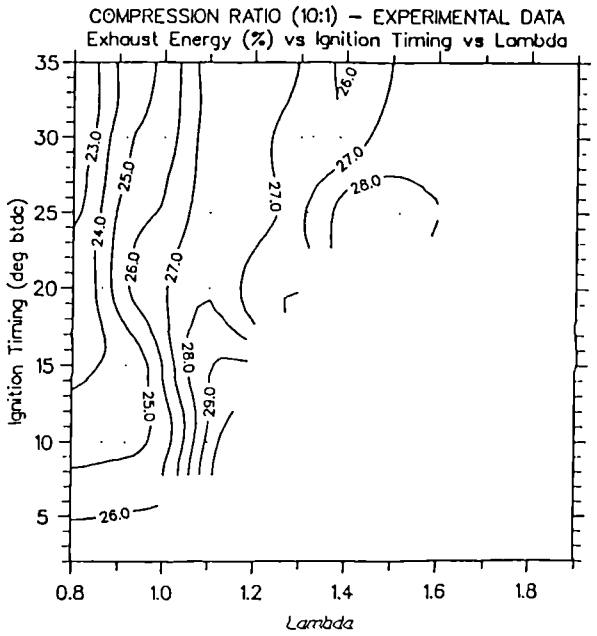

Fig. 4.25a The baseline exhaust energy (%) as a function of the air fuel ratio and the ignition timing.

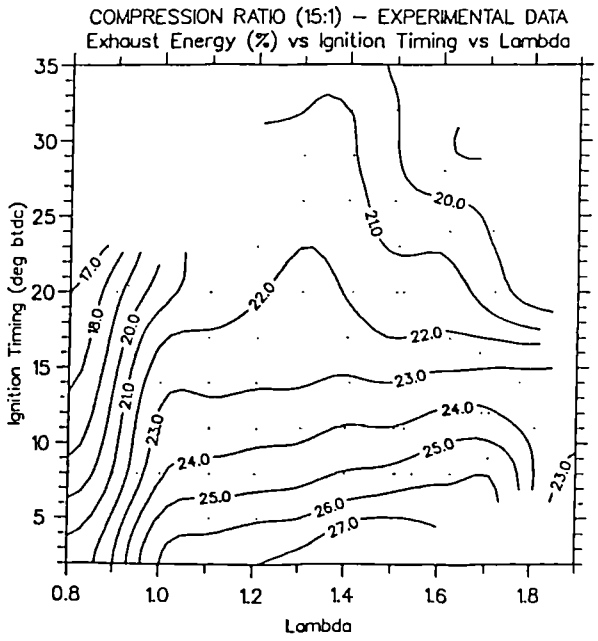

Fig. 4.25b The FBHCR exhaust energy (%) with a compression ratio of 14.7, as a function of the air fuel ratio and the ignition timing.

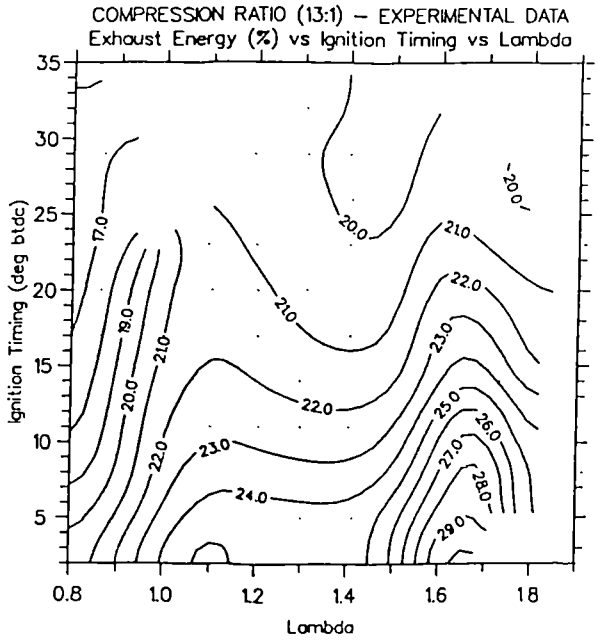

Fig. 4.25c The FBHCR exhaust energy (%) with a compression ratio of 13.0, as a function of the air fuel ratio and the ignition timing.

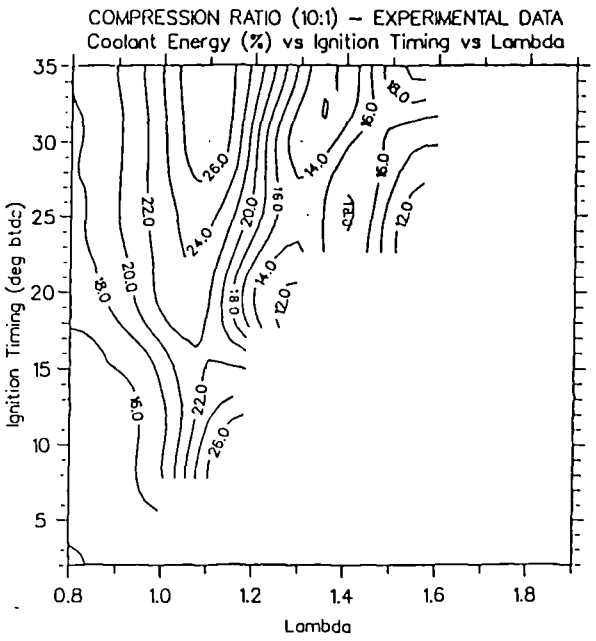

Fig. 4.26a The baseline coolant energy (%) as a function of the air fuel ratio and the ignition timing.

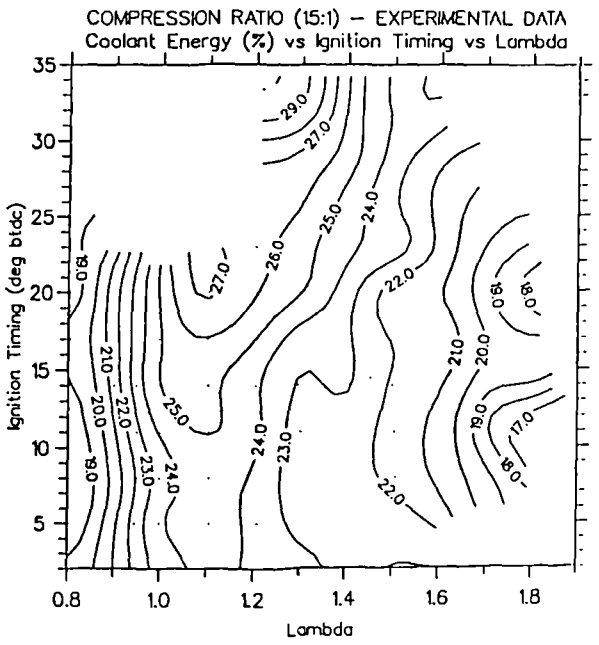

Fig. 4.26b The FBHCR coolant energy (%) with a compression ratio of 14.7, as a function of the air fuel ratio and the ignition timing.

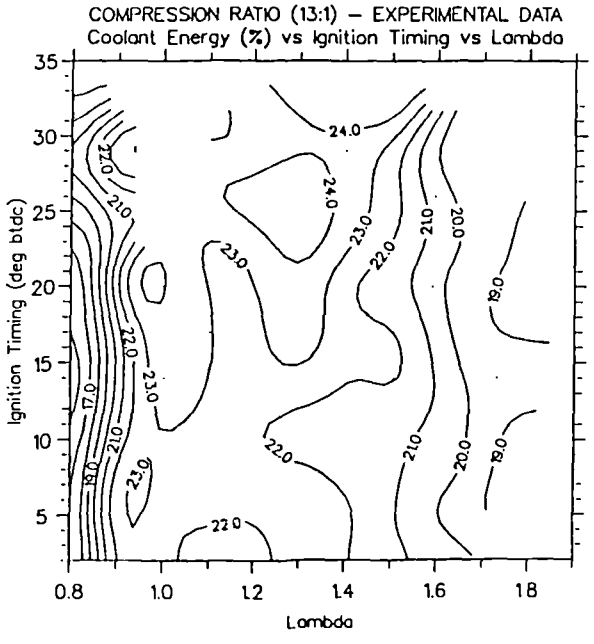

Fig. 4.26c The FBHCR coolant energy (%) with a compression ratio of 13.0, as a function of the air fuel ratio and the ignition timing.

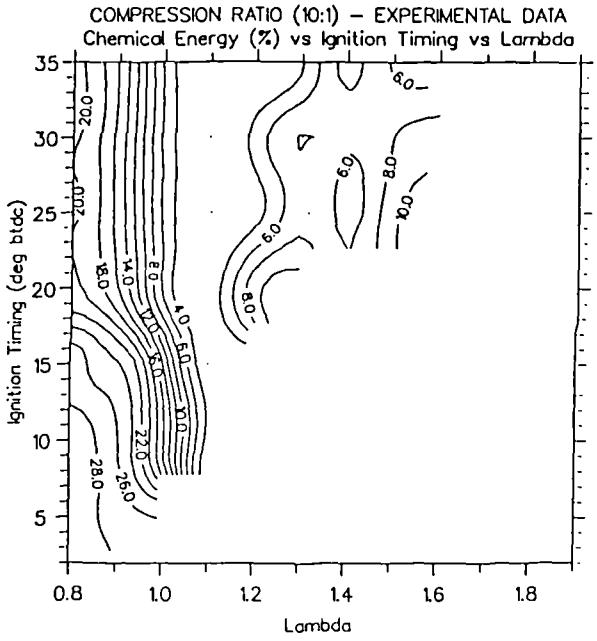

Fig. 4.27a The baseline exhaust chemical energy (%) as a function of the air fuel ratio and the ignition timing.

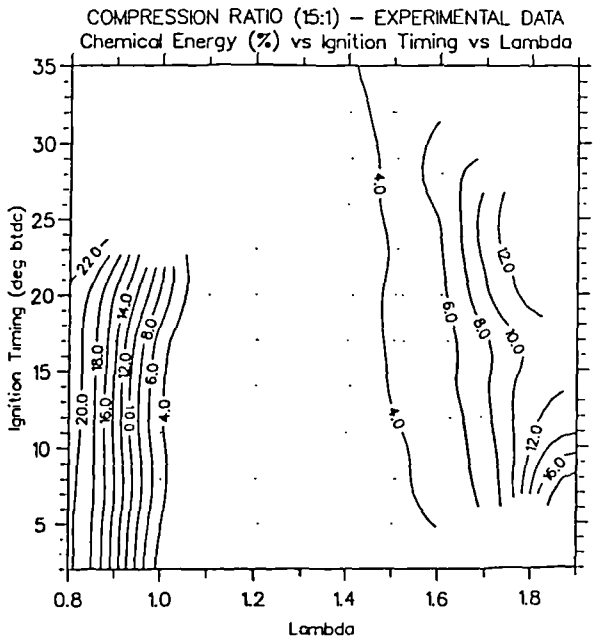

Fig. 4.27b The FBHCR exhaust chemical energy (%) with a compression ratio of 14.7, as a function of the air fuel ratio and the ignition timing.

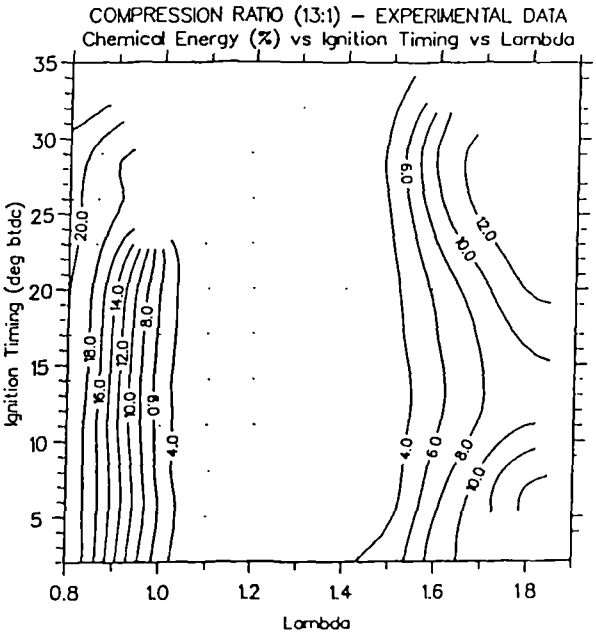

Fig. 4.27c The FBHCR exhaust chemical energy (%) with a compression ratio of 13.0, as a function of the air fuel ratio and the ignition timing.

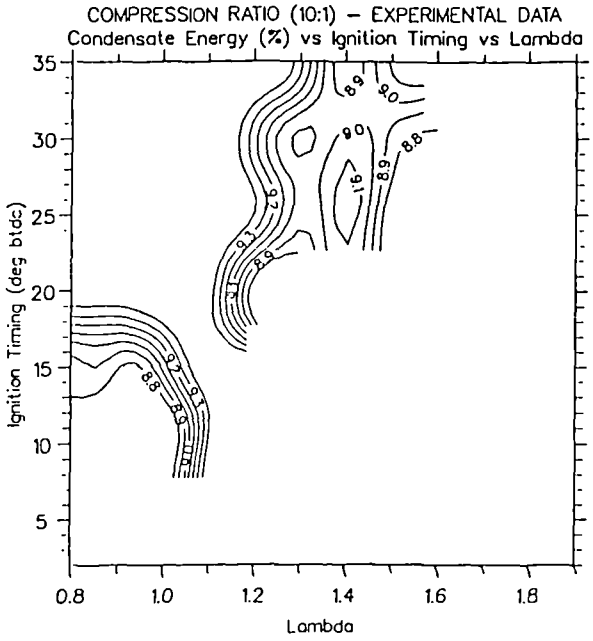

Fig. 4.28a The baseline exhaust condensate energy (%) as a function of the air fuel ratio and the ignition timing.

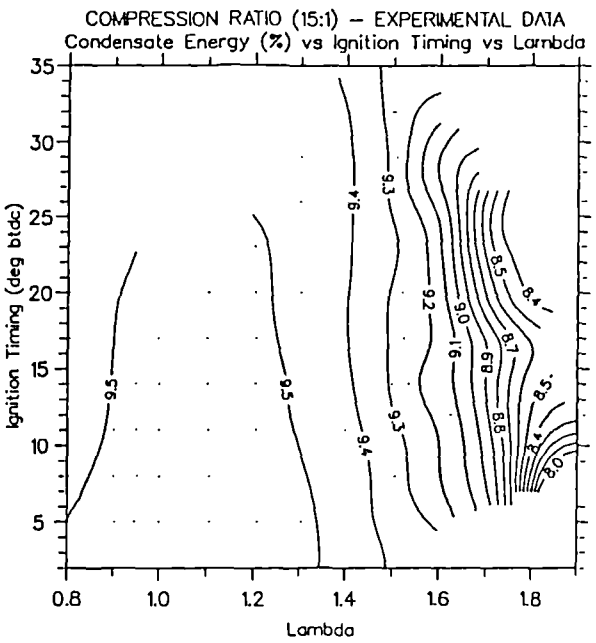

Fig. 4.28b The FBHCR exhaust condensate energy (%) with a compression ratio of 14.7, as a function of the air fuel ratio and the ignition timing.

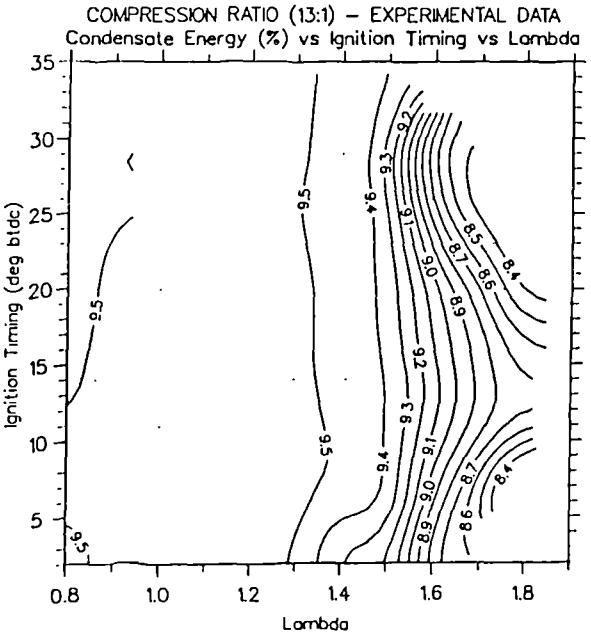

Fig. 4.28c The FBHCR exhaust condensate energy (%) with a compression ratio of 13.0, as a function of the air fuel ratio and the ignition timing.

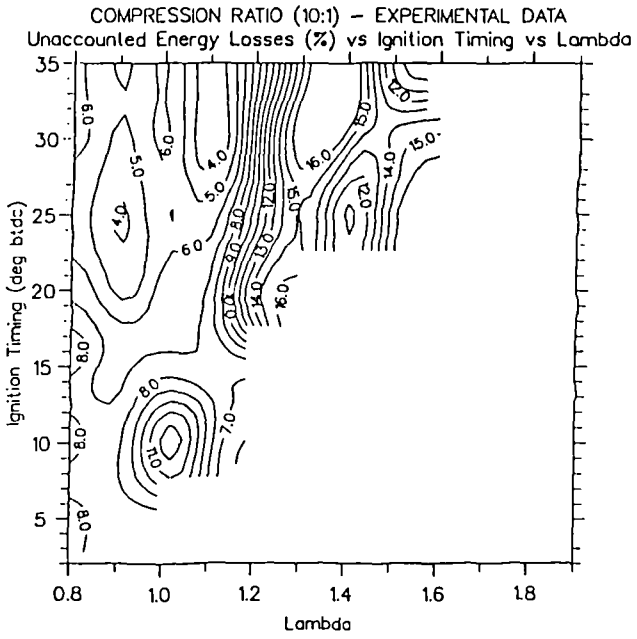

Fig. 4.29a The baseline unaccounted energy (%) as a function of the air fuel ratio and the ignition timing.

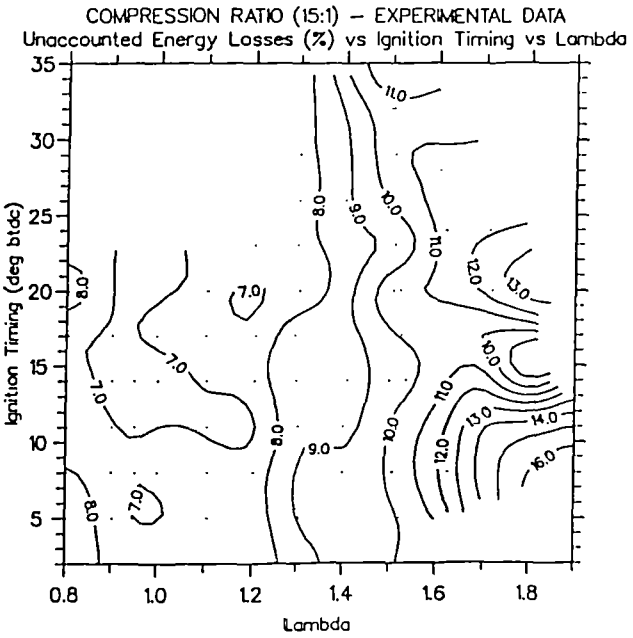

Fig. 4.29b The FBHCR unaccounted energy (%) with a compression ratio of 14.7, as a function of the air fuel ratio and the ignition timing.

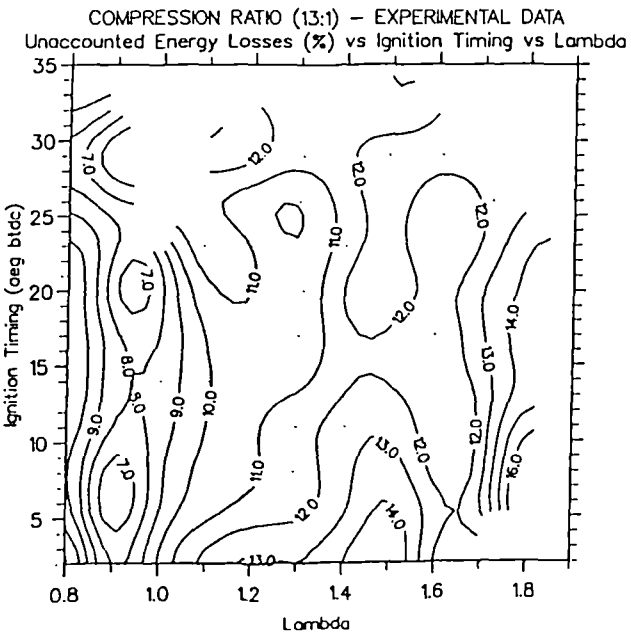

Fig. 4.29c The FBHCR unaccounted energy (%) with a compression ratio of 13.0, as a function of the air fuel ratio and the ignition timing.

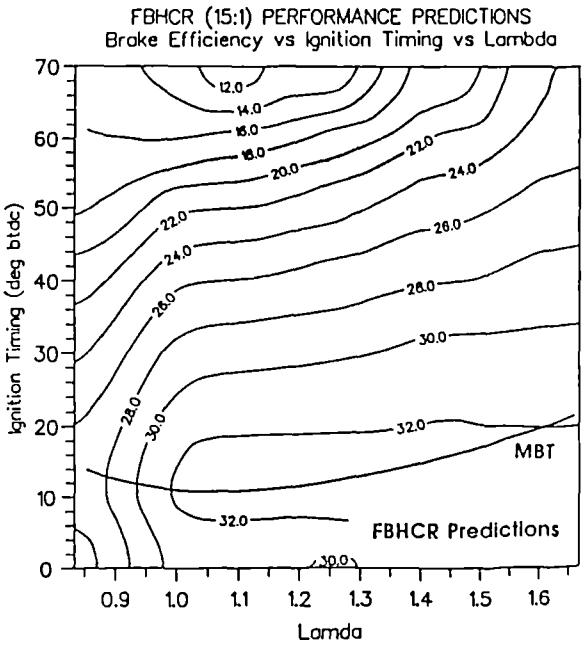

Fig. 5.1 The originally predicted FBHCR brake efficiency (%) with a compression ratio of 14.7, as a function of the air fuel ratio and the ignition timing.

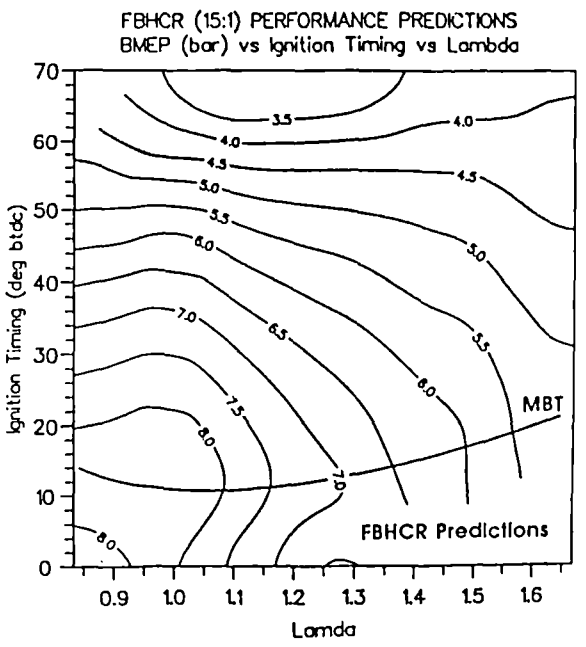

Fig. 5.2 The originally predicted FBHCR bmep (bar) with a compression ratio of 14.7, as a function of the air fuel ratio and the ignition timing.

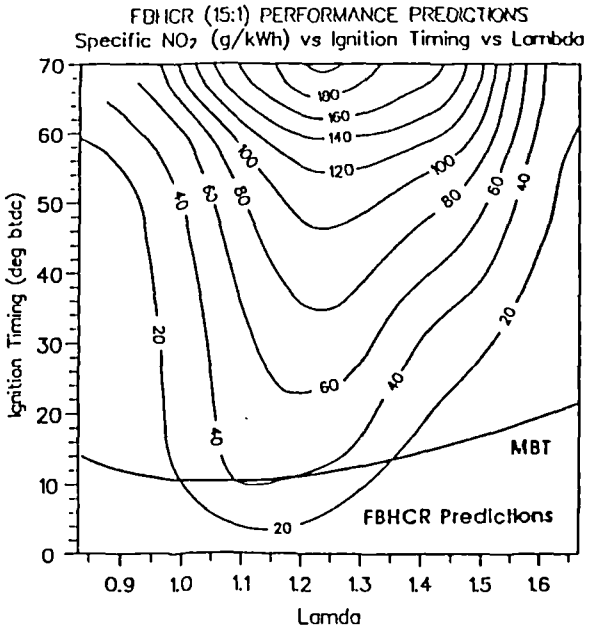

Fig. 5.3 The originally predicted FBHCR brake specific NO_2 emissions (g/kWh) with a compression ratio of 14.7, as a function of the air fuel ratio and the ignition timing.

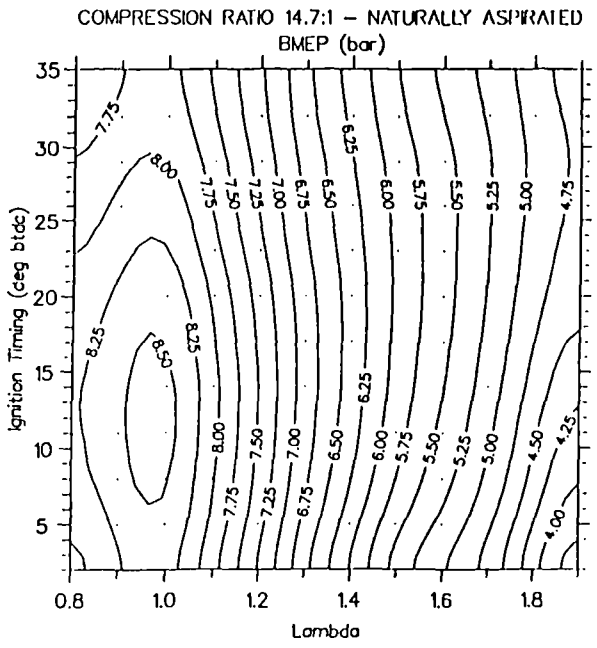

Fig. 5.4 The re-tuned simulation, predicted FBHCR bmep (bar) with a compression ratio of 14.7, as a function of the air fuel ratio and the ignition timing.

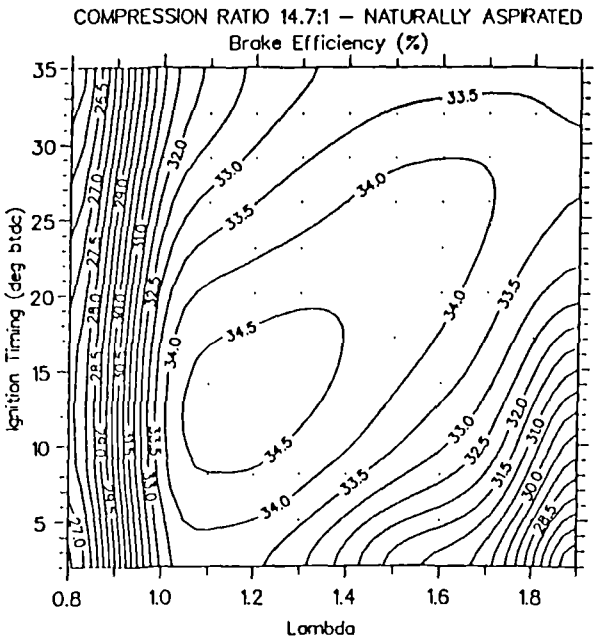

Fig. 5.5 The re-tuned simulation predicted FBHCR brake efficiency (%) with a compression ratio of 14.7, as a function of the air fuel ratio and the ignition timing.

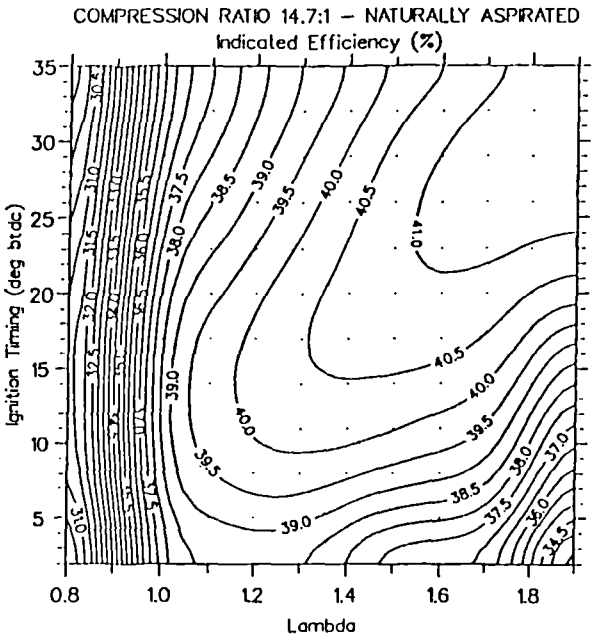

Fig. 5.6 The re-tuned simulation predicted FBHCR indicated efficiency (%) with a compression ratio of 14.7, as a function of the air fuel ratio and the ignition timing.

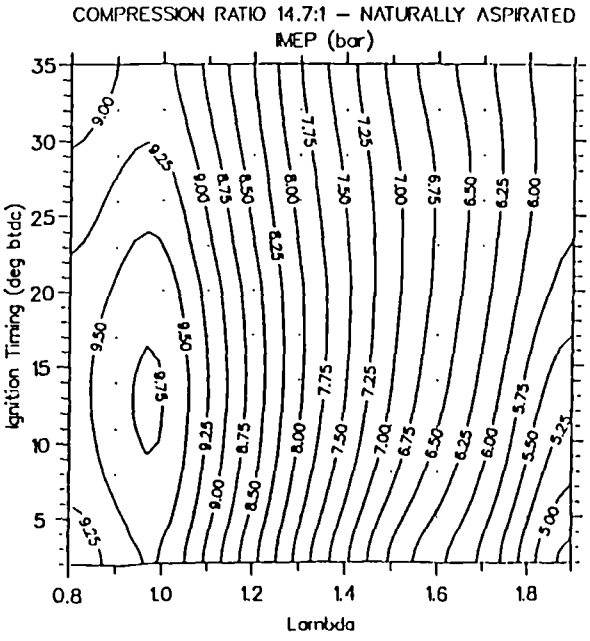

Fig. 5.7 The re-tuned simulation predicted FBHCR imep (bar) with a compression ratio of 14.7, as a function of the air fuel ratio and the ignition timing.

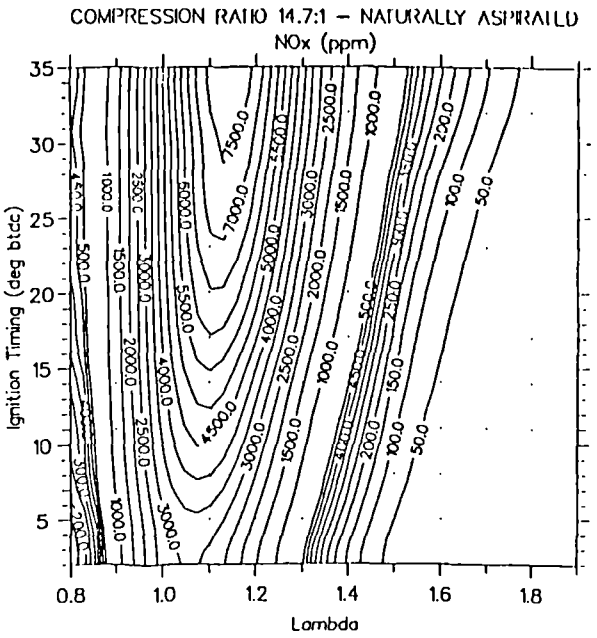

Fig. 5.8 The re-tuned simulation predicted FBHCR volumetric NO_2 emissions (ppm) with a compression ratio of 14.7, as a function of the air fuel ratio and the ignition timing.

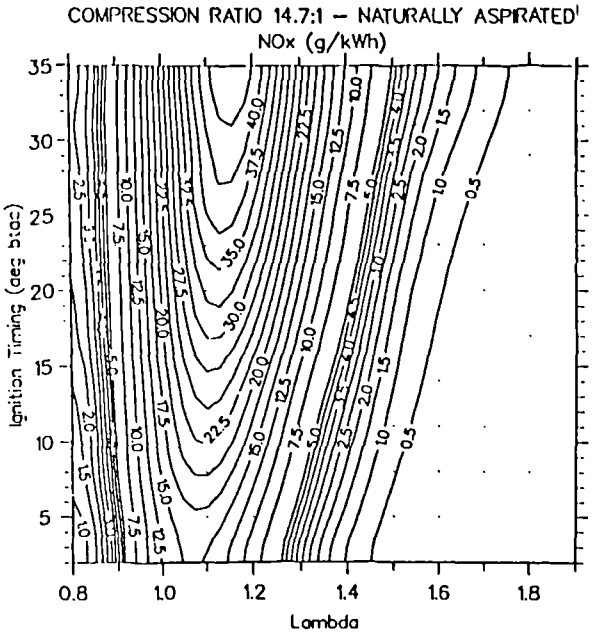

Fig. 5.9 The re-tuned simulation predicted FBHCR brake specific NO_2 emissions (g/kWh) with a compression ratio of 14.7, as a function of the air fuel ratio and the ignition timing.

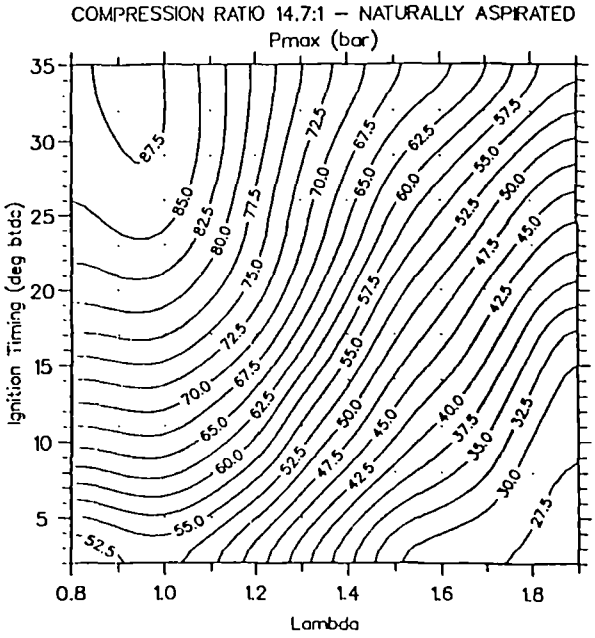

Fig. 5.10 The re-tuned simulation predicted FBHCR maximum pressure (bar) with a compression ratio of 14.7, as a function of the air fuel ratio and the ignition timing.

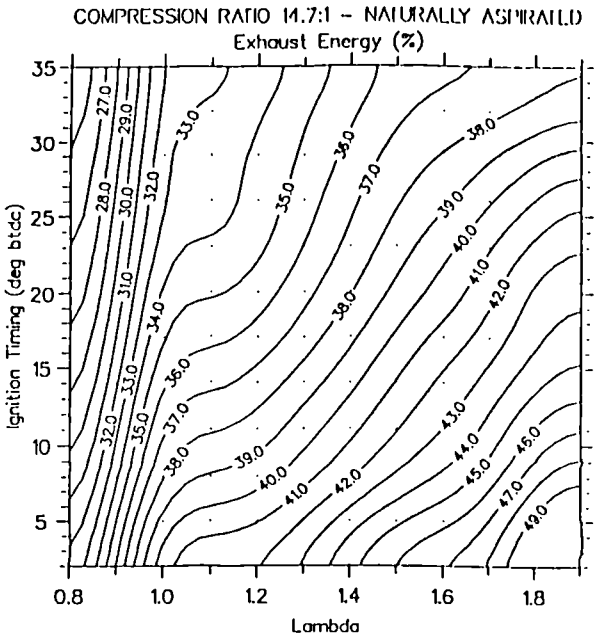

Fig. 5.11a The re-tuned simulation predicted FBHCR exhaust energy (%) with a compression ratio of 14.7, as a function of the air fuel ratio and the ignition timing.

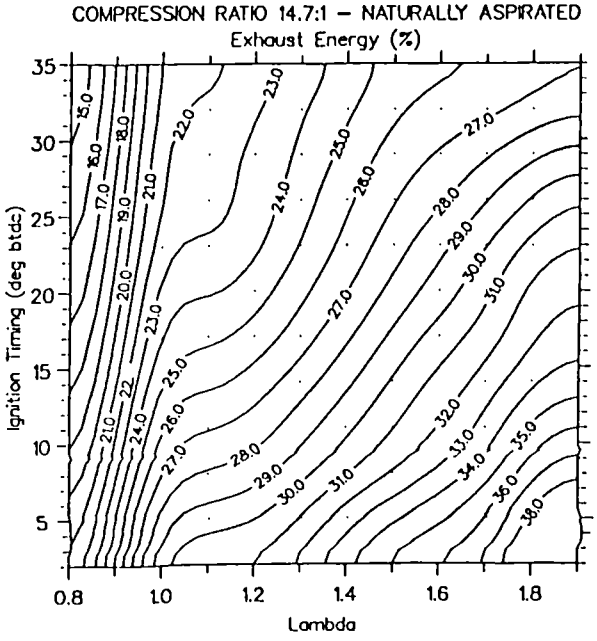

Fig. 5.11b The re-tuned simulation predicted FBHCR exhaust energy percentage (using the lower calorific value for methane) with a compression ratio of 14.7, as a function of the air fuel ratio and the ignition timing.

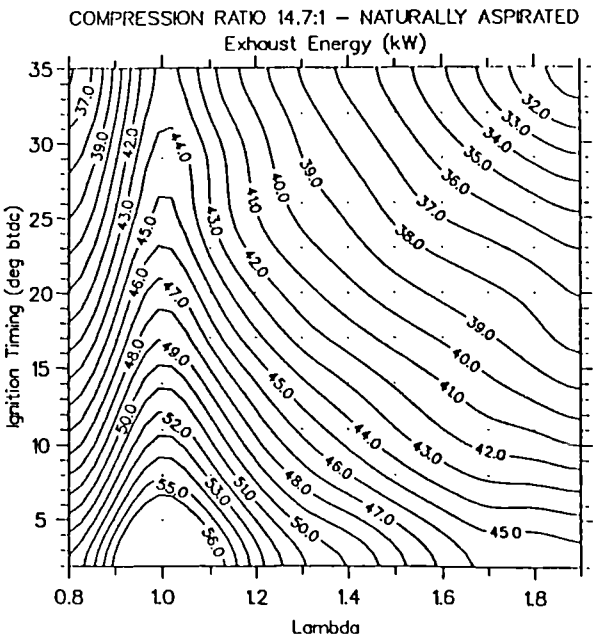

Fig. 5.12a The re-tuned simulation predicted FBHCR exhaust energy (kW) with a compression ratio of 14.7, as a function of the air fuel ratio and the ignition timing.

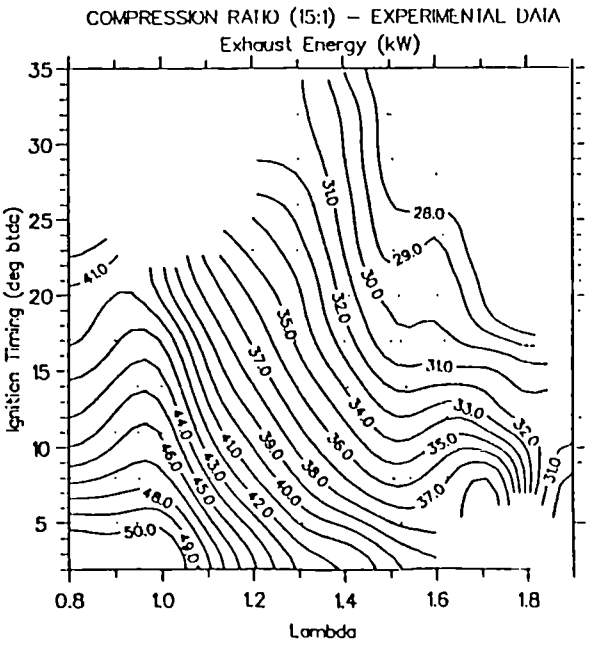

Fig. 5.12b The experimental FBHCR exhaust energy (kW) with a compression ratio of 14.7, as a function of the air fuel ratio and the ignition timing.

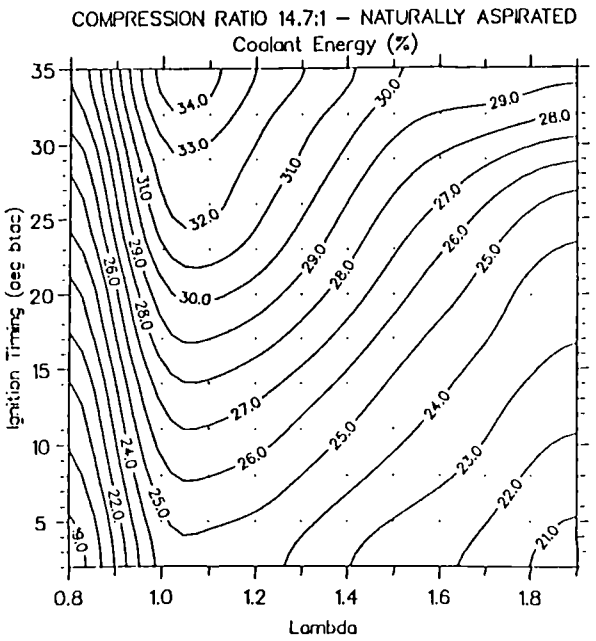

Fig. 5.13 The re-tuned simulation predicted FBHCR coolant energy (%) with a compression ratio of 14.7, as a function of the air fuel ratio and the ignition timing.

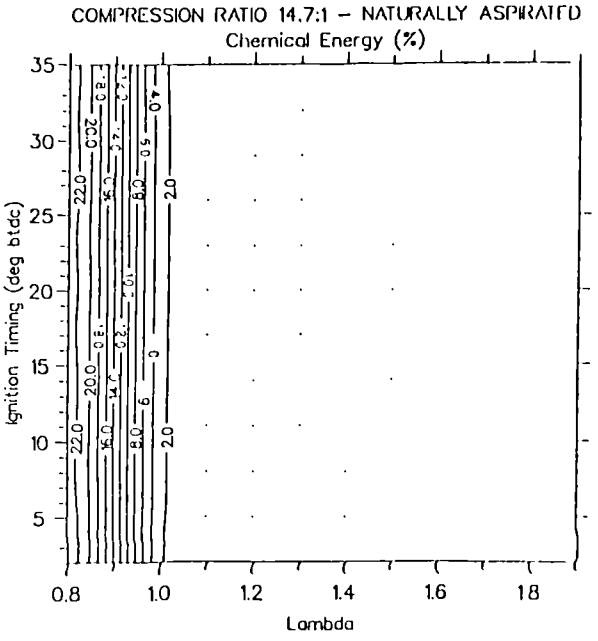

Fig. 5.14 The re-tuned simulation predicted FBHCR chemical energy (%) with a compression ratio of 14.7, as a function of the air fuel ratio and the ignition timing.

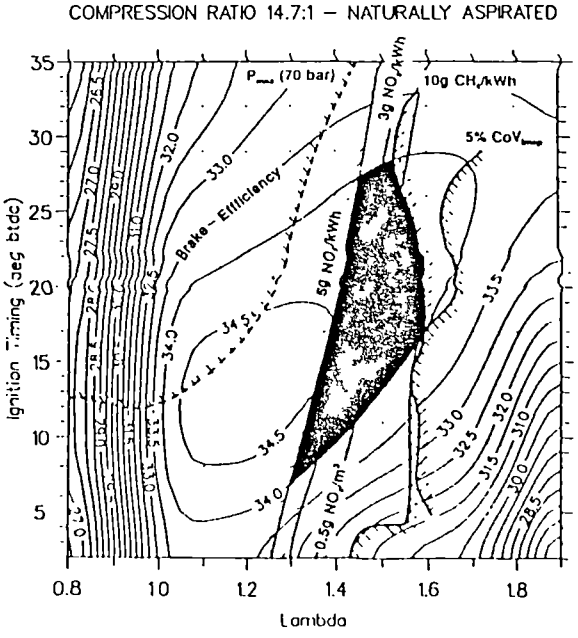

Fig. 5.15 Identification of operating windows with the simulation FBHCR NO_x (g/kWh) and brake efficiency, within typical operational and emissions constraints.

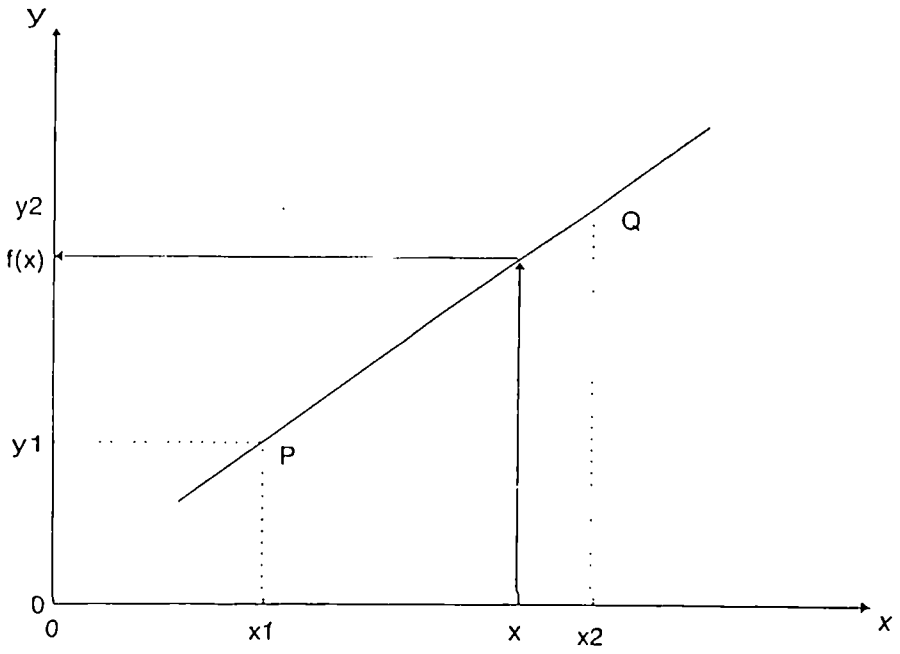

Fig. 5.16 An example of Linear Interpolation.

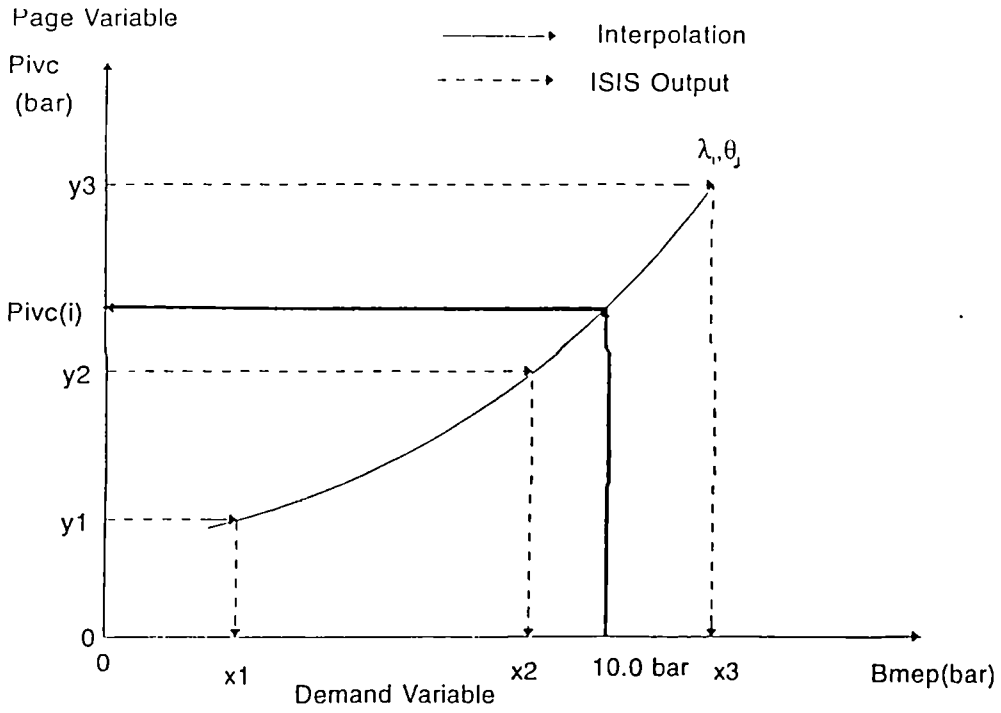

Fig. 5.17a Selection of the Pivc at a particular operating point of 10 bar using Lagrangian interpolation.

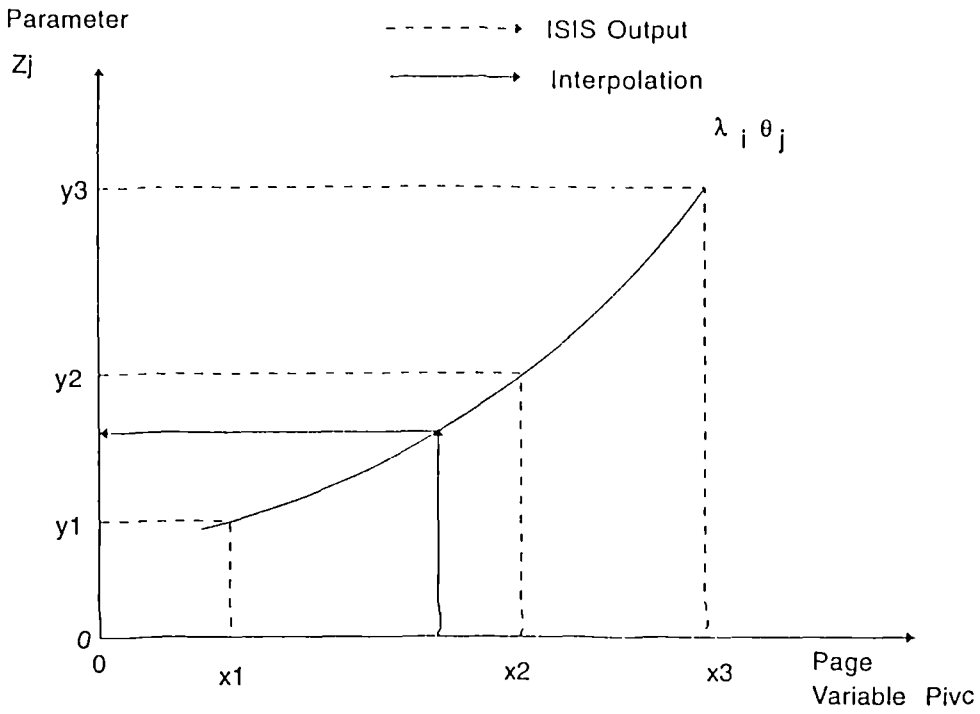

Fig. 5.17b Finding the Z parameter at the particular Pivc that is required to give a bmep of 10 bar.

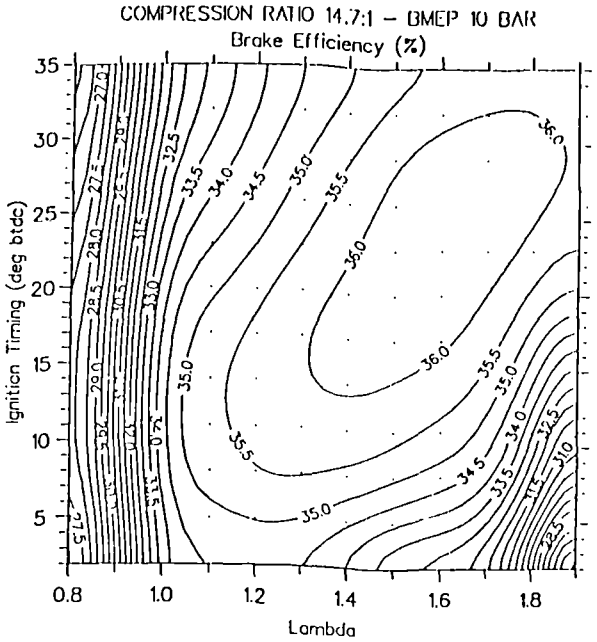

Fig. 5.18 The predicted turbocharged brake efficiency (%) at a bmep of 10 bar, with a compression ratio of 14.7, as a function of the air fuel ratio and the ignition timing.

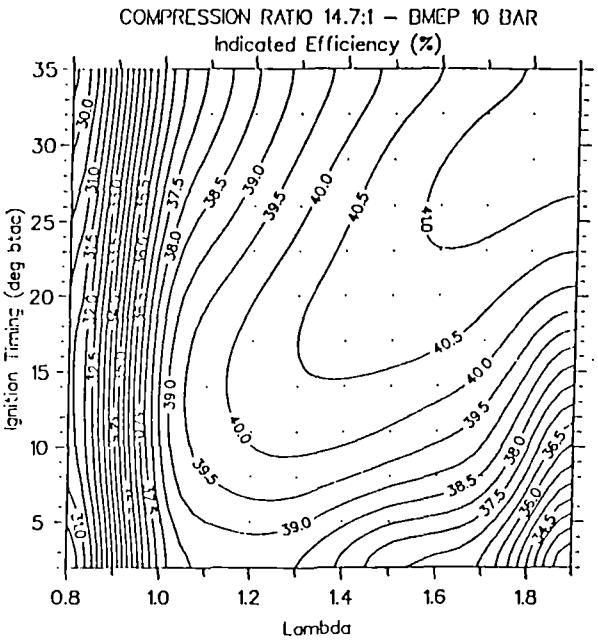

Fig. 5.19 The predicted turbocharged indicated efficiency (%) at a bmep of 10 bar, with a compression ratio of 14.7, as a function of the air fuel ratio and the ignition timing.

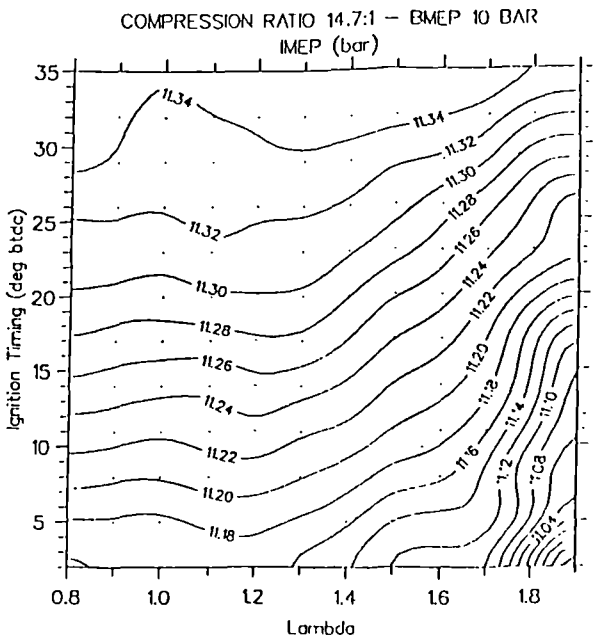

Fig. 5.20 The predicted turbocharged imep (bar) at a bmep of 10 bar, with a compression ratio of 14.7, as a function of the air fuel ratio and the ignition timing.

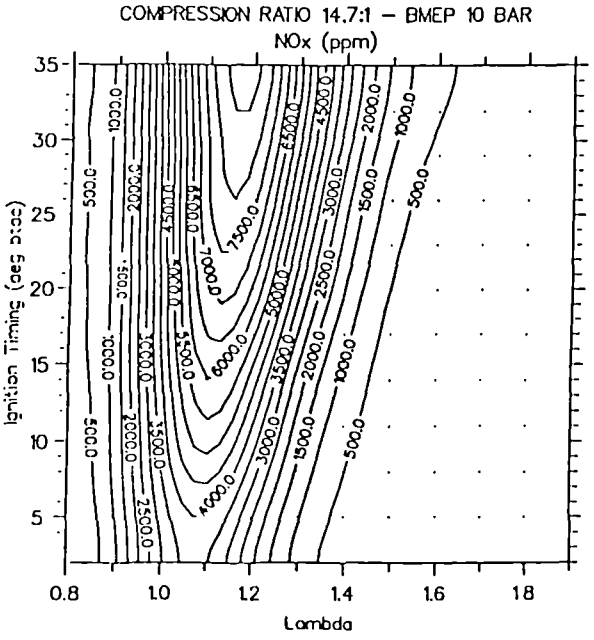

Fig. 5.21 The predicted turbocharged volumetric NO_x emissions (ppm) at a bmep of 10 bar, with a compression ratio of 14.7, as a function of the air fuel ratio and the ignition timing.

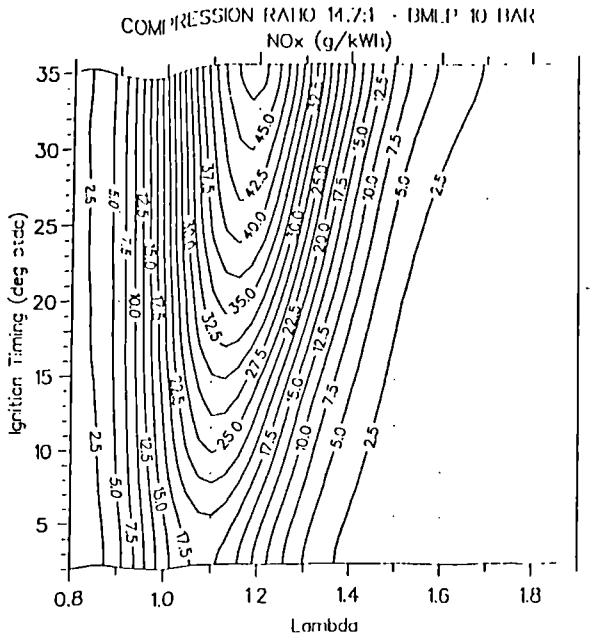

Fig. 5.22 The predicted turbocharged brake specific NO_x emissions (g/kWh) at a bmep of 10 bar, with a compression ratio of 14.7, as a function of the air fuel ratio and the ignition timing.

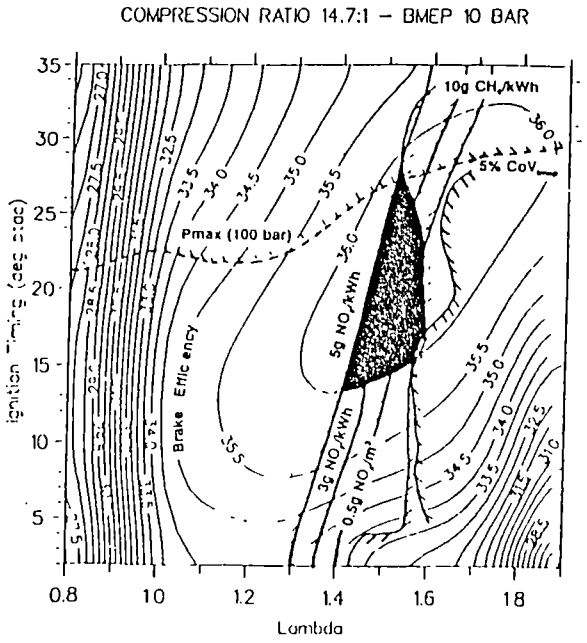

Fig. 5.24 Identification of operating windows with the turbocharged simulation NO_x (g/kWh) and brake efficiency, within typical operational and emissions constraints.

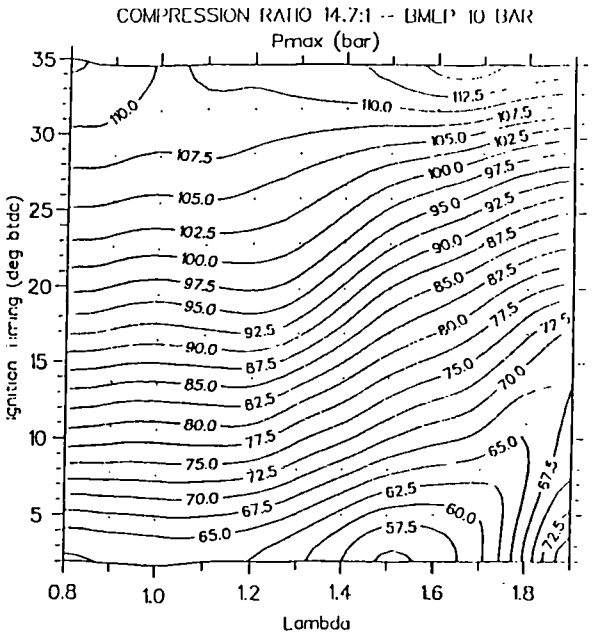

Fig. 5.23 The predicted turbocharged maximum pressure (bar) at a bmep of 10 bar, with a compression ratio of 14.7, as a function of the air fuel ratio and the ignition timing.

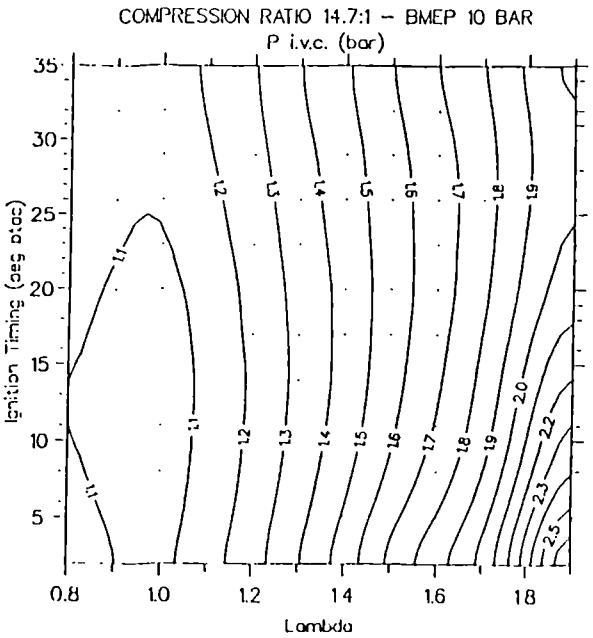

Fig. 5.25 The predicted boost pressure at inlet valve closure (bar) required to give a bmep of 10 bar, with a compression ratio of 14.7, plotted as a function of the air fuel ratio and the ignition timing.

APPENDIX A

ENGINE TECHNICAL SPECIFICATION

Model	6 cylinder (Natural gas)
Working cycle	4 stroke - normally aspirated
Valves	Overhead
Firing order	1,5,3,6,2,4
Direction of rotation	Clockwise facing front of engine
Swept volume	6200cc (380 cu.in.)
Bore	107mm (4.22 in.)
Stroke	115mm (4.52 in.)
Compression ratio	11 - 1
Combustion chamber	Machined in piston
Ignition timing	Static advance at present 19° btdc
Valve timing	Camshaft and crankshaft gear timing marks
Power and torque	See power curves
Approx. dry weight	475 kg (1045 lbs.) light flywheel
	526 kg (1160 lbs.) heavy flywheel
Height	1025 mm
width	624 mm
Length	1086 mm

POWER CURVES

BS 5514/1/77
ISO 3046

4 BLADE
475mm FAN

ENGINE MODEL. DOVERGAS S.I.6 NG

ENGINE TYPE DESIGNATION	DECLARED OUTPUT			
	POWER OUTPUT & SPEED		MAX TORQUE & SPEED	
		R.P.M		R.P.M
CONTINUOUS (2)	84 kW	2600	347 Nm	1200
INTERMITTENT(1)	93.3 kW	2600	386 Nm	1200

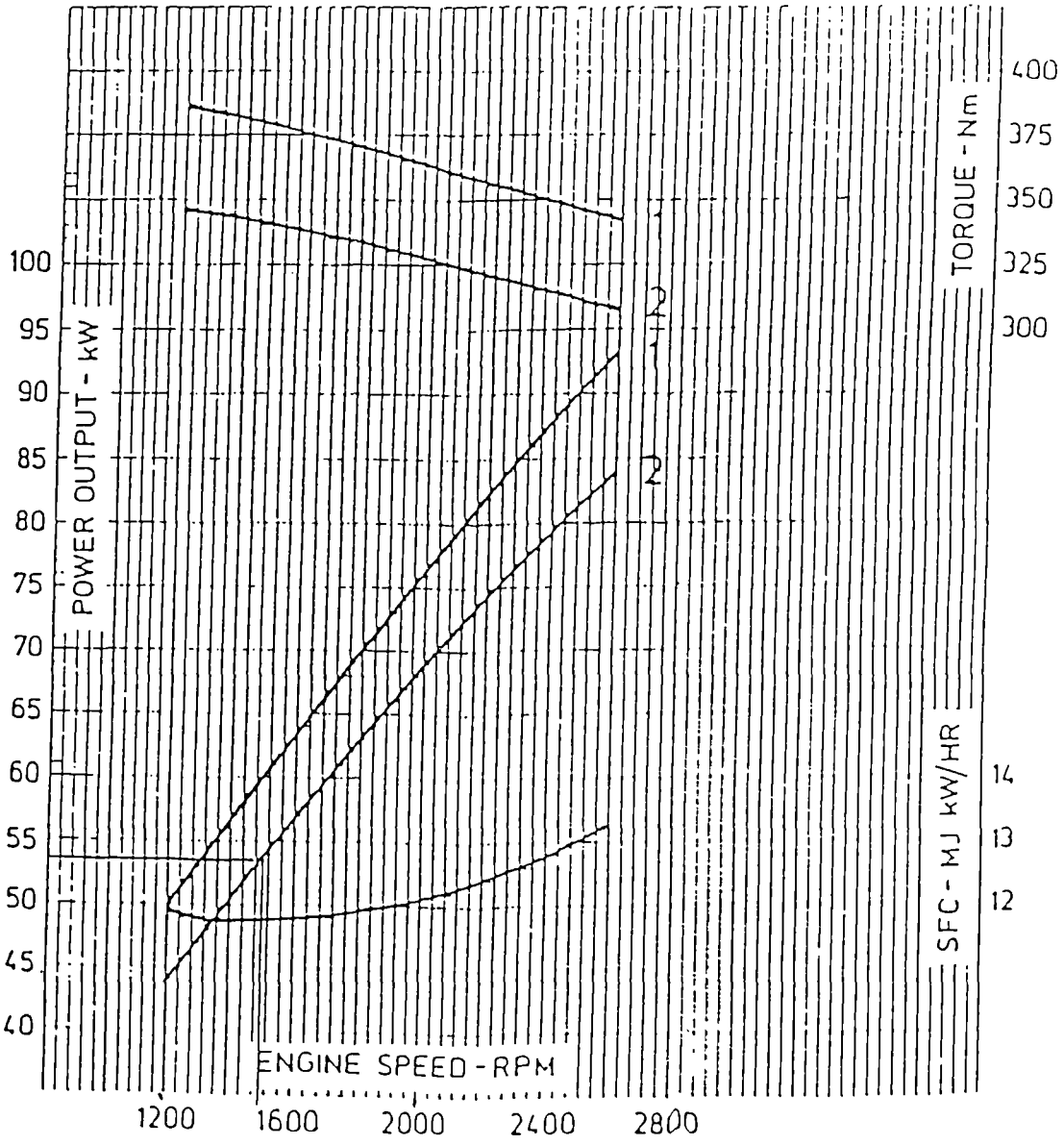

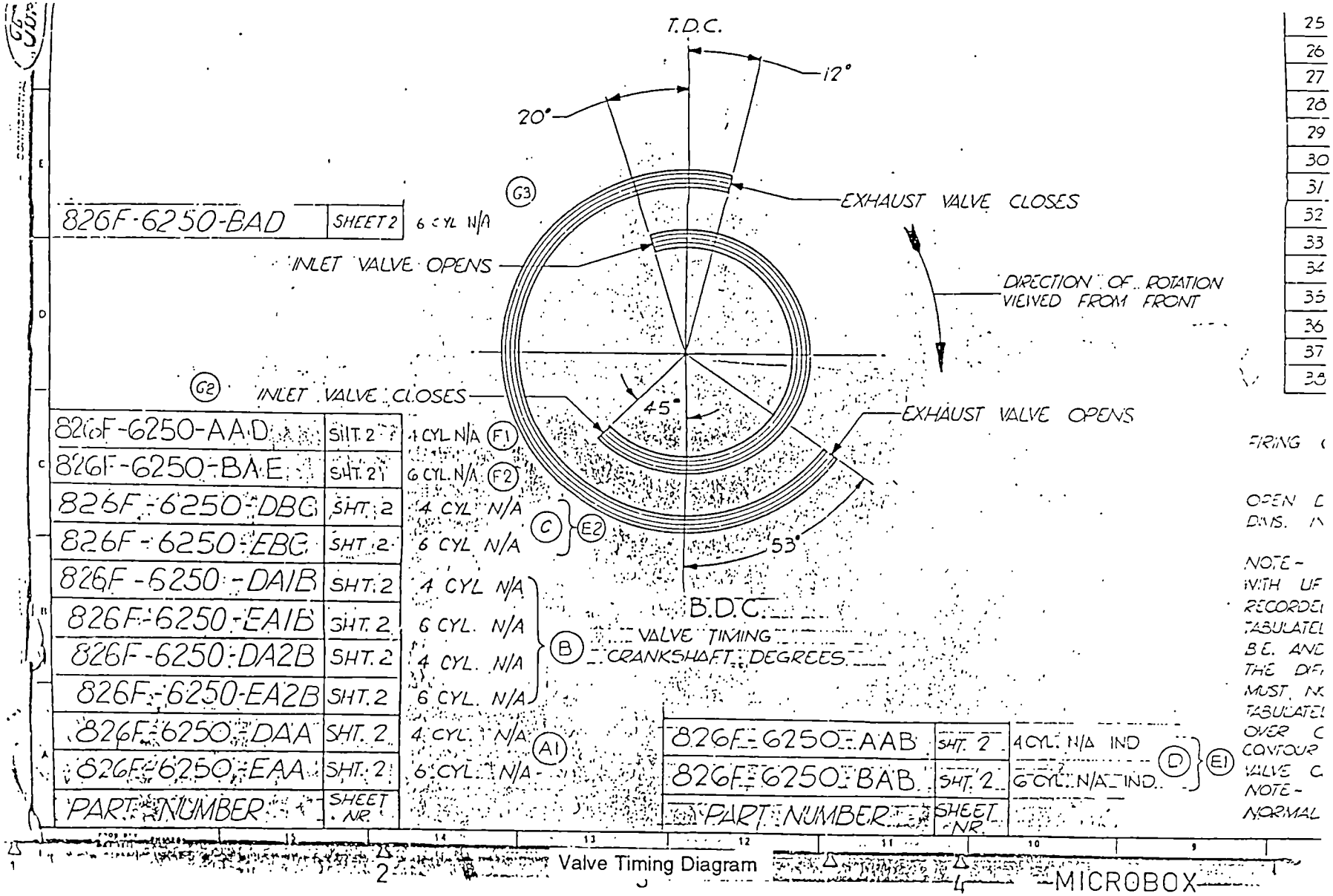

Valve Timing Diagram

LUBRICATION SYSTEM

TYPE

Pressure fed by sliding vane pump.
Minimum 1.054 Kgs.cm² (15 lbs.sq.in.)
3.515 to 3.866 Kgs.cm² (50 to 55 lbs.sq.in.) at normal operating speeds.
Sump capacity (inc. filter) front, rear or shallow well:
S.I.4 9.1 litres (16 pints)
S.I.6 13.7 litres (24 pints)
Oil filter capacity:
S.I.4 .85 litres (1.5 pints)
S.I.6 1.14 litres (2 pints)
Oil temperature 74°—116°C (165°—240°F)
Grade of lubricant:
Above 32°C (90°F) SAE 30 or 20W/40
—7°C to 30°C (20°F to 90°F) 20W/40
10W/30 (or SAE 20 Series 111)
Below —1°C (30°F) SAE 10W or 10W/30
Note:— These oils must be supplement 1, heavy duty or Series T11.

VALVE GEAR

Valve clearance, inlet and exhaust 0.38mm (0.015in.) hot.
Valve seat angle 30° — 30°30'.
Valve face angle 29°15' — 29°30'.
Valve seat inserts Standard Diesel.

VALVES

Petrol and L.P.G., standard Ford diesel valves (unless Stellite faced specified).
Natural Gas (also petrol and L.P.G. where specified) stellite faced.
Maximum valve protrusion above face of cylinder head 0.65mm (0.025in.).
Maximum piston protrusion above face of block 0.015mm (0.006in.).
Note:— To ensure that valves do not contact the top of the piston, piston and valve protrusion must be checked accurately.

BOLT TIGHTENING TORQUES

Main Bearing Cap Bolts	15.89 to 16.58 kg.m.	(115 to 120 lb.ft.)
Connecting Rod Bolts (where fitted)	11.75 to 12.44 kg.m.	(85 to 90 lb.ft.)
Cylinder Head Bolts	14.51 to 15.20 kg.m.	(105 to 110 lb.ft.)
Flywheel to C/Shaft Flange Bolts	11.06 to 12.44 kg.m.	(80 to 90 lb.ft.)
Gear to Camshaft Bolt	20.7 to 21.4 kg.m.	(150 to 155 lb.ft.)
Oil Pan Drain Plug	4.84 to 5.53 kg.m.	(35 to 40 lb.ft.)
Rocker Shaft Bracket Bolts	2.35 to 3.04 kg.m.	(17 to 22 lb.ft.)
Front Housing to Cylinder Block (including Camshaft Thrust Plate)	3.45 to 4.15 kg.m.	(25 to 30 lb.ft.)
Front Cover to Front Housing	0.83 to 1.11 kg.m.	(6 to 8 lb.ft.)
Oil Pan to Cylinder Block	3.04 to 3.32 kg.m.	(22 to 24 lb.ft.)
Crankshaft Centre Bolt	33.20 kg.m.	(240 lb.ft.)
Exhaust Manifold Retaining Bolts	2.35 to 3.04 kg.m.	(17 to 22 lb.ft.)
Inlet Manifold Retaining Bolts	2.35 to 3.04 kg.m.	(17 to 22 lb.ft.)
Engine Mounting Bolts	4.15 to 4.84 kg.m.	(30 to 35 lb.ft.)
Oil Pick-up Support Bolts	0.415 to 0.553 kg.m.	(3 to 4 lb.ft.)
Valve Rocker Cover Bolts	1.66 to 2.4 kg.m.	(12 to 18 lb.ft.)
Fuel Lift Pump Mounting Bolts	1.66 to 2.07 kg.m.	(12 to 15 lb.ft.)
Water Pump Mounting Bolts	1.66 to 2.07 kg.m.	(12 to 15 lb.ft.)
Water Outlet Housing Mounting Bolts	1.66 to 2.07 kg.m.	(12 to 15 lb.ft.)

COOLING SYSTEM

WATER PUMP
Type – Centrifugal impeller
Belt Drive – Single or twin
Drive Ratios – Single Belt 1,35:1 & 1,67:1; Twin Belt 1,32:1 & 1,67:1

Water Pump Flow Rates

Engine Speed (rpm)	1200	1500	1800	2000	2400	2500	2600
Drive Ratio 1,32:1							
Litre/sec	0,39	0,96	1,31	1,53	1,78	1,85	1,94
Pressure (bar)	0,56	0,61	0,65	0,69	0,75	0,77	0,80
Drive Ratio 1,35:1							
Litre/sec	0,42	1,00	1,35	1,56	1,82	1,90	1,99
Pressure (bar)	0,56	0,61	0,65	0,69	0,75	0,77	0,80
Drive Ratio 1,67:1							
Litre/sec	0,98	1,44	1,70	1,88	2,24	2,32	2,65
Pressure (bar)	0,61	0,67	0,72	0,76	0,88	0,92	1,02

Coolant Capacity – less radiator
S.I.4 – 8,23 litre; S.I.6 – 9,95 litre.

Antifreeze
– Ford Spec SSM-97B-9102A – 50 per cent solution.

Optimum Operating Temperature
99°C

Temperature Sender Unit
– Thread 3/8 – 18 NPTF

Single Thermostat System
Commence Opening – 82°C; Fully Open – 94°C

LUBRICATION SYSTEM

PUMP
High output bi-rotor screw driven from camshaft.

FILTER
Vertical 'spin-on' cannister. Capacity 1 litre.
Oil capacity including filter, S.I.4 – 9,1 litres.
S.I.6 – 13,6 litres front and rear well, 17,2 litres shallow.

Oil pressure (min.)	1600 r.p.m.	2.8 bar (40 lbs sq.in.)
	2000 r.p.m.	3.2 bar (47 lbs sq.in.)
Oil temp (max.)	116°C (241°F)	
Oil grade (viscosity)	Below 20°C	SAE 10W
	Between 0 & 32°C	SAE 20W/20
	Above 30°C	SAE 30

DORSET S.I.4 & S.I.6
ELECTRICAL SYSTEM

12 volt negative earth.

CHARGING
Alternator.

STARTING
Lucas co-axial sealed, or unsealed pre engaged.

IGNITION
12 volt coil. Lumenition electronic optional.

DISTRIBUTOR
Drive from oil pump.
Advance mechanism, Petrol, mechanical and vacuum advance. Natural Gas and L.P.G. no mechanical or vacuum advance.
Contact breaker setting (where applicable) 0.38mm (0.015in.).

STATIC ADVANCE

L.P.G. and Natural Gas	19° B.T.D.C.
Petrol	6° B.T.D.C.

SPARK PLUGS
L.P.G. Motorcraft A.E.6.C
Petrol and Natural Gas Motorcraft A.E.2.C

Spark plug gap:	Petrol and L.P.G.	0.65mm (0.025in.)
	Natural Gas	0.45mm (0.018in.)

COOLING SYSTEM

WATER PUMP
Belt driven centrifugal impeller.
Maximum free flow at 2500 R.P.M.
100 litres (22 gallons) per minute with 1.35—1 ratio pulley.
161 litres (35.5 gallons) per minute with 1.67—1 ratio pulley.
Optimum operating temperature 90° C (195° F).

Engine coolant capacity:	S.I.4	7.54 litres (13.25 pints)
	S.I.6	9.95 litres (17.5 pints)

PETROL PUMP (where fitted)
Operating pressure: 0.1055 to 0.1406 Kgs.cm^2 (1½ to 2 lbs.sq.in.).

DOVERGAS

Principal Dimensions

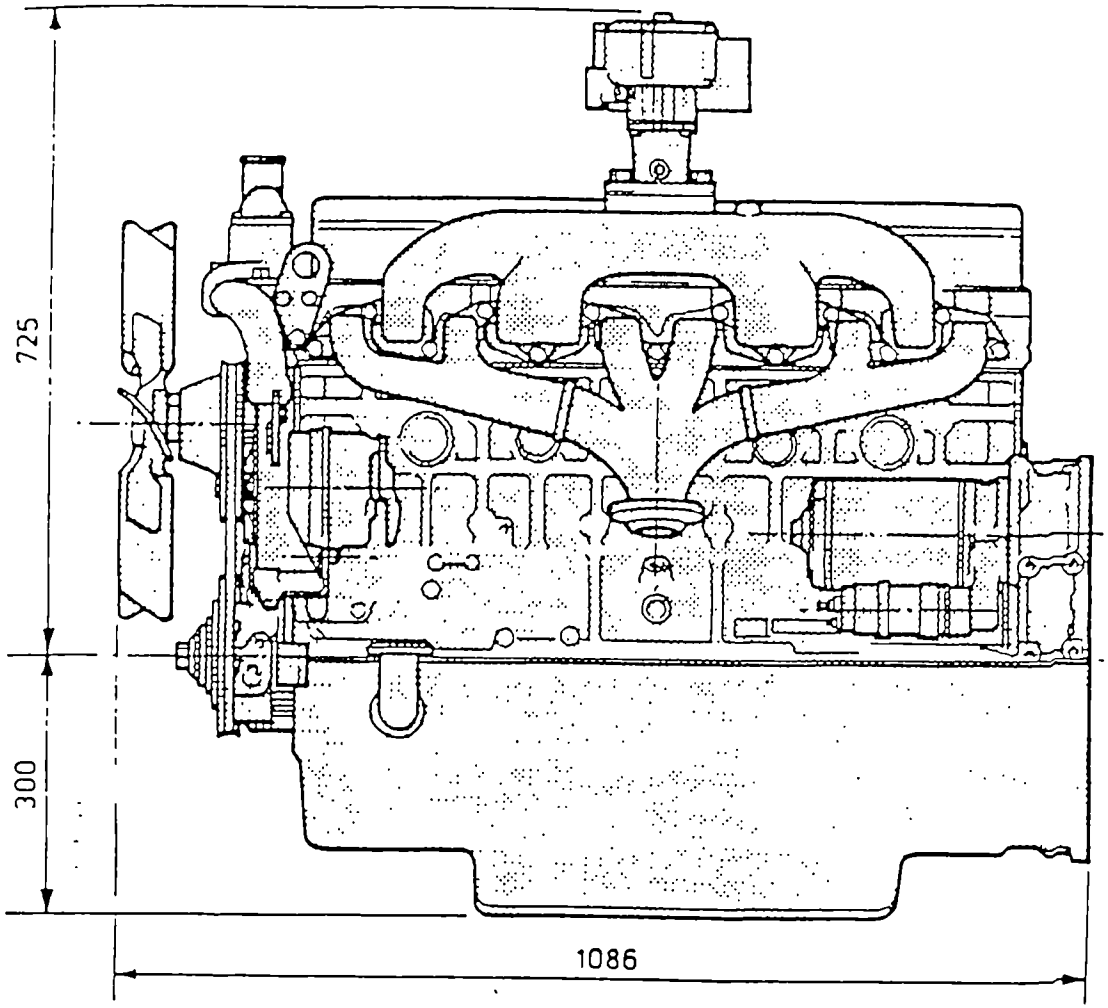

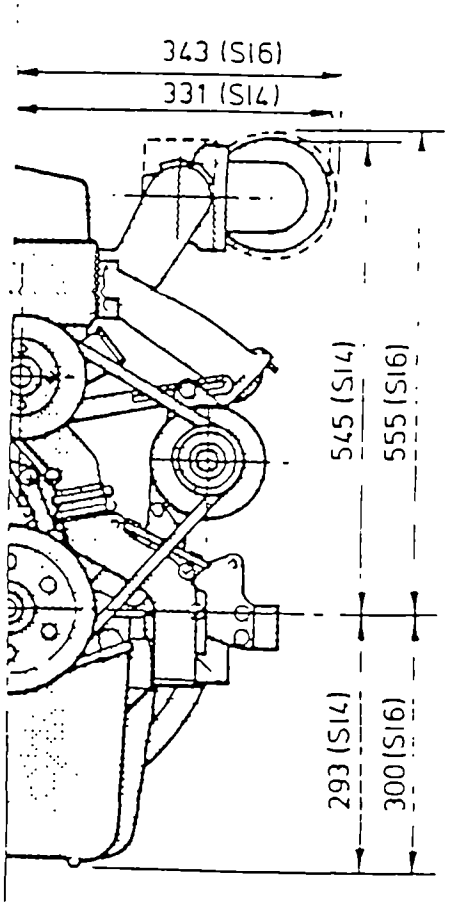

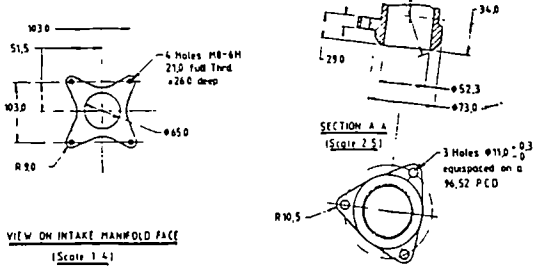

VIEW ON INTAKE MANIFOLD FACE
(Scale 1.4)

VIEWS SHOWING EXHAUST MANIFOLD OUTLET

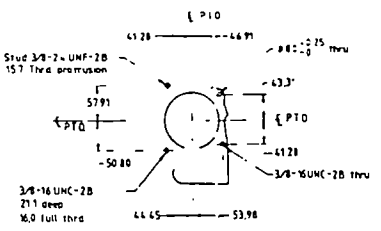

VIEW ON ARROW A
STD PTO MTG FACE
(Scale 1.4)

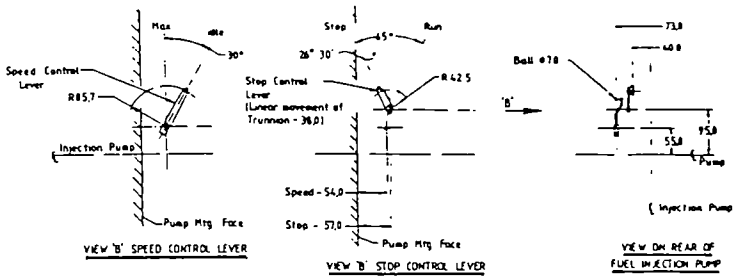

VIEW 'B' SPEED CONTROL LEVER

VIEW 'B' STOP CONTROL LEVER

VIEW ON REAR OF
FUEL INJECTION PUMP

VIEWS SHOWING INJECTION PUMP CONTROL LEVERS (AUTOMOTIVE & G.P. Pumps)

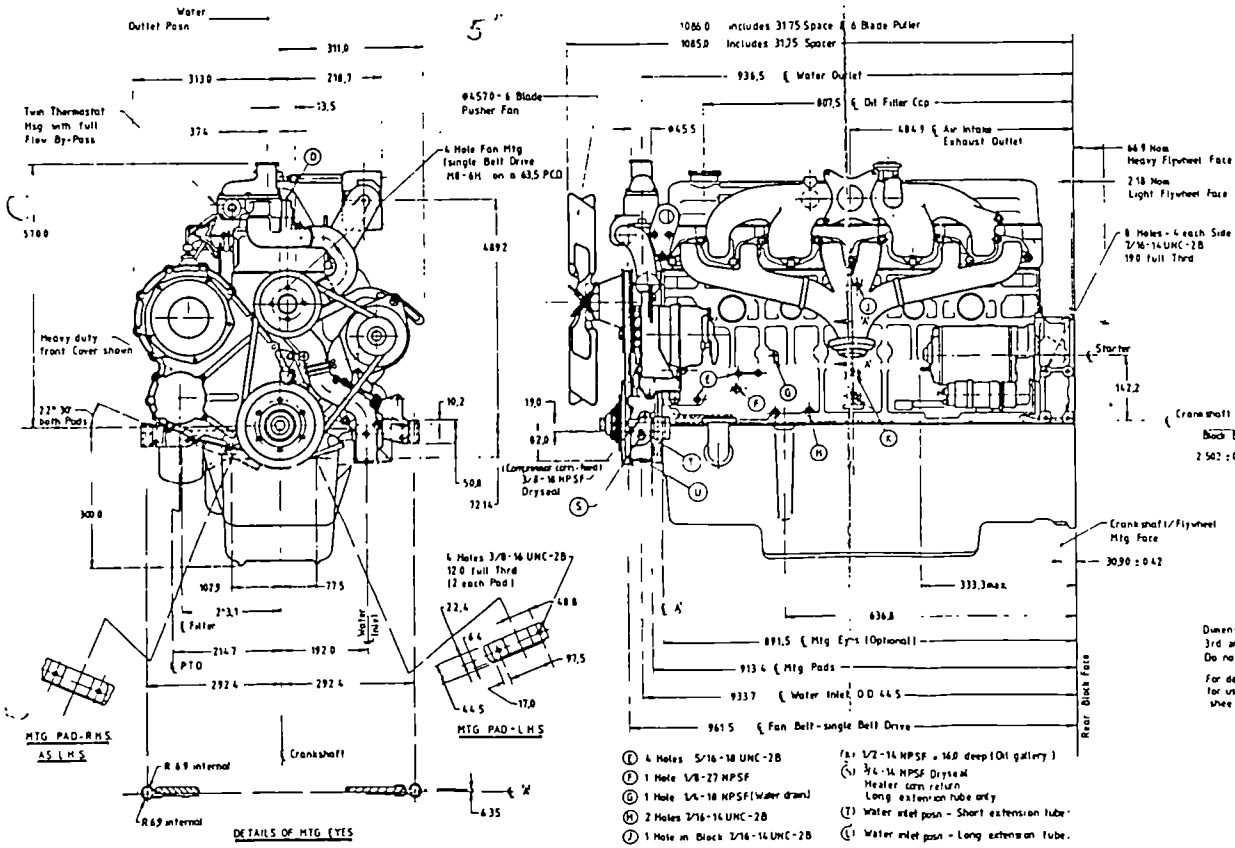

Dimensions are in millimetres
3rd angle projection
Do not scale

For details of optional equipment
for use with this engine see
sheet 6 thru 7

Ford

VERTRAULICH — CONFIDENTIAL

0 25 50 75 100 125 150 175 200 225 250 mm

OBEN ANGEGEBENER MASSSTAB NUR ALS BEZUGSMASS
ABOVE SCALE FOR REFERENCE ONLY

REFERENCES

DR	DATE Mar 80	CA	APP
NICHT ABMESSEN	MASSSTAB 1 5 SCALE	DO NOT SCALE	

PART NAME
INSTALLATION - ENGINE ASSY - 6 CYL
2723/5 NORMALLY ASPIRATED

TEILNUMMER/PART NR
IND-250

Sht 2 of 21

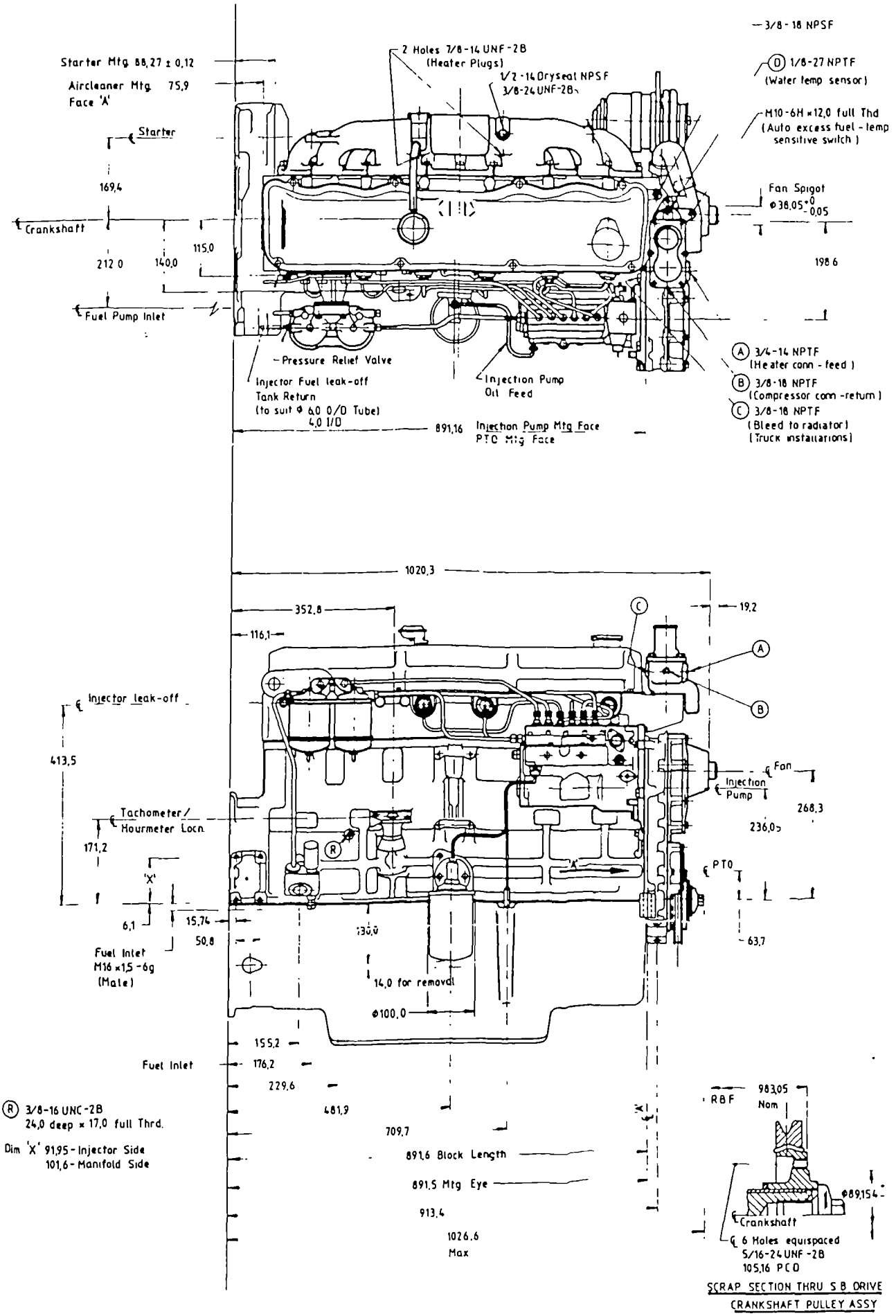

SCRAP SECTION THRU S B DRIVE
CRANKSHAFT PULLEY ASSY

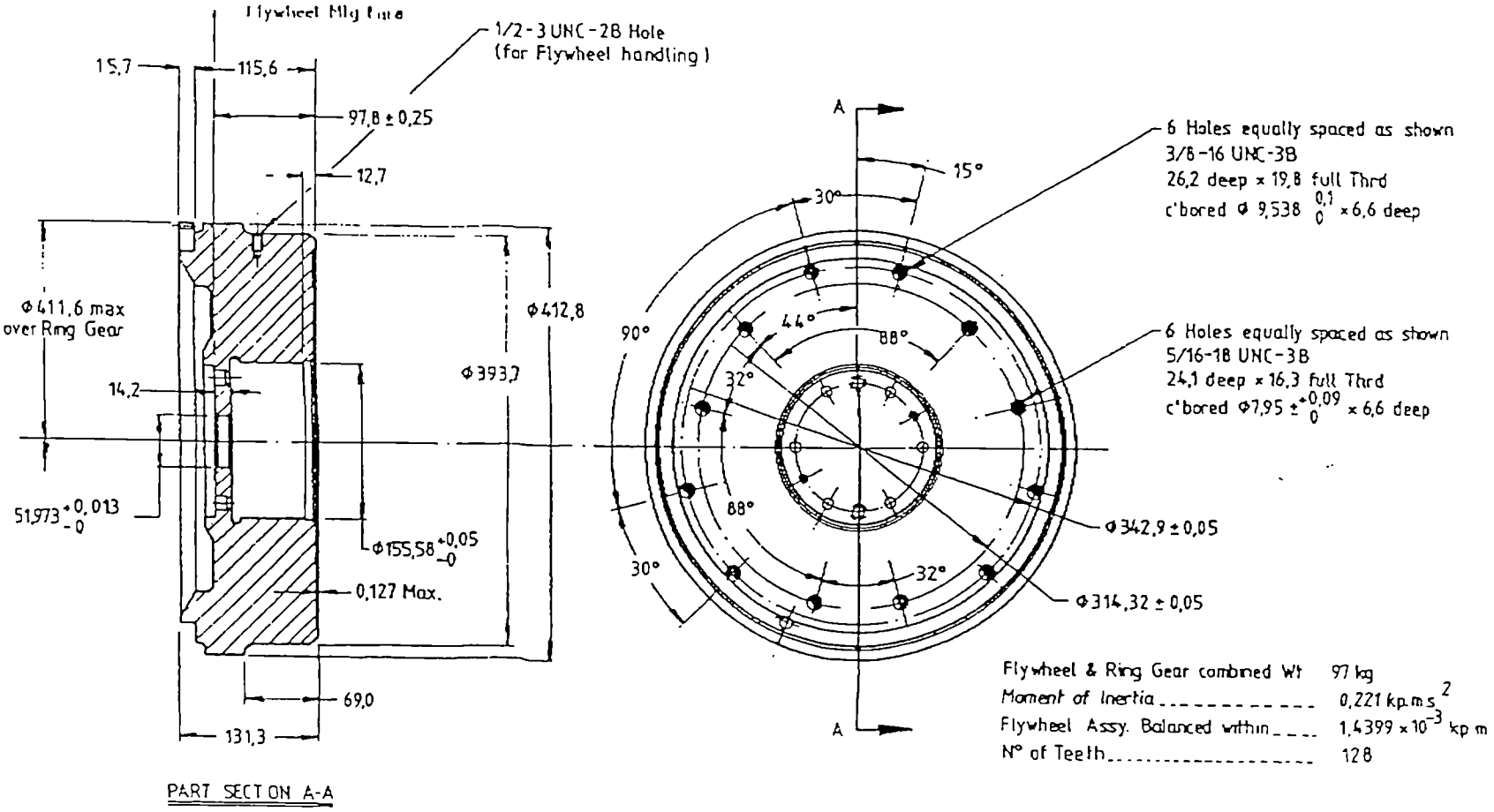

Flywheel, 90,7 kg: Tapped for 279 mm and 305 mm clutches. Use with all engines.
Schwungrad, 90,7 kg: Gewindelöcher für Kupplung 279 mm und 305 mm ϕ. Für die Verwendung mit allen Motoren.

DRG No. B 01

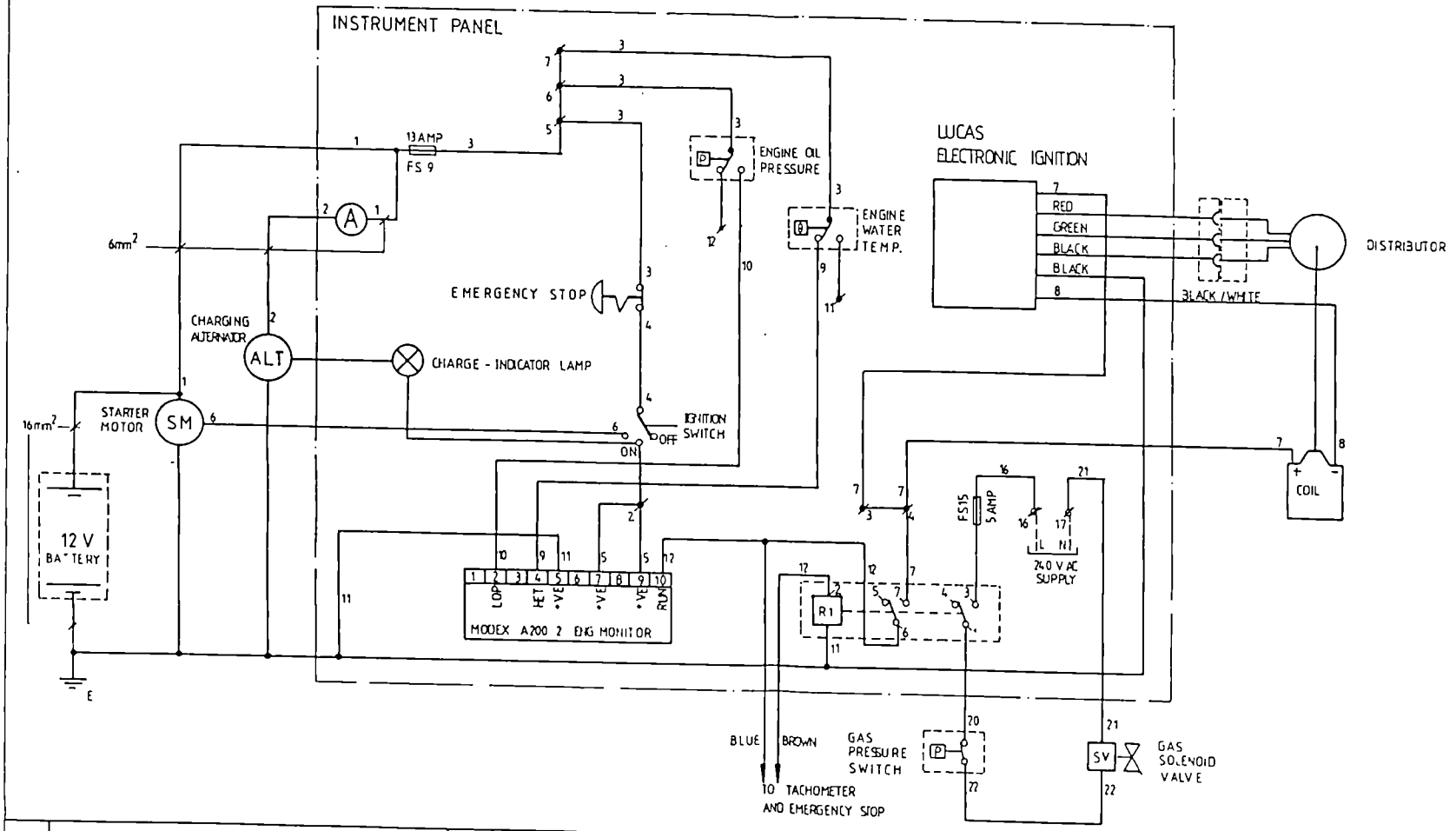

No	DESCRIPTION	CHK'D	APP'D	DATE
REVISIONS				

GAS ENGINE

INSTRUMENT PANEL (WIRING DIAGRAM)

DRAWN	TRACED	CHECKED	APPROVED	DATE	SCALE
S STROELE				13 06 91	NTS

DRAWING No. B 01

DRG No. B 02

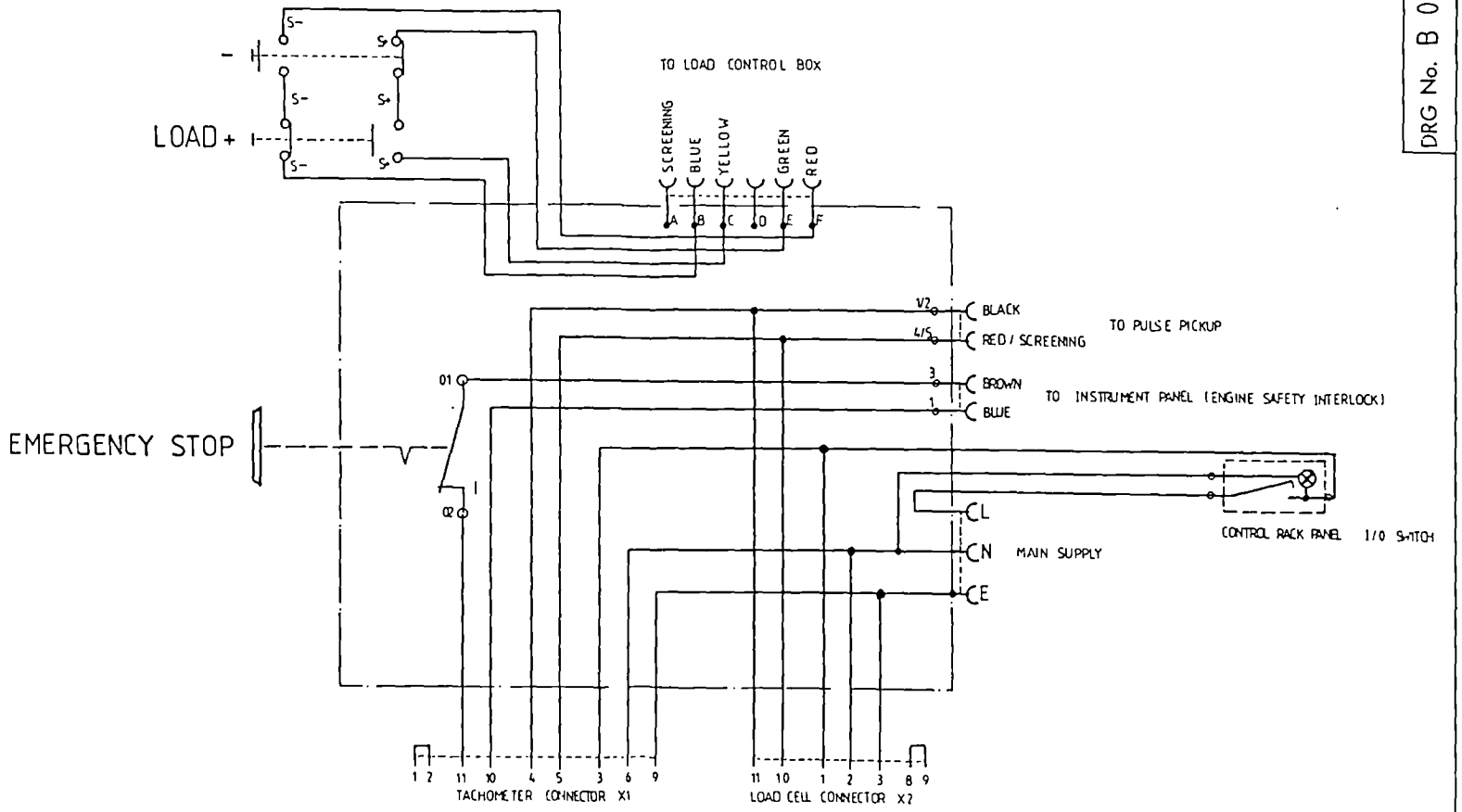

No	DESCRIPTION	CHK'D	APP'D	DATE

REVISIONS

GAS ENGINE

TACHO AND LOAD CELL (WIRING DIAGRAM)

DRAWN	TRACED	CHECKED	APPROVED	DATE	SCALE
S STR ELE				13 06 91	NTS

DRAWING No. B 02

Note: This diagram must not be used without reference to the relevant clauses.

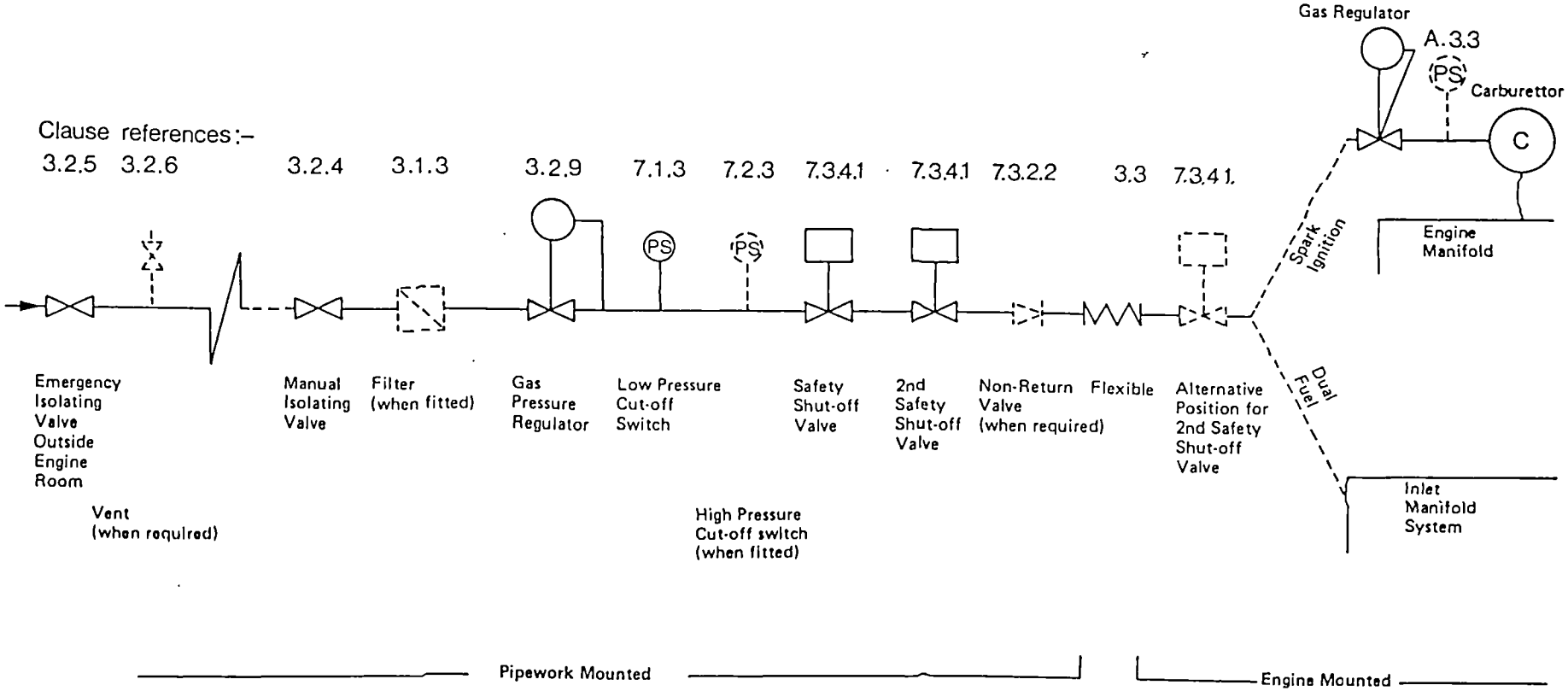

DIAGRAMMATIC REPRESENTATION OF THE RELATIVE POSITIONS OF CONTROLS WHICH MAY BE REQUIRED IN THE GAS SUPPLY TO AN ENGINE.

The Layrub Range

Layrub Block

Pre-compressed rubber blocks form the basis of all Layrub coupling and shaft designs. Natural rubber of 60/65 duro hardness is the standard material, but alternative mixes are available and neoprene blocks are used where additional damping is required or where the presence of mineral oils presents a special hazard. The blocks accommodate movement in all directions, making these couplings exceptionally tolerant of relative shaft displacements and providing controlled torsional stiffness for the correct tuning of systems subject to torsional vibration excitation. Flexible shafts, consisting of two Layrub couplings connected either by a fixed length tube or a splined centre shaft, will tolerate very large relative movement with minimal shaft reaction forces and moments.

Approved by leading Classification Societies and Government Agencies, these couplings and shafts have been proven in the field over many years and have earned their reputation as world leaders in a wide range of industries and applications.

Section of Block

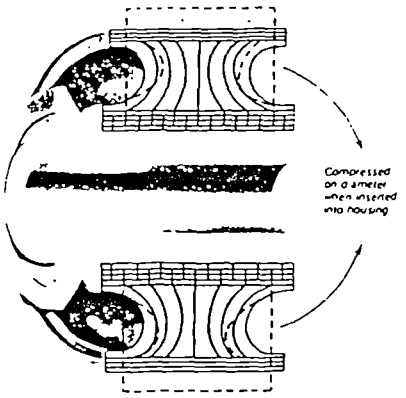

Layrub Coupling Range

All standard couplings and shafts are based on one of the constructions shown here and the power rating charts opposite give a preliminary size selection based on a service factor of 3.0, which meets most applications other than engine test dynamometers, reciprocating compressors and other severe duties dealt with more fully under 'Selection' on page 4.

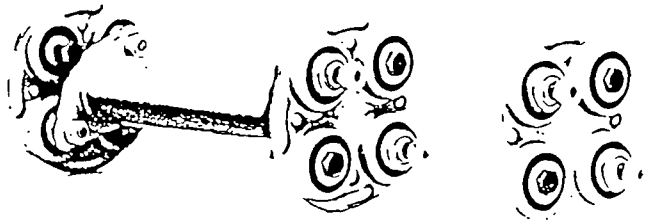

Two-four series
(two bolts in each flange,
four resilient blocks)

Three-six series
(three bolts in each flange,
six resilient blocks)

Six-six series
(six bolts in each flange,
six resilient blocks)
and
Multi-point
(larger sizes including
8/8, 9/9, 10/10, 12/12)

Standard Couplings

Two-four series

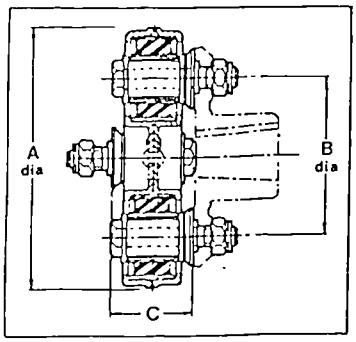

Type of Trunnion Block	Maximum Momentary Torque Nm.	A Dia.	B PCD	C
40	147	102	65.0	41.5
50	235	128	81.0	47.5
60+	392	153	96.8	57.0
65	598	167	104.8	57.0
70	735	178	109.5	68.5
80	1080	203	125.4	68.5
90	1492	229	141.3	76.0
100	1898	254	157.1	79.5
105	2712	270	157.1	92.0
120	3254	305	187.3	92.0

Three-six series

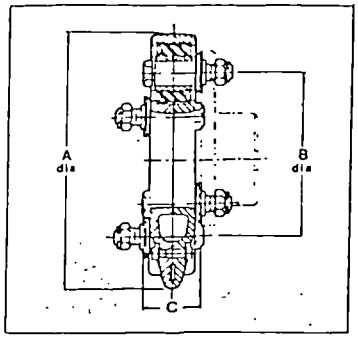

Type of Trunnion Block	Maximum Momentary Torque Nm.	A Dia.	B PCD	C
70	1356	220	139.7	68.5
80	2034	251	160.3	68.5
90	3119	286	188.9	76.0
100	4340	350	241.3	79.5
120	5831	353	225.4	92.0
140	8140	423	279.4	101.5

Six-six series

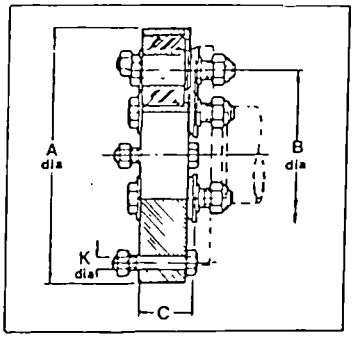

Type of Trunnion Block	Maximum Momentary Torque Nm.	A Dia.	B PCD	C	K
40	515	115	76 2	32 5	M8
50	814	145	95 3	37.0	M10
60+	1373	172	114.3	45.0	M10
65	2170	191	127.0	45.0	M12
70	2848	210	139.7	53.0	M12
70+	3530	210	139.7	53.0	M12
80	4462	253	171.5	55.0	M12
90	6102	276	188.9	61.0	M16
100	7306	296	200.0	65.0	M16
120	11797	346	228.6	73 0	M16
140	14900	394	260.3	80.5	M20

Companion Flanges

For coupling shaft ends, companion flanges are available to suit all standard Layrub flexible coupling assemblies, and full details are given on separate leaflets.

Flywheel mounting

Layflange couplings are available in certain sizes for direct flywheel to shaft mounting. Brief details are given here, and a separate leaflet is available.

Couplings for minimum space requirements

The Layshaft couplings described on page 6 provide a low cost solution for shaft to shaft applications where the couplings must fit into a minimum space envelope.

Blind assembly

All coupling sizes can be supplied with sliding sleeve pins to permit blind assembly. Details on request.

Trunnion blocks

Standard Layrub pre-compressed flexible blocks within a steel shell are available for building into existing machinery flanges or for use in other applications requiring flexible bushings such as torque reaction rods.

Balancing

Layrub flexible shafts are balanced for normal engine and electric motor speeds. Special balancing available to order.

THE LAYFLANGE COUPLING FOR FLYWHEEL MOUNTING

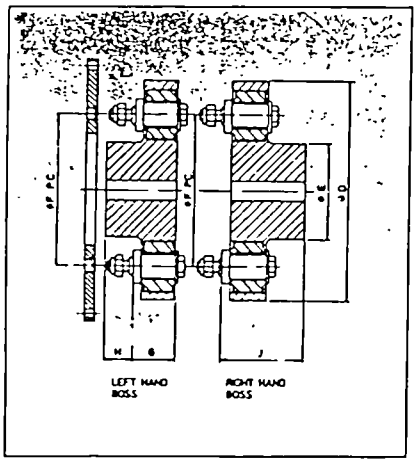

Layflange Coupling Size	Max Momentary Torque Nm	D	E	F	G	H (LH only)	J (RH only)	SAE Adaptor Reference 11½	14	18	Max Speed r/min
60+3/3	940	225	100	158.8	48	26	85	157210	158511	-	2500
60+4/4	1250	225	100	158.8	48	26	85	157210	158511	-	2500
60+6/6	1880	225	100	158.8	48	26	85	157210	158511	-	2500
80-3/3	2700	295	125	203 0	59	41	111	156975	156976	156977	2000
80-4/4	3600	295	125	203 0	59	41	111	156975	156976	156977	2000
80-6/6	5400	295	125	203 0	59	41	111	156975	156976	156977	2000
80+6/6	5700	295	125	203 0	59	41	111	156975	156976	156977	2000

Power Ratings

Two-four series

Service factor = 3.0

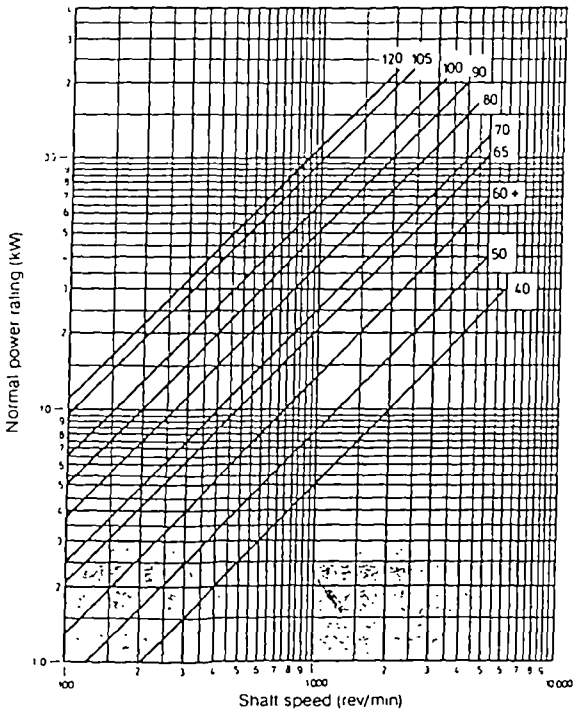

Six-six and Multi-point series

Service factor = 3.0

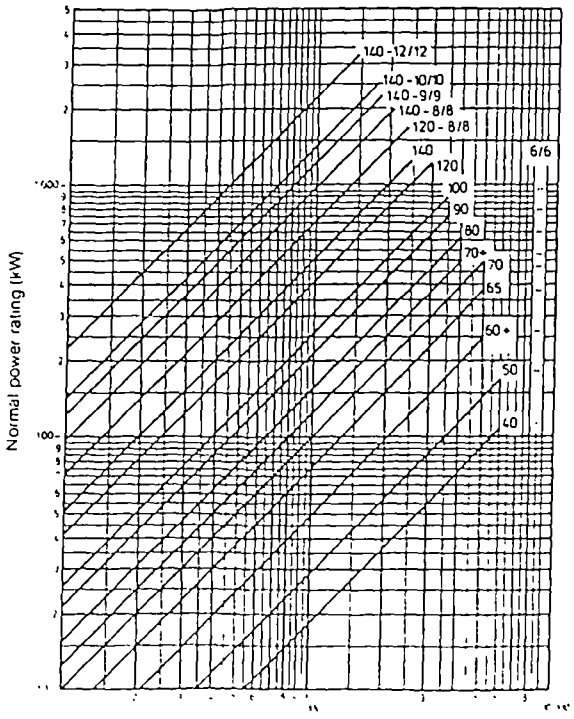

Three-six series

Service factor = 3.0

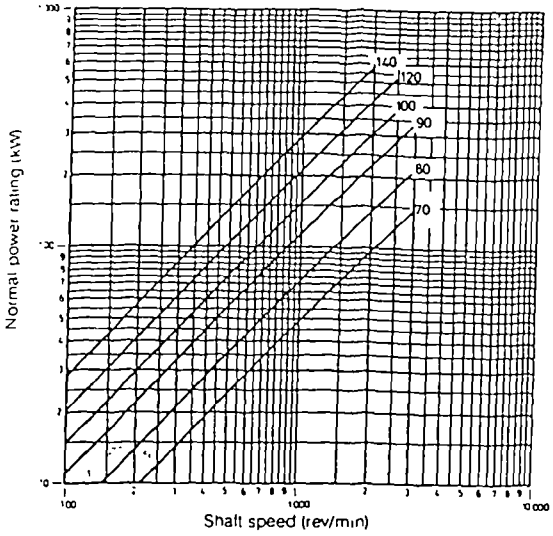

Preliminary Selection

Given the transmitted power and speed, a preliminary choice of coupling size (to suit most applications), may be made from these charts and the corresponding 'maximum momentary torques' for each size are given in the tables on page 5. If a service factor (maximum momentary torque ÷ normal transmitted torque) other than 3.0 is required, the initial selection should be made on the basis of the 'maximum momentary torque' expected in the application.

Maximum Momentary Torque

If this figure is exceeded, the Layrub blocks may be damaged, so it is important to make a realistic assessment of the peak torque which the couplings or shaft will have to transmit. This may be produced on start up by, for example, a high starting torque electric motor or a reciprocating engine, especially when connected to a driven machine of high inertia relative to the prime mover. The maximum torque may be produced by the load such as that due to a short circuit torque or out-of-phase paralleling in alternators, or by stalling. Braking may also be responsible for high coupling torques, especially where the coupling is interposed between the brake and the load or the principal inertia in the system.

Selection

Choosing the best type

Having made a preliminary selection based on the power ratings given on the previous page, it will be seen that the Layrub range provides more than one choice at most powers and speeds. Other considerations may indicate the best type for a given application For example, to transmit 100kW at 1500 rev/min, with a service factor of 3.0, the charts give the following choices

The stiffness values (which are given on the relevant data sheets for each series) relate to one coupling, so that the given value is halved for flexible shafts having a coupling at each end If these technical properties do not determine the optimum ho ce, then other factors such as cost or standardisat on (where one of the blocks is already held in stock for an he application, for example) will become decisive

Coupling Size	Outside Dia mm	Max Speed rev/min	Static Axial Stiffness N/mm	Dyn Torsional Stiffness MNm/rad	Max Shaft angle (deg)
105-2/4	270	2500	700	0 017	3 5
80-3/6	260	3000	600	0 027	2 5
65-6/6	191	5000	1900	0 054	1 0

Torsional Vibration

In order to ensure satisfactory operation, it is essential to carry out TV calculations for the whole transmission system. Inertia and stiffness values for all Layrub couplings are given on separate data sheets together with permissible vibratory torque amplitudes.

Continuous vibratory torque amplitude should not exceed ± max torque rating ÷ 6. Twiflex will be pleased to check torsional vibration compatibility if inertia and torsional stiffness details for the rest of the system can be provided.

In most sizes, alternative hardness grades and materials for the Layrub blocks are available, providing a choice of stiffness and damping factors as follows:

Block material	Dyn. torsional stiffness factor	Static axial stiffness factor	Damping	
			Dyn. Magnifier M	Rel. damping factor Ψ
Nat Rubber 50/55	0.6	0 6	1 4	0 45
Nat Rubber 60/65	1.0	1 0	1 2	0 52
Nat Rubber 70/75	1.75	1 35	9	0 70
Neoprene 60/65	1.4	1 0	8	0 79

Maximum speed

Values for single couplings are indicated in the rating tables on page 3. Maximum speeds for sliding shafts and special builds may be different and Twiflex will be pleased to advise.

Hostile Environment

Although natural rubber is attacked by mineral oils, it operates satisfactorily in the oil mist atmosphere of an engine room environment, but should not be exposed to frequent splashing or total immersion The following table summarises the tolerance range of the blocks

Material	Natural Rubber (all mixes)	Neoprene
Ambient temp range Deg C:	-40 to +60	-40 to +80
Resistance to:		
Mineral Oils	poor	excellent
Vegetable Oils	excellent	poor

Overload protection

Where high acc.dental overloads may occur, it is worth considering the use of a torque limiting device such as a shear pin coupling or a clutch The Twiflex centrifugal clutch coupling provides effective protection against momentary overloads, but if a sustained overload is possible, the air-start variant of the clutch is worth considering because of its ability to protect the whole of the power train and to provide a definable maximum torque above which the clutch will automatically disengage itself

Shaft alignment

Maximum continuous shaft displacements, radial axial, and conical for sing e couplings and shafts are given in the data sheets for each type Where expected al gnment errors, drift or thermal growth or flexibly mounted machinery may cause movements exceeding the stated values for a sing e coupling, a close-coupled assembly ('short shaft') can be used to increase the permissible radial and axial coupling deflections

Momentary excursions up to twice the continuous displacements are acceptable where they occur at insufficient frequency to cause a heat build up, for example during starts. Higher displacements may al o be used at low speeds or by increasing the service factor

Layrub

2/4 Series Couplings

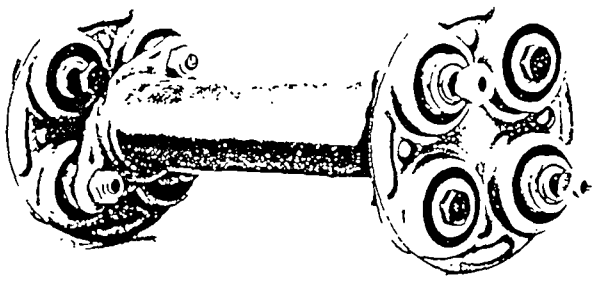

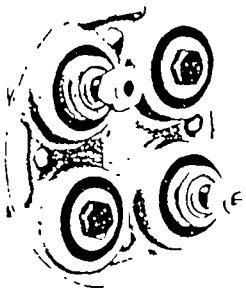

Description

The 2/4 is the type most commonly used, chiefly on account of its general adaptability to widely varying conditions. It also offers the least resistance to axial displacement, a useful feature where excessive plunge has to be accommodated, or where the length between the units it connects cannot be controlled to close limits on production. This type also has a high degree of articulation therefore, suitable for shaft arrangements requiring angular misalignment.

The coupling housings are produced from high quality ductile steel, having four pockets or recesses formed in each half, spaced equidistant both radially and circumferentially. The depth of each pocket is equal to that of half the rubber block, so that when the two half pressings are assembled the blocks are fully supported by the pressing itself.

Typical Applications

Dumper Trucks	Tractors	Automotive P.T.O.s
Excavators	Rolling Mills	Dynamometers
Rollers	Commercial Vehicles	Marine P.T.O.s
Cranes	Electric Vehicles	Diesel Auxiliary Drives

Type of Trunnion Block	Coupling Assembly Number	Maximum Torque Nm	Normal Torque Nm	Maximum Vibratory Torque Nm	Dynamic Torsional Stiffness Kp cm rad	Static Axial Stiffness Kp cm	Static Radial Stiffness Kp cm	Static Conical Stiffness Kp cm deg	Inertia Kg cm S²
40	32003	147	49	24 5	024 x 10⁶	200	1500	15	008
50	32004	235	78	39 2	016 x 10⁶	180	700	18	019
60–	32007	392	131	65 3	041 x 10⁶	270	1200	36	051
65	32008	598	199	100	065 x 10⁶	320	1600	47	072
70	32009	735	245	122	079 x 10⁶	320	1800	69	116
80	32011	1080	360	180	12 x 10⁶	410	2000	85	207
90	32014	1492	497	249	17 x 10⁶	480	2300	91	374
100	32015	1898	633	316	19 x 10⁶	430	2100	160	600
105	32016	2712	904	452	17 x 10⁶	720	2000	200	883
120	32017	3254	1085	542	26 x 10⁶	720	2000	220	1 517

* Normal torque based on a service factor of 3

* Maximum vibratory torque based frequency [illegible]

All stiffness values are for natural rubber [illegible]

Type of Trunnion Block	Maximum Shaft Angles		Maximum Extension or Compression per Coupling with $\theta_1°$ and $\theta_2°$ (mm)		Maximum Radial Mis-alignment (mm)	Maximum Speed of Single Couplings (rpm)	DIMENSIONS (mm)							Weight
	Con-tinuous $\theta_1°$	Mom-entary $\theta_2°$	$\theta_1°$	$\theta_2°$			A	B	C	D	E dia.	F	G dia.	Kg
40	2°	5°	1·2	3·2	0·3	6000	102	32·54	41·5	10	solid	18·5	29 0	0 6
50	3 5°	8°	1·6	4·0	0·3	5000	128	40·48	47·5	10	22	20	34 5	1 0
60+	3·5°	8°	2·4	6·4	0·4	5000	153	48·42	57 0	10	solid	26	42 0	1·7
65	3·5°	8°	2·4	6·4	0·4	5000	167	52·39	57·0	12·5	solid	26	42 5	2 3
70	3 5°	8°	2 4	6·4	0 4	5000	178	54·77	68·5	16	solid	31	42 5	3·1
80	3·5°	8°	3 2	7·9	0·5	4500	203	62·71	68 5	16	solid	24	49 5	4 2
90	3 5°	8°	3·2	7·9	0·5	4000	229	70·64	76 0	19	solid	27	58 5	5 9
100	3 5°	8°	3 2	7·9	0 6	3500	254	78·56	79 5	19	solid	28	63 5	7 5
105	3 5	8	4 0	9·5	0 6	2500	270	78·56	92 0	25	solid	32	47 0	11 3
120	3 5°	8°	4·0	9 5	0 6	2000	305	93 66	92 0	25	solid	32	75 5	13 6

For speeds in excess of specified values or maximum shaft speeds, please consult our Engineering Department

Laycock Engineering Ltd

Archer Road, Millhouses, Sheffield S8 0JY Telephone (0742) 368221 Telex 54255

A GKN company

JWMS/283:2M

Printed in E

HEENAN & FROUDE LIMITED ENGINEERS, WORCESTER ENGLAND

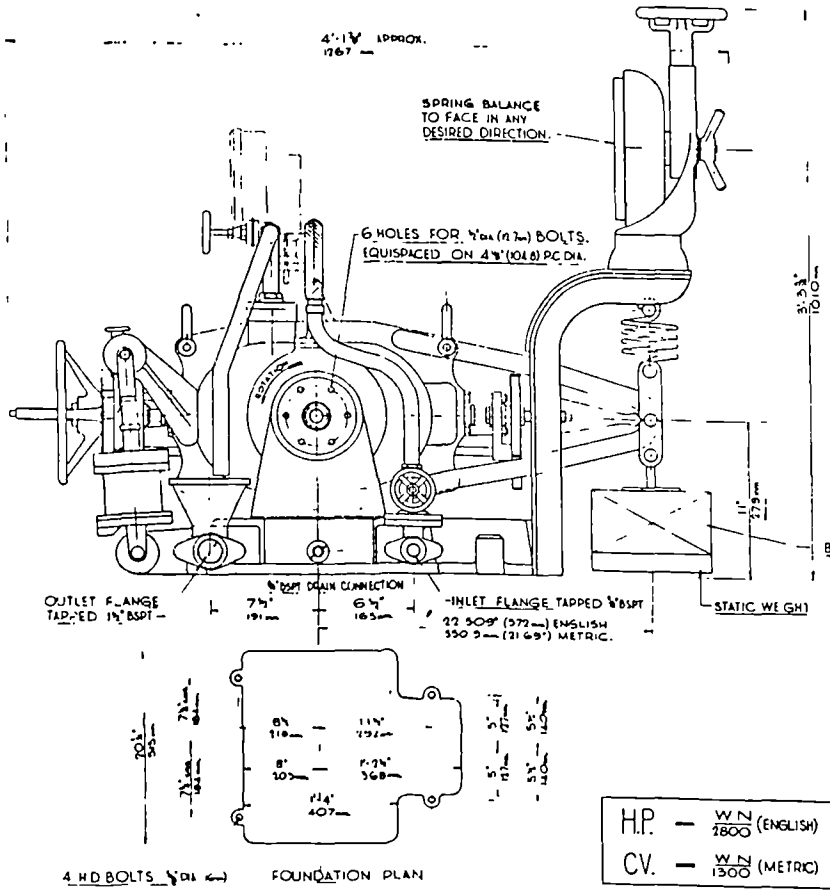

TACHOMETER MOUNTING PROVISION. TACHOMETER & WORM-DRIVE NOT SUPPLIED BY H&F LTD UNLESS SPECIALLY ORDERED.

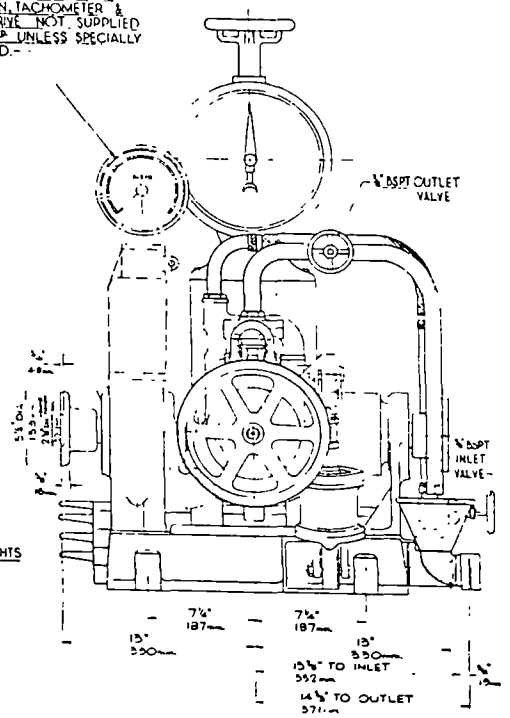

THIS DYNAMOMETER SHAFT IS NOT DESIGNED TO WITHSTAND HEAVY BENDING MOMENTS DUE TO THE WEIGHT OF ENGINE FLYWHEELS ETC.

H.P. — $\frac{W.N}{2800}$ (ENGLISH)

CV. — $\frac{W.N}{1300}$ (METRIC)

APPROXIMATE SHIPPING		SPECIFICATION.	
NETT WEIGHT	GROSS WEIGHT	CUBAGE.	
952 LB.	1234 LB.	41 CU.FT.	
432 KG.	559 KG.	1.16 CU.M.	

THIS DRAWING MUST NOT BE SCALED

FROUDE PATENT HYDRAULIC DYNAMOMETER - SIZE D P X 3

THIS DRAWING IS NOT CERTIFIED

Designed and Manufactured by Dynamometer ...

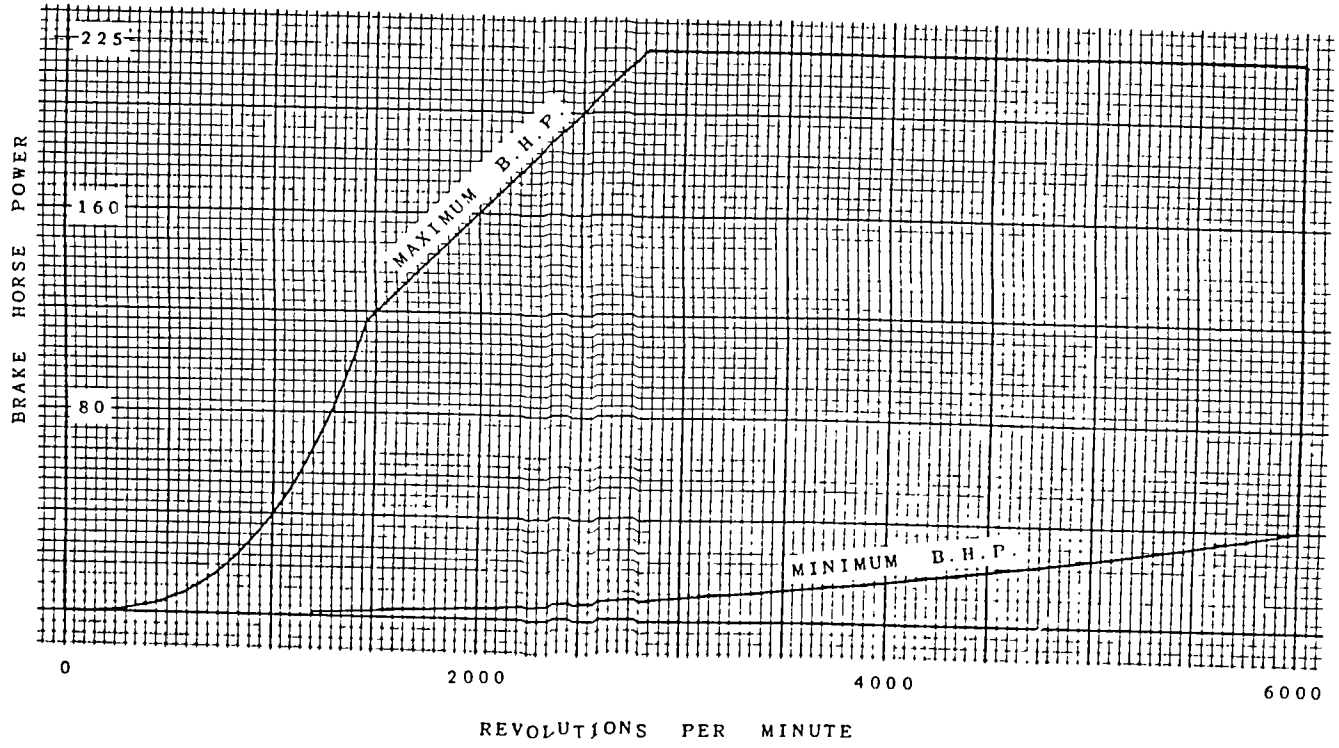

DIAGRAM OF MAXIMUM AND MINIMUM
BRAKE HORSE POWER ABSORBED BY
FROUDE PATENT HYDRAULIC DYNAMOMETER
SIZE D p X 3 (OPEN FLOW)

CURVE NO.
SS 3/8463

AIR FLOW RIG CALCULATIONS

DATE:28 May 1992

ENGINE DATA

ENGINE TYPE:

PORT TYPE:	Swirl	RATED ENGINE SPEED-RPM:	1500
TEST LOCATION:	Brunel	CAPACITY/CYL-cc:	1034.217
CARBURETTOR:	No	BORE-mm:	107
MANIFOLD:	No	STROKE-mm:	115
INT VALVES/CYL:	1	CON-ROD CENTRES-mm:	203
SEAT ANGLE-DEG:	30	INNER VALVE SEAT DIA-MM:	45.3
		L/R RATIO:	0

CAMSHAFT DATA

CAMSHAFT PART NO: Ford_Dover
ROCKER RATIO: 1.4
VALVE CLEARANCE: .4

TEST DATA

TEST DATE:	24 April 1991	AMBIENT PRESSURE-mmHG:	765
TEST NO :	1	PORT DEPRESSION-MMH2O:	252
CYL NO :	1	AMBIENT TEMP.-Deg.C:	18

ORIFICE PLATE DIA mm: 60

IMPULSE METER SWIRL READINGS USED

TEST RESULTS

1.RICARDO VALVE LIFT DEPENDENT MODEL
-CONSTANT PRESSURE DROP OVER PORT
-INTEGRATED FROM IVO TO IVC

SWIRL RATIO = 2.009
GULP FACTOR = 0.322
MEAN FLOW COEFFICIENT = 0.291
CYCLE FLOW COEFFICIENT= 1.322

2.THIEN(AVL)PISTON DEPENDENT MODEL
-FLOW=PISTON SPEED*AREA
-INTEGRATED FROM TDC TO BDC

SWIRL RATIO = 2.750
GULP FACTOR = 0.288
MEAN FLOW COEFFICIENT= 0.325

VALVE LIFT (MM)	N-D LIFT (L/D)	AIRFLOW LTR/S	AIRFLOW CFM	SWIRL RPM	SWIRL Nss	FLOW COEFF	N-D SWIRL	COEFF OF PERF	COEFF OF DISCH	THETE (DEG)	SWIRL NO EISELLE	SWIRL NO AVL
1.00	0.022	9.00	19.07	291	0.480	0.0877	0.0513	0.9933	1.0519	1.75	1.632	1.116
2.00	0.044	14.49	30.70	424	1.125	0.1412	0.0747	0.8007	0.8716	3.16	1.476	1.010
3.00	0.066	19.23	40.74	696	2.450	0.1875	0.1226	0.7112	0.7744	5.84	1.825	1.248
4.00	0.088	25.61	54.26	1158	5.425	0.2496	0.2039	0.7169	0.7717	9.67	2.278	1.559
5.00	0.110	30.89	65.45	1575	8.900	0.3011	0.2773	0.7013	0.7411	13.50	2.569	1.758
6.00	0.132	35.11	74.39	1919	12.325	0.3423	0.3379	0.6761	0.6977	17.16	2.754	1.884
7.00	0.155	38.70	81.99	2239	15.850	0.3772	0.3943	0.6531	0.6547	20.88	2.916	1.995
8.00	0.177	42.61	89.27	2611	20.350	0.4153	0.4598	0.6476	0.6262	24.79	3.088	2.113
9.00	0.199	45.44	96.27	2912	24.200	0.4429	0.5127	0 6342	0.5893	28.51	3.229	2.209
10.00	0.221	47.52	100.67	3170	27.550	0.4632	0.5581	0.6195	0.5504	32.14	3.361	2.299
11.00	0.243	49.43	104.72	3423	30.950	0.4818	0.6028	0.6105	0.5166	35.66	3.490	2.387
12.00	0.265	51.00	108.05	3623	33.800	0.4971	0.6389	0.6017	0.4848	38.76	3.580	2.449
TEST DATA AT MAXIMUM VALVE LIFT												
10.62	0.235	0.0487	103.20	3328	29.670	0.4748	0.5860	0.6139	0.5293	34.33	3.441	2.354

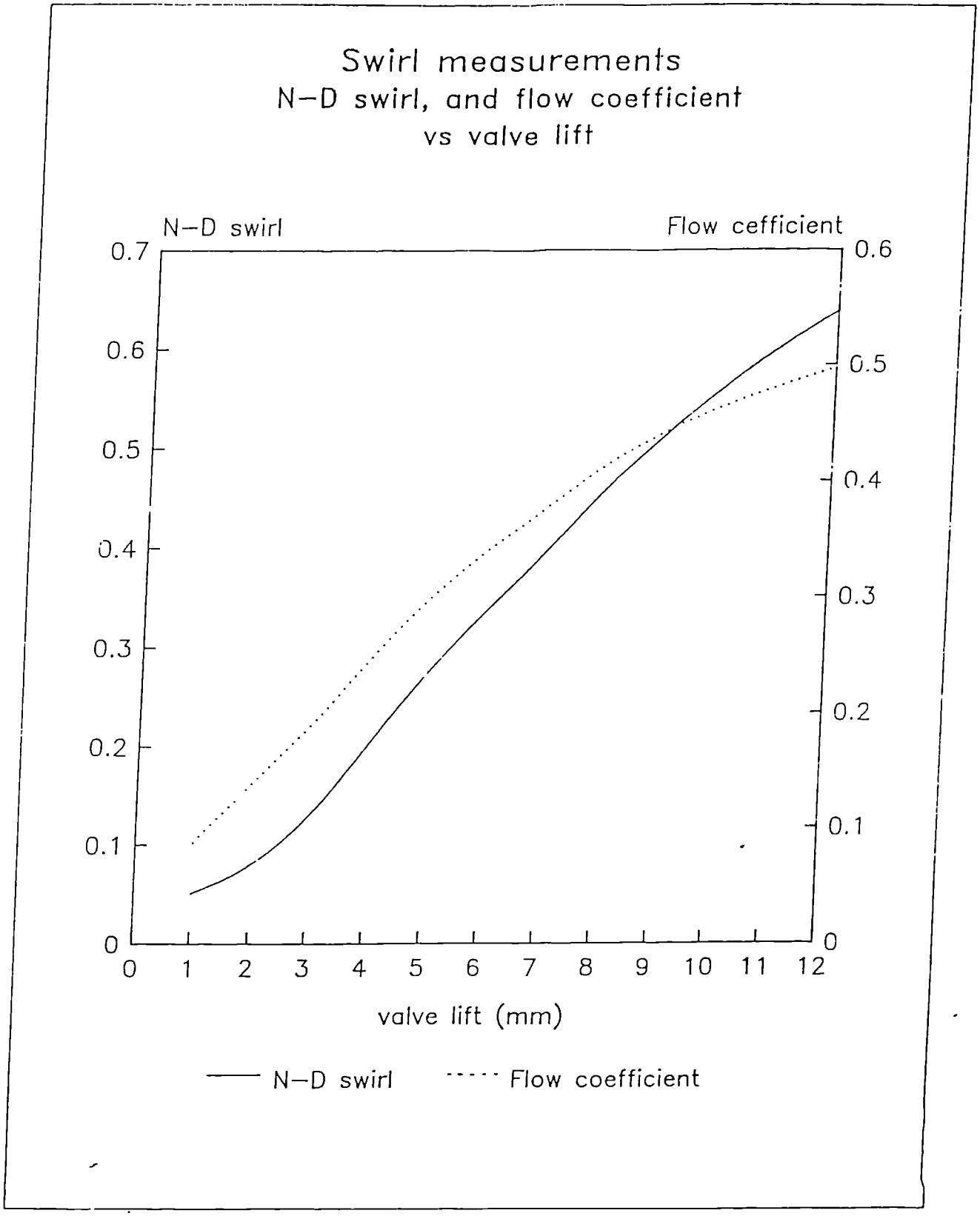
Swirl measurements
N–D swirl, and flow coefficient
vs valve lift
N–D swirl
Flow cefficient
0.7
0.6
0.5
0.4
0.3
0.2
0.1
0
0.6
0.5
0.4
0.3
0.2
0.1
0
0 1 2 3 4 5 6 7 8 9 10 11 12
valve lift (mm)
N–D swirl
Flow coefficient

RICARDO MOMENTUM SUMMATION METHOD

The method used by Ricardo is presented in some detail by Beard (1984), the assumptions are:

i) Flow is adiabatic and incompressible.

ii) The moment of momentum is conserved (there are no viscous losses in the cylinder).

iii) Volumetric efficiency of 100% per cent.

iv) If a paddle wheel is used, the swirl is a forced vortex.

v) If a paddle wheel is used, the axial velocity within the cylinder is uniform.

vi) The pressure drop across the port is constant during induction.

vii) Flow only occurs between inlet valve opening and closing, and hence flow rate at any time is dependent only on valve lift.

Hence the Ricardo swirl ratio, (R_s) i.e. the ratio of the swirl speed at induction to the engine crankshaft speed, is defined as:

$$R_s = \frac{L_D \int_{\alpha_1}^{\alpha_2} C_F(\alpha)\, N_R(\alpha)\, d\alpha}{\left[\int_{\alpha_1}^{\alpha_2} C_F(\alpha)\, d\alpha\right]^2}$$

where: $\alpha 1$ = inlet valve opening

$\alpha 2$ = inlet valve closing

engine shape factor

$$L_D = \frac{BS}{nD^2}$$

where: B = bore, S = stroke, n = number of inlet valves, D = inlet valve throat diameter

and port flow coefficient

$$C_F = V/(A_p v_o)$$

where V = volumetric flow rate, A_p = valve perimeter area, and v_0 the velocity in a frictionless nozzle for a given pressure drop is given by:

$$v_0 = \sqrt{2\Delta P/\rho}\ , \qquad \Delta P = \textit{Pressure drop across the valve}$$

The Ricardo defined mean flow coefficient is equal to the sum of the flow coefficients between inlet valve opening and inlet valve closing divided by the angle between these two events:

$$C_{F(MEAN)} = \frac{\int_{\alpha_1}^{\alpha_2} C_F(\alpha)\, d\alpha}{\alpha_2 - \alpha_1}$$

Kistler Pressure Transducer

3 6001 9 82 1 2

QUARZKRISTALL HOCHTEMPERATUR DRUCKAUFNEHMER
CAPTEUR DE PRESSION A QUARTZ POUR TEMPERATURES ELEVEES
QUARTZ HIGH TEMPERATURE PRESSURE TRANSDUCER

6001

Quarzkristall Druckaufnehmer zum Messen dynamischer und quasistatischer Drucke bis 250 bar bei Temperaturen bis zu 350 °C

Capteur de pression à quartz pour mesurer des pressions dynamiques et quasi statiques jusqu'à 250 bar sous des temperatures pouvant atteindre 350 °C

Quartz pressure transducer for measuring dynamic and quasistatic pressures up to 250 bar at temperatures up to 350° C

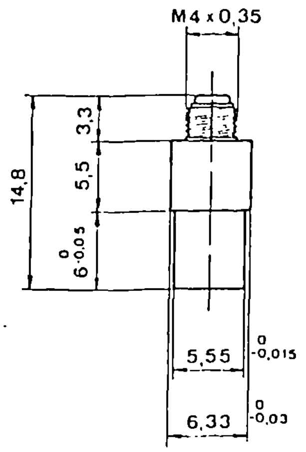

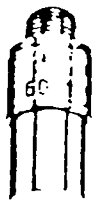

2 : 1

TECHNISCHE DATEN — DONNEES TECHNIQUES — TECHNICAL DATA

Bereich	Gamme	Range	bar	0 ..250
Kalibrierte Teilbereiche	Gammes partielles étalonnées	Calibrated partial ranges	bar	0 . 25
			bar	0 2,5
Überlast	Surcharge	Overload	bar	350
Ansprechschwelle	Seuil de réponse	Threshold	bar	<0,002
Empfindlichkeit	Sensibilité	Sensitivity	pC/bar	≈ -15
Eigenfrequenz	Fréquence propre	Natural frequency	kHz	>150
Linearität } für Bereich [illegible]	Linéarité } [illegible]	Linearity } for range and [illegible]	% FSO	<±0 8
Hysterese } und Teilb[illegible]	Hysterésis } gamme partielle	Hysteresis } partial range	% FSO	<0 5
Beschleunigungsempfindlichkeit	Sensibilité aux accélérations:	Acceleration sensitivity.		
axial	axiales	axial	bar/g	<0,001
normal zur Achse	normales [illegible]	transverse	bar/g	<0,0001
Stossfestigkeit	Résistance au choc	Shock resistance	g	5000
Thermische Empfindlichkeitsänderung	Décalage thermique de la sensibilité	Thermal sensitivity shift		
20 ..100°C	20 ..100°C	20 ..100°C	%	≈ +0,5
20 ..350°C	20 ..350°C	20 ..350°C	%	≈ +3
200 ±50°C	200 ±50°C	200 ±50°C	%	≈ ±1
Kalibriert im Bereich	Etalonné dans la gamme	Calibrated in range	°C	20 ..350
Betriebstemperaturbereich	Gamme de température d'utilisation	Operating temperature range	°C	-196 ..350
Transient Temperaturfehler	Erreur transitoire due à la température	Transient temperature error	bar	<-1 5
(Propanflamme intermittierend [illegible])	(flamme au propane intermittente [illegible])	(propane flame intermittent [illegible])		
Isolationswiderstand:	Résistance d'isolation:	Insulation resistance:		
bei 20°C	à 20°C	at 20°C	TΩ	>10
bei 350°C	à 350°C	at 350°C	TΩ	>0,01
Gewicht	Poids	Weight	g	1 8

1 bar = 10⁵ Pa (Pascal) [illegible] 1 TΩ (Teraohm) = 10^{12} Ω

Polystable® Quarzkristallelemente sind international durch Patente geschützt

Les éléments à quartz Polystable® sont l'objet de brevets internationaux

Polystable® quartz elements are internationally patented

3.6001 9.82 2

JK

Type

5675

5711
5713
5715

5717

5719

5721
5723
5725
5727

5729
573

574

575

580

580

582

590

590

590

590

595
595

595

60

60

60

63

64

64

6C

6C

BESCHREIBUNG

Die Membrane übertragt den Druck auf das Polystable® Quarzkristall Messelement und ist mit dem Aufnehmergehause bundig und dicht verschweisst. Die patentierte Konstruktion ist sehr unempfindlich gegen rasche Temperaturanderungen im Messmedium. Der Stecker ist dicht und hat einen Keramikisolator. Der Aufnehmer besteht aus gehartetem, korrosionsfestem CrNi-Stahl; die Membrane ist aus rostfreiem 18-8 CrNi-Stahl.

ANWENDUNG

Dieser Aufnehmer eignet sich besonders zum Messen dynamischer Drucke bei Temperaturen bis zu 350 °C und benotigt sehr wenig Platz fur den Einbau. Anwendungen finden sich in Nukleartechnik, Heissdampfsystemen, Verbrennungsvorgangen, Explosionen usw. Dieser Typ kann auch zum Messen von Kraften verwendet werden (0 ... 200N).

MONTAGE

Der Aufnehmer kann mittels luftgekühlter Steckernippel Typ 6461 (Fig. 1) eingebaut werden. Teflonisolierte Kabelstecker können verwendet werden, solange die Umgebungstemperaturen unter 200 °C bleiben. Andernfalls beraten wir Sie gerne aufgrund Ihrer Einbauvorschläge über die Verwendung von Kabeln oder Spezialsteckernippeln (Fig. 2). Uber Standard-Einbaumaterial informieren folgende Datenblatter:

Adapter	4.015
Steckernippel	4.014
Werkzeuge	4.012
Kabel	15.011

DESCRIPTION

La membrane transmet la pression sur l'element de mesure à quartz Polystable® et est soude de façon etanche et arrase au boîtier du capteur La construction brevetee est pratiquement insensible face aux variations brutales de température dans le fluide soumis à mesure La prise est etanche et possède un isolant en ceramique Le capteur est realise en acier nickel/chrome trempe resistant à la corrosion, la membrane est en acier inoxydable nickel/chrome 18 8

APPLICATION

Ce capteur convient particulierement a la mesure de pressions dynamiques sous des températures pouvant atteindre jusqu'a 350° C et ne requiert que peu de place pour son montage. Les applications essentielles se trouvent dans la recherche nucleaire, les systèmes de vapeurs surchauffees, les phenomenes de combustion, les explosions etc. Ce type de capteur peut aussi être utilisé pour la mesure de forces (0 . 200N).

MONTAGE

Le capteur peut être monte au moyen d'un ecrou connecteur type 6461 (figure 1) refroidi par air. Les prises de câble à isolant teflon peuvent être utilisees tant que la température ambiante reste inferieure à 200°C. Dans les autres cas nous vous conseillerons volontiers, en nous basant sur vos projets de montage, sur l'emploi de câbles ou de connecteurs speciaux (figure 2) Les notices techniques suivantes fournissent des précisions sur les accessoires de montage standard:

Adaptateurs	4 015
Ecrous connecteurs	4.014
Outillage	4 012
Câbles	15.011

DESCRIPTION

The diaphragm transmits the pressure to the Polystable® quartz element and is welded flush and tight to the transducer body The patented design has a very low sensitivity to rapid temperature changes in the fluid

The connector is tight and has a ceramic insulator The transducer is made of hardened, corrosion resistant CrNi steel, the diaphragm is of stainless 18 8 CrNi steel

APPLICATION

This transducer is ideal for measuring dynamic pressures at temperatures up to 350 C and requires a minimum of mounting space Applications are in nuclear research, superheated steam systems, internal combustion, explosions and so on

This type may also be used for measuring forces (0 ... 200N)

MOUNTING

The transducer can be mounted with air cooled connecting nipples type 6461 (fig. 1). Teflon insulated cable connectors may be used if ambient air temperatures stay below 200 C For other cases, please submit details of the proposed installation and we will advise whether cables or special extension nipples are to be preferred (fig 2).

The following data sheets inform on standard mounting material

Adaptors	4 015
Connecting Nipples	4 014
Tools	4 012
Cables	15 011

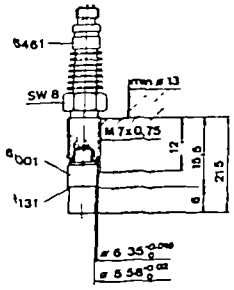

Fig. 1 Standard Einbau
Montage standard
Standard mounting

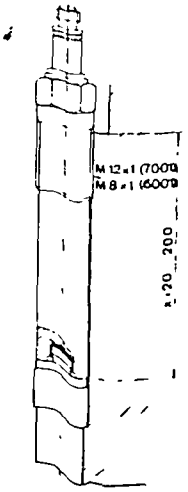

Fig. Spezialmontage
Montage
Special mounting

APPENDIX B

The Use of the Wiebe Function in Combustion Analysis

The Wiebe function is a convenient means of generating the 'S' shaped curves, that are produced when calculating the cumulative mass fration burnt (mfb) in spark ignition engine combustion. The Wiebe function is defined by the following equation:

$$mfb = 1 - \exp(-a*(theta)**(m+1))$$

where theta is the fraction of the burn duration
and a and m are constants, with typical values of 5 and 2

The Wiebe function is constrained to pass through the values (0,0) and close to (1,1). The constants a and m can be determined analytically if the values of mfb and theta are known at two other locations. Convenient values are the 10% and 90% mfb values, since these are usually well defined in a combustion analysis. Lower values of mfb are sensitive to errors in the pressure transducer datum pressure level, and higher values of mfb are sensitive to the choice of polytropic index in the Rassweiler and Withrow combustion analysis.

However, whilst the 10% and 90% mass fraction burnt crank angles are likely to be well defined, these angles need to be normalised by the total burn period. Examination of an experimental mass fraction burnt plot, will show that the total burn period can be difficult to define. The errors associated with the uncertainty in identifying the total burn period are illustrated in the following example.

Consider a mass fraction burn curve with a period of 60 degrees, with a = 5 and m = 2; the mass fraction burn results are included in the following table, along with the consequences of incorrectly identifying the burn period as 50 degrees and 70 degrees.

Inspection of the table, shows that there are no differences in the computed values of the mfb, but that if too short a burn period is selected, then the mfb does not reach unity. However, when the Wiebe parameters are used in a simulation program, the crank angle will increment beyond the nominal period of combustion, and no errors should be introduced. The Wiebe parameter a is subject to significant changes in numerical value, but these are a reflection of the change in nominal burn period, as:

$$a/(\text{burn period})^{**}(m+1) = \text{const}$$

(Perhaps it would be better to fix a value for a, (such as 5), and then compute the burn period)

In conclusion, it must be remembered that the Wiebe function is solely a means of modelling an observed burn rate, and that the best ways of characterising the burn rate will be the 0-10% and 10-90% burn times. The Wiebe parameters and the burn period are not an appropriate way of characterising the burn rate.

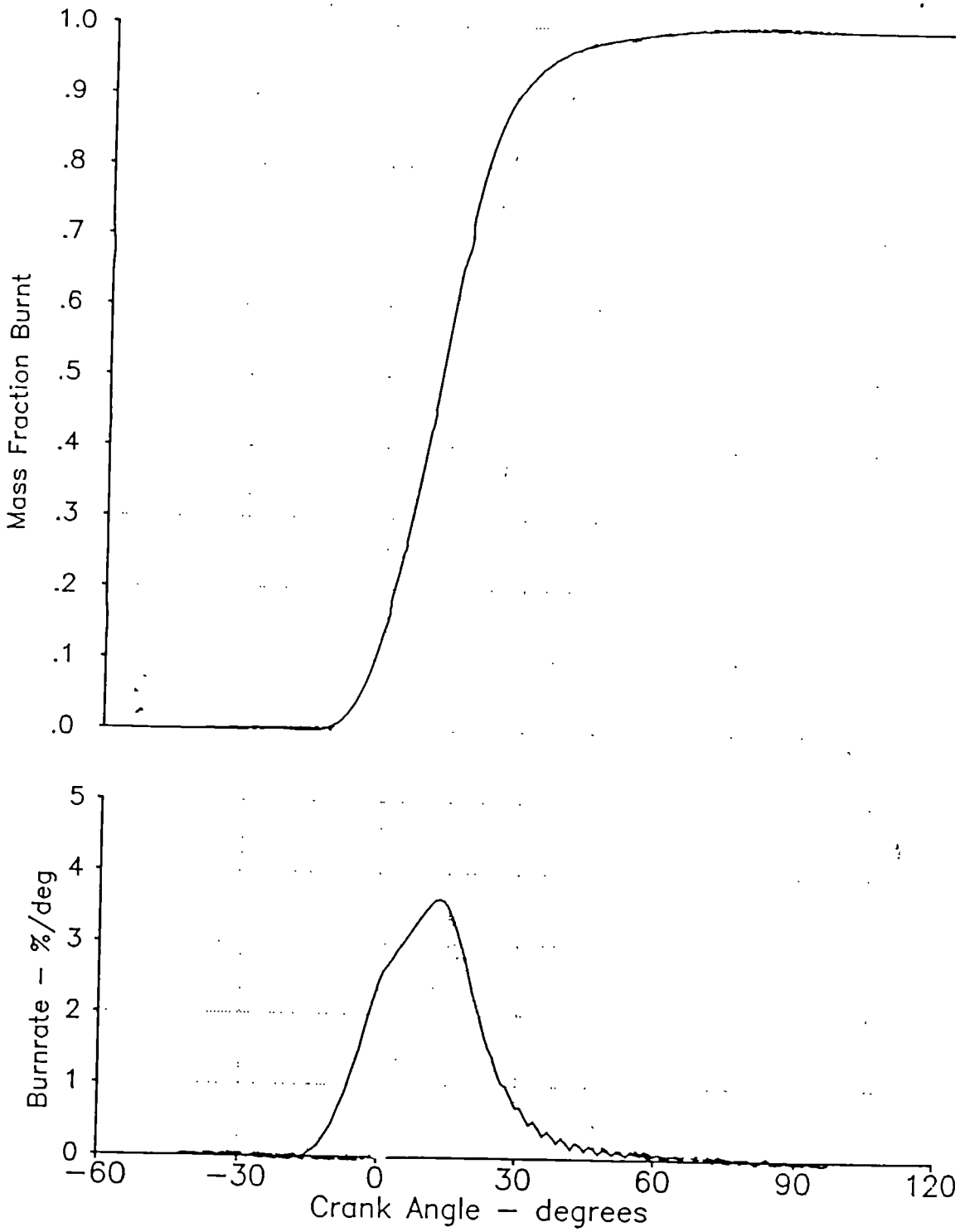
1.0
.9
.8
.7
.6
.5
.4
.3
.2
.1
.0
Mass Fraction Burnt
5
4
3
2
1
0
Burnrate – %/deg
−60
−30
0
30
60
90
120
Crank Angle – degrees

Wiebe parameters, a = 4.99, m = 2.00; Burn Period = 60.0

Theta	MFB
.0	.000000
5.0	.002906
10.0	.022967
15.0	.075336
20.0	.169312
25.0	.303765
30.0	.464908
35.0	.629361
40.0	.772584
45.0	.878510
50.0	.944458
55.0	.978642
60.0	.993210

Wiebe parameters, a = 2.89, m = 2.00; Burn Period = 50.0

Theta	MFB
.0	.000000
5.0	.002906
10.0	.022967
15.0	.075336
20.0	.169312
25.0	.303765
30.0	.464908
35.0	.629361
40.0	.772584
45.0	.878510
50.0	.944458

Wiebe parameters, a = 7.92, m = 2.00; Burn Period = 70.0

Theta	MFB
.0	.000000
5.0	.002906
10.0	.022967
15.0	.075336
20.0	.169312
25.0	.303765
30.0	.464908
35.0	.629361
40.0	.772584
45.0	.878510
50.0	.944458
55.0	.978642
60.0	.993210
65.0	.998246
70.0	.999638

COMPOSITION OF NATURAL GAS IN NORTH THAMES REGION File 2.2.8

The "Typical Composition" given below is that for the gas that will be supplied from 1.10.86, and the "Range of Composition" indicates the limits of variations that might occur in the course of time due to changes in the proportions of gas derived from the various production sources. If more precise information is required for special reasons at any particular time, the Scientific Services Manager should be consulted.

It should be remembered that the only statutory limitations relating to the quality of gas supplies are: the Calorific Value should be at, or above, the Declared Calorific Value, the Hydrogen Sulphide content should be less than 3.3 ppm, and the gas should have a "distinctive smell".

	Typical Composition Vol. %	Range of Composition Vol %
Nitrogen	3.1	1.2 to 3.4
Helium	0.0	0.0 to 0.1
Carbon dioxide	0.4	0.1 to 0.7
Methane	92.8	91.0 to 95.0
Ethane	2.8	2.6 to 3.6
Propane	0.6	0.5 to 1.0
Butanes	0.2	0.1 to 0.4
Pentane and heavier hydrocarbons (including traces of aromatic compounds)	0.1	0.1 to 0.3

The natural gas may also contain some or all of the following compounds:-

Hydrogen sulphide	0.0 ppm	0 to 3 ppm
Methyl-ethyl sulphide	0.1 ppm	0.1 to 0.6 ppm
Di-ethyl sulphide	4.4 ppm	3 to 10 ppm
Ethyl mercaptan	0.5 ppm	0.3 to 0.7 ppm
Tertiary butyl mercaptan	0.9 ppm	0.5 to 1.4 ppm
Water	50.0 ppm	40 to 2000 ppm
Methanol	100.0 ppm	0 to 200 ppm
Monc-ethylene glycol	up to 90 mg/m^3	

The specific gravity (relative to dry air) will normally be between 0.595 and 0.605.

w.e.	CV	N2	CO_2	CH_4	C_2H_6	C_3H_8	iC4	nC4	C5+
27/11/91	38.3	2.40	0.23	93.62	2.89	0.55	0.09	0.12	0.10
25/ 3/92	38.1	2.68	0.36	93.10	2.96	0.59	0.10	0.13	0.08
29/ 7/92	38.3	2.23	0.11	94.06	2.84	0.48	0.08	0.11	0.09
5/ 8/92	38.4	2.32	0.18	93.62	2.98	0.57	0.10	0.13	0.10
9/ 9/92	38.4	2.41	0.35	93.52	2.88	0.53	0.09	0.12	0.10
21/10/92	38.3	2.35	0.31	93.57	2.89	0.57	0.09	0.12	0.10
10/ 2/92	38.4	2.34	0.31	93.45	2.97	0.60	0.10	0.13	0.10

```
c       PROGRAM DOVERGAS.FOR
c
c       This program converts raw experimental input data to give useful
C       measurements of energy, emissions and combustion performance of the
c       Dovergas SI6 gas engine

        REAL    NOxV(200), Lamda(200), Speed(200), Power(200), Tmg(200)
        REAL    TClIn(200), TClout(200), TPrimary(200), TFuel(200)
        REAL    TAir(200), TMixin(200), TExout(200), TOilgly(200)
        REAL    TOilsmp(200)
        REAL    Airflrt(200), Clflrt(200)
        REAL    CO(200), CO2(200), O2(200), HC(200)
        REAL    Mthne(200), Time(200), Pgup(200), Pgdn(200)
        REAL    Hmdty(200)
        REAL    Torque(200), bmep(200)
        REAL    Imep(200), COVimep(200), Pmax(200), COVpmax(200)
        REAL    Mfb1(200), Mfb10(200), Mfb90(200), Mfb1090(200)
        REAL    fmep(200), etam(200), etab(200), etai(200)
        REAL    mFuel(200), vFuel(200), Pbaro(200), Pabs(200)
        REAL    QCl(200), QEx(200)
        REAL    AFRV(200), AFRG(200), etav(200)
        REAL    CO2gkWh(200), COgkWh(200), HCgkWh(200)
        REAL    NOxh(200), NOxgkWh(200), NOxcorgkwh(200)
        REAL    Pdry(200), Powercorr(200)
        REAL    VSwept, CalVal, Cbn, Hdn, Oxn, Ntn, ffimep
        REAL    mfb,mfb2
        REAL    mexhaust, raz, ian
        REAL    COgMJth,COgCum
        REAL    CO2gMJth,CO2gCum
        REAL    HCgMJth,HCgCum
        REAL    NOxgMJth,NOxgCum,NOxcgMJth,NOxcgCum
        REAL    MCbn,MHdn,MOxn,MNtn,Mgas
        REAL    N2,H2,H2O
        REAL    Nmol(8)
        REAL    Cv(8,4)
        REAL    H,QChm
        REAL    Ho
        REAL    KExout, KDtm, mfCV

        CHARACTER*15 Engine
        CHARACTER*15 FileIn
        CHARACTER*15 Firstout
        CHARACTER*15 Secondout
        CHARACTER*15 Thirdout
        CHARACTER*15 Fourthout

c       Coefficients for calculating the molar heat capacity at
c       constant volume (kJ/kmolK) from the absolute temperature K
c       derived from (Stone 1992,adapted from Reid et al.(1977)
c
c       CO2:
              Cv(1,1)=11.477
              Cv(1,2)=7.342E-2
              Cv(1,3)=-56.01E-6
              Cv(1,4)=17.15E-9
c       CO:
              Cv(2,1)=22.550
              Cv(2,2)=-1.285E-2
              Cv(2,3)= 27.89E-6
              Cv(2,4)=-12.71E-9
```

```
c       O2:
                Cv(3,1)=19.786
                Cv(3,2)=-3.680E-6
                Cv(3,3)=17.46E-6
                Cv(3,4)=-10.65E-9
c       HC(CH4):
                Cv(4,1)=10.933
                Cv(4,2)=5.216E-2
                Cv(4,3)=11.97E-6
                Cv(4,4)=-11.31E-9
c       NOx(NO):
                Cv(5,1)=21.0357
                Cv(5,2)=-9.378E-4
                Cv(5,3)=9.747E-6
                Cv(5,4)=-4.187E-9
c       H2:
                Cv(6,1)=18.824
                Cv(6,2)=9.272E-3
                Cv(6,3)=-13.81E-6
                Cv(6,4)=7.644E-9
c       H2O:
                Cv(7,1)=23.928
                Cv(7,2)=1.924E-3
                Cv(7,3)=10.56E-6
                Cv(7,4)=3.596E-9
c       N2:
                Cv(8,1)=22.836
                Cv(8,2)=-1.356E-2
                Cv(8,3)=26.80E-6
                Cv(8,4)=-11.68E-9
c
c
        WRITE(*,*) 'This program is capable of differentiating units'
        WRITE(*,*) 'of Power(kW) from Torque(Nm).'
        WRITE(*,*)
        WRITE(*,*) 'What is the Engine parameter filename ?    '
        WRITE(*,*)
        WRITE(*,*) 'The Engine parameter file contains the fuel'
        WRITE(*,*) 'composition expressed as an equivalent molecular'
        WRITE(*,*) 'formula, from which the equivalent molecular'
        WRITE(*,*) 'weight is calculated'
        READ(*,'(A)') Engine
        WRITE(*,*)
        WRITE(*,*)
        WRITE(*,*) 'What is the INPUT filename ?    '
        READ(*,'(A)') FileIn
        WRITE(*,*) 'What is the first OUTPUT filename ?    '
        READ(*,'(A)') Firstout
        WRITE(*,*) 'What is the second OUTPUT filename ?    '
        READ(*,'(A)') Secondout
        WRITE(*,*) 'What is the third OUTPUT filename ?    '
        READ(*,'(A)') Thirdout
        WRITE(*,*) 'What is the fourth OUTPUT filename ?    '
        READ(*,'(A)') Fourthout
        OPEN(3,File=Engine)
        OPEN(4,File=FileIn)
        OPEN(11,File=Firstout,status = 'new')
        OPEN(12,File=Secondout,status = 'new')
        OPEN(13,File=Thirdout,status = 'new')
        OPEN(14,File=Fourthout,status = 'new')
```

```
c
      Pi = 4.0*Atan(1.0)
c     Reference Temperature(British Gas)
      TRef=288.15

c     Molecular weights
      MCbn=12.011
      MHdn=1.008
      MOxn=15.999
      MNtn=14.007
c
c
      READ(3,*, ERR=4445) VSwept,CalVal,Cbn,Hdn,Oxn,Ntn,ffimep,TALuft
     $ ,TDtm,Clcomp,Tfcorr
      KDtm = TDtm + 273.15
      WRITE(*,*) VSwept,CalVal,Cbn,Hdn,Oxn,Ntn,ffimep,TALuft,TDtm
     $ ,Clcomp,Tfcorr

      Mgas=Cbn*MCbn+Hdn*MHdn+Oxn*MOxn+Ntn*MNtn
      R=8314.3/Mgas
      IF ((Mgas.GT.19).AND.(Mgas.LT.15)) then
      WRITE(*,*) 'The value of the MOLECULAR WEIGHT is out of'
      WRITE(*,*) 'range (15 to 19 kg/kmol). Enter 1 if you wish'
      WRITE(*,*) 'to continue'
      READ(*,*) IMwt
      IF (IMwt.NE.1) GO TO 4447
      ENDIF
c     Next lines: sv=stoichiometric volumetric A:F ratio
c                 sg=stoichiometric gravimetric A:F ratio
c
      AFRsv = (Cbn+(Hdn/2.0-Oxn)/2.0)/0.2095
      AFRsg =2896.0*(2.0*Cbn+Hdn/2.0-Oxn)/
     $       (41.90*((Cbn*12.011)+(Oxn*15.999)+(Ntn*14.007)+
     $       (Hdn*1.008)))
c
      CalValg = CalVal*R*TRef/101325
c
      WRITE(11,1000)
      WRITE(11,1010)
      WRITE(12,2000)
      WRITE(12,2010)
      WRITE(13,3000)
      WRITE(13,3010)
      WRITE(14,4000)
      WRITE(14,4010)

      Do 11 i=1,200
      READ(4,*,end=20)  NOxV(i), Lamda(i), Speed(i), Power(i), Tmg(i)
     $                , TClIn(i), TClout(i), TPrimary(i), TFuel(i),
     $                  TAir(i), TMixin(i), TExout(i), TOilgly(i),
     $                  TOilsmp(i),
     $                  Airflrt(i), Clflrt(i),
     $                  CO(i), CO2(i), O2(i), HC(i),
     $                  Mthne(i), Time(i), Pgup(i), Pgdn(i),
     $                  Hmdty(i),
     $                  Imep(i), COVimep(i), Pmax(i), COVpmax(i),
     $                  Mfb1(i), Mfb10(i), Mfb90(i), Pbaro(i)
c
c     Correction for fuel temperature
      Tfuel(i)=Tfuel(i)-Tfcorr
```

```
c       The next line corrects for dynamometer
c       zero reading offset
c       Power(i) = Power(i)-1.95

        IF (Power(i).GT.100) then
        Torque(i)=Power(i)
        Power(i) = Torque(i)*2.0*Pi*Speed(i)/60000
        ENDIF

        Torque(i) = Power(i)*1000*60/(2.0*Pi*Speed(i))
        bmep(i) = 1200*Power(i)/(speed(i)*VSwept)
        imep(i) = imep(i)*ffimep
        fmep(i) = Imep(i)-bmep(i)
        etam(i) = bmep(i)/Imep(i)
        Pabs(i) = Pbaro(i)*0.001333224 + Pgdn(i)*25.4*9.81E-5
        vfuel(i)= (Mthne(i)/Time(i))*0.02831685
        mFuel(i) = vFuel(i)*Pabs(i)*100000/(R*(TFuel(i)+273))
        etab(i)= Power(i)/(mFuel(i)*CalValg)
        etaI(i)= etab(i)/etam(i)
        AFRV(i)=Lamda(i)*AFRsv
        AfRG(i)=Lamda(i)*AFRsg
        mexhaust=mfuel(i)*(1+AFRG(i))
        Airflrt(i)=mfuel(i)*AFRg(i)*1000
        etav(i)=vfuel(i)*AFRV(i)*120000/(VSwept*speed(i))
c
c       Next lines: Calculation of Heat Flow to Coolant
c                   Coolant = mixture of WATER and ETHYLENE GLYCOL
c                   cpW obtained from Thermodynamic and Transport
c                   Properties of Fluids, Rogers and Mayhew.
c                   cpEG obtained from Heat Transfer, FJ Bayley
c                   JM Owen AB Turner.
c                   RhoCool obtained from Specific Gravities
c                   of Ethylene Glycol Solutions..
        TCl=(TClin(i)+TClOut(i))/2.0
        cpEG=2.474+((2.742-2.474)/60)*(TCl-40)
        cpW =4.179+((4.219-4.179)/60)*(TCl-40)
        cpCl=(Clcomp*cpEG+(100-Clcomp)*cpW)/100
        RhoCool=1084-0.701*TClout(i)+(Clcomp-52)*1.025
        QCl(i)=Clflrt(i)*RhoCool*cpCl*(TClout(i)-TClin(i))/60000
c
c       Next lines: SAE Handbook(Vol 3 Section 25 Item 3)
c                   NOx correction to reference Inlet air humidity
c
        A = 0.044/(Lamda(i)*AFRSg)-0.0038
        B = (-0.116/(Lamda(i)*AFRSg))+0.0053
        ABK = 1+(7*A*(hmdty(i)-10.714))+(1.8*B*(Tair(i)-29.444))
        NOxh(i) = NOxV(i)/ABK
c
c       Next lines: Calculation of brake specific emissions(g/kWh)
c
        raz=(CO2(i)+CO(i)+(HC(i)/10000))/Cbn
        bsfc=mFuel(i)*3600000/Power(i)
        ian=bsfc/(raz * Mgas)
        COgkwh(i)=CO(i)*(MCbn+MOxn)*ian
        CO2gkwh(i)=CO2(i)*(MCbn+2*MOxn)*ian
        HCgkwh(i)=HC(i)*(MCbn+4*MHdn)*ian/10000
        NOxgkwh(i)=NOxV(i)*(MNtn+2*MOxn)*ian/10000
        NOxcorgkwh(i)=NOxh(i)*(MNtn+2*MOxn)*ian/10000
c
c       Next lines: Conversion to grams per MegaJoule(thermal)
```

```
c
      COgMJth  =COgkwh(i)*1000000 /(CalValg*bsfc)
      CO2gMJth =CO2gkwh(i)*1000000 /(CalValg*bsfc)
      HCgMJth  =HCgkwh(i) *1000000 /(CalValg*bsfc)
      NOxgMJth =NOxgkwh(i)*1000000 /(CalValg*bsfc)
      NOxcgMJth =NOxcorgkwh(i)*1000000 /(CalValg*bsfc)

c
c     TALuft Calculations (The Laws Demand's, Stationary Combustion
c                          Engines and the Environmental Protection Act,
c                          IMechE 1992, 1-12, T O R Shaw
c
      TAOx=0
      IF (Lamda(i).LE.1) Go To 676
c     TAx=2.0*CO2(i)+CO(i)-HC(i)/5000.0
c     The above equation was replaced by the one below (ie containing the
c     NOxV/10000 term) subsequently to plotting the results
      TAx=2.0*CO2(i)+CO(i)+NOxV(i)/10000-HC(i)/5000.0
      TAOx=(raz*(-Hdn/2.0+Oxn+0.418*AFRV(i))-TAx)/2.0

676   COgCum  =CO(i) *((20.9-TALuft)/(20.9-TAOx))*12.49
      CO2gCum =CO2(i)*((20.9-TALuft)/(20.9-TAOx))*19.64
      HCgCum  =HC(i) *((20.9-TALuft)/(20.9-TAOx))*0.714/1000.0
      NOxgCum =NOxV(i)*((20.9-TALuft)/(20.9-TAOx))*2.053/1000.0
      NOxcgCum =NOxh(i)*((20.9-TALuft)/(20.9-TAOx))*2.053/1000.0

c     Power correction: SAE Handbook Vol3 Section25 Item10
c                      (Also SAE J1349 Jun85, Engine Power Test
c                       Code - SI and Diesel)
      Pdry(i)=Pbaro(i)*0.133224 /(1+(hmdty(i)*29/18000))
     Powercorr(i)=Power(i)*(1.18*(99/Pdry(i))*sqrt((Tair(i)+273)/298)
    $  -0.18)

c
c     Next lines: Calculation of Heat Flow to Exhaust
c                 Convert all % and ppm to kmol/s
c                 Measured:CO2,CO,HC,O2,NOx   Calculated:N2,H2,H2O

      H2O = (Hdn*(CO2(i)+CO(i)+HC(i)/10000)/(2*Cbn))-2*HC(i)/10000
      H2 = 0
      IF (Lamda(i).LE.1) then
      H2 = ((Hdn*(CO2(i)+CO(i)+HC(i)/10000)/(2*Cbn))-2*HC(i)/10000)*
    $       CO(i)/(CO(i)+3.5*CO2(i))
      H2O = 3.5*CO2(i)*H2/CO(i)
      ENDIF
      N2 = 100-(CO2(i)+CO(i)+O2(i)+(HC(i)+NOxV(i))/10000 + H2)
      CF = mFuel(i)*Cbn/(Mgas*(CO2(i)+CO(i)+(HC(i)/10000)))

      Nmol(1)=CF*CO2(i)
      Nmol(2)=CF*CO(i)
      Nmol(3)=CF*O2(i)
      Nmol(4)=CF*HC(i)/10000
      Nmol(5)=CF*NOxV(i)/10000
      Nmol(6)=CF*H2
      Nmol(7)=CF*H2O
      Nmol(8)=CF*N2

      KExout=TExout(i)+273

      Ho=0
```

```
      HHo=0
      Do 21 ij=1,8
      H=(8.3143+KExout*(Cv(ij,1)+KExout*(Cv(ij,2)/2+KExout*
     $      (Cv(ij,3)/3+Cv(ij,4)/4*KExout))))*Nmol(ij)
      Ho=Ho+H
      HH=(8.3143+KDtm*(Cv(ij,1)+KDtm*(Cv(ij,2)/2+KDtm*
     $      (Cv(ij,3)/3+Cv(ij,4)/4*KDtm))))*Nmol(ij)
      HHo=HHo+HH
21    Continue


c     Next lines: Calculation of Chemical Energy in the exhaust.
c                 Oxidation of CO, HC, NOx, H2.
c                 Qcond=Heat loss owing to latent heat of water

      QChm=(Nmol(2)*282990)+(Nmol(4)*802310)+(Nmol(5)*
     $ 90290)+(Nmol(6)*241830)
      Qex(i)=Ho - HHo
      Qcond=Nmol(7)*43990
c
c     Next lines: Calculation of Energy Outputs as percentages of
c                 Total Fuel Energy Input
c
      mfCV=mFuel(i)*CalValg
      Wb=100*Power(i)/mfCV
      Qc=100*QCl(i)/mfCV
      Qe=100*QEx(i)/mfCV
      QCm=100*Qchm/mfCV
      Qcnd=100*Qcond/mfCV
      Qout=(1-((Power(i)+QCl(i)+QEx(i)+QChm+Qcond)/mfCV))*100

      Mfb1(i)=Mfb1(i)+Tmg(i)-180
      Mfb10(i)=Mfb10(i)+Tmg(i)-180
      Mfb90(i)=Mfb90(i)+Tmg(i)-180
      Mfb1090(i)=Mfb90(i)-Mfb10(i)
c
      theta1=Mfb10(i)
      theta2=Mfb90(i)
      mfb=0.1
      mfb2=0.9
      period=(int( theta1 + theta2 +15 )/10)*10.0
      theta1=theta1/period
      theta2=theta2/period
      Wiebem=(alog(alog(1-mfb)/alog(1-mfb2))/alog(theta1/theta2))-1
      Wiebea=-alog(1-mfb)/(theta1**(Wiebem+1))

c
c     First Output File (measurements)
c

      WRITE(11,1020)    Lamda(i), Tmg(i), Speed(i),
     $                  TClIn(i), TClout(i), TPrimary(i), TFuel(i),
     $                  TAir(i), TMixin(i), TExout(i), TOilgly(i),
     $                  TOilsmp(i), Airflrt(i), Clflrt(i),
     $                  Mthne(i), Time(i),
     $                  Pgup(i), Pgdn(i), Hmdty(i),
     $                  mFuel(i), vFuel(i), Pbaro(i), Pabs(i),
     $                  AFRV(i), AFRG(i)
c    $                  period,Wiebea,Wiebem
```

```
1000    FORMAT(3X,'AFR',3X,'Tmg',2X,'Speed',7X,
     $         'Temperatures (DegC)',11X,
     $         'Airflrt',1X,'Clflrt',3X,
     $         'Mthne',1X,'Time',1X,
     $         'Pgup',1X,'Pgdn',1X,'Hmdty',2X,
     $         'mFuel',1X,'vFuel',2X,'Pbaro',2X,'Pabs',3X,
     $         'AFRV',3X,'AFRG',3X)
c    $         'period',1X,'Wiebea',1X,'Wiebem')

1010    FORMAT(2X,'Lmda',1X,'DegBTDC',1X,'RPM',2X,
     $         'In',1X,'Out',1X,'Pmy',1X,'Fuel',1X,
     $         'Air',1X,'Mix',1X,'Exh',2X,'Gly',2X,
     $         'Smp',1X,'g/sec',1X,'l/min',4X,
     $         'cuft',2X,'Sec',1X,
     $         'in/WG',1X,'in/RL',1X,'g/kg',2X,
     $         'kg/s',2X,'cum/s',3X, 'mmHg',3X,'bar',4X)
c    $         'vol',3X,'grav',1X)

1020    FORMAT(F7.3, F5.0, F7.0,
     $         F4.0, F4.0, F4.0, F4.0,
     $         F4.0, F4.0, F5.0, F5.0,
     $         F5.0, F5.1, F6.1,
     $         F8.0, F6.1,
     $         F5.1, F5.2  F5.0,
     $         F7.4, F7.4, F7.1, F7.3,
     $         F7.2, F7.2)
c    $         F7.1,F7.2,F7.2)

c
c       Second Output File (combustion analysis)
c

        WRITE(12,2020)   Lamda(i), Tmg(i),
     $                   bmep(i), Imep(i), COVimep(i), Pmax(i),
     $                   COVpmax(i), Mfb1(i), Mfb10(i), Mfb90(i),
     $                   Mfb1090(i),
     $                   fmep(i), etam(i), etab(i), etai(i), etav(i),
     $                   Torque(i), Power(i)

2000    FORMAT(3X,'AFR',3X,'Tmg',2X,
     $         'bmep',1X,'Imep',1X,'COVimep',2X,'Pmax',1X,
     $         'COVpmax',1X,'MFB1%',1X,'MFB10%',1X,'MFB90%'1X,
     $         'MFB1090%'1X,
     $         'fmep',1X,'etam',1X,'etab',2X,'etai',3X,'etav',1X,
     $         'Trque',1X,'Pwr')

2010    FORMAT(2X,'Lmda',1X,'DegBTDC',1X,
     $         'bar',1X,'bar',5X,'%',5X,'bar',5X,
     $         '%',7X,'Degree crank angle',8X,
     $         'bar',3X,'%',5X,'%',5X,'%',5X,'%',4X,
     $         'Nm',3X,'kW')

2020    FORMAT(F7.3, F5.0,
     $         F6.2, F5.2, F8.3, F6.1,
     $         F6.1, F7.1, F7.1, F6.1,
     $         F8.1,
     $         F7.2, F5.2, F6.3, F6.3, F6.2,
     $         F7.1, F6.2)

c
```

```
c       Third Output File (exhaust emissions)
c

        WRITE(13,3020)   Lamda(i), Tmg(i),
     $                   NOxV(i), NOxh(i),
     $                   NOxgkWh(i), NOxgMJth, NOxgCum,
     $                   NOxcorgkWh(i), NOxcgMJth, NOxcgCum,
     $                   bsfc,
     $                   HC(i),HCgkWh(i), HCgMJth, HCgCum,
     $                   CO2(i), CO2gkWh(i), CO2gMJth, CO2gCum,
     $                   CO(i), COgkWh(i), COgMJth, COgCum,
     $                   O2(i), TAOx,
     $                   Power(i), Powercorr(i)

3000    FORMAT(2X,'AFR',3X,'Tmg',4X,
     $          'NOxv',1X,'NOxcorv',10X,
     $          'NOxg',16X,'NOxcorg',9X,
     $          'bsfc',4X,
     $          'HCv',10X,'HCg',10X,
     $          'CO2v',10X,'CO2g',12X,
     $          'COv',12X,'COg',9X,
     $          'O2v',3X,'TAOx',3X,
     $          'Pwr',2X,'Pwrcorr')

3010    FORMAT(2X,'Lmda',1X,'DegBTDC',2X,
     $          'ppm',4X,'ppm',3X,
     $          'g/kWh',2X,'g/MJth',1X,'g/cum',4X,
     $          'g/kWh',1X,'g/MJth',2X,'g/cum',2X,
     $          'g/kWh',3X,
     $          'ppm',3X,'g/kWh',1X,'g/MJth',1X,'g/cum',4X,
     $          '%',3X,'g/kWh',3X,'g/MJth',1X,'g/cum',5X,
     $          '%',4X,'g/kWh',3X,'g/MJth',1X,'g/cum',3X,
     $          '%',5X,'%',5X,
     $          'kW',3X,'kW')

3020    FORMAT(F6.3, F6.0,
     $          F7.0, F7.0,
     $          F6.1, F7.3, F8.3,
     $          F8.1, F7.3, F8.3,
     $          F9.3,
     $          F7.0, F6.2, F6.2, F6.2,
     $          F7.2, F8.2, F7.2, F8.2,
     $          F6.2, F8.2, F7.2, F7.2,
     $          F6.2, F7.2,
     $          F6.1, F6.1)

c
c       Fourth Output File (energy balance)
c

        WRITE(14,4020)   Lamda(i), Tmg(i),
     $                   fmep(i), etam(i), etab(i), etai(i), etav(i),
     $                   Torque(i), Power(i), QCl(i), QEx(i), QChm,
     $                   Qcond, Wb, Qc, Qe, QCm, Qcnd,
     $                   Qout, mfCV

4000    FORMAT(3X,'AFR',3X,'Tmg',2X,
     $          'fmep',1X,'etam',1X,'etab',2X,'etai',3X,'etav',1X,
     $          'Trque',2X,'Pwr',5X,'QCl',4X,'QEx',3X,'QChm',3X,
     $          'Qcond',3X,'Wb',3X,'Qc',4X,'Qe',4X,'QCm',3X,'Qcnd',3X,
```

```
     $        'Qout',2X,'mfCV')

 4010   FORMAT(2X,'Lmda',1X,'DegBTDC',1X,
     $        'bar',3X,'%',5X,'%',5X,'%',5X,'%',4X,
     $        'Nm',4X,'kW',6X,'kW',5X,'kW',5X,'kW',4X,
     $        'kW',5X,'%',5X,'%',5X,'%',5X,'%',5X,'%',7X,
     $        '%',4X,'kW')


 4020   FORMAT(F7.3, F5.0,
     $        F6.2, F5.2, F6.3, F6.3, F6.2,
     $        F7.1, F6.2, F7.2, F7.2, F7.2,
     $        F7.2, F6.2, F6.2, F6.2, F6.2, F6.2,
     $        F7.2, F7.2)

c
11      Continue
        WRITE(*,*) 'Input file has more than 200 lines'
20      Continue
c
        go to 4446
4444    Write(*,*) 'error in opening file engine'
4445    write(*,*) 'Cannot read variable'
4446    write(*,*) 'analysis finished'

4447    END
```

```
*******************************************************************************
*****                                                                     ******
*****                  DEFINITIONS OF VARIABLES                           ******
*****                                                                     ******
*******************************************************************************
*       Variable        Unit                    Input file    Output file

*       Lamda(A:F ratio)                            -             -
*       Tmg(timing)     Deg(btdc)                   -             -
*       Speed           rpm                         -             -
*       Power           kW                          -             -
*       Powercorr       kW                                        -
*       Torque          Nm                          -             -
*       Vswept          litres                      *             -
*       CalVal(higher)  kJ/cubic metre              *             -
*       CalValg         kJ/kg
*       bmep            bar                                       -
*       imep            bar                         -             -
*       fmep            bar                                       -
*       COVimep         %                           -             -
*       Pmax            bar                         -             -
*       COVpmax         %                           -             -
*       Clflrt          litres/minute               -
*       Airflrt         g/s                         -
*       vFuel (vflrt)   cubic m/s                                 -
*       mFuel (mflrt)   kg/s                                      -
*       mfCV            kW                                        -
*       Bsfc            g/kWh                                     -
*       RhoCool         kg/cubic metre                            -
*       cpCl            kJ/kgK
```

*	Mthne	cubic feet	-	-
*	Pbaro	mm mercury	-	-
*	Pabs	bar		-
*	Pgup	inches red liquid	-	-
*	Pgdn	inches water	-	-
*	Hmdty	g/kg dry air	-	-
*	Pdry (dry air)	Pascal	-	
*	Temperatures	degrees C	-	-
*	AFRV(Vol)			-
*	AFRG(Grav)			-
*	MFB	Deg crank angle	-	-
*	Eta*(efficiency)	%		-
*				
*	Emissions			
*	Volumetric	%,ppm(NOx corrected to SAE)	-	-
*	Gravimetric	g/kWh,g/MJ(thermal)		-
*	TAOx	g/m3(TAluft specified O2)	*	-
*	QCl(ht output)	kW		-
*	QEx(ht output)	kW		-
*	QChm(ht output)	kW		-
*	Qcond(ht output)	kW		-
*	Qc	%		-
*	Qe	%		-
*	Qcm	%		-
*	Qcnd	%		-
*	Qout	%		-
*	Wb	%		-

Dovergas baseline 10:1 experimental results (output from the program Dovergas.for)

AFR	Tmg	Speed	Temperatures (DegC)								Airflrt	Clflrt	Mthne	Time	Pgup	Pgdn	Hmdty	mFuel	vFuel	Pbaro	Pabs	AFRV	AFRG
Lmda	DegBTDC	RPM	In	Out	Pmy	Fuel	Air	Mix	Exh	Gly	Smp g/sec	l/min	cuft	Sec	in/WG	in/RL	g/kg	kg/s	cum/s	mmHg	bar		
1.601	55.	1539.	46.	84.	83.	20.	30.	33.	500.	92.	83.	69.1	7.2	10.	77.2	19.0	3.50	10.	.0027	.0037	765.0	1.029	15.41	25.97
1.618	60.	1489.	45.	83.	82.	20.	30.	33.	478.	92.	84.	72.6	3.0	10.	74.2	18.8	3.00	10.	.0028	.0038	765.0	1.027	15.57	26.24
1.515	25.	1461.	46.	84.	83.	20.	30.	33.	532.	90.	82.	67.8	7.4	10.	74.7	18.0	4.50	10.	.0028	.0038	765.0	1.031	14.58	24.57
1.513	30.	1511.	48.	84.	83.	19.	30.	33.	538.	90.	80.	70.5	10.6	10.	71.8	19.0	3.75	10.	.0029	.0039	765.0	1.029	14.56	24.54
1.491	35.	1478.	50.	84.	83.	19.	30.	33.	546.	91.	83.	66.5	15.7	10.	75.3	18.8	5.50	10.	.0028	.0038	765.0	1.034	14.35	24.18
1.512	40.	1502.	50.	84.	83.	19.	29.	33.	548.	91.	81.	67.2	15.0	10.	75.6	18.8	5.25	10.	.0027	.0037	765.0	1.033	14.55	24.52
1.501	45.	1499.	51.	84.	84.	20.	30.	33.	543.	92.	83.	66.9	14.5	10.	74.7	18.0	3.25	10.	.0027	.0038	765.0	1.028	14.45	24.34
1.514	45.	1501.	50.	83.	83.	19.	29.	32.	542.	88.	75.	66.8	16.1	10.	76.3	18.0	5.75	8.	.0027	.0037	766.0	1.036	14.57	24.55
1.500	50.	1501.	51.	84.	83.	19.	29.	32.	540.	89.	77.	66.6	16.9	10.	75.8	18.3	5.75	8.	.0027	.0037	766.0	1.036	14.44	24.33
1.500	50.	1500.	52.	84.	84.	20.	30.	33.	540.	92.	84.	66.5	16.2	10.	75.1	20.0	3.25	10.	.0027	.0038	765.0	1.028	14.44	24.33
1.503	55.	1502.	52.	84.	83.	19.	29.	32.	537.	90.	79.	66.6	17.9	10.	76.0	20.0	6.00	8.	.0027	.0037	766.0	1.036	14.47	24.38
1.500	55.	1499.	52.	85.	84.	20.	30.	34.	539.	92.	85.	66.0	17.9	10.	75.7	18.8	3.25	10.	.0027	.0037	765.0	1.028	14.44	24.33
1.500	60.	1493.	52.	85.	84.	20.	30.	34.	538.	90.	81.	65.7	13.4	10.	76.0	20.0	3.00	10.	.0027	.0037	765.0	1.027	14.44	24.33
1.497	65.	1501.	53.	85.	84.	20.	30.	33.	537.	91.	83.	65.7	18.3	10.	75.9	19.5	3.00	10.	.0027	.0037	765.0	1.027	14.41	24.28
1.501	70.	1497.	54.	85.	84.	20.	30.	33.	536.	93.	84.	66.0	19.4	10.	75.7	19.0	3.00	10.	.0027	.0037	765.0	1.027	14.45	24.34
1.396	25.	1500.	51.	83.	82.	18.	28.	32.	598.	80.	65.	64.6	18.5	10.	72.7	17.5	4.25	8.	.0029	.0039	766.0	1.032	13.44	22.64
1.385	30.	1518.	29.	83.	82.	22.	32.	35.	538.	92.	83.	66.5	4.4	10.	69.4	19.0	5.50	8.	.0030	.0041	766.0	1.035	13.33	22.46
1.402	30.	1490.	51.	83.	82.	18.	29.	32.	562.	87.	75.	63.4	18.2	10.	74.4	17.5	4.50	8.	.0028	.0038	766.0	1.032	13.49	22.74
1.401	35.	1502.	28.	83.	82.	22.	32.	36.	528.	92.	83.	63.4	5.2	10.	73.5	19.0	5.00	8.	.0028	.0039	766.0	1.034	13.48	22.72
1.400	40.	1500.	29.	84.	83.	22.	31.	35.	564.	92.	82.	62.7	5.6	10.	74.1	19.0	3.75	8.	.0028	.0038	766.0	1.031	13.48	22.71
1.398	45.	1502.	29.	84.	83.	22.	31.	35.	563.	92.	82.	62.9	6.0	10.	73.8	19.0	3.75	8.	.0028	.0038	766.0	1.031	13.46	22.67
1.401	50.	1503.	32.	84.	83.	22.	32.	35.	560.	92.	83.	62.6	6.0	10.	74.2	18.3	3.50	8.	.0028	.0038	766.0	1.030	13.48	22.72
1.422	50.	1425.	37.	85.	84.	22.	31.	36.	555.	101.	92.	62.9	6.2	10.	75.5	19.0	4.50	8.	.0027	.0038	770.0	1.038	13.69	23.06
1.415	60.	1485.	37.	85.	84.	22.	32.	36.	526.	102.	92.	65.1	6.0	10.	72.5	18.0	4.00	8.	.0028	.0039	770.0	1.037	13.62	22.95
1.316	25.	1452.	31.	83.	82.	22.	32.	36.	570.	93.	85.	65.8	6.9	10.	66.7	19.0	5.50	8.	.0031	.0042	766.0	1.035	12.67	21.34
1.325	30.	1451.	32.	83.	83.	22.	32.	36.	563.	95.	86.	65.6	7.0	10.	67.3	18.5	5.50	8.	.0031	.0042	766.0	1.035	12.75	21.49
1.300	30.	1481.	31.	84.	83.	22.	32.	36.	569.	93.	85.	64.4	6.6	10.	67.3	18.5	5.50	8.	.0031	.0042	766.0	1.035	12.51	21.08
1.300	35.	1502.	30.	84.	83.	22.	33.	36.	597.	93.	83.	63.0	8.3	10.	68.4	18.5	5.50	9.	.0030	.0041	762.0	1.030	12.51	21.08
1.298	40.	1504.	31.	84.	83.	22.	32.	36.	594.	93.	84.	62.8	9.6	10.	68.5	19.0	5.50	9.	.0030	.0041	762.0	1.030	12.49	21.05
1.295	45.	1506.	32.	84.	83.	22.	32.	36.	594.	94.	85.	62.5	10.0	10.	68.7	19.0	5.50	9.	.0030	.0041	762.0	1.030	12.46	21.00
1.290	50.	1499.	32.	84.	83.	22.	32.	36.	594.	94.	85.	62.0	10.0	10.	69.3	18.0	5.50	8.	.0030	.0041	766.0	1.035	12.42	20.92
1.305	50.	1464.	41.	85.	84.	22.	32.	37.	589.	108.	98.	60.3	14.0	10.	72.0	18.0	3.00	8.	.0028	.0039	770.0	1.034	12.56	21.16
1.302	60.	1478.	40.	85.	84.	22.	32.	36.	562.	108.	98.	61.9	14.0	10.	70.0	18.0	3.00	8.	.0029	.0040	770.0	1.034	12.53	21.12
1.202	20.	1501.	29.	83.	82.	22.	33.	37.	592.	94.	85.	65.6	7.0	10.	60.7	18.8	5.50	9.	.0034	.0047	762.0	1.030	11.57	19.49
1.206	25.	1502.	31.	84.	83.	21.	33.	37.	634.	95.	86.	63.6	11.0	10.	63.1	18.8	5.50	9.	.0032	.0045	762.0	1.030	11.61	19.56
1.200	35.	1502.	33.	84.	83.	22.	33.	37.	627.	95.	87.	61.8	14.0	10.	64.3	17.9	5.50	9.	.0032	.0044	762.0	1.030	11.55	19.46
1.202	40.	1502.	33.	84.	83.	22.	33.	36.	624.	95.	86.	61.6	15.0	10.	64.7	18.3	5.50	9.	.0032	.0044	762.0	1.030	11.57	19.49
1.200	50.	1460.	44.	86.	85.	22.	32.	37.	618.	106.	98.	60.7	18.6	10.	66.0	18.0	4.50	8.	.0031	.0043	770.0	1.038	11.55	19.46
1.230	60.	1423.	43.	86.	84.	22.	33.	37.	596.	107.	98.	60.0	17.5	10.	68.5	18.0	4.50	8.	.0030	.0041	770.0	1.038	11.84	19.95
1.100	0.	1505.	43.	85.	85.	19.	32.	36.	879.	80.	66.	65.7	20.9	10.	56.5	17.0	4.50	8.	.0037	.0050	770.0	1.038	10.59	17.84
1.100	10.	1504.	42.	84.	83.	15.	26.	31.	804.	80.	67.	64.1	22.0	10.	58.8	17.0	4.50	9.	.0036	.0048	771.0	1.039	10.59	17.84
1.101	15.	1503.	34.	84.	83.	22.	33.	37.	710.	97.	88.	62.9	15.0	10.	57.4	17.8	1.50	9.	.0035	.0049	762.0	1.020	10.60	17.86
1.101	20.	1500.	34.	84.	83.	22.	33.	38.	688.	98.	89.	62.2	16.0	10.	58.1	18.0	1.60	9.	.0035	.0049	762.0	1.020	10.60	17.86

1.102	25.	1505.	34.	84.	83.	23.	34.	38.	675.	96.	89.	62.0	17.0	10.	58.7	17.8	5.50	9.	.0035	.0048	762.0	1.030	10.61	17.87
1.099	30.	1500.	34.	84.	83.	23.	34.	38.	670.	96.	89.	61.2	19.0	10.	59.4	19.3	5.75	9.	.0034	.0048	762.0	1.030	10.58	17.82
1.101	35.	1506.	35.	85.	84.	23.	33.	37.	665.	97.	89.	61.0	19.0	10.	59.6	17.5	5.25	9.	.0034	.0048	762.0	1.029	10.60	17.86
1.098	40.	1500.	36.	85.	84.	22.	33.	37.	662.	97.	89.	60.2	18.0	10.	60.4	17.0	5.25	9.	.0034	.0047	762.0	1.029	10.57	17.81
1.084	50.	1451.	47.	86.	85.	22.	35.	39.	673.	104.	98.	59.8	24.2	10.	60.5	17.5	4.50	8.	.0034	.0047	770.0	1.038	10.43	17.58
1.083	60.	1509.	48.	87.	85.	22.	33.	38.	669.	107.	99.	61.3	24.0	10.	59.0	17.0	4.50	8.	.0035	.0048	770.0	1.038	10.42	17.56
1.049	0.	1383.	45.	85.	84.	22.	34.	40.	642.	106.	103.	65.0	6.3	10.	54.0	17.0	4.50	9.	.0038	.0052	771.0	1.039	10.10	17.01
1.037	10.	1493.	45.	86.	85.	22.	34.	39.	721.	107.	103.	65.4	16.0	10.	53.0	16.5	4.50	9.	.0039	.0053	771.0	1.039	9.98	16.82
1.003	20.	1489.	48.	86.	85.	21.	33.	38.	754.	99.	93.	62.9	22.7	10.	53.5	17.0	4.50	9.	.0039	.0053	771.0	1.039	9.65	16.27
1.000	25.	1518.	49.	86.	85.	22.	33.	39.	736.	107.	102.	63.1	22.8	10.	53.0	17.5	4.50	9.	.0039	.0053	771.0	1.039	9.63	16.22
1.000	30.	1499.	49.	86.	85.	22.	33.	38.	719.	110.	104.	63.4	23.0	10.	52.8	17.5	4.50	9.	.0039	.0054	771.0	1.039	9.63	16.22
1.000	35.	1506.	49.	86.	85.	22.	34.	39.	711.	110.	105.	62.5	23.0	10.	53.5	17.5	4.50	9.	.0039	.0053	771.0	1.039	9.63	16.22
1.000	40.	1496.	50.	86.	85.	22.	34.	39.	708.	111.	105.	61.9	25.6	10.	54.0	17.5	4.50	9.	.0038	.0052	771.0	1.039	9.63	16.22
1.000	45.	1501.	50.	87.	85.	22.	33.	39.	706.	112.	105.	61.9	25.7	10.	54.0	16.5	4.50	9.	.0038	.0052	771.0	1.039	9.63	16.22
1.000	50.	1509.	52.	86.	85.	22.	35.	40.	710.	112.	104.	61.9	29.6	10.	54.0	17.5	4.50	9.	.0038	.0052	771.0	1.039	9.63	16.22
1.002	60.	1457.	52.	87.	86.	22.	34.	39.	708.	108.	101.	62.1	30.3	10.	54.0	17.0	4.50	9.	.0038	.0052	771.0	1.039	9.64	16.25
.915	0.	1485.	62.	86.	85.	24.	35.	41.	734.	95.	89.	66.4	26.6	10.	45.4	16.5	5.00	9.	.0045	.0062	764.0	1.031	8.81	14.84
.917	5.	1506.	61.	86.	85.	24.	35.	40.	695.	97.	90.	67.2	26.6	10.	45.0	16.0	5.00	9.	.0045	.0063	764.0	1.031	8.83	14.87
.917	10.	1498.	61.	85.	85.	24.	35.	40.	661.	98.	92.	66.7	27.0	10.	45.3	16.5	5.00	9.	.0045	.0062	764.0	1.031	8.83	14.87
.916	15.	1491.	62.	85.	84.	24.	35.	40.	632.	102.	97.	66.7	27.7	10.	45.2	17.5	4.75	9.	.0045	.0063	764.0	1.030	8.82	14.86
.923	20.	1509.	72.	88.	87.	25.	36.	41.	702.	98.	90.	64.2	47.1	10.	47.2	16.0	5.00	10.	.0043	.0060	764.0	1.031	8.88	14.97
.915	25.	1496.	71.	88.	87.	25.	36.	41.	684.	98.	91.	62.3	46.3	10.	48.2	16.0	5.00	10.	.0042	.0059	764.0	1.031	8.81	14.84
.917	30.	1506.	72.	89.	88.	25.	36.	41.	679.	99.	93.	62.8	45.0	10.	48.0	16.0	5.00	10.	.0042	.0059	764.0	1.031	8.83	14.87
.923	35.	1503.	73.	89.	89.	25.	36.	41.	677.	100.	94.	62.1	50.2	10.	48.8	16.8	4.50	10.	.0041	.0058	764.0	1.030	8.88	14.97
.925	40.	1494.	74.	89.	89.	25.	36.	41.	676.	100.	94.	61.5	50.1	10.	49.3	17.0	4.50	10.	.0041	.0057	764.0	1.030	8.90	15.00
.924	45.	1482.	75.	91.	89.	25.	36.	41.	676.	101.	95.	60.6	51.1	10.	50.0	17.0	4.50	10.	.0040	.0057	764.0	1.030	8.89	14.99
.928	50.	1451.	76.	93.	91.	25.	36.	41.	674.	103.	99.	59.7	51.3	10.	51.0	17.0	4.50	10.	.0040	.0056	764.0	1.030	8.93	15.05
.925	55.	1502.	78.	95.	93.	25.	36.	41.	682.	103.	98.	60.7	52.3	10.	50.0	17.5	4.50	10.	.0040	.0057	764.0	1.030	8.90	15.00
.925	60.	1496.	79.	97.	95.	25.	36.	41.	684.	105.	99.	58.7	53.1	10.	51.7	17.0	4.50	10.	.0039	.0055	764.0	1.030	8.90	15.00
.927	65.	1513.	81.	99.	97.	25.	36.	41.	691.	106.	102.	60.4	53.0	10.	50.3	16.5	4.50	10.	.0040	.0056	764.0	1.030	8.92	15.03
.928	70.	1486.	82.	101.	99.	25.	36.	41.	694.	107.	103.	59.5	53.2	10.	51.2	17.0	4.75	10.	.0040	.0055	764.0	1.030	8.93	15.05
.863	0.	1484.	64.	86.	85.	24.	36.	42.	744.	97.	91.	63.2	30.6	10.	44.9	15.8	4.00	10.	.0045	.0063	764.0	1.029	8.31	14.00
.860	5.	1497.	65.	86.	85.	24.	35.	40.	706.	101.	96.	64.4	31.8	10.	43.9	16.3	4.00	10.	.0046	.0065	764.0	1.029	8.28	13.95
.866	10.	1491.	62.	86.	84.	23.	34.	39.	666.	96.	89.	63.5	27.2	10.	45.1	16.5	4.00	10.	.0045	.0063	765.0	1.030	8.34	14.05
.856	15.	1501.	74.	89.	88.	23.	35.	40.	719.	101.	95.	60.5	51.8	10.	46.8	16.5	4.00	10.	.0044	.0061	765.0	1.030	8.24	13.88
.864	20.	1501.	62.	86.	85.	19.	31.	36.	690.	92.	88.	62.0	32.1	10.	46.7	17.5	4.00	10.	.0044	.0061	765.0	1.030	8.32	14.01
.866	25.	1495.	62.	86.	85.	20.	32.	36.	676.	94.	89.	61.2	32.8	10.	47.3	17.5	4.00	10.	.0044	.0060	765.0	1.030	8.34	14.05
.866	30.	1498.	63.	86.	85.	19.	31.	36.	669.	95.	89.	61.3	34.4	10.	47.3	16.0	3.75	10.	.0044	.0060	765.0	1.029	8.34	14.05
.865	35.	1504.	65.	86.	86.	20.	32.	36.	666.	97.	89.	61.1	37.5	10.	47.2	17.8	4.00	10.	.0044	.0060	765.0	1.030	8.33	14.03
.865	40.	1499.	66.	87.	86.	20.	32.	37.	665.	91.	33.	60.2	39.5	10.	47.9	17.0	3.75	10.	.0043	.0059	765.0	1.029	8.33	14.03
.866	45.	1501.	67.	87.	86.	20.	32.	37.	665.	98.	92.	60.3	42.3	10.	47.9	17.5	3.75	10.	.0043	.0059	765.0	1.029	8.34	14.05
.865	50.	1500.	68.	88.	87.	20.	32.	37.	666.	99.	93.	59.9	45.6	10.	48.2	17.5	4.00	10.	.0043	.0059	765.0	1.030	8.33	14.03
.865	55.	1502.	70.	89.	87.	20.	32.	37.	668.	100.	94.	59.1	50.0	10.	48.8	17.0	3.75	10.	.0042	.0058	765.0	1.029	8.33	14.03
.866	60.	1494.	71.	89.	88.	20.	32.	37.	670.	101.	95.	59.1	50.0	10.	48.9	18.0	4.00	10.	.0042	.0058	765.0	1.030	8.34	14.05
.866	65.	1506.	73.	92.	90.	20.	32.	37.	677.	103.	97.	59.3	52.0	10.	48.8	18.0	4.00	10.	.0042	.0058	765.0	1.030	8.34	14.05

.856	70.	1502.	79.	97.	96.	23.	34.	39.	681.	99.	90.	57.4	52.0	10.	49.3	16.5	4.25	10.	.0041	.0057	765.0	1.031	8.24	13.88
.800	20.	1504.	60.	85.	85.	19.	31.	36.	686.	90.	83.	63.6	27.9	10.	42.2	16.5	4.50	10.	.0049	.0067	765.0	1.031	7.70	12.97
.799	25.	1499.	60.	85.	85.	19.	31.	35.	664.	91.	85.	63.1	28.0	10.	42.4	16.5	4.50	10.	.0049	.0067	765.0	1.031	7.69	12.96
.793	30.	1501.	60.	86.	85.	19.	31.	35.	649.	92.	86.	62.9	28.0	10.	42.3	16.0	4.50	10.	.0049	.0067	765.0	1.031	7.63	12.86
.795	35.	1498.	61.	86.	85.	19.	31.	35.	640.	92.	85.	63.0	30.4	10.	42.3	17.0	4.50	10.	.0049	.0067	765.0	1.031	7.65	12.89
.796	40.	1504.	62.	86.	85.	19.	31.	35.	636.	93.	86.	62.6	31.9	10.	42.6	17.0	4.00	10.	.0049	.0067	765.0	1.030	7.66	12.91
.792	45.	1497.	63.	86.	85.	19.	31.	35.	632.	95.	86.	62.3	33.5	10.	42.6	15.5	4.25	10.	.0048	.0066	765.0	1.031	7.62	12.84
.790	50.	1500.	63.	86.	85.	19.	31.	35.	632.	96.	87.	62.0	34.3	10.	42.7	16.0	4.00	10.	.0048	.0066	765.0	1.030	7.60	12.81
.789	55.	1504.	64.	86.	85.	19.	31.	35.	631.	96.	89.	61.8	36.4	10.	42.8	16.0	4.50	10.	.0048	.0066	765.0	1.031	7.59	12.80
.796	60.	1492.	66.	87.	86.	19.	31.	35.	632.	97.	90.	61.6	40.5	10.	43.3	17.0	4.00	10.	.0048	.0065	765.0	1.030	7.66	12.91
.807	10.	1502.	53.	84.	84.	20.	32.	37.	692.	92.	87.	66.3	20.2	10.	40.7	16.0	5.00	10.	.0051	.0070	765.0	1.032	7.77	13.09
.822	15.	1507.	53.	84.	82.	19.	31.	36.	653.	94.	87.	67.4	20.3	10.	40.9	15.0	4.50	10.	.0051	.0069	765.0	1.031	7.91	13.33

AFR	Tmg	bmep	COVimep	Pmax	COVpmax	MFB1%	MFB10%	MFB90%	MFB1090%	etam	etab	etav	Trque	Pwr
Lmda	DegBTDC	bar	%	bar	%	Degree crank angle				%	%	%	Nm	kW
1.601	55.	4.83	25.767	38.0	14.1	38.2	46.0	76.6	30.6	.73	.275	.71	238.3	38.40
1.618	60.	4.34	45.735	35.3	20.6	41.5	51.7	82.3	30.6	.74	.230	.77	214.2	33.40
1.515	25.	4.74	7.580	34.2	8.3	16.5	23.6	50.1	26.5	.60	.247	.73	234.0	35.80
1.513	30.	4.91	1.368	37.4	6.8	19.3	26.2	52.7	26.5	.64	.254	.74	242.1	38.30
1.491	35.	5.55	1.135	40.2	5.8	21.3	28.8	55.4	26.6	.74	.293	.71	273.9	42.40
1.512	40.	5.61	4.328	40.7	6.4	24.5	32.4	60.1	27.7	.76	.302	.70	276.6	43.50
1.501	45.	5.76	1.078	44.1	5.3	26.1	34.4	63.3	28.9	.78	.309	.71	284.1	44.60
1.514	45.	5.56	1.172	41.8	6.0	27.5	35.7	64.7	29.0	.76	.301	.70	274.2	43.10
1.500	50.	5.61	1.222	43.5	5.8	30.3	38.8	68.8	30.0	.78	.302	.70	276.7	43.50
1.500	50.	5.64	13.626	45.2	5.3	29.6	38.9	67.9	29.0	.70	.304	.70	278.2	43.70
1.503	55.	5.53	1.461	45.2	5.2	33.4	42.1	73.3	31.2	.78	.299	.69	272.7	42.90
1.500	55.	5.55	1.673	46.6	5.1	32.2	41.1	72.5	31.4	.78	.302	.70	273.9	43.00
1.500	60.	5.46	2.135	47.7	5.0	35.6	44.7	77.4	32.7	.77	.297	.70	269.3	42.10
1.497	65.	5.33	9.692	48.9	6.5	37.9	47.5	81.1	33.6	.78	.291	.69	262.7	41.30
1.501	70.	5.24	13.085	49.5	8.1	41.2	51.1	85.8	34.7	.79	.284	.70	258.3	40.50
1.396	25.	5.78	2.033	33.5	8.1	16.5	23.3	49.7	26.4	.77	.299	.68	285.2	44.80
1.385	30.	5.29	16.857	40.3	9.0	16.8	24.1	48.8	24.7	.71	.267	.69	261.1	41.50
1.402	30.	5.75	1.128	39.6	5.9	17.6	24.8	50.1	25.3	.76	.302	.67	283.9	44.30
1.401	35.	4.94	4.318	42.5	5.8	18.9	26.8	52.4	25.6	.67	.261	.67	243.5	38.30
1.400	40.	5.86	4.316	42.8	5.6	22.0	30.3	57.3	27.0	.81	.313	.66	289.0	45.40
1.398	45.	5.75	4.395	44.5	5.4	24.4	33.0	61.4	28.4	.81	.306	.67	283.6	44.60
1.401	50.	5.61	4.468	45.2	5.5	27.6	36.5	66.3	29.8	.81	.301	.66	277.0	43.60
1.422	50.	6.15	2.088	47.5	4.8	27.3	35.8	64.7	28.9	.91	.316	.70	303.6	45.30
1.415	60.	5.11	4.736	50.9	4.4	31.8	42.3	71.7	29.4	.71	.263	.69	252.1	39.20
1.316	25.	5.63	1.608	45.6	4.4	12.6	19.5	41.0	21.5	.67	.261	.72	277.5	42.20
1.325	30.	5.72	27.186	47.0	4.5	14.2	23.7	47.1	23.4	.58	.267	.72	282.3	42.90
1.300	30.	5.531	6.617	49.3	3.5	14.3	23.9	46.0	22.1	.53	.264	.69	272.7	42.30
1.300	35.	6.35	1.874	49.4	4.0	15.8	23.6	48.3	24.7	.81	.314	.67	313.4	49.30
1.298	40.	6.20	2.574	51.4	3.9	17.6	25.7	52.3	26.6	.81	.308	.66	306.0	48.20
1.295	45.	6.01	3.478	53.1	3.7	19.7	28.0	56.1	28.1	.82	.299	.66	296.8	46.80
1.290	50.	5.86	4.627	54.5	3.4	22.2	30.6	59.7	29.1	.84	.292	.65	289.2	45.40
1.305	50.	6.07	2.679	49.0	4.2	25.0	33.6	62.0	28.4	.93	.306	.65	299.4	45.90
1.302	60.	5.12	5.904	51.9	4.2	28.5	37.5	68.4	30.9	.94	.254	.66	252.6	39.10
1.202	20.	6.05	3.003	46.4	4.4	9.8	16.9	36.8	19.9	.65	.265	.70	298.4	46.90
1.206	25.	7.05	2.293	48.4	3.6	11.8	18.6	39.1	20.5	.82	.320	.67	347.8	54.70
1.200	35.	6.64	2.679	51.2	3.6	17.9	25.1	47.2	22.1	.80	.309	.66	327.4	51.50
1.202	40.	6.44	2.293	48.4	3.6	26.8	33.6	54.1	20.5	.75	.301	.65	317.9	50.00
1.200	50.	6.56	6.006	57.0	3.0	20.4	28.5	53.4	24.9	1.09	.302	.66	323.8	49.50
1.230	60.	5.62	7.337	59.4	2.8	25.4	34.4	58.7	24.3	1.00	.261	.67	277.2	41.30
1.100	0.	4.85	10.354	21.5	16.7	17.4	21.1	51.5	30.4	.71	.195	.68	239.2	37.70
1.100	10.	6.34	346.661	22.6	14.6	2.2	6.5	26.0	19.5	6.01	.261	.66	313.0	49.30
1.101	15.	7.46	2.656	43.9	5.3	8.5	14.8	33.9	19.1	.79	.313	.67	367.9	57.90
1.101	20.	7.54	2.844	53.3	4.3	11.1	17.2	36.0	18.8	.80	.319	.67	371.8	58.40

1.102	25.	7.47	6.296	53.9	2.9	10.6	17.7	37.1	19.4	.79	.318	.66	368.6	58.10
1.099	30.	7.28	3.949	56.9	2.9	11.2	18.2	39.1	20.9	.83	.313	.65	359.1	56.40
1.101	35.	7.03	5.936	59.0	3.7	12.4	19.7	42.2	22.5	.85	.305	.65	346.8	54.70
1.098	40.	6.79	4.531	60.7	2.7	14.1	21.5	45.1	23.6	.86	.296	.64	334.9	52.60
1.084	50.	6.95	6.918	64.2	2.5	18.5	25.8	46.7	20.9	1.16	.291	.65	342.9	52.10
1.083	60.	5.62	9.781	67.2	.8	22.8	31.1	50.1	19.0	1.03	.239	.64	277.2	43.80
1.049	0.	3.41	21.335	21.8	12.8	17.8	21.1	49.4	28.3	.45	.122	.74	168.5	24.40
1.037	10.	5.34	1.791	32.4	7.5	11.7	17.6	39.7	22.1	.54	.202	.69	263.5	41.20
1.003	20.	7.861	1.069	40.6	5.9	18.1	23.0	42.8	19.8	.78	.298	.66	388.0	60.50
1.000	25.	8.031	5.495	50.6	4.8	14.4	20.6	40.7	20.1	.79	.308	.66	396.3	63.00
1.000	30.	8.13	1.369	56.0	2.7	15.3	21.4	42.7	21.3	.83	.307	.67	401.3	63.00
1.000	35.	7.99	2.105	59.1	2.6	15.9	22.3	46.3	24.0	.84	.307	.65	394.4	62.20
1.000	40.	7.80	2.956	61.1	2.7	17.1	24.0	49.6	25.6	.86	.301	.65	384.9	60.30
1.000	45.	7.52	4.475	62.5	2.5	18.7	25.7	51.3	25.6	.89	.291	.65	370.9	58.30
1.000	50.	7.16	5.382	66.2	2.3	20.7	28.2	50.7	22.5	.93	.278	.65	353.1	55.80
1.002	60.	6.40	12.446	68.9	.7	22.0	29.4	45.2	15.8	1.34	.240	.67	315.9	48.20
.915	0.	4.12	7.011	21.0	2.1	8.9	15.0	46.1	31.1	.51	.134	.72	203.2	31.60
.917	5.	4.91	4.975	26.0	9.4	7.3	14.3	40.5	26.2	.53	.161	.71	242.2	38.20
.917	10.	5.53	1.584	34.6	8.0	8.8	14.8	36.9	22.1	.57	.182	.71	272.8	42.80
.916	15.	5.96	2.153	43.8	5.7	8.8	15.1	34.6	19.5	.61	.194	.72	294.0	45.90
.923	20.	7.66	3.169	51.1	3.5	9.5	15.7	33.8	18.1	.81	.265	.68	377.8	59.70
.915	25.	7.67	3.573	55.8	2.7	10.3	16.8	35.2	18.4	.83	.269	.67	378.5	59.30
.917	30.	7.57	3.851	58.9	2.7	11.0	17.9	37.6	19.7	.85	.265	.67	373.5	58.90
.923	35.	7.37	4.292	60.9	2.5	12.0	19.1	40.4	21.3	.88	.262	.66	363.4	57.20
.925	40.	7.10	3.792	62.5	2.3	20.0	23.3	49.9	26.6	.90	.254	.66	350.3	54.80
.924	45.	6.83	4.689	64.2	2.0	16.3	23.9	46.9	23.0	.86	.246	.66	337.0	52.30
.928	50.	6.51	6.683	65.8	1.4	17.1	24.7	45.9	21.2	.95	.234	.66	321.2	48.80
.925	55.	6.20	8.314	66.6	.6	18.4	26.4	45.8	19.4	1.01	.226	.65	305.8	48.10
.925	60.	5.76	10.220	66.5	.6	19.7	28.1	45.5	17.4	1.08	.216	.63	284.1	44.50
.927	65.	5.36	11.708	66.2	.6	20.7	29.5	44.3	14.8	1.23	.198	.64	264.5	41.90
.928	70.	4.86	21.718	65.9	.5	22.2	31.4	46.5	15.1	1.20	.180	.64	239.7	37.30
.863	0.	3.73	10.311	20.9	1.7	9.1	15.2	47.6	32.4	.48	.121	.68	184.0	28.60
.860	5.	4.49	6.464	24.4	9.7	9.0	15.0	42.1	27.1	.51	.143	.69	221.3	34.70
.866	10.	5.30	1.581	35.6	7.5	8.2	14.2	35.9	21.7	.55	.172	.68	261.3	40.80
.856	15.	7.27	2.135	43.9	5.8	8.8	15.1	34.6	19.5	.74	.246	.64	358.8	56.40
.864	20.	7.67	2.897	51.5	3.5	9.5	15.8	33.8	18.0	.80	.256	.65	378.5	59.50
.866	25.	7.68	4.088	56.2	2.7	10.2	16.9	35.4	18.5	.81	.259	.65	378.8	59.30
.866	30.	7.56	3.870	59.1	2.7	11.0	18.0	37.6	19.6	.85	.255	.65	372.9	58.50
.865	35.	7.40	4.271	61.2	2.7	12.3	19.5	40.7	21.2	.87	.251	.64	365.1	57.50
.865	40.	7.17	5.418	62.8	2.4	14.0	21.5	44.1	22.6	.87	.246	.64	353.6	55.50
.866	45.	6.85	3.805	64.5	2.1	15.5	23.0	45.0	22.0	.91	.235	.64	337.8	53.10
.865	50.	6.53	5.186	65.8	1.8	17.4	25.1	46.5	21.4	.93	.226	.63	322.1	50.60
.865	55.	6.21	6.949	67.1	.8	18.6	26.8	46.0	19.2	.98	.218	.62	306.4	48.20
.866	60.	5.84	9.361	67.3	.4	19.9	28.4	45.7	17.3	1.06	.204	.63	288.3	45.10
.866	65.	5.42	11.484	67.1	.5	20.9	29.8	45.2	15.4	1.19	.190	.62	267.6	42.20

.856	70.	5.12	12.436	66.7	.5	22.0	31.2	45.0	13.8	1.40	.183	.61	252.4	39.70
.800	20.	7.27	1.021	40.4	7.5	14.4	20.7	42.2	21.5	.74	.219	.67	358.7	56.50
.799	25.	7.61	1.480	49.8	4.5	13.4	20.4	40.6	20.2	.78	.230	.66	375.2	58.90
.793	30.	7.61	1.895	53.4	4.1	14.9	22.2	43.2	21.0	.79	.230	.66	375.4	59.00
.795	35.	7.57	1.895	53.4	4.1	19.9	27.2	48.2	21.0	.79	.228	.66	373.6	58.60
.796	40.	7.45	3.160	58.4	4.0	18.3	26.2	50.2	24.0	.82	.227	.66	367.6	57.90
.792	45.	7.28	4.177	60.3	3.8	20.5	28.6	53.7	25.1	.83	.221	.65	359.1	56.30
.790	50.	7.17	4.904	62.5	3.4	22.6	30.9	56.6	25.7	.87	.219	.65	354.0	55.60
.789	55.	6.90	5.005	64.1	3.1	24.9	33.6	59.1	25.5	.88	.211	.65	340.3	53.60
.796	60.	6.64	5.835	66.7	2.6	26.1	35.3	58.8	23.5	.93	.204	.65	327.7	51.20
.807	10.	4.02	4.506	24.2	10.4	11.3	17.3	47.8	30.5	.46	.117	.70	198.4	31.20
.822	15.	5.09	1.565	34.3	9.8	11.7	18.1	42.1	24.0	.53	.149	.70	250.9	39.60

AFR	Tmg	NOxv	NOxcorv	NOxg			NOxcorg			HCv	HCg			CO2v	CO2g			COv	COg			O2v	TAOx
Lmda	DegBTDC	ppm	ppm	g/kWh	g/MJth	g/cum	g/kWh	g/MJth	g/cum	ppm	g/kWh	g/MJth	g/cum	%	g/kWh	g/MJth	g/cum	%	g/kWh	g/MJth	g/cum	%	%
1.601	55.	700.	688.	7.3	.553	1.901	7.1	.544	1.868	5520.	19.96	1.52	5.21	5.95	590.13	45.00	154.55	.10	6.31	.48	1.65	11.30	8.88
1.618	60.	750.	737.	9.8	.624	2.105	9.6	.613	2.069	8370.	38.05	2.43	8.17	5.35	667.23	42.55	143.62	.09	7.14	.46	1.54	12.10	9.27
1.515	25.	210.	207.	2.5	.168	.535	2.4	.166	.526	7570.	30.87	2.12	6.71	5.68	635.48	43.58	138.43	.07	4.98	.34	1.08	10.70	8.09
1.513	30.	320.	315.	3.5	.249	.810	3.5	.245	.797	6260.	24.12	1.70	5.51	6.00	634.11	44.67	145.22	.08	5.38	.38	1.23	10.60	8.00
1.491	35.	590.	581.	5.3	.433	1.441	5.2	.426	1.418	3500.	11.00	.90	2.97	6.67	574.93	46.84	155.85	.09	4.94	.40	1.34	9.40	7.54
1.512	40.	700.	690.	7.5	.633	1.572	7.4	.624	1.548	2900.	10.90	.91	2.26	5.39	555.84	46.64	115.78	.09	5.91	.50	1.23	9.50	6.36
1.501	45.	1000.	984.	8.7	.743	2.385	8.5	.732	2.347	1700.	5.14	.44	1.41	6.75	559.82	48.01	153.99	.10	5.28	.45	1.45	9.80	7.21
1.514	45.	1000.	968.	8.5	.714	2.490	8.2	.691	2.409	2220.	6.60	.55	1.92	6.99	569.96	47.73	166.47	.10	5.19	.43	1.51	10.00	7.79
1.500	50.	1100.	1065.	9.3	.784	2.679	9.0	.759	2.593	1740.	5.15	.43	1.47	7.05	572.23	48.06	164.27	.10	5.17	.43	1.48	9.90	7.50
1.500	50.	1250.	1230.	10.9	.925	2.984	10.8	.910	2.937	1740.	5.32	.45	1.44	6.78	568.15	47.99	154.84	.10	5.33	.45	1.45	9.60	7.23
1.503	55.	1400.	1355.	12.5	1.033	3.354	12.1	1.000	3.246	1720.	5.34	.44	1.43	6.80	578.65	48.01	155.84	.10	5.42	.45	1.46	10.00	7.27
1.500	55.	1400.	1378.	12.4	1.039	3.340	12.2	1.023	3.287	1820.	5.62	.47	1.51	6.74	571.08	47.86	153.84	.11	5.93	.50	1.60	9.40	7.22
1.500	60.	1900.	1870.	17.1	1.412	4.518	16.9	1.389	4.447	1750.	5.50	.45	1.45	6.74	581.13	47.90	153.32	.11	6.04	.50	1.59	9.20	7.17
1.497	65.	1900.	1870.	17.8	1.441	4.459	17.6	1.418	4.389	1740.	5.70	.46	1.42	6.60	592.98	47.87	148.19	.11	6.29	.51	1.57	9.50	6.99
1.501	70.	2100.	2067.	20.0	1.581	4.954	19.7	1.556	4.875	1630.	5.42	.43	1.34	6.66	607.32	47.96	150.30	.11	6.38	.50	1.58	9.80	7.06
1.396	25.	1100.	1067.	9.4	.776	2.423	9.1	.753	2.350	1900.	5.63	.47	1.46	7.14	580.65	48.17	150.43	.07	3.62	.30	.94	9.30	6.08
1.385	30.	1700.	1648.	16.0	1.185	3.937	15.5	1.149	3.816	6160.	20.21	1.50	4.96	6.80	612.07	45.35	150.65	.07	4.01	.30	.99	9.70	6.80
1.402	30.	1500.	1454.	12.1	1.017	3.410	11.7	.986	3.306	2700.	7.61	.64	2.13	7.36	568.69	47.72	160.06	.07	3.44	.29	.97	9.50	6.54
1.401	35.	1900.	1840.	18.9	1.373	4.502	18.3	1.329	4.361	7650.	26.58	1.93	6.30	6.39	608.96	44.16	144.85	.07	4.25	.31	1.01	10.30	7.12
1.400	40.	2100.	2035.	16.2	1.408	4.703	15.7	1.364	4.557	1540.	4.14	.36	1.20	7.54	556.41	48.36	161.54	.09	4.23	.37	1.23	8.30	6.32
1.398	45.	2500.	2423.	20.2	1.721	5.509	19.6	1.668	5.339	1400.	3.95	.34	1.07	7.35	569.44	48.41	154.95	.09	4.44	.38	1.21	8.65	6.09
1.401	50.	2900.	2809.	23.2	1.942	6.479	22.5	1.881	6.276	1430.	3.99	.33	1.11	7.55	577.96	48.37	161.37	.10	4.87	.41	1.36	8.20	6.29
1.422	50.	2100.	2033.	14.0	1.228	5.270	13.5	1.189	5.103	2950.	6.85	.60	2.57	8.52	542.92	47.66	204.53	.11	4.46	.39	1.68	7.20	7.89
1.415	60.	2350.	2275.	19.6	1.435	6.307	19.0	1.389	6.106	9400.	27.40	2.00	8.77	7.51	600.45	43.86	192.83	.10	5.09	.37	1.63	9.30	8.74
1.316	25.	2050.	1993.	19.1	1.382	4.562	18.6	1.344	4.435	7700.	25.01	1.81	5.96	6.91	615.63	44.57	147.12	.06	3.40	.25	.81	9.00	6.23
1.325	30.	2900.	2818.	26.5	1.969	6.409	25.8	1.913	6.228	6880.	21.93	1.63	5.29	6.94	606.95	45.07	146.73	.06	3.34	.25	.81	8.70	6.13
1.300	30.	2700.	2626.	25.1	1.835	5.851	24.4	1.785	5.692	7280.	23.57	1.73	5.49	6.89	611.92	44.80	142.84	.06	3.39	.25	.79	9.00	5.84
1.300	35.	2600.	2537.	19.2	1.671	5.287	18.7	1.631	5.160	990.	2.54	.22	.70	7.95	560.29	48.89	154.65	.07	3.14	.27	.87	7.10	4.85
1.298	40.	3600.	3512.	27.1	2.312	7.292	26.4	2.256	7.115	1070.	2.81	.24	.75	7.95	571.76	48.84	154.06	.07	3.20	.27	.86	7.30	4.79
1.295	45.	4100.	4001.	31.3	2.599	8.306	30.5	2.537	8.105	1120.	2.98	.25	.79	8.04	586.31	48.76	155.83	.08	3.71	.31	.99	7.00	4.79
1.290	50.	4300.	4185.	34.2	2.768	8.617	33.3	2.694	8.386	1070.	2.97	.24	.75	7.93	602.83	48.84	152.03	.07	3.39	.27	.85	7.10	4.61
1.305	50.	4000.	3890.	25.3	2.150	8.712	24.6	2.091	8.473	1500.	3.30	.28	1.14	9.47	571.96	48.69	197.33	.09	3.46	.29	1.19	5.60	5.91
1.302	60.	3800.	3696.	28.7	2.023	9.089	27.9	1.967	8.840	8150.	21.46	1.51	6.78	8.90	642.76	45.32	203.64	.09	4.14	.29	1.31	7.00	7.25
1.202	20.	2500.	2453.	21.2	1.565	5.182	20.8	1.535	5.085	9980.	29.57	2.18	7.20	7.31	594.11	43.77	144.97	.03	1.55	.11	.38	8.20	5.15
1.206	25.	3700.	3629.	24.5	2.177	7.016	24.0	2.136	6.882	1500.	3.46	.31	.99	8.67	548.54	48.80	157.28	.05	2.01	.18	.58	6.00	3.69
1.200	35.	4300.	4219.	30.2	2.592	8.008	29.7	2.543	7.858	990.	2.43	.21	.64	8.50	571.71	49.01	151.44	.06	2.57	.22	.68	6.00	3.37
1.202	40.	4400.	4317.	31.0	2.592	8.246	30.4	2.543	8.090	1000.	2.46	.21	.65	8.70	586.22	49.03	155.98	.06	2.57	.22	.68	5.60	3.48
1.200	50.	5000.	4888.	29.9	2.505	9.757	29.2	2.449	9.538	1760.	3.67	.31	1.19	10.18	581.90	48.80	190.05	.06	2.18	.18	.71	4.30	4.17
1.230	60.	5000.	4885.	35.1	2.547	10.578	34.3	2.488	10.333	5560.	13.60	.99	4.09	9.63	646.22	46.93	194.90	.06	2.56	.19	.77	4.80	5.47
1.100	0.	1000.	983.	8.4	.457	1.746	8.3	.449	1.717	210.	.62	.03	.13	11.36	916.84	49.62	189.78	.05	2.57	.14	.53	2.10	2.21
1.100	10.	2000.	1945.	12.6	.914	3.488	12.3	.889	3.393	280.	.62	.04	.17	11.31	682.27	49.46	188.71	.08	3.07	.22	.85	2.00	2.18
1.101	15.	3550.	3506.	21.9	1.899	6.093	21.6	1.876	6.017	750.	1.61	.14	.45	9.64	568.26	49.34	158.28	.04	1.50	.13	.42	3.80	1.88
1.101	20.	4300.	4247.	26.3	2.334	7.356	26.0	2.305	7.265	760.	1.62	.14	.45	9.50	556.59	49.33	155.47	.04	1 49	.13	.42	4.70	1.82

1.102	25.	5000.	4948.	31.0	2.739	8.549	30.6	2.710	8.460	880.	1.90	.17	.52	9.40	556.84	49.26	153.76	.04	1.51	.13	.42	3.80	1.81
1.099	30.	5300.	5246.	33.6	2.919	9.024	33.3	2.889	8.933	880.	1.95	.17	.52	9.35	566.97	49.25	152.30	.04	1.54	.13	.41	4.20	1.73
1.101	35.	5200.	5135.	34.1	2.889	8.870	33.7	2.854	8.760	930.	2.13	.18	.55	9.26	581.63	49.22	151.11	.04	1.60	.14	.42	4.40	1.76
1.098	40.	5650.	5581.	38.4	3.160	9.592	38.0	3.121	9.475	920.	2.18	.18	.54	9.20	598.67	49.22	149.42	.04	1.66	.14	.41	4.65	1.67
1.084	50.	5600.	5550.	31.4	2.537	9.658	31.1	2.515	9.573	1890.	3.69	.30	1.13	11.27	603.76	48.85	185.95	.06	2.05	.17	.63	2.00	1.97
1.083	60.	5200.	5131.	35.7	2.370	9.307	35.3	2.339	9.183	5400.	12.94	.86	3.36	10.85	713.26	47.31	185.78	.06	2.51	.17	.65	3.20	2.66
1.049	0.	550.	547.	9.5	.320	1.276	9.4	.318	1.268	30000.	180.42	6.09	24.20	5.89	971.70	32.82	130.70	.07	7.35	.25	.99	12.10	6.83
1.037	10.	1350.	1343.	10.7	.602	2.596	10.7	.598	2.583	14620.	40.59	2.27	9.78	9.70	738.71	41.35	178.47	.55	26.66	1.49	6.44	4.60	3.93
1.003	20.	3000.	2984.	15.4	1.271	4.785	15.3	1.264	4.760	1020.	1.82	.15	.57	11.49	563.00	46.56	175.32	.73	22.77	1.88	7.08	1.00	.43
1.000	25.	3000.	2985.	14.7	1.262	4.686	14.7	1.256	4.662	1140.	1.95	.17	.62	11.51	541.26	46.33	171.98	.78	23.35	2.00	7.41	.70	.00
1.000	30.	3700.	3682.	18.3	1.561	5.779	18.2	1.554	5.750	1190.	2.06	.18	.65	11.50	544.89	46.42	171.83	.75	22.62	1.93	7.13	.60	.00
1.000	35.	4000.	3993.	19.7	1.684	6.247	19.7	1.682	6.237	1250.	2.15	.18	.68	11.49	542.55	46.28	171.68	.78	23.44	2.00	7.41	.60	.00
1.000	40.	4400.	4393.	22.3	1.863	6.872	22.3	1.859	6.861	1300.	2.30	.19	.71	11.56	560.78	46.81	172.72	.64	19.76	1.65	6.08	.70	.00
1.000	45.	4500.	4478.	23.6	1.907	7.028	23.5	1.898	6.993	1350.	2.47	.20	.73	11.57	581.22	46.91	172.87	.61	19.50	1.57	5.80	.60	.00
1.000	50.	5000.	5008.	27.3	2.112	7.809	27.4	2.115	7.822	1380.	2.63	.20	.75	11.59	606.20	46.83	173.17	.63	20.97	1.62	5.99	.60	.00
1.002	60.	5400.	5390.	34.6	2.307	8.522	34.5	2.302	8.507	1280.	2.86	.19	.70	11.61	711.05	47.44	175.29	.48	18.71	1.25	4.61	6.80	.22
.915	0.	66.	67.	.9	.033	.103	.9	.033	.105	11090.	51.13	1.91	6.02	6.05	765.15	28.55	90.40	3.42	275.29	10.27	32.50	6.10	.00
.917	5.	100.	102.	1.1	.050	.156	1.1	.051	.159	11440.	44.42	1.99	6.21	6.02	641.17	28.67	89.95	3.32	225.05	10.06	31.55	5.80	.00
.917	10.	130.	132.	1.3	.065	.203	1.3	.066	.206	11500.	39.85	2.01	6.25	6.02	572.26	28.87	89.95	3.24	196.03	9.89	30.79	6.20	.00
.916	15.	240.	244.	2.3	.122	.375	2.3	.124	.381	11770.	38.56	2.08	6.39	5.93	532.89	28.78	88.60	3.18	181.88	9.82	30.22	6.70	.00
.923	20.	900.	923.	6.3	.463	1.406	6.5	.475	1.441	1300.	3.17	.23	.71	7.01	469.34	34.52	104.74	3.00	127.84	9.40	28.51	3.10	.00
.915	25.	900.	924.	6.1	.456	1.406	6.3	.468	1.442	1400.	3.31	.25	.76	7.14	463.77	34.61	106.68	3.02	124.85	9.32	28.70	3.20	.00
.917	30.	910.	934.	6.1	.451	1.421	6.3	.463	1.458	1460.	3.42	.25	.79	7.25	466.35	34.39	108.33	3.13	128.14	9.45	29.74	2.80	.00
.923	35.	1000.	1025.	6.7	.487	1.562	6.9	.500	1.601	1500.	3.50	.25	.81	7.54	482.10	35.15	112.66	3.02	122.90	8.96	28.70	2.90	.00
.925	40.	1100.	1127.	7.8	.554	1.718	8.0	.567	1.761	1500.	3.73	.26	.81	7.28	496.40	35.05	108.77	2.94	127.59	9.01	27.94	2.90	.00
.924	45.	1200.	1230.	8.8	.604	1.874	9.1	.620	1.921	1510.	3.88	.27	.82	7.24	510.58	34.89	108.18	2.97	133.31	9.11	28.22	3.40	.00
.928	50.	1400.	1434.	10.7	.695	2.187	10.9	.712	2.240	1480.	3.94	.26	.80	7.42	541.60	35.22	110.87	2.95	137.05	8.91	28.03	3.50	.00
.925	55.	1550.	1589.	12.1	.758	2.421	12.4	.777	2.481	1430.	3.88	.24	.78	7.62	566.99	35.65	113.85	2.91	137.81	8.66	27.65	3.40	.00
.925	60.	1600.	1640.	13.1	.789	2.499	13.5	.809	2.561	1350.	3.86	.23	.73	7.53	591.04	35.52	112.51	2.92	145.87	8.77	27.75	3.70	.00
.927	65.	1700.	1742.	15.0	.826	2.655	15.3	.846	2.721	1270.	3.90	.22	.69	7.71	649.88	35.82	115.20	2.91	156.12	8.60	27.65	3.50	.00
.928	70.	1750.	1793.	17.3	.864	2.733	17.7	.885	2.801	1200.	4.14	.21	.65	7.54	713.85	35.62	112.66	2.91	175.35	8.75	27.65	3.60	.00
.863	0.	52.	54.	.8	.025	.081	.8	.026	.084	11340.	57.27	1.92	6.16	6.00	831.18	27.83	89.65	3.63	320.05	10.72	34.49	5.90	.00
.860	5.	65.	67.	.8	.031	.102	.8	.032	.104	11590.	49.29	1.96	6.30	5.96	695.35	27.61	89.05	3.66	271.77	10.79	34.78	5.40	.00
.866	10.	100.	102.	1.0	.050	.156	1.1	.051	.159	11400.	41.65	1.99	6.19	5.80	581.34	27.74	86.66	3.50	223.28	10.65	33.26	6.30	.00
.856	15.	130.	133.	.9	.062	.203	.9	.064	.208	1190.	2.91	.20	.65	7.15	479.97	32.84	106.83	3.60	153.81	10.53	34.21	3.40	.00
.864	20.	210.	211.	1.3	.091	.328	1.3	.091	.329	1510.	3.22	.23	.82	8.27	483.14	34.35	123.57	3.60	133.86	9.52	34.21	3.30	.00
.866	25.	420.	424.	2.5	.182	.656	2.6	.184	.662	1570.	3.30	.24	.85	8.25	476.19	34.28	123.27	3.61	132.62	9.55	34.30	3.10	.00
.866	30.	560.	562.	3.4	.241	.875	3.4	.242	.877	1670.	3.54	.25	.91	8.34	484.60	34.34	124.61	3.62	133.87	9.49	34.40	3.30	.00
.865	35.	620.	625.	4.0	.277	.968	4.0	.279	.977	1670.	3.73	.26	.91	7.88	482.83	33.69	117.74	3.63	141.56	9.88	34.49	2.80	.00
.865	40.	640.	645.	4.2	.285	1.000	4.2	.287	1.008	1790.	4.07	.28	.97	7.91	493.35	33.70	118.19	3.63	144.10	9.84	34.49	2.90	.00
.866	45.	700.	706.	4.8	.311	1.093	4.8	.314	1.103	1790.	4.25	.28	.97	7.95	518.03	33.84	118.78	3.60	149.30	9.75	34.21	3.10	.00
.865	50.	720.	726.	5.2	.327	1.125	5.3	.330	1.134	1710.	4.32	.27	.93	7.84	543.68	34.06	117.14	3.48	153.59	9.62	33.07	3.10	.00
.865	55.	760.	767.	5.7	.344	1.187	5.7	.347	1.197	1660.	4.33	.26	.90	7.84	560.96	33.93	117.14	3.53	160.75	9.72	33.54	3.20	.00
.866	60.	800.	807.	6.2	.352	1.249	6.3	.355	1.260	1610.	4.36	.25	.87	8.11	602.04	34.11	121.18	3.60	170.09	9.64	34.21	3.00	.00
.866	65.	860.	867.	7.1	.378	1.343	7.2	.381	1.355	1480.	4.29	.23	.80	8.17	648.98	34.31	122.07	3.57	180.49	9.54	33.92	2.90	.00

.856	70.	1000.	1021.	9.5	.482	1.562	9.7	.492	1.594	1280.	4.24	.22	.70	7.22	656.46	33.29	107.88	3.48	201.38	10.21	33.07	3.90	.00
.800	20.	135.	136.	.9	.055	.211	.9	.055	.212	2020.	4.70	.29	1.10	7.25	462.89	28.21	108.33	5.38	218.62	13.32	51.12	2.60	.00
.799	25.	130.	131.	.9	.054	.203	.9	.055	.204	2130.	4 86	.31	1.16	6.87	429.97	27.48	102.65	5.40	215.10	13.75	51.31	3.30	.00
.793	30.	140.	141.	.9	.058	.219	.9	.058	.220	2230.	5.01	.32	1.21	7.09	437.31	27.89	105.93	5.38	211.20	13.47	51.12	3.30	.00
.795	35.	165.	166.	1.1	.067	.258	1.1	.068	.260	2340.	5.26	.33	1.27	7.16	441.51	27.99	106.98	5.38	211.14	13.38	51.12	2.90	.00
.796	40.	170.	171.	1.1	.069	.266	1.1	.070	.267	2360.	5.33	.34	1.28	7.19	445.37	28.10	107.43	5.35	210.92	13.31	50.84	2.90	.00
.792	45.	190.	191.	1.3	.080	.297	1.3	.080	.299	2390.	5.69	.35	1.30	6.82	445.15	27.33	101.90	5.40	224.33	13.77	51.31	3.20	.00
.790	50.	200.	202.	1.4	.083	.312	1.4	.083	.315	2370.	5.63	.34	1.29	6.91	450.29	27.34	103.25	5.47	226.87	13.78	51.98	2.90	.00
.789	55.	200.	202.	1.4	.082	.312	1.4	.083	.315	2370.	5.80	.34	1.29	7.08	475.22	27.88	105.79	5.36	228.98	13.44	50.93	3.30	.00
.796	60.	215.	217.	1.6	.089	.336	1.6	.089	.338	2270.	5.74	.33	1.23	7.06	489.89	27.81	105.49	5.39	238.04	13.51	51.22	3.50	.00
.807	10.	36.	36.	.5	.016	.056	.5	.016	.057	14240.	67.27	2.19	7.73	5.67	734.72	23.92	84.72	4.74	390.92	12.73	45.04	6.10	.00
.822	15.	110.	111.	1.2	.048	.172	1.2	.048	.173	13160.	48.35	2.00	7.15	6.07	611.82	25.33	90.69	4.58	293.81	12.16	43.52	5.80	.00

AFR	Tmg	etam	etab	etav	Trque	Pwr	QCl	QEx	QChm	Qcond	Wb	Qc	Qe	QCm	Qcnd	Qout	mfCV
Lmda	DegBTDC	%	%	%	Nm	kW	kW	kW	kW	kW	%	%	%	%	%	%	kW
1.601	55.	.73	.275	.71	238.3	38.40	14.79	26.65	11.48	12.40	27.45	10.57	19.05	8.21	8.86	25.86	139.89
1.618	60.	.74	.230	.77	214.2	33.40	6.16	27.11	18.50	12.17	22.96	4.23	18.64	12.72	8.36	33.08	145.47
1.515	25.	.60	.247	.73	234.0	35.80	15.20	30.13	15.90	12.37	24.69	10.48	20.78	10.97	8.53	24.55	145.00
1.513	30.	.64	.254	.74	242.1	38.30	20.65	31.14	13.48	13.23	25.36	13.67	20.62	8.93	8.76	22.66	151.02
1.491	35.	.74	.293	.71	273.9	42.40	28.91	29.11	7.19	13.31	29.33	20.00	20.13	4.97	9.20	16.36	144.57
1.512	40.	.76	.302	.70	276.6	43.50	27.62	34.62	7.49	13.24	30.21	19.18	24.04	5.20	9.19	12.17	144.00
1.501	45.	.78	.309	.71	284.1	44.60	25.93	29.29	4.06	13.66	30.87	17.95	20.28	2.81	9.45	18.64	144.47
1.514	45.	.76	.301	.70	274.2	43.10	28.78	27.96	4.78	13.43	30.15	20.13	19.56	3.34	9.39	17.43	142.96
1.500	50.	.78	.302	.70	276.7	43.50	30.22	28.00	3.96	13.61	30.24	21.01	19.46	2.75	9.46	17.09	143.87
1.500	50.	.70	.304	.70	278.2	43.70	28.11	28.82	4.14	13.58	30.41	19.56	20.05	2.88	9.45	17.65	143.71
1.503	55.	.78	.299	.69	272.7	42.90	31.06	28.55	4.12	13.58	29.87	21.62	19.88	2.87	9.45	16.31	143.63
1.500	55.	.78	.302	.70	273.9	43.00	32.02	28.58	4.36	13.45	30.17	22.47	20.05	3.06	9.44	14.82	142.54
1.500	60.	.77	.297	.70	269.3	42.10	23.97	28.40	4.32	13.40	29.67	16.90	20.02	3.05	9.45	20.92	141.87
1.497	65.	.78	.291	.69	262.7	41.30	31.76	28.86	4.40	13.42	29.06	22.35	20.31	3.10	9.44	15.74	142.11
1.501	70.	.79	.284	.70	258.3	40.50	32.64	28.70	4.22	13.48	28.43	22.91	20.15	2.96	9.46	16.09	142.45
1.396	25.	.77	.299	.68	285.2	44.80	32.09	32.95	4.19	14.16	29.87	21.39	21.97	2.79	9.44	14.54	149.99
1.385	30.	.71	.267	.69	261.1	41.50	12.73	29.35	12.48	13.81	26.68	8.18	18.87	8.02	8.87	29.38	155.57
1.402	30.	.76	.302	.67	283.9	44.30	31.57	28.80	5.40	13.70	30.21	21.53	19.64	3.68	9.35	15.60	146.64
1.401	35.	.67	.261	.67	243.5	38.30	15.32	27.73	14.99	12.67	26.10	10.44	18.90	10.22	8.64	25.70	146.72
1.400	40.	.81	.313	.66	289.0	45.40	16.50	28.42	3.55	13.78	31.29	11.37	19.59	2.45	9.50	25.80	145.09
1.398	45.	.81	.306	.67	283.6	44.60	17.68	29.10	3.50	13.86	30.61	12.13	19.97	2.40	9.51	25.38	145.72
1.401	50.	.81	.301	.66	277.0	43.60	16.74	28.06	3.56	13.77	30.13	11.57	19.39	2.46	9.51	26.93	144.71
1.422	50.	.91	.316	.70	303.6	45.30	16.01	24.63	5.22	13.42	31.60	11.17	17.19	3.65	9.37	27.03	143.34
1.415	60.	.71	.263	.69	252.1	39.20	15.49	24.45	15.90	12.82	26.29	10.39	16.40	10.66	8.60	27.65	149.09
1.316	25.	.67	.261	.72	277.5	42.20	19.25	31.91	15.50	14.09	26.07	11.89	19.71	9.58	8.70	24.06	161.90
1.325	30.	.58	.267	.72	282.3	42.90	19.16	31.35	14.09	14.13	26.73	11.94	19.54	8.78	8.80	24.21	160.48
1.300	30.	.53	.264	.69	272.7	42.30	18.76	31.79	14.83	14.04	26.36	11.69	19.81	9.24	8.75	24.15	160.48
1.300	35.	.81	.314	.67	313.4	49.30	24.03	31.98	2.69	15.03	31.41	15.31	20.38	1.71	9.57	21.61	156.94
1.298	40.	.81	.308	.66	306.0	48.20	27.29	31.71	3.02	14.99	30.75	17.41	20.23	1.93	9.56	20.11	156.74
1.295	45.	.82	.299	.66	296.8	46.80	27.90	31.30	3.22	14.94	29.94	17.85	20.02	2.06	9.56	20.56	156.30
1.290	50.	.84	.292	.65	289.2	45.40	27.90	31.55	3.15	14.89	29.17	17.93	20.27	2.02	9.56	21.05	155.66
1.305	50.	.93	.306	.65	299.4	45.90	33.21	26.10	3.18	14.29	30.65	22.17	17.43	2.13	9.54	18.08	149.76
1.302	60.	.94	.254	.66	252.6	39.10	33.94	24.81	12.72	13.66	25.38	22.03	16.11	8.26	8.87	19.35	154.04
1.202	20.	.65	.265	.70	298.4	46.90	20.26	34.34	20.01	15.03	26.52	11.46	19.42	11.32	8.50	22.78	176.82
1.206	25.	.82	.320	.67	347.8	54.70	31.27	35.03	3.67	16.27	32.03	18.31	20.51	2.15	9.53	17.48	170.78
1.200	35.	.80	.309	.66	327.4	51.50	38.34	34.41	2.96	15.99	30.86	22.97	20.62	1.77	9.58	14.19	166.87
1.202	40.	.75	.301	.65	317.9	50.00	41.07	33.43	2.91	15.91	30.11	24.73	20.13	1.75	9.58	13.69	166.07
1.200	50.	1.09	.302	.66	323.8	49.50	42.17	28.81	3.63	15.62	30.19	25.72	17.57	2.21	9.53	14.78	163.97
1.230	60.	1.00	.261	.67	277.2	41.30	40.60	26.65	8.89	14.46	26.14	25.70	16.87	5.63	9.15	16.51	157.98
1.100	0.	.71	.195	.68	239.2	37.70	47.37	49.89	.77	18.73	19.48	24.48	25.78	.40	9.68	20.18	193.50
1.100	10.	6.01	.261	.66	313.0	49.30	49.84	43.49	1.19	18.27	26.10	26.38	23.02	.63	9.67	14.20	188.92
1.101	15.	.79	.313	.67	367.9	57.90	40.29	40.83	2.23	17.82	31.26	21.75	22.04	1.20	9.62	14.13	185.24
1.101	20.	.80	.319	.67	371.8	58.40	42.97	39.21	2.40	17.60	31.90	23.48	21.42	1.31	9.62	12.27	183.05

1.102	25.	.79	.318	.66	368.6	58.10	45.66	38.38	2.76	17.52	31.85	25.03	21.04	1.51	9.60	10.97	182.44
1.099	30.	.83	.313	.65	359.1	56.40	51.03	37.74	2.80	17.32	31.27	28.30	20.93	1.55	9.60	8.34	180.34
1.101	35.	.85	.305	.65	346.8	54.70	51.05	37.47	2.88	17.23	30.47	28.43	20.87	1.61	9.60	9.03	179.55
1.098	40.	.86	.296	.64	334.9	52.60	47.42	37.06	2.94	17.05	29.60	26.68	20.86	1.66	9.60	11.61	177.71
1.084	50.	1.16	.291	.65	342.9	52.10	51.03	32.53	3.86	17.05	29.13	28.53	18.19	2.16	9.53	12.47	178.87
1.083	60.	1.03	.239	.64	277.2	43.80	50.62	33.06	9.04	16.92	23.88	27.60	18.02	4.93	9.22	16.35	183.42
1.049	0.	.45	.122	.74	168.5	24.40	13.61	39.41	61.78	12.75	12.16	6.78	19.64	30.79	6.35	24.27	200.66
1.037	10.	.54	.202	.69	263.5	41.20	35.43	39.17	26.55	17.27	20.15	17.33	19.16	12.99	8.45	21.92	204.45
1.003	20.	.78	.298	.66	388.0	60.50	46.66	40.64	5.90	19.54	29.77	22.96	20.00	2.90	9.61	14.76	203.23
1.000	25.	.79	.308	.66	396.3	63.00	45.65	39.43	8.39	19.63	30.81	22.33	19.28	4.11	9.60	13.86	204.45
1.000	30.	.83	.307	.67	401.3	63.00	46.06	38.52	8.41	19.72	30.67	22.42	18.75	4.09	9.60	14.46	205.42
1.000	35.	.84	.307	.65	394.4	62.20	46.06	37.38	8.65	19.43	30.71	22.74	18.46	4.27	9.59	14.23	202.54
1.000	40.	.86	.301	.65	384.9	60.30	49.90	37.00	7.65	19.24	30.05	24.87	18.44	3.81	9.59	13.24	200.66
1.000	45.	.89	.291	.65	370.9	58.30	51.48	36.90	7.51	19.24	29.05	25.66	18.39	3.74	9.59	13.57	200.66
1.000	50.	.93	.278	.65	353.1	55.80	54.55	37.07	7.77	19.23	27.81	27.18	18.47	3.87	9.58	13.08	200.66
1.002	60.	1.34	.240	.67	315.9	48.20	57.47	37.41	5.35	19.25	24.02	28.64	18.64	2.67	9.59	16.44	200.66
.915	0.	.51	.134	.72	203.2	31.60	34.78	49.05	62.42	20.34	13.43	14.79	20.85	26.54	8.65	15.74	235.22
.917	5.	.53	.161	.71	242.2	38.20	36.21	46.46	63.00	20.42	16.10	15.26	19.58	26.55	8.61	13.91	237.31
.917	10.	.57	.182	.71	272.8	42.80	35.29	43.53	62.10	20.25	18.16	14.98	18.47	26.36	8.59	13.44	235.64
.916	15.	.61	.194	.72	294.0	45.90	34.72	41.56	62.82	20.19	19.44	14.71	17.60	26.61	8.55	13.08	236.07
.923	20.	.81	.265	.68	377.8	59.70	41.25	46.70	37.18	21.57	26.48	18.29	20.71	16.49	9.57	8.46	225.49
.915	25.	.83	.269	.67	378.5	59.30	43.06	43.72	36.21	21.10	26.87	19.51	19.81	16.41	9.56	7.85	220.72
.917	30.	.85	.265	.67	373.5	58.90	41.87	42.81	36.98	21.20	26.55	18.87	19.30	16.67	9.56	9.06	221.87
.923	35.	.88	.262	.66	363.4	57.20	43.98	41.40	34.47	20.82	26.25	20.18	19.00	15.82	9.56	9.20	217.92
.925	40.	.90	.254	.66	350.3	54.80	41.17	41.86	34.40	20.59	25.42	19.10	19.42	15.96	9.55	10.55	215.58
.924	45.	.86	.246	.66	337.0	52.30	44.80	41.32	34.35	20.30	24.60	21.07	19.43	16.16	9.55	9.19	212.61
.928	50.	.95	.234	.66	321.2	48.80	47.80	39.93	32.89	19.92	23.41	22.93	19.15	15.78	9.56	9.17	208.44
.925	55.	1.01	.226	.65	305.8	48.10	48.76	40.90	32.50	20.32	22.63	22.94	19.24	15.29	9.56	10.32	212.52
.925	60.	1.08	.216	.63	284.1	44.50	52.43	39.98	31.72	19.68	21.63	25.49	19.44	15.42	9.57	8.45	205.69
.927	65.	1.23	.198	.64	264.5	41.90	52.36	41.13	31.79	20.22	19.84	24.80	19.48	15.06	9.58	11.25	211.17
.928	70.	1.20	.180	.64	239.7	37.30	55.49	41.17	31.72	19.90	17.96	26.72	19.83	15.27	9.58	10.64	207.67
.863	0.	.48	.121	.68	184.0	28.60	36.71	49.62	65.07	20.51	12.05	15.47	20.91	27.42	8.64	15.49	237.26
.860	5.	.51	.143	.69	221.3	34.70	36.44	47.41	67.42	20.93	14.29	15.01	19.53	27.77	8.62	14.78	242.78
.866	10.	.55	.172	.68	261.3	40.80	35.57	44.15	65.72	20.44	17.18	14.97	18.59	27.67	8.61	12.99	237.53
.856	15.	.74	.246	.64	358.8	56.40	42.57	46.33	41.83	21.95	24.64	18.59	20.24	18.27	9.59	8.68	228.94
.864	20.	.80	.256	.65	378.5	59.50	41.97	41.55	38.58	22.25	25.59	18.05	17.87	16.60	9.57	12.31	232.48
.866	25.	.81	.259	.65	378.8	59.30	42.89	39.84	38.25	21.89	25.91	18.74	17.41	16.71	9.57	11.66	228.84
.866	30.	.85	.255	.65	372.9	58.50	43.13	39.15	38.26	21.92	25.51	18.81	17.07	16.68	9.56	12.38	229.34
.865	35.	.87	.251	.64	365.1	57.50	42.97	39.88	39.93	21.86	25.12	18.77	17.42	17.44	9.55	11.69	228.89
.865	40.	.87	.246	.64	353.6	55.50	45.28	39.14	39.43	21.54	24.59	20.06	17.34	17.47	9.54	10.99	225.69
.866	45.	.91	.235	.64	337.8	53.10	46.20	39.15	39.09	21.55	23.52	20.46	17.34	17.31	9.54	11.82	225.79
.865	50.	.93	.226	.63	322.1	50.60	49.82	39.57	38.24	21.42	22.56	22.21	17.64	17.05	9.55	11.00	224.33
.865	55.	.98	.218	.62	306.4	48.20	51.94	39.08	38.04	21.14	21.78	23.47	17.65	17.19	9.55	10.36	221.35
.866	60.	1.06	.204	.63	288.3	45.10	49.23	38.39	37.49	21.14	20.40	22.27	17.36	16.96	9.56	13.46	221.12
.866	65.	1.19	.190	.62	267.6	42.20	54.07	38.98	37.00	21.22	19.03	24.39	17.58	16.69	9.57	12.73	221.71

.856	70.	1.40	.183	.61	252.4	39.70	51.34	41.22	38.84	20.83	18.26	23.61	18.96	17.86	9.58	11.74	217.45
.800	20.	.74	.219	.67	358.7	56.50	37.97	43.17	62.01	24.56	21.94	14.74	16.76	24.08	9.54	12.94	257.53
.799	25.	.78	.230	.66	375.2	58.90	38.10	41.96	64.15	24.39	23.01	14.88	16.39	25.06	9.53	11.14	256.02
.793	30.	.79	.230	.66	375.4	59.00	39.62	40.44	63.07	24.47	22.96	15.42	15.74	24.54	9.52	11.82	256.99
.795	35.	.79	.228	.66	373.6	58.60	41.38	39.51	62.78	24.43	22.82	16.12	15.38	24.44	9.51	11.72	256.80
.796	40.	.82	.227	.66	367.6	57.90	41.71	38.91	61.96	24.25	22.71	16.36	15.26	24.31	9.51	11.85	254.93
.792	45.	.83	.221	.65	359.1	56.30	42.00	39.23	64.48	24.21	22.10	16.49	15.40	25.32	9.50	11.19	254.72
.790	50.	.87	.219	.65	354.0	55.60	43.00	38.81	64.31	24.18	21.86	16.91	15.26	25.29	9.51	11.18	254.33
.789	55.	.88	.211	.65	340.3	53.60	43.67	38.55	62.39	24.13	21.12	17.21	15.19	24.59	9.51	12.37	253.74
.796	60.	.93	.204	.65	327.7	51.20	46.42	38.15	61.81	23.85	20.43	18.53	15.23	24.67	9.52	11.63	250.57
.807	10.	.46	.117	.70	198.4	31.20	33.97	46.93	87.36	22.61	11.72	12.76	17.63	32.82	8.49	16.57	266.18
.822	15.	.53	.149	.70	250.9	39.60	34.14	43.30	81.55	22.85	14.90	12.85	16.29	30.69	8.60	16.67	265.72

Dovergas FBHCR 15:1 experimental results

AFR	Tmg	Speed	Temperatures (DegC)								Airflrt	Clflrt	Mthne	Time	Pgup	Pgdn	Hmdty	mFuel	vFuel	Pbaro	Pabs	AFRV	AFRG
Lmda	DegBTDC	RPM	In	Out	Pmy	Fuel	Air	Mix	Exh	Gly	Smp g/sec	l/min	cuft	Sec	in/WG	in/RL	g/kg	kg/s	cum/s	mmHg	bar		
1.526	2.	1506.	63.	86.	86.	26.	37.	41.	660.	93.	88. 66.5	24.9	10.	75.0	23.5	5.00	9.	.0027	.0038	761.5	1.028	14.72	24.90
1.523	5.	1505.	62.	86.	85.	26.	36.	41.	610.	93.	88. 64.7	23.3	10.	77.0	23.0	5.00	9.	.0026	.0037	761.5	1.028	14.69	24.85
1.543	8.	1501.	61.	85.	85.	26.	36.	40.	577.	93.	86. 65.1	21.7	10.	77.5	22.5	5.00	9.	.0026	.0037	761.5	1.028	14.88	25.17
1.525	11.	1504.	62.	85.	85.	25.	36.	40.	547.	93.	86. 65.0	21.9	10.	77.0	23.0	5.00	9.	.0026	.0037	761.5	1.028	14.71	24.88
1.535	14.	1511.	61.	85.	84.	25.	36.	39.	523.	93.	86. 63.8	21.7	10.	79.0	23.0	5.00	9.	.0025	.0036	761.5	1.028	14.81	25.04
1.524	17.	1500.	61.	85.	84.	25.	36.	39.	504.	92.	86. 62.9	21.6	10.	79.5	23.0	5.00	9.	.0025	.0036	761.5	1.028	14.70	24.86
1.520	20.	1496.	61.	85.	85.	25.	36.	39.	489.	92.	85. 62.3	22.0	10.	80.0	23.5	5.00	9.	.0025	.0035	761.5	1.028	14.66	24.80
1.493	2.	1492.	66.	87.	86.	27.	38.	42.	639.	89.	84. 65.1	27.7	10.	75.0	22.5	5.00	9.	.0027	.0038	764.5	1.032	14.40	24.36
1.509	8.	1516.	66.	86.	86.	26.	37.	40.	570.	85.	75. 66.1	26.6	10.	75.0	23.0	5.00	9.	.0027	.0038	764.5	1.032	14.56	24.62
1.498	14.	1508.	66.	86.	86.	26.	36.	39.	522.	80.	69. 65.1	25.9	10.	75.5	23.5	5.00	9.	.0027	.0038	764.5	1.032	14.45	24.44
1.505	20.	1502.	65.	86.	86.	26.	35.	38.	480.	73.	63. 64.6	20.9	10.	76.5	24.0	5.00	9.	.0026	.0037	764.5	1.032	14.52	24.55
1.499	26.	1506.	65.	86.	86.	26.	36.	38.	476.	78.	66. 63.1	25.2	10.	78.0	23.5	5.00	11.	.0026	.0036	764.5	1.032	14.46	24.46
1.497	32.	1504.	66.	86.	86.	26.	36.	39.	477.	83.	79. 63.0	28.0	10.	78.0	24.0	5.00	11.	.0026	.0036	764.5	1.032	14.44	24.42
1.391	2.	1514.	64.	86.	86.	26.	37.	42.	642.	95.	89. 64.0	27.8	10.	71.0	23.0	4.50	9.	.0028	.0040	761.5	1.026	13.42	22.69
1.399	8.	1498.	64.	86.	85.	25.	37.	41.	582.	96.	89. 63.7	27.1	10.	72.0	22.5	4.50	9.	.0028	.0039	761.5	1.026	13.50	22.83
1.399	11.	1502.	64.	86.	85.	26.	36.	40.	557.	97.	91. 63.0	27.0	10.	72.5	23.0	4.50	9.	.0028	.0039	761.5	1.026	13.50	22.83
1.408	14.	1500.	63.	86.	85.	25.	36.	40.	536.	97.	91. 63.2	27.2	10.	73.0	22.5	4.50	9.	.0028	.0039	761.5	1.026	13.58	22.97
1.402	17.	1505.	64.	86.	85.	25.	36.	40.	524.	97.	92. 62.9	27.7	10.	73.0	22.5	4.50	9.	.0028	.0039	761.5	1.026	13.52	22.87
1.412	20.	1498.	64.	86.	85.	25.	36.	40.	513.	94.	89. 62.1	27.1	10.	74.5	23.0	4.50	9.	.0027	.0038	761.5	1.026	13.62	23.04
1.401	26.	1499.	64.	86.	85.	26.	36.	40.	505.	96.	90. 61.8	28.5	10.	74.0	23.0	4.50	9.	.0027	.0038	761.5	1.026	13.51	22.86
1.408	29.	1495.	64.	86.	85.	25.	36.	40.	498.	97.	90. 61.5	29.8	10.	75.0	23.0	4.50	9.	.0027	.0038	761.5	1.026	13.58	22.97
1.403	32.	1509.	65.	86.	86.	25.	36.	40.	496.	97.	90. 61.3	31.0	10.	75.0	23.0	4.50	9.	.0027	.0038	761.5	1.026	13.53	22.89
1.302	2.	1497.	63.	86.	85.	22.	33.	38.	655.	90.	85. 62.9	28.7	10.	68.0	23.0	4.50	10.	.0030	.0042	756.0	1.019	12.56	21.24
1.306	5.	1497.	63.	85.	85.	22.	32.	37.	625.	89.	84. 63.1	28.3	10.	68.0	23.0	4.50	10.	.0030	.0042	756.0	1.019	12.60	21.31
1.299	8.	1506.	63.	85.	85.	22.	32.	37.	601.	89.	82. 63.7	28.1	10.	67.0	23.0	4.50	10.	.0030	.0042	756.0	1.019	12.53	21.19
1.302	11.	1503.	63.	85.	84.	21.	32.	36.	578.	86.	80. 63.2	28.0	10.	68.0	23.0	4.50	10.	.0030	.0042	756.0	1.019	12.56	21.24
1.298	14.	1501.	63.	85.	85.	21.	32.	35.	561.	83.	72. 63.0	28.6	10.	68.0	23.0	4.50	10.	.0030	.0042	756.0	1.019	12.52	21.18
1.294	17.	1492.	62.	85.	85.	21.	31.	34.	547.	73.	61. 62.8	27.6	10.	68.0	23.0	4.50	10.	.0030	.0042	756.0	1.019	12.48	21.11
1.303	20.	1504.	65.	87.	86.	26.	37.	41.	543.	97.	92. 61.2	32.0	10.	69.5	22.5	4.50	9.	.0029	.0041	761.5	1.026	12.57	21.26
1.299	23.	1499.	66.	87.	86.	26.	37.	41.	537.	97.	92. 60.6	32.1	10.	70.0	23.0	4.50	9.	.0029	.0040	761.5	1.026	12.53	21.19
1.300	26.	1496.	66.	87.	86.	26.	37.	41.	530.	98.	92. 60.7	34.1	10.	70.0	22.5	4.50	9.	.0029	.0040	761.5	1.026	12.54	21.21
1.301	29.	1503.	65.	86.	85.	23.	34.	37.	523.	93.	87. 59.9	33.8	10.	71.0	23.0	4.75	11.	.0028	.0040	754.5	1.018	12.55	21.23
1.301	32.	1501.	65.	87.	86.	23.	33.	37.	515.	96.	89. 59.9	35.9	10.	71.0	23.0	4.75	11.	.0028	.0040	754.5	1.018	12.55	21.23
1.209	2.	1493.	65.	86.	85.	24.	34.	39.	676.	96.	90. 61.8	33.8	10.	64.0	21.5	5.00	10.	.0031	.0044	756.0	1.020	11.66	19.73
1.208	5.	1499.	65.	86.	85.	23.	34.	39.	647.	96.	90. 61.9	33.9	10.	64.0	21.5	5.00	10.	.0031	.0044	756.0	1.020	11.65	19.71
1.202	8.	1495.	64.	86.	85.	23.	34.	38.	623.	97.	91. 61.6	32.5	10.	64.0	21.5	5.00	10.	.0031	.0044	756.0	1.020	11.60	19.61
1.204	11.	1495.	64.	86.	85.	23.	34.	38.	602.	97.	91. 61.2	33.1	10.	64.5	22.5	5.00	10.	.0031	.0044	756.0	1.020	11.61	19.64
1.203	14.	1506.	65.	86.	85.	23.	34.	38.	586.	97.	91. 61.1	33.5	10.	64.5	22.5	4.50	10.	.0031	.0044	756.0	1.019	11.60	19.63
1.204	17.	1502.	65.	86.	85.	23.	34.	38.	573.	97.	91. 60.7	34.9	10.	65.0	22.0	4.50	10.	.0031	.0044	756.0	1.019	11.61	19.64
1.202	20.	1500.	65.	86.	85.	23.	34.	38.	564.	96.	89. 60.1	35.9	10.	65.5	22.0	4.50	10.	.0031	.0043	756.0	1.019	11.60	19.61
1.201	23.	1497.	65.	86.	86.	22.	33.	37.	557.	95.	89. 59.8	36.3	10.	66.0	22.0	4.50	10.	.0031	.0043	756.0	1.019	11.59	19.59
1.100	2.	1504.	67.	87.	86.	23.	34.	39.	708.	97.	92. 61.9	39.2	10.	59.0	22.0	4.50	10.	.0034	.0048	766.0	1.032	10.61	17.95
1.107	5.	1499.	66.	86.	85.	22.	33.	38.	676.	98.	92. 61.4	39.2	10.	60.0	22.5	4.50	10.	.0034	.0047	766.0	1.032	10.68	18.06

1.106	8.	1499.	66.	86.	85.	22.	33.	38.	653.	98.	93.	61.4	38.4
1.104	11.	1501.	65.	86.	85.	22.	33.	38.	634.	98.	93.	60.5	38.6
1.103	14.	1499.	66.	86.	85.	21.	32.	37.	619.	98.	93.	59.6	39.1
1.100	17.	1504.	66.	86.	85.	21.	33.	37.	607.	98.	91.	60.0	41.1
1.103	20.	1496.	66.	87.	85.	21.	31.	36.	595.	96.	89.	59.6	41.4
1.003	2.	1500.	71.	88.	87.	24.	36.	41.	745.	99.	97.	61.5	48.4
1.000	5.	1503.	70.	88.	87.	23.	35.	40.	721.	99.	96.	61.0	49.0
1.000	8.	1500.	71.	88.	87.	23.	35.	40.	700.	99.	95.	61.0	48.8
.999	11.	1499.	71.	88.	87.	23.	35.	39.	682.	97.	93.	60.8	50.3
.999	14.	1499.	71.	89.	87.	23.	35.	39.	666.	95.	90.	60.3	51.1
.997	17.	1498.	72.	89.	88.	22.	33.	38.	654.	92.	89.	60.4	51.6
.950	2.	1497.	68.	87.	86.	23.	35.	40.	727.	99.	97.	61.3	42.9
.947	5.	1500.	68.	87.	86.	23.	35.	40.	704.	100.	97.	61.7	43.6
.952	8.	1503.	68.	87.	86.	23.	34.	39.	684.	100.	97.	61.4	44.3
.950	11.	1503.	68.	87.	86.	23.	34.	39.	669.	101.	97.	61.3	44.9
.949	14.	1502.	69.	88.	87.	23.	34.	39.	656.	99.	96.	61.2	45.7
.903	2.	1499.	67.	87.	86.	22.	34.	39.	713.	98.	95.	62.7	41.6
.903	5.	1505.	67.	87.	86.	22.	34.	39.	688.	99.	95.	62.7	42.0
.900	8.	1502.	68.	87.	86.	22.	33.	38.	667.	99.	96.	62.5	42.3
.901	11.	1506.	68.	87.	86.	22.	33.	38.	650.	100.	97.	62.6	43.4
.900	14.	1507.	68.	87.	86.	22.	33.	38.	636.	100.	97.	61.9	44.7
.900	17.	1493.	68.	87.	86.	22.	33.	38.	626.	100.	95.	61.2	45.0
.902	20.	1498.	69.	88.	86.	21.	32.	37.	620.	96.	91.	61.6	47.0
.807	2.	1507.	65.	86.	85.	21.	32.	38.	719.	96.	92.	60.5	36.3
.803	5.	1493.	65.	86.	85.	21.	32.	37.	683.	98.	92.	60.9	35.9
.803	8.	1503.	65.	86.	85.	20.	32.	36.	651.	102.	97.	61.1	36.6
.801	11.	1500.	65.	86.	85.	20.	31.	36.	626.	103.	101.	60.2	36.9
.802	14.	1508.	65.	86.	85.	19.	33.	36.	608.	107.	107.	61.2	38.5
.804	17.	1501.	65.	86.	85.	19.	30.	34.	598.	106.	105.	60.7	39.4
.803	20.	1500.	65.	85.	84.	17.	29.	33.	589.	93.	89.	61.7	38.4
.799	23.	1484.	65.	86.	85.	18.	30.	34.	582.	103.	101.	59.8	39.1
1.900	8.	1468.	58.	84.	83.	17.	28.	32.	473.	89.	86.	76.1	12.6
1.808	11.	1558.	59.	84.	84.	17.	28.	31.	500.	90.	83.	75.6	14.8
1.773	14.	1529.	60.	85.	84.	17.	28.	31.	503.	90.	82.	71.7	18.9
1.709	17.	1632.	60.	85.	84.	17.	28.	31.	493.	90.	82.	69.7	19.2
1.760	20.	1510.	59.	84.	83.	17.	27.	30.	433.	90.	84.	71.8	16.5
1.504	2.	1483.	66.	86.	86.	27.	39.	43.	632.	93.	89.	63.5	29.2
1.501	5.	1514.	66.	86.	86.	27.	38.	42.	602.	92.	85.	65.1	28.4
1.505	8.	1502.	66.	86.	85.	26.	37.	41.	569.	90.	86.	64.6	27.5
1.504	11.	1498.	66.	86.	85.	26.	37.	40.	540.	89.	83.	64.2	27.1
1.499	14.	1499.	66.	86.	85.	25.	36.	40.	521.	87.	77.	63.8	27.4
1.503	17.	1498.	66.	86.	85.	25.	36.	39.	504.	82.	71.	63.5	27.2
1.509	23.	1504.	66.	86.	85.	28.	38.	42.	492.	96.	91.	62.9	30.0
1.499	26.	1500.	67.	86.	86.	28.	38.	41.	485.	97.	91.	62.3	30.2
1.507	29.	1506.	65.	86.	85.	25.	36.	39.	473.	77.	65.	62.7	26.8

10.	60.0	22.5	4.75	10.	.0034	.0047	766.0	1.033	10.67	18.04
10.	60.0	22.0	4.50	10.	.0034	.0047	756.0	1.019	10.65	18.01
10.	61.0	22.5	4.50	10.	.0033	.0046	756.0	1.019	10.64	18.00
10.	60.5	22.5	4.50	10.	.0033	.0047	756.0	1.019	10.61	17.95
10.	61.0	22.5	4.50	10.	.0033	.0046	756.0	1.019	10.64	18.00
10.	54.0	21.5	4.50	8.	.0038	.0052	767.0	1.034	9.68	16.36
10.	54.5	21.5	4.50	8.	.0037	.0052	767.0	1.034	9.65	16.32
10.	54.5	22.0	4.50	8.	.0037	.0052	767.0	1.034	9.65	16.32
10.	54.5	22.0	4.50	10.	.0037	.0052	766.0	1.032	9.64	16.30
10.	55.0	22.0	4.50	10.	.0037	.0051	766.0	1.032	9.64	16.30
10.	55.0	22.0	4.50	10.	.0037	.0051	766.0	1.032	9.62	16.27
10.	51.5	20.5	5.50	9.	.0040	.0055	765.5	1.034	9.16	15.50
10.	51.0	21.5	5.50	9.	.0040	.0056	765.0	1.034	9.14	15.45
10.	51.5	21.5	5.50	9.	.0040	.0055	765.0	1.034	9.18	15.53
10.	51.5	21.5	5.50	9.	.0040	.0055	765.0	1.034	9.16	15.50
10.	51.5	21.0	5.50	9.	.0040	.0055	765.0	1.034	9.15	15.48
10.	48.0	21.0	5.50	9.	.0043	.0059	765.0	1.034	8.71	14.73
10.	48.0	21.0	5.50	7.	.0043	.0059	765.0	1.034	8.71	14.73
10.	48.0	21.5	5.50	7.	.0043	.0059	765.0	1.034	8.68	14.68
10.	48.0	21.5	5.50	7.	.0043	.0059	765.0	1.034	8.69	14.70
10.	48.5	21.0	5.50	7.	.0042	.0058	765.0	1.034	8.68	14.68
10.	49.0	21.5	5.50	7.	.0042	.0058	765.0	1.034	8.68	14.68
10.	49.0	21.0	5.50	7.	.0042	.0058	765.0	1.034	8.70	14.72
10.	44.5	19.5	4.00	8.	.0046	.0064	765.5	1.031	7.78	13.17
10.	44.0	19.5	4.00	8.	.0046	.0064	765.5	1.031	7.75	13.10
10.	44.0	20.5	4.00	8.	.0047	.0064	765.5	1.031	7.75	13.10
10.	44.5	20.0	4.00	8.	.0046	.0064	765.5	1.031	7.73	13.07
10.	44.0	20.0	4.00	8.	.0047	.0064	765.5	1.031	7.74	13.08
10.	44.5	19.5	4.00	8.	.0046	.0064	765.5	1.031	7.76	13.12
10.	44.0	20.5	4.00	8.	.0047	.0064	765.5	1.031	7.75	13.10
10.	45.0	20.0	4.00	8.	.0046	.0063	765.5	1.031	7.71	13.04
10.	83.5	22.5	4.50	5.	.0025	.0034	756.5	1.020	18.33	31.00
10.	80.0	22.5	4.50	5.	.0026	.0035	756.5	1.020	17.44	29.50
10.	82.7	23.0	4.50	5.	.0025	.0034	756.5	1.020	17.10	28.93
10.	82.0	23.5	4.50	5.	.0025	.0035	756.5	1.020	16.49	27 88
10.	82.0	23.5	4.50	5.	.0025	.0035	756.5	1.020	16.98	28.71
10.	78.0	23.5	5.00	7.	.0026	.0036	770.0	1.039	14.51	24.54
10.	76.0	23.0	5.00	7.	.0027	.0037	770.0	1.039	14.48	24.49
10.	77.0	22.5	5.00	7.	.0026	.0037	770.0	1.039	14.52	24.55
10.	77.5	23.5	5.00	7.	.0026	.0037	770.0	1.039	14.51	24.54
10.	78.0	23.0	5.00	7.	.0026	.0036	770.0	1.039	14.46	24.46
10.	78.5	23.0	5.00	7.	.0026	.0036	770.0	1.039	14.50	24.52
10.	78.8	22.5	5.00	7.	.0026	.0036	770.0	1.039	14.56	24.62
10.	79.0	23.0	5.00	7.	.0025	.0036	770.0	1.039	14.46	24.46
10.	79.0	23.0	5.00	9.	.0026	.0036	763.0	1.030	14.54	24.59

1.503	32.	1504.	65.	86.	85.	26.	37.	40.	467.	86.	75.	61.6	27.7	10.	80.0	23.0	5.00	9.	.0025	.0035	763.0	1.030	14.50	24.52
1.490	35.	1552.	65.	86.	85.	26.	37.	41.	474.	89.	83.	63.0	28.1	10.	77.5	23.0	5.00	9.	.0026	.0037	763.0	1.030	14.37	24.31
1.625	8.	1540.	60.	85.	85.	17.	27.	31.	564.	92.	85.	71.7	21.2	10.	76.0	22.5	4.50	7.	.0027	.0037	758.0	1.022	15.68	26.51
1.625	12.	1551.	60.	85.	84.	17.	27.	30.	531.	92.	84.	70.7	21.1	10.	77.0	22.5	4.50	7.	.0027	.0037	758.0	1.022	15.68	26.51
1.620	17.	1547.	60.	85.	84.	16.	28.	31.	498.	97.	91.	69.0	21.8	10.	79.0	22.0	4.50	7.	.0026	.0036	758.0	1.022	15.63	26.43
1.605	20.	1558.	60.	84.	84.	16.	28.	31.	484.	93.	86.	69.2	22.2	10.	78.0	22.5	4.50	7.	.0026	.0036	758.0	1.022	15.48	26.19
1.617	24.	1560.	60.	85.	84.	17.	26.	30.	473.	95.	86.	70.9	21.6	10.	76.5	22.5	4.50	7.	.0027	.0037	758.0	1.022	15.60	26.38
1.603	28.	1557.	60.	85.	84.	17.	26.	30.	430.	94.	88.	66.3	20.9	10.	81.0	23.5	4.50	7.	.0025	.0035	758.0	1.022	15.46	26.15
1.705	9.	1653.	60.	85.	84.	18.	27.	31.	573.	92.	84.	78.1	20.3	10.	73.0	23.5	4.50	6.	.0028	.0039	759.0	1.023	16.45	27.82
1.690	12.	1605.	60.	85.	84.	17.	27.	30.	542.	92.	84.	74.6	19.2	10.	76.0	22.0	4.50	6.	.0027	.0037	759.0	1.023	16.30	27.57
1.708	16.	1605.	60.	85.	84.	17.	27.	30.	505.	92.	83.	75.4	19.5	10.	76.0	23.0	4.50	6.	.0027	.0037	759.0	1.023	16.48	27.87
1.716	20.	1560.	59.	84.	84.	17.	27.	30.	442.	93.	84.	72.9	18.8	10.	79.0	22.5	4.50	7.	.0026	.0036	759.0	1.023	16.55	28.00
1.710	24.	1525.	58.	84.	83.	18.	27.	30.	426.	94.	87.	69.3	18.2	10.	82.5	23.0	4.50	6.	.0025	.0034	759.0	1.023	16.50	27.90
1.706	12.	1480.	59.	85.	84.	17.	27.	30.	512.	92.	86.	69.8	15.0	10.	82.0	23.0	4.50	6.	.0025	.0035	759.0	1.023	16.46	27.83
1.685	16.	1446.	59.	84.	84.	17.	27.	30.	482.	91.	85.	65.8	18.7	10.	86.0	23.0	4.50	6.	.0024	.0033	759.0	1.023	16.25	27.49

AFR	Tmg	bmep	COVimep	Pmax	COVpmax	MFB1%	MFB10%	MFB90%	MFB1090%	etam	etab	etav	Trque	Pwr
Lmda	DegBTDC	bar	%	bar	%	Degree crank angle				%	%	%	Nm	kW
1.526	2.	4.13	7.426	31.4	.2	11.9	15.6	41.3	25.7	.72	.227	.71	204.0	32.17
1.523	5.	4.93	4.945	31.5	1.2	11.5	15.2	38.1	22.9	.79	.278	.69	243.0	38.30
1.543	8.	5.05	4.403	32.7	5.2	12.3	15.8	37.4	21.6	.80	.286	.70	249.0	39.14
1.525	11.	5.43	3.165	37.0	8.4	12.6	16.2	36.1	19.9	.83	.305	.70	268.0	42.21
1.535	14.	5.47	4.391	39.0	8.8	14.5	18.0	37.4	19.4	.86	.317	.68	270.0	42.72
1.524	17.	5.63	2.291	43.5	7.7	15.4	19.0	37.4	18.4	.87	.326	.68	278.0	43.67
1.520	20.	5.63	1.831	48.0	7.6	16.3	20.1	37.6	17.5	.87	.327	.67	278.0	43.55
1.493	2.	4.86	11.757	31.8	.9	9.4	13.4	35.6	22.2	.73	.265	.71	240.0	37.50
1.509	8.	5.57	2.079	37.4	8.2	10.5	14.2	33.5	19.3	.79	.307	.70	275.0	43.66
1.498	14.	6.00	1.298	48.3	7.0	12.0	15.6	32.6	17.0	.84	.331	.70	296.0	46.74
1.505	20.	6.04	1.433	57.0	5.1	13.7	17.7	33.9	16.2	.86	.336	.69	298.0	46.87
1.499	26.	5.86	1.488	61.5	4.7	16.3	20.9	36.7	15.8	.88	.334	.67	289.0	45.58
1.497	32.	5.68	1.580	67.4	3.1	19.7	23.1	38.6	15.5	.88	.323	.67	280.0	44.10
1.391	2.	5.37	2.248	32.9	5.2	7.9	12.2	31.8	19.6	.73	.281	.68	265.0	42.01
1.399	8.	6.08	1.269	42.6	7.8	9.1	12.9	30.2	17.3	.82	.319	.69	300.0	47.06
1.399	11.	6.26	1.499	47.9	7.3	9.9	13.7	29.9	16.2	.85	.332	.68	309.0	48.60
1.408	14.	6.28	1.756	52.3	5.9	10.5	14.4	30.3	15.9	.87	.334	.68	310.0	48.69
1.402	17.	6.38	1.970	57.6	5.1	11.1	15.1	30.4	15.3	.89	.341	.67	315.0	49.65
1.412	20.	6.28	2.215	61.6	4.7	11.8	16.1	31.1	15.0	.90	.341	.67	310.0	48.63
1.401	26.	6.12	2.410	65.1	3.5	15.3	19.8	34.8	15.0	.89	.331	.67	302.0	47.41
1.408	29.	5.94	2.342	69.1	2.7	14.4	19.3	35.5	16.2	.90	.323	.66	293.0	45.87
1.403	32.	5.82	1.981	71.2	1.8	15.1	20.2	38.4	18.2	.89	.320	.66	287.0	45.35
1.302	2.	6.08	1.417	37.2	7.8	6.7	10.9	28.3	17.4	.77	.300	.68	300.0	47.03
1.306	5.	6.45	1.184	43.8	7.0	7.0	11.0	27.0	16.0	.81	.318	.68	318.0	49.85
1.299	8.	6.79	1.232	49.2	7.2	8.1	11.9	27.0	15.1	.85	.332	.68	335.0	52.83
1.302	11.	6.87	1.440	55.1	6.1	8.4	12.3	26.9	14.6	.88	.339	.67	339.0	53.36
1.298	14.	6.91	1.631	61.0	5.0	8.7	12.7	26.8	14.1	.89	.340	.67	341.0	53.60
1.294	17.	6.93	1.826	66.5	3.7	8.9	13.1	26.8	13.7	.91	.339	.67	342.0	53.43
1.303	20.	6.65	2.456	68.9	3.3	9.9	14.2	28.1	13.9	.91	.339	.66	328.0	51.66
1.299	23.	6.55	3.202	72.0	2.4	10.4	14.9	29.6	14.7	.91	.335	.65	323.0	50.70
1.300	26.	6.49	3.547	73.9	1.9	11.0	15.7	32.2	16.5	.92	.331	.66	320.0	50.13
1.301	29.	6.32	3.515	74.9	1.8	11.6	16.7	34.4	17.7	.91	.328	.64	312.0	49.11
1.301	32.	5.86	3.515	74.9	1.8	14.6	19.7	37.4	17.7	.84	.304	.65	289.0	45.43
1.209	2.	6.69	1.138	41.4	6.7	6.0	10.3	26.0	15.7	.81	.311	.67	330.0	51.59
1.208	5.	7.03	.943	48.7	6.6	6.2	10.2	24.8	14.6	.85	.327	.67	347.0	54.47
1.202	8.	7.22	.880	54.3	5.7	7.0	10.9	24.9	14.0	.88	.335	.66	356.0	55.73
1.204	11.	7.42	1.087	60.7	5.4	7.2	11.1	24.5	13.4	.92	.347	.66	366.0	57.30
1.203	14.	7.34	1.192	65.4	4.2	7.9	12.0	25.1	13.1	.92	.346	.65	362.0	57.09
1.204	17.	7.36	1.359	70.2	3.4	8.3	12.6	25.7	13.1	.94	.349	.65	363.0	57.10
1.202	20.	7.17	1.756	73.8	2.6	8.9	13.2	26.6	13.4	.94	.343	.65	354.0	55.61
1.201	23.	6.97	2.702	77.6	2.1	9.0	13.6	27.5	13.9	.94	.334	.64	344.0	53.93
1.100	2.	7.22	.847	46.1	6.4	5.5	9.6	24.1	14.5	.82	.307	.66	356.0	56.07
1.107	5.	7.50	.713	52.6	5.7	5.8	9.8	23.6	13.8	.86	.322	.65	370.0	58.08

1.106	8.	7.70	.823	58.8	5.2	6.4	10.4	23.6	13.2	.89	.331	.65	380.0	59.65
1.104	11.	7.78	.992	64.4	4.5	6.9	10.9	23.9	13.0	.91	.339	.65	384.0	60.36
1.103	14.	7.74	1.336	70.3	3.8	7.2	11.3	24.0	12.7	.92	.342	.64	382.0	59.96
1.100	17.	7.60	1.789	75.3	3.2	7.9	12.1	24.5	12.4	.92	.334	.64	375.0	59.06
1.103	20.	7.46	2.187	81.1	2.2	8.0	12.3	24.3	12.0	.95	.329	.64	368.0	57.65
1.003	2.	7.82	.528	50.7	5.7	5.0	9.1	22.9	13.8	.82	.305	.65	386.0	60.63
1.000	5.	8.11	.439	57.2	5.6	5.7	9.5	22.7	13.2	.85	.318	.65	400.0	62.96
1.000	8.	8.25	.840	64.4	4.9	6.0	9.8	22.4	12.6	.87	.323	.65	407.0	63.93
.999	11.	8.35	1.253	70.3	3.7	6.6	10.5	22.7	12.2	.89	.327	.65	412.0	64.67
.999	14.	8.37	1.455	75.6	3.3	7.2	11.2	23.2	12.0	.91	.331	.64	413.0	64.83
.997	17.	8.23	2.060	82.1	2.6	7.2	11.3	23.0	11.7	.93	.324	.64	406.0	63.69
.950	2.	7.84	.531	50.3	5.9	5.3	9.4	23.1	13.7	.83	.290	.65	387.0	60.67
.947	5.	8.19	.407	57.3	5.2	5.9	9.8	22.7	12.9	.86	.300	.65	404.0	63.46
.952	8.	8.37	.756	64.1	4.6	6.3	10.1	22.5	12.4	.89	.310	.65	413.0	65.00
.950	11.	8.45	1.218	70.5	4.0	6.4	10.4	22.5	12.1	.91	.313	.65	417.0	65.63
.949	14.	8.45	1.449	75.5	3.3	7.1	11.1	23.1	12.0	.93	.313	.65	417.0	65.59
.903	2.	7.70	.761	48.0	6.9	5.7	10.0	24.4	14.4	.82	.265	.66	380.0	59.65
.903	5.	8.11	.524	55.4	5.3	6.2	10.2	23.6	13.4	.86	.280	.66	400.0	63.04
.900	8.	8.33	.618	61.6	5.3	6.9	10.8	23.7	12.9	.88	.287	.66	411.0	64.65
.901	11.	8.43	1.010	69.2	4.5	7.1	11.0	23.2	12.2	.91	.291	.66	416.0	65.61
.900	14.	8.43	1.203	74.7	3.7	7.6	11.6	23.5	11.9	.92	.294	.65	416.0	65.65
.900	17.	8.35	1.534	79.4	2.7	8.0	12.2	24.2	12.0	.93	.292	.65	412.0	64.41
.902	20.	8.25	1.892	83.0	2.2	8.4	12.7	25.4	12.7	.95	.288	.65	407.0	63.85
.807	2.	6.40	.898	44.2	7.3	6.5	10.8	26.0	15.2	.69	.205	.64	316.0	49.87
.803	5.	7.09	.749	52.2	6.8	6.5	10.6	24.7	14.1	.77	.222	.65	350.0	54.72
.803	8.	7.60	.728	58.5	6.0	7.4	11.4	24.6	13.2	.82	.239	.64	375.0	59.02
.801	11.	7.90	.825	64.6	5.3	8.0	12.0	24.7	12.7	.86	.251	.63	390.0	61.26
.802	14.	8.01	1.031	71.0	4.2	8.6	12.6	24.7	12.1	.89	.252	.64	395.0	62.38
.804	17.	8.07	1.156	76.1	3.3	8.8	13.0	24.9	11.9	.91	.255	.64	398.0	62.56
.803	20.	8.03	1.313	80.4	2.4	9.2	13.6	25.8	12.2	.92	.249	.64	396.0	62.20
.799	23.	7.95	1.779	82.7	1.7	9.6	14.2	27.7	13.5	.95	.251	.63	392.0	60.92
1.900	8.	3.34	48.258	31.4	.3	18.5	21.2	46.9	25.7	.90	.195	.82	165.0	25.37
1.808	11.	4.36	21.590	31.9	2.7	17.3	20.2	44.0	23.8	.85	.258	.77	215.0	35.08
1.773	14.	5.07	13.851	34.7	8.3	16.7	19.9	41.1	21.2	.87	.305	.74	250.0	40.03
1.709	17.	5.55	9.451	39.9	9.8	17.1	20.5	39.9	19.4	.89	.354	.68	274.0	46.83
1.760	20.	4.86	28.037	38.6	12.5	20.4	23.7	43.9	20.2	.85	.287	.75	240.0	37.95
1.504	2.	4.86	3.669	31.9	1.1	9.1	13.1	34.9	21.8	.73	.272	.69	240.0	37.27
1.501	5.	5.35	2.232	34.6	6.8	9.1	13.0	32.7	19.7	.77	.297	.69	264.0	41.86
1.505	8.	5.68	1.609	39.7	8.0	9.9	13.5	31.8	18.3	.80	.316	.69	280.0	44.04
1.504	11.	5.92	1.236	49.2	6.7	8.2	12.3	28.9	16.6	.84	.331	.68	292.0	45.81
1.499	14.	6.06	1.236	49.2	6.7	11.8	15.5	32.1	16.6	.86	.340	.68	299.0	46.94
1.503	17.	6.08	1.253	53.5	5.7	12.5	16.4	32.7	16.3	.87	.343	.68	300.0	47.06
1.509	23.	5.94	1.473	61.6	4.4	13.8	18.1	33.5	15.4	.89	.341	.67	293.0	46.15
1.499	26.	5.92	1.633	65.2	3.7	14.4	19.2	34.2	15.0	.90	.340	.67	292.0	45.87
1.507	29.	5.63	1.554	63.8	4.2	17.3	22.1	38.1	16.0	.87	.325	.67	278.0	43.84

1.503	32.	5.47	6.494	65.4	5.0	19.1	23.9	39.7	15.8	.87	.320	.66	270.0	42.52
1.490	35.	5.27	1.522	69.3	2.4	18.7	24.0	40.4	16.4	.85	.308	.65	260.0	42.26
1.625	8.	4.97	9.213	36.2	8.3	10.7	14.5	34.4	19.9	.71	.276	.73	245.0	39.51
1.625	12.	5.37	9.120	40.7	8.3	12.2	15.9	34.9	19.0	.79	.305	.72	265.0	43.04
1.620	17.	5.57	9.072	45.9	7.2	14.5	18.3	36.2	17.9	.83	.322	.70	275.0	44.55
1.605	20.	5.68	1.390	51.3	6.1	15.2	19.2	36.3	17.1	.84	.326	.70	280.0	45.68
1.617	24.	5.59	1.480	56.7	5.8	16.5	20.8	37.3	16.5	.84	.317	.72	276.0	45.09
1.603	28.	5.37	1.475	61.7	4.4	17.5	22.3	38.3	16.0	.82	.322	.67	265.0	43.21
1.705	9.	4.22	16.725	33.2	5.3	12.9	16.5	38.4	21.9	.68	.242	.75	208.0	36.01
1.690	12.	4.80	11.823	36.5	7.9	13.5	17.0	37.6	20.6	.75	.278	.73	237.0	39.83
1.708	16.	5.07	15.813	40.3	8.9	15.7	19.2	38.5	19.3	.81	.293	.74	250.0	42.02
1.716	20.	4.99	3.456	44.5	9.3	17.8	21.4	39.8	18.4	.78	.291	.74	246.0	40.19
1.710	24.	4.66	18.346	44.3	13.1	21.6	25.3	43.8	18.5	.77	.279	.72	230.0	36.73
1.706	12.	4.97	9.296	34.3	6.8	14.7	18.1	39.4	21.3	.82	.286	.74	245.0	37.97
1.685	16.	5.19	3.115	41.1	8.4	15.3	18.8	38.0	19.2	.81	.306	.72	256.0	38.76

AFR	Tmg	NOxv	NOxcorv	NOxg			NOxcorg			HCv	HCg			CO2v	CO2g			COv	COg			O2v	TAOx
Lmda	DegBTDC	ppm	ppm	g/kWh	g/MJth	g/cum	g/kWh	g/MJth	g/cum	ppm	g/kWh	g/MJth	g/cum	%	g/kWh	g/MJth	g/cum	%	g/kWh	g/MJth	g/cum	%	%
1.526	2.	65.	63.	.7	.042	.176	.6	.041	.170	2640.	9.43	.60	2.49	7.71	755.15	47.68	199.79	.08	4.99	.31	1.32	9.10	8.85
1.523	5.	85.	82.	.7	.054	.234	.7	.052	.227	3080.	8.82	.68	2.95	7.82	614.21	47.40	206.28	.09	4.50	.35	1.51	8.90	9.06
1.543	8.	135.	130.	1.1	.087	.380	1.1	.084	.367	3550.	10.09	.80	3.47	7.58	591.25	46.93	204.09	.11	5.46	.43	1.88	9.30	9.30
1.525	11.	185.	179.	1.4	.121	.501	1.4	.117	.484	3170.	8.54	.72	2.98	7.52	556.04	47.13	194.70	.11	5.18	.44	1.81	9.40	8.84
1.535	14.	260.	251.	1.9	.171	.724	1.9	.165	.699	4320.	11.28	.99	4.18	7.35	526.33	46.33	195.82	.12	5.47	.48	2.03	9.80	9.18
1.524	17.	440.	425.	3.2	.285	1.216	3.0	.276	1.175	4090.	10.22	.92	3.93	7.49	513.19	46.47	198.02	.13	5.67	.51	2.19	9.70	9.09
1.520	20.	660.	638.	4.8	.439	1.771	4.7	.424	1.712	3670.	9.36	.85	3.42	7.34	513.38	46.65	188.42	.13	5.79	.53	2.12	9.60	8.73
1.493	2.	90.	87.	.8	.057	.236	.7	.055	.228	2240.	6.71	.49	2.04	7.94	652.21	47.97	198.82	.08	4.18	.31	1.27	8.60	8.43
1.509	8.	160.	155.	1.2	.103	.424	1.2	.100	.409	2520.	6.64	.57	2.32	7.73	558.86	47.70	195.84	.09	4.14	.35	1.45	9.10	8.57
1.498	14.	400.	387.	2.8	.259	1.046	2.7	.251	1.013	2800.	6.87	.63	2.55	7.65	515.18	47.39	191.46	.11	4.71	.43	1.75	9.20	8.42
1.505	20.	780.	755.	5.6	.525	2.014	5.4	.508	1.950	2960.	7.43	.69	2.66	7.31	503.56	47.07	180.54	.13	5.70	.53	2.04	9.80	8.26
1.499	26.	1350.	1347.	9.5	.883	3.530	9.5	.881	3.521	3230.	7.95	.74	2.94	7.50	506.25	46.91	187.62	.14	6.01	.56	2.23	8.90	8.42
1.497	32.	2150.	2145.	15.5	1.392	5.630	15.5	1.388	5.616	3250.	8.18	.73	2.96	7.57	522.71	46.87	189.64	.15	6.59	.59	2.39	8.70	8.43
1.391	2.	230.	224.	1.8	.139	.541	1.7	.135	.526	2060.	5.55	.43	1.68	8.33	616.16	48.16	187.38	.08	3.77	.29	1.14	7.60	7.02
1.399	8.	520.	506.	3.6	.315	1.232	3.5	.306	1.198	2000.	4.77	.42	1.65	8.31	543.97	48.13	188.31	.09	3.75	.33	1.30	7.80	7.12
1.399	11.	750.	730.	5.0	.464	1.761	4.9	.451	1.714	2130.	4.97	.46	1.74	8.11	519.48	47.96	182.21	.10	4.08	.38	1.43	8.20	7.00
1.408	14.	1000.	973.	6.8	.627	2.361	6.6	.610	2.296	2260.	5.32	.49	1.86	7.97	514.90	47.80	180.03	.11	4.52	.42	1.58	8.40	7.08
1.402	17.	1400.	1362.	9.1	.862	3.310	8.9	.839	3.220	2320.	5.27	.50	1.91	8.09	503.80	47.68	182.99	.13	5.15	.49	1.87	8.10	7.09
1.412	20.	1500.	1459.	9.8	.928	3.582	9.5	.903	3.483	2330.	5.32	.50	1.94	8.04	503.17	47.60	183.67	.14	5.58	.53	2.03	8.40	7.23
1.401	26.	2250.	2189.	15.2	1.397	5.274	14.8	1.359	5.131	2250.	5.30	.49	1.83	8.02	518.34	47.64	179.83	.14	5.76	.53	2.00	8.10	6.97
1.408	29.	2500.	2431.	17.4	1.562	5.885	16.9	1.519	5.724	2240.	5.43	.49	1.83	7.97	530.24	47.64	179.49	.14	5.93	.53	2.01	8.20	7.03
1.403	32.	3000.	2919.	21.3	1.891	6.979	20.7	1.840	6.790	2210.	5.47	.49	1.79	7.89	535.61	47.57	175.59	.15	6.48	.58	2.12	8.40	6.87
1.302	2.	440.	436.	3.0	.249	.944	3.0	.246	.935	1240.	2.93	.24	.93	9.01	584.98	48.71	184.97	.08	3.31	.28	1.04	6.50	5.69
1.306	5.	680.	673.	4.3	.377	1.478	4.2	.373	1.463	1400.	3.07	.27	1.06	9.17	551.14	48.64	190.73	.08	3.06	.27	1.06	6.20	5.89
1.299	8.	1100.	1089.	6.6	.610	2.373	6.6	.604	2.349	1560.	3.27	.30	1.17	9.14	526.31	48.51	188.66	.09	3.30	.30	1.18	6.20	5.77
1.302	11.	1500.	1485.	8.9	.841	3.239	8.8	.833	3.206	1720.	3.57	.34	1.29	9.01	513.58	48.35	186.11	.10	3.63	.34	1.31	6.50	5.78
1.298	14.	2000.	1980.	11.8	1.120	4.294	11.7	1.108	4.251	1720.	3.55	.34	1.28	9.03	511.28	48.35	185.47	.10	3.60	.34	1.31	6.30	5.70
1.294	17.	2500.	2474.	15.0	1.412	5.320	14.8	1.398	5.265	1770.	3.70	.35	1.31	8.94	512.43	48.31	181.98	.10	3.65	.34	1.29	6.60	5.56
1.303	20.	3000.	2938.	18.8	1.767	6.353	18.4	1.731	6.222	1800.	3.93	.37	1.33	8.55	512.14	48.18	173.21	.11	4.19	.39	1.42	7.20	5.49
1.299	23.	3300.	3233.	20.8	1.932	6.966	20.4	1.893	6.824	1820.	4.00	.37	1.34	8.60	518.06	48.17	173.66	.11	4.22	.39	1.41	7.10	5.44
1.300	26.	3800.	3723.	24.3	2.238	8.002	23.8	2.192	7.839	1820.	4.07	.37	1.33	8.55	523.86	48.17	172.24	.11	4.29	.39	1.41	7.20	5.40
1.301	29.	4200.	4220.	26.8	2.442	8.890	26.9	2.453	8.933	1870.	4.16	.38	1.38	8.65	527.40	48.10	175.15	.12	4.66	.42	1.55	6.60	5.48
1.301	32.	4600.	4621.	31.7	2.672	9.734	31.8	2.684	9.778	1930.	4.63	.39	1.42	8.65	569.75	48.07	175.10	.12	5.03	.42	1.54	6.70	5.47
1.209	2.	1450.	1442.	8.9	.773	2.824	8.9	.769	2.809	1090.	2.34	.20	.74	9.60	566.21	48.95	178.87	.06	2.25	.19	.71	4.90	4.14
1.208	5.	2000.	1990.	11.6	1.059	3.895	11.6	1.054	3.875	1200.	2.44	.22	.81	9.65	537.58	48.90	179.81	.06	2.13	.19	.71	4.90	4.14
1.202	8.	2600.	2587.	14.7	1.365	5.039	14.6	1.359	5.015	1350.	2.66	.25	.91	9.72	524.66	48.83	180.22	.06	2.06	.19	.71	4.90	4.06
1.204	11.	3100.	3085.	17.3	1.665	5.998	17.2	1.657	5.968	1550.	3.01	.29	1.04	9.47	504.54	48.65	175.29	.07	2.37	.23	.82	5.20	4.03
1.203	14.	3600.	3582.	19.9	1.913	6.971	19.8	1.903	6.936	1600.	3.08	.30	1.08	9.56	505.11	48.59	177.09	.08	2.69	.26	.94	5.30	4.04
1.204	17.	4000.	3980.	22.1	2.141	7.740	22.0	2.131	7.702	1670.	3.22	.31	1.12	9.47	500.18	48.49	175.31	.09	3.03	.29	1.06	5.20	4.03
1.202	20.	4200.	4179.	23.6	2.247	8.110	23.5	2.236	8.070	1720.	3.37	.32	1.16	9.47	509.40	48.47	174.94	.09	3.08	.29	1.06	5.30	4.00
1.201	23.	4300.	4274.	24.5	2.275	8.312	24.4	2.261	8.263	1720.	3.42	.32	1.16	9.58	523.21	48.48	177.16	.09	3.13	.29	1.06	5.20	4.01
1.100	2.	3000.	2997.	16.7	1.423	5.236	16.7	1.422	5.231	1070.	2.07	.18	.65	10.81	575.02	49.05	180.51	.06	2.03	.17	.64	2.90	2.20
1.107	5.	3500.	3488.	18.7	1.675	6.151	18.6	1.669	6.130	1200.	2.24	.20	.73	10.71	547.48	49.03	180.06	.05	1.63	.15	.53	3.10	2.33

1.106	8.	4000.	3986.	20.8	1.914	7.025	20.7	1.907	7.001	1340.	2.43	.22	.82	10.69	532.20	48.92	179.60	.06	1.90	.17	.64	3.00	2.31	
1.104	11.	4500.	4485.	22.7	2.141	7.886	22.6	2.134	7.860	1420.	2.50	.24	.87	10.74	518.51	48.89	180.05	.06	1.84	.17	.64	3.10	2.27	
1.103	14.	5000.	4983.	25.0	2.375	8.759	24.9	2.367	8.729	1600.	2.79	.27	.97	10.74	514.27	48.81	179.99	.06	1.83	.17	.64	3.10	2.27	
1.100	17.	5400.	5394.	27.6	2.564	9.418	27.6	2.561	9.407	1580.	2.82	.26	.96	10.74	526.06	48.78	179.20	.07	2.18	.20	.74	3.20	2.18	
1.103	20.	5500.	5470.	28.6	2.613	9.625	28.5	2.599	9.572	1600.	2.90	.27	.97	10.73	534.41	48.77	179.63	.07	2.22	.20	.75	3.20	2.25	
1.003	2.	2500.	2508.	13.0	1.104	3.974	13.1	1.107	3.986	1630.	2.97	.25	.90	11.33	565.61	47.86	172.30	.30	9.53	.81	2.90	1.30	.37	
1.000	5.	2800.	2801.	14.0	1.235	4.373	14.0	1.235	4.374	1600.	2.78	.25	.87	11.32	540.30	47.74	169.14	.33	10.02	.89	3.14	1.10	.00	
1.000	8.	3000.	3001.	14.7	1.316	4.686	14.7	1.317	4.687	1660.	2.83	.25	.90	11.35	530.96	47.64	169.59	.35	10.42	.94	3.33	1.30	.00	
.999	11.	3200.	3231.	15.4	1.402	4.998	15.6	1.416	5.046	1710.	2.88	.26	.93	11.39	525.37	47.75	170.18	.32	9.39	.85	3.04	1.20	.00	
.999	14.	3300.	3332.	15.8	1.453	5.154	16.0	1.467	5.204	1790.	2.99	.27	.97	11.35	519.79	47.79	169.59	.30	8.74	.80	2.85	1.30	.00	
.997	17.	3400.	3411.	16.5	1.484	5.310	16.5	1.489	5.327	1890.	3.20	.29	1.03	11.35	526.44	47.39	169.59	.39	11.51	1.04	3.71	1.40	.00	
.950	2.	500.	507.	2.5	.203	.781	2.6	.206	.791	1630.	2.87	.23	.89	10.76	519.69	41.80	160.77	1.90	58.41	4.70	18.05	1.40	.00	
.947	5.	540.	547.	2.6	.217	.843	2.6	.220	.855	1670.	2.81	.23	.91	10.79	497.57	41.48	161.22	2.00	58.70	4.89	19.00	1.20	.00	
.952	8.	620.	626.	2.9	.252	.968	2.9	.254	.977	1840.	3.02	.26	1.00	10.81	486.93	41.99	161.52	1.83	52.46	4.52	17.39	1.30	.00	
.950	11.	660.	666.	3.1	.271	1.031	3 1	.274	1.040	1890.	3.11	.27	1.03	10.74	485.00	42.23	160.47	1.74	50.01	4.35	16.53	1.60	.00	
.949	14.	650.	656.	3.1	.266	1.015	3.1	.268	1.025	1960.	3.21	.28	1.06	10.71	481.04	41.85	160.02	1.84	52.60	4.58	17.48	1.50	.00	
.903	2.	540.	547.	2.8	.209	.843	2.9	.212	.855	1840.	3.38	.25	1.00	9.94	501.42	36.86	148.52	3.31	106.27	7.81	31.45	1.30	.00	
.903	5.	620.	619.	3.1	.239	.968	3.1	.239	.967	1920.	3.32	.26	1.04	9.99	474.44	36.85	149.26	3.32	100.35	7.80	31.55	1.30	.00	
.900	8.	630.	627.	3.1	.245	.984	3.1	.244	.979	2100.	3.58	.28	1.14	9.85	460.34	36.67	147.17	3.32	98.75	7.87	31.55	1.40	.00	
.901	11.	660.	656.	3.1	.254	1.031	3.1	.253	1.025	2310.	3.84	.31	1.25	9.95	453.42	36.66	148.67	3.34	96.87	7.83	31.74	1.20	.00	
.900	14.	680.	676.	3.2	.262	1.062	3.2	.261	1.056	2310.	3.80	.31	1.25	9.94	448.66	36.67	148.52	3.33	95.66	7.82	31.64	1.40	.00	
.900	17.	680.	676.	3.3	.263	1.062	3.2	.262	1.056	2310.	3.85	.31	1.25	9.88	451.88	36.61	147.62	3.33	96.93	7.85	31.64	1.60	.00	
.902	20.	750.	742.	3.6	.290	1.171	3.6	.287	1.159	2370.	4.00	.32	1.29	9.90	458.17	36.67	147.92	3.31	97.50	7.80	31.45	1.50	.00	
.807	2.	135.	136.	.8	.048	.211	.9	.048	.212	2800.	6.12	.35	1.52	8.78	526.39	29.98	131.19	5.53	211.01	12.02	52.55	1.10	.00	
.803	5.	150.	151.	.9	.053	.234	.9	.054	.236	2800.	5.62	.35	1.52	8.80	484.28	29.92	131.48	5.57	195.09	12.05	52.93	1.10	.00	
.803	8.	160.	161.	.8	.056	.250	.9	.057	.252	2990.	5.54	.37	1.62	8.77	445.67	29.60	131.04	5.69	184.03	12.22	54.07	1.20	.00	
.801	11.	170.	170.	.9	.060	.266	.9	.060	.266	3260.	5.77	.40	1.77	8.70	422.40	29.45	129.99	5.69	175.83	12.26	54.07	1.20	.00	
.802	14.	190.	193.	1.0	.067	.297	1.0	.068	.301	3390.	5.98	.42	1.84	8.68	419.94	29.37	129.69	5.70	175.51	12.28	54.16	1.20	.00	
.804	17.	185.	184.	.9	.065	.289	.9	.064	.287	3510.	6.04	.43	1.91	8.74	412.61	29.27	130.59	5.78	173.67	12.32	54.92	1.30	.00	
.803	20.	200.	198.	1.0	.070	.312	1.0	.069	.309	3680.	6.51	.45	2.00	8.74	424.09	29.38	130.59	5.71	176.34	12.22	54.26	1.20	.00	
.799	23.	180.	179.	.9	.063	.281	.9	.063	.280	3780.	6.65	.46	2.05	8.62	415.89	28.96	128.80	5.83	179.02	12.46	55.40	1.20	.00	
1.900	8.	9.	8.	.1	.007	.051	.1	.006	.047	14470.	69.91	3.79	28.75	5.37	711.76	38.56	293.47	.12	10.12	.55	4.17	12.80	15.19	
1.808	11.	9.	8.	.1	.006	.040	.1	.006	.037	9530.	33.15	2.38	14.58	6.19	590.62	42.39	260.54	.13	7.89	.57	3.48	11.40	13.48	
1 773	14.	13.	12.	.1	.009	.054	.1	.008	.050	8580.	24.70	2.09	12.42	6.46	510.23	43.20	257.16	.13	6.54	.55	3.29	11.20	13.06	
1.709	17.	32.	30.	.2	.022	.115	.2	.020	.106	5310.	12.78	1.26	6.62	7.02	463.51	45.52	240.57	.13	5.46	.54	2.83	10.80	11.79	
1.760	20.	70.	65.	.6	.050	.286	.6	.046	.265	9820.	30.64	2.44	13.94	6.21	531.47	42.30	242.50	.12	6.54	.52	2.98	12.30	12.90	
1.504	2.	75.	71.	.6	.045	.209	.6	.042	.197	2570.	7.07	.53	2.49	8.40	633.57	47.83	223.71	.09	4.32	.33	1.52	7.50	9.17	
1.501	5.	110.	104.	.8	.066	.303	.8	.062	.287	2330.	5.87	.49	2.23	8.40	580.62	47.97	221.36	.09	3.96	.33	1.51	7.50	9.05	
1.505	8.	180.	170.	1.2	.108	.499	1.2	.102	.473	2680.	6.40	.56	2.59	8.30	543.39	47.70	220.31	.10	4.17	.37	1.69	7.70	9.14	
1.504	11.	280.	265.	1.8	.169	.776	1.7	.160	.735	2910.	6.66	.61	2.81	8.23	516.91	47.50	218.32	.11	4.40	.40	1.86	7.70	9.13	
1.499	14.	460.	436.	2.9	.275	1.274	2.8	.261	1.208	2960.	6.54	.62	2.85	8.28	502.19	47.43	219.36	.12	4.63	.44	2.02	7.70	9.11	
1.503	17.	670.	635.	4.2	.405	1.856	4.0	.384	1.760	3060.	6.77	.64	2.95	8.18	496.22	47.29	216.78	.13	5.02	.48	2.19	7.90	9.12	
1.509	23.	1150.	1088.	7.5	.706	3.173	7.1	.668	3.002	3080.	6.97	.66	2.96	8.02	497.61	47.12	211.72	.15	5.92	.56	2.52	7.90	9.07	
1.499	26.	1500.	1420.	9.7	.918	4.079	9.2	.869	3.861	2960.	6.69	.63	2.80	8.05	499.28	47.14	209.40	.16	6.32	.60	2.65	7.90	8.90	
1.507	29.	1550.	1503.	10.7	.952	4.236	10.4	.933	4.109	3190.	7.66	.69	3.03	7.91	520.93	46.97	206.82	.16	6.71	.60	2.66	8.50	8.96	

1.503	32.	1800.	1745.	12.5	1.113	4.986	12.1	1.079	4.833	4220.	10.24	.91	4.07	7.84	521.86	46.37	207.77	.16	6.78	.60	2.70	8.60	9.12
1.490	35.	2300.	2231.	16.7	1.427	6.145	16.2	1.384	5.960	3400.	8.60	.74	3.16	7.89	547.65	46.84	201.65	.16	7.07	.60	2.60	8.50	8.68
1.625	8.	22.	21.	.2	.015	.069	.2	.014	.065	3890.	11.69	.90	4.23	7.40	610.29	46.78	221.32	.09	4.72	.36	1.71	9.60	10.46
1.625	12.	34.	32.	.3	.023	.106	.3	.021	.100	3800.	10.39	.88	4.11	7.37	552.75	46.76	219.39	.10	4.77	.40	1.89	9.90	10.41
1.620	17.	90.	85.	.7	.060	.275	.6	.057	.260	3500.	9.11	.82	3.71	7.33	523.47	46.87	213.96	.11	5.00	.45	2.04	9.80	10.20
1.605	20.	200.	189.	1.5	.135	.594	1.4	.128	.562	3520.	9.12	.83	3.64	7.26	515.94	46.77	206.24	.12	5.43	.49	2.17	10.10	9.91
1.617	24.	340.	323.	2.6	.228	1.043	2.5	.217	.991	4280.	11.39	1.00	4.57	7.19	524.95	46.22	211.00	.13	6.04	.53	2.43	10.00	10.26
1.603	28.	520.	494.	4.0	.358	1.579	3.8	.340	1.500	5940.	15.96	1.43	6.27	6.84	504.15	45.04	198.73	.13	6.10	.54	2.40	10.50	10.15
1.705	9.	19.	18.	.2	.013	.070	.2	.012	.065	5470.	18.80	1.26	6.98	7.19	677.89	45.58	252.21	.12	7.20	.48	2.68	9.90	12.00
1.690	12.	23.	21.	.2	.015	.081	.2	.014	.075	4800.	14.39	1.11	5.87	7.25	596.04	46.00	244.03	.12	6.28	.48	2.57	10.00	11.62
1.708	16.	34.	32.	.3	.023	.119	.3	.022	.111	5300.	15.64	1.27	6.47	6.91	559.20	45.53	231.97	.12	6.18	.50	2.56	10.40	11.60
1.716	20.	82.	78.	.7	.059	.289	.7	.056	.274	7670.	23.97	1.94	9.41	6.30	540.20	43.72	212.60	.11	6.00	.49	2.36	11.40	11.65
1.710	24.	140.	130.	1.3	.103	.501	1.2	.096	.465	9530.	31.60	2.45	11.85	6.00	545.83	42.31	205.27	.11	6.37	.49	2.39	11.70	11.77
1.706	12.	28.	26.	.2	.020	.097	.2	.018	.091	5860.	18.00	1.43	7.09	6.74	567.98	45.09	224.45	.12	6.44	.51	2.54	10.70	11.52
1.685	16.	58.	54.	.5	.040	.199	.4	.037	.185	5970.	16.86	1.43	7.13	6.85	530.52	45.09	225.13	.12	5.92	.50	2.51	10.60	11.40

AFR	Tmg	etam	etab	etav	Trque	Pwr	QCl	QEx	QChm	Qcond	Wb	Qc	Qe	QCm	Qcnd	Qout	mfCV
Lmda	DegBTDC	%	%	%	Nm	kW	kW	kW	kW	kW	%	%	%	%	%	%	kW
1.526	2.	.72	.227	.71	204.0	32.17	31.22	32.83	4.67	13.24	22.73	22.06	23.19	3.30	9.36	19.36	141.53
1.523	5.	.79	.278	.69	243.0	38.30	30.47	28.45	5.19	12.83	27.78	22.10	20.64	3.76	9.31	16.41	137.85
1.543	8.	.80	.286	.70	249.0	39.14	28.36	26.76	6.11	12.66	28.58	20.71	19.53	4.46	9.24	17.48	136.96
1.525	11.	.83	.305	.70	268.0	42.21	27.45	25.50	5.66	12.84	30.52	19.84	18.44	4.09	9.29	17.83	138.32
1.535	14.	.86	.317	.68	270.0	42.72	28.36	23.53	7.39	12.32	31.69	21.04	17.45	5.48	9.14	15.20	134.82
1.524	17.	.87	.326	.68	278.0	43.67	28.23	22.02	6.97	12.29	32.60	21.07	16.44	5.20	9.18	15.51	133.97
1.520	20.	.87	.327	.67	278.0	43.55	28.76	21.47	6.48	12.27	32.71	21.60	16.13	4.87	9.22	15.47	133.13
1.493	2.	.73	.265	.71	240.0	37.50	31.75	30.97	3.95	13.33	26.48	22.42	21.87	2.79	9.41	17.02	141.61
1.509	8.	.79	.307	.70	275.0	43.66	29.04	27.31	4.56	13.32	30.73	20.44	19.22	3.21	9.37	17.03	142.08
1.498	14.	.84	.331	.70	296.0	46.74	28.28	24.30	5.15	13.18	33.12	20.04	17.22	3.65	9.34	16.64	141.14
1.505	20.	.86	.336	.69	298.0	46.87	23.95	22.19	5.73	12.96	33.65	17.19	15.93	4.12	9.30	19.81	139.30
1.499	26.	.88	.334	.67	289.0	45.58	28.88	21.02	6.04	12.68	33.36	21.14	15.39	4.42	9.28	16.42	136.62
1.497	32.	.88	.323	.67	280.0	44.10	30.57	20.91	6.20	12.68	32.28	22.38	15.30	4.54	9.28	16.22	136.62
1.391	2.	.73	.281	.68	265.0	42.01	33.35	31.74	3.73	14.10	28.14	22.34	21.26	2.50	9.44	16.33	149.32
1.399	8.	.82	.319	.69	300.0	47.06	32.51	27.76	3.71	13.96	31.85	22.01	18.79	2.51	9.45	15.39	147.74
1.399	11.	.85	.332	.68	309.0	48.60	32.39	26.40	4.05	13.79	33.24	22.15	18.06	2.77	9.43	14.36	146.23
1.408	14.	.87	.334	.68	310.0	48.69	34.10	25.32	4.40	13.72	33.42	23.40	17.37	3.02	9.41	13.38	145.72
1.402	17.	.89	.341	.67	315.0	49.65	33.23	24.25	4.60	13.71	34.07	22.81	16.64	3.15	9.41	13.92	145.72
1.412	20.	.90	.341	.67	310.0	48.63	32.51	23.21	4.61	13.43	34.06	22.77	16.26	3.23	9.41	14.28	142.79
1.401	26.	.89	.331	.67	302.0	47.41	34.19	22.88	4.65	13.49	33.09	23.87	15.97	3.25	9.42	14.41	143.27
1.408	29.	.90	.323	.66	293.0	45.87	35.75	22.36	4.66	13.35	32.34	25.21	15.76	3.29	9.42	13.99	141.83
1.403	32.	.89	.320	.66	287.0	45.35	35.52	22.40	4.80	13.36	31.98	25.04	15.79	3.38	9.42	14.39	141.83
1.302	2.	.77	.300	.68	300.0	47.03	35.98	32.53	2.43	14.98	29.98	22.93	20.73	1.55	9.55	15.26	156.90
1.306	5.	.81	.318	.68	318.0	49.85	33.94	30.20	2.67	14.96	31.77	21.63	19.25	1.70	9.53	16.11	156.90
1.299	8.	.85	.332	.68	335.0	52.83	33.70	29.16	3.08	15.16	33.18	21.17	18.31	1.94	9.52	15.89	159.24
1.302	11.	.88	.339	.67	339.0	53.36	33.58	27.65	3.45	14.95	33.89	21.33	17.56	2.19	9.50	15.52	157.43
1.298	14.	.89	.340	.67	341.0	53.60	34.30	26.57	3.53	14.95	34.05	21.79	16.88	2.24	9.50	15.54	157.43
1.294	17.	.91	.339	.67	342.0	53.43	34.59	25.91	3.73	14.94	33.94	21.97	16.46	2.37	9.49	15.77	157.43
1.303	20.	.91	.339	.66	328.0	51.66	38.41	25.68	3.96	14.46	33.86	25.18	16.84	2.59	9.48	12.05	152.55
1.299	23.	.91	.335	.65	323.0	50.70	36.79	25.02	3.99	14.36	33.48	24.29	16.52	2.63	9.48	13.59	151.46
1.300	26.	.92	.331	.66	320.0	50.13	39.09	24.72	4.10	14.36	33.10	25.81	16.32	2.71	9.48	12.59	151.46
1.301	29.	.91	.328	.64	312.0	49.11	38.73	23.74	4.19	14.17	32.84	25.90	15.88	2.80	9.48	13.11	149.56
1.301	32.	.84	.304	.65	289.0	45.43	43.09	23.26	4.35	14.16	30.37	28.81	15.56	2.91	9.47	12.88	149.56
1.209	2.	.81	.311	.67	330.0	51.59	38.73	34.22	2.26	15.87	31.12	23.36	20.64	1.36	9.57	13.94	165.78
1.208	5.	.85	.327	.67	347.0	54.47	38.84	32.32	2.52	15.90	32.75	23.35	19.43	1.51	9.56	13.40	166.34
1.202	8.	.88	.335	.66	356.0	55.73	38.99	30.59	2.82	15.88	33.51	23.44	18.39	1.70	9.55	13.41	166.34
1.204	11.	.92	.347	.66	366.0	57.30	39.71	29.54	3.32	15.72	34.72	24.06	17.90	2.01	9.52	11.79	165.05
1.203	14.	.92	.346	.65	362.0	57.09	38.39	28.28	3.49	15.69	34.63	23.29	17.15	2.12	9.52	13.29	164.85
1.204	17.	.94	.349	.65	363.0	57.10	39.99	27.41	3.72	15.56	34.90	24.45	16.76	2.28	9.51	12.10	163.58
1.202	20.	.94	.343	.65	354.0	55.61	41.14	26.65	3.80	15.43	34.25	25.34	16.42	2.34	9.51	12.14	162.33
1.201	23.	.94	.334	.64	344.0	53.93	41.59	25.89	3.76	15.37	33.36	25.73	16.02	2.33	9.51	13.05	161.65
1.100	2.	.82	.307	.66	356.0	56.07	42.81	36.66	2.45	17.50	30.71	23.45	20.08	1.34	9.59	14.84	182.58
1.107	5.	.86	.322	.65	370.0	58.08	42.80	34.32	2.66	17.25	32.24	23.76	19.05	1.48	9.57	13.90	180.14

1.106	8.	.89	.331	.65	380.0	59.65	41.93	32.83	3.01	17.23	33.09	23.26	18.22	1.67	9.56	14.20	180.25
1.104	11.	.91	.339	.65	384.0	60.36	44.23	31.07	3.16	16.99	33.94	24.87	17.47	1.77	9.55	12.38	177.82
1.103	14.	.92	.342	.64	382.0	59.96	42.69	29.70	3.45	16.74	34.17	24.33	16.92	1.97	9.54	13.08	175.50
1.100	17.	.92	.334	.64	375.0	59.06	44.87	29.19	3.57	16.88	33.38	25.36	16.50	2.02	9.54	13.21	176.95
1.103	20.	.95	.329	.64	368.0	57.65	47.45	28.23	3.59	16.74	32.85	27.04	16.09	2.04	9.54	12.44	175.50
1.003	2.	.82	.305	.65	386.0	60.63	45.02	40.39	4.55	19.00	30.46	22.61	20.29	2.29	9.55	14.80	199.07
1.000	5.	.85	.318	.65	400.0	62.96	48.23	38.46	5.54	18.90	31.81	24.37	19.44	2.80	9.55	12.03	197.91
1.000	8.	.87	.323	.65	407.0	63.93	45.39	36.91	5.80	18.89	32.30	22.94	18.65	2.93	9.54	13.63	197.91
.999	11.	.89	.327	.65	412.0	64.67	46.79	35.63	5.66	18.86	32.72	23.67	18.03	2.86	9.54	13.18	197.65
.999	14.	.91	.331	.64	413.0	64.83	50.32	34.36	5.61	18.67	33.10	25.69	17.54	2.86	9.53	11.27	195.85
.997	17.	.93	.324	.64	406.0	63.69	48.01	33.46	6.46	18.72	32.41	24.43	17.03	3.29	9.53	13.32	196.52
.950	2.	.83	.290	.65	387.0	60.67	44.54	38.53	17.73	20.02	28.95	21.25	18.39	8.46	9.56	13.38	209.53
.947	5.	.86	.300	.65	404.0	63.46	45.26	37.03	18.61	20.20	30.01	21.41	17.51	8.80	9.55	12.72	211.45
.952	8.	.89	.310	.65	413.0	65.00	45.99	35.62	17.47	19.98	31.04	21.96	17.01	8.34	9.54	12.10	209.40
.950	11.	.91	.313	.65	417.0	65.63	46.61	34.93	17.02	19.97	31.34	22.26	16.68	8.13	9.53	12.05	209.40
.949	14.	.93	.313	.65	417.0	65.59	47.46	33.90	17.85	19.96	31.32	22.66	16.19	8.52	9.53	11.77	209.40
.903	2.	.82	.265	.66	380.0	59.65	45.44	38.85	30.97	21.52	26.46	20.16	17.24	13.74	9.55	12.87	225.43
.903	5.	.86	.280	.66	400.0	63.04	45.87	36.99	31.02	21.51	27.96	20.35	16.41	13.76	9.54	11.97	225.43
.900	8.	.88	.287	.66	411.0	64.65	43.91	35.76	31.61	21.48	28.68	19.48	15.86	14.02	9.53	12.43	225.43
.901	11.	.91	.291	.66	416.0	65.61	45.06	34.33	31.76	21.44	29.10	19.99	15.23	14.09	9.51	12.08	225.43
.900	14.	.92	.294	.65	416.0	65.65	46.40	33.08	31.40	21.22	29.43	20.80	14.83	14.07	9.51	11.36	223.11
.900	17.	.93	.292	.65	412.0	64.41	46.72	32.19	31.23	21.00	29.17	21.15	14.58	14.14	9.51	11.45	220.83
.902	20.	.95	.288	.65	407.0	63.85	48.81	31.89	31.24	21.07	28.81	22.03	14.39	14.10	9.51	11.16	221.58
.807	2.	.69	.205	.64	316.0	49.87	41.59	39.57	53.15	23.09	20.50	17.10	16.26	21.85	9.49	14.79	243.26
.803	5.	.77	.222	.65	350.0	54.72	41.14	37.36	53.92	23.35	22.24	16.72	15.19	21.92	9.49	14.44	246.03
.803	8.	.82	.239	.64	375.0	59.02	41.94	35.05	55.17	23.41	23.91	16.99	14.20	22.35	9.48	13.07	246.87
.801	11.	.86	.251	.63	390.0	61.26	42.28	33.01	55.16	23.10	25.10	17.32	13.52	22.60	9.46	12.00	244.09
.802	14.	.89	.252	.64	395.0	62.38	44.12	32.25	56.28	23.42	25.18	17.81	13.02	22.72	9.45	11.82	247.71
.804	17.	.91	.255	.64	398.0	62.56	45.15	30.99	55.99	23.14	25.54	18.43	12.65	22.86	9.45	11.06	244.93
.803	20.	.92	.249	.64	396.0	62.20	41.91	31.03	56.79	23.53	24.94	16.80	12.44	22.77	9.44	13.61	249.42
.799	23.	.95	.251	.63	392.0	60.92	44.80	29.73	56.66	22.92	25.07	18.43	12.23	23.32	9.43	11.52	243.04
1.900	8.	.90	.195	.82	165.0	25.37	17.82	21.72	25.36	9.89	19.50	13.70	16.70	19.50	7.61	23.00	130.06
1.808	11.	.85	.258	.77	215.0	35.08	20.13	23.66	16.93	11.37	25.84	14.83	17.43	12.47	8.38	21.05	135.75
1.773	14.	.87	.305	.74	250.0	40.03	25.72	22.67	14.47	11.21	30.48	19.59	17.26	11.02	8.54	13.11	131.32
1.709	17.	.89	.354	.68	274.0	46.83	26.13	21.88	9.04	11.91	35.36	19.73	16.52	6.82	8.99	12.58	132.44
1.760	20.	.85	.287	.75	240.0	37.95	22.45	19.07	16.86	11.05	28.66	16.95	14.40	12.73	8.35	18.92	132.44
1.504	2.	.73	.272	.69	240.0	37.27	31.88	28.21	4.12	12.88	27.18	23.25	20.57	3.01	9.39	16.60	137.13
1.501	5.	.77	.297	.69	264.0	41.86	31.01	27.29	3.90	13.25	29.74	22.03	19.39	2.77	9.42	16.65	140.74
1.505	8.	.80	.316	.69	280.0	44.04	30.03	25.26	4.46	13.07	31.60	21.54	18.12	3.20	9.38	16.16	139.37
1.504	11.	.84	.331	.68	292.0	45.81	29.59	23.54	4.85	12.94	33.08	21.37	17.00	3.50	9.35	15.71	138.48
1.499	14.	.86	.340	.68	299.0	46.94	29.92	22.28	4.95	12.90	34.00	21.67	16.14	3.59	9.34	15.26	138.05
1.503	17.	.87	.343	.68	300.0	47.06	29.70	21.36	5.20	12.80	34.31	21.65	15.57	3.79	9.33	15.35	137.17
1.509	23.	.89	.341	.67	293.0	46.15	32.76	20.69	5.42	12.62	34.09	24.20	15.28	4.00	9.32	13.11	135.37
1.499	26.	.90	.340	.67	292.0	45.87	31.34	20.20	5.32	12.60	33.99	23.23	14.97	3.94	9.34	14.54	134.94
1.507	29.	.87	.325	.67	278.0	43.84	30.71	19.78	5.74	12.57	32.46	22.73	14.65	4.25	9.30	16.61	135.08

1.503	32.	.87	.320	.66	270.0	42.52	31.74	19.06	7.15	12.21	31.99	23.87	14.33	5.38	9.18	15.24	132.94
1.490	35.	.85	.308	.65	260.0	42.26	32.20	20.14	6.27	12.73	30.79	23.46	14.68	4.57	9.28	17.22	137.23
1.625	8.	.71	.276	.73	245.0	39.51	28.85	27.61	6.95	13.16	27.60	20.15	19.28	4.85	9.19	18.93	143.17
1.625	12.	.79	.305	.72	265.0	43.04	28.71	25.31	6.79	13.00	30.46	20.32	17.91	4.81	9.20	17.31	141.31
1.620	17.	.83	.322	.70	275.0	44.55	29.67	22.94	6.28	12.76	32.23	21.46	16.60	4.54	9.24	15.92	138.21
1.605	20.	.84	.326	.70	280.0	45.68	29.01	22.53	6.52	12.92	32.63	20.72	16.10	4.66	9.23	16.66	139.99
1.617	24.	.84	.317	.72	276.0	45.09	29.39	22.15	7.96	12.99	31.70	20.67	15.57	5.60	9.13	17.33	142.24
1.603	28.	.82	.322	.67	265.0	43.21	28.44	18.78	10.41	11.96	32.16	21.17	13.98	7.75	8.90	16.03	134.34
1.705	9.	.68	.242	.75	208.0	36.01	27.63	29.24	10.13	13.37	24.21	18.57	19.66	6.81	8.99	21.76	148.74
1.690	12.	.75	.278	.73	237.0	39.83	26.13	26.30	8.67	13.01	27.79	18.23	18.35	6.05	9.07	20.52	143.36
1.708	16.	.81	.293	.74	250.0	42.02	26.54	24.73	9.86	12.88	29.31	18.51	17.25	6.88	8.98	19.06	143.36
1.716	20.	.78	.291	.74	246.0	40.19	25.58	20.79	14.08	11.89	29.14	18.54	15.07	10.21	8.62	18.42	137.92
1.710	24.	.77	.279	.72	230.0	36.73	25.74	19.08	16.81	10.98	27.91	19.55	14.50	12.77	8.34	16.93	131.61
1.706	12.	.82	.286	.74	245.0	37.97	21.22	23.59	10.19	11.82	28.58	15.97	17.76	7.67	8.90	21.13	132.87
1.685	16.	.81	.306	.72	256.0	38.76	25.44	20.54	9.73	11.27	30.60	20.08	16.21	7.68	8.90	16.53	126.69

Dovergas FBHCR 13:1 experimental results

AFR	Tmg	Speed	Temperatures (DegC)								Airflrt	Clflrt	Mthne	Time	Pgup	Pgdn	Hmdty	mFuel	vFuel	Pbaro	Pabs	AFRV	AFRG
Lmda	DegBTDC	RPM	In	Out	Pmy	Fuel	Air	Mix	Exh	Gly	Smp g/sec	l/min	cuft	Sec	in/WG	in/RL	g/kg	kg/s	cum/s	mmHg	bar		
.799	2.	1510.	67.	84.	83.	13.	25.	30.	496.	94.	87. 34.0	27.3	10.	81.0	27.0	6.00	8.	.0026	.0035	765.0	1.035	7.73	13.05
1.900	2.	1510.	67.	84.	83.	13.	25.	30.	496.	94.	87. 81.0	27.3	10.	81.0	27.0	6.00	8.	.0026	.0035	765.0	1.035	18.37	31.03
1.900	35.	1510.	67.	84.	83.	13.	25.	30.	496.	94.	87. 81.0	27.3	10.	81.0	27.0	6.00	8.	.0026	.0035	765.0	1.035	18.37	31.03
1.775	8.	1492.	67.	84.	84.	15.	25.	32.	552.	98.	91. 76.1	26.3	10.	81.0	29.0	6.00	5.	.0026	.0035	775.0	1.048	17.16	28.99
1.726	11.	1505.	68.	84.	84.	15.	24.	31.	544.	97.	90. 71.3	27.9	10.	83.0	28.0	6.00	8.	.0025	.0034	765.0	1.035	16.69	28.19
1.730	14.	1506.	67.	84.	84.	14.	24.	30.	522.	96.	89. 72.1	27.8	10.	82.5	26.0	6.00	8.	.0026	.0034	765.0	1.035	16.73	28.25
1.755	17.	1510.	67.	84.	83.	13.	25.	30.	496.	94.	87. 74.8	27.3	10.	81.0	27.0	6.00	8.	.0026	.0035	765.0	1.035	16.97	28.66
1.750	20.	1500.	68.	85.	84.	16.	26.	30.	470.	100.	95. 75.2	27.5	10.	80.5	26.5	6.00	5.	.0026	.0035	775.0	1.048	16.92	28.58
1.752	23.	1511.	68.	85.	84.	15.	26.	30.	455.	100.	93. 75.6	27.2	10.	80.5	28.5	6.00	5.	.0026	.0035	775.0	1.048	16.94	28.61
1.711	8.	1484.	68.	85.	85.	16.	27.	32.	598.	91.	84. 71.7	27.8	10.	82.5	27.5	6.00	5.	.0026	.0034	775.0	1.048	16.55	27.94
1.703	11.	1502.	68.	85.	85.	16.	27.	31.	561.	92.	84. 72.3	28.3	10.	81.5	27.0	6.00	5.	.0026	.0035	775.0	1.048	16.47	27.81
1.703	14.	1502.	68.	85.	85.	15.	26.	31.	532.	92.	84. 72.5	28.0	10.	81.5	26.0	6.00	5.	.0026	.0035	775.0	1.048	16.47	27.81
1.707	17.	1505.	68.	85.	85.	15.	26.	30.	510.	92.	84. 73.2	27.4	10.	81.0	27.0	6.00	5.	.0026	.0035	775.0	1.048	16.51	27.88
1.717	20.	1507.	68.	85.	85.	15.	26.	30.	484.	93.	85. 73.6	27.2	10.	81.0	28.0	6.00	5.	.0026	.0035	775.0	1.048	16.60	28.04
1.725	23.	1519.	67.	85.	84.	15.	26.	29.	462.	96.	86. 73.9	26.9	10.	81.0	27.0	6.00	5.	.0026	.0035	775.0	1.048	16.68	28.17
1.720	26.	1521.	67.	85.	84.	15.	25.	29.	442.	94.	84. 72.8	26.0	10.	82.0	26.5	6.00	5.	.0026	.0035	775.0	1.048	16.63	28.09
1.610	2.	1500.	71.	86.	85.	17.	29.	33.	634.	92.	87. 71.2	36.0	10.	78.0	27.5	6.00	5.	.0027	.0036	775.0	1.048	15.57	26.29
1.620	5.	1502.	71.	86.	85.	17.	28.	33.	609.	92.	86. 72.5	33.0	10.	77.0	27.5	6.00	5.	.0027	.0037	775.0	1.048	15.67	26.46
1.619	8.	1495.	70.	86.	85.	17.	28.	32.	588.	92.	86. 71.6	32.7	10.	78.0	27.5	6.00	5.	.0027	.0036	775.0	1.048	15.66	26.44
1.618	11.	1493.	70.	86.	85.	17.	27.	32.	566.	92.	86. 70.6	32.3	10.	79.0	27.5	6.00	5.	.0027	.0036	775.0	1.048	15.65	26.42
1.596	17.	1506.	70.	86.	85.	16.	27.	31.	514.	93.	85. 69.9	32.5	10.	79.0	26.5	6.00	5.	.0027	.0036	775.0	1.048	15.43	26.07
1.590	20.	1511.	70.	86.	85.	16.	26.	31.	496.	93.	85. 69.2	31.2	10.	79.5	26.5	6.00	5.	.0027	.0036	775.0	1.048	15.38	25.97
1.596	23.	1511.	69.	86.	85.	16.	27.	31.	477.	93.	85. 69.0	30.3	10.	80.0	27.5	6.00	5.	.0026	.0035	775.0	1.048	15.43	26.07
1.594	26.	1509.	69.	86.	85.	16.	27.	30.	458.	92.	85. 68.9	30.1	10.	80.0	26.5	6.00	5.	.0026	.0035	775.0	1.048	15.41	26.03
1.609	29.	1496.	69.	85.	85.	16.	27.	30.	448.	92.	85. 68.7	29.7	10.	81.0	27.5	6.00	5.	.0026	.0035	775.0	1.048	15.56	26.28
1.510	2.	1480.	72.	86.	85.	15.	26.	30.	647.	96.	86. 67.6	39.0	10.	77.5	27.5	6.00	6.	.0027	.0037	775.0	1.048	14.60	24.66
1.502	5.	1476.	72.	86.	85.	15.	26.	30.	618.	97.	87. 67.7	38.7	10.	77.0	26.5	6.00	6.	.0028	.0037	775.0	1.048	14.52	24.53
1.502	8.	1507.	72.	86.	85.	14.	25.	29.	588.	99.	88. 68.8	40.0	10.	76.0	26.5	6.00	6.	.0028	.0037	775.0	1.048	14.52	24.53
1.500	11.	1509.	72.	86.	85.	14.	26.	30.	563.	97.	88. 68.8	40.1	10.	76.0	27.0	6.00	6.	.0028	.0037	775.0	1.048	14.51	24.50
1.505	14.	1500.	71.	86.	85.	14.	25.	31.	541.	96.	87. 68.1	39.3	10.	77.0	27.5	6.00	6.	.0028	.0037	775.0	1.048	14.55	24.58
1.505	17.	1500.	71.	86.	85.	13.	26.	30.	526.	94.	84. 67.4	39.0	10.	78.0	27.5	6.00	6.	.0027	.0036	775.0	1.048	14 55	24.58
1.508	20.	1507.	71.	85.	85.	13.	25.	29.	513.	91.	81. 67.6	39.1	10.	78.0	26.5	6.00	6.	.0027	.0036	775.0	1.048	14.58	24.63
1.505	23.	1506.	71.	85.	85.	13.	25.	29.	508.	82.	70. 67.0	40.3	10.	78.5	27.5	6.00	6.	.0027	.0036	775.0	1.048	14.55	24.58
1.504	26.	1507.	72.	86.	85.	15.	25.	28.	493.	96.	84. 66.9	41.3	10.	78.0	26.5	6.00	6.	.0027	.0036	775.0	1.048	14.54	24.56
1.494	29.	1501.	72.	86.	86.	15.	25.	28.	488.	96.	84. 66.1	41.2	10.	78.5	26.0	6.00	6.	.0027	.0036	775.0	1.048	14.45	24.40
1.496	32.	1508.	72.	87.	86.	15.	26.	28.	486.	97.	85. 65.7	42.4	10.	79.0	26.5	6.00	6.	.0027	.0036	775.0	1.048	14.47	24.43
1.432	2.	1461.	72.	86.	86.	15.	26.	30.	624.	96.	86. 68.5	42.6	10.	72.5	26.5	6.00	7.	.0029	.0039	774.0	1.047	13.85	23.39
1.413	5.	1502.	72.	87.	86.	15.	26.	30.	617.	96.	85. 69.0	42.0	10.	71.0	26.5	6.00	7.	.0030	.0040	774.0	1.047	13.66	23.08
1.404	8.	1499.	72.	86.	85.	15.	26.	29.	589.	96.	85. 67.1	42.6	10.	72.5	26.0	6.00	7.	.0029	.0039	774.0	1.047	13.58	22.93
1.403	11.	1507.	72.	86.	85.	15.	26.	29.	570.	96.	84. 67.6	42.6	10.	72.0	28.5	6.00	7.	.0029	.0039	774.0	1.047	13.57	22.91
1.4 0	14.	1497.	72.	86.	85.	15.	25.	29.	548.	96.	83. 67.0	42.5	10.	73.0	25.5	6.00	7.	.0029	.0039	774.0	1.047	13.63	23.03
1.405	17.	1509.	72.	86.	86.	15.	25.	28.	535.	95.	82. 67.2	43.7	10.	72.5	26.5	6.00	7.	.0029	.0039	774.0	1.047	13.59	22.95
1.402	20.	1499.	73.	86.	86.	15.	25.	28.	527.	95.	82. 66.1	44.6	10.	73.5	26.5	6.00	7.	.0029	.0039	774.0	1.047	13.56	22.90

1.402	23.	1506.	73.	87.	86.	15.	25.	29.	521.	94.	81.	66.1	45.1	10.	73.5	27.5	6.00	7.	.0029	.0039	774.0	1.047	13.56	22.90
1.405	26.	1502.	73.	87.	86.	14.	26.	28.	515.	92.	80.	65.6	45.3	10.	74.5	26.5	6.00	7.	.0029	.0038	774.0	1.047	13.59	22.95
1.400	29.	1505.	73.	87.	86.	14.	25.	28.	514.	89.	77.	65.4	45.7	10.	74.5	25.5	6.00	7.	.0029	.0038	774.0	1.047	13.54	22.86
1.406	32.	1505.	74.	87.	86.	14.	25.	28.	517.	86.	73.	65.3	50.1	10.	75.0	26.5	6.00	7.	.0028	.0038	775.0	1.048	13.60	22.96
1.307	2.	1480.	75.	88.	87.	19.	29.	34.	656.	99.	89.	65.4	51.8	10.	68.5	27.0	6.00	9.	.0031	.0041	776.0	1.050	12.64	21.35
1.301	5.	1505.	75.	88.	87.	19.	29.	33.	634.	99.	89.	65.6	51.4	10.	68.0	26.5	6.00	9.	.0031	.0042	776.0	1.050	12.58	21.25
1.293	8.	1501.	75.	88.	87.	18.	29.	33.	609.	99.	89.	64.9	49.6	10.	68.5	28.0	6.00	9.	.0031	.0041	776.0	1.050	12.50	21.12
1.297	11.	1502.	75.	87.	86.	18.	28.	32.	588.	99.	89.	64.7	51.1	10.	69.0	28.5	6.00	9.	.0031	.0041	776.0	1.050	12.54	21.18
1.296	14.	1499.	75.	88.	87.	18.	28.	32.	570.	100.	89.	64.6	51.8	10.	69.0	27.0	6.00	9.	.0031	.0041	776.0	1.050	12.53	21.17
1.300	17.	1502.	75.	88.	87.	18.	28.	32.	558.	100.	90.	64.3	53.0	10.	69.5	26.5	6.00	9.	.0030	.0041	776.0	1.050	12.57	21.23
1.309	20.	1507.	75.	88.	87.	18.	28.	32.	546.	100.	90.	64.3	52.5	10.	70.0	28.0	6.00	9.	.0030	.0040	776.0	1.050	12.66	21.38
1.302	23.	1502.	75.	88.	87.	18.	27.	31.	543.	100.	89.	64.0	54.5	10.	70.0	26.5	6.00	9.	.0030	.0040	776.0	1.050	12.59	21.26
1.301	26.	1496.	75.	88.	87.	18.	27.	32.	540.	100.	89.	63.0	54.6	10.	71.0	25.5	6.00	9.	.0030	.0040	776.0	1.050	12.58	21.25
1.308	29.	1497.	77.	89.	87.	17.	27.	31.	535.	99.	89.	63.0	54.6	10.	71.5	27.0	6.00	9.	.0029	.0040	774.0	1.047	12.65	21.36
1.304	32.	1505.	77.	89.	88.	17.	28.	33.	540.	98.	91.	62.8	55.8	10.	71.5	26.5	6.00	9.	.0029	.0040	774.0	1.047	12.61	21.30
1.202	2.	1514.	80.	91.	90.	20.	31.	36.	655.	103.	95.	64.1	57.8	10.	64.0	27.5	6.00	8.	.0033	.0044	775.0	1.048	11.62	19.63
1.206	5.	1508.	79.	91.	90.	19.	30.	36.	657.	103.	96.	64.6	57.0	10.	64.0	25.5	6.00	9.	.0033	.0044	776.0	1.050	11.66	19.70
1.200	8.	1510.	29.	91.	89.	19.	30.	34.	634.	104.	95.	64.3	56.9	10.	64.0	27.5	6.00	9.	.0033	.0044	776.0	1.050	11.60	19.60
1.206	11.	1500.	79.	91.	89.	19.	30.	34.	612.	104.	95.	63.6	55.5	10.	65.0	28.0	6.00	9.	.0032	.0044	776.0	1.050	11.66	19.70
1.203	14.	1507.	80.	92.	91.	19.	29.	34.	598.	105.	97.	63.4	57.1	10.	65.0	28.0	6.00	9.	.0032	.0044	776.0	1.050	11.63	19.65
1.202	17.	1500.	80.	92.	91.	19.	30.	34.	587.	106.	98.	63.4	56.9	10.	65.0	27.5	6.00	9.	.0032	.0044	776.0	1.050	11.62	19.63
1.201	20.	1498.	81.	93.	92.	19.	30.	34.	581.	106.	99.	62.9	57.1	10.	65.5	26.0	6.00	9.	.0032	.0043	776.0	1.050	11.61	19.61
1.197	23.	1497.	81.	93.	92.	19.	29.	34.	575.	106.	99.	62.2	56.0	10.	66.0	27.5	6.00	9.	.0032	.0043	776.0	1.050	11.58	19.55
1.196	26.	1501.	82.	95.	93.	19.	30.	34.	570.	106.	98.	61.7	56.8	10.	66.5	27.0	6.00	9.	.0032	.0043	776.0	1.050	11.57	19.53
1.192	29.	1508.	82.	94.	93.	19.	29.	33.	570.	102.	94.	62.4	57.6	10.	65.5	28.5	6.00	9.	.0032	.0043	776.0	1.050	11.53	19.47
1.100	2.	1506.	83.	95.	94.	20.	32.	36.	713.	104.	95.	62.6	57.3	10.	60.0	26.0	6.00	8.	.0035	.0047	775.0	1.048	10.64	17.96
1.101	5.	1504.	82.	95.	94.	20.	31.	36.	689.	103.	94.	62.6	57.0	10.	60.0	26.0	6.00	8.	.0035	.0047	775.0	1.048	10 65	17.98
1.106	8.	1498.	82.	95.	94.	19.	32.	36.	665.	102.	92.	62.6	56.3	10.	60.5	26.0	6.00	8.	.0035	.0047	775.0	1.048	10.70	18.06
1.100	11.	1503.	82.	95.	94.	19.	31.	35.	647.	101.	91.	62.3	56.8	10.	60.5	27.0	6.00	8.	.0035	.0047	775.0	1.048	10.64	17.96
1.104	14.	1503.	83.	96.	94.	19.	31.	35.	634.	98.	88.	62.5	57.1	10.	60.5	27.0	6.00	8.	.0035	.0047	775.0	1.048	10.68	18.03
1.101	17.	1498.	83.	96.	95.	19.	30.	34.	625.	96.	87.	61.8	56.8	10.	61.0	27.0	6.00	8.	.0034	.0046	775.0	1.048	10.65	17.98
1.101	20.	1503.	84.	97.	96.	18.	30.	34.	621.	89.	79.	62.5	57.5	10.	60.5	28.5	6.00	8.	.0035	.0047	775.0	1.048	10.65	17.98
1.092	23.	1507.	83.	96.	95.	18.	29.	33.	617.	83.	71.	63.1	57.8	10.	59.5	27.5	6.00	8.	.0035	.0048	775.0	1.048	10.56	17.83
1.003	2.	1486.	41.	84.	83.	20.	31.	36.	726.	101.	93.	62.2	19.0	10.	55.0	25.5	6.00	8.	.0038	.0051	775.0	1.048	9.70	16.38
.994	5.	1491.	42.	84.	83.	20.	32.	36.	702.	102.	94.	62.2	19.0	10.	54.5	26.0	6.00	8.	.0038	.0052	775.0	1.048	9.61	16.23
1.001	8.	1507.	42.	84.	83.	20.	32.	36.	684.	102.	96.	62.1	19.5	10.	55.0	27.0	6.00	8.	.0038	.0051	775.0	1.048	9.68	16.35
1.000	11.	1507.	42.	84.	83.	20.	31.	35.	667.	102.	94.	62.0	20.0	10.	55.0	25.5	6.00	8.	.0038	.0051	775.0	1.048	9.67	16.33
1.001	14.	1494.	42.	84.	83.	20.	31.	35.	655.	102.	94.	61.5	20.9	10.	55.5	25.5	6.00	8.	.0038	.0051	775.0	1.048	9.68	16.35
.998	17.	1502.	42.	84.	83.	21.	32.	36.	647.	102.	93.	61.7	20.9	10.	55.0	26.5	6.00	8.	.0038	.0051	775.0	1.048	9.65	16.30
.999	20.	1511.	43.	85.	84.	22.	32.	36.	642.	101.	92.	60.5	20.2	10.	56.0	25.5	6.00	8.	.0037	.0051	775.0	1.048	9.66	16.32
.918	2.	1506.	39.	84.	83.	17.	27.	31.	727.	99.	91.	61.9	20.5	10.	50.5	25.0	2.50	5.	.0041	.0056	772.0	1.035	8.88	14.99
.925	5.	1498.	39.	84.	83.	17.	28.	32.	697.	99.	90.	61.2	20.7	10.	51.5	25.0	2.50	5.	.0040	.0055	772.0	1.035	8.94	15.11
.924	8.	1495.	39.	84.	82.	17.	27.	31.	675.	99.	91.	61.1	21.0	10.	51.5	25.5	2.50	5.	.0040	.0055	772.0	1.035	8.94	15.09
.920	11.	1496.	39.	84.	82.	16.	27.	31.	657.	100.	92.	60.8	19.1	10.	51.7	25.0	2.50	5.	.0040	.0055	772.0	1.035	8.90	15.03
.920	14.	1494.	42.	85.	83.	18.	29.	32.	648.	99.	90.	62.1	19.6	10.	50.4	24.5	3.00	7.	.0041	.0056	773.0	1.038	8.90	15.03

.917	17.	1492.	42.	85.	85.	18.	29.	33.	638.	100.	91.	61.7	19.6	10.	50.6	25.0	3.00	7.	.0041	.0056	773.0	1.038	8.87	14.98
.923	20.	1498.	40.	84.	82.	16.	26.	31.	629.	100.	91.	59.9	23.5	10.	52.7	24.5	2.50	5.	.0040	.0054	772.0	1.035	8.93	15.07
.861	2.	1492.	37.	83.	82.	16.	26.	31.	710.	97.	89.	61.7	17.4	10.	47.7	25.0	2.50	5.	.0044	.0059	772.0	1.035	8.33	14.06
.861	5.	1503.	37.	82.	81.	15.	26.	30.	685.	98.	89.	62.2	22.3	10.	47.5	25.5	2.50	5.	.0044	.0060	772.0	1.035	8.33	14.06
.863	8.	1495.	37.	82.	81.	15.	26.	30.	662.	98.	89.	61.9	20.2	10.	47.8	26.0	2.50	5.	.0044	.0059	772.0	1.035	8.35	14.09
.864	11.	1499.	37.	82.	81.	14.	25.	29.	641.	99.	89.	61.9	17.1	10.	48.0	24.5	2.50	5.	.0044	.0059	772.0	1.035	8.36	14.11
.860	14.	1504.	41.	84.	83.	18.	29.	32.	626.	98.	88.	61.9	17.0	10.	47.3	24.5	3.00	7.	.0044	.0060	773.0	1.038	8.32	14.05
.862	17.	1494.	40.	84.	83.	17.	29.	32.	616.	91.	80.	61.8	16.0	10.	47.6	26.0	3.00	7.	.0044	.0059	773.0	1.038	8.34	14.08
.861	20.	1502.	38.	82.	81.	13.	26.	30.	620.	96.	90.	61.9	17.2	10.	48.0	26.5	2.50	5.	.0044	.0059	772.0	1.035	8.33	14.06
.858	23.	1497.	38.	82.	81.	12.	25.	30.	616.	93.	87.	61.9	18.0	10.	48.0	26.5	2.50	5.	.0044	.0059	772.0	1.035	8.30	14.01
.860	26.	1497.	38.	82.	80.	12.	25.	29.	616.	89.	81.	62.1	19.7	10.	48.0	24.5	2.50	5.	.0044	.0059	772.0	1.035	8.32	14.05
.866	29.	1493.	41.	84.	83.	15.	26.	30.	606.	77.	66.	62.4	23.8	10.	47.7	25.0	3.00	7.	.0044	.0059	773.0	1.038	8.37	14.14
.806	2.	1493.	38.	84.	83.	18.	29.	33.	718.	98.	89.	61.3	10.0	10.	45.0	24.0	5.50	7.	.0047	.0063	773.0	1.044	7.79	13.16
.808	5.	1503.	38.	84.	83.	17.	29.	32.	680.	98.	89.	61.8	11.2	10.	45.0	24.0	5.50	6.	.0047	.0063	775.0	1.047	7.81	13.20
.807	8.	1503.	38.	84.	82.	17.	28.	32.	656.	99.	89.	62.4	12.0	10.	44.5	24.0	5.50	6.	.0047	.0064	775.0	1.047	7.80	13.18
.807	11.	1503.	38.	84.	82.	17.	28.	32.	628.	99.	89.	61.8	13.0	10.	45.0	24.0	5.50	6.	.0047	.0063	775.0	1.047	7.80	13.18
.805	14.	1503.	38.	84.	82.	17.	28.	32.	613.	100.	89.	61.6	12.5	10.	45.0	24.0	5.50	6.	.0047	.0063	775.0	1.047	7.78	13.15
.805	17.	1493.	38.	84.	82.	17.	28.	32.	600.	100.	90.	61.6	14.5	10.	45.0	23.0	5.50	6.	.0047	.0063	775.0	1.047	7.78	13.15
.803	20.	1506.	39.	84.	82.	17.	28.	31.	594.	100.	90.	61.4	14.0	10.	45.0	24.0	5.50	6.	.0047	.0063	775.0	1.047	7.77	13.11
.803	23.	1492.	39.	84.	82.	16.	27.	31.	587.	101.	92.	61.7	15.0	10.	45.0	24.0	5.50	6.	.0047	.0063	775.0	1.047	7.77	13.11
.805	26.	1505.	39.	84.	82.	16.	28.	31.	588.	102.	94.	61.8	17.1	10.	45.0	23.0	5.50	6.	.0047	.0063	775.0	1.047	7.78	13.15
.806	29.	1502.	40.	84.	82.	16.	29.	33.	595.	100.	94.	62.0	18.1	10.	45.0	26.0	6.00	6.	.0047	.0063	775.0	1.048	7.79	13.16
.809	32.	1504.	40.	84.	83.	16.	28.	32.	596.	98.	91.	62.2	18.5	10.	45.0	25.5	6.00	8.	.0047	.0063	775.0	1.048	7.82	13.21

AFR	Tmg	bmep	COVimep	Pmax	COVpmax	MFB1%	MFB10%	MFB90%	MFB1090%	etam	etab	etav	Trque	Pwr
Lmda	DegBTDC	bar	%	bar	%	Degree crank angle				%	%	%	Nm	kW
.799	2.	4.60	29.873	32.7	10.3	6.7	10.0	30.4	20.4	.86	.260	.35	227.0	35.89
1.900	2.	4.60	29.873	32.7	10.3	6.7	10.0	30.4	20.4	.86	.260	.82	227.0	35.89
1.900	35.	4.60	29.873	32.7	10.3	39.7	43.0	63.4	20.4	.86	.260	.82	227.0	35.89
1.775	8.	3.14	59.762	29.7	.8	26.3	28.6	53.7	25.1	.89	.174	.78	155.0	24.22
1.726	11.	4.05	22.406	29.9	2.4	22.1	24.8	47.2	22.4	.81	.235	.73	200.0	31.52
1.730	14.	4.50	24.556	30.8	5.8	21.3	24.3	45.5	21.2	.85	.259	.74	222.0	35.01
1.755	17.	4.60	29.873	32.7	10.3	21.7	25.0	45.4	20.4	.86	.260	.76	227.0	35.89
1.750	20.	4.52	46.281	35.0	14.6	22.6	26.2	46.1	19.9	.89	.251	.77	223.0	35.03
1.752	23.	4.52	51.113	38.7	18.0	22.1	26.6	44.8	18.2	.89	.252	.76	223.0	35.29
1.711	8.	3.61	22.901	29.7	.5	22.2	24.8	48.2	23.4	.75	.203	.74	178.0	27.66
1.703	11.	4.30	10.612	30.3	3.7	20.0	23.0	44.3	21.3	.78	.242	.74	212.0	33.35
1.703	14.	4.78	14.672	32.5	8.8	19.3	22.5	42.2	19.7	.82	.269	.74	236.0	37.12
1.707	17.	5.01	12.895	35.5	11.1	19.8	23.1	42.0	18.9	.84	.280	.74	247.0	38.93
1.717	20.	4.95	20.954	38.6	13.6	20.7	24.4	42.6	18.2	.83	.277	.75	244.0	38.51
1.725	23.	4.78	33.837	41.3	17.0	21.7	26.0	43.5	17.5	.84	.270	.74	236.0	37.54
1.720	26.	4.74	25.070	46.5	14.6	22.1	26.6	43.1	16.5	.81	.272	.73	234.0	37.27
1.610	2.	3.49	25.168	29.8	.3	25.6	27.8	55.0	27.2	.84	.189	.73	172.0	27.02
1.620	5.	3.95	22.116	29.9	.4	21.8	24.3	49.1	24.8	.83	.211	.74	195.0	30.67
1.619	8.	4.52	6.449	30.6	4.4	15.5	18.7	39.3	20.6	.78	.244	.74	223.0	34.91
1.618	11.	4.97	6.449	30.6	4.4	18.9	21.9	42.4	20.5	.85	.271	.73	245.0	38.30
1.596	17.	5.45	8.300	37.6	11.3	18.9	22.4	40.5	18.1	.88	.299	.71	269.0	42.42
1.590	20.	5.53	16.984	41.7	12.0	19.3	23.1	40.5	17.4	.91	.306	.70	273.0	43.20
1.596	23.	5.39	15.379	45.0	12.5	20.4	24.6	41.4	16.8	.88	.300	.70	266.0	42.09
1.594	26.	5.15	17.955	49.6	12.2	21.0	25.5	41.5	16.0	.85	.286	.70	254.0	40.14
1.609	29.	4.93	15.165	53.3	10.8	21.9	26.9	42.0	15.1	.82	.275	.70	243.0	38.07
1.510	2.	4.30	3.249	30.0	1.6	14.1	17.3	36.5	19.2	.65	.226	.70	212.0	32.86
1.502	5.	5.07	2.047	32.5	7.1	13.2	16.5	34.1	17.6	.73	.264	.70	250.0	38.64
1.502	8.	5.47	1.476	37.0	8.2	13.2	16.6	33.2	16.6	.78	.287	.70	270.0	42.61
1.500	11.	5.82	1.588	42.9	7.8	13.2	16.6	32.1	15.5	.83	.305	.69	287.0	45.35
1.505	14.	6.00	1.842	48.4	6.2	13.3	17.0	31.6	14.6	.86	.317	.69	296.0	46.50
1.505	17.	6.04	2.244	53.1	5.6	13.6	17.5	31.7	14.2	.89	.322	.68	298.0	46.81
1.508	20.	6.06	2.719	57.7	5.2	13.9	18.3	31.9	13.6	.91	.325	.68	299.0	47.19
1.505	23.	6.02	3.139	62.1	4.3	14.0	18.9	32.1	13.2	.93	.324	.67	297.0	46.84
1.504	26.	6.00	3.183	65.2	3.8	14.4	20.1	32.8	12.7	.95	.324	.68	296.0	46.71
1.494	29.	5.96	3.736	68.7	3.0	15.0	20.8	33.2	12.4	.96	.322	.67	294.0	46.21
1.496	32.	5.86	3.649	70.5	2.2	15.7	21.8	34.1	12.3	.97	.320	.67	289.0	45.64
1.432	2.	5.23	2.173	31.4	5.8	12.2	15.7	33.3	17.6	.73	.255	.72	258.0	39.47
1.413	5.	5.80	1.691	36.8	8.8	11.7	15.3	31.4	16.1	.79	.284	.70	286.0	44.98
1.404	8.	6.16	1.680	41.7	7.7	12.2	15.7	30.8	15.1	.84	.308	.68	304.0	47.72
1.403	11.	6.45	2.080	47.9	7.0	12.3	15.8	30.0	14.2	.88	.321	.69	318.0	50.18
1.410	14.	6.55	2.640	52.8	5.9	12.2	16.1	29.8	13.7	.91	.329	.68	323.0	50.64
1.405	17.	6.59	2.866	58.4	5.3	12.1	16.4	29.6	13.2	.94	.331	.68	325.0	51.36
1.402	20.	6.57	3.200	62.5	4.5	12.2	17.0	29.8	12.8	.96	.333	.67	324.0	50.86

1.402	23.	6.53	3.644	66.2	3.8	12.9	18.0	30.4	12.4	.98	.332	.67	322.0	50.78
1.405	26.	6.43	4.155	68.9	2.9	13.6	19.1	31.3	12.2	1.00	.329	.67	317.0	49.86
1.400	29.	6.32	4.255	71.0	2.5	14.5	20.1	32.1	12.0	1.01	.325	.66	312.0	49.17
1.406	32.	6.16	3.851	72.5	2.0	15.1	21.0	33.2	12.2	.99	.318	.66	304.0	47.91
1.307	2.	5.68	2.153	29.2	7.4	11.5	15.0	31.1	16.1	.89	.267	.68	280.0	43.40
1.301	5.	6.36	2.003	39.6	7.8	11.0	14.6	29.7	15.1	.85	.303	.67	314.0	49.49
1.293	8.	6.75	1.804	45.7	7.2	11.1	14.7	28.8	14.1	.90	.321	.67	333.0	52.34
1.297	11.	6.85	2.437	51.1	5.8	11.4	15.1	28.6	13.5	.92	.329	.66	338.0	53.16
1.296	14.	6.99	2.348	56.4	5.8	11.5	15.5	28.5	13.0	.96	.335	.66	345.0	54.16
1.300	17.	6.97	2.486	62.0	4.9	11.4	15.8	28.1	12.3	.99	.337	.66	344.0	54.11
1.309	20.	6.89	2.955	66.3	4.0	11.4	16.3	28.3	12.0	1.01	.337	.66	340.0	53.66
1.302	23.	6.85	3.405	69.8	3.3	11.9	17.1	28.8	11.7	1.03	.334	.66	338.0	53.16
1.301	26.	6.75	4.178	73.1	2.4	12.6	17.8	29.3	11.5	1.04	.332	.65	333.0	52.17
1.308	29.	6.63	5.045	73.8	1.9	13.6	19.0	30.6	11.6	1.05	.328	.65	327.0	51.26
1.304	32.	6.47	5.085	75.0	1.3	13.9	19.6	31.9	12.3	1.04	.322	.64	319.0	50.28
1.202	2.	6.55	2.097	37.4	7.4	10.6	14.1	29.0	14.9	.85	.296	.66	323.0	51.21
1.206	5.	6.89	1.656	43.0	7.2	10.4	14.0	28.1	14.1	.89	.309	.66	340.0	53.69
1.200	8.	7.24	1.366	49.0	6.7	10.6	14.1	27.5	13.4	.94	.325	.66	357.0	56.45
1.206	11.	7.34	1.700	54.6	5.6	10.6	14.4	27.2	12.8	.97	.333	.66	362.0	56.86
1.203	14.	7.38	1.652	60.1	4.8	10.7	14.8	27.1	12.3	.99	.336	.65	364.0	57.44
1.202	17.	7.38	1.949	65.5	4.2	10.9	15.2	26.9	11.7	1.02	.334	.65	364.0	57.18
1.201	20.	7.34	2.131	70.2	3.4	11.1	15.6	27.0	11.4	1.05	.335	.65	362.0	56.79
1.197	23.	7.24	2.428	73.4	2.6	11.4	16.4	27.5	11.1	1.07	.332	.64	357.0	55.97
1.196	26.	7.11	3.043	75.7	1.9	12.2	17.2	28.5	11.3	1.08	.330	.64	351.0	55.17
1.192	29.	6.95	4.644	77.1	1.1	12.6	17.9	30.2	12.3	1.07	.319	.64	343.0	54.17
1.100	2.	6.89	1.052	44.0	6.6	8.9	12.6	25.8	13.2	.83	.291	.65	340.0	53.62
1.101	5.	7.46	.891	50.2	5.6	9.2	12.8	25.2	12.4	.89	.314	.65	368.0	57.96
1.106	8.	7.70	.960	55.8	4.9	9.7	13.2	25.1	11.9	.92	.325	.65	380.0	59.61
1.100	11.	7.84	1.189	62.0	4.4	9.9	13.5	24.9	11.4	.95	.332	.64	387.0	60.91
1.104	14.	7.92	1.605	67.2	4.1	10.0	14.0	25.1	11.1	.98	.335	.64	391.0	61.54
1.101	17.	7.90	1.997	72.9	3.2	9.8	14.0	24.8	10.8	1.02	.336	.64	390.0	61.18
1.101	20.	7.82	2.317	76.5	2.0	10.2	14.7	25.5	10.8	1.03	.330	.64	386.0	60.75
1.092	23.	7.80	2.700	77.9	.2	10.2	15.1	28.0	12.9	1.05	.325	.65	385.0	60.76
1.003	2.	7.50	.706	47.8	6.1	8.7	12.4	25.0	12.6	.83	.286	.65	370.0	57.58
.994	5.	7.90	.655	54.5	5.3	9.0	12.6	24.4	11.8	.87	.300	.65	390.0	60.89
1.001	8.	8.13	.894	60.5	4.8	9.4	12.9	24.2	11.3	.90	.315	.64	401.0	63.28
1.000	11.	8.27	1.487	66.1	4.4	9.4	13.2	24.2	11.0	.94	.320	.64	408.0	64.39
1.001	14.	8.37	1.873	72.1	3.9	9.3	13.4	24.1	10.7	.98	.324	.64	413.0	64.61
.998	17.	8.35	2.253	76.3	2.2	9.6	13.9	24.5	10.6	1.02	.323	.64	412.0	64.80
.999	20.	8.21	2.383	77.6	.4	9.7	14.3	26.3	12.0	1.04	.327	.63	405.0	64.08
.918	2.	7.44	.671	47.6	5.8	8.6	12.2	24.7	12.5	.83	.265	.64	367.0	57.88
.925	5.	7.78	.795	52.7	5.2	8.6	12.3	26.3	14.0	.89	.281	.64	384.0	60.24
.924	8.	8.11	1.048	59.1	4.6	9.1	12.6	24.0	11.4	.94	.292	.64	400.0	62.62
.920	11.	8.25	1.461	65.8	4.4	8.9	12.7	23.5	10.8	.98	.298	.63	407.0	63.76
.920	14.	8.51	1.792	72.1	3.6	9.1	13.3	23.8	10.5	1.01	.300	.65	420.0	65.71

.917	17.	8.45	2.115	76.2	2.2	9.4	13.8	24.2	10.4	1.04	.299	.64	417.0	65.15
.923	20.	8.17	2.227	77.8	1.5	9.1	14.0	24.6	10.6	1.08	.301	.62	403.0	63.22
.861	2.	7.26	1.721	42.2	7.1	10.1	13.9	27.7	13.8	.82	.241	.64	358.0	55.93
.861	5.	7.80	1.596	49.3	6.0	10.1	13.8	26.7	12.9	.88	.259	.64	385.0	60.60
.863	8.	8.19	1.119	57.0	5.5	9.9	13.7	25.6	11.9	.93	.272	.64	404.0	63.25
.864	11.	8.41	1.310	64.2	4.9	10.1	13.9	25.0	11.1	.97	.280	.64	415.0	65.14
.860	14.	8.35	1.541	68.5	4.2	10.3	14.4	25.4	11.0	.99	.278	.64	412.0	64.89
.862	17.	8.37	1.882	74.1	3.2	10.3	14.8	25.3	10.5	1.02	.278	.64	413.0	64.61
.861	20.	8.31	2.066	77.8	1.4	10.2	15.2	25.6	10.4	1.06	.276	.63	410.0	64.49
.858	23.	8.19	2.316	78.6	.2	10.5	15.7	27.7	12.0	1.07	.271	.63	404.0	63.33
.860	26.	8.07	3.074	78.7	.1	11.2	16.4	30.9	14.5	1.09	.267	.63	398.0	62.39
.866	29.	8.03	5.706	77.9	.2	11.7	17.1	35.1	18.0	1.10	.265	.64	396.0	61.91
.806	2.	6.49	1.854	36.9	10.0	11.8	15.5	31.1	15.6	.74	.203	.64	320.0	50.03
.808	5.	7.26	1.877	44.8	7.6	11.1	14.9	28.8	13.9	.82	.227	.63	358.0	56.35
.807	8.	7.78	1.866	51.6	6.2	11.3	15.0	27.9	12.9	.88	.241	.64	384.0	60.44
.807	11.	8.09	2.015	57.9	5.5	11.3	15.3	27.5	12.2	.93	.253	.63	399.0	62.80
.805	14.	8.23	1.881	64.2	4.8	11.3	15.5	27.3	11.8	.97	.258	.63	406.0	63.90
.805	17.	8.23	2.199	70.3	3.9	11.2	15.8	27.0	11.2	1.00	.256	.64	406.0	63.48
.803	20.	8.21	1.805	74.4	3.5	11.8	16.6	27.7	11.1	1.02	.257	.63	405.0	63.87
.803	23.	8.15	2.696	77.1	1.1	12.2	17.3	28.6	11.3	1.04	.252	.63	402.0	62.81
.805	26.	8.11	3.070	77.6	.3	12.8	18.2	30.9	12.7	1.07	.253	.63	400.0	63.04
.806	29.	7.90	4.462	77.7	.1	13.5	18.9	33.4	14.5	1.09	.246	.63	390.0	61.34
.809	32.	7.76	6.781	77.9	.2	14.0	19.6	36.7	17.1	1.06	.242	.63	383.0	60.32

AFR	Tmg	NOxv	NOxcorv	NOxg			NOxcorg			HCv	HCg			CO2v	CO2g			COv	COg			O2v	TAOx
Lmda	DegBTDC	ppm	ppm	g/kWh	g/MJth	g/cum	g/kWh	g/MJth	g/cum	ppm	g/kWh	g/MJth	g/cum	%	g/kWh	g/MJth	g/cum	%	g/kWh	g/MJth	g/cum	%	%
.799	2.	20.	19.	.2	.013	.031	.2	.013	.030	8510.	26.93	1.94	4.62	7.00	607.71	43.86	104.59	.11	6.08	.44	1.05	9.70	.00
1.900	2.	20.	19.	.2	.013	.128	.2	.013	.123	8510.	26.93	1.94	18.90	7.00	607.71	43.86	427.65	.11	6.08	.44	4.27	9.70	15.79
1.900	35.	20.	19.	.2	.013	.128	.2	.013	.123	8510.	26.93	1.94	18.90	7.00	607.71	43.86	427.65	.11	6.08	.44	4.27	9.70	15.79
1.775	8.	1.	1.	.0	.001	.005	.0	.001	.004	11530.	55.86	2.70	19.32	6.49	862.53	41.76	299.08	.11	9.30	.45	3.22	9.70	14.12
1.726	11.	3.	3.	.0	.002	.012	.0	.002	.012	7780.	26.95	1.76	11.21	7.14	678.38	44.37	282.89	.11	6.65	.44	2.77	8.90	13.02
1.730	14.	5.	5.	.0	.003	.021	.0	.003	.020	7600.	23.83	1.71	11.05	7.19	618.44	44.50	287.52	.11	6.02	.43	2.80	9.20	13.09
1.755	17.	20.	19.	.2	.013	.088	.2	.013	.086	8510.	26.93	1.94	13.09	7.00	607.71	43.86	296.26	.11	6.08	.44	2.96	9.70	13.52
1.750	20.	32.	30.	.3	.022	.131	.3	.021	.122	9700.	33.81	2.36	13.86	6.40	611.99	42.74	251.55	.10	6.09	.43	2.50	9.40	12.96
1.752	23.	62.	57.	.6	.043	.268	.6	.040	.248	10810.	37.09	2.60	16.23	6.38	600.43	42.09	263.49	.10	5.99	.42	2.63	9.60	13.34
1.711	8.	9.	8.	.1	.007	.031	.1	.006	.028	7510.	34.37	1.94	8.92	6.16	773.28	43.71	201.33	.12	9.59	.54	2.49	8.80	11.35
1.703	11.	10.	9.	.1	.007	.032	.1	.007	.030	5680.	21.93	1.48	6.40	6.31	668.30	44.98	195.55	.12	8.09	.54	2.36	8.30	10.82
1.703	14.	14.	13.	.1	.010	.050	.1	.009	.046	6170.	19.83	1.48	7.62	6.85	604.00	45.10	232.83	.11	6.17	.46	2.38	8.20	11.71
1.707	17.	20.	19.	.2	.014	.071	.2	.013	.066	6130.	19.02	1.48	7.57	6.81	579.49	45.10	231.23	.11	5.96	.46	2.38	8.50	11.70
1.717	20.	38.	35.	.3	.026	.141	.3	.024	.131	7310.	22.90	1.76	9.42	6.71	576.62	44.39	237.90	.10	5.47	.42	2.25	8.50	12.09
1.725	23.	70.	65.	.6	.048	.279	.6	.045	.258	9830.	31.62	2.37	13.61	6.45	569.14	42.71	245.69	.10	5.62	.42	2.42	9.20	12.70
1.720	26.	95.	88.	.9	.067	.368	.8	.063	.341	10310.	33.81	2.55	13.88	6.22	559.59	42.21	230.31	.10	5.73	.43	2.35	9.30	12.47
1.610	2.	16.	15.	.2	.011	.051	.2	.010	.047	7900.	36.28	1.90	8.75	6.68	841.63	44.08	203.41	.09	7.22	.38	1.74	7.30	10.64
1.620	5.	24.	22.	.3	.017	.077	.3	.015	.072	7840.	32.20	1.89	8.78	6.66	750.34	44.04	205.23	.10	7.17	.42	1.96	7.90	10.77
1.619	8.	30.	28.	.3	.020	.095	.3	.019	.088	6190.	21.72	1.47	6.80	6.93	666.96	45.14	209.40	.11	6.74	.46	2.11	7.70	10.57
1.618	11.	44.	41.	.4	.030	.136	.4	.028	.126	4970.	15.61	1.17	5.35	7.09	611.02	45.95	209.89	.11	6.03	.45	2.07	7.40	10.35
1.596	17.	130.	121.	1.1	.089	.383	1.0	.083	.356	4760.	13.77	1.14	4.88	6.99	554.51	46.03	197.21	.11	5.55	.46	1.97	7.60	9.83
1.590	20.	190.	177.	1.5	.131	.559	1.4	.121	.520	5010.	14.11	1.20	5.13	6.98	539.31	45.87	196.49	.11	5.41	.46	1.97	7.80	9.81
1.596	23.	200.	186.	1.7	.141	.594	1.6	.131	.551	6240.	18.43	1.54	6.44	6.65	538.73	44.93	188.79	.11	5.67	.47	1.99	8.30	9.90
1.594	26.	280.	260.	2.5	.200	.849	2.3	.186	.787	8100.	25.41	2.02	8.54	6.37	548.12	43.59	184.70	.11	6.02	.48	2.03	8.50	10.13
1.609	29.	300.	278.	2.8	.217	.931	2.6	.201	.863	8770.	28.98	2.21	9.46	6.22	563.76	43.05	184.62	.11	6.35	.48	2.08	8.90	10.38
1.510	2.	13.	12.	.1	.007	.041	.1	.007	.038	4510.	13.65	.86	4.91	9.03	749.67	47.12	270.41	.08	4.23	.27	1.52	7.50	10.47
1.502	5.	25.	23.	.2	.014	.072	.2	.013	.067	2010.	5.37	.39	2.01	8.98	658.70	48.37	246.56	.08	3.73	.27	1.40	7.00	9.53
1.502	8.	45.	42.	.3	.025	.131	.3	.024	.123	2260.	5.52	.44	2.28	9.03	605.16	48.20	250.97	.09	3.84	.31	1.59	7.20	9.66
1.500	11.	100.	94.	.7	.056	.290	.6	.053	.273	2460.	5.66	.48	2.48	8.98	566.62	48.04	249.27	.10	4.02	.34	1.77	7.10	9.65
1.505	14.	175.	165.	1.1	.098	.511	1.1	.093	.481	2620.	5.84	.51	2.66	8.91	544.41	47.94	248.79	.10	3.89	.34	1.78	7.20	9.72
1.505	17.	280.	263.	1.8	.158	.819	1.7	.148	.770	2770.	6.08	.54	2.82	8.86	533.55	47.75	247.84	.12	4.60	.41	2.13	7.30	9.74
1.508	20.	400.	377.	2.5	.227	1.170	2.4	.214	1.102	2860.	6.27	.57	2.91	8.79	528.59	47.68	246.01	.12	4.59	.41	2.14	7.40	9.74
1.505	23.	650.	612.	4.1	.369	1.888	3.9	.347	1.779	2770.	6.08	.55	2.80	8.79	529.06	47.68	244.29	.13	4.98	.45	2.30	7.40	9.66
1.504	26.	800.	752.	5.1	.456	2.311	4.8	.428	2.171	2780.	6.14	.55	2.79	8.75	530.02	47.66	241.85	.13	5.01	.45	2.29	7.50	9.60
1.494	29.	1000.	940.	6.4	.570	2.837	6.0	.536	2.665	2680.	5.95	.53	2.64	8.73	531.71	47.61	236.90	.15	5.81	.52	2.59	7.50	9.39
1.496	32.	1250.	1173.	8.0	.716	3.540	7.6	.672	3.323	2670.	5.99	.53	2.63	8.69	534.94	47.60	235.44	.15	5.88	.52	2.58	7.40	9.37
1.432	2.	160.	152.	1.2	.084	.454	1.1	.079	.431	4750.	12.23	.87	4.69	9.43	666.18	47.11	256.19	.08	3.60	.25	1.38	6.70	9.41
1.413	5.	230.	218.	1.5	.122	.609	1.5	.116	.577	2970.	6.95	.55	2.73	9.47	607.83	47.98	239.69	.08	3.27	.26	1.29	6.20	8.56
1.404	8.	320.	304.	2.0	.171	.816	1.9	.163	.774	1950.	4.26	.36	1.73	9.45	566.39	48.43	230.48	.09	3.43	.29	1.40	6.20	8.10
1.403	11.	500.	474.	3.0	.267	1.277	2.8	.253	1.212	2000.	4.16	.37	1.78	9.48	541.54	48.36	231.62	.10	3.64	.32	1.55	5.90	8.12
1.410	14.	670.	636.	4.0	.362	1.720	3.8	.343	1.632	2150.	4.43	.40	1.92	9.32	527.17	48.16	228.89	.12	4.32	.39	1.87	6.20	8.18
1.405	17.	1025.	973	6.0	.552	2.612	5.7	.524	2.479	2100.	4.28	.39	1.86	9.36	523.69	48.19	228.17	.12	4.27	.39	1.86	6.10	8.09
1.402	20	1100.	1044.	6.4	.594	2.784	6.1	.564	2.643	2100.	4.28	.40	1.85	9.31	520.98	48.13	225.42	.13	4.63	.43	2.00	6.20	8.00

1.402	23.	1650.	1566.	9.7	.892	4.167	9.2	.846	3.955	2100.	4.29	.40	1.84	9.31	521.78	48.13	224.94	.13	4.64	.43	2.00	6.20	7.98
1.405	26.	1900.	1803.	11.3	1.034	4.796	10.7	.981	4.550	2070.	4.29	.39	1.82	9.24	525.59	48.08	223.13	.14	5.07	.46	2.15	6.30	7.97
1.400	29.	2250.	2136.	13.5	1.217	5.649	12.8	1.155	5.362	2050.	4.28	.39	1.79	9.30	533.18	48.10	223.37	.14	5.11	.46	2.14	6.20	7.90
1.406	32.	2450.	2325.	15.2	1.342	6.146	14.4	1.274	5.833	1980.	4.28	.38	1.73	9.18	544.40	48.11	220.30	.14	5.28	.47	2.14	6.30	7.89
1.307	2.	480.	470.	3.3	.242	1.096	3.2	.237	1.073	1920.	4.54	.34	1.52	10.09	653.86	48.58	220.31	.08	3.30	.25	1.11	4.60	6.60
1.301	5.	670.	656.	4.1	.341	1.497	4.0	.334	1.466	1350.	2.85	.24	1.05	10.04	580.72	48.84	214.59	.08	2.95	.25	1.09	4.50	6.29
1.293	8.	1000.	980.	5.7	.508	2.213	5.6	.497	2.168	1450.	2.87	.26	1.12	10.04	545.85	48.75	212.54	.09	3.11	.28	1.21	4.50	6.15
1.297	11.	1380.	1351.	7.7	.707	3.062	7.6	.692	2.999	1610.	3.15	.29	1.24	9.93	532.55	48.66	210.77	.09	3.07	.28	1.21	4.70	6.19
1.296	14.	1800.	1763.	9.9	.921	3.988	9.7	.902	3.906	1670.	3.20	.30	1.29	9.92	521.95	48.58	210.27	.10	3.35	.31	1.35	4.80	6.17
1.300	17.	2200.	2154.	12.1	1.131	4.891	11.8	1.108	4.789	1720.	3.29	.31	1.33	9.86	517.82	48.50	209.69	.11	3.68	.34	1.49	4.90	6.22
1.309	20.	2600.	2546.	14.5	1.352	5.818	14.2	1.324	5.698	1760.	3.41	.32	1.37	9.74	518.06	48.46	208.52	.11	3.72	.35	1.50	5.10	6.31
1.302	23.	3000.	2937.	16.7	1.547	6.666	16.3	1.514	6.526	1760.	3.41	.32	1.36	9.83	522.99	48.48	208.95	.11	3.72	.35	1.49	4.90	6.21
1.301	26.	3400.	3329.	19.1	1.760	7.532	18.7	1.723	7.374	1860.	3.64	.34	1.43	9.78	524.87	48.42	207.27	.11	3.76	.35	1.48	4.90	6.17
1.308	29.	3400.	3329.	19.3	1.762	7.595	18.9	1.725	7.436	1820.	3.61	.33	1.41	9.77	531.08	48.44	208.79	.11	3.81	.35	1.49	5.10	6.29
1.304	32.	3600.	3525.	20.9	1.871	7.984	20.5	1.833	7.818	1820.	3.69	.33	1.40	9.74	541.46	48.43	206.64	.11	3.89	.35	1.48	5.00	6.18
1.202	2.	1350.	1312.	7.9	.647	2.695	7.6	.628	2.620	1580.	3.21	.26	1.10	10.66	593.49	48.84	203.62	.07	2.48	.20	.85	3.20	4.55
1.206	5.	1750.	1719.	9.8	.845	3.482	9.7	.830	3.420	1140.	2.23	.19	.79	10.62	570.99	49.04	202.16	.07	2.40	.21	.85	3.20	4.50
1.200	8.	2400.	2357.	12.8	1.155	4.737	12 6	1.135	4.653	1240.	2.31	.21	.85	10.65	543.10	49.04	201.10	.06	1.95	.18	.72	3.20	4.36
1.206	11.	3000.	2946.	15.7	1.455	5.956	15.5	1.429	5.849	1360.	2.49	.23	.94	10.55	529.71	48.93	200.37	.07	2.24	.21	.85	3.40	4.46
1.203	14.	3600.	3532.	18.7	1.742	7.120	18.3	1.710	6.986	1450.	2.62	.24	1.00	10.55	523.43	48.84	199.60	.08	2.53	.24	.96	3.30	4.39
1.202	17.	4200.	4125.	21.9	2.030	8.290	21.5	1.994	8.143	1510.	2.74	.25	1.04	10.56	525.59	48.82	199.39	.08	2.53	.24	.96	3.20	4.36
1.201	20.	4600.	4518.	24.0	2.229	9.052	23.6	2.190	8.891	1500.	2.73	.25	1.03	10.52	524.67	48.77	198.04	.09	2.86	.27	1.08	3.30	4.31
1.197	23.	5000.	4906.	26.3	2.429	9.766	25.8	2.383	9.583	1450.	2.66	.25	.98	10.50	528.57	48.79	196.19	.09	2.88	.27	1.07	3.20	4.19
1.196	26.	5400.	5305.	28.6	2.619	10.533	28.1	2.573	10.347	1510.	2.79	.26	1.02	10.51	531.85	48.77	196.11	.09	2.90	.27	1.07	3.20	4.16
1.192	29.	5200.	5103.	28.4	2.516	10.111	27.8	2.469	9.922	1590.	3.03	.27	1.08	10.54	550.14	48.78	196.05	.08	2.66	.24	.95	3.10	4.11
1.100	2.	2600.	2548.	14.5	1.171	4.599	14.2	1.147	4.507	1620.	3.15	.25	1.00	11.36	605.69	48.93	192.21	.06	2.04	.16	.65	1.30	2.44
1.101	5.	3200.	3130.	16.5	1.440	5.632	16.1	1.408	5.508	1190.	2.14	.19	.73	11.41	562.48	49.12	192.10	.06	1.88	.16	.64	1.40	2.35
1.106	8.	3700.	3625.	18.6	1.675	6.535	18.2	1.641	6.402	1170.	2.05	.18	.72	11.35	544.75	49.16	191.76	.05	1.53	.14	.54	1.40	2.42
1.100	11.	4100.	4006.	20.0	1.845	7.196	19.6	1.803	7.032	1280.	2.18	.20	.78	11.40	532.19	49.08	191.42	.06	1.78	.16	.64	1.30	2.30
1.104	14.	4500.	4396.	21.9	2.036	7.929	21.4	1.989	7.746	1350.	2.29	.21	.83	11.33	526.37	49.04	190.99	.06	1.77	.17	.64	1.40	2.37
1.101	17	4700.	4583.	22.8	2.126	8.252	22.2	2.073	8.047	1400.	2.36	.22	.85	11.33	524.92	49.02	190.30	.06	1.77	.17	.64	1.40	2.31
1.101	20.	4800.	4681.	23.6	2.160	8.430	23.0	2.106	8.221	1400.	2.40	.22	.86	11.39	534.84	49.03	191.37	.06	1.79	.16	.64	1.30	2.31
1.092	23.	4900.	4770.	24.3	2.190	8.516	23.7	2.132	8.290	1370.	2.37	.21	.83	11.46	543.53	49.00	190.53	.07	2.11	.19	.74	1.10	2.12
1.003	2.	1950.	1919.	9.9	.789	3.180	9.8	.776	3.130	1910.	3.39	.27	1.08	11.53	561.14	44.62	179.89	1.17	36.24	2.88	11.61	.00	.88
.994	5.	2250.	2223.	10.9	.907	3.514	10.8	.896	3.472	1820.	3.07	.26	.99	11.56	535.14	44.59	172.72	1.19	35.06	2.92	11.31	.00	.00
1.001	8.	2700.	2666.	12.6	1.098	4.361	12.4	1.084	4.306	1710.	2.78	.24	.96	11.61	516.89	45.17	179.41	1.04	29.47	2.58	10.22	.00	.69
1.000	11.	3000.	2953.	13.8	1.225	4.686	13.6	1.206	4.612	1630.	2.61	.23	.89	11.66	512.13	45.54	174.22	.95	26.56	2.36	9.03	.00	.00
1.001	14.	3100.	3051.	14.0	1.265	4.996	13.8	1.245	4.918	1710.	2.70	.24	.96	11.62	503.68	45.35	179.17	.99	27.31	2.46	9.71	.00	.65
.998	17.	3200.	3160.	14.5	1.305	4.998	14.4	1.289	4.936	1730.	2.74	.25	.94	11.63	505.41	45.39	173.77	.98	27.11	2.43	9.31	.00	.00
.999	20.	3400.	3358.	15.4	1.393	5.310	15.2	1.375	5.244	1700.	2.68	.24	.92	11.62	501.91	45.54	173.62	.94	25.84	2.34	8.93	.00	.00
.918	2.	1350.	1294.	6.8	.499	2.108	6.5	.479	2.022	2260.	3.96	.29	1.23	11.18	537.69	39.54	167.05	2.70	82.65	6.08	25.66	.00	.00
.925	5.	1800.	1732.	8.6	.672	2.811	8.3	.646	2.705	1950.	3.25	.25	1.06	11.08	506.77	39.55	165.55	2.70	78.60	6.13	25.66	.00	.00
.924	8.	2050.	1965.	9.4	.765	3.202	9.0	.733	3.069	1950.	3.13	.25	1.06	11.08	487.48	39.55	165.55	2.70	75.61	6.13	25.66	.00	.00
.920	11.	2250.	2157.	10.2	.839	3.514	9.7	.805	3.369	2010.	3.16	.26	1.09	11.08	478.37	39.54	165.55	2.70	74.19	6.13	25.66	.00	.00
.920	14.	1000.	974.	4.4	.368	1.562	4.3	.358	1.521	2160.	3.32	.28	1.17	10.96	462.48	38.57	163.76	3.00	80.57	6.72	28.51	.00	.00

.917	17.	1050.	1023.	4.6	.385	1.640	4.5	.375	1.597	2230.	3.44	.29	1.21	10.93	462.11	38.36	163.31	3.06	82.34	6.84	29.08	.00	.00
.923	20.	2500.	2386.	11.1	.930	3.905	10.6	.887	3.727	2230.	3.46	.29	1.21	11.17	475.73	39.74	166.90	2.63	71.29	5.95	24.99	.00	.00
.861	2.	280.	268.	1.5	.098	.437	1.4	.094	.419	2380.	4.33	.29	1.29	10.17	507.39	33.94	151.95	4.54	144.16	9.64	43.14	.00	.00
.861	5.	310.	297.	1.5	.107	.484	1.4	.103	.464	2370.	3.98	.29	1.29	10.27	472.84	34.00	153.45	4.56	133.62	9.61	43.33	.00	.00
.863	8.	350.	335.	1.6	.121	.547	1.5	.116	.524	2530.	4.03	.30	1.37	10.29	449.97	33.99	153.75	4.56	126.91	9.59	43.33	.00	.00
.864	11.	380.	362.	1.7	.130	.594	1.6	.124	.566	2610.	4.01	.31	1.42	10.37	437.42	34.05	154.94	4.56	122.42	9.53	43.33	.00	.00
.860	14.	340.	333.	1.5	.118	.531	1.5	.116	.520	2780.	4.36	.34	1.51	9.94	427.77	33.06	148.52	4.78	130.93	10.12	45.42	.00	.00
.862	17.	320.	313.	1.4	.111	.500	1.4	.109	.489	2830.	4.45	.34	1.54	9.94	428.50	33.07	148.52	4.77	130.87	10.10	45.32	.00	.00
.861	20.	350.	335.	1.6	.120	.547	1.5	.115	.524	2860.	4.46	.34	1.55	10.20	436.29	33.51	152.40	4.70	127.95	9.83	44.66	.00	.00
.858	23.	340.	324.	1.5	.116	.531	1.5	.111	.507	2930.	4.65	.35	1.59	10.16	442.10	33.23	151.80	4.80	132.94	9.99	45.61	.00	.00
.860	26.	350.	334.	1.6	.120	.547	1.5	.114	.521	2960.	4.77	.35	1.61	10.16	448.68	33.22	151.80	4.80	134.91	9.99	45.61	.00	.00
.866	29.	380.	366.	1.8	.132	.594	1.7	.127	.572	2800.	4.60	.34	1.52	10.05	452.83	33.36	150.16	4.70	134.78	9.93	44.66	.00	.00
.806	2.	120.	118.	.7	.040	.187	.7	.040	.184	4720.	9.81	.55	2.56	9.18	523.52	29.50	137.16	5.87	213.06	12.01	55.78	.00	.00
.808	5.	140.	138.	.7	.047	.219	.7	.046	.215	3010.	5.57	.35	1.63	9.45	479.87	30.28	141.20	5.82	188.10	11.87	55.30	.00	.00
.807	8.	170.	166.	.8	.057	.266	.8	.056	.260	2950.	5.14	.34	1.60	9.40	449.32	30.07	140.45	5.90	179.49	12.01	56.06	.00	.00
.807	11.	185.	181.	.9	.062	.289	.9	.060	.282	3110.	5.16	.36	1.69	9.38	426.82	30.01	140.15	5.90	170.87	12.02	56.06	.00	.00
.805	14.	195.	191.	.9	.065	.305	.9	.064	.298	3320.	5.39	.39	1.80	9.36	417.21	29.85	139.85	5.95	168.80	12.08	56.54	.00	.00
.805	17.	205.	200.	1.0	.068	.320	.9	.067	.313	3490.	5.70	.41	1.90	9.36	419.54	29.82	139.85	5.95	169.74	12.06	56.54	.00	.00
.803	20.	205.	200.	1.0	.068	.320	.9	.066	.313	3630.	5.87	.42	1.97	9.36	415.25	29.70	139.85	6.00	169.42	12.12	57.01	.00	.00
.803	23.	200.	194.	.9	.066	.312	.9	.065	.304	3710.	6.13	.43	2.02	9.29	420.89	29.50	138.81	6.05	174.45	12.23	57.49	.00	.00
.805	26.	210.	205.	1.0	.070	.328	1.0	.068	.321	3710.	6.09	.43	2.02	9.33	420.08	29.55	139.40	6.05	173.37	12.20	57.49	.00	.00
.806	29.	215.	211.	1.0	.071	.336	1.0	.070	.330	3780.	6.36	.43	2.05	9.20	424.66	29.03	137.46	6.23	183.03	12.51	59.20	.00	.00
.809	32.	230.	226.	1.1	.076	.359	1.1	.074	.353	3660.	6.25	.42	1.99	9.29	435.30	29.27	138.81	6.18	184.30	12.39	58.72	.00	.00

AFR	Tmg	etam	etab	etav	Trque	Pwr	QCl	QEx	QChm	Qcond	Wb	Qc	Qe	QCm	Qcnd	Qout	mfCV
Lmda	DegBTDC	%	%	%	Nm	kW	kW	kW	kW	kW	%	%	%	%	%	%	kW
.799	2.	.86	.260	.35	227.0	35.89	26.06	22.23	14.34	11.91	25.98	18.87	16.09	10.38	8.62	20.06	138.14
1.900	2.	.86	.260	.82	227.0	35.89	26.06	22.23	14.05	11.91	25.98	18.87	16.09	10.17	8.62	20.27	138.14
1.900	35.	.86	.260	.82	227.0	35.89	26.06	22.23	14.05	11.91	25.98	18.87	16.09	10.17	8.62	20.27	138.14
1.775	8.	.89	.174	.78	155.0	24.22	25.11	26.03	19.43	11.40	17.43	18.07	18.74	13.98	8.20	23.58	138.95
1.726	11.	.81	.235	.73	200.0	31.52	25.08	24.12	12.39	11.68	23.55	18.73	18.02	9.25	8.72	21.73	133.87
1.730	14.	.85	.259	.74	222.0	35.01	26.54	23.04	12.18	11.82	25.90	19.64	17.05	9.01	8.75	19.65	135.15
1.755	17.	.86	.260	.76	227.0	35.89	26.06	22.23	14.05	11.91	25.98	18.87	16.09	10.17	8.62	20.27	138.14
1.750	20.	.89	.251	.77	223.0	35.03	26.26	21.94	17.06	11.69	25.14	18.85	15.75	12.24	8.39	19.63	139.32
1.752	23.	.89	.252	.76	223.0	35.29	25.97	20.86	18.78	11.55	25.24	18.58	14.92	13.44	8.26	19.57	139.81
1.711	8.	.75	.203	.74	178.0	27.66	26.54	30.72	13.95	11.72	20.35	19.53	22.59	10.26	8.62	18.65	135.95
1.703	11.	.78	.242	.74	212.0	33.35	27.02	28.87	10.92	12.22	24.23	19.64	20.98	7.93	8.88	18.34	137.62
1.703	14.	.82	.269	.74	236.0	37.12	26.74	25.38	10.87	12.26	26.88	19.36	18.38	7.87	8.88	18.63	138.09
1.707	17.	.84	.280	.74	247.0	38.93	26.16	24.31	10.94	12.33	28.02	18.83	17.50	7.87	8.88	18.91	138.95
1.717	20.	.83	.277	.75	244.0	38.51	25.97	22.65	12.85	12.12	27.71	18.69	16.30	9.25	8.72	19.32	138.95
1.725	23.	.84	.270	.74	236.0	37.54	27.18	21.25	17.09	11.65	27.02	19.56	15.29	12.30	8.39	17.44	138.95
1.720	26.	.81	.272	.73	234.0	37.27	26.27	20.19	18.12	11.38	27.16	19.14	14.71	13.21	8.29	17.50	137.25
1.610	2.	.84	.189	.73	172.0	27.02	30.36	32.86	14.17	12.39	18.85	21.19	22.93	9.89	8.65	18.49	143.29
1.620	5.	.83	.211	.74	195.0	30.67	27.83	31.69	14.34	12.56	21.13	19.18	21.84	9.88	8.65	19.33	145.16
1.619	8.	.78	.244	.74	223.0	34.91	29.41	29.66	11.20	12.73	24.36	20.52	20.70	7.81	8.88	17.72	143.29
1.618	11.	.85	.271	.73	245.0	38.30	29.05	27.85	8.97	12.80	27.07	20.53	19.68	6.34	9.04	17.33	141.48
1.596	17.	.88	.299	.71	269.0	42.42	29.23	25.03	8.80	12.86	29.88	20.59	17.63	6.20	9.06	16.64	141.97
1.590	20.	.91	.306	.70	273.0	43.20	28.06	23.71	9.16	12.74	30.62	19.89	16.81	6.49	9.03	17.16	141.08
1.596	23.	.88	.300	.70	266.0	42.09	28.94	22.86	11.48	12.40	30.02	20.64	16.30	8.19	8.85	16.00	140.20
1.594	26.	.85	.286	.70	254.0	40.14	28.75	21.83	14.90	12.03	28.63	20.50	15.57	10.63	8.58	16.09	140.20
1.609	29.	.82	.275	.70	243.0	38.07	26.70	21.12	16.06	11.73	27.49	19.28	15.25	11.60	8.47	17.90	138.46
1.510	2.	.65	.226	.70	212.0	32.86	30.72	28.71	6.62	13.39	22.63	21.15	19.77	4.56	9.22	22.68	145.22
1.502	5.	.73	.264	.70	250.0	38.64	30.48	28.04	3.29	13.84	26.44	20.85	19.18	2.25	9.47	21.80	146.16
1.502	8.	.78	.287	.70	270.0	42.61	31.50	26.56	3.73	14.04	28.67	21.20	17.87	2.51	9.45	20.29	148.60
1.500	11.	.83	.305	.69	287.0	45.35	31.58	25.15	4.09	14.01	30.52	21.25	16.93	2.75	9.43	19.12	148.60
1.505	14.	.86	.317	.69	296.0	46.50	33.15	23.69	4.31	13.80	31.70	22.60	16.15	2.94	9.41	17.21	146.67
1.505	17.	.89	.322	.68	298.0	46.81	32.89	22.66	4.60	13.64	32.22	22.64	15.59	3.17	9.39	16.99	145.30
1.508	20.	.91	.325	.68	299.0	47.19	30.79	22.05	4.78	13.63	32.48	21.19	15.17	3.29	9.38	18.49	145.30
1.505	23.	.93	.324	.67	297.0	46.84	31.73	21.63	4.71	13.55	32.44	21.98	14.98	3.26	9.39	17.94	144.37
1.504	26.	.95	.324	.68	296.0	46.71	32.53	20.87	4.77	13.54	32.37	22.54	14.46	3.31	9.39	17.93	144.29
1.494	29.	.96	.322	.67	294.0	46.21	32.45	20.48	4.73	13.47	32.23	22.63	14.29	3.30	9.40	18.15	143.37
1.496	32.	.97	.320	.67	289.0	45.64	35.77	20.32	4.75	13.39	32.04	25.11	14.26	3.34	9.40	15.87	142.46
1.432	2.	.73	.255	.72	258.0	39.47	33.55	28.31	7.13	14.28	25.46	21.64	18.26	4.60	9.21	20.83	155.04
1.413	5.	.79	.284	.70	286.0	44.98	35.43	28.88	4.79	14.86	28.41	22.38	18.24	3.03	9.39	18.55	158.31
1.404	8.	.84	.308	.68	304.0	47.72	33.55	26.93	3.34	14.71	30.78	21.64	17.37	2.15	9.49	18.57	155.04
1.403	11.	.88	.321	.69	318.0	50.18	33.55	25.91	3.50	14.81	32.15	21.49	16.59	2.24	9.48	18.04	156.11
1.410	14.	.91	.329	.68	323.0	50.64	33.47	24.53	3.84	14.58	32.89	21.74	15.93	2.49	9.47	17.49	153.98
1.405	17.	.94	.331	.68	325.0	51.36	34.42	23.88	3.84	14.69	33.13	22.20	15.40	2.48	9.47	17.32	155.04
1.402	20.	.96	.333	.67	324.0	50.86	32.63	23.18	3.87	14.48	33.26	21.34	15.16	2.53	9.47	18.25	152.93

1.402	23.	.98	.332	.67	322.0	50.78	35.53	22.84	3.96	14.48	33.21	23.23	14.93	2.59	9.47	16.57	152.93
1.405	26.	1.00	.329	.67	317.0	49.86	35.68	22.39	3.99	14.34	32.93	23.57	14.79	2.63	9.47	16.60	151.40
1.400	29.	1.01	.325	.66	312.0	49.17	36.00	22.23	3.99	14.35	32.48	23.78	14.68	2.64	9.48	16.95	151.40
1.406	32.	.99	.318	.66	304.0	47.91	36.66	22.51	3.96	14.28	31.82	24.35	14.95	2.63	9.48	16.78	150.58
1.307	2.	.89	.267	.68	280.0	43.40	37.92	30.84	3.21	15.42	26.75	23.37	19.01	1.98	9.50	19.39	162.26
1.301	5.	.85	.303	.67	314.0	49.49	37.62	30.01	2.48	15.62	30.28	23.02	18.36	1.51	9.56	17.27	163.45
1.293	8.	.90	.321	.67	333.0	52.34	36.31	28.35	2.71	15.54	32.15	22.30	17.41	1.66	9.55	16.93	162.81
1.297	11.	.92	.329	.66	338.0	53.16	34.53	27.09	3.01	15.40	32.89	21.37	16.76	1.86	9.53	17.59	161.63
1.296	14.	.96	.335	.66	345.0	54.16	37.92	26.02	3.21	15.39	33.51	23.46	16.10	1.99	9.52	15.43	161.63
1.300	17.	.99	.337	.66	344.0	54.11	38.79	25.22	3.39	15.28	33.72	24.18	15.71	2.11	9.52	14.76	160.47
1.309	20.	1.01	.337	.66	340.0	53.66	38.43	24.56	3.53	15.16	33.68	24.12	15.41	2.21	9.51	15.06	159.32
1.302	23.	1.03	.334	.66	338.0	53.16	39.89	24.22	3.56	15.16	33.37	25.04	15.20	2.23	9.51	14.64	159.32
1.301	26.	1.04	.332	.65	333.0	52.17	39.97	23.78	3.73	14.93	33.21	25.44	15.14	2.37	9.50	14.33	157.08
1.308	29.	1.05	.328	.65	327.0	51.26	36.92	23.38	3.66	14.84	32.83	23.65	14.98	2.34	9.51	16.69	156.12
1.304	32.	1.04	.322	.64	319.0	50.28	37.73	23.71	3.70	14.84	32.20	24.17	15.19	2.37	9.51	16.57	156.12
1.202	2.	.85	.296	.66	323.0	51.21	35.85	31.63	2.86	16.50	29.63	20.74	18.30	1.65	9.54	20.14	172.85
1.206	5.	.89	.309	.66	340.0	53.69	38.56	32.11	2.32	16.64	30.92	22.20	18.49	1.33	9.58	17.48	173.66
1.200	8.	.94	.325	.66	357.0	56.45	194.40	30.61	2.51	16.63	32.51	111.94	17.63	1.45	9.57	-73.09	173.66
1.206	11.	.97	.333	.66	362.0	56.86	37.54	28.96	2.81	16.35	33.25	21.95	16.94	1.64	9.56	16.65	170.99
1.203	14.	.99	.336	.65	364.0	57.44	38.63	28.07	3.08	16.34	33.59	22.59	16.42	1.80	9.55	16.04	170.99
1.202	17.	1.02	.334	.65	364.0	57.18	38.50	27.38	3.26	16.33	33.44	22.51	16.01	1.91	9.55	16.58	170.99
1.201	20.	1.05	.335	.65	362.0	56.79	38.64	26.87	3.35	16.20	33.47	22.77	15.84	1.97	9.55	16.40	169.69
1.197	23.	1.07	.332	.64	357.0	55.97	37.89	26.36	3.32	16.09	33.23	22.50	15.66	1.97	9.55	17.08	168.40
1.196	26.	1.08	.330	.64	351.0	55.17	41.64	25.84	3.44	15.96	33.01	24.91	15.46	2.06	9.55	15.01	167.14
1.192	29.	1.07	.319	.64	343.0	54.17	38.99	26.18	3.52	16.19	31.92	22.98	15.43	2.07	9.54	18.06	169.69
1.100	2.	.83	.291	.65	340.0	53.62	38.79	35.92	3.08	17.61	29.08	21.04	19.48	1.67	9.55	19.18	184.38
1.101	5.	.89	.314	.65	368.0	57.96	41.78	34.40	2.55	17.67	31.44	22.66	18.66	1.38	9.59	16.28	184.38
1.106	8.	.92	.325	.65	380.0	59.61	41.27	32.87	2.55	17.59	32.49	22.49	17.91	1.39	9.59	16.12	183.48
1.100	11.	.95	.332	.64	387.0	60.91	41.64	31.59	2.81	17.57	33.20	22.69	17.22	1.53	9.58	15.78	183.48
1.104	14.	.98	.335	.64	391.0	61.54	41.87	30.90	2.99	17.56	33.54	22.82	16.84	1.63	9.57	15.60	183.48
1.101	17.	1.02	.336	.64	390.0	61.18	41.65	30.08	3.07	17.41	33.62	22.89	16.53	1.69	9.57	15.71	181.97
1.101	20.	1.03	.330	.64	386.0	60.75	42.17	30.07	3.11	17.61	33.00	22.90	16.33	1.69	9.57	16.51	184.11
1.092	23.	1.05	.325	.65	385.0	60.76	42.38	30.17	3.16	17.92	32.46	22.64	16.12	1.69	9.57	17.53	187.20
1.003	2.	.83	.286	.65	370.0	57.58	45.34	36.95	8.88	19.19	28.63	22.54	18.37	4.41	9.54	16.51	201.14
.994	5.	.87	.300	.65	390.0	60.89	44.30	35.63	12.00	19.38	30.00	21.83	17.56	5.91	9.55	15.16	202.98
1.001	8.	.90	.315	.64	401.0	63.28	45.47	34.40	8.11	19.22	31.46	22.61	17.10	4.03	9.56	15.24	201.14
1.000	11.	.94	.320	.64	408.0	64.39	46.64	33.41	10.02	19.23	32.01	23.19	16.61	4.98	9.56	13.65	201.14
1.001	14.	.98	.324	.64	413.0	64.61	48.74	32.33	7.87	19.04	32.42	24.45	16.22	3.95	9.55	13.41	199.32
.998	17.	1.02	.323	.64	412.0	64.80	48.74	32.00	10.39	19.15	32.33	24.31	15.96	5.18	9.55	12.66	200.45
.999	20.	1.04	.327	.63	405.0	64.08	47.11	31.11	9.90	18.75	32.66	24.01	15.86	5.04	9.55	12.87	196.21
.918	2.	.83	.265	.64	367.0	57.88	51.15	37.52	24.22	20.83	26.47	23.39	17.16	11.08	9.53	12.37	218.64
.925	5.	.89	.281	.64	384.0	60.24	51.65	35.09	23.62	20.47	28.10	24.09	16.37	11.02	9.55	10.88	214.39
.924	8.	.94	.292	.64	400.0	62.62	52.39	33.68	23.66	20.47	29.21	24.44	15.71	11.03	9.55	10.06	214.39
.920	11.	.98	.298	.63	407.0	63.76	47.65	32.51	23.75	20.45	29.75	22.24	15.17	11.08	9.54	12.22	214.30
.920	14.	1.01	.300	.65	420.0	65.71	46.78	32.25	26.37	20.87	30.02	21.37	14.74	12.05	9.54	12.28	218.86

.917	17.	1.04	.299	.64	417.0	65.15	46.78	31.42	26.79	20.78	29.89	21.46	14.41	12.29	9.53	12.42	218.00
.923	20.	1.08	.301	.62	403.0	63.22	57.35	30.10	23.01	20.03	30.07	27.28	14.32	10.95	9.53	7.86	210.24
.861	2.	.82	.241	.64	358.0	55.93	44.35	36.85	39.80	22.13	24.08	19.09	15.86	17.14	9.53	14.30	232.28
.861	5.	.88	.259	.64	385.0	60.60	55.61	35.28	39.93	22.31	25.89	23.76	15.07	17.06	9.53	8.69	234.06
.863	8.	.93	.272	.64	404.0	63.25	50.37	33.49	39.81	22.15	27.19	21.66	14.40	17.11	9.52	10.11	232.59
.864	11.	.97	.280	.64	4 5.0	65.14	42.64	31.99	39.65	22.12	28.03	18.35	13.76	17.06	9.52	13.29	232.43
.860	14.	.99	.278	.64	412.0	64.89	40.57	31.35	42.55	22.16	27.82	17.39	13.44	18.24	9.50	13.59	233.21
.862	17.	1.02	.278	.64	413.0	64.61	39.05	30.62	42.42	22.09	27.79	16.79	13.17	18.24	9.50	14.51	232.54
.861	20.	1.06	.276	.63	410.0	64.49	41.96	30.73	41.38	22.16	27.65	17.99	13.17	17.74	9.50	13.95	233.24
.858	23.	1.07	.271	.63	404.0	63.33	43.91	30.47	42.30	22.23	27.06	18.76	13.02	18.07	9.50	13.59	234.06
.860	26.	1.09	.267	.63	398.0	62.39	48.06	30.47	42.34	22.22	26.66	20.53	13.02	18.09	9.49	12.21	234.06
.866	29.	1.10	.265	.64	396.0	61.91	56.79	30.07	41.81	22.18	26.52	24.33	12.88	17.91	9.50	8.86	233.47
.806	2.	.74	.203	.64	320.0	50.03	25.49	38.31	56.41	23.14	20.29	10.34	15.53	22.87	9.38	21.58	246.60
.808	5.	.82	.227	.63	358.0	56.35	28.55	35.98	53.51	23.56	22.71	11.51	14.50	21.57	9.50	20.21	248.08
.807	8.	.88	.241	.64	384.0	60.44	30.59	34.70	54.71	23.83	24.09	12.19	13.83	21.81	9.50	18.57	250.87
.807	11.	.93	.253	.63	399.0	62.80	33.14	32.45	54.36	23.54	25.31	13.36	13.08	21.91	9.49	16.85	248.08
.805	14.	.97	.258	.63	406.0	63.90	31.87	31.37	54.96	23.51	25.76	12.84	12.64	22.15	9.48	17.12	248.08
.805	17.	1.00	.256	.64	406.0	63.48	36.96	30.49	55.14	23.48	25.59	14.90	12.29	22.23	9.47	15.53	248.08
.803	20.	1.02	.257	.63	405.0	63.87	34.93	30.00	55.58	23.46	25.75	14.08	12.09	22.40	9.46	16.22	248.08
.803	23.	1.04	.252	.63	402.0	62.81	37.42	29.65	56.42	23.53	25.23	15.03	11.91	22.67	9.45	15.71	248.94
.805	26.	1.07	.253	.63	400.0	63.04	42.66	29.67	56.26	23.53	25.32	17.14	11.92	22.60	9.45	13.57	248.94
.806	29.	1.09	.246	.63	390.0	61.34	44.18	30.06	57.95	23.55	24.61	17.72	12.06	23.25	9.45	12.90	249.24
.809	32.	1.06	.242	.63	383.0	60.32	45.15	30.11	57.17	23.57	24.20	18.12	12.08	22.94	9.46	13.21	249.24

11 Specific Gravities of Aqueous Ethylene Glycol Solutions

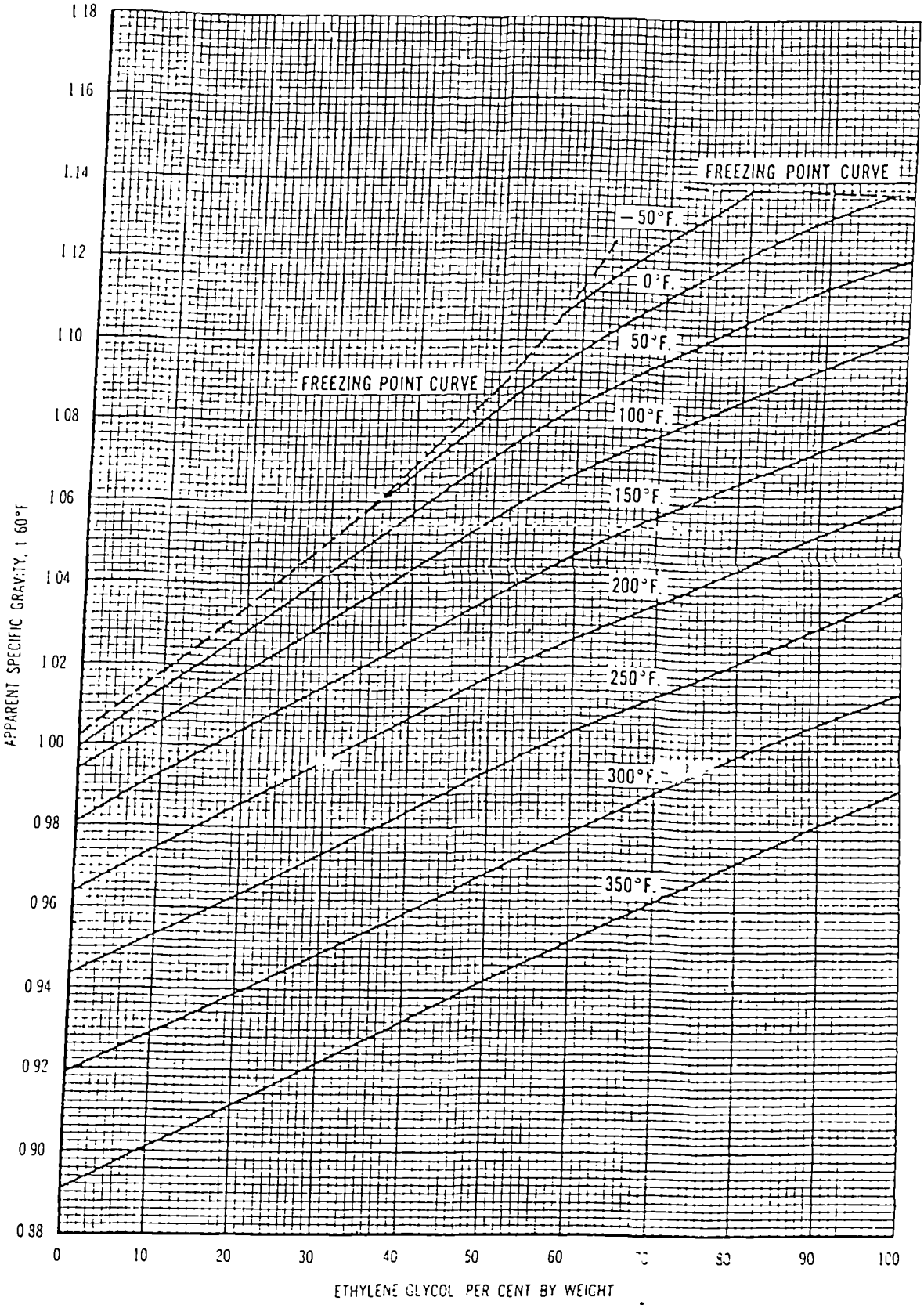

[°C]	[bar]	10^{-3}[m³/kg]	[kJ/kg	K]	10^{-6}[kg/m s]		10^{-6}[kW/m K]		$(Pr)_f$	$(Pr)_g$
0.01	0.006112	0.10002	4.210	1.86	1752	8.49	569	16.3	12.96	0.97
5	0.008719	0.10001	4.204	1.86	1501	8.66	578	16.7	10.92	0.96
10	0.01227	0.10003	4.193	1.86	1300	8.83	587	17.1	9.29	0.96
15	0.01704	0.10010	4.186	1.87	1136	9.00	595	17.5	7.99	0.96
20	0.02337	0.10018	4.183	1.87	1002	9.18	603	17.9	6.95	0.96
25	0.03166	0.10030	4.181	1.88	890	9.35	611	18.3	6.09	0.96
30	0.04242	0.10044	4.179	1.88	797	9.52	618	18.7	5.39	0.96
35	0.05622	0.10060	4.178	1.88	718	9.70	625	19.1	4.80	0.96
40	0.07375	0.10079	4.179	1.89	651	9.87	632	19.5	4.30	0.96
45	0.09582	0.10099	4.181	1.89	594	10.0	638	19.9	3.89	0.95
50	0.1233	0.1012	4.182	1.90	544	10.2	643	20.4	3.54	0.95
55	0.1574	0.1015	4.183	1.90	501	10.4	648	20.8	3.23	0.95
60	0.1992	0.1017	4.185	1.91	463	10.6	653	21.2	2.97	0.95
65	0.2501	0.1020	4.188	1.92	430	10.7	658	21.6	2.74	0.95
70	0.3116	0.1023	4.191	1.93	400	10.9	662	22.0	2.53	0.96
75	0.3855	0.1026	4.194	1.94	374	11.1	666	22.5	2.36	0.96
80	0.4736	0.1029	4.198	1.95	351	11.3	670	22.9	2.20	0.96
85	0.5780	0.1032	4.203	1.96	330	11.4	673	23.3	2.06	0.96
90	0.7011	0.1036	4.208	1.97	311	11.6	676	23.8	1.94	0.96
95	0.8453	0.1040	4.213	1.99	294	11.8	678	24.3	1.83	0.97
100	1.01325	0.1044	4.219	2.01	279	12.0	681	24.8	1.73	0.97
105	1.208	0.1048	4.226	2.03	265	12.2	683	25.3	1.64	0.98
110	1.433	0.1052	4.233	2.05	252	12.4	684	25.8	1.56	0.99
115	1.691	0.1056	4.240	2.07	241	12.6	686	26.3	1.49	0.99
120	1.985	0.1060	4.248	2.09	230	12.8	687	26.8	1.42	1.00
125	2.321	0.1065	4.26	2.12	220	13.0	687	27.3	1.36	1.01
130	2.701	0.1070	4.27	2.15	211	13.2	688	27.8	1.31	1.02
135	3.131	0.1075	4.28	2.18	203	13.4	688	28 3	1.26	1.03
140	3.614	0 1080	4.29	2.21	195	13.5	688	28.8	1.22	1.04
145	4.155	0 1085	4.30	2.25	188	13.7	687	29.4	1.18	1.05
150	4.760	0.1091	4.32	2.29	181	13.9	687	30.0	1.14	1.07
160	6.181	0 1102	4.35	2.38	169	14.2	684	31.3	1.07	1.09
170	7.920	0 1114	4.38	2.49	159	14.6	681	32.6	1.02	1.12
180	10.03	0.1128	4.42	2.62	149	15.0	676	34.1	0.97	1.15
190	12.55	0 1142	4.46	2.76	141	15.3	671	35.7	0.94	1.18
200	15.55	0.1157	4.51	2.91	134	15.7	665	37.5	0.91	1.22
210	19.08	0.1173	4.56	3.07	127	16.0	657	39.4	0.88	1.25
220	23.20	0.1190	4.63	3.25	121	16.3	648	41.5	0.86	1.28
230	27.98	0 1209	4.70	3.45	116	16.7	639	43.9	0.85	1.31
240	33.48	0.1229	4.78	3.68	111	17.1	628	46.5	0.84	1.35
250	39.78	0.1251	4.87	3.94	107	17.5	616	49.5	0.85	1.39
260	46.94	0.1276	4.98	4.22	103	17.9	603	52.8	0.85	1.43
270	55.05	0.1302	5.10	4.55	99	18.3	589	56.6	0.86	1.47
280	64.19	0.1332	5.24	4.98	96	18.8	574	61.0	0.88	1.53
290	74.45	0.1366	5.42	5.46	93	19.3	558	66.0	0.90	1.60
300	85.92	0.1404	5.65	6.18	90	19.8	541	72.0	0.94	1.70
320	112.9	0.1499								
340	146.1	0.1639								
360	186.7	0.1894								
370	210.5	0.2225								
374.15	221.2	0.317								

The values for saturated water can be used with good accuracy above saturation pressure. The values for saturated steam can be used with only moderate accuracy below saturation pressure at temperatures greater than 200 °C.

Table A5 —*contd.*

T, °C	ρ, kg/m³	C_p, kJ/kg K	$\nu \times 10^6$, m²/s	k, W/m K	β, K^{-1}	P
			Engine oil			
0	899	1·796	4,280	0·147		47,100
20	888	1·880	900	0·145	0·00070	10,400
40	876	1·964	240	0·144		2,870
60	864	2·047	84	0·140		1,050
80	852	2·131	37	0·138		490
100	840	2·219	20	0·137		276
120	829	2·307	12	0·135		175
140	817	2·395	8	0·133		116
160	806	2·483	6	0·132		84
			Ethylene glycol			
0	1,131	2·294	57·5	0·242		615
20	1,117	2·382	19·2	0·249	0·00065	204
40	1,102	2·474	8·69	0·256		93
60	1,088	2·562	4·75	0·260		51
80	1,078	2·650	2·98	0·261		32
100	1,059	2·742	2·03	0·263		22
			Eutectic calcium chloride solution (29·9% Ca)			
−50	1,320	2·608	36·3	0·402		312
−40	1,315	2·636	24·9	0·415		208
−30	1,311	2·661	17·1	0·429		139
−20	1,306	2·688	11·0	0·445		87·1
−10	1,301	2 713	6·96	0·459		53·6
0	1,296	2·738	4·40	0·472		33·0
10	1,292	2·763	3·35	0·485		24·6
20	1,287	2 788	2·72	0 498		19·6
30	1,282	2 814	2 27	0·511		16 0
40	1,278	2 839	1 92	0 523		13 3
50	1,273	2 868	1·65	0 535		11·3
To convert to	lb/ft³	Btu/lb °R	ft²/s	Btu/ft h °R	°R^{-1}	—
Multiply by	0 06243	0 2388	10·76	0·5778	0 5556	1

35 Volume Per Cent vs Weight Per Cent of Aqueous Ethylene Glycol Solutions

Glycol, % by		Glycol, % by		Glycol, % by		Glycol, % by		Glycol, % by	
wt.	vol.	wt.	vol.	wt.	vol.	wt.	vol.	wt.	vol.
0	0.0	20	18.4	40	37 8	60	58.0	80	78.9
1	0.9	21	19.3	41	38 8	61	59.1	81	79.9
2	1.8	22	20.3	42	39.8	62	60.1	82	81.0
3	2.7	23	21.2	43	40.8	63	61.1	83	82.0
4	3.6	24	22.2	44	41 8	64	62.2	84	83.1
5	4.5	25	23.2	45	42.8	65	63.2	85	84.1
6	5.4	26	24.1	46	43.8	66	64.2	86	85.2
7	6.3	27	25.1	47	44.8	67	65.3	87	86.2
8	7.2	28	26.0	48	45.8	68	66.3	88	87.3
9	8.2	29	27.0	49	46.8	69	67.4	89	88.4
10	9.1	30	28.0	50	47.8	70	68.4	90	89.4
11	10 0	31	28.9	51	48.8	71	69.4	91	90.5
12	10.9	32	29.9	52	49.8	72	70.5	92	91.5
13	11.9	33	30.9	53	50.9	73	71.5	93	92.6
14	12.8	34	31.9	54	51 9	74	72 6	94	93.6
15	13.7	35	32 8	55	52.9	75	73 6	95	94.7
16	14 6	36	33 8	56	53.9	76	74.7	96	95.8
17	15.6	37	34.8	57	55.0	77	75.7	97	96 8
18	16 5	38	35.8	58	56.0	78	76.8	98	97.9
19	17 5	39	36 8	59	57.0	79	77.8	99	98.9
20	18.4	40	37.8	60	58.0	80	78.9	100	100

EVALUATION OF THE FLOW OF HEAT ENERGY FROM THE TEST CELL

The test cell was ventilated by a cold air duct (open to atmosphere) and an extractor fan and duct (also open to atmosphere). The inlet and the outlet ducts were situated at opposite corners of the test cell. With the engine operating at the rated load, speed and temperature, the temperature difference between the incoming air and the extracted air was 9.5°C. This was measured with a mercury in glass thermometer.

The air flow measurement was made with the aid of a digital turbine air flow meter which was placed in front of the cold air duct. The effective flow area of the duct was divided into 25 equal rectangles and the flow meter was placed in the centre of each rectangle. An average flow rate was taken of the 25 readings. This was calculated to be 4.86m/s.

This flow rate was first converted to a volume flow rate. The volume flow rate was then used to calculate the mass flow rate. Given the temperature rise and the mass flow rate it then becomes possible to evaluate an energy flow rate. This was done in the following way:

Flow rate x cross-sectional area = volume flow rate

$4.86 \times 0.297 = 1.442\ m^3/s$

From $PV = mRT$

$P = m/V\ RT$

$P = \rho RT$

$\rho = P/RT$

where P = 774.55/750 = 1.0327 bar, R = Specific gas constant = 0.2871 kJ/kgK

T = ambient temperature = 19.5°C, ρ = density of air

Substituting: $\rho = 1.0327 \times 10^5 / 0.2871(273+19.5)$

$= 1.230\ kg/m^3$

since $\rho = m/V$ is also true for flow rates

$\dot{m} = 1.442 \times 1.230$

$\rho = 1.773\ kg/s$

$\dot{Q} = \dot{m} Cp \Delta T$

Where Q = Heat flow (kW), m = mass flow (kg/s),

Cp = specific heat capacity of air (ambient temp), ΔT = temperature difference

Substituting: $= 1.773 \times 1005 \times 9.5$

$\dot{Q} = 16.92\ kW$

APPENDIX C

Interpolation Program Outputs

Bore 10.70 cm
Stroke 11.50 cm
Conrod length 20.30 cm
No. cylinders 06
Inlet valve diameter 4.50 cm
Inlet valves/cyl 01
Blowby coefficient .25 1/s
File with 10% and 90% burn data used (NBR=3): mfb1090.sea
Fuel is methane
Higher Calorific Value used
The Hohenberg heat transfer correlation is used
with a weighting factor of .75 for the unburnt
gas, and .75 for the burnt gas
The fmep weighting factor used is .75
The cylinder wall temperature is 450.
The emissions are quoted as dry emissions except for H2O which is quoted as a
wet emission
The brake specific emissions are quoted as wet emissions

Page 1, Pressure at Inlet Valve Closure of 0.9 bar

Lamb	Ig. Ang dbtdc	Inl P Bar	IMEP Bar	BMEP Bar	ETA %	P MAX Bar	B. Pwr kW	H. Loss kW	B. Torq Nm	bsfc g/kWh	ETA B %	NOe ppm	NOX ppm	O2 %	CO kg/kWh	CO2 EMISSIONS	NO2
0.80	35.0	0.90	8.74	7.49	28.37	86.68	58	35.07	370	267	24.30	3	323	0.01	0.201	0.409	0.0018
0.90	35.0	0.90	9.01	7.75	32.42	88.62	60	37.83	383	233	27.88	4	1032	0.01	0.095	0.482	0.0054
1.00	35.0	0.90	9.16	7.90	36.21	88.10	61	39.58	390	208	31.23	248	4198	0.06	0.003	0.559	0.0211
1.10	35.0	0.90	8.67	7.43	37.40	84.03	58	35.69	367	202	32.04	1457	8204	2.04	0.001	0.549	0.0447
1.20	35.0	0.90	8.21	6.99	38.38	79.23	54	32.14	345	199	32.66	1962	7661	3.73	0.001	0.539	0.0451
1.30	35.0	0.90	7.75	6.54	38.98	75.46	51	29.53	323	197	32.89	2296	4113	5.15	0.001	0.535	0.0262
1.40	35.0	0.90	7.33	6.13	39.51	71.84	48	27.25	303	196	33.06	2542	1698	6.35	0.001	0.532	0.0117
1.50	35.0	0.90	6.95	5.77	40.00	68.50	45	25.27	285	195	33.20	2728	650	7.36	0.001	0.530	0.0048
1.60	35.0	0.90	6.61	5.43	40.39	66.59	42	23.66	268	195	33.21	2882	263	8.25	0.001	0.530	0.0021
1.70	35.0	0.90	6.30	5.14	40.78	63.60	40	22.11	254	195	33.25	3009	99	9.03	0.001	0.529	0.0008
1.80	35.0	0.90	6.02	4.87	41.13	59.53	38	20.62	241	195	33.29	3116	35	9.72	0.001	0.529	0.0003
1.90	35.0	0.90	5.74	4.60	41.25	55.68	36	19.47	227	196	33.11	3208	13	10.34	0.001	0.532	0.0001
0.80	32.0	0.90	8.84	7.59	28.70	86.43	59	34.41	375	263	24.64	3	316	0.01	0.199	0.403	0.0017
0.90	32.0	0.90	9.12	7.86	32.82	88.43	61	37.14	388	229	28.28	4	1026	0.01	0.094	0.476	0.0053
1.00	32.0	0.90	9.26	8.00	36.59	88.47	62	39.06	395	205	31.60	248	4187	0.06	0.003	0.553	0.0208
1.10	32.0	0.90	8.74	7.49	37.67	84.34	58	35.32	370	201	32.30	1457	8164	2.04	0.001	0.545	0.0441
1.20	32.0	0.90	8.26	7.03	38.58	78.94	55	31.84	347	197	32.86	1962	7446	3.73	0.001	0.536	0.0435
1.30	32.0	0.90	7.79	6.58	39.18	74.23	51	29.15	325	196	33.12	2296	3805	5.15	0.001	0.531	0.0241
1.40	32.0	0.90	7.38	6.19	39.79	70.01	48	26.73	306	194	33.38	2542	1475	6.35	0.001	0.527	0.0100
1.50	32.0	0.90	7.01	5.84	40.35	66.29	45	24.62	289	193	33.59	2732	529	7.38	0.001	0.524	0.0039
1.60	32.0	0.90	6.67	5.51	40.79	63.40	43	22.88	272	193	33.68	2882	196	8.25	0.001	0.523	0.0015
						ETC											
1.10	5.0	0.90	9.06	7.92	39.06	54.92	61	27.24	391	190	34.17	1457	3693	2.04	0.001	0.515	0.0189
1.20	5.0	0.90	8.41	7.30	39.31	50.05	57	24.99	361	190	34.10	1962	1650	3.73	0.001	0.516	0.0093
1.30	5.0	0.90	7.81	6.71	39.28	45.07	52	22.99	331	192	33.76	2296	545	5.15	0.001	0.521	0.0034
1.40	5.0	0.90	7.20	6.12	38.80	39.12	47	21.17	302	196	33.01	2542	150	6.35	0.001	0.533	0.0010
1.50	5.0	0.90	6.67	5.62	38.36	34.09	44	19.61	277	201	32.31	2732	39	7.38	0.001	0.545	0.0003
1.60	5.0	0.90	6.25	5.21	38.23	31.73	40	18.42	257	204	31.85	2886	13	8.27	0.001	0.553	0.0001
1.70	5.0	0.90	5.87	4.83	37.98	29.39	37	17.34	239	207	31.28	3013	4	9.05	0.001	0.563	0.0001
1.80	5.0	0.90	5.37	4.34	36.66	27.22	34	16.15	214	219	29.66	3120	1	9.74	0.001	0.593	0.0001
1.90	5.0	0.90	4.74	3.72	34.12	27.27	29	14.97	184	242	26.76	3211	0.1	10.36	0.001	0.658	0.0001
0.80	2.0	0.90	8.95	7.84	29.05	48.38	61	25.35	387	255	25.44	3	48	0.01	0.192	0.390	0.0003

0.90	2.0	0.90	9.35	8.22	33.64	51.33	64	27.30	406	219	29.60	5	563	0.01	0.090	0.454	0.0028
1.00	2.0	0.90	9.62	8.49	38.01	52.79	66	28.81	419	193	33.55	248	2878	0.06	0.003	0.521	0.0135
1.10	2.0	0.90	8.91	7.80	38.43	49.59	60	26.51	385	193	33.62	1457	2986	2.04	0.001	0.523	0.0155
1.20	2.0	0.90	8.25	7.16	38.55	44.53	56	24.31	354	194	33.44	1963	1220	3.73	0.001	0.526	0.0070
1.30	2.0	0.90	7.65	6.57	38.49	40.30	51	22.42	325	196	33.06	2296	397	5.15	0.001	0.532	0.0025
1.40	2.0	0.90	7.01	5.95	37.77	34.62	46	20.65	294	202	32.08	2542	105	6.35	0.001	0.549	0.0007
1.50	2.0	0.90	6.43	5.40	37.01	29.28	42	19.11	267	209	31.06	2732	25	7.38	0.001	0.567	0.0002
1.60	2.0	0.90	6.03	5.00	36.86	27.34	39	17.95	247	212	30.59	2886	8	8.27	0.001	0.575	0.0001
1.70	2.0	0.90	5.68	4.65	36.74	27.17	36	16.95	230	215	30.11	3013	3	9.05	0.001	0.585	0.0001
1.80	2.0	0.90	5.17	4.14	35.31	27.22	32	15.84	205	229	28.31	3120	1	9.74	0.001	0.622	0.0001
1.90	2.0	0.90	4.54	3.51	32.64	27.27	27	14.73	174	257	25.28	3211	0.1	10.36	0.001	0.696	0.0001

Page 2, Pressure at Inlet Valve Closure of 1.25 bar

Lamb	Ig. Ang dbtdc	Inl P Bar	IMEP Bar	BMEP Bar	ETA %	P MAX Bar	B. Pwr kW	H. Loss kW	B. Torq Nm	bsfc g/kWh	ETA B %	NOe ppm	NOX ppm	O2 %	CO kg/kWh	CO2 EMISSIONS	NO2
0.80	35.0	1.25	11.69	10.32	28.49	116.54	80	45.28	510	258	25.15	2	280	0.01	0.195	0.395	0.0025
0.90	35.0	1.25	12.05	10.67	32.55	119.12	83	48.80	527	225	28.82	4	874	0.01	0.092	0.467	0.0044
1.00	35.0	1.25	12.25	10.87	36.35	118.43	84	51.04	537	201	32.26	233	3936	0.05	0.003	0.542	0.0192
1.10	35.0	1.25	11.59	10.23	37.53	112.99	79	46.09	506	196	33.14	1457	8228	2.04	0.001	0.531	0.0433
1.20	35.0	1.25	10.97	9.64	38.49	106.51	75	41.56	476	192	33.82	1963	9016	3.73	0.001	0.520	0.0512
1.30	35.0	1.25	10.34	9.03	39.08	101.46	70	38.23	446	190	34.22	2297	5652	5.15	0.001	0.516	0.0347
1.40	35.0	1.25	9.78	8.49	39.60	96.62	66	35.33	419	189	34.37	2542	2506	6.35	0.001	0.512	0.0166
1.50	35.0	1.25	9.28	8.00	40.08	92.17	62	32.81	395	188	34.57	2733	993	7.38	0.001	0.509	0.0070
1.60	35.0	1.25	8.82	7.55	40.46	89.61	59	30.77	373	187	34.65	2883	411	8.25	0.001	0.508	0.0031
1.70	35.0	1.25	8.40	7.15	40.84	85.63	55	28.80	353	187	34.77	3010	159	9.03	0.001	0.506	0.0013
1.80	35.0	1.25	8.03	6.80	41.17	80.19	53	26.90	336	186	34.87	3117	57	9.72	0.001	0.505	0.0005
1.90	35.0	1.25	7.64	6.44	41.28	75.07	50	25.45	318	187	34.76	3208	22	10.34	0.001	0.507	0.0002
0.80	32.0	1.25	11.82	10.45	28.81	116.19	81	44.44	516	255	25.48	2	277	0.01	0.192	0.390	0.0015
0.90	32.0	1.25	12.19	10.81	32.94	118.86	84	47.92	534	222	29.22	4	869	0.01	0.091	0.460	0.0043
1.00	32.0	1.25	12.37	11.00	36.72	118.92	85	50.37	543	199	32.63	233	3926	0.05	0.003	0.536	0.0189
1.10	32.0	1.25	11.67	10.32	37.80	113.35	80	45.60	510	194	33.40	1457	8213	2.04	0.001	0.527	0.0429
1.20	32.0	1.25	11.03	9.70	38.68	106.10	75	41.17	479	191	34.02	1963	8843	3.73	0.001	0.517	0.0499
1.30	32.0	1.25	10.40	9.09	39.28	99.80	71	37.75	449	189	34.35	2297	5271	5.15	0.001	0.512	0.0322
1.40	32.0	1.25	9.85	8.56	39.87	94.16	66	34.68	423	187	34.68	2542	2188	6.35	0.001	0.508	0.0143
1.50	32.0	1.25	9.36	8.09	40.41	89.19	63	31.99	400	186	34.96	2733	812	7.38	0.001	0.504	0.0057
1.60	32.0	1.25	8.90	7.65	40.84	85.33	59	29.78	378	185	35.11	2883	308	8.25	0.001	0.501	0.0023

ETC

1.10	5.0	1.25	12.07	10.86	39.08	73.84	84	35.28	537	184	35.16	1457	4798	2.04	0.001	0.500	0.0238
1.20	5.0	1.25	11.21	10.02	39.32	67.30	78	32.41	495	184	35.16	1963	2359	3.73	0.001	0.500	0.0129
1.30	5.0	1.25	10.39	9.23	39.27	60.64	72	29.88	456	186	34.89	2296	812	5.15	0.001	0.504	0.0049
1.40	5.0	1.25	9.58	8.45	38.78	52.70	66	27.57	417	190	34.21	2542	230	6.35	0.001	0.514	0.0015
1.50	5.0	1.25	8.87	7.77	38.33	45.97	60	25.59	384	193	33.57	2733	63	7.38	0.001	0.524	0.0005
1.60	5.0	1.25	8.32	7.23	38.18	42.82	56	24.08	357	195	33.19	2886	20	8.27	0.001	0.530	0.0002
1.70	5.0	1.25	7.80	6.73	37.92	39.68	52	22.70	332	198	32.69	3013	7	9.05	0.001	0.538	0.0001
1.80	5.0	1.25	7.13	6.07	36.59	37.39	47	21.19	300	208	31.12	3120	2	9.74	0.001	0.566	0.0001
1.90	5.0	1.25	6.30	5.24	34.04	37.46	41	19.69	259	229	28.29	3211	0.1	10.36	0.001	0.622	0.0001
0.80	2.0	1.25	11.92	10.75	29.06	65.01	83	32.84	531	248	26.19	2	63	0.01	0.187	0.379	0.0003
0.90	2.0	1.25	12.45	11.26	33.65	68.98	87	35.33	556	213	30.43	4	630	0.01	0.087	0.442	0.0030
1.00	2.0	1.25	12.82	11.62	38.03	70.97	90	37.26	574	188	34.47	232	3267	0.05	0.002	0.507	0.0149
1.10	2.0	1.25	11.87	10.69	38.43	66.66	83	34.34	528	187	34.60	1457	3987	2.04	0.001	0.508	0.0201
1.20	2.0	1.25	10.99	9.83	38.55	59.88	76	31.54	486	188	34.49	1963	1758	3.73	0.001	0.510	0.0098
1.30	2.0	1.25	10.18	9.05	38.47	54.23	70	29.15	447	190	34.18	2296	592	5.15	0.001	0.515	0.0036
1.40	2.0	1.25	9.32	8.22	37.74	46.64	64	26.90	406	195	33.27	2542	161	6.35	0.001	0.529	0.0011
1.50	2.0	1.25	8.56	7.43	36.96	39.49	58	24.95	370	201	32.31	2733	40	7.38	0.001	0.545	0.0003

1.60	2.0	1.25	8.02	6.95	36.81	37.24	54	23.48	343	203	31.91	2886	13	8.27	0.001	0.552	0.0001
1.70	2.0	1.25	7.55	6.48	36.68	37.32	50	22.20	320	206	31.50	3013	4	9.05	0.001	0.559	0.0001
1.80	2.0	1.25	6.87	5.80	35.23	37.39	45	20.79	287	218	29.76	3120	1	9.74	0.001	0.591	0.0001
1.90	2.0	1.25	6.03	4.96	32.54	37.46	38	19.38	245	242	26.80	3211	0.1	10.36	0.001	0.657	0.0001

Page 3, Pressure at Inlet Valve Closure of 1.60 bar

Lamb	Ig. Ang dbtdc	Inl P Bar	IMEP Bar	BMEP Bar	ETA %	P MAX Bar	B. Pwr kW	H. Loss kW	B. Torq Nm	bsfc g/kWh	ETA B %	NOe ppm	NOX ppm	O2 %	CO kg/kWh	CO2 EMISSIONS	NO2
0.80	35.0	1.60	14.39	12.92	28.53	144.49	100	54.68	638	253	25.60	2	250	0.01	0.191	0.388	0.0013
0.90	35.0	1.60	14.83	13.34	32.60	147.67	103	58.88	659	221	29.32	3	775	0.01	0.090	0.459	0.0039
1.00	35.0	1.60	15.08	13.59	36.39	146.83	105	61.54	671	198	32.80	221	3755	0.05	0.002	0.533	0.0180
1.10	35.0	1.60	14.26	12.80	37.56	140.09	99	55.66	632	192	33.71	1457	8171	2.04	0.001	0.522	0.0423
1.20	35.0	1.60	13.50	12.07	38.51	132.08	94	50.26	596	188	34.43	1963	9811	3.73	0.001	0.511	0.0547
1.30	35.0	1.60	12.72	11.31	39.09	125.85	88	46.31	559	187	34.77	2297	7140	5.15	0.001	0.506	0.0431
1.40	35.0	1.60	12.02	10.64	39.59	119.90	83	42.86	526	185	35.04	2542	3450	6.35	0.001	0.502	0.0224
1.50	35.0	1.60	11.40	10.04	40.06	114.41	78	39.87	496	184	35.28	2733	1425	7.38	0.001	0.499	0.0099
1.60	35.0	1.60	10.83	9.48	40.43	111.27	74	37.44	468	183	35.40	2883	605	8.25	0.001	0.497	0.0045
1.70	35.0	1.60	10.32	8.99	40.80	106.37	70	35.09	444	183	35.54	3010	240	9.04	0.001	0.495	0.0019
1.80	35.0	1.60	9.86	8.55	41.12	99.67	66	32.84	422	182	35.68	3117	88	9.73	0.001	0.493	0.0007
1.90	35.0	1.60	9.38	8.10	41.22	93.38	63	31.11	400	182	35.60	3208	35	10.34	0.001	0.495	0.0003
0.80	32.0	1.60	14.55	13.08	28.85	144.04	101	53.68	646	250	25.92	2	248	0.01	0.189	0.383	0.0013
0.90	32.0	1.60	15.01	13.52	32.99	147.33	105	57.83	668	218	29.71	3	771	0.01	0.089	0.453	0.0038
1.00	32.0	1.60	15.23	13.74	36.76	147.42	107	60.75	679	196	33.16	221	3746	0.05	0.002	0.528	0.0178
1.10	32.0	1.60	14.36	12.90	37.83	140.53	100	55.07	637	191	33.97	1457	8163	2.04	0.001	0.518	0.0419
1.20	32.0	1.60	13.56	12.13	38.70	131.57	94	49.80	599	187	34.62	1963	9695	3.73	0.001	0.508	0.0538
1.30	32.0	1.60	12.78	11.38	39.28	123.81	88	45.73	562	185	34.98	2297	6725	5.15	0.001	0.503	0.0403
1.40	32.0	1.60	12.10	10.73	39.86	116.86	83	42.08	530	184	35.34	2542	3032	6.35	0.001	0.498	0.0195
1.50	32.0	1.60	11.50	10.15	40.39	110.74	79	38.88	501	182	35.66	2733	1170	7.38	0.001	0.494	0.0080
1.60	32.0	1.60	10.93	9.60	40.80	105.98	74	36.26	474	181	35.84	2883	455	8.25	0.001	0.491	0.0033
					ETC												
1.10	5.0	1.60	14.82	13.54	39.04	91.58	105	42.74	669	182	35.67	1457	5735	2.04	0.001	0.493	0.0281
1.20	5.0	1.60	13.76	12.51	39.26	83.50	97	39.35	618	182	35.70	1963	3151	3.73	0.001	0.493	0.0170
1.30	5.0	1.60	12.76	11.54	39.20	75.29	89	36.34	570	183	35.46	2297	1138	5.15	0.001	0.496	0.0067
1.40	5.0	1.60	11.75	10.57	38.70	65.49	82	33.59	522	186	34.81	2542	334	6.35	0.001	0.506	0.0022
1.50	5.0	1.60	10.88	9.74	38.23	57.19	76	31.24	481	190	34.21	2733	93	7.38	0.001	0.515	0.0007
1.60	5.0	1.60	10.20	9.07	38.08	53.31	70	29.44	448	192	33.86	2887	31	8.27	0.001	0.520	0.0002
1.70	5.0	1.60	9.57	8.45	37.81	49.45	66	27.81	417	194	33.40	3013	11	9.06	0.001	0.527	0.0001
1.80	5.0	1.60	8.74	7.63	36.47	47.36	59	26.01	377	204	31.85	3120	3	9.75	0.001	0.553	0.0001
1.90	5.0	1.60	7.72	6.61	33.90	47.44	51	24.22	327	223	29.05	3212	1	10.36	0.001	0.606	0.0001
0.80	2.0	1.60	14.65	13.41	29.03	80.60	104	39.82	662	244	26.58	2	80	0.01	0.184	0.374	0.0004
0.90	2.0	1.60	15.30	14.04	33.62	85.51	109	42.79	694	210	30.86	3	665	0.01	0.086	0.436	0.0031
1.00	2.0	1.60	15.74	14.47	37.99	88.00	112	45.09	715	186	34.93	221	3450	0.05	0.002	0.501	0.0155
1.10	2.0	1.60	14.58	13.33	38.38	82.68	103	41.63	658	185	35.10	1457	4911	2.04	0.001	0.501	0.0244
1.20	2.0	1.60	13.49	12.27	38.48	74.30	95	38.31	606	185	35.02	1963	2376	3.73	0.001	0.503	0.0130
1.30	2.0	1.60	12.49	11.31	38.39	67.32	88	35.46	559	187	34.75	2297	832	5.15	0.001	0.507	0.0050
1.40	2.0	1.60	11.43	10.28	37.65	57.98	80	32.79	508	192	33.87	2542	234	6.35	0.001	0.520	0.0016
1.50	2.0	1.60	10.49	9.38	36.86	49.15	73	30.47	463	197	32.94	2733	60	7.38	0.001	0.534	0.0004
1.60	2.0	1.60	9.83	8.72	36.70	47.16	68	28.72	431	199	32.57	2887	20	8.27	0.001	0.541	0.0002
1.70	2.0	1.60	9.25	8.14	36.56	47.26	63	27.21	402	202	32.19	3013	7	9.06	0.001	0.547	0.0001
1.80	2.0	1.60	8.41	7.31	35.10	47.36	57	25.52	361	213	30.49	3120	2	9.75	0.001	0.577	0.0001
1.90	2.0	1.60	7.38	6.27	32.41	47.44	49	23.84	310	235	27.56	3212	0.1	10.36	0.001	0.639	0.0001

Output from PLI, with interpolation for bmep of 10bar

Lamb	Ig. Ang dbtdc	Inl P Bar	IMEP Bar	BMEP Bar	ETA %	P MAX Bar	B. Pwr kW	H. Loss kW	B. Torq Nm	bsfc g/kWh	ETA B %	NOe ppm	NOX ppm	O2 %	CO kg/kWh	CO2 EMISSIONS	NO2
.80	35.00	1.21	11.36	10.00	28.48	113.12	77.5	44.12	494	258	25.07	2	284.39	.01	.20	.40	1.53
.90	35.00	1.17	11.35	10.00	32.53	112.03	77.8	46.27	493	226	28.64	4	906.27	.01	.09	.47	4.59
1.00	35.00	1.14	11.34	10.00	36.32	109.45	77.2	47.67	493	202	32.00	237	4006.80	.05	.00	.55	19.70
1.10	35.00	1.22	11.35	10.00	37.52	110.58	77.2	45.23	494	196	33.07	1457	8229.12	2.04	.00	.53	43.40
1.20	35.00	1.30	11.35	10.00	38.50	110.27	77.8	42.85	493	191	33.94	1963	9164.13	3.73	.00	.52	51.86
1.30	35.00	1.40	11.35	10.00	39.10	111.79	77.6	41.66	494	188	34.46	2297	6275.76	5.15	.00	.51	38.20
1.40	35.00	1.49	11.36	10.00	39.60	112.92	77.9	40.61	494	185	34.90	2542	3146.17	6.35	.00	.50	20.53
1.50	35.00	1.59	11.36	10.00	40.06	113.97	77.6	39.73	494	184	35.27	2733	1415.30	7.38	.00	.50	9.83
1.60	35.00	1.70	11.36	9.99	40.40	117.17	77.9	39.25	493	182	35.49	2882	668.49	8.25	.00	.50	4.97
1.70	35.00	1.80	11.36	9.98	40.73	117.87	78.7	38.57	493	182	35.64	3009	296.94	9.05	.00	.49	2.30
1.80	35.00	1.91	11.35	9.96	41.00	116.12	75.9	37.87	491	182	35.75	3116	123.41	9.75	.00	.49	.88
1.90	35.00	2.04	11.34	9.93	41.02	114.89	77.9	37.78	490	181	35.51	3208	57.04	10.34	.00	.50	.43
.80	32.00	1.19	11.35	10.00	28.80	111.46	77.5	42.86	493	256	25.37	2	282.69	.01	.19	.39	1.53
.90	32.00	1.15	11.34	10.00	32.91	110.42	77.6	44.95	493	223	29.00	4	907.56	.01	.09	.46	4.53
1.00	32.00	1.13	11.33	10.00	36.69	108.65	77.1	46.58	493	200	32.33	237	4006.73	.05	.00	.54	19.46
1.10	32.00	1.21	11.34	10.00	37.79	110.02	77.5	44.43	494	194	33.30	1457	8212.37	2.04	.00	.53	43.03
1.20	32.00	1.29	11.34	10.00	38.69	109.21	77.3	42.23	493	190	34.12	1963	8972.77	3.73	.00	.52	50.49
1.30	32.00	1.39	11.35	10.00	39.29	109.29	77.9	40.91	494	187	34.67	2297	5835.65	5.15	.00	.51	35.34
1.40	32.00	1.48	11.35	10.00	39.87	109.18	77.2	39.59	494	184	35.18	2542	2725.66	6.35	.00	.50	17.60
1.50	32.00	1.57	11.35	10.00	40.39	109.16	77.8	38.38	493	182	35.63	2733	1140.34	7.38	.00	.49	7.81
1.60	32.00	1.68	11.34	10.00	40.78	110.26	77.1	37.60	493	180	35.91	2882	491.28	8.25	.00	.49	3.54
						ETC											
1.00	5.00	1.05	11.17	9.99	38.64	67.07	77.2	33.33	493	187	34.52	240	3384.13	.05	.00	.51	15.36
1.10	5.00	1.14	11.19	10.00	39.08	68.23	77.2	32.90	494	185	34.91	1457	4480.90	2.04	.00	.50	22.38
1.20	5.00	1.25	11.19	10.00	39.32	67.17	77.8	32.35	494	184	35.15	1963	2353.22	3.73	.00	.50	12.87
1.30	5.00	1.36	11.18	10.00	39.25	65.49	77.8	32.02	494	184	35.14	2296	911.31	5.15	.00	.50	5.45
1.40	5.00	1.50	11.17	10.00	38.73	62.02	77.8	31.96	493	186	34.70	2542	302.76	6.35	.00	.51	1.99
1.50	5.00	1.65	11.14	10.00	38.21	58.69	78.2	31.99	493	189	34.25	2732	97.61	7.38	.00	.51	.73
1.60	5.00	1.79	11.13	9.99	38.01	58.70	76.7	32.20	493	192	33.94	2887	38.57	8.27	.00	.52	.16
1.70	5.00	1.94	11.15	9.96	37.65	58.50	78.7	32.57	492	194	33.42	3013	15.88	9.08	.00	.53	.10
1.80	5.00	2.19	11.13	9.89	36.15	63.83	77.0	33.69	487	213	31.42	3120	4.70	9.79	.00	.56	.10
1.90	5.00	2.61	11.02	9.71	33.16	74.98	68.6	36.19	483	244	26.94	3220	8.61	10.36	.00	.67	.10
.80	2.00	1.16	11.15	10.00	29.06	60.67	77.2	30.89	493	249	26.02	2	58.80	.01	.19	.38	.29
.90	2.00	1.10	11.16	10.00	33.65	61.59	77.3	31.98	493	215	30.13	4	605.35	.01	.09	.45	2.93
1.00	2.00	1.06	11.16	9.99	38.03	61.47	77.5	32.86	493	190	34.04	239	3086.32	.05	.00	.51	14.26
1.10	2.00	1.16	11.16	10.00	38.43	62.53	77.5	32.45	493	188	34.40	1457	3746.18	2.04	.00	.51	18.99
1.20	2.00	1.27	11.17	10.00	38.55	60.88	77.3	32.01	494	187	34.54	1963	1796.91	3.73	.00	.51	10.00
1.30	2.00	1.39	11.15	10.00	38.44	59.70	77.5	31.79	494	188	34.48	2296	684.97	5.15	.00	.51	4.14
1.40	2.00	1.55	11.14	10.00	37.67	56.42	77.8	31.98	494	192	33.82	2542	222.67	6.35	.00	.52	1.52
1.50	2.00	1.72	11.11	9.99	36.81	52.35	77.9	32.30	492	196	33.01	2732	68.04	7.38	.00	.53	.43
1.60	2.00	1.87	11.11	9.97	36.57	54.89	78.2	32.60	493	199	32.63	2885	26.83	8.27	.00	.54	.35
1.70	2.00	2.03	11.10	9.94	36.33	59.15	77.5	33.02	491	203	32.08	3013	13.40	9.09	.00	.55	.10
1.80	2.00	2.30	11.00	9.87	34.69	66.65	77.9	34.30	484	220	29.80	3120	6.98	9.80	.00	.60	.10
1.90	2.00	2.77	10.88	9.64	31.76	79.34	85.8	37.39	484	269	24.57	3222	.10	10.36	.00	.73	.10